AD 298-061

# THE THERMAL PROPERTIES OF TWENTY-SIX SOLID MATERIALS TO 5000°F OR THEIR DESTRUCTION TEMPERATURES

TECHNICAL DOCUMENTARY REPORT NO. ASD-TDR-62-765
August 1962

Directorate of Materials and Processes
Aeronautical Systems Division
Air Force Systems Command
Wright-Patterson Air Force Base, Ohio

Project No. 7381, Task No. 738103

(Prepared under Contract No. AF 33(616)-7319
by the Southern Research Institute, Birmingham, Alabama)

REPRODUCED BY
NATIONAL TECHNICAL
INFORMATION SERVICE
U S DEPARTMENT OF COMMERCE
SPRINGFIELD, VA 22161

# NOTICES

When Government drawings, specifications, or other data are used for any purpose other than in connection with a definitely related Government procurement operation, the United States Government thereby incurs no responsibility nor any obligation whatsoever; and the fact that the Government may have formulated, furnished, or in any way supplied the said drawings, specifications, or other data, is not to be regarded by implication or otherwise as in any manner licensing the holder or any other person or corporation, or conveying any rights or permission to manufacture, use, or sell any patented invention that may in any way be related thereto.

Qualified requesters may obtain copies of this report from the Armed Services Technical Information Agency, (ASTIA), Arlington Hall Station, Arlington 12, Virginia.

This report has been released to the Office of Technical Services, U. S. Department of Commerce, Washington 25, D. C., in stock quantities for sale to the general public.

Copies of this report should not be returned to the Aeronautical Systems Division unless return is required by security considerations, contractual obligations, or notice on a specific document.

# FOREWORD

AF 33(657)-767

This work was performed by Southern Research Institute under USAF Contract No. AF 33(616)-7319. ~~The contract was initiated under Project No. 7381,~~ "Materials Application," Task No. ~~738103,~~ "Data Collection and Correlation." The work was administered under the direction of the Directorate of Materials and Processes, Deputy for Technology, Aeronautical Systems Division, Wright-Patterson Air Force Base, Ohio. Mr. ~~Hyman Marcus~~ R. K. Boward was the project engineer.

This report covers work conducted from ~~1 May 1960 to 31 April 1962.~~ 1 Jan 1962 to 31 Dec 1962

This report supplements WADD TR 60-924 and includes much additional information concerning materials reported in that program.

This program was under the specific direction of C. D. Pears and the general direction of Sabert Oglesby.

J. G. Allen made the determinations of electrical resistivity and thermoelectric voltage and was responsible for the arduous task of assembling all of the data in a final report.

D. S. Neel performed the thermal conductivity on the S. R. I. equipment, treated the data for expansion and heat capacity, and prepared most of the tables.

W. H. Mann made all runs on the GFE thermal conductivity apparatus.

P. H. Rhodes, Jr., made all emittance runs and established the computer programs for the emittance, heat capacity, and thermoelectric voltage.

David Osment made all runs on thermal expansion and heat capacity.

Dr. W. J. Barrett directed all of the analysis of density and chemical properties.

S. G. Holder, J. O. Honeycutt, Jr., and C. A. Willhelm, Jr., prepared the specimens for photomicrographs and prepared the formal structure analysis.

# ABSTRACT

The thermal expansion, heat capacity, thermal conductivity, total normal emittance, electric resistivity, and thermoelectric voltage were investigated for 26 refractory materials, including the borides, carbides, nitrides, oxides, ATJ graphite, tungsten, and alloys of molybdenum and columbium. The temperature range was from 500°F to 5000°F. In addition to these thermophysical properties, the density, chemical analysis before and after temperature exposure, and microscopic pictures before and after temperature exposure are included to define the materials and assist in the analysis of the data.

This technical documentary report has been reviewed and is approved.

JULES I. WITTEBORT
Chief, Thermophysics Branch
Physics Laboratory
Directorate of Materials and Processes

## TABLE OF CONTENTS

Page

INTRODUCTION . . . . . . . . . . . . . . . . . . . . . . 1

THE 5000°F FURNACES . . . . . . . . . . . . . . . . . . 2

TEMPERATURE MEASUREMENT IN THE 5000°F FURNACE . 3

THE SPECIMEN MATERIALS AND THEIR GENERAL PERFORMANCE. . . . . . . . . . . . . . . . . . . . . . 4

PHOTOMICROGRAPHIC EVALUATION OF SELECTED CERAMICS, REFRACTORY METALS, AND REFRACTORY ALLOYS . . . . . . . . . . . . . . . . . . . . . . . 7

- General . . . . . . . . . . . . . . . . . . . . . . 7
- Preparation of Specimens . . . . . . . . . . . . . 7
- Toxic Specimen Materials . . . . . . . . . . . . . 8

CHEMICAL ANALYSIS . . . . . . . . . . . . . . . . . . 8

- Preparation of Samples . . . . . . . . . . . . . . 9
- Methods of Analysis . . . . . . . . . . . . . . . . 9
  - Metals. . . . . . . . . . . . . . . . . . . . . 9
  - Carbon . . . . . . . . . . . . . . . . . . . . 9
  - Nitrogen. . . . . . . . . . . . . . . . . . . . 9
  - Boron . . . . . . . . . . . . . . . . . . . . . 9
  - Emission Spectrography. . . . . . . . . . . . . 9

DENSITY MEASUREMENTS. . . . . . . . . . . . . . . . . 10

THERMAL EXPANSION. . . . . . . . . . . . . . . . . . . 10

- Apparatus and Procedure. . . . . . . . . . . . . . 10
- Error Analysis . . . . . . . . . . . . . . . . . . 12
- Data and Results . . . . . . . . . . . . . . . . . 12

## TABLE OF CONTENTS (Continued)

Page

HEAT CAPACITY . . . . . . . . . . . . . . . . . . . . . 15

Apparatus and Procedure. . . . . . . . . . . . . . . . . 15
Error Analysis . . . . . . . . . . . . . . . . . . . . . 17
Data and Results . . . . . . . . . . . . . . . . . . . . 18

SRI THERMAL CONDUCTIVITY . . . . . . . . . . . . . . . . 20

Apparatus and Procedure. . . . . . . . . . . . . . . . . 20
Error Analysis . . . . . . . . . . . . . . . . . . . . . 24
Data and Results . . . . . . . . . . . . . . . . . . . . 24

GFE THERMAL CONDUCTIVITY. . . . . . . . . . . . . . . . 29

Apparatus and Procedure. . . . . . . . . . . . . . . . . 29
Data and Results . . . . . . . . . . . . . . . . . . . . 32

TOTAL NORMAL EMITTANCE TO 5000°F . . . . . . . . . . . 33

General . . . . . . . . . . . . . . . . . . . . . . . . 33
Description of Apparatus . . . . . . . . . . . . . . . . 34
Calibration Procedure . . . . . . . . . . . . . . . . . 35
Operating Procedure. . . . . . . . . . . . . . . . . . . 36
Emittance Calculation . . . . . . . . . . . . . . . . . 38
Error Analysis . . . . . . . . . . . . . . . . . . . . . 38
Data and Results. . . . . . . . . . . . . . . . . . . . 39

ELECTRICAL RESISTIVITY. . . . . . . . . . . . . . . . . 43

General . . . . . . . . . . . . . . . . . . . . . . . . 43
Apparatus and Procedure. . . . . . . . . . . . . . . . . 43
Error Analysis . . . . . . . . . . . . . . . . . . . . . 45
Data and Results. . . . . . . . . . . . . . . . . . . . 46

THERMOELECTRIC VOLTAGE . . . . . . . . . . . . . . . . . 48

General . . . . . . . . . . . . . . . . . . . . . . . . 48
Apparatus and Procedure. . . . . . . . . . . . . . . . . 49
Error Analysis . . . . . . . . . . . . . . . . . . . . . 49
Data and Results . . . . . . . . . . . . . . . . . . . . 50

TABLE OF CONTENTS (Continued)

Page

CONCLUSIONS . . . . . . . . . . . . . . . . . . . . . . . . 53

# LIST OF ILLUSTRATIONS

| Figure No. | | Page |
|---|---|---|
| 1 | Schematic Cross Section of Furnaces No. 1 and No. 2 Employing Helical Graphite Heaters and Pressure and Vacuum Capability . . . . . . . . | 56 |
| 2 | Schematic Cross Section of 5000°F Furnaces No. 3, No. 4, and No. 8 Employing Helical Graphite Heaters for Atmospheric Pressure Operation . . . . . . . . . . . . . . . . . . . . . | 57 |
| 3 | Relation of Furnace Temperature and Input Power . . . . . . . . . . . . . . . . . . . . . | 58 |
| 4 | Furnace Number 1 with Expansion Apparatus Installed . . . . . . . . . . . . . . . . . . . . . | 59 |
| 5 | Furnace Number 8 with Thermal Conductivity Apparatus Installed . . . . . . . . . . . . . . . | 60 |
| 6 | Furnace Number 4 with Heat Capacity Apparatus Installed . . . . . . . . . . . . . . . . . . . . . | 61 |
| 7 | Schematic Cross Section of Electrical Property Furnace Employing Tubular Graphite Heater . . . | 62 |
| 8 | Electrical Property Furnace with Electrical Resistivity Apparatus Installed . . . . . . . . . . | 63 |
| 9 | Electrical Property Furnace with Thermoelectric Voltage Apparatus Installed . . . . . . . . . . . | 64 |
| 10 | Temperature Calibration Curves for Optical Pyrometer . . . . . . . . . . . . . . . . . . . . | 65 |
| 11 | Picture of Tantalum, Tungsten Wire, Tungsten Sheet, and Part of Arc-Cast Tungsten Specimen After Exposure to 5000°F (Specimens in Listed Order from 3 to 4 on the Scale) . . . . . . . . . . | 66 |
| 12 | Photomicrographs of Hafnium Diboride . . . . . . | 67 |
| 13 | Photomicrographs of Thorium Tetraboride . . . . | 67 |

LIST OF ILLUSTRATIONS (Continued).

| Figure No. | | Page |
|---|---|---|
| 14 | Photomicrographs of Titanium Diboride . . . . . | 68 |
| 15 | Photomicrographs of Tungsten Boride . . . . . . . | 68 |
| 16 | Photomicrographs of Zirconium Diboride . . . . . | 69 |
| 17 | Photomicrographs of Columbium Carbide . . . . . | 69 |
| 18 | Photomicrographs of Dimolybdenum Carbide . . . | 70 |
| 19 | Photomicrographs of Hafnium Carbide . . . . . . | 70 |
| 20 | Photomicrographs of Tantalum Carbide. . . . . . | 71 |
| 21 | Photomicrographs of Titanium Carbide . . . . . . , | 71 |
| 22 | Photomicrographs of Tungsten Carbide . . . . . . | 72 |
| 23 | Photomicrographs of Vanadium Carbide. . . . . . | 72 |
| 24 | Photomicrographs of Zirconium Carbide . . . . . | 73 |
| 25 | Photomicrographs of Boron Nitride. . . . . . . . | 73 |
| 26 | Photomicrographs of Hafnium Nitride. . . . . . . | 74 |
| 27 | Photomicrographs of Silicon Nitride . . . . . . . | 74 |
| 28 | Photomicrographs of Tantalum Nitride . . . . . . . | 75 |
| 29 | Photomicrographs of Titanium Nitride . . . . . . | 75 |
| 30 | Photomicrographs of Zirconium Nitride. . . . . . | 76 |
| 31 | Photomicrographs of Beryllium Oxide . . . . . . . | 76 |
| 32 | Photomicrographs of Cerium Dioxide. . . . . . . . | 77 |
| 33 | Photomicrographs of Hafnium Dioxide . . . . . . | 77 |

## LIST OF ILLUSTRATIONS (Continued).

| Figure No. | | Page |
|---|---|---|
| 34 | Photomicrographs of Magnesium Oxide | 78 |
| 35 | Photomicrographs of Thorium Dioxide | 78 |
| 36 | Photomicrographs of Zirconium Dioxide | 79 |
| 37 | Photomicrographs of Columbium +0.5% Zirconium | 79 |
| 38 | Photomicrographs of Molybdenum +0.5% Titanium | 80 |
| 39 | Photomicrographs of Tungsten (Carborundum) | 80 |
| 40 | Photomicrographs of Tungsten (General Electric) | 81 |
| 41 | Photomicrographs of ATJ Graphite | 81 |
| 42 | Photomicrographs of Zirconium Silicate | 82 |
| 43 | Picture of the Graphite Dilatometer Tubes for Measuring Thermal Expansion to 5000°F | 83 |
| 44 | Thermal Expansion of Hafnium Diboride | 84 |
| 45 | Thermal Expansion of Thorium Tetraboride | 85 |
| 46 | Thermal Expansion of Titanium Diboride | 86 |
| 47 | Thermal Expansion of Tungsten Boride | 87 |
| 48 | Thermal Expansion of Dimolybdenum Carbide | 88 |
| 49 | Thermal Expansion of Titanium Carbide | 89 |
| 50 | Thermal Expansion of Tungsten Carbide | 90 |
| 51 | Thermal Expansion of Vanadium Carbide | 91 |
| 52 | Thermal Expansion of Boron Nitride | 92 |
| 53 | Thermal Expansion of Tantalum Nitride | 93 |

## LIST OF ILLUSTRATIONS (Continued).

| Figure No. | | Page |
|---|---|---|
| 54 | Thermal Expansion of Beryllium Oxide | 94 |
| 55 | Thermal Expansion of Cerium Dioxide | 95 |
| 56 | Thermal Expansion of Hafnium Dioxide | 96 |
| 57 | Thermal Expansion of Magnesium Oxide | 97 |
| 58 | Thermal Expansion of Thorium Dioxide | 98 |
| 59 | Thermal Expansion of Zirconium Dioxide | 99 |
| 60 | Thermal Expansion of Columbium +0.5% Zirconium | 100 |
| 61 | Thermal Expansion of Molybdenum +0.5% Titanium | 101 |
| 62 | Ice Calorimeter, Drop Type - Specimens to 5000°F | 102 |
| 63 | Picture of Ice Calorimeter Jacket and Drop Valve | 103 |
| 64 | Picture of Ice Mantle | 104 |
| 65 | Specimen Holder and Drop Rig for Insertion into Top of Furnaces | 105 |
| 66 | Mercury Displacement Due to Sapphire and 304 Stainless Steel Basket | 106 |
| 67 | Heat Capacity of ATJ Graphite and Tungsten from WADD TR 60-924 by New Equations with Some Reference Values | 107 |
| 68 | Enthalpy and Heat Capacity of Hafnium Diboride | 108 |
| 69 | Enthalpy and Heat Capacity of Thorium Tetraboride | 109 |
| 70 | Enthalpy and Heat Capacity of Titanium Diboride | 110 |
| 71 | Enthalpy and Heat Capacity of Tungsten Boride | 111 |

# LIST OF ILLUSTRATIONS

| Figure No. | | Page |
|---|---|---|
| 72 | Enthalpy and Heat Capacity of Dimolybdenum Carbide | 112 |
| 73 | Enthalpy and Heat Capacity of Titanium Carbide | 113 |
| 74 | Enthalpy and Heat Capacity of Tungsten Carbide | 114 |
| 75 | Enthalpy and Heat Capacity of Vanadium Carbide | 115 |
| 76 | Enthalpy and Heat Capacity of Boron Nitride | 116 |
| 77 | Enthalpy and Heat Capacity of Tantalum Nitride | 117 |
| 78 | Enthalpy and Heat Capacity of Beryllium Oxide | 118 |
| 79 | Enthalpy and Heat Capacity of Cerium Dioxide | 119 |
| 80 | Enthalpy and Heat Capacity of Hafnium Dioxide | 120 |
| 81 | Enthalpy and Heat Capacity of Magnesium Oxide | 121 |
| 82 | Enthalpy and Heat Capacity of Thorium Dioxide | 122 |
| 83 | Enthalpy and Heat Capacity of Zirconium Dioxide | 123 |
| 84 | Enthalpy and Heat Capacity of Columbium +0.5% Zirconium | 124 |
| 85 | Enthalpy and Heat Capacity of Molybdenum +0.5% Titanium | 125 |
| 86 | Cross-section Schematic of the Thermal Conductivity Apparatus | 126 |
| 87 | Picture of the Radial Thermal Conductivity Apparatus | 127 |
| 88 | Thermal Conductivity of Hafnium Diboride | 128 |
| 89 | Thermal Conductivity of Thorium Tetraboride | 128 |

## LIST OF ILLUSTRATIONS (Continued)

Figure No. Page

90 Thermal Conductivity of Titanium Diboride . . . . 129

91 Thermal Conductivity of Tungsten Boride . . . . . 129

92 Thermal Conductivity of Zirconium Diboride . . . 130

93 Thermal Conductivity of Dimolybdenum Carbide . . 130

94 Thermal Conductivity of Hafnium Carbide. . . . . 131

95 Thermal Conductivity of Titanium Carbide . . . . 131

96 Thermal Conductivity of Tungsten Carbide . . . . 132

97 Thermal Conductivity of Vanadium Carbide . . . . 132

98 Thermal Conductivity of Boron Nitride . . . . . . 133

99 Thermal Conductivity of Tantalum Nitride. . . . . 133

100 Thermal Conductivity of Beryllium Oxide . . . . . 134

101 Thermal Conductivity of Cerium Dioxide . . . . . 134

102 Thermal Conductivity of Hafnium Dioxide . . . . . 135

103 Thermal Conductivity of Magnesium Oxide . . . . 135

104 Thermal Conductivity of Thorium Dioxide. . . . . 136

105 Thermal Conductivity of Zirconium Dioxide . . . . 136

106 Thermal Conductivity of Columbium +0.5% Zirconium. . . . . . . . . . . . . . . . . . . . 137

107 Thermal Conductivity of Molybdenum +0.5% Titanium . . . . . . . . . . . . . . . . . . . . 137

108 Thermal Conductivity of Tungsten . . . . . . . . . 138

109 Thermal Conductivity of ATJ Graphite . . . . . . 138

## LIST OF ILLUSTRATIONS (Continued)

Figure No. Page

110 Picture of GFE Furnace with Thermal Conductivity Apparatus Installed . . . . . . . . . . . . . . . . 139

111 Thermal Conductivity Specimen for GFE . . . . . 140

112 GFE Thermal Conductivity Specimens Showing Different Hole Configurations . . . . . . . . . . . 141

113 Exposed GFE Thermal Conductivity Specimen . . . 142

114 Thermal Conductivity of Cerium Dioxide with GFE Apparatus . . . . . . . . . . . . . . . . . . 143

115 Thermal Conductivity of Magnesium Oxide with GFE Apparatus . . . . . . . . . . . . . . . . . . 143

116 Thermal Conductivity of Zirconium Dioxide with GFE Apparatus . . . . . . . . . . . . . . . . 144

117 Thermal Conductivity of Columbium +0.5% Zirconium with GFE Apparatus . . . . . . . . . . . 144

118 Thermal Conductivity of Molybdenum +0.5% Titanium with GFE Apparatus . . . . . . . . . . . 145

119 Thermal Conductivity of ATJ Graphite Using 1" and $2\frac{1}{2}$" Diameter Specimens . . . . . . . . . . . 145

120 Picture of the Apparatus for Measuring Total Normal Emittance . . . . . . . . . . . . . . . . . 146

121 Cross Section of Emittance Apparatus with Flat Coil Furnace . . . . . . . . . . . . . . . . . . 147

122 Schematic of 160-Junction Thermopile in Emissivity Equipment . . . . . . . . . . . . . . . 148

123 Cross Section of Emittance Apparatus with Black Body Furnace . . . . . . . . . . . . . . . . 149

## LIST OF ILLUSTRATIONS (Continued)

| Figure No. | | Page |
|---|---|---|
| 124 | Black Body Calibration Curve . . . . . . . . . . . | 150 |
| 125 | Calculation Standards for Total Normal Emittance . | 151 |
| 126 | Correction for Mirror and Sapphire Window in Emittance Apparatus . . . . . . . . . . . . . . . | 152 |
| 127 | Correction for Brightness Temperature to True Temperature . . . . . . . . . . . . . . . . . . | 153 |
| 128 | Calculation Standards for Total Normal Emittance . | 154 |
| 129 | Total Normal Emittance of Hafnium Diboride . . . | 155 |
| 130 | Total Normal Emittance of Thorium Tetraboride. . | 155 |
| 131 | Total Normal Emittance of Titanium Diboride . . . | 156 |
| 132 | Total Normal Emittance of Tungsten Boride. . . . | 156 |
| 133 | Total Normal Emittance of Zirconium Diboride . . | 157 |
| 134 | Total Normal Emittance of Columbium Carbide . . | 157 |
| 135 | Total Normal Emittance of Dimolybdenum Carbide. | 158 |
| 136 | Total Normal Emittance of Hafnium Carbide. . . . | 158 |
| 137 | Total Normal Emittance of Tantalum Carbide . . . | 159 |
| 138 | Total Normal Emittance of Titanium Carbide . . . | 159 |
| 139 | Total Normal Emittance of Tungsten Carbide . . . | 160 |
| 140 | Total Normal Emittance of Vanadium Carbide . . . | 160 |
| 141 | Total Normal Emittance of Zirconium Carbide. . . | 161 |
| 142 | Total Normal Emittance of Boron Nitride . . . . . | 161 |

## LIST OF ILLUSTRATIONS (Continued)

| Figure No. | | Page |
|---|---|---|
| 143 | Total Normal Emittance of Hafnium Nitride | 162 |
| 144 | Total Normal Emittance of Tantalum Nitride | 162 |
| 145 | Total Normal Emittance of Titanium Nitride | 163 |
| 146 | Total Normal Emittance of Beryllium Oxide | 163 |
| 147 | Total Normal Emittance of Cerium Dioxide | 164 |
| 148 | Total Normal Emittance of Hafnium Dioxide | 164 |
| 149 | Total Normal Emittance of Magnesium Oxide | 165 |
| 150 | Total Normal Emittance of Thorium Dioxide | 165 |
| 151 | Total Normal Emittance of Zirconium Dioxide | 166 |
| 152 | Total Normal Emittance of Columbium +0.5% Zirconium | 166 |
| 153 | Total Normal Emittance of Molybdenum +0.5% Titanium | 167 |
| 154 | Total Normal Emittance of Tungsten (Carborundum) (Complete Data Including Dark Spots and Whiskers) | 167 |
| 155 | Total Normal Emittance of Tungsten (Reliable Data Unconfounded by Dark Spots or Whiskers) | 168 |
| 156 | Standard Electrical Resistivity Specimen | 169 |
| 157 | Apparatus for Measurement of Electrical Resistivity | 170 |
| 158 | Electrical Resistivity of Graphite Illustrating the Effect of Specimen Size upon Resistivity | 171 |
| 159 | Electrical Resistivity of Nickel | 172 |

## LIST OF ILLUSTRATIONS (Continued)

| Figure No. | | Page |
|---|---|---|
| 160 | Electrical Resistivity of Armco Iron . . . . . . . . | 173 |
| 161 | Electrical Resistivity of Tungsten . . . . . . . . . | 174 |
| 162 | Electrical Resistivity of Hafnium Diboride . . . . | 175 |
| 163 | Electrical Resistivity of Thorium Tetraboride. . . | 175 |
| 164 | Electrical Resistivity of Titanium Diboride . . . . | 176 |
| 165 | Electrical Resistivity of Tungsten Boride . . . . . | 176 |
| 166 | Electrical Resistivity of Zirconium Diboride . . . | 177 |
| 167 | Electrical Resistivity of Columbium Carbide . . . | 177 |
| 168 | Electrical Resistivity of Dimolybdenum Carbide . . | 178 |
| 169 | Electrical Resistivity of Hafnium Carbide. . . . . | 178 |
| 170 | Electrical Resistivity of Tantalum Carbide . . . . | 179 |
| 171 | Electrical Resistivity of Titanium Carbide . . . . | 179 |
| 172 | Electrical Resistivity of Tungsten Carbide . . . . | 180 |
| 173 | Electrical Resistivity of Vanadium Carbide . . . . | 180 |
| 174 | Electrical Resistivity of Zirconium Carbide. . . . | 181 |
| 175 | Electrical Resistivity of Hafnium Nitride . . . . . | 181 |
| 176 | Electrical Resistivity of Tantalum Nitride . . . . | 182 |
| 177 | Electrical Resistivity of Titanium Nitride. . . . . | 182 |
| 178 | Electrical Resistivity of Columbium +0.5% Zirconium. . . . . . . . . . . . . . . . . . . . | 183 |
| 179 | Electrical Resistivity of Molybdenum +0.5% Titanium . . . . . . . . . . . . . . . . . . . | 183 |

## LIST OF ILLUSTRATIONS (Continued)

| Figure No. | | Page |
|---|---|---|
| 180 | Electrical Resistivity of Tungsten (Supplied by Carborundum) | 184 |
| 181 | Electrical Resistivity of Tungsten (Supplied by General Electric) | 184 |
| 182 | Apparatus for Measurement of Thermoelectric Voltage | 185 |
| 183 | Thermoelectric Voltage for Hafnium Diboride (ATJ Graphite Reference, Density = 1.73 g/cc) | 186 |
| 184 | Thermoelectric Voltage for Thorium Tetraboride (ATJ Graphite Reference, Density = 1.73 g/cc) | 187 |
| 185 | Thermoelectric Voltage for Titanium Diboride (ATJ Graphite Reference, Density = 1.73 g/cc) | 188 |
| 186 | Thermoelectric Voltage for Tungsten Boride (ATJ Graphite Reference, Density = 1.73 g/cc) | 189 |
| 187 | Thermoelectric Voltage for Zirconium Diboride (ATJ Graphite Reference, Density = 1.73 g/cc) | 190 |
| 188 | Thermoelectric Voltage for Columbium Carbide (ATJ Graphite Reference, Density = 1.73 g/cc) | 191 |
| 189 | Thermoelectric Voltage for Dimolybdenum Carbide (ATJ Graphite Reference, Density = 1.73 g/cc) | 192 |
| 190 | Thermoelectric Voltage for Hafnium Carbide (ATJ Graphite Reference, Density = 1.73 g/cc) | 193 |
| 191 | Thermoelectric Voltage for Tantalum Carbide (ATJ Graphite Reference, Density = 1.73 g/cc) | 194 |
| 192 | Thermoelectric Voltage for Titanium Carbide (ATJ Graphite Reference, Density = 1.73 g/cc) | 195 |
| 193 | Thermoelectric Voltage for Tungsten Carbide (ATJ Graphite Reference, Density = 1.73 g/cc) | 196 |

## LIST OF ILLUSTRATIONS (Continued)

| Figure No. | | Page |
|---|---|---|
| 194 | Thermoelectric Voltage for Vanadium Carbide (ATJ Graphite Reference, Density 1.73 g/cc) . . . | 197 |
| 195 | Thermoelectric Voltage for Zirconium Carbide (ATJ Graphite Reference, Density = 1.73 g/cc) . . | 198 |
| 196 | Thermoelectric Voltage for Boron Nitride (ATJ Graphite Reference, Density = 1.73 g/cc) . . | 199 |
| 197 | Thermoelectric Voltage for Hafnium Nitride (ATJ Graphite Reference, Density = 1.73 g/cc) . . | 200 |
| 198 | Thermoelectric Voltage for Titanium Nitride (ATJ Graphite Reference, Density = 1.73 g/cc) . . | 201 |
| 199 | Thermoelectric Voltage for Beryllium Oxide (ATJ Graphite Reference, Density = 1.73 g/cc) . . | 202 |
| 200 | Thermoelectric Voltage for Cerium Dioxide (ATJ Graphite Reference, Density = 1.73 g/cc) . . | 203 |
| 201 | Thermoelectric Voltage for Hafnium Dioxide (ATJ Graphite Reference, Density = 1.73 g/cc) . . | 204 |
| 202 | Thermoelectric Voltage for Magnesium Oxide (ATJ Graphite Reference, Density = 1.73 g/cc) . . | 205 |
| 203 | Thermoelectric Voltage for Thorium Dioxide (ATJ Graphite Reference, Density = 1.73 g/cc) . . | 206 |
| 204 | Thermoelectric Voltage for Zirconium Dioxide (ATJ Graphite Reference, Density = 1.73 g/cc) . . | 207 |
| 205 | Thermoelectric Voltage for Columbium +0.5% Zirconium (ATJ Graphite Reference, Density = 1.73 g/cc) . . . . . . . . . . . . . . . | 208 |
| 206 | Thermoelectric Voltage for Molybdenum +0.5% Titanium (ATJ Graphite Reference, Density = 1.73 g/cc) . . . . . . . . . . . . . . . | 209 |

## LIST OF ILLUSTRATIONS (Continued)

**Figure No.** **Page**

207 Thermoelectric Voltage for Tungsten (Carborundum) (ATJ Graphite Reference, Density = 1.73 g/cc) . . 210

208 Thermoelectric Voltage for Tungsten (Supplied by General Electric) (ATJ Graphite Reference, Density = 1.73 g/cc) . . . . . . . . . . . . . . . 211

209 Thermoelectric Voltage for ATJ Graphite (ATJ Graphite Reference, Density = 1.73 g/cc) . . 212

210 Thermoelectric Voltage for Platinum +12.2% Rhodium (ATJ Graphite Reference, Density = 1.73 g/cc) . . . . . . . . . . . . . . . 213

# LIST OF TABLES

| Table No. | | Page |
|---|---|---|
| 1 | Properties of the Materials Evaluated in the Work | 215 |
| 2 | Data Interpreted from Photomicrographs of Non Toxic Refractory Materials | 217 |
| 3 | Data Interpreted from Photomicrographs of Toxic Refractory Materials | 218 |
| 4 | Chemical Analysis of Specimens Before and After Exposure | 219 |
| 5 | Densities of Specimens Before and After Exposure | 221 |
| 6 | Thermal Expansion of Hafnium Diboride | 222 |
| 7 | Thermal Expansion of Thorium Tetraboride | 223 |
| 8 | Thermal Expansion of Titanium Diboride | 224 |
| 9 | Thermal Expansion of Tungsten Boride | 225 |
| 10 | Thermal Expansion of Dimolybdenum Carbide | 226 |
| 11 | Thermal Expansion of Titanium Carbide | 227 |
| 12 | Thermal Expansion of Tungsten Carbide | 228 |
| 13 | Thermal Expansion of Vanadium Carbide | 230 |
| 14 | Thermal Expansion of Boron Nitride | 231 |
| 15 | Thermal Expansion of Tantalum Nitride | 233 |
| 16 | Thermal Expansion of Beryllium Oxide | 234 |
| 17 | Thermal Expansion of Cerium Dioxide | 235 |

## LIST OF TABLES (Continued)

| Table No. | | Page |
|---|---|---|
| 18 | Thermal Expansion of Hafnium Dioxide | 237 |
| 19 | Thermal Expansion of Magnesium Oxide | 243 |
| 20 | Thermal Expansion of Thorium Dioxide | 244 |
| 21 | Thermal Expansion of Zirconium Dioxide | 245 |
| 22 | Thermal Expansion of Columbium +0.5% Zirconium | 249 |
| 23 | Thermal Expansion of Molybdenum +0.5% Titanium | 250 |
| 24 | Equations Expressing the Heat Capacity and Enthalpy as Functions of Temperature | 251 |
| 25 | Enthalpy and Heat Capacity Data for Hafnium Diboride | 252 |
| 26 | Enthalpy and Heat Capacity Data for Thorium Tetraboride | 253 |
| 27 | Enthalpy and Heat Capacity Data for Titanium Diboride | 254 |
| 28 | Enthalpy and Heat Capacity Data for Tungsten Boride | 255 |
| 29 | Enthalpy and Heat Capacity Data for Dimolybdenum Carbide | 256 |
| 30 | Enthalpy and Heat Capacity Data for Titanium Carbide | 257 |
| 31 | Enthalpy and Heat Capacity Data for Tungsten Carbide | 258 |
| 32 | Enthalpy and Heat Capacity Data for Vanadium Carbide | 259 |

## LIST OF TABLES (Continued)

| Table No. | | Page |
|---|---|---|
| 33 | Enthalpy and Heat Capacity Data for Boron Nitride. . | 260 |
| 34 | Enthalpy and Heat Capacity Data for Tantalum Nitride | 261 |
| 35 | Enthalpy and Heat Capacity Data for Beryllium Oxide . . . . . . . . . . . . . . . . . . . . . . . | 262 |
| 36 | Enthalpy and Heat Capacity Data for Cerium Dioxide . . . . . . . . . . . . . . . . . . . . . | 263 |
| 37 | Enthalpy and Heat Capacity Data for Hafnium Dioxide . . . . . . . . . . . . . . . . . . . . . | 264 |
| 38 | Enthalpy and Heat Capacity Data for Magnesium Oxide . . . . . . . . . . . . . . . . . . . . . . | 265 |
| 39 | Enthalpy and Heat Capacity Data for Thorium Dioxide . . . . . . . . . . . . . . . . . . . . . | 266 |
| 40 | Enthalpy and Heat Capacity Data for Zirconium Dioxide . . . . . . . . . . . . . . . . . . . . . | 267 |
| 41 | Enthalpy and Heat Capacity Data for Columbium +0.5% Zirconium. . . . . . . . . . . . . . . . . . | 268 |
| 42 | Enthalpy and Heat Capacity Data for Molybdenum +0.5% Titanium . . . . . . . . . . . . . . . . . . | 269 |
| 43 | Thermal Conductivity Data for Hafnium Diboride . . | 270 |
| 44 | Thermal Conductivity Data for Thorium Tetraboride . . . . . . . . . . . . . . . . . . | 272 |
| 45 | Thermal Conductivity Data for Titanium Diboride . . | 273 |
| 46 | Thermal Conductivity Data for Tungsten Boride . . . | 275 |

## LIST OF TABLES (Continued)

| Table No. | | Page |
|---|---|---|
| 47 | Thermal Conductivity Data for Dimolybdenum Carbide | 277 |
| 48 | Thermal Conductivity Data for Hafnium Carbide | 280 |
| 49 | Thermal Conductivity Data for Titanium Carbide | 281 |
| 50 | Thermal Conductivity Data for Tungsten Carbide | 283 |
| 51 | Thermal Conductivity Data for Vanadium Carbide | 284 |
| 52 | Thermal Conductivity Data for Boron Nitride | 286 |
| 53 | Thermal Conductivity Data for Tantalum Nitride | 288 |
| 54 | Thermal Conductivity Data for Beryllium Oxide | 290 |
| 55 | Thermal Conductivity Data for Cerium Dioxide | 292 |
| 56 | Thermal Conductivity Data for Hafnium Dioxide | 293 |
| 57 | Thermal Conductivity Data for Magnesium Oxide | 294 |
| 58 | Thermal Conductivity Data for Thorium Dioxide | 295 |
| 59 | Thermal Conductivity Data for Zirconium Dioxide | 296 |
| 60 | Thermal Conductivity Data for Columbium +0.5% Zirconium | 297 |
| 61 | Thermal Conductivity Data for Molybdenum +0.5% Titanium | 298 |
| 62 | Thermal Conductivity Data for Cerium Dioxide with GFE Apparatus | 299 |
| 63 | Thermal Conductivity Data for Magnesium Oxide with GFE Apparatus | 300 |

## LIST OF TABLES (Continued)

| Table No. | | Page |
|---|---|---|
| 64 | Thermal Conductivity Data for Zirconium Dioxide With GFE Apparatus . . . . . . . . . . . . . . . . | 301 |
| 65 | Thermal Conductivity Data for Columbium +0.5% Zirconium With GFE Apparatus . . . . . . . . . . . . | 302 |
| 66 | Thermal Conductivity Data for Molybdenum +0.5% Titanium With GFE Apparatus . . . . . . . . . . . . | 303 |
| 67 | Total Normal Emittance of Hafnium Diboride . . . . | 304 |
| 68 | Total Normal Emittance of Thorium Tetraboride. . . | 306 |
| 69 | Total Normal Emittance of Titanium Diboride . . . . | 307 |
| 70 | Total Normal Emittance of Tungsten Boride. . . . . | 308 |
| 71 | Total Normal Emittance of Zirconium Diboride . . . | 309 |
| 72 | Total Normal Emittance of Columbium Carbide . . . | 310 |
| 73 | Total Normal Emittance of Dimolybdenum Carbide. . | 312 |
| 74 | Total Normal Emittance of Hafnium Carbide. . . . . | 314 |
| 75 | Total Normal Emittance of Tantalum Carbide . . . . | 316 |
| 76 | Total Normal Emittance of Titanium Carbide . . . . | 318 |
| 77 | Total Normal Emittance of Tungsten Carbide . . . . | 320 |
| 78 | Total Normal Emittance of Vanadium Carbide . . . . | 322 |
| 79 | Total Normal Emittance of Zirconium Carbide. . . . | 324 |
| 80 | Total Normal Emittance of Boron Nitride . . . . . . | 326 |

## LIST OF TABLES (Continued)

Table No. Page

81 Total Normal Emittance of Hafnium Nitride . . . . . 327

82 Total Normal Emittance of Tantalum Nitride . . . . 329

83 Total Normal Emittance of Titanium Nitride . . . . 330

84 Total Normal Emittance of Beryllium Oxide. . . . . 332

85 Total Normal Emittance of Cerium Dioxide . . . . . 333

86 Total Normal Emittance of Hafnium Dioxide. . . . . 336

87 Total Normal Emittance of Magnesium Oxide . . . . 337

88 Total Normal Emittance of Thorium Dioxide . . . . 338

89 Total Normal Emittance of Zirconium Dioxide. . . . 339

90 Total Normal Emittance of Columbium +0.5% Zirconium. . . . . . . . . . . . . . . . . . . . 341

91 Total Normal Emittance of Molybdenum +0.5% Titanium . . . . . . . . . . . . . . . . . . . . 342

92 Total Normal Emittance of Tungsten . . . . . . . . . 343

93 The Probable Error that can be Anticipated in the Electrical Resistivity Data. Basic Data is the Electrical Resistivity at Temperature Ordinates. . . 345

94 Electrical Resistivity Data for Hafnium Diboride . . 347

95 Electrical Resistivity Data for Thorium Tetraboride . . . . . . . . . . . . . . . . . . . . 349

96 Electrical Resistivity Data for Titanium Diboride . . 350

## LIST OF TABLES (Continued)

| Table No. | | Page |
|---|---|---|
| 97 | Electrical Resistivity Data for Tungsten Boride . . . | 352 |
| 98 | Electrical Resistivity Data for Zirconium Diboride . | 353 |
| 99 | Electrical Resistivity Data for Columbium Carbide . | 354 |
| 100 | Electrical Resistivity Data for Dimolybdenum Carbide | 356 |
| 101 | Electrical Resistivity Data for Hafnium Carbide . . . | 358 |
| 102 | Electrical Resistivity Data for Tantalum Carbide . . | 361 |
| 103 | Electrical Resistivity Data for Titanium Carbide. . . | 362 |
| 104 | Electrical Resistivity Data for Tungsten Carbide. . . | 364 |
| 105 | Electrical Resistivity Data for Vanadium Carbide . . | 366 |
| 106 | Electrical Resistivity Data for Zirconium Carbide . . | 368 |
| 107 | Electrical Resistivity Data for Boron Nitride . . . . | 370 |
| 108 | Electrical Resistivity Data for Hafnium Nitride . . . | 371 |
| 109 | Electrical Resistivity Data for Tantalum Nitride. . . | 372 |
| 110 | Electrical Resistivity Data for Titanium Nitride . . . | 373 |
| 111 | Electrical Resistivity Data for Beryllium Oxide . . . | 374 |
| 112 | Electrical Resistivity Data for Cerium Dioxide . . . | 375 |
| 113 | Electrical Resistivity Data for Hafnium Dioxide . . . | 376 |
| 114 | Electrical Resistivity Data for Magnesium Oxide . . | 377 |
| 115 | Electrical Resistivity Data for Thorium Dioxide . . . | 378 |

## LIST OF TABLES (Continued)

| Table No. | | Page |
|---|---|---|
| 116 | Electrical Resistivity Data for Zirconium Dioxide . . | 379 |
| 117 | Electrical Resistivity Data for Columbium +0.5% Zirconium. . . . . . . . . . . . . . . . . . . . . | 380 |
| 118 | Electrical Resistivity Data for Molybdenum +0.5% Titanium . . . . . . . . . . . . . . . . . . . . | 382 |
| 119 | Electrical Resistivity Data for Tungsten (Supplied by Carborundum). . . . . . . . . . . . . . . . . | 385 |
| 120 | Electrical Resistivity Data for Tungsten (Supplied by General Electric) . . . . . . . . . . . . . . . | 387 |
| 121 | The Probable Error that can be Anticipated in the Thermoelectric Voltage Data. Basic Data is the Voltage Output per Degree Temperature Differential at Temperature Ordinates . . . . . . . . . . . . | 388 |
| 122 | Thermoelectric Voltage Data for Hafnium Diboride . | 389 |
| 123 | Thermoelectric Voltage Data for Thorium Tetraboride . . . . . . . . . . . . . . . . . . . . | 390 |
| 124 | Thermoelectric Voltage Data for Titanium Diboride . | 391 |
| 125 | Thermoelectric Voltage Data for Tungsten Boride . . | 392 |
| 126 | Thermoelectric Voltage Data for Zirconium Diboride. . . . . . . . . . . . . . . . . . . . . . | 394 |
| 127 | Thermoelectric Voltage Data for Columbium Carbide | 395 |
| 128 | Thermoelectric Voltage Data for Dimolybdenum Carbide . . . . . . . . . . . . . . . . . . . . . | 396 |
| 129 | Thermoelectric Voltage Data for Hafnium Carbide . . | 397 |

## LIST OF TABLES (Continued)

| Table No. | | Page |
|---|---|---|
| 130 | Thermoelectric Voltage Data for Tantalum Carbide . | 398 |
| 131 | Thermoelectric Voltage Data for Titanium Carbide . | 400 |
| 132 | Thermoelectric Voltage Data for Tungsten Carbide . | 402 |
| 133 | Thermoelectric Voltage Data for Vanadium Carbide . | 403 |
| 134 | Thermoelectric Voltage Data for Zirconium Carbide . | 405 |
| 135 | Thermoelectric Voltage Data for Boron Nitride . . . | 406 |
| 136 | Thermoelectric Voltage Data for Hafnium Nitride . . | 407 |
| 137 | Thermoelectric Voltage Data for Titanium Nitride . . | 408 |
| 138 | Thermoelectric Voltage Data for Beryllium Oxide . . | 409 |
| 139 | Thermoelectric Voltage Data for Cerium Dioxide . . | 410 |
| 140 | Thermoelectric Voltage Data for Hafnium Dioxide . . | 411 |
| 141 | Thermoelectric Voltage Data for Magnesium Oxide . | 412 |
| 142 | Thermoelectric Voltage Data for Thorium Dioxide . . | 413 |
| 143 | Thermoelectric Voltage Data for Zirconium Dioxide . | 414 |
| 144 | Thermoelectric Voltage Data for Columbium +0.5% Zirconium. . . . . . . . . . . . . . . . . . . . | 415 |
| 145 | Thermoelectric Voltage Data for Molybdenum +0.5% Titanium . . . . . . . . . . . . . . . . . . . . | 416 |
| 146 | Thermoelectric Voltage Data for Platinum +12.2% Rhodium . . . . . . . . . . . . . . . . . . . . | 417 |

## LIST OF TABLES (Continued)

Table No. Page

147 Thermoelectric Voltage Data for Tungsten (Carborundum). . . . . . . . . . . . . . . . . . . 418

148 Thermoelectric Voltage Data for Tungsten (General Electric) . . . . . . . . . . . . . . . . . 419

149 Thermoelectric Voltage Data for ATJ Graphite . . . 420

# THE THERMAL PROPERTIES OF TWENTY-SIX SOLID MATERIALS TO 5000°F OR THEIR DESTRUCTION TEMPERATURES

## INTRODUCTION

The scope of this work was the determination from 2000°F to 5000°F of the thermal conductivity, thermal expansion, heat capacity, total normal emittance, electrical resistivity, and the thermoelectric voltage of twenty-six refractory materials. The densities and the chemical compositions, before and after exposure, were determined, also. Some of the thermal properties of eight of the materials were previously evaluated and reported in WADD TR 60-924. In the course of that work, techniques were developed for reliable furnace operation at temperatures slightly greater than 5000°F. Methods were also developed for measuring the thermal properties of refractory materials at these temperatures. Of considerable interest in this work is the data showing the behavior of some of the refractory materials at these extremely high temperatures. This material behavior not only influenced the thermal property data to a great extent, but also indicated some of the difficulties that might be encountered in structural applications of these materials.

In this report, the equipment that was used in the thermal property measurements is described in considerable detail. The techniques for measuring temperature, and the calibration procedures, are presented, also.

Considerable data are included to supplement the information in WADD TR 60-924. For example, this report contains the electrical resistivity, thermoelectric voltage, emittance, photomicrographic plates, and other additional data of the materials investigated in that prior program.

---

Manuscript released by authors August 1962 for publication as an ASD Technical Documentary Report.

# THE 5000°F FURNACES

The furnaces used in the thermal property measurements were designed, built, and operated by Southern Research Institute prior to initiation of work under this contract. During the work, many improvements were incorporated to extend the temperature range and improve the heater life. At the conclusion of the work, several furnaces were available with two of one type capable of operating under pressure or vacuum and three of a second type capable of operating only at atmospheric pressure. The latter are very flexible and permit heater changeout in a few minutes. Details of both types of furnaces are shown in Figures 1 and 2. All furnaces can operate at over 5000°F on most heating loads and at 5500°F under low heat loss conditions.

The heater design was rather thoroughly investigated. A simple slotted tube was an effective heater configuration, but provision had to be made for thermal expansion during a run by permitting the electrodes to move. A helical carbon heating element permitted the use of fixed electrodes without introducing serious handling or cost problems. The helical heater configuration, with its longer service life, was incorporated in both types of furnaces. The electrical design of the heater was found to be very important. Using configurations requiring relatively low current and high voltage (150 amps at 70 volts), the current would rise sharply at 4000°F furnace temperatures suggesting a current bypass in the ionized gas around the heater element. At higher currents and lower voltages (700 amps at 15 volts), the current bypass was not noted and the furnace temperature increased with input power at a fairly uniform rate to over 5000°F; see Figure 3.

Generally, CS graphite, as produced by National Carbon Company, was used for the heater element. Different batches were quite different in electrical properties, machineability, and apparent texture so that some minor changes in heater design were required occasionally between batches.

Zirconia end plugs and spacers around the heater and inner tube proved effective. Generally, the graphite and zirconia were compatible if the temperature range at their contact points was kept below 3500°F. Deterioration of the zirconia, resulting from the carbon vapors in the gas phase, was not excessive. If the two materials were permitted to contact physically within a zone at over 3500°F, the deterioration of the zirconia was quite rapid.

All of the graphite heaters seemed to contain some silica, magnesia, calcia, sulphur, and other contaminants that vaporized out of the heaters and could be found after a run condensed on the colder (2500°F) parts of the tubes.

Different purge gases were employed, including helium, argon, and nitrogen. Since no major difference in performance was noted, helium was selected as the primary purge. This gas was dried by a desiccant, but no serious effort was made to clean it further since the heater life was considered satisfactory. Usually, purge rates of about 5 to 20 scfh were employed.

No difficulty was experienced with the water-cooled copper electrodes that were operated at current densities up to 300 amps per square inch. Undoubtedly, these electrodes could be made smaller and operated at even higher current densities.

Pictures of the different furnaces with the different apparatuses installed are shown in Figures 4, 5, and 6.

The final configuration for the furnace used to measure electrical resistivity and thermoelectric voltage is shown in Figure 7. This furnace employed the slotted tube design for the heater and was capable of operating to 5000°F on either AC or DC power. The slotted heater made it possible to use a variety of arrangements for determining conditions in the hot zone. Mounting the furnace in the vertical plane helped to facilitate the removal and placement of specimens. The furnace set up for electrical resistivity and thermoelectric voltage is shown in Figures 8 and 9, respectively. Heater life in this furnace was short compared to the life of the helical-type furnaces but was considered satisfactory. However, since the insulating material in the annulus came in direct contact with the heater, some difficulty was encountered when changing the heater.

## TEMPERATURE MEASUREMENT IN THE 5000°F FURNACE

The temperatures in the furnaces were determined with chromel-alumel thermocouples to 2000°F and by optical pyrometer readings through optical sight glasses with sapphire windows to 5000°F.

In addition to the actual temperature calibration runs, cross checks were obtained during data runs between the optical pyrometer and the thermocouples above 1500°F.

In previous investigations, the influence of the physical aspects of the sight tube on the resulting temperature reading was determined. As general conclusions, the temperature reading was independent of the distance of the focusing lens of the pyrometer from the source within the range of 5 to 20 inches with a normal deviation of about 10°F to 15°F. However, the diameter of the sight tube had a major influence. Tubes larger than $\frac{1}{2}$" diameter had no effect. Tubes smaller than $\frac{1}{4}$" did reduce the temperature reading by as much as 100°F to 200°F at about 3500°F. In between $\frac{1}{4}$" and $\frac{1}{2}$", the diameter of the tube had the influence of reducing the temperature by an amount dependent, also, on the tube length. Any sight tube in this critical range or smaller should be calibrated in place in the furnace or errors as large as 100°F to 500°F can result.

During runs, measurements with optical pyrometers were made by viewing the specimen through a sight window. Windows of synthetic sapphire were used in the furnaces and introduced an error in the observed optical readings. To correct these readings, the windows were calibrated by comparing readings through the windows to readings with no window. The target used for calibration was the center of an inductively heated graphite crucible with a black body depth to diameter ratio of six to one. The correction curve for the synthetic sapphire sight window is shown in Figure 10. With a steady pyrometer mount and the cavity-type target, variation in pyrometer readings was about 10°F at the 4000°F level with a constant source temperature.

For work under this contract, the true temperatures above 1500°F were taken as the corrected optical readings. Earlier investigations with high temperature thermocouples established these couples to be internally inconsistent and unreliable when compared with the optical pyrometer.

Although the furnace environment was important in the performance of the thermocouples, the chromel-alumel couples were found to be reliable for repeated runs within the life of the couple. As additional protection, double-bore alumina 0.070" diameter tubes were employed.

## THE SPECIMEN MATERIALS AND THEIR GENERAL PERFORMANCE

The refractory materials evaluated in this program were ordered under specifications requiring a maximum density, purity, and strength while employing a forming process compatible with either laboratory or production line techniques. Particle size was left to the discrimination of the supplier. Reliable performance as components at 5000°F was emphasized and the price left open. Generally, the best product for the current state of the art was anticipated. The suppliers were informed of the particular properties to be measured.

More than one supplier was found for every material; however, the price range and delivery dates were often orders of magnitude different. In every case, the supplier was selected either on the basis of a probable premium product, experience in a particular field, or a more firm guarantee of performance.

Within the very rigid confines of proprietary rights, all suppliers were very cooperative and assisted greatly in the over-all performance by expediting deliveries. In spite of this, the very nature of the work of producing the specimens resulted in some delays.

The specimen sizes were selected on the basis of maximum compatibility between the thermal property measurement apparatuses and the ability to produce a sound specimen. Some suppliers could not produce a piece bigger than one-inch diameter nor longer than about three diameters. Other suppliers questioned the homogeneity that could be anticipated for special shapes and sizes. As a compromise, solid pieces about $\frac{3}{4}$" diameter by $\frac{3}{4}$" or 3" long were selected as the goal. Southern Research Institute then shaped the specimens with diamond grinding and ultrasonic drilling equipment.

The general information on all materials is presented in Table 1. All pressed materials were pressed in the axial direction. The table contains one column listing the theoretical melting temperature and another listing the temperature at which the specimens failed in these evaluations. Only four of the materials performed at over 5000°F. This was not the furnace limit but that of the specimen materials. For a few materials, such as tantalum carbide, the temperature range could have been extended to over 5000°F without melting the specimen; however, since the specimens failed at 4800°F in a fashion such as fracturing or exploding that precluded any further measurements, the runs were concluded. Most of the specimens failed by disassociation, incipient melting, excessive softening, or a similar mechanism that indicated absolute material failure.

After the runs, the specimens were examined carefully to determine the type of failure and the possible contamination that may have resulted from carbon vapor in the furnace atmosphere. Generally, it did not appear that the presence of the trace carbon vapors actually caused any failures or induced premature temperature deterioration at other than the surface of the material. One exception was noted. The tungsten specimen melted at about

5000°F. Since the pure crystal melts at over 6000°F, it was probable that the carbon eutectic was formed. It is not known whether most of the carbon came from the furnace vapors or was in the material before exposure. Figure 11 shows some small specimens of tungsten supplied by four different suppliers and exposed to 4940°F. In one instance, the tungsten specimen melted internally and broke through the solid shell, or skeleton, of the surface material.

There is considerable evidence that many of these materials with crystal melting points of over 5000°F were actually fired during forming at considerably below the melting temperature of their crystals and even considerably below 5000°F. First, the data that was obtained on the thermophysical properties shifted considerably after the temperatures exceeded 4500°F to 5000°F. Reruns then indicated repeat data up to the level of the maximum temperature of the previous run and then again the data would shift. Second, heat soaking the specimens quite dramatically improved their subsequent performance in resistance to fracture and shifted their absolute thermophysical properties.

The maximum temperatures to which a material was taken during a run depended primarily upon the material itself. The expansion of each material was determined first to find the point of failure for the material. This was either the melting of the material or an inflection in the expansion curve indicating a rather drastic change of state of the material. The other properties were determined to this point of failure. In the case of the electrical resistivity specimens, an effort was made to stop the runs before the failure occurred so that the specimen for thermoelectric voltage determinations could be cut from the same piece of stock.

The maximum temperature for the toxic materials was held to 3500°F, except for the expansion determinations, because of the hazard of excessive boil off of vapors above this temperature. This maximum was necessary because of personnel health protection.

Specific details on the materials are presented in subsequent sections as they relate to the chemistry, structure, and measurement of the particular properties; however, the nature of the materials, furnaces, and measurements should be kept in mind during the discussion of all observations.

# PHOTOMICROGRAPHIC EVALUATION OF SELECTED CERAMICS, REFRACTORY METALS, AND REFRACTORY ALLOYS

## General

This evaluation of selected ceramics, refractory metals, and refractory alloys was directly derived from an interpretation based solely on photomicrographic evidence. Photomicrographs representative of the starting material microstructures before an exposure or heat soak were reviewed as well as photomicrographs of temperature-exposed structures. The materials were placed in two categories of (1) nontoxic and (2) toxic to warn the reader of the hazards involved and to distinguish between the nontoxics that were subjected to extensive study and the toxics that were subjected to less repetitive examination.

Microstructures were evaluated individually and collectively as the groups: (1) carbides, (2) metals and alloys, (3) diborides and boride, (4) nitrides, and (5) dioxides and oxide. Individual interpretations of structure were based on three criteria: line discontinuities (LD), random discontinuities (RD), and cracks (C). Collective or group interpretations were based on the over-all density of discontinuities, both line and random, and on cracking. See Figures 12 through 42.

## Preparation of Specimens

To prepare the specimen materials for photomicrographic examination, the specimen was first ground flat on a surface grinder using a 120 grit diamond wheel. Next, it was polished on lapping wheels impregnated with diamond compounds (AB Metati) of various sizes using mineral spirits as the lubricant. The first polishing wheel was a lead lap impregnated with diamond compound 14 microns in size to remove grinding marks made by the 120 grit diamond wheel.

The specimen was lapped on a series of maple wood wheels impregnated with diamond compound of eight microns and one micron, respectively. Between each lapping operation the specimen was rotated 90° to remove last traces of polishing scratches.

The ceramographic and metallographic test data on the nontoxic refractory materials are presented in Table 2. Tantalum carbide showed the best microstructure before and after exposure. This structure was the most uniform and had very few random discontinuities. Columbium carbide, on the other hand, showed the worst structure after exposure. This material cracked generally and severely. Before heat soaking, it showed coarse LD.

As a group, however, the carbide microstructures held up the best after exposure, with the distinct exceptions of CbC, $Mo_2C$, and WC. TaC, HfC, ZrC, VC, and TiC maintained their structural integrity. Collectively, the refractory alloys ranked as a close second to the carbides, but tungsten metal from two sources showed transaggregate cracks. The diborides and boride group ranked third and were followed by the nitrides. The dioxides and oxide group were worst, both before and after exposure; however, only small changes of coarse discontinuities occurred after exposure since the starting structures were poor. Zirconium silicate was structurally unsound both before and after exposure, and it was ranked last among all refractory materials evaluated. Extremely large and numerous voids developed in the material after exposure. Furthermore, the voids were connected by large cracks.

### Toxic Specimen Materials

The microstructures of the three toxic refractory materials were evaluated individually and ranked collectively in the following order: (1) tetraboride, and (2) oxide and dioxide. Individual interpretations of structure were based on three criteria: random discontinuities (RD), cracks (C), and fusion of aggregates. Data on the toxic materials are shown in Table 3.

Thorium tetraboride showed the best microstructure before and after exposure. This structure was composed of distinctly outlined aggregates, and no fusion of aggregates was evident. The beryllium oxide microstructure was rated second and the thorium dioxide last because of transaggregate and interaggregate cracks. With the exception of this cracking, there were essentially no microstructural changes in all materials after heat exposure.

## CHEMICAL ANALYSIS

Table 4 gives the results of chemical analysis of the materials before exposure (as received from the manufacturer) and after exposure in the furnaces. Comments regarding specific results are included as footnotes to the tables.

## Preparation of Samples

Discs ranging in thickness from one mm to five or six mm were cut from the cylindrical specimens with a diamond wheel. Any extraneous material adhering to the outer surface was removed and the discs were degreased with xylene. The samples were then crushed in a hardened steel mortar to pass a 100-mesh screen.

## Methods of Analysis

The publication, "The Analysis of Refractory Borides, Carbides, Nitrides, and Silicides," by Owen H. Kriege, Los Alamos Scientific Laboratory (LA-2306), was used as a general guide for methods of analysis.

Metals. In general the metals were determined by gravimetric methods, either with the aid of a suitable precipitant, or, in those instances where nonvolatile impurities were low, simply by ignition to an oxide. Some of the results given for the metals are likely to be high because of contamination of the weighing form by impurities. No corrections have been made for such errors.

Carbon. Carbon was determined in all samples after exposure and in most samples before exposure. The samples were burned in an oxygen atmosphere, and the carbon dioxide was absorbed by Ascarite and weighed.

Nitrogen. After some experimentation with various methods, nitrogen was finally determined by the Dumas method, using a Coleman Automatic Nitrogen Analyzer. For the nitrides one to 10 mg samples were taken, and for other materials, 20 to 60 mg. The samples were heated in the combustion tube at 1100°C with a mixture of sodium and potassium carbonates. The method worked satisfactorily for all of the nitrides, including boron nitride.

Boron. Boron was determined by the customary method of alkalimetric titration in the presence of mannitol.

Emission Spectrography. A semiquantitative method, estimated on the basis of past experience with other materials to give results within one-half to two times the true values, was used. All samples were mixed with graphite as a matrix material. Sample line intensities were compared visually with those of standards made from Spex-Mix. Samples and standards were exposed on the same plate. Because the method is semiquantitative, no corrections for impurities were made in estimating the major metallic component of the samples.

## DENSITY MEASUREMENTS

Densities were determined by three different methods. Two of these methods gave "apparent" density; the volume of the specimen was not corrected for the volume of voids or air-filled space. The experimental values by these two methods were generally in good agreement. The third method gave "true" density; voids were filled, insofar as was possible, with the immersion liquid, xylene, in which the specimens were weighed. See Table 5. Values for the "true" density were, in many instances, significantly higher than the "apparent" densities. The differences were taken as a measure of porosity of the samples.

## THERMAL EXPANSION

### Apparatus and Procedure

Thermal expansion measurements were made on all specimens, axially, in graphite tube dilatometers to over 5000°F or the destruction point of the material. The dilatometers consisted of (1) graphite tubes into which the specimens were placed; (2) graphite rods, which transmitted specimen motions to the dial gages; (3) short stainless steel tube and rod extensions; and (4) the dial gages. The dilatometers were self-contained units that were placed in the high temperature furnaces with the dilatometers hung from the top flanges of the furnaces and not in contact with the furnace inner parts. A typical dilatometer assembly and the dilatometer parts are shown in Figure 43.

Dilatometer tubes and rods were machined from National Carbon Company's Grade CS graphite stock. The effective lengths of the dilatometer tubes were equal to the combined lengths of the specimens and the dilatometer rods. The stainless steel tube and rod extensions were of equal effective lengths, eliminating errors due to the differences in coefficients of expansion. The dial gages used in the dilatometry apparatus were graduated in 0.0001" divisions. The mechanical accuracy of the B. C. Ames Company Model 212 shockless dial gages is stated by the manufacturer to be ±0.001" for any given reading at any point in the range.

The dial gage movements during any expansion run were corrected by the movement of the length of graphite dilatometer tube corresponding to the specimen length. The true total elongation of the specimen was equal to the sum of the dial gage movement and the calibrated movement of the graphite dilatometer over the specimen length. Other than in the specimen zone, the expansion of all dilatometer parts was cancelled by an equal expansion of a corresponding part of the same material at the same temperature.

Careful measurement of the graphite dilatometer parts before and after temperature exposures indicated a permanent change in length on the initial high temperature exposure. No significant dimensional changes occurred on subsequent exposures, so a preliminary heat-soaking run at 5300°F to 5700°F was standard procedure for new graphite dilatometer parts.

In preparing a specimen for the thermal expansion run, the ends were ground to a radius equal to the specimen length. This provided that one end of the specimen could shift without causing any change in dial gage indication. Most specimens were wrapped in tungsten or tantalum foil to provide protection from carbon pickup from the gas phase and the dilatometer parts.

Temperature measurements at the center of the specimen were made with chromel-alumel thermocouples to 1500°F and optical pyrometer above 1500°F.

Furnace No. 1, previously described and shown in Figures 1 and 4, was used for the thermal expansion measurements.

The specimen, and usually the dilatometer tube and rod, were measured for initial length before assembly of the dilatometer unit. The dial gage housing was anchored to the stainless steel extension tube, and the dial gage was zeroed. The unit was then inserted into the furnace and hung from the top. The bell glass was attached, the furnace sealed and evacuated several times, and purged with helium gas. At this point, the power was turned on, and the furnace heat-up started. The furnace was evacuated several more times while below 800°F to remove boil off and assure an inert atmosphere.

Data points were taken at approximately 250-500°F intervals throughout most of the temperature range. At a given power setting at least three times the theoretical soak time was allowed for complete elimination of specimen temperature gradients.

Throughout all runs, careful attention was directed to the indication of inflections in the expansion of specimens. When slope changes were evident, readings were taken much more regularly to insure true analysis of specimen behavior.

Data points were taken at less frequent intervals during the cooling period on most runs. The room temperature zero return was recorded on all runs and compared to the original zero setting.

At the completion of all runs, the specimen length was measured and recorded. On most runs, the tube and rod were measured to determine the permanent change in length. The conditions of the specimens following the runs were very carefully observed and recorded.

The thermal expansion data recorded during all specimen runs provided dial gage readings at given absolute temperatures. The treatment of the raw data required that the dial readings (observed total elongation) be converted to observed unit elongation, that the unit correction for the expansion of the graphite dilatometer tube be applied, and that the correction be algebraically added to the observed unit elongation to obtain the corrected specimen unit elongation.

## Error Analysis

From a study of the calibration runs and the specimen data obtained, results were repeatable to about 0.00025 in./in. at any given finite temperature range; and rod, tube, and specimen growth accountability was within 0.0005 in./in. over the entire exposure. The agreement with standards was also good so that the accuracy was estimated within 5%. For a thorough discussion of the error analysis refer to WADD TR 60-924.

## Data and Results

The thermal expansion data are included in Tables 6 through 23 and plotted in the graphs of Figures 44 through 61. For those runs in which the specimen was not melted or otherwise destroyed, the initial and final lengths are shown as measured by a micrometer to within ± 0.001". If the curve of unit expansion versus temperature contained a straight line portion, a tangent coefficient of expansion was shown on the curve; otherwise, over-all (or secant) coefficients were noted over a fairly large temperature range.

Practically all of the materials exhibited linear expansions up to within about 1000°F of their ultimate exposure temperatures. Usually, the materials then shrunk, expanded, and proceeded to either fracture or melt just prior to the maximum temperature. The maximum temperature was easily defined in most cases when the specimen fractured or melted. In the remaining few cases, the growth or expansion rate became so great with increasing temperature that the run was stopped and the appearance of the specimen confirmed that the material was no longer structurally sound.

For some materials, the growths and shrinkages were related to structure changes, additional sintering, densification or some other known physical event. For other materials, the growths or shrinkages were unexpected and were not explained by post exposure chemical or micrographic analysis. In spite of these anomalies, the thermal expansion data provided the good indication of the performance of the material at high temperature and pointed out some of the difficulties that could be expected in other measurements.

The expansions of the different borides were orderly and linear up to about 4000°F. All materials had coefficients within the range of $4.2 \times 10^{-6}$ to $5 \times 10^{-6}$ in./in./°F.

Above 4500°F, all of the borides deteriorated. Most of these materials have crystals that should be stable to over 5000°F so the failures were undoubtedly in the grain boundaries and in the poor structure between the crystallites. The photomicrographs confirmed this between grain and across void failure. From this observation, it can be deduced that the expansion was probably dependent on the between-grain structure. From the post exposure chemical analysis, there was no change in composition that should have influenced the thermal expansion. Only the thorium tetraboride and zirconium diboride (TR 60-924) gave evidence of densification.

The expansions of the carbides were linear up to about 4000°F with coefficients ranging from about 2.9 to $5.0 \times 10^{-6}$ in./in./°F. Although several of the carbides were sound to 4500°F, only hafnium carbide performed to 5000°F. At the top temperatures, all of the materials had considerable growth excepting hafnium carbide and zirconium carbide which shrank but did not densify appreciably. From the chemical analysis, there was little change in composition before and after the exposures; however, the photomicrographs revealed considerable rearrangement of the carbide phase with migration to grain boundaries and changes in the dispersion size and shape. These structural changes could have accompanied and irreversibly altered the thermal motions. The four carbides, $Mo_2C$, TiC, WC, and VC, all had the previously mentioned slope increases a few hundred degrees below their deterioration temperatures. There was some evidence of melting on all of the specimens after exposure. It is interesting to note that the tungsten carbide specimen had a sharp expansion slope change at 3900°F, then still an additional slope change at about 4700-4800°F, but did not show signs of melting until about 4960°F, the top exposure temperature. Literature references give a decomposition temperature for WC of 4760-4770°F. Further investigation of the literature (Leo Brewer, et al, The Chemistry and Metallurgy of Miscellaneous Materials - Thermodynamics, McGraw-Hill, 1950) reveals that WC decomposes to form $W_2C$ and carbon at 4761°F and $W_2C$ melts at 4941°F. From this information, it would seem that the tungsten carbide specimen decomposed and that the final material, $W_2C$, began melting at about 4960°F, the maximum exposure. A comparison of the initial and final densities and chemical analyses did not confirm any transformation to $W_2C$.

The expansions of the nitrides were rather linear up to 2000°F to 3000°F with coefficient ranging from $1.9 \times 10^{-6}$ to $5.0 \times 10^{-6}$ in./in./°F. Whereas the motions of the silicon nitride and boron nitride became erratic at slightly above 3000°F, all other nitrides performed in some more orderly fashion to well over 4000°F. The thermal motions over 3000°F were somewhat erratic, indicating decomposition and phase changes, and there were some large shrinkages and growths; however, the materials did remain structurally integral. The photomicrographs revealed that the structures macrocracked rather seriously and that the phases changed in size and distribution. These influences undoubtedly introduced irreversible motions. From the chemical analysis, there was appreciable carbon pickup in the tantalum nitride; however, up to 3500°F, this contamination was essentially zero and did not influence the data. All of the nitrides densified, although some cracked and let the structure open so that the expansion indicated a growth as for boron nitride.

The expansions of the oxides were typically unpredictable, with reasonably linear behavior up to a temperature (depending on the material) and coefficients ranging from about $4 \times 10^{-6}$ to $7.9 \times 10^{-6}$ in./in./°F. These values were a little higher than for the other refractory types. At temperatures above the linear thermal response, the thermal motions were erratic undulating either as a growth or shrinkage. From the photomicrographs, the crystallites were rather loosely bonded by smaller crystallites and an amorphous structure with many voids. This interconnecting structure probably accounted for a large part of the total expansion. After exposure, many cracks were observed, which had introduced irreversible thermal motions. This same phenomena was recorded for the hafnia and would probably be true for all of the oxides. The phase change for the zirconia is well described in the literature and the considerable increase in the expansion coefficient on reruns of the same specimen was probably evidence of irreversible phase shifts. All of the oxides densified somewhat, although the beryllia and magnesia structures opened with gross surface cracks. There was no chemical change in the composition that would have influenced the thermal expansion.

For the ATJ graphite, tungsten, columbium-0.5 zirconium and molybdenum-0.5 titanium, the coefficients ranged from about $2 \times 10^{-6}$ to $3 \times 10^{-6}$ in./in./°F for all but the columbium alloy, which had a high value of $5.45 \times 10^{-6}$ in./in./°F. For the graphite, there was no large inflection in the thermal motion at the higher temperatures, although there was an irreversible growth. In similar graphites, SRI has noted irreversible shrinkages depending on the specific history of the graphite. Data published by National Carbon Company on ATJ are about 10% higher; however, this deviation is far less than the deviation shown for the heat treatment of a single sample. The refractory metals all experienced a severe shrinkage at the higher temperatures well before melting started, although only the columbium alloy indicated much densification from the density measurements. The chemical analyses indicated some carbon pickup during the exposures, but the photomicrographs indicated primarily a surface effect and little change in the grains of the structure. The macrocracking was undoubtedly irreversible. For tungsten, WADC TR 56-423 reports coefficients ranging from $2.1 \times 10^{-6}$ to $3.3 \times 10^{-6}$ in./in./°F. On many other tungstens, SRI has obtained values of $2.1 \times 10^{-6}$ to $2.6 \times 10^{-6}$; however, a value of only $2.0 \times 10^{-6}$ was found for this arc cast specimen. Apparently, the range for tungsten is broad. The shrinkage of the tungsten between 3000°F and 4000°F probably is related to the softening temperature and void closure. For the molybdenum and columbium alloys, the temperatures at which the gross shrinkages started corresponded with the annealing temperatures of the main elements.

The thermal expansions of most of these refractory materials generally followed the classic laws up to 2000°F to 3000°F with the normal lattice expansions with increasing temperatures and lattice energy levels. The crystallites (and matrix phases) probably expanded in an orderly fashion with some loss of motion in the interconnecting structure or dispersions. At the higher temperatures, the thermal motions were probably influenced rather severely by annealing, macrocracking, intercrystallite refinement, and other phenomena related to the type of structure obtained for hot-pressed and pressed and sintered materials.

## HEAT CAPACITY

### Apparatus and Procedure

The apparatus used for heat capacity employed the drop technique in which the specimen was heated in a tube-type graphite furnace and then dropped in an ice calorimeter in which an ice mantle had been frozen around the cup. The heat from the specimen was sensed as the change in volume as some of the ice melted. The annulus containing the flooded ice mantle communicated with the atmosphere through a mercury column so that the change in volume was read directly on a calibrated glass tube to provide a volumetric mercury accounting system. The flutter valve immediately above the cup is a major feature and blocked radiation losses from the specimen up the drop tube. This heat was conducted to the cup wall and ice mantle. The details of the furnace were presented in an earlier section of this report, see Figures 2 and 6. A cross section of the apparatus is shown in Figure 62. Detailed pictures of the ice calorimeter, the ice mantel, and the drop rig are shown in Figures 63, 64, and 65.

In operation, the specimen (normally $\frac{3}{4}$" in diameter by about $\frac{3}{4}$" long) was enclosed in a basket and tungsten or tantalum foil when required for protection from carbon vapor, heated to desired temperature, and dropped into the ice calorimeter. Typical data showing the mercury displacement as a function of time before, during and after the drop are plotted in Figure 66. The mercury displacement was a measure of the amount of ice on the mantle that had melted; the time was measured from any selected interval after freezing the mantle and permitting the subcooling to equilibrate at 32°F. For the first 30 minutes or so, the slope was a measure of the heat loss from the system. At the time of the specimen drop, the slope increased sharply. After the specimen had cooled to 32°F, the curve flattened out to the same slope that existed before the drop. The heat removed from the specimen and basket was proportional to the displacement of the two slopes before and after the drop. To determine the enthalpy of the specimen alone, it was necessary to know the effect of the drop basket, radiation losses, drop losses, and unknowns upon the system. These factors were determined by making runs with the drop basket alone. The mercury displacement caused by dropping the basket included the above-mentioned losses and provided a convenient way to correct for system unknown. The mercury displacement units were calculated so that one cc theoretically was equivalent to 3.5 Btu.

Material: Synthetic Sapphire at 1503°F

From Figure 66, total displacement = 5.95 cc
From Figure 66, basket displacement = 0.[illegible] cc
By subtraction, displacement due to specimen = 5.35 cc
Specimen Weight = 21.765 grams = 0.048 lbs

$$\text{Enthalpy} = \frac{5.35 \times 3.5}{0.048} = 390 \text{ Btu/lb (Reference } 32°\text{F)}$$

Drops were made at 500°F temperature increments and enthalpy versus temperature plots obtained. Different techniques have been employed to reduce the enthalpy data to heat capacity versus temperature information. First, the slopes of the enthalpy plots were read from the curves at 1000°F total increments around a mean temperature. This slope was the average heat capacity of the material at this temperature. This technique has the major advantage of being insensitive to small, odd inflections in the curve and yet, provides reliable data that is not distorted by the practical inability to write a precise equation that matches the enthalpy plot throughout its entire range. The solid curves were plotted using this technique.

As a second method of treating the enthalpy data to obtain heat capacity versus temperature information, cubic equations were written for the least squares curve fit of the enthalpy plot, and the heat capacity was found by differentiation of the enthalpy equation. Unfortunately, most of the enthalpy data, over the wide temperature ranges employed, had several inflections so that the equation actually fit precisely only at a few points of intersection rather than over the entire range. Since heat capacity is the derivative of the enthalpy plot, any deviation of the equation from the observed data introduced a magnified error in heat capacity. Further, this equation did not anticipate the theoretical behavior.

Finally, a technique was selected that does not provide the best definition of the enthalpy data over the entire temperature range but does anticipate the theoretical behavior and is consistent with methods recommended by WADC TR 57-308 and K. K. Kelley in USBM Bulletin 584. The enthalpy data were fitted by a least squares treatment of $H_1 - H_2 = aT + bT^2 + c/T + d$. The derivative of this equation provided a relation for heat capacity that was adjusted in the lower temperature range by resolving for the value of c to make the plot of the equation pass through the heat capacity value obtained graphically at 500°F for each material. This is similar to the technique of Kelley in making the equation pass through a known value at zero reference temperature. All data from past reports and TR 60-924 have been converted to this data treatment and the equations included in the figures herein and in Table 24 for the materials of TR 60-924. The equations are good from 500°F to within about 500°F of the top exposure temperatures but cannot be extrapolated.

## Error Analysis

A compilation of all errors indicated that the apparatus was accurate to well within 5% error over the entire temperature range. Comparison of Southern Research Institute data on copper, Linde synthetic sapphire, ATJ graphite, and many other isolated check points on the specimen materials all confirmed the accuracy. For a thorough discussion of the error analysis and the data on copper and sapphire, refer to WADD TR 60-924. For the reference data on ATJ graphite and tungsten, see Figure 67. These data are discussed in the next section.

## Data and Results

Data for the heat capacities of the materials are presented in Tables 25 through 42 and Figures 68 through 85. Reference values are included on the curves. In the figures, the enthalpy above the reference temperature of 32°F was plotted against specimen drop temperature and an equation developed for the data. The heat capacity curve was developed and plotted on a second part of the same figure. It is emphasized that the heat capacity equation presents instantaneous values since the slope of the enthalpy curve at a given temperature is plotted as heat capacity. Mean data can be obtained from the enthalpy curve, which would be the over-all capacity from 32°F to a selected temperature; however, the instantaneous data are probably preferred by most designers and data analysts. Recall that there is some hazard in presenting instantaneous data in that the heat capacity curve may show excessive undulating character or excessive linearization that is not strictly a property of the material, and that data at a temperature immediately above or below any one temperature influences the slope at a finite temperature range as obtained by this analytical approach.

The heat capacity values for the borides were orderly, increasing with temperature for all materials except for titanium diboride above 3500°F, and tantalum boride and zirconium boride above 2000°F. For these materials the values became about constant. An inspection of the enthalpy data for these borides reveals that there was considerable scatter above 3000°F. From the photomicrographs, the dispersion phases did change at the higher temperatures and new interfaces were formed. This same physical behavior was noted for the tungsten boride for which the data tended to behave similarly. The heat capacity values at 3000°F ranged between 0.1 and 0.2 Btu/lb/°F for the borides with titanium boride a little higher and tungsten boride a little lower.

The enthalpy data for the carbides contained a minimum scatter to the higher temperatures and the heat capacities increased uniformly with temperature and became essentially constant above 3000°F to 3500°F. Two exceptions were zirconium carbide and vanadium carbide, which had increasing values through the high temperature range. The vanadium carbide had a rather large decrease in density after the high temperature exposures. The photomicrographs for these materials revealed relatively little change in their structures. The heat capacities of the columbium carbide, dimolybdenum carbide, and tungsten carbide were orderly even though the pictures indicated rather severe changes in the dispersion phase and the formation of new interfaces. The values of the carbides ranged from about 0.1 Btu/lb/°F to 0.4 Btu/lb/°F with hafnium carbide, tantalum carbide, and tungsten carbide being on the low side.

The heat capacities of all the nitrides increased with increasing temperature initially and then became fairly constant at above about 2000°F to 3000°F. The enthalpy data for the zirconium nitride had considerable scatter. This material showed considerable degradation at above 3000°F. All of the nitrides contained considerable dispersions and formed new interfaces so the normal increase in lattice energy with increasing temperature might not be expected. The large densification of the tantalum nitride and titanium nitride undoubtedly influenced the ability of the lattices to store energy and distorted the character of the heat capacity curve. The heat capacity of the nitrides at 3000°F ranged from about 0.08 to 0.3 Btu/lb/°F with tantalum lower and boron nitride much higher at about 0.45 Btu/lb/°F.

The heat capacities of the oxides increased with temperature initially and then tended to become constant. Generally, the data scatter was high, probably because of the temperature-time dependence of the poorly developed structure between the crystallites as shown in the photomicrographs. The values for the oxides at 3000°F ranged from about 0.08 Btu/lb/°F for thoria to almost 0.6 Btu/lb/°F for beryllia. The other oxide materials had values ranging from about 0.1 to 0.3 Btu/lb/°F at 3000°F. Literature data (WADC TR 58-476) for MgO and $ZrO_2$ give comparable specific heat values for these materials at 1500°F and 2000°F, respectively. At 1500°F for MgO, the literature value is about 0.32 Btu/lb/°F, as compared to Southern Research Institute data of 0.31 Btu/lb/°F. At 2000°F for $ZrO_2$, the literature shows a specific heat of about 0.154 whereas Southern Research Institute data are about 0.162 Btu/lb/°F. On $ZrO_2$, the influence of a phase transformation was expected, as had been found in other zirconias in the 2000°F to 2500°F temperature range, but was not noticeable in the data. Observe the curves for the different zirconias.

For the ATJ graphite, tungsten, columbium-0.5 zirconium, and molybdenum-0.5 titanium, the heat capacities increased with temperature initially and then became either linear or constant at above 2500°F. Apparently, the densification of the columbium alloy, the formation of the many interfaces in the tungsten, and the changes in the dispersion phases did not introduce sharp inflections in the heat capacity-temperature curves; however, these factors may have influenced the freedom of the lattice to vibrate and store energy on an accumulative basis of temperature-time and thus influenced the over-all shapes of the curves. For the graphite, the agreement between Ubbelohde and the SRI values was excellent, as shown in Figure 67, when using the SRI equation. The graphical data of SRI contained more character, but the agreement was still good. For the tungsten, the agreement between the Rembar and the SRI values was excellent at above 1000°F when using the SRI equation. The agreement with WADC TR 56-423 was not so good with that data being about 13% lower; however, the data from WADC TR 56-423 provided a heat capacity curve concave upward contrary to theoretical expectations and as would be obtained if low enthalpy values were obtained in the mid and higher temperature vicinities. As discussed by Kelley, the drop method should retain its precision at higher temperatures whereas the direct measurement of heat capacity at different temperatures and the summation of these values results in an accumulation of errors with the same problems of data treatment. The graphical data of SRI for tungsten were a little higher in the mid-temperature range and a little lower in the high-temperature range. Of course, the same equations should be used for a strict comparison of data between different investigators. For the alloys, no good reference data were found. There is no evidence that the carbon pickup in the materials influenced the heat capacities. The small amount of additional carbon entered as dispersions or surface effects and contributed only on a weight percentage basis and not by influencing the basic lattice arrangements. Other factors such as intercrystallite lattice growths and void alterations were undoubtedly much more significant.

During this program, it was found that all materials of the "same" composition do not have the same heat capacities. For example, a zirconium diboride from another investigator had enthalpy values 16% higher at 1300°F when both were analyzed in the SRI equipment. Further, some pressed and sintered tungstens from another source were found to have heat capacities much lower than that of the arc cast material in this program and in good agreement with values from WADC TR 56-423.

The data in the tables for enthalpy and drop temperature include the weight of the specimens before and after each drop. These data provide valuable information on the stability of the material as the weight loss can be obtained as a function of temperature. The times at temperature were not held constant but were usually about 15 minutes with one to two hours required to reach the temperature level.

## SRI THERMAL CONDUCTIVITY

### Apparatus and Procedure

Thermal conductivity measurements were made to 5000°F with a radial heat flow apparatus that utilized a miniaturized specimen $\frac{3}{4}$" long. A cross-section schematic and a picture of the conductivity apparatus are shown in Figures 86 and 87, respectively. The apparatus consisted primarily of (1) water calorimeter that passed through the center of the specimen; (2) guards made from the specimen material at both ends of the specimen to prevent axial heat losses; (3) optical or thermocouple temperature measuring devices in the specimen; and (4) an external heat source. The water calorimeter provided a heat sink at the center of the specimen to create a substantial heat flow through the material. Thermocouples mounted $\frac{1}{4}$" apart in the calorimeter water stream measured the increase in the temperature of the water as it passed through the gage portion of the specimen. By also metering the water flow through the calorimeter, all variables necessary for calculating heat flow were determined. The total radial heat flow through the $\frac{1}{4}$" specimen gage section into the calorimeter was calculated from the standard relation of $Q = MC\Delta T$. In this particular case, M was the weight of water flowing per hour, C was unity for water, and $\Delta T$ was the temperature rise of the water as it passed through the gage section.

The specimen configuration was $\frac{3}{4}$" long, $\frac{3}{4}$" outside diameter, $\frac{1}{4}$" inside diameter, with $\frac{3}{8}$" deep, 0.073" diameter holes on radii of $\frac{3}{16}$" and $\frac{5}{16}$" permit temperature measurement within the specimen, Guards of specimen material, generally $\frac{3}{8}$" and $\frac{3}{4}$" long, were placed above and below the specimen, respectively, to maintain a constant radial temperature gradient over a sufficient axial distance and minimize axial heat flow. Graphite tubes filled with thermatomic carbon were placed next to the specimen guards and further insulated the system. The graphite tubes also held the specimens in alignment. The combined effect of specimen guards and excellent thermatomic carbon insultation permitted a minimum axial temperature gradient not detectable by optical pyrometer readings sensitive to 10°F.

To provide controlled radial heat flow from the $\frac{1}{4}$" inside diameter of the specimen to the $\frac{7}{32}$" outside diameter of the water calorimeter tube, the annulus was packed with copper, graphite, or lamp black. The filled annulus permitted heat flow through the material and, also, provided a positive method of centering the water calorimeter within the specimen. Generally, copper granules were preferred as the packing on low temperature runs to increase the heat flow, and graphite lathe dust on high temperature runs. Some exceptions were encountered, especially on materials with a high conductivity. To prevent swamping of the calorimeter by excessive heat flow in these cases, low conductivity packing materials were used.

Up to 2000°F, the specimen temperatures were measured with chromel-alumel thermocouples. At high temperatures, optical sight tubes were aligned to view the bottoms of the specimen temperature holes from the top of the furnace. The temperature drop across the $\frac{1}{8}$" specimen distance was then read with an optical pyrometer sighted through a right-angle mirror device.

In the prior Figure 87 showing a typical conductivity calorimeter apparatus ready for insertion in a furnace for a run, the specimen and specimen guards can be seen at the center of the unit. The specimen guards were shouldered within the graphite extension tubes that contained lamp black insulation. A water-cooled, stainless-steel section can be seen at the top of the unit. This section provided permanent optical sight tubes to within about $2\frac{1}{2}$" of the guard specimen, in addition to a permanent mount for the right-angle mirror device. Within the short graphite tube between the water-cooled section and the top specimen guard, graphite sight tubes were fitted. The remainder of the annulus was filled with lamp black insulation.

For the 2000°F temperature range, several thermocouple readings were made along with the optical pyrometer readings as a check. The thermocouples were placed in the specimen through the graphite and water-cooled tubes. This arrangement permitted crosschecking without the inconvenience of an additional run.

During thermal conductivity runs, the following data were recorded: (1) power input; (2) specimen face temperature; (3) specimen temperatures in the gage section at the $\frac{3}{16}$" and $\frac{5}{16}$" radii; (4) temperature of the water in the calorimeter at two points $\frac{1}{4}$" apart axially within the specimen center; and (5) flow rate of the water through the calorimeter. Several readings (four to six) were made at each general temperature range to establish data scatter, to eliminate the error due to stray points, and to determine the influence of water flow rates through the calorimeter and provide a method of observing internal consistency in the data. Generally, a series of readings were made about every 500°F through the temperature range.

All thermocouple readings were measured on a Leeds and Northrup K-2 null balance potentiometer used in conjunction with a galvanometer of 0.43 microvolts per mm deflection sensitivity. All optically measured temperatures were read with a Leeds and Northrup Type 8622 optical pyrometer. The flow rate of the calorimeter water was measured with either a Fischer and Porter Stabl-Vis Flowrator or Brooks Instrument Company flowmeter.

The thermal conductivity values for the materials evaluated under this contract were computed from the relation

$$K = \frac{Q}{A\Delta T/L}$$

where Q was the heat flow to the calorimeter within the specimen gage section; A was the log mean cylindrical area between the $\frac{5}{16}$" and $\frac{3}{16}$" radius circles through which the Q passed; $\Delta T$ was the specimen temperature change between the $\frac{5}{16}$" and $\frac{3}{16}$" radius circles; and L was the radial distance ($\frac{1}{8}$") over which specimen $\Delta T$ was measured.

Q, in the above equation, was determined from the measured calorimeter water flow and temperature increase in the specimen test section. A was calculated directly for the particular specimen configuration to be 0.00267 square feet; L was known to be 0.125". The specimen $\Delta T$ was used directly in the heat transfer relation. A sample calculation follows:

$H_2O$ Flow = 17.0 gph

$H_2O\Delta T$ = 3.14°F

Specimen $\Delta T$ = 182°F

Specimen Mean = 1810°F

Substituting in the initial equation gives:

$$Q = Mc\Delta T = \frac{17\ \text{gal} \times 8.33\ \text{lb}\ 1\ \text{Btu} \times 3.14^\circ\text{F}}{\text{hr} \qquad \text{gal}\ \text{lb}\ ^\circ\text{F}}$$

$$Q = 444.2\ \text{Btu/hr}$$

Solving the heat transfer equation for K gives:

$$K = \frac{Q}{A\Delta T/L}$$

$$K = \frac{444.2\ \text{Btu} \times 0.125\ \text{in.}}{\text{hr} \qquad 0.00267\ \text{ft}^2 \times 182^\circ\text{F}}$$

$$K = 114.3\ \text{Btu/hr/ft}^2/^\circ\text{F/in.}$$

On high temperature runs where the specimen ΔT was measured through the optical sight tubes, both of which had absolute temperature loss, the effective temperature of the specimen test section was determined from the specimen outer face temperature as a reference. For the specimen configuration used, the radial distance from the specimen face to the log mean of the test section was $\frac{1}{8}$", a length about equal to the distance between the two specimen temperature measuring points. To obtain the mean specimen temperature, 83% of the measured temperature drop was subtracted from the specimen face temperature. The 83% value was arrived at by the ratio of the log mean area of the outer $\frac{1}{8}$" section to the log mean area of the $\frac{1}{8}$" section where the specimen ΔT was measured.

## Error Analysis

A review of the different errors indicated that the systematic errors were small and the random errors somewhat larger. From this analysis and the runs on the "standards," the scatter was estimated at 10% and the absolute error at less than 7%. For most materials, the probable error was in the range of from 5% to 7%, based on the deviation of observed data points from the smooth curve fit of the data. For a detailed error analysis refer to "A Radial Heat Flow Method for the Measurement of Thermal Conductivity to 5200°F," a paper by W. H. Mann, Jr., and C. D. Pears presented at the Invitational Conference on Thermal Conductivity Methods at Battelle Memorial Institute on October 26, 27, and 28, 1961.

## Data and Results

The data for the thermal conductivity are presented in Tables 43 through 61 and plotted in the graphs of Figures 88 through 109. At least duplicate runs were made for all materials. In many cases, runs were made on both heat-soaked and unheat-soaked materials that were not homogeneous as indicated by the photomicrographs and density and chemical analysis before and after the exposures. For the better materials, the scatter was considerably less.

Reference data are included on several of the graphs indicating values obtained by other investigators. In most cases, comparative data were not available. In practically all cases, the investigator had not reported sufficient information on the specific structure and chemistry of the material.

A few graphs are presented on materials that were reruns of the prior program under WADD TR 60-924.

During thermal conductivity runs, the specimens, even though only $\frac{3}{4}$" in diameter, still had rather severe thermal gradients present between outside and inside diameters. Materials with high internal stresses are prone to break easily when exposed to such gradients and quite often fracture at comparatively low temperatures (2000°F) before data can be obtained in the 3000-5000°F range. Heat treatment of specimens prior to data runs proved to be very helpful in relieving internal stresses and improving the thermal shock resistance.

To establish the heat soak procedure, the materials were evaluated first for thermal expansion. These data provided knowledge on melting points, deterioration points, and points of definite inflection in thermal expansion. Using this information as a base, materials were programmed for one of the following heat treatments: (1) at 4000°F (for 30 minutes), heated slowly and cooled slowly; (2) at 500°F below the temperatures at which melting or deterioration occurred during expansion runs (for 30 minutes), heated slowly and cooled slowly; or (3) at about 100°F below the temperature at which the initial marked inflection of the expansion curve occurred (for 30 minutes), heated slowly and cooled slowly. The lowest temperature of the three choices was selected for each material in an effort to prevent damage during the heat treating process.

Even though extreme care was taken in heat soaking the specimens, some damage occurred on a few materials. Most specimens were undamaged, however, and undoubtedly had improved thermal shock resistance. Of the materials that were heat treated, only hafnium diboride and tantalum nitride were appreciably damaged. One of the three pieces of hafnium diboride was damaged beyond use and was replaced with a new piece of material. The two guard pieces were slightly damaged also, but were cut to provide suitable surfaces for use. One of the tantalum nitride samples broke in half during the heat treating process. This specimen broke just as did several of the refractory materials that were not heat soaked in prior work. The new pieces of hafnium diboride and tantalum nitride were both heat treated at temperatures lower than on the initial heat treatment. Possibly, the initial treatment was at a temperature higher than should have been selected. Both were soaked at 4000°F initially, which was less than 500°F of the melting or deterioration point of the material; however, expansion curve inflections were very near the 4000°F points (see Figures 44 and 53), indicating that some material change occurred in that range. Extreme care was taken on all subsequent heat treatments to prevent recurrences of specimen damage.

Following is a tabulation of heat treatment temperatures for the ten materials:

| | |
|---|---|
| Hafnium Diboride | - 4000°F, then new piece at 3500°F |
| Titanium Diboride | - 3800°F |
| Tungsten Boride | - 3500°F |
| Dimolybdenum Carbide | - 3200°F |
| Titanium Carbide | - 4050°F |
| Tungsten Carbide | - 3875°F |
| Vanadium Carbide | - 3675°F |
| Tantalum Nitride | - 4000°F, then new piece at 3000°F |
| Molybdenum-0.5 Titanium | - 2800°F |
| Columbium-0.5 Zirconium | - 3350°F |

Following the heat treatment process, the small radially spaced temperature measuring holes were drilled in the specimens. These holes were not drilled prior to heat treatment because the holes act as crack initiators.

It is difficult to determine the influence of the structures of the materials on the measurement of conductivity. As mentioned, practically all materials had severe dispersions and macrocracks. Certainly if a temperature measurement hole were located close to a nonuniformity, an error was introduced in the measurement by the distorted temperature gradient. The scatter in the data was probably introduced, primarily, by these heterogeneities.

The conductivities of the boride materials generally decreased with increasing temperature and then increased somewhat. All had a value of about 300 Btu/hr/ft$^2$/°F/in. except zirconium diboride, which was about 30% lower. The matrices of the thorium tetraboride, tungsten boride, and zirconium diboride materials became more continuous and the dispersions agglomerated a little with temperature. These behaviors probably would increase the conductivity. The borides may behave as a polycrystalline graphite with lattice vibrating controlling at the lower temperature and electron conduction permitting the higher conductivity at the higher temperatures. Certainly, there were enough grain boundaries to scatter the lattice vibrations and prevent the normal operation of this mechanism. A rerun of the zirconium diboride is shown and provided data in good agreement with that in the prior report, WADD TR 60-924.

The conductivities of most of the carbides behaved similarly with decreasing values with increasing temperature at the lower level and then increasing values at higher temperatures. An exception was the tungsten carbide with a curve convex upwards. The development of the gross macrocrack system in tungsten carbide may have caused the decreasing rate of increase in conductivity. Both dimolybdenum carbide and columbium carbide had similar macrocrack systems that probably accounted for the large scatter in their data. There were aligned discontinuities and macrocracks in about all of the carbides similar to those found in the borides that undoubtedly disrupted the thermal gradients and introduced scatter in the data. The duplicate runs should have eliminated the probability of gross errors from this cause.

A rerun was made of the hafnium carbide reported previously in WADD TR 60-924. Note that the new data provided a fairly smooth extension of the old data from about 2000°F to 4700°F. Apparently, the higher data for the one run in the prior report was on a specimen that contained undetected macrocracks, which severely distorted the thermal gradient. This material did have rather severe aligned discontinuities.

Whereas the conductivities of the boron nitride and silicon nitride decreased a little with increasing temperature to values of about 120 and 50 Btu/hr/ft$^2$/°F/in. at 3000°F, respectively, the values for titanium nitride, tantalum nitride, and hafnium nitride increased to about 150 Btu/hr/ft$^2$/°F/in. at 3000°F and for the tantalum nitride on up to 4700°F. The tantalum nitride had a heavy dispersion and considerable densification at temperature. All of the nitrides contained gross dispersions as viewed in the photomicrographs and had many aligned discontinuities that probably developed into macrocracks with temperature exposure. The data for the boron nitride were in good agreement with data in WADC TR 58-476. The minimum scatter for this material was indicative of data obtained on a fairly sound structure. Observe from the photomicrograph that this material was fairly homogeneous and, when it cracked, the failure was gross and easily detected.

Except for the hafnia, the conductivities of the oxides decreased with increasing temperature, as expected for the lattice vibration mechanism of dielectrics, but then increased at the higher temperatures. This increase was probably related with the introduction of the electron transfer as the materials became better electrical conductors at above 3000°F. Although the Wiedemann-Franz law does not apply strictly even at the lower temperatures, it was completely reversed at above 3000°F. Obviously, another mechanism prevailed. The numerous grain boundaries and the poor structure between the crystallites undoubtedly scattered the lattice vibration and did not permit that mechanism to operate ideally. The conductivity values for most of the oxides were about 10 to 20 Btu/hr/ft$^2$/°F/in. at 3000°F with ceria a little low at 5 Btu/hr/ft$^2$/°F/in. and beryllia a little high at about 75 Btu/hr/ft$^2$/°F/in. The literature values for thoria, zirconia, hafnia, and magnesia are in fair agreement; however, the literature values for beryllia are about 30% higher at 3000°F than for one specimen and twice as high for another. The beryllia investigated under this program had a theoretical density of better than 99%; however, the density is not necessarily a good measure of the conductivity of a material. Observe from the photomicrographs of this beryllia that it was unsound with crystallites poorly connected by voids and an agglomerate phase. Obviously the thermal conductivity would be influenced more by the agglomerate phase, which was continuous throughout the structure, than by the properties of the crystallite (the particles). As for the other oxides, there also was very little particle deformation and diffusion bonding. The structures were more like packed sand with only spot bonding. In spite of these photomicrographic observations, the materials were visually dense, smooth, strong and represented the current state of the commercial art in forming and fabrication. The conductivities were probably more influenced by the structure and macrocracks than by any other property. The conductivity curve for beryllia had a marked inflection at about 2100°F, the temperature of a phase change in this material; however, the other properties did not indicate an inflection at this temperature.

The conductivities of the ATJ graphite, tungsten, columbium-0.5 zirconium and molybdenum-0.5 titanium decreased with temperature to values at 3000°F of about 500 Btu/hr/ft$^2$/°F/in. for the tungsten and 150 to 200 Btu/hr/ft$^2$/°F/in. for the ATJ and the columbium and molybdenum alloys. Above 3000°F, the conductivities of these materials increased somewhat. In these polycrystalline structures, it seems logical that the electron transfer was responsible for the increasing conductivities at the higher temperatures. For the graphite, the structure contained voids, inclusions and a poorly developed lattice between the crystallites. Also, there were many macrocrack systems. Undoubtedly, the conductivity data contained scatter resulting from the distortion of the temperature gradient by these discontinuities near the temperature measurement holes.

For the tungsten and the two alloys of columbium and molybdenum, the data scatter was fairly small. All contained dispersions and aligned discontinuities; however, only the tungsten macrocracked severely. For the tungsten, the products of two different suppliers behaved similarly as to the behavior of the structure with temperature exposures. Generally, all of the metals densified and showed a slight carbon pickup at above 3500°F. The densification may have contributed to the increased conductivity at the higher temperatures. It is doubtful if the carbon pickup seriously influenced the data even above 3500°F since the carbon appeared to go into the dispersions and the dispersions were so gross. Observe for the tungsten and ATJ graphite that the data on the new specimens were somewhat different than that reported in WADD TR 60-924. For the tungsten, the values were a little higher and the curve smoother. For the graphite, the conductivity of the new batch of material, at the higher temperatures, was appreciably higher. For the same batch of material, the values were the same regardless of the specimen size of $\frac{3}{4}$" or 1". The lower values for the ATJ of the prior report were confirmed during this program. These bands probably represent the range of data that can be obtained for the "same" refractory materials of this type.

The conductivity data were surprisingly consistent within families of materials, and the scatter was essentially dependent on the homogeneity of the material. There was evidence that the development of macrocrack systems introduced errors in the data that could be detected only by duplicate and triplicate runs. The chemical and structural histories of the material must be recorded in the description to provide a means of analyzing the results and applying them to design or material study applications.

## GFE THERMAL CONDUCTIVITY

### Apparatus and Procedure

The GFE thermal conductivity furnace was extensively modified to provide a flexible furnace capable of operation to over 5000°F.

The entire internal structure of the original furnace was removed and rebuilt with components similar to those in the other 5000°F furnaces and described in the prior section of this report. As a result of the internal changes made, several external modifications became necessary. These changes were primarily plumbing and the replacement of the original furnace top. The revised top permitted better accessibility to the work area without removing the top. The modified furnace was run at atmospheric pressure with a helium environment. The interior of the furnace was patterned after Furnaces Number 1 and 2 shown in Figure 1, and a photograph of the furnace and associated equipment are shown in Figure 110.

In addition to the furnace itself, the thermal conductivity apparatus consisted of (1) the specimen, (2) an axial flow water calorimeter, which passed through the center of the specimen, (3) proper guarding for the specimen, and (4) optical or thermocouple temperature measuring within the specimen.

The specimen configuration was 3" long, $2\frac{1}{2}$" outside diameter, $\frac{3}{4}$" inside diameter, with six holes for temperature measurements. A sketch of the GFE specimen is shown in Figure 111. A photograph of two specimens with different hole orientations is shown in Figure 112. The specimen on the left had the holes on the same radial lines; this orientation was later revised to that shown on the right. To minimize axial heat flow and maintain a constant radial temperature gradient within the specimen, graphite guard cylinders filled with thermatomic carbon were placed on the top and bottom of the specimen. The top cylinder had small graphite sight tubes located to be in alignment with the temperature holes in the specimen.

The original counterflow calorimeter that came with the GFE equipment was replaced with the axial flow calorimeter developed by SRI. The counterflow calorimeter was composed of a stainless steel tube surrounding a glass tube with a coil spring placed in the annulus and a roughened surface on the inner tube to produce turbulent flow. The water temperature differential was measured by thermocouples placed axially one inch apart in the annulus. Water entered in the inner tube and exited from the annulus.

The axial flow calorimeter developed by SRI has been described in a prior section of this report.

Unlike the SRI conductivity apparatus, the GFE specimen assembly was performed within the furnace prior to a run. The axial calorimeter and lower graphite guard cylinder were left in the furnace after a run and only the specimen and upper guard cylinder removed. New specimens were set in place and the annulus between the calorimeter and specimen was packed with the appropriate packing material. For the runs made, graphite particles were used as the packing material. The upper packed cylinder was placed on the specimen and the sight holes aligned. The top water-cooled section, normally used with the SRI apparatus to extend the temperature sight holes, was not necessary with the GFE equipment.

During thermal conductivity runs, the following data were recorded: (1) power input, (2) specimen face temperature when above 2000°F, (3) specimen temperature at the six thermocouple and optical sight holes, (4) water temperature in the calorimeter at two points $\frac{1}{4}$" apart, and (5) water flow rate through the calorimeter. Several readings, usually four, at different water flow rates were made at each temperature level. Temperatures within the specimen at the six points were taken alternately between the hot and cold ones. The number of readings taken at the temperature levels was established by the data scatter, and selected to minimize the influence of random error and permit the observation of internal consistency in the data.

Monitoring equipment used for temperatures and flow rates was identical to those used with the SRI conductivity apparatus and described in another section of this report.

The thermal conductivity for the materials was computed, as with SRI conductivity apparatus from the equation:

$$K = \frac{Q}{A \Delta T / L}$$

where Q was the heat to the calorimeter within the specimen gage section; A was the log mean area between the $1\frac{1}{8}$" and $\frac{1}{2}$" radius circles through which the Q flowed; $\Delta T$ was specimen temperature change between the average of the three temperatures at the $1\frac{1}{8}$" radius and the three temperatures at the $\frac{1}{2}$" radius; and L was the radial distance ($\frac{5}{8}$") over which the specimen $\Delta T$ was measured.

Q, in the above equation, was determined from the measured water flow and temperature increase of the water; A was calculated directly as 0.00841 ft$^2$; L is 0.625". A sample calculation follows:

| | |
|---|---|
| $H_2O$ Flow | = 15.7 gph |
| $H_2O \Delta T$ | = 0.64°F |
| Specimen $\Delta T$ | = 730°F |
| Specimen Mean | = 2406°F |

Substitution in the equation:

$$Q = Mc\Delta T = \frac{15.7 \text{ gal}}{\text{hr}} \times \frac{8.33 \text{ lb}}{\text{gal}} \times \frac{1 \text{ Btu}}{\text{lb °F}} \times 0.64°\text{F}$$

$$Q = 83.6 \text{ Btu/hr}$$

Solving the heat transfer equation for K:

$$K = \frac{Q}{A\Delta T/L} = \frac{83.6 \text{ Btu} \times 0.625 \text{ in.}}{\text{hr} \times 0.00841 \text{ ft}^2 \times 730°\text{F}}$$

$$K = 8.5 \text{ Btu/hr/ft}^2/°\text{F/in.}$$

For temperature measurements with the optical pyrometer, the specimen mean temperature was determined from a relationship between the outer face temperature, the specimen $\Delta T$, and the log mean area of the specimen. This relationship established the mean temperature as the true face temperature minus 0.595 times the specimen $\Delta T$.

Data and Results

The thermal conductivity data were obtained in the GFE equipment to establish operability of the apparatus, to obtain confirming data on some of the materials, to observe the temperature distortion (or lack of it) by measuring each radial temperature gradient at three positions, and to observe the influence of the size of the specimen on the property.

The equipment was checked out at 5400°F with a graphite specimen and then data obtained on ATJ graphite, magnesia, zirconia, ceria, molybdenum-0.5 titanium and columbium-0.5 zirconium. For all materials except the magnesia, the data compared well with that obtained in the SRI equipment, see Tables 62 through 66 and Figures 114 through 119 for the data.

The conductivity of the ATJ graphite was about 15% higher than that obtained in the smaller one inch specimen in the SRI equipment. Recall that this SRI data was considerably higher than that obtained on another $\frac{3}{4}$" SRI specimen and another 1" SRI specimen. Apparently, there was no size effect, and the difference of 15% could be expected from the different specimens of the same material. Unfortunately, this result was not anticipated, and specimens of different sizes were not cut from the same block; however, density profiles indicated that even a single block may have quite different densities (perhaps 25% difference).

For the zirconia and ceria, the agreement of the data with that of the SRI equipment was excellent. This might be expected since these commercial materials are fairly repetitive in structure, and the cross bonding between crystallites is so poor that other minor differences would have little influence.

For the magnesia, the lower values for the GFE equipment cannot be explained. The soundness of the structures seemed quite different visually and to scraping, but this difference did not show in the photomicrographs. The structure between the crystallites in both specimens was so discontinuous that differences were difficult to detect.

For the alloys of columbium and molybdenum, the conductivities of the large specimens were in good agreement with the smaller ones of the SRI equipment. Since both materials had gross dispersions and neither macrocracked severely, the size of the specimen should have had little influence.

The GFE equipment performed well and provided confirming data for several of the materials. There was no consistent indication of size effect of the specimen on the data; however, the larger specimens fractured more often and were almost invariably broken during the cooling cycle. For all of the runs, the variation in temperature gradient between the "clean" holes around a common diameter of the specimen was perhaps 15%. Often a hole would become "dirty" and a clear optical view was not present. In these cases, the data were not consistent with the data from the other holes. As with the SRI apparatus, the holes had to be stepped to provide concentric ledges that permitted an optical line of sight and gave visual indication that the hole was clean.

Generally, the GFE equipment was more difficult to assemble for a run and the specimen was more prone to break; however, the data were considered reliable.

## TOTAL NORMAL EMITTANCE TO 5000°F

### General

Emittance was measured by comparing the energy received by a radiometer from the sample to that received from a black body cavity maintained at the same temperature.

The equipment may be divided into three main parts: the induction heating furnace, the radiometer, and the temperature measurement equipment. Figure 120 shows a picture of the complete equipment.

## Description of Apparatus

A cross section of the apparatus is shown in Figure 121. The specimen (1) was supported in the center of the flat concentrator induction coil (2) by a zirconia cylinder filled with fine zirconia grog and tungsten wires (3). The zirconia cylinder rested on a crucible filled with coarse zirconia grog (4). The radiometer (5) viewed the specimen from directly above through a water-cooled tube (6). A water-cooled optical valve (7) was used to blank off the specimen from the radiometer. Optical-temperature readings were taken through the main port (8), which was pushed in to view the specimen through a mirror (9) from directly above. When radiometer readings were taken, the main port was pulled out and away from the line of sight of the radiometer. Auxiliary port (10) was used to view the specimen directly as a check for the main port. Both viewing ports contained sapphire windows. The portion of the furnace above the specimen (11) was water-cooled to eliminate any possibility of energy being reflected back onto the specimen surface. The emittance furnace was built of steel and sealed with "O" rings so that a vacuum can be obtained.

The radiometer, see Figure 122, was constructed according to Snyder[1] and Gier[2] with some modifications. The receiver element consisted of approximately 160 turns of No. 40 AWG bare-constantan wire (104 turns per inch) wound around a plastic insulator strip about 2" long by $1\frac{5}{8}$" wide by $\frac{5}{16}$" thick. Silver was electroplated in several stages onto the constantan coil so that two $\frac{1}{8}$" wide lines of silver-constantan junctions, $\frac{1}{2}$" apart, were formed on the same side of the coil and across all of the wire turns. The remainder of the entire coil was silver plated. Each of the two lines of junctions was covered with a thin, narrow strip of black paper. One of these junction lines was designated as the active or "hot" junction and was placed to receive energy from the sample. The other was shielded and termed the passive or "cold" junction.

In order to shield the element from extraneous radiation, a cylindrical housing was placed immediately around the thermopile. The front of the housing contained a rectangular opening $\frac{1}{4}$" by $1\frac{1}{2}$" to allow the element to "see" the specimen. The actual limiting of the receiver field was accomplished by this rectangular slit and the $\frac{1}{4}$" round stop (12) just above the specimen. Additional stops in the water-cooled tube were installed as as added insurance to further minimize spurious reflections. The radiometer viewed the specimen directly. This eliminated the possibility of dirty lenses affecting the reading and, also, eliminated the spectral selectivity of the different types of materials used as windows.

---

[1] Snyder, N. W., Gier, J. T., and Dunkle, R. V., "Total Normal Emissivity Measurements on Aircraft Materials Between 100°and 1000°F," Trans. of the A. S. M. E., Vol. 77, 1955, p. 1011

[2] Gier, J. T., and Boelter, L. M. K., "The Silver-Constantan Plated Thermopile," Temperature - Its Measurement and Control in Science and Industry, American Institute of Physics, 1941, p. 1284.

The voltage generated by the receiver was measured with a Type K-3 Leeds and Northrup potentiometer in conjunction with an L and N Type 2430 DC galvanometer of 0.43 microvolts per millimeter deflection sensitivity. Temperatures were measured with a Leeds and Northrup portable potentiometer.

The receiver element was calibrated against a carbon-filament lamp of known radiation[3] and demonstrated a sensitivity of 8.66 Btu/hr/sq ft/millivolt.

The radiometer was checked, also, against an Eppley thermopile with 12 bismuth-silver junctions and a 1-mm quartz window and agreed within 10% scatter of data points. By factory calibration, the sensitivity of the Eppley thermopile was 0.048 microvolts/microwatt/sq cm.

The optical pyrometers used were L and N catalog type 8622 calibrated in accordance with the International Critical Table of 1948 for an emittance of unity.

## Calibration Procedure

To calibrate the radiometer for black body radiation, a black body cavity with a 6 to 1 aspect ratio made from graphite was used. The black body cavity was insulated by zirconia grog and lamp black placed in the annulus between the black body and the load coil, see Figure 123.

The accurate determinations of the specimen and black body temperatures are essential to good data. For the cavity-type black body, the temperatures were determined relatively easily by (1) thermocouples placed in the bottom of the cavity; (2) thermocouples dropped into the cavity; and (3) optical pyrometer observations. Up to 3000°F, agreement to within 15°F has been obtained regularly between these three readings. Above 3000°F, the agreement between tungsten-rhenium couples and the optical pyrometer was generally within 50°F or the repeatability of this type of thermocouple. Actually, the optical readings had no error other than those of the instrument calibration and the human error, which appeared to provide a readout scatter of about 10°F at 4000°F.

---

[3] Lamp No. C584, calibrated by the National Bureau of Standards and reported in NBC Report 132737 A, July 1, 1952.

Radiometer output versus temperature for black body radiation was plotted in Figure 124. Notice that the output was essentially linear from 2000°F to 5000°F with a slight curvature below 2000°F. As in house standards, the emittance of 304 stainless steel, tarnished tungsten, and graphite were measured, see Figure 125. The emittance of the stainless steel ranged from 0.15 at 700°F to 0.67 at 2000°F. These values were in close agreement with the literature values. The sanded CS graphite, also, checked out closely with the literature with values from 0.95 to 0.98.

The calibration curve was used in all emittance calculations and was checked periodically to assure its continued accuracy. Small graphite black body cavities of aspect ratio 3 to 1 and 1 to 1 were situated in place of the specimen in the emittance furnace to check the calibration curve. The outputs of the small cavities approximated those of the large one within the accuracy of one per cent or close enough for periodic checks.

## Operating Procedure

The specimen was placed directly on the surface provided by the zirconia tube, grog, and tungsten wires. However, if the material of interest could not be heated inductively, tungsten and tantalum heating discs were placed under the specimen with the specimen in contact with the tungsten disc.

The furnace was evacuated to 15 mm of Hg and filled with high-purity, dry argon. This operation was carried out at least twice to assure an inert atmosphere. Throughout the run a slight pressure was maintained in the furnace by an argon purge, which was brought in through the radiometer enclosure and exhausted from the furnace housing, see Figure 121. In addition to maintaining an inert atmosphere, the purge flow tended to keep fumes away from the radiometer.

The temperature of the specimen was raised and maintained at the desired point by transferring energy to the specimen through the induction coil. About three hours were required to complete a single run with the temperature increasing stepwise but in uniform intervals. At each temperature level, a radiometer reading was taken in conjunction with the temperature readings.

To obtain the radiometer reading, the following procedure was followed: As the specimen was heated, the blank-off valve was shut so that the thermopile could see no impulse. When the specimen temperature reached steady state, a zero reading was obtained for the thermopile output. This reading was usually in the order of ± 0.002 millivolts. The blank-off valve was then opened, and the thermopile output increased several fold in a few seconds. The reading leveled off as heat was transferred down the wires to the cold junction. The radiometer output was taken at the peak reading immediately after steady state. The net reading for that temperature was obtained as the difference between the zero and steady-state reading.

If the blank-off valve were left open, the thermopile output would decrease slowly with time. After about 10 minutes, this reading might decrease by 50%; however, if the blank-off valve were shut and a new zero reading obtained, the difference between this new output and zero reading would be about the same as the original readings. The variation might be about 5% to 10%. The shift in readings was a result of the heating of the cold junctions. To further minimize this influence, a helium purge was introduced immediately below the upper stop. Later, this purge was moved to the thermopile housing. This purge also eliminated any convection heating of the thermopile junctions by the hot gases "chimneying" up from the specimen zone. It was necessary to watch the specimen at each temperature to insure that no smoking existed since only slight smoking affected the radiometer reading by as much as 75%.

The purge to the radiometer housing had no influence on the readings within the ranges at which the purge was operated. To determine this limit, the purge rate was increased to about 10 times the normal metered reading, and a small shift in readings of less than 1% was noted.

The temperature of the specimen was monitored by (1) thermocouples mounted directly on the target surface (usually held in place by a small zirconia pad), and (2) optical pyrometer readings on the target surface. Low temperature readings were made with thermocouples; however, in the intermediate temperature range from 1600°F to 2700°F a cross check was made between the thermocouple readings and the optical readings. Unfortunately, a surface temperature measurement with thermocouples leaves much to be desired and discrepancies of at least 50°F often occurred between the thermocouple and optical readings. The high-temperature measurements were made with an optical pyrometer. A main-port optical and an auxiliary-port optical-temperature reading were taken at each temperature level. The auxiliary-port temperature was normally used only as a check; however, if conditions warranted, such as a dirty main-port window or mirror, the auxiliary-port value was used. Usually very good agreement was maintained between the main-port and auxiliary-port optical readings.

## Emittance Calculation

The optical temperature readings were corrected to obtain true temperatures. The main-port reading was corrected for the sapphire window and mirror, while the auxiliary-port reading was corrected for the sapphire window and the angle at which the port views the specimen. The above corrections are shown as curves in Figure 126.

After assuming an arbitrary-initial emittance value, the brightness temperature was corrected for this assumed emittance, see Figure 127. The black body output was then read at this "true" temperature from Figure 124. The ratio of the observed specimen radiometer output to the black body output was calculated and was the emittance of the material at that temperature. If the assumed emittance was correct, the calculated value agreed with it; if not, the calculated value was used as the former assumed value and the process repeated until the assumed emittance value agreed with the calculated value. This iterative process converged on the correct emittance value, assuming gray body distribution of most of the energy at the particular temperature. The above process was programmed for analysis by a digital computer.

## Error Analysis

The above procedure for determining emittance was strictly correct only for those materials which radiated as gray bodies, since the total emittance was assumed to be equal to the spectral emittance at the wavelength of the pyrometer. This approximation was used above to convert the brightness temperature to true temperature.

The error in emittance values for non-gray materials varied depending on the difference between the 0.665 micron spectral and the total emittance, and the distribution of radiant energy within the particular spectrum. If the deviation from gray body became very great at temperatures up to 2500°F, it was indicated by the thermocouple measurements. On materials of low emittance, such as tungsten, the emittance values calculated by this procedure could be in error by as much as 20% at the highest temperatures. However, it is believed that for most materials, the accuracy is within 10%. Several things indicated that the accuracy of the emittance values was good. First, the radiometer output versus temperature curves were orderly and almost linear with only normal data scatter. Second, the data obtained on two samples of the same material were in close agreement. Third, the values of emittances for the check samples agreed very well with the literature, see Figures 125 and 128.

A statistical analysis of the data accuracy is of interest. Generally, the probable error in each black-body reading was about 4%, and the probable error in each specimen reading was about 8%. If the data points were used to calculate emittance, the maximum probable error was about 12%. The curve-fitting approach undoubtedly reduced this maximum to about 5%. As a general conclusion, the accuracy of the measuring system was well within the range of variation as experienced by different surface finishes on the same material, the changing chemistry of the surface at the high temperatures, surface temperature measurements, and other variables.

## Data and Results

The data and graphs for the total normal emittance are included in Tables 67 through 92 and Figures 129 through 155, respectively. The condition of the specimen is noted at the different temperature levels, whether there was fuming, whisker growing, or some other phenomena. Also, duplicate runs on different specimens and repeat runs on the same specimen are presented. When the material remained stable, the duplication was within 0.05 emittance; whereas, when the material changed appreciably, the data might shift considerably.

Recall that there was no graphite, silica, or other materials present in the apparatus that could contaminate the specimen—at temperatures up to at least 4500°F. Above 4500°F, there may have been some reaction between some of the specimens and the zirconia, tungsten, or tantalum that were used to support the specimen. Since there were no contaminants, the photomicrographs shown in the report must be considered as indicative only of phase changes, structure changes, cracking and other temperature phenomena but not of carbon, silicon, or any other such contamination. Also, the chemical analysis shown for post exposure does not apply for carbon pickup but probably does for element loss at the same temperature. The density measurements should apply since densification is primarily a temperature-time relation.

The emittances of the borides increased with temperature at the lower temperature levels (as for metals) and then decreased with temperature to near 5000°F. At 4000°F, the values ranged from a low of about 0.35 for tungsten boride to a high of 0.75 for hafnium diboride. For the titanium diboride and tungsten boride, there were sharp increases in emittance initiating at about 4800°F with decreasing values as the temperature was increased a few hundred degrees further. Black crystals or surface changes seemed to appear on these surfaces and then disappear. This phenomena, which is described later, was better recorded for the tungsten element, and may be the same as observed for the boride in that vapors from the specimen were condensing near the surface and then being reabsorbed in the specimen upon recontact.

For the carbides, the emittances generally increased with temperature at the lower level and then decreased as the temperature approached 4500°F. Above 4500°F, the behavior depended on the specific material. Duplicate runs were obtained on several materials with good agreement between runs in most cases. Several of the materials blistered, smoked and developed a surface with an uneven appearance. During the heating cycles, various surface phenomena were noted on some of the materials. At temperatures between 2400°F and 3500°F, small dark spots appeared on the tantalum carbide. At times, the spots moved about similar to the action of drops of a boiling liquid on a hot, flat surface. At 3500°F, the dark spots disappeared. A rerun of the original specimen was made to determine the effect of the dark spots on the measured emittance. Below 2500°F, the emittance of the rerun material was lower than for the original run. However, the emittance was about the same in the temperature range where the spots were present. During the run on titanium carbide, dark spots somewhat similar to those above were noted at 3300°F. In this case the spots were stationary and appeared to be small blisters on the surface of the specimen. Dimolybdenum carbide and vanadium carbide both appeared to swell up in the center (or form a single large blister covering the entire surface). A second specimen of dimolybdenum carbide was run, but this specimen appeared to blister as before. This second run was halted before the melting point was reached in order to examine the specimen. It was very porous with a large blister about $\frac{1}{4}$" high on the surface. Small dark spots appeared on zirconium carbide at 4300°F.

For the nitrides, the emittances generally decreased with increasing temperatures (similar to ceramics) to values near 0.5 at 4000°F. There was little smoking, fuming or development of spottiness on the surface; however, a few of the specimens cracked. All of the materials were melted except the boron nitride, which vaporized. Duplicate runs on the hafnium nitride and titanium nitride provided fair agreement.

The emittances for the oxides were strictly dependent on the material and could not be categorized. The beryllia and magnesia smoked seriously at about 3500°F with the emittance increasing from a value of about 0.5. The hafnia had a constant value of about 0.8 from 1500°F to 4000°F. The emittances of the ceria, thoria, and zirconia all increased very sharply with increasing temperature at about 1700°F for the ceria and 3000°F for the thoria and zirconia. Note the high values for ceria and low values for thoria, which make these materials good additivies for blending a desired emittance. The zirconia deserves special attention. In helium, the emittance of zirconia increased sharply at about 3000°F from about 0.4 to 0.9 and remained high to over 4000°F. In air, the emittance of zirconia remained fairly low and increased only slightly to about 0.5 at 3500°F. During the run in air, the air was deleted and the emittance immediately increased to 0.8 at about 2600°F. Upon reintroducing the air, the value decreased again to less than 0.4. This same immediate response of emittance value to the presence or absence of air was noted at about 3500°F. On several runs, the specimen was quenched from 3500°F in the helium and air environments, respectively. When quenched in helium, the surface was gray. When quenched in air, the surface was the characteristic yellow. Since the zirconia contained many impurities (in ppm), the chemical analyses of the surface could not be defined precisely and did not reveal the cause of the color change; however, probably either a suboxide was forming or some material contaminant (such as iron) was diffusing to the surface and remaining there to vaporize off slowly in helium or immediately burn off in air.

For the tungsten, columbium-0.5 zirconium, and molybdenum -0.5 titanium, the emittances were lower than for most of the other refractories and decreased as the temperature increased from 2000°F toward 5000°F. The columbium and molybdenum alloys behaved orderly with values of about 0.25 at 4500°F. At this temperature, the value for molybdenum may have started to increase. During initial heating of the tungsten, black soot-like particles appeared on the surface of the specimen. In Run No. 1, a large pile of particles formed at the surface while in Run No. 2 only a small number appeared. These particles were collected on one run. In both cases, the particles disappeared at temperatures of about 3000°F. After disappearance of the particles, the temperature was reduced to obtain emittance values at 2500°F. The emittance values obtained while the particles were on the surface were high as indicated, but the curve was not extended through these points since the values obviously were not representative of tungsten. From 2500°F to 4800°F, the emittance of tungsten was about 0.23. At the higher temperatures, the temperature began to decrease even though the induction power input to the specimen was increased. At the same time, higher values of emittance were obtained. Further power increases resulted in higher temperature and decreased values of emittance. A maximum temperature of 5100°F at an emittance of 0.43 was reached. After the runs, large dendritic whisker formations were noted on the surfaces of the materials. Figure 155 includes only that data for tungsten that is considered to be representative of the base material and not confounded by either the dark spots at the lower temperature or the whiskers at the higher temperature. This curve should be used for design purposes.

For all of the refractory materials, the surfaces for the reported data remained clean after the temperature exposure. In many cases, there was a grayish or satin finish as often found after high temperature exposures. The tungsten was shiny, as is characteristic. For some of the runs, difficulties were encountered in maintaining the clean surfaces and reruns were necessary. A clean surface for commercial refractory materials requires some definition. A careful inspection of the photomicrographs revealed that the materials were not homogeneous and contained many different phases, dispersion and voids. Obviously, the compounds and alloys were not completely formed; rather, some phases were rich in one element and other phases rich in another. Further, the chemical analyses revealed that most of the materials contained contaminants, which could melt and migrate to the surface. Since emittance is essentially a surface phenomenon, the influence of voids, phase smearing during machining and the migration of only a small amount of contaminant could influence the data quite drastically. Some of these influences were described for the tungsten, for example. In view of these difficulties, a clean surface was determined as one that was not contaminated by external sources and that was dependent on the condition of the commercial materials and the temperature-time history of the run.

Great care was exercised to eliminate contamination by machining, handling and operating environmental conditions. The mechanical finishes were obtained with diamond cutoff wheels at high speeds and low feeds producing a finish of about 20 microinches. For this general finish and at temperatures above 2000°F, a considerable variation in surface finish had little influence on emittance.

No evidence of transmittance was found for any of the materials. Several possible indications were monitored. In the thermal conductivity phase, the conductivity was not noted to increase drastically (by Stefan Boltzman) at the higher temperatures. Under the microscope, no particle transparency was noted with angle lighting, although beryllia did seem to introduce some diffusion. Further, the temperature drop through the emittance specimens was observed both by optical pyrometer and by noting the melting of the heating disc, and the temperature differences from the bottom to the top surfaces were about as expected for the known thermal conductivity and the radiance from the upper surface. Specifically, however, there can be no assurance that the transmittance was absolutely negligible.

The emittances of most of the materials behaved about as expected up to about 2200°F with the values for the ceramic types decreasing with temperature and the values for the metal types increasing with temperature. Exceptions were the dimolybdenum carbide, hafnium carbide, titanium nitride, ceria and hafnia. Above 2500°F, the classic relations did not sustain, generally, and the emittances tended to vary either up or down and then converge on a value between 0.3 and 0.6 at 5000°F rather than unity. It seems doubtful that the classic explanations of radiation, which have been developed for well ordered lattices, should be precise on materials that present a surface that is not well ordered. At the higher temperatures, the structure densification and chemistry of the surface probably have a major role in establishing the emittance.

## ELECTRICAL RESISTIVITY

### General

Electrical resistivity was determined to 5000°F on unexposed specimens $\frac{3}{4}$" in diameter by 3" long that were radiantly heated in a graphite heater tube. The heater power supply was varied using either a rectified D. C. or 60 cycle A. C. A sketch of the specimen can be seen in Figure 156.

### Apparatus and Procedure

During the run, spring-loaded graphite rods pressed against the ends of the specimen and extended beyond the ends of the heater tube to permit the external completion of the electrical circuit through the specimen, see Figure 157. Direct current was applied to the specimen to provide a voltage potential across the $1\frac{1}{2}$" gage section. This gage potential was detected by tungsten probes that contacted tungsten pins pressed into holes radially drilled into the center line of the specimen. Due to some Thomson effect and some A. C. coupling with the heater resulting from either A. C. power or A. C. ripple in the rectified D. C., a small potential was present across the gage length before the D. C. voltage was applied to the specimen. This potential was called the open circuit gage length potential and was accounted for during the calculations.

A sample calculation follows:

True Closed Circuit Gage Length Potential = Observed Closed Circuit Gage Length Potential — Open Circuit Gage Length Potential

Electrical Resistivity = $\frac{MVA}{Il}$ x 1000 Micro ohms-cm

MV = True Closed Circuit Gage Length Potential in Millivolts

I = Current Flow Through Specimen in Amps

A = Cross Sectional Area of Specimen in Square Centimeters

l = Gage Length of Specimen in Centimeters

**Substituting:**

-2.008 millivolts = Open Circuit Gage Length Potential

-1.052 millivolts = Observed Closed Circuit Gage Length Potential

5.80 amperes = I

2.853 $cm^2$ = A

3.810 cm = l

True Closed Circuit Gage Length Potential = -1.052 -(-2.008)

= 0.956 millivolts

$$\text{Electrical Resistivity} = \frac{0.956 \text{ millivolts} \times 2.853 \text{ cm}^2}{5.80 \text{ amps} \times 3.810 \text{ cm}} \times 1000$$

$$= 123.39 \text{ micro ohms-cm}$$

Temperatures were measured with thermocouples from room temperature to 2000°F and with optical pyrometers from 2000°F up. Several data points were calculated at each temperature to establish statistical reliability to the data.

## Error Analysis

The introduction of errors into the determination of electrical resistivity arose from (1) deviations in implementation from the theoretical assumptions of the system and (2) errors in the readings themselves. The latter possibility was minimized by taking several readings at each temperature setting to establish a statistical reliability to the data.

Much study was conducted to establish the optimum means of taking voltage readings across the gage length of the specimen. It was concluded that the best method was to press-fit tungsten pins in holes drilled into the center line of the specimen. This technique provided an average value for the voltage across the cross section of the specimen and compensated for skin effects. The per cent error involved in this configuration was negligible as verified by the observation that the electrical resistivity was found not to depend on specimen size within the limitations imposed by furnace design. Figure 158 shows results obtained on CS graphite cut from the same stock and varying in diameter from $\frac{1}{4}$" to $\frac{3}{4}$". No trend was apparent in the data, with scatter accounting for the small differences encountered.

The current in the specimen circuit was varied from practically zero to approximately 60 amperes with no significant change in the electrical resistivity. Most of the runs were made with 5-10 amperes in the measuring circuit. The instrument used to measure the current flow could be read to the nearest 0.01 ampere. Therefore, the current could be read to 0.2%.

The probe locations for measuring the potential drop across the specimen were located $\frac{3}{4}$" on each side of the center line of the furnace hot zone and should have been at the same temperature; however, this was not exactly the case. This temperature difference, which varied around 20°F, caused a potential due to the thermoelectric effect. This potential plus the potential induced in the specimen by the A. C. power or the ripple in the D. C. power to the heater was determined by taking a reading of the potential across the gage length of the specimen before the current was applied to the specimen circuit. This potential varied from 0.2% up to approximately 300% of the true potential across the gage length, and was taken into account during the calculation of the resistivity.

The voltage measurements were made with a Leeds and Northrup Type K-2 potentiometer. With this instrument it was possible to read voltages of .001 millivolts. An error of about 0.02% was introduced in these readings.

The measurement of the gage length and diameter of the specimen was made to within 0.001". These measurements introduced a possible error of approximately 0.02%.

Since this equipment was designed to measure the resistivities of conductors, it was difficult to measure, with any great degree of accuracy, the resistivities of the materials with dielectric characteristics. The measured resistivities of these dielectrics varied as much as one order of magnitude with that found published in the literature. However, for the materials not exceeding a resistivity value of about 1000 micro ohms-cm, the accuracy was within 5%. Several things indicated that the accuracy of the electrical resistivity values was good. First, the resistivity versus temperature curves were orderly. Second, the values of the calibration materials agreed very well with the literature, see Figures 159, 160, and 161. Third, the data obtained on additional runs of the same material were in close agreement.

A statistical analysis of the data is given in Table 93. The standard deviation shown by this analysis was 7.2 and the probable error 4.86%. Assuming the absolute error of the data was approximately ½ of the probable error, an error of about 2.43% would be expected.

## Data and Results

The data for the electrical resistivity are shown in Tables 94 through 120 and the graphs in Figures 162 through 181. For many of the materials, duplicate data were obtained, usually with excellent agreement. Cooling cycle data are included for several of the materials. Some reference data from the literature are included on the curves for comparison.

The electrical resistivities of the borides increased about linearly with temperature to 75 to 125 micro ohm-centimeters at 3000°F. The cooling data were in fair agreement with the heating data, suggesting no serious changes in structure as was also noted in the thermal expansion data over these temperature ranges. Apparently the macrocracks had no significant effect. Observe for the zirconium diboride that some similar materials reported in the literature have similar values at room temperature but quite divergent values at slightly higher temperatures.

The resistivities of the carbides were similar to those of the borides, linearly increasing (except for dimolybdenum carbide) to slightly higher values of 100 to 175 micro ohm-centimeters at 3000°F. The hafnium carbide, titanium carbide, and tantalum carbide increased linearly on up to about 4000°F to 4500°F; however, the curves for columbium carbide and zirconium carbide had rather sharp inflections at the higher temperatures. For these materials, the photomicrographs revealed that there were considerable changes in the nature of the dispersions after the temperature exposures; however, the changes were not the same for the two materials. For the columbium carbide, the dispersions agglomerated and formed macrocrack extensions; this structure change would suggest the increase in resistivity that was observed. For the zirconium carbide, the dispersion became finer and less aligned; this structure change would suggest an increased resistivity for becoming finer but a decreased resistivity for becoming less aligned. Actually, the resistivity of the zirconium carbide decreased and then increased a little. For the dimolybdenum carbide, the resistivity was quite irregular as suggested by the development of the gross cracking and continuity of the crack system. The literature data on the titanium carbide was not in good agreement but that data was on a 1-mm wire, which undoubtedly had a quite different structure.

For the nitrides, the resistivities at 3000°F were higher for hafnium nitride, tantalum nitride, and titanium nitride than for the borides and carbides, and the curves for all nitrides that were conductors were not linear. All of the curves had rather sharp inflections at about 2500°F. The temperature levels of these inflections were in rather close agreement with the inflections in the thermal expansion curves suggesting that the changes in structure, which were primarily changes in phase size and the development of macrocracks through the aligned discontinuities, were responsible. Resistivity curves are not included for the boron nitride and silicon nitride since these materials were essentially dielectrics at up to about 3000°F, and this program did not include measurements on dielectrics. The values for the dielectrics that were obtained are shown in the tables; however, these data are not precise at the lower temperatures and should be used only to determine the temperature level (around 3000°F) at which the materials were becoming conductors. The literature data for titanium nitride was quite different but was on a 2-mm wire specimen.

Since they were dielectrics at up to about 3000°F at least, the resistivities for the oxides were not plotted in the graphs. As for the nitrides, the data in the tables are useful for establishing the temperatures (about 3000°F) at which the oxides became conductors.

For the metallic elements and alloys, the resisitivities at 3000°F were lower at about 50 to 100 micro ohm-centimeters, except for the columbium alloy, which was high at about 130 micro ohm-centimeters. As discussed elsewhere, the resistivities of the graphites decreased with increasing temperature and then became essentially constant at about 600 micro ohm-centimeters to over 4000°F at which temperature level the values began increasing again. For the metals, the resistivities were essentially linear with temperature and had excellent agreement between the heating and cooling cycles and for different runs. From the expansion data, there was little change in structure over these temperature ranges. Most of the changes in structure observed from the photomicrographs probably occurred at the higher temperatures. The literature data on the tungsten element was in excellent agreement. The literature data on the main elements of the alloys provides some comparison of the influence of alloying. The resistivities of the elements were quite low.

The Wiedemann-Franz law did not apply for any of the materials over a significant portion of the temperature range. Since all of the materials contained many phases and dispersions, and since the crystallites were usually imperfectly bonded, the major resistance was probably at the electron jump between crystallites. Ubbelohde and Lewis[4] suggested this property of polycrystalline graphite, which has a somewhat similar structure. From the photomicrographs, the most tortuous electrical path was probably through the porous and contaminant-containing structure usually bonding the crystallites and grains in the materials.

## THERMOELECTRIC VOLTAGE

### General

Thermoelectric voltage measurements were made to 5000°F on specimens $\frac{3}{4}$" in diameter and $1\frac{1}{2}$" in length. This voltage is the combination of the Thomson effect of the temperature gradient in a given material and the Peltier effect at the interfaces with a reference material, which was ATJ graphite in this program. Wherever possible, the thermoelectric specimen was cut from the specimen exposed previously to measure electrical resistivity. Care was taken to have the ends of the material as smooth and square as possible to obtain the best possible electrical connection.

---

[4] Graphite and Its Crystal Compounds, Oxford University Press, 1960.

## Apparatus and Procedure

During the run, the lower portion of the specimen was shielded partially from the radiant output of the heater by a graphite cylinder. This shielding caused the lower junction of the specimen to be at a temperature 50°F to 200°F lower than the unshielded end. The magnitude of this temperature difference was found to depend primarily upon the specimen characteristics, primarily thermal conductivity.

The specimen was suspended between two spring-loaded ATJ graphite extension rods, which came into direct contact with the specimen, see Figure 182. By measuring the temperature of the specimen at the interfaces with the graphite extension rods, the temperature difference between the two junctions was determined. The voltage output was measured by an electronic galvanometer connected to water-cooled electrodes on the ends of the graphite rods with the plus terminal connected to the extension rod from the hot end of the specimen.

The voltage output ($\Delta V$) was actually the algebraic sum of the Thomson effect plus the output of the hot junction minus the cold junction. By dividing the voltage output ($\Delta V$) by the temperature between the two junctions ($\Delta T$), a curve was obtained of $\Delta V / \Delta T$ versus the mean temperature of the specimen. A least-squares curve fit of these data points was found and integrated to give the equation of a curve of voltage output versus temperature. Zero voltage output was assumed at 3000°F.

During a run, the following data were recorded: (1) power input to the furnace; (2) temperature of hot and cold junction; and (3) millivolt output of the hot and cold junctions. When the voltage output reading was taken, the power supply to the furnace was interrupted to eliminate superimposed voltages induced by either the A. C. power or A. C. ripple in the rectified D. C. power to the furnace heater.

Temperature measurements were made with a Leeds and Northrup Type 8622 optical pyrometer. The voltage output was measured using a Kintel Electronic Galvanometer, Model 204A.

## Error Analysis

In the measurement of thermoelectric voltage, there were two possible sources for the introduction of errors: (1) deviations from the theoretical assumptions of the system; (2) errors in the observed readings.

The latter of the sources was minimized by taking several readings at each temperature setting and by the use of a computer to obtain a least-squares curve fit for the data.

The temperature readings were obtained at the junction of the specimen and graphite supports with an optical pyrometer, with which it was possible to measure to within ±10°F of the true temperature at 4000°F. This reading introduced an error of 0.5% to 1.0%, depending upon the temperature level. The specimen and support temperatures undoubtedly were not exactly the same at the junction. About $\frac{1}{2}$" from the interface, the support temperature was occasionally as much as 75°F lower than that of the specimen. However, the interfaces were ground flat and pressed tightly together (about 20 pounds force) so it was assumed that the interfaces of the two materials were at the same temperature at the points of contact. This assumption was confirmed by the observation that varying the configuration and thermal gradients at the ends of the support rods did not influence the data. Due to the large temperature gradient in the specimen, the movement of the hot wire of the optical pyrometer toward the center of the specimen by only about 60 mils produced a significant difference in the temperature readings. This error was minimized by the multiple readings and the intent of the operator to position the hot wire in approximately the same place each time a reading was taken. There was some error introduced by the voltage gradient difference in the two graphite extension rods; however, both calculations and experimentally varying the gradients showed this error to be immeasurably small. The Thomson effect is small for graphite.

The voltage output of the specimen was measured to the nearest .05 millivolts. The accuracy of the instrument, depending upon the magnitude of the output, varied from 1.6% to 2.0%. To prevent any spurious readings due to induced voltages in the specimen, the power to the heater was interrupted when a reading was taken.

Table 121 shows a statistical analysis of the data. The standard deviation was found to be 7.14 and the probable error 4.82%. Assuming that the absolute error of the readings was approximately $\frac{1}{2}$ of the probable error, the error would be 2.41%. The accuracy of the thermoelectric voltage output per degree Fahrenheit was estimated to be within 5%.

## Data and Results

The data for the thermoelectric voltage are presented in Tables 122 through 149 and plotted in the graphs of Figures 183 through 210.

Two plots are included for each material. The first (upper) plot is the incremental output in millivolts per °F temperature change, across the specimen length between the ATJ graphite support rods, versus temperature. The second (lower) plot is the total output in millivolts, assuming a 3000°F reference, versus temperature. The equations for both curves are included on the graphs.

Recall that the total output curve was obtained by writing a mathematical equation for the incremental output curve and then integrating to obtain the cumulative output voltage with 3000°F assumed as the point of zero voltage output. This assumption of zero total output at 3000°F is important in reading and analyzing the data. For example, the output of two materials selected at random cannot be obtained by subtracting the difference in outputs at the same temperature from the total output curves; rather, the change in total output of two materials can be observed in reference to the graphite over a small temperature increment about a selected temperature on the abscissa. If the change in output voltage of two materials is of opposite sign or has a large algebraic difference, then these two materials may produce large thermoelectric voltages and should be investigated further. It makes little difference in application whether the voltage changes were causing the absolute voltages to converge or diverge since a large potential could be obtained at some temperature near the selected temperature at which the large change was noted. Another method is necessary to analyze the data where there is no large change in the total output around a selected temperature. For these cases, the absolute total output voltages can be compared and if they are significantly different, the materials would probably be good voltage generators and should be investigated.

This technique of data presentation was selected because the task of establishing the relation with each of the 26 materials as a reference would be monumental and was not intended. Further, the purpose of this program was to screen the materials against a single reference to determine which ones might be good thermoelectric voltage providers. With the first order information in this report, plus the electrical resistivity presented elsewhere in this report, the potential of a pair of materials as generators of thermoelectric power can be estimated by calculating the power coefficient.

The voltage outputs of the borides increased rather uniformly with temperature at above 2500°F. Generally the output changes were small at about 0 to 15 millivolts per 1000°F. On a rerun of the tungsten boride, the total output voltage shifted completely and decreased with increasing temperature converging to the incremental output of the first exposure at about 3500°F. This same phenomena of a reversed output was found for the tungsten element.

For the carbides, the characters of the total output voltage curves were quite different and demonstrated no material family uniformity. Except for zirconium carbide, titanium carbide, and tungsten carbide, the values were about 10 to 20 millivolts per 1000°F and fairly linearly increasing with temperature. A rerun of the vanadium carbide provided less output in the temperature range of 2000°F to 3000°F. The output of the zirconium carbide was about 20 millivolts per 1000°F, only decreasing with increasing temperature. This material, with one of the others, might make a good voltage provider. The outputs of the tungsten carbide and titanium carbide had larger values of about 30 to 50 millivolts per 1000°F at up to about 3000°F. Above 3000°F, the outputs changed little on up to above 4000°F. With the large incremental outputs and the negative slopes, these materials might be good voltage providers, particularly at the lower temperatures. With fair linearity and the negative values, the columbium carbide may also be a worthwhile candidate in conjunction with one of the other materials.

The voltage outputs of the nitrides decreased with increasing temperature and then increased slightly at above about 3000°F to the maximum temperature. Up to 3000°F, the outputs of the titanium nitride and hafnium nitride were comparable with the carbides at about 20 millivolts per 1000°F; however, the output for the boron nitride was higher at about 300 millivolts per 1000°F. Unfortunately, this material also has a high electrical resistivity and so would have a high internal power loss as a thermoelectric power provider.

The voltage outputs for the oxides were exceptionally high over at least parts of the temperature range with ranges of from 80 millivolts per 1000°F for the beryllia from 2000°F to 3000°F to 12,000 millivolts per 1000°F for the hafnia from 2000°F to 3000°F. The other oxides ranged from 250 to 1500 millivolts per 1000°F over temperature increments below the level of 3000°F. Above 3000°F, none of the oxides had such large output changes. This is unfortunate since some of the materials became fair electrical conductors at the higher temperatures. Perhaps some of the oxides, such as hafnia, still offer a potential as thermoelectric power generators, particularly if their lattice structures can be improved. Above 2000°F, the outputs for all of the oxides, except hafnia and thoria, decreased with increasing temperature. The values for the two exceptions increased with temperature. Undoubtedly, the hafnia and thoria would be large voltage (not power) providers with any of the other materials over the temperature interval from 2000°F to 3000°F. The data for the zirconia were erratic at up to 2800°F and should not be used. Probably, the lattice shift was not stable until the higher temperature was obtained. Zirconia shifts from monoclinic to hexagonal and cubic at the higher temperatures and reverts upon cooling unless thoroughly stabilized. It is doubtful if this material were thoroughly stabilized as witnessed from the large inflection in the curve for thermal expansion versus temperature.

The outputs for the two tungstens, columbium-0.5 zirconium and molybdenum-0.5 titanium were about the same at 20 millivolts per 1000°F at temperatures up to about 3000°F for the alloys and 4000°F for the tungstens. The outputs decreased with increasing temperature for all of these metals except one tungsten for which it increased. Both tungstens were rerun to confirm the opposite slopes. No explanation for this behavior was found in the photomicrographs, the chemical analysis, or a study of the other properties. Since the tungsten crystal is body centered cubic, there should be no large difference from crystal orientation. The only difference was in the method of formation of the materials, which might have introduced undetectable structure (not crystal) differences such as minute microcracks filled with a tungsten oxide or some other material that introduced a series of small voltage cells and provided an output voltage dependent on this phenomena rather than the metallic composition and normal lattice.

The data for the ATJ graphite and platinum-12.2 rhodium are included to provide reference information. The small output for the ATJ was an accumulation of material differences, surface effects at the interface with the ATJ support rods, and Thomson effect down the support rods. For precise calculations, these effects would have to be corrected for in all of the data; however, for screening purposes, the effect was considered negligible. The data on the platinum provides a reference to a material that is well reported in the literature and should provide a reference for other investigators.

## CONCLUSIONS

The specific conclusions were included in the discussion of data and results for each particular property. Generally, apparatuses have been developed, calibrated, and demonstrated for the determination of several of the thermophysical properties of materials. The temperature range for these studies has been extended to 5000°F with good engineering precision. Finer precisions of, say, $\frac{1}{2}\%$, as are often needed in some laboratory studies, have not been obtained.

While it is true that refractory materials for 5000°F service are relatively new and need much developmental effort, a single material from a single supplier does not have the wide variations in a property that the literature seems to suggest. For example, the literature may report data varying by several hundred per cent for the same chemical compound and density. This large deviation was not found in this program (with one or two rare exceptions) when investigating different specimens from the same lot or even when comparing the same material from different sources — when the photomicrographs revealed the same general structures. This observation suggests that photomicrographs, and chemical and density analysis, should accompany all thermophysical property data of this type.

There also is some doubt to the accepted procedure of correcting properties to a theoretical density and expecting the results to agree. Probably, this technique is adequate only when the voids that are causing a reduced density are distributed in a preferred fashion. More likely, the lower density is indicative of an unsound structure between the crystallites, inadequate diffusion, contaminants that may isolate the crystallites, and other phenomena that will influence the property far more than the mere presence of voids.

The thermal and environmental history of refractory materials is extremely important in obtaining data of this type. This history should be controlled and recorded even through the actual measurements. This procedure was established during the program but, unfortunately, not recorded for all measurements. At the high temperatures, only trace contaminants in the environment can have gross effects on some of the properties. Most of the materials contained contaminants of small quantity that boiled out during heating and otherwise confounded the control of environment.

During the program, several high temperature "standards" were established. Considerable work is necessary to obtain standards and some general agreement among investigators on this phase. Regardless of philosophy, the consumer of the data must judge results that are different and assign the difference to either the technique or the material. Standards will help in this judgment.

During the program, numerous contacts were received from other reliable investigators who were investigating some of the properties of these refractory materials at the lower temperature vicinity. The agreement in data was usually good over the range of common temperatures. In practically every case in which differences existed, they were traced to some physical cause induced by material differences, exposure conditions, or some other condition that could be altered to obtain agreement. Of course, this agreement could be no better than the accumulative error of the two systems.

Now that the state of the art has been extended to 5000°F, the temperature capability should be extended to 6500°F. Aerospace applications are now requiring these higher temperatures. Also, better environmental simulation is necessary to assure that the material is subjected to the same condition as will be met in application. The thermophysical properties are not basic entities at these higher temperatures but are transient with the material and a function of many variables, which must be controlled and known.

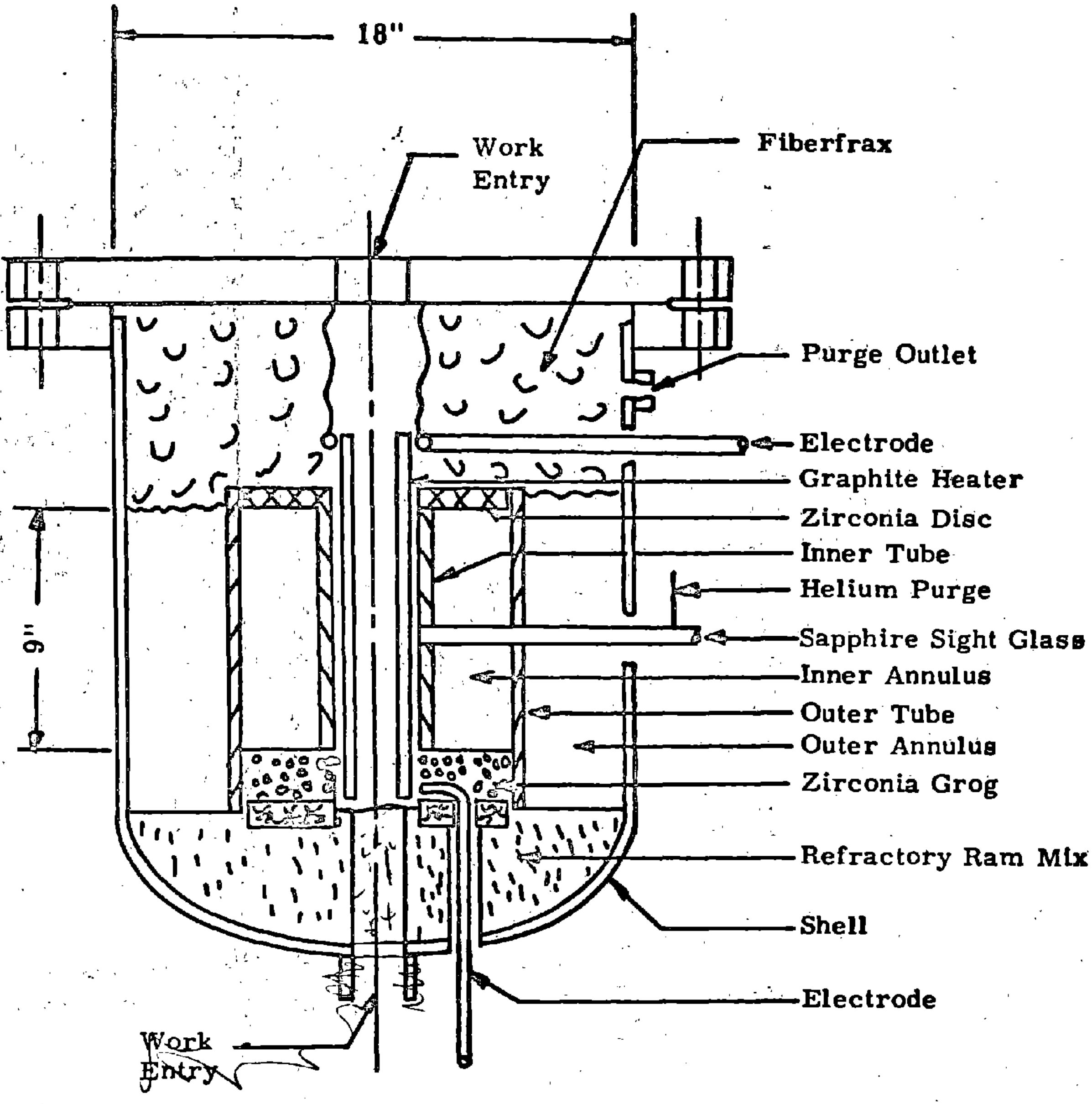

Figure 1. Schematic Cross Section of Furnaces No. 1 and No. 2 Employing Helical Graphite Heaters and Pressure and Vacuum Capability.

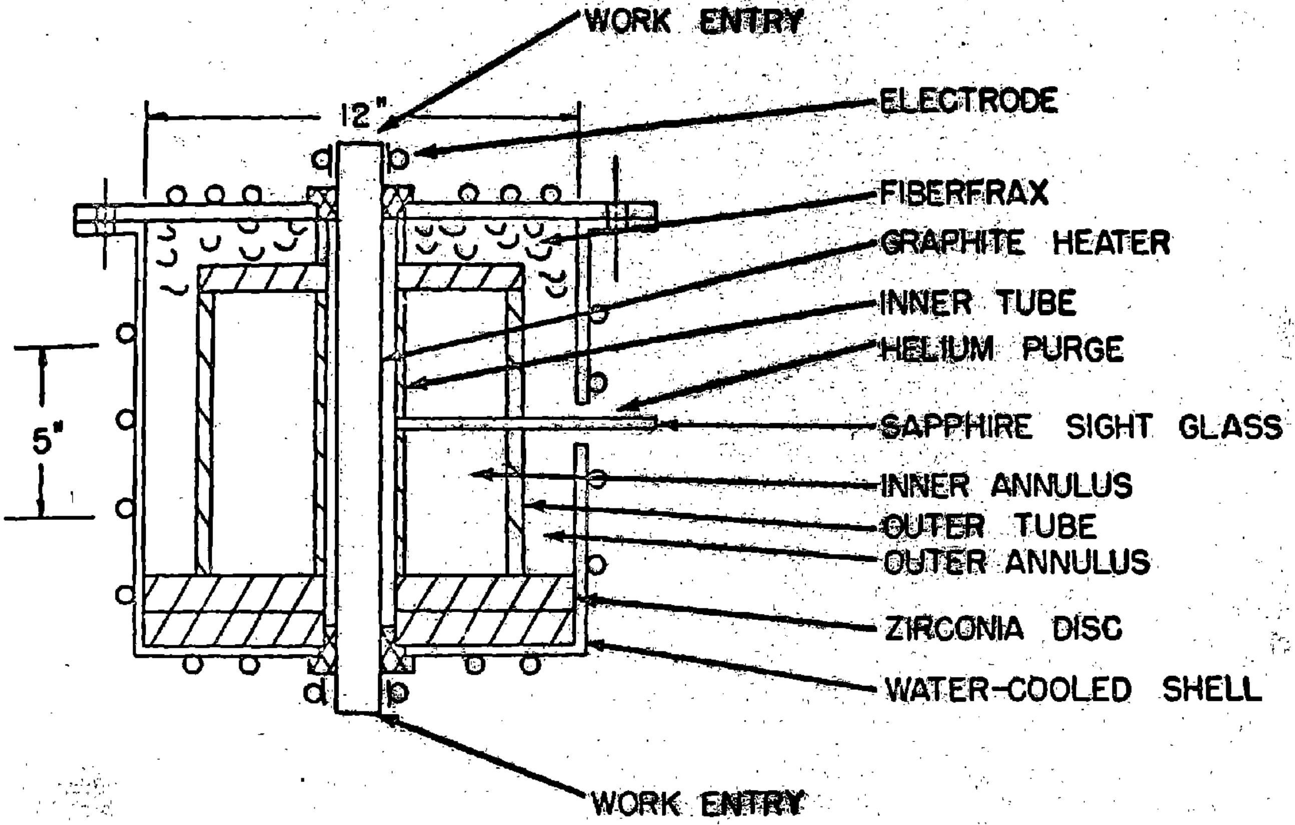

Figure 2. Schematic Cross Section of 5000°F Furnaces No. 3, No. 4, and No. 8 Employing Helical Graphite Heaters for Atmospheric Pressure Operation.

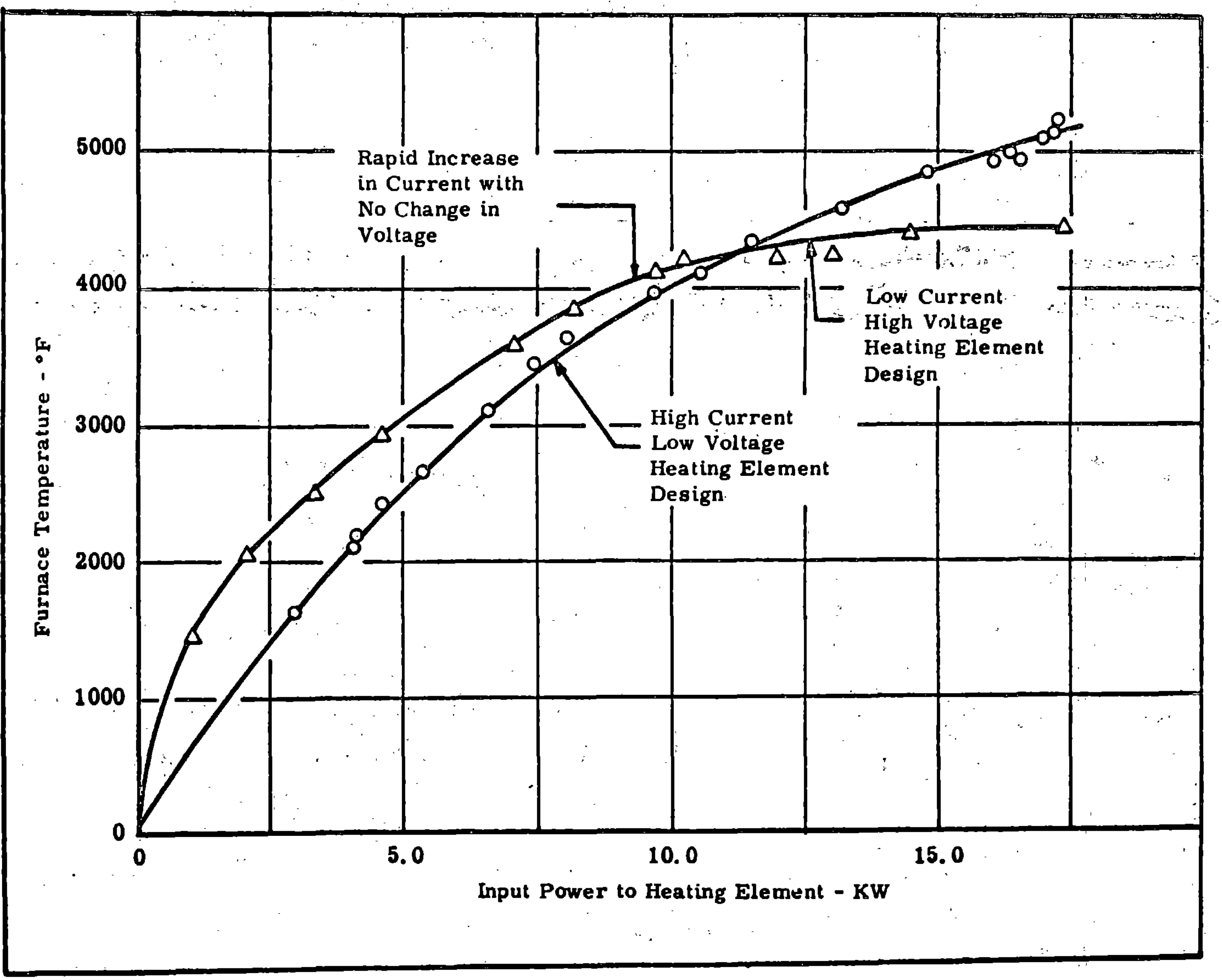

Figure 3. Relation of Furnace Temperature and Input Power.

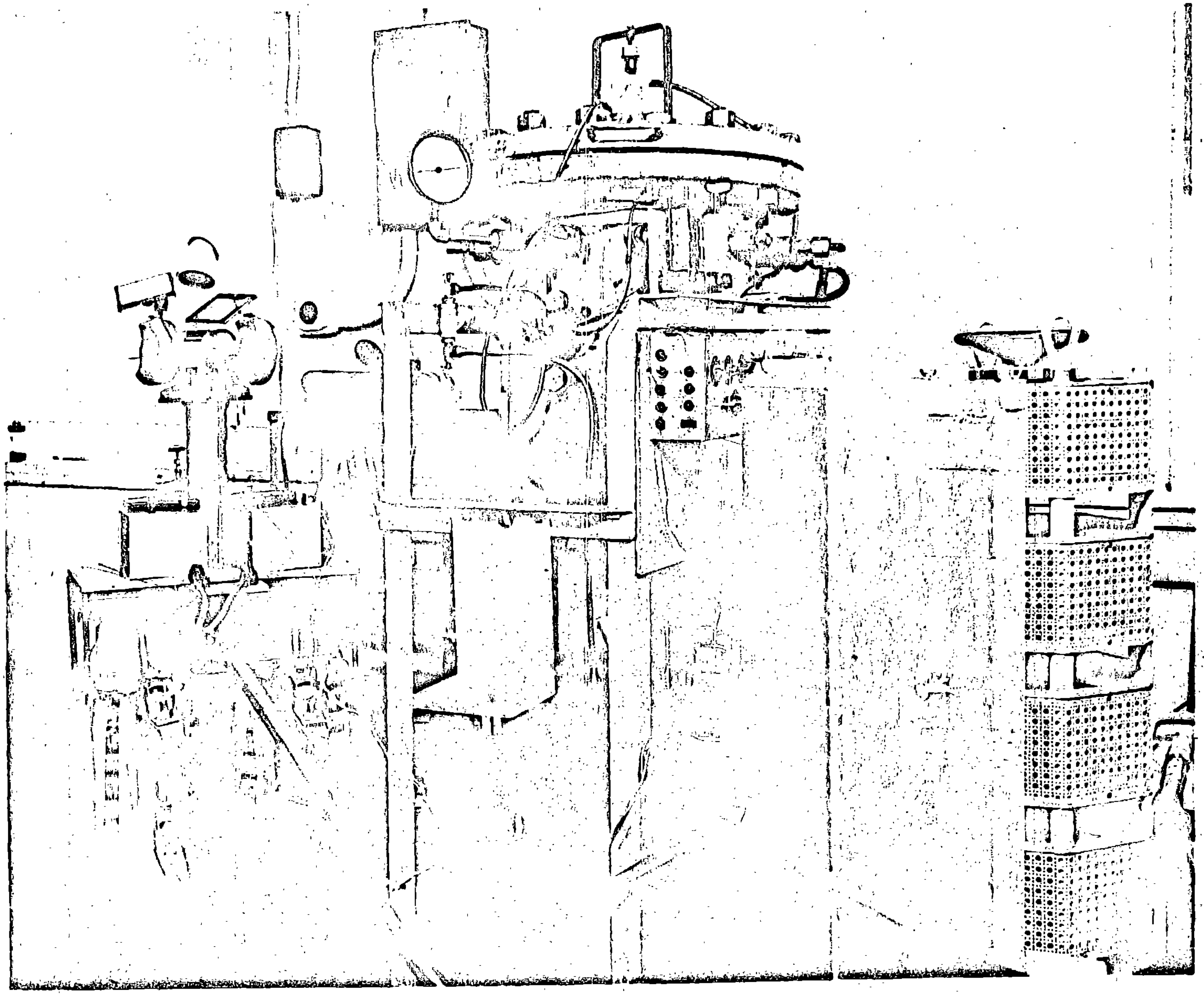

Figure 4. Furnace Number 1 with Expansion Apparatus Installed.

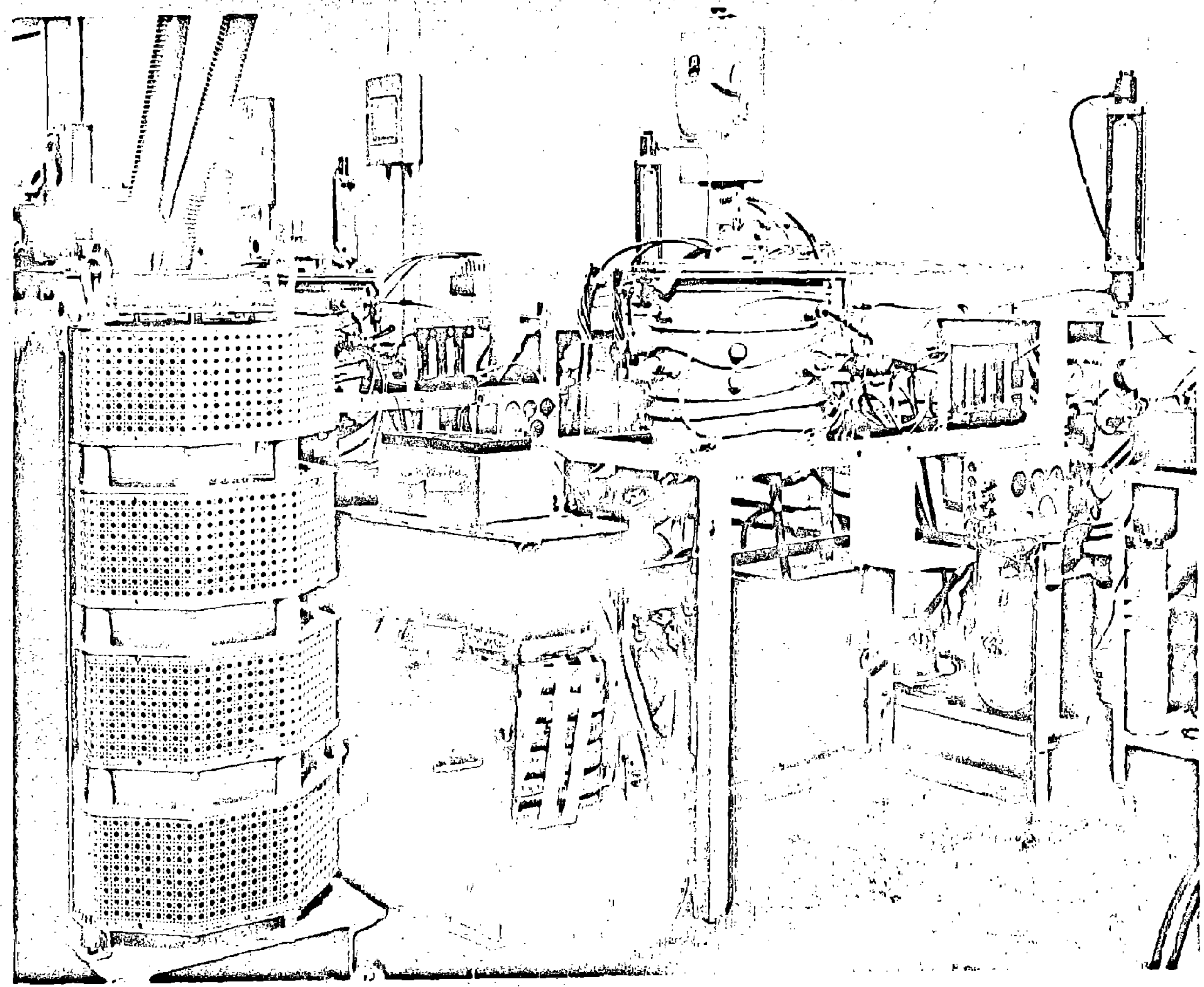

Figure 5. Furnace Number 8 with Thermal Conductivity Apparatus Installed.

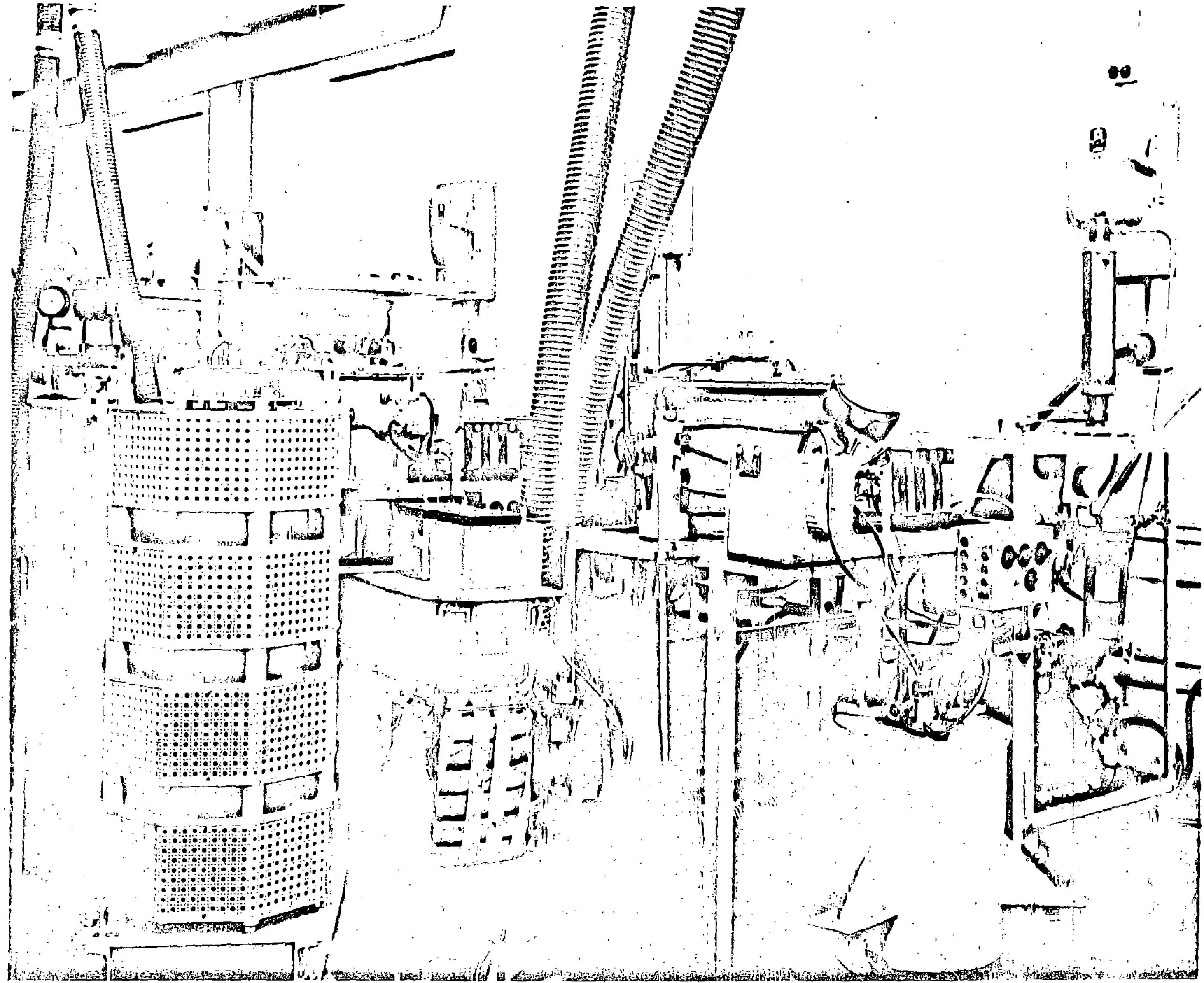

Figure 6. Furnace Number 4 with Heat Capacity Apparatus Installed.

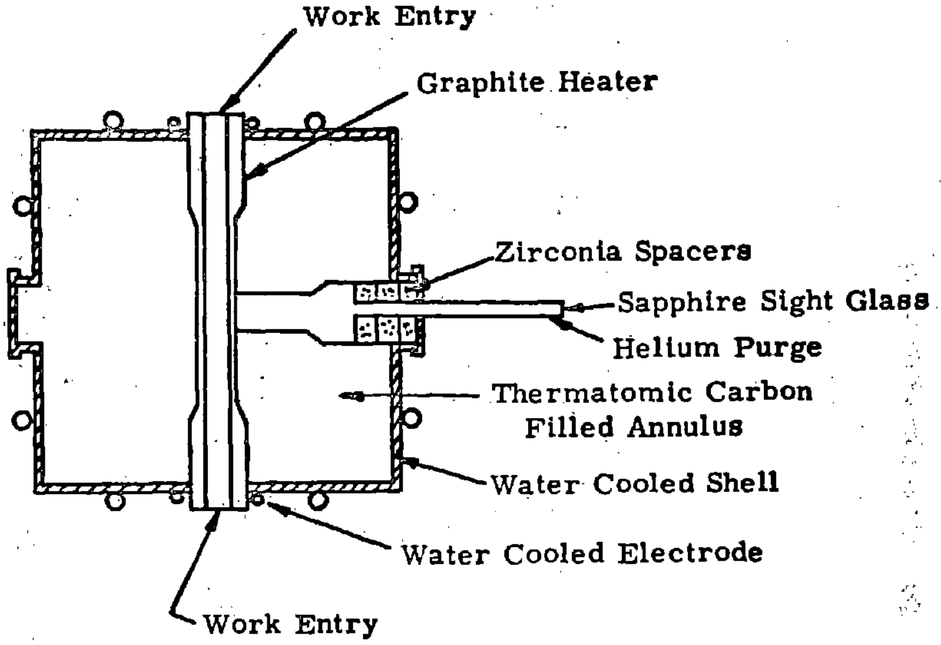

Figure 7. Schematic Cross Section of Electrical Property Furnace Employing Tubular Graphite Heater.

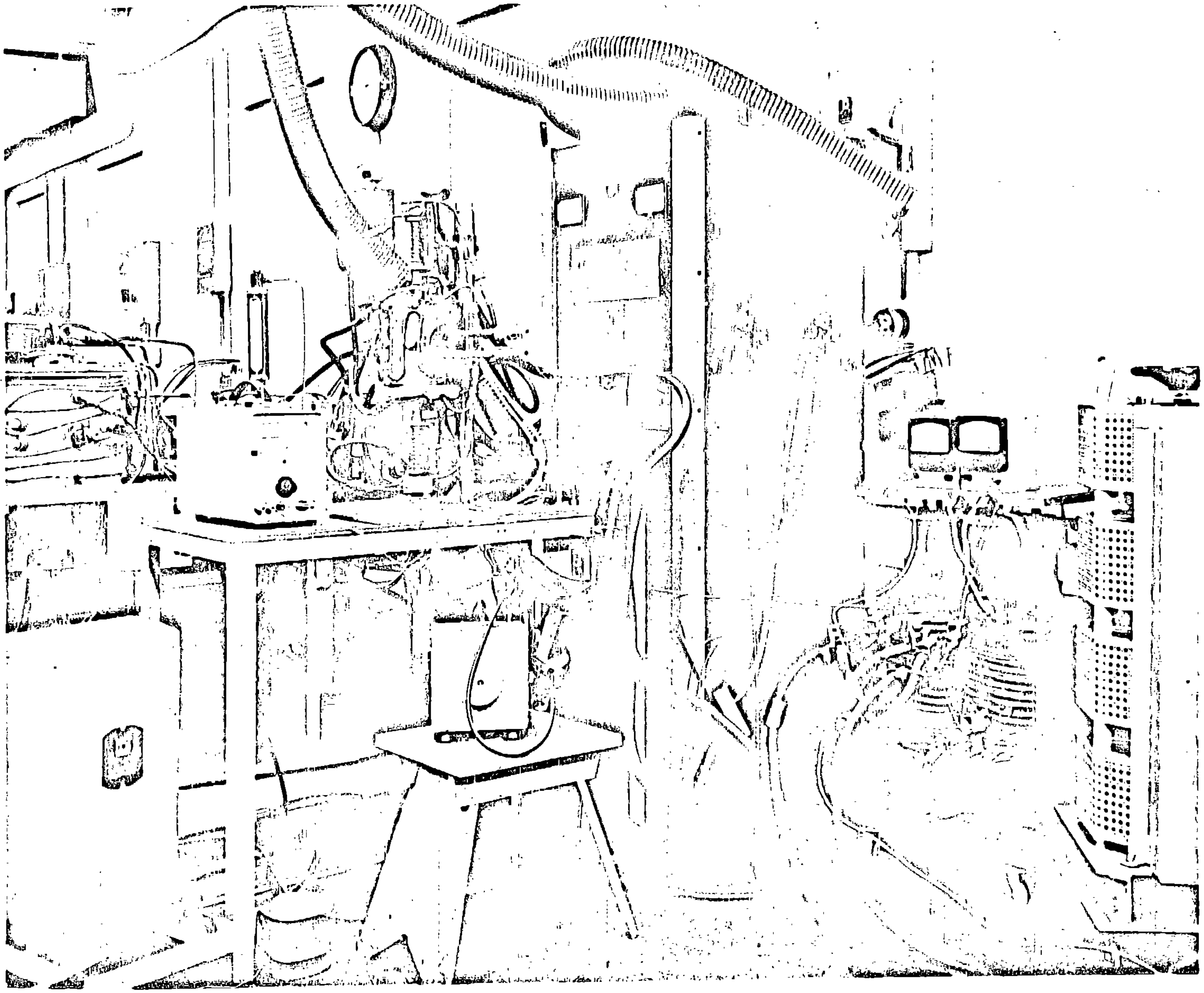

Figure 8. Electrical Property Furnace with Electrical Resistivity Apparatus Installed.

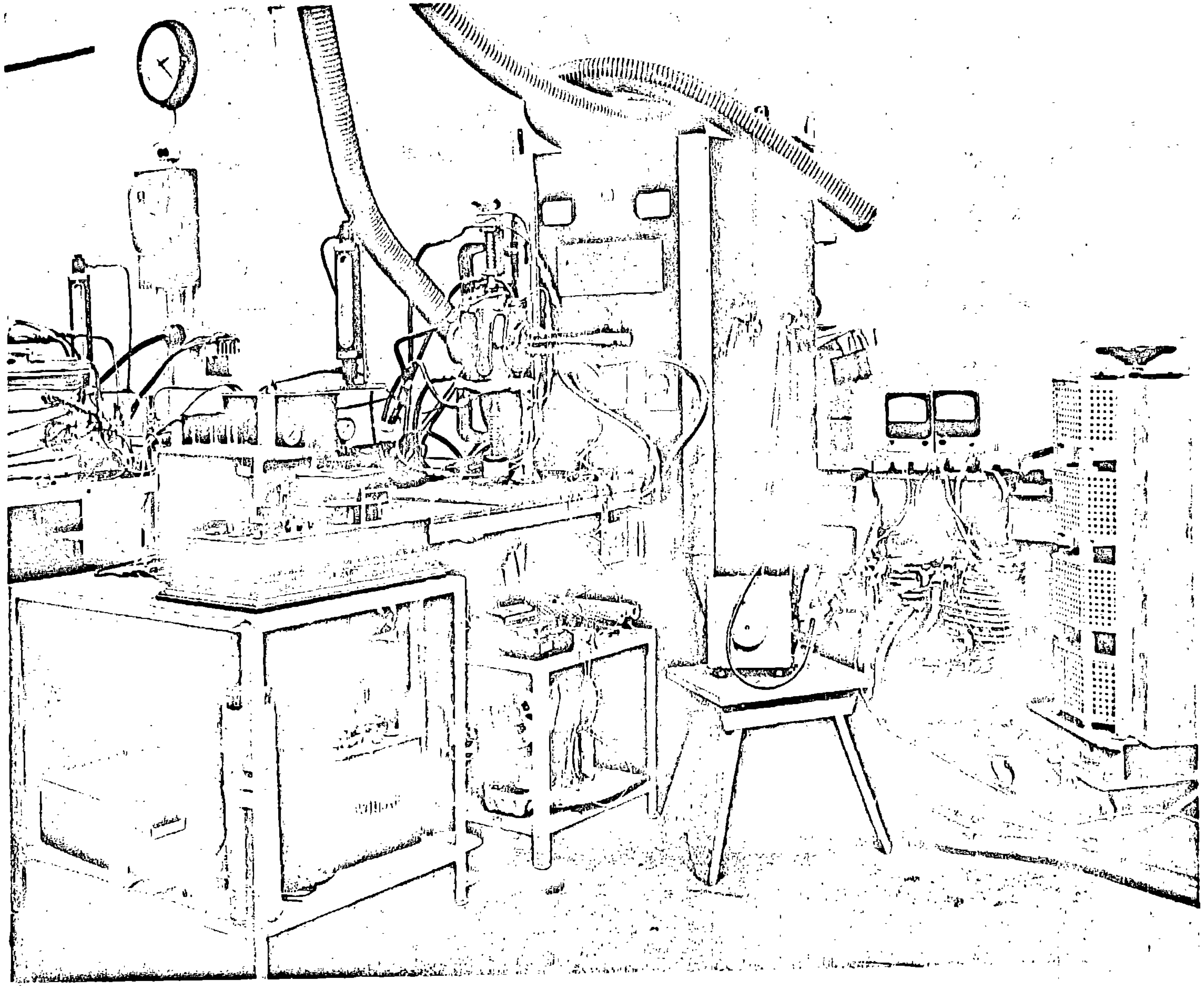

Figure 9. Electrical Property Furnace with Thermoelectric Voltage Apparatus Installed.

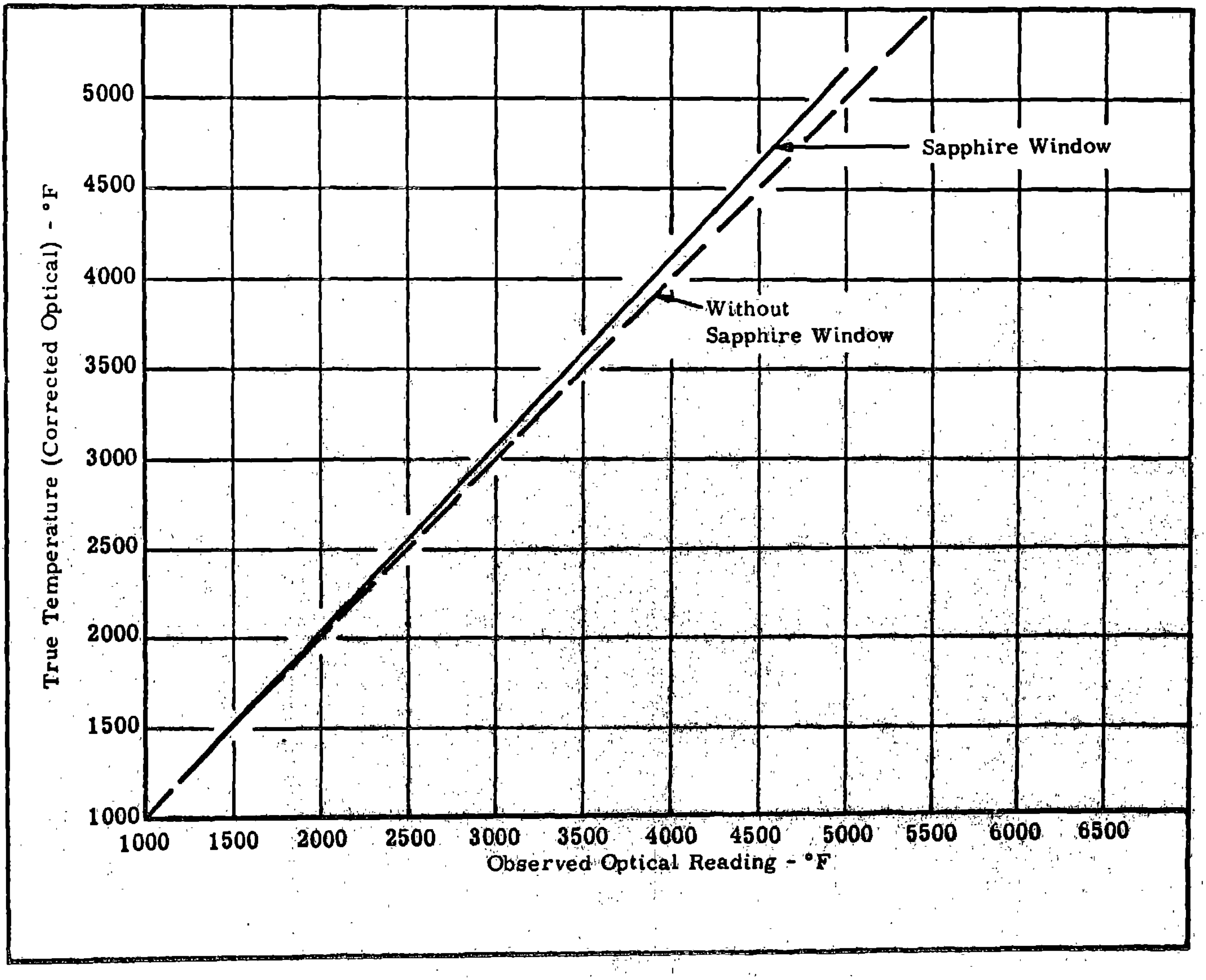

Figure 10. Temperature Calibration Curves for Optical Pyrometer.

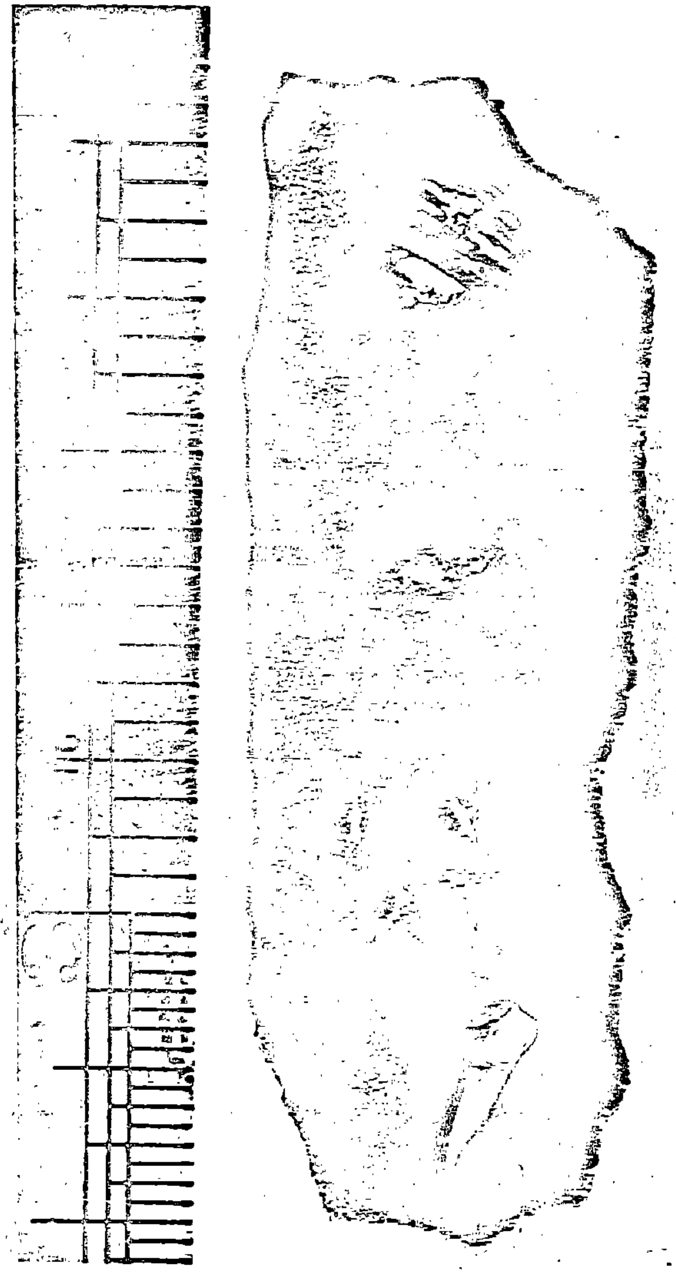

Figure 11. Picture of Tantalum, Tungsten Wire, Tungsten Sheet, and Part of Arc-Cast Tungsten Specimen After Exposure to 5000°F (Specimens in Listed Order from 3 to 4 on the Scale).

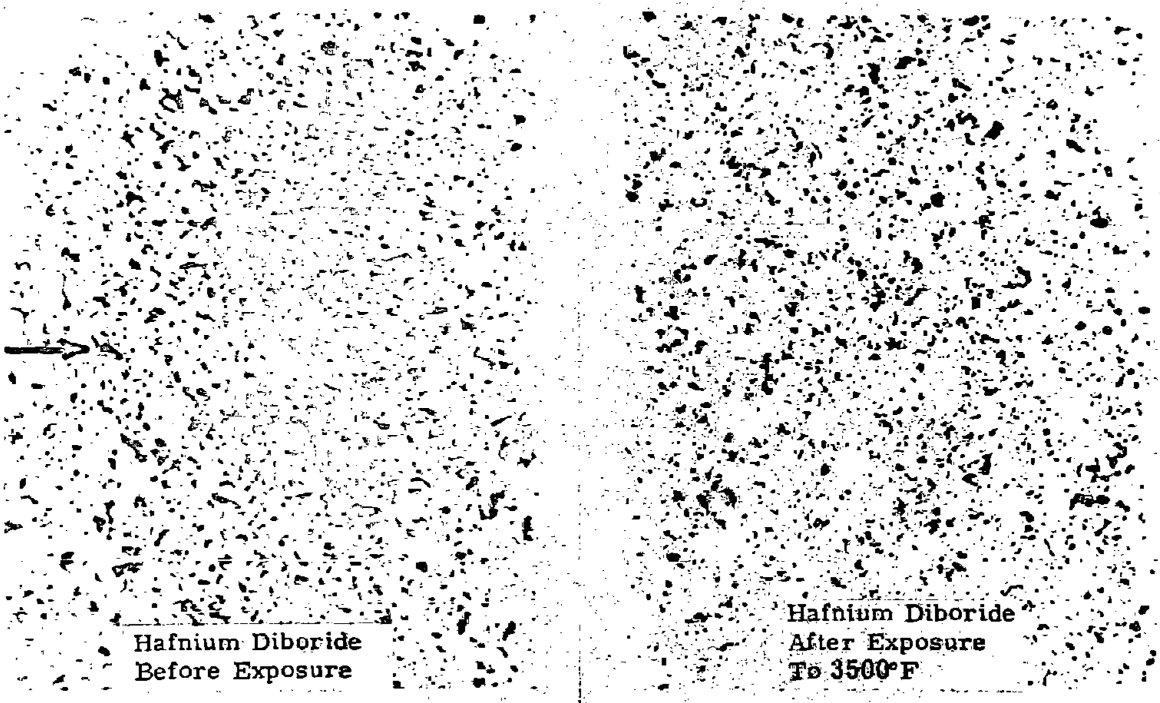

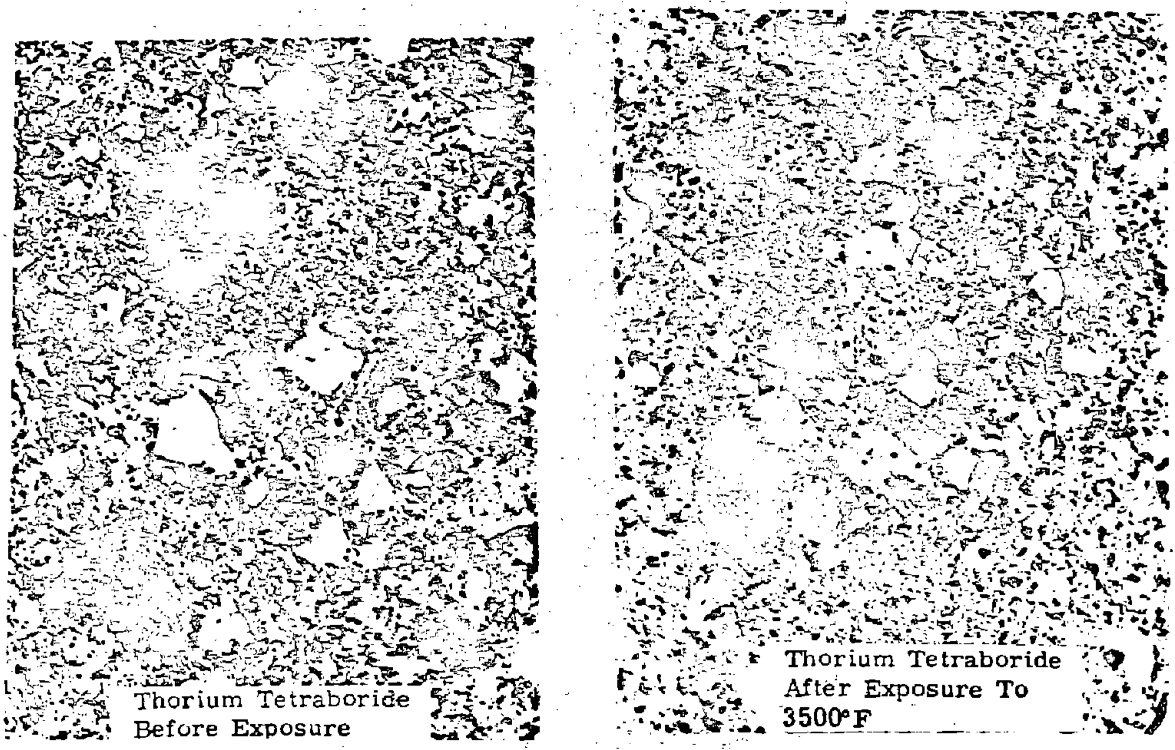

(Top) Figure 12. Photomicrographs of Hafnium Diboride.

(Bottom) Figure 13. Photomicrographs of Thorium Tetraboride.

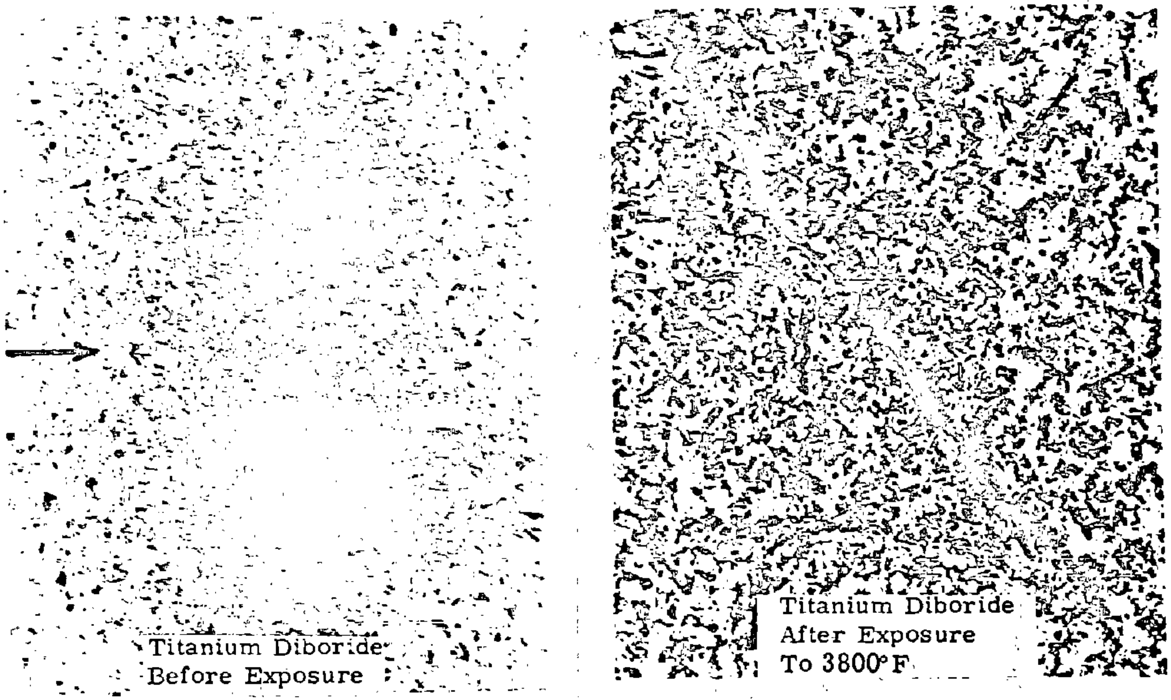

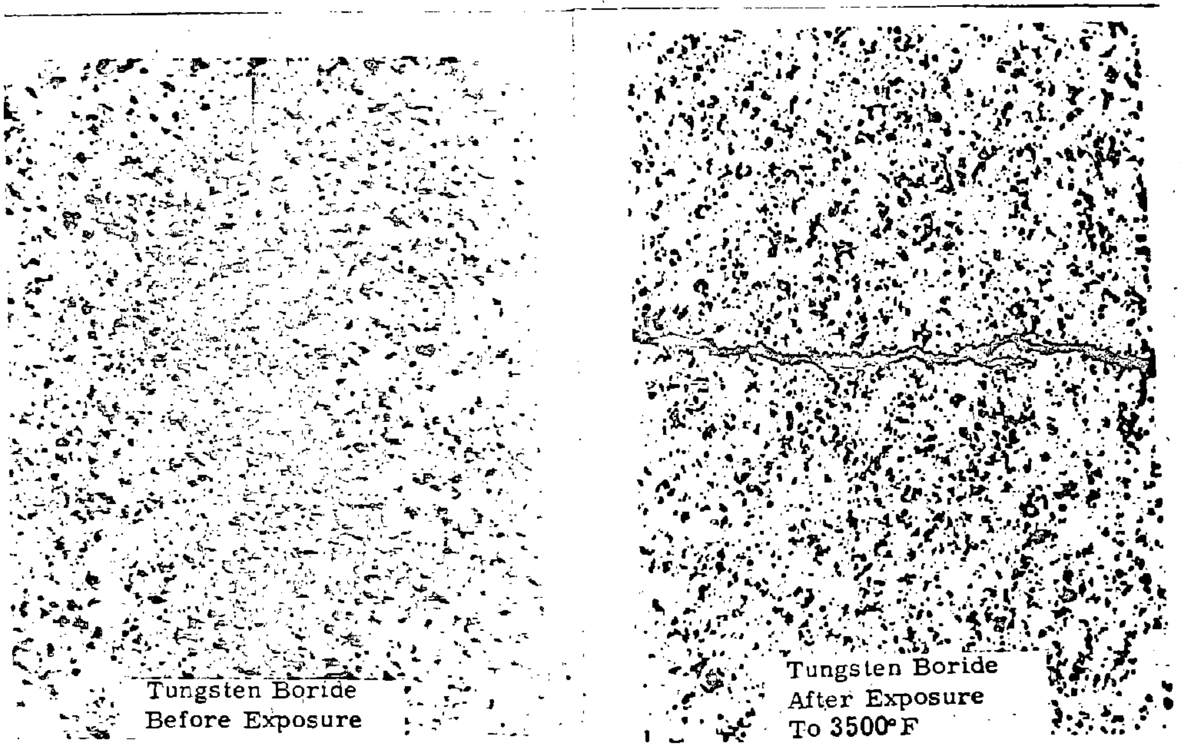

(Top) Figure 14. Photomicrographs of Titanium Diboride.

(Bottom) Figure 15. Photomicrographs of Tungsten Boride.

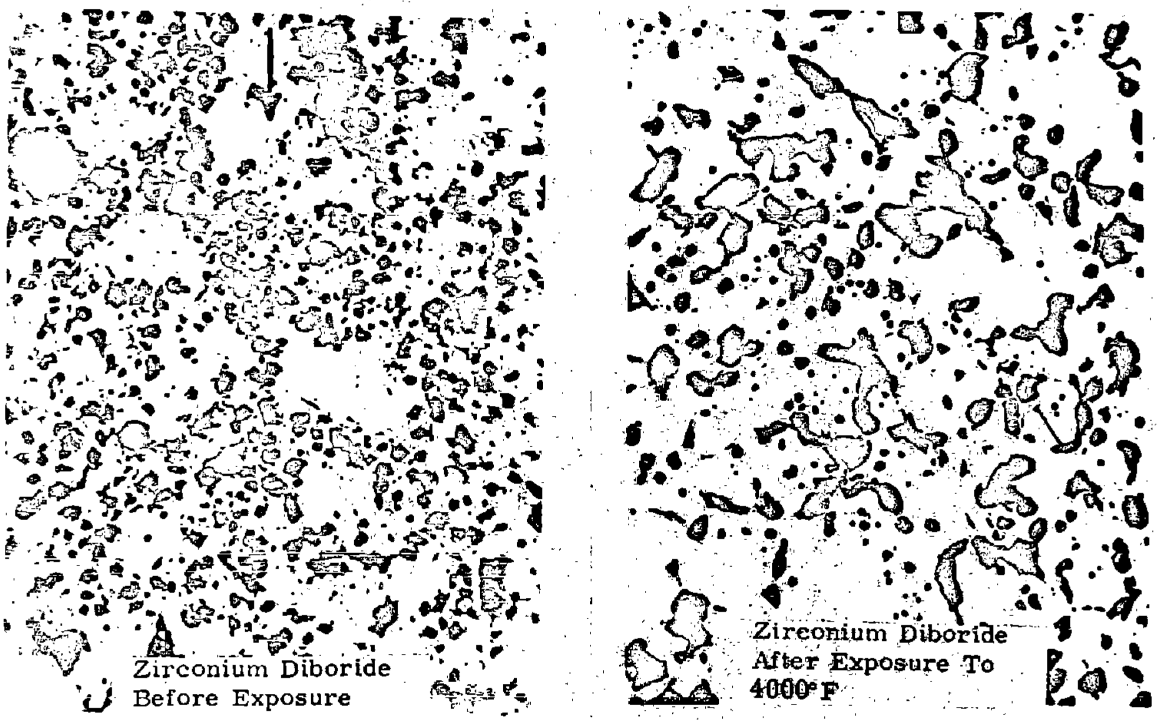

Zirconium Diboride
Before Exposure

Zirconium Diboride
After Exposure To
4000°F

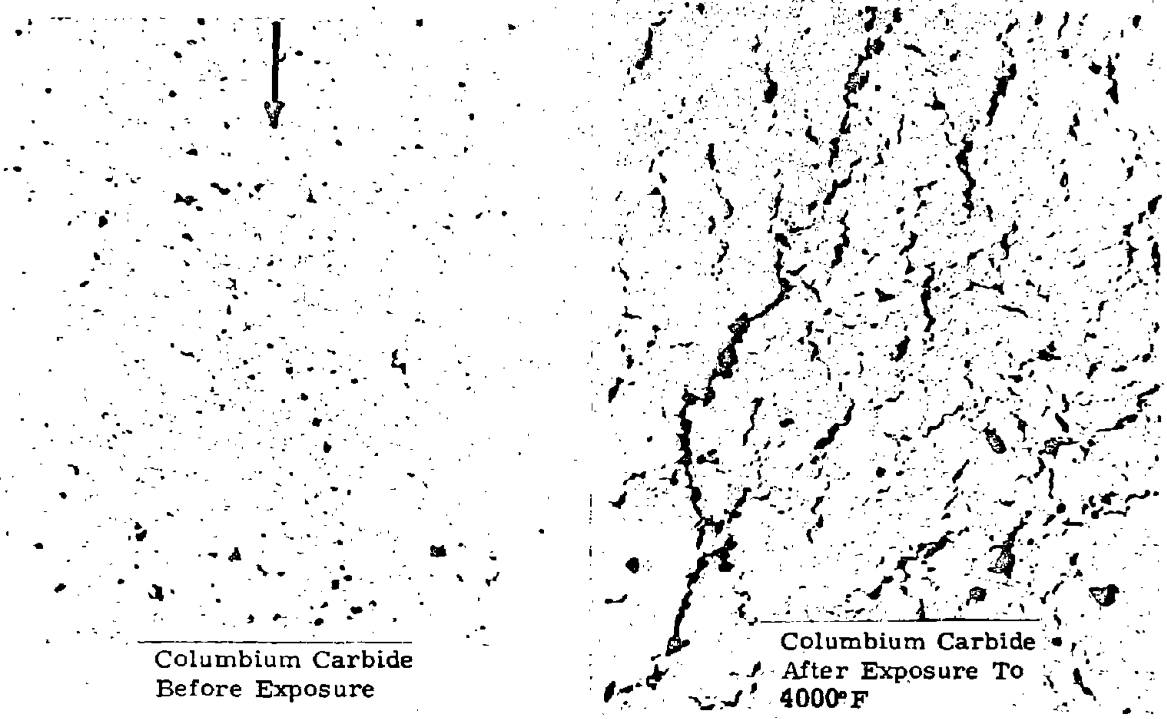

Columbium Carbide
Before Exposure

Columbium Carbide
After Exposure To
4000°F

(Top) Figure 16. Photomicrographs of Zirconium Diboride.

(Bottom) Figure 17. Photomicrographs of Columbium Carbide.

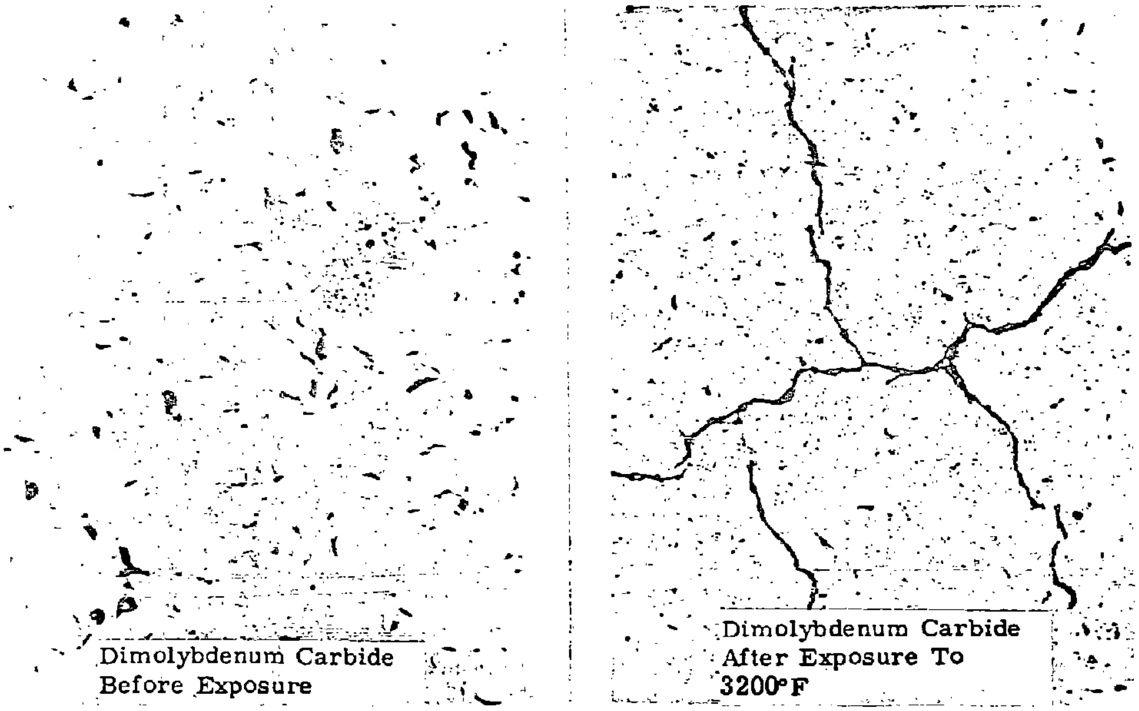

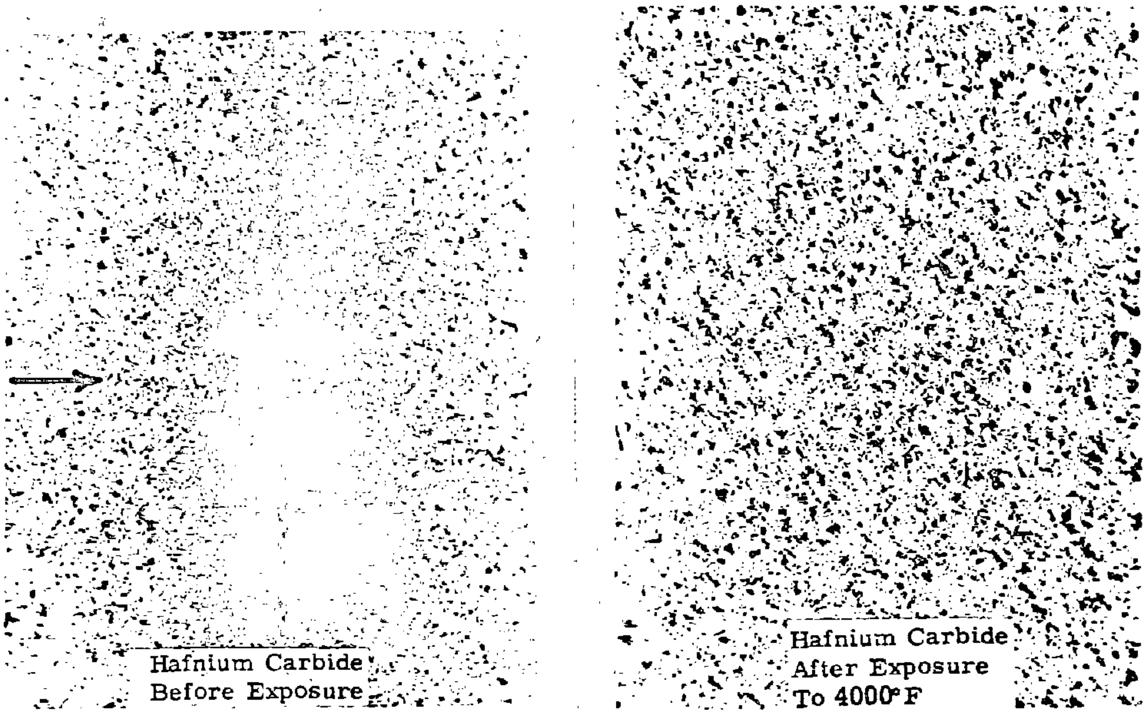

(Top) Figure 18. Photomicrographs of Dimolybdenum Carbide.

(Bottom) Figure 19. Photomicrographs of Hafnium Carbide.

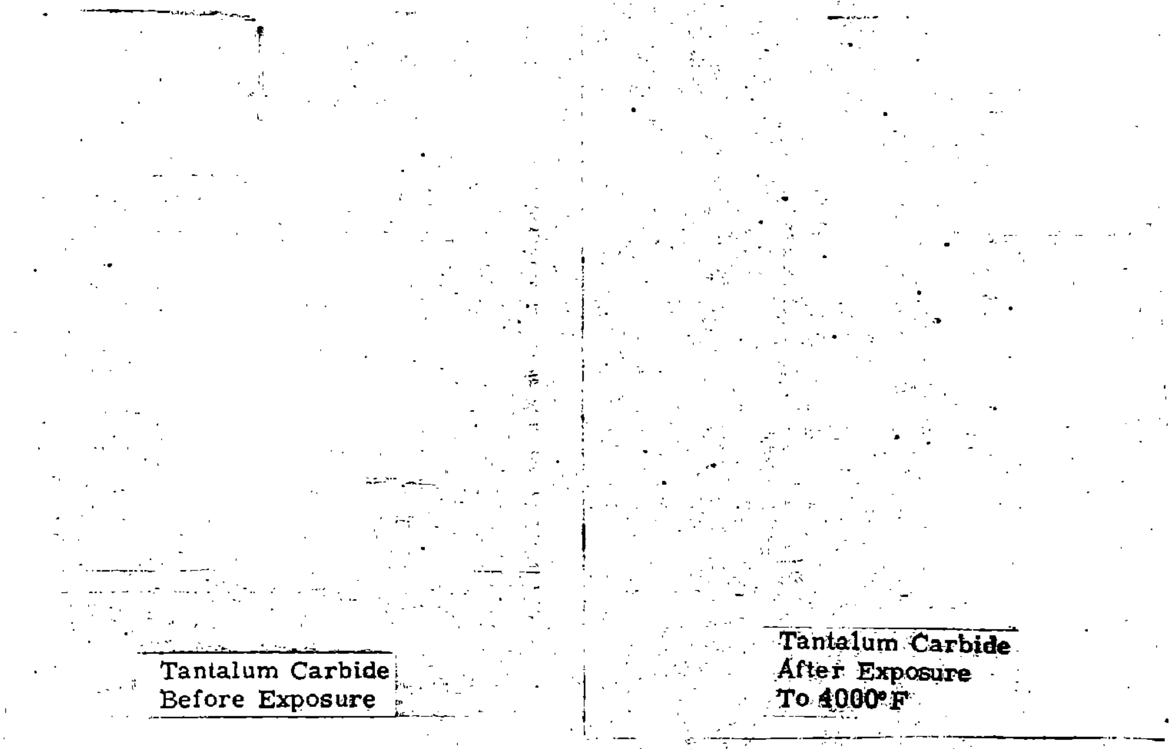

Tantalum Carbide
Before Exposure

Tantalum Carbide
After Exposure
To 4000°F

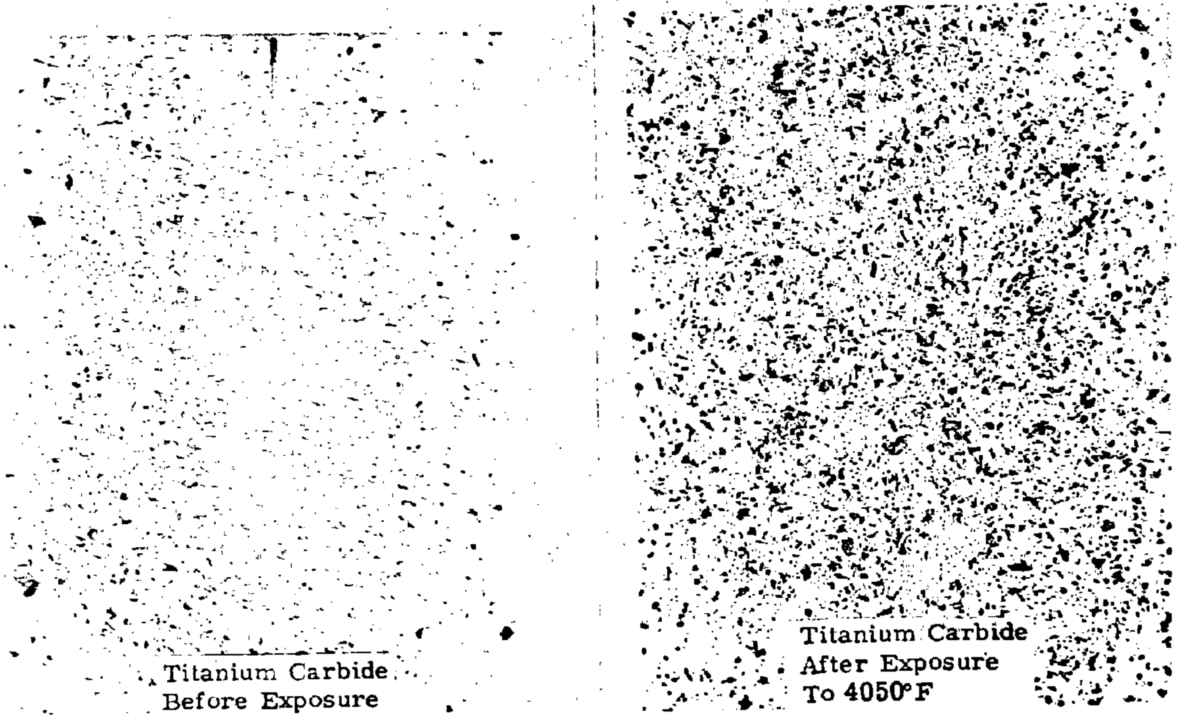

Titanium Carbide
Before Exposure

Titanium Carbide
After Exposure
To 4050°F

(Top) Figure 20. Photomicrographs of Tantalum Carbide.

(Bottom) Figure 21. Photomicrographs of Titanium Carbide.

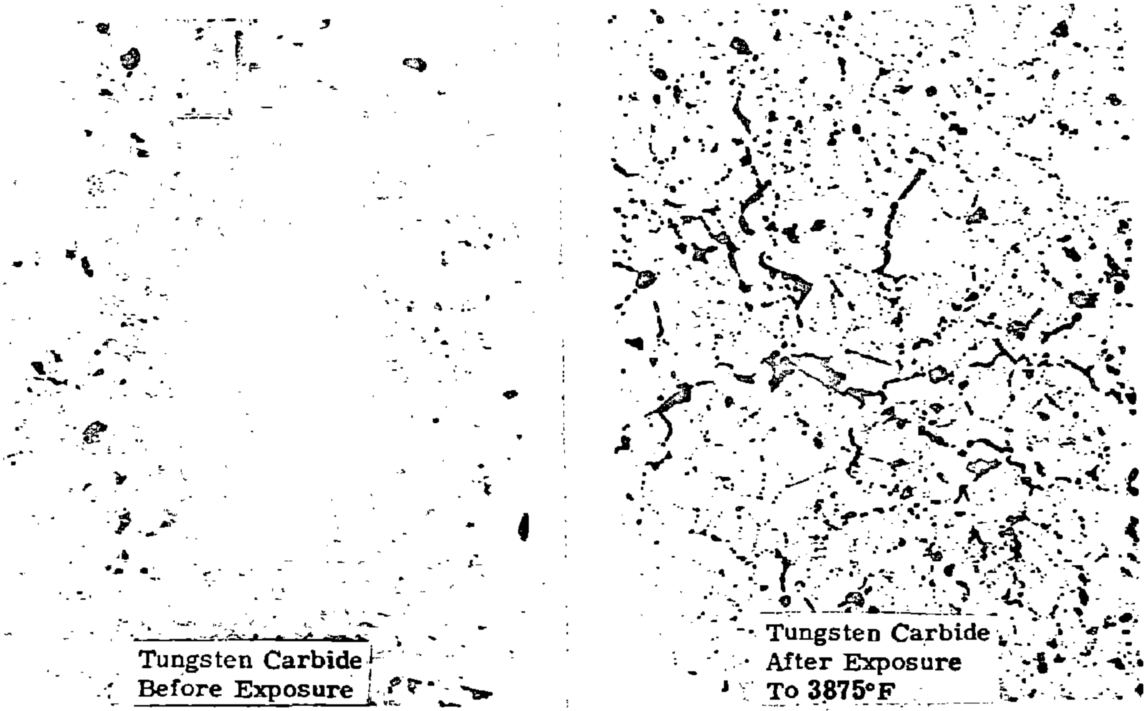

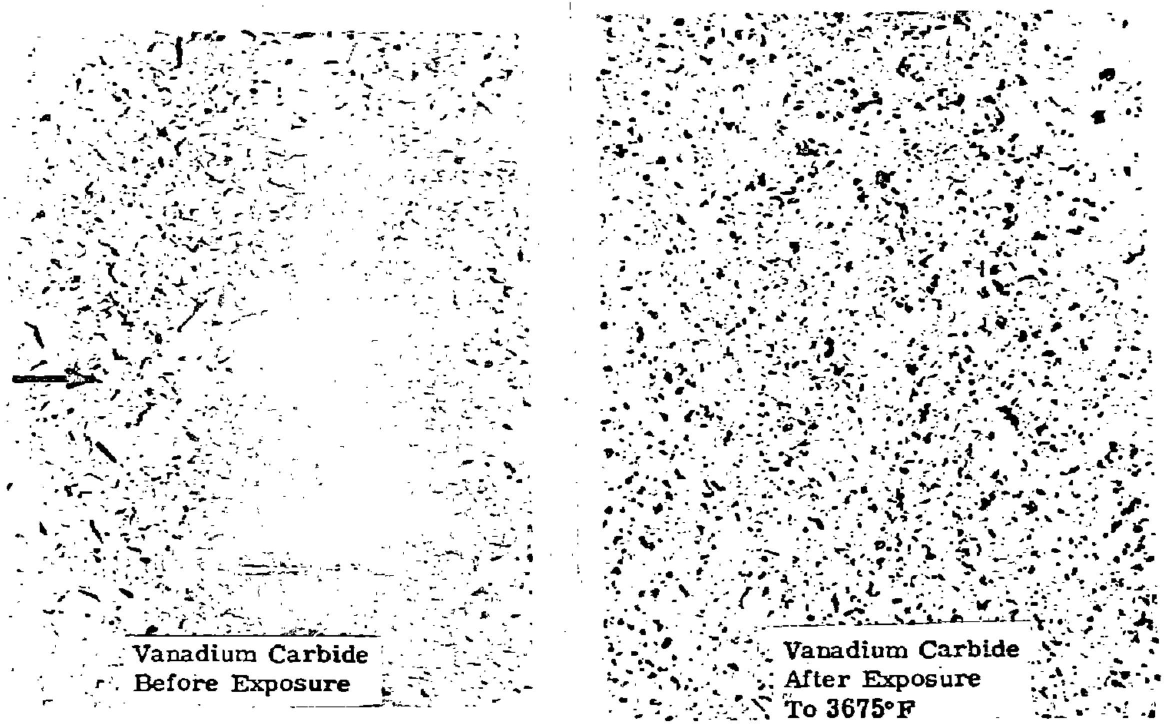

(Top) Figure 22. Photomicrographs of Tungsten Carbide.

(Bottom) Figure 23. Photomicrographs of Vanadium Carbide.

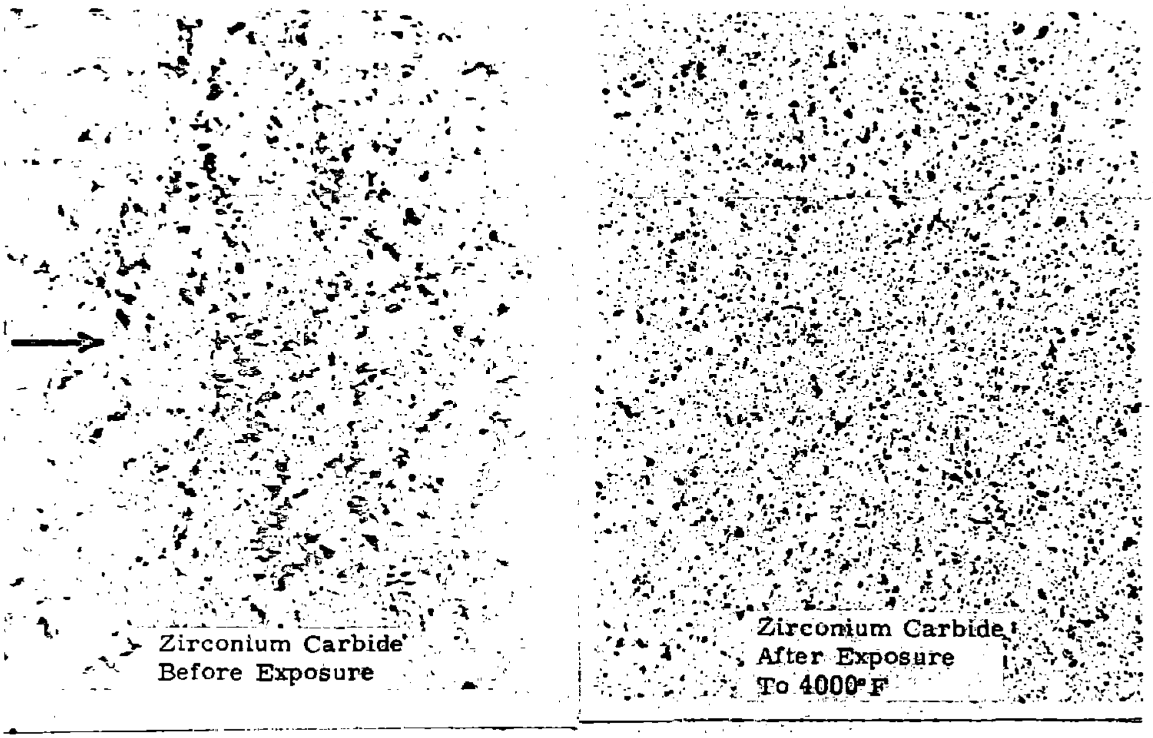

Zirconium Carbide Before Exposure

Zirconium Carbide After Exposure To 4000°F

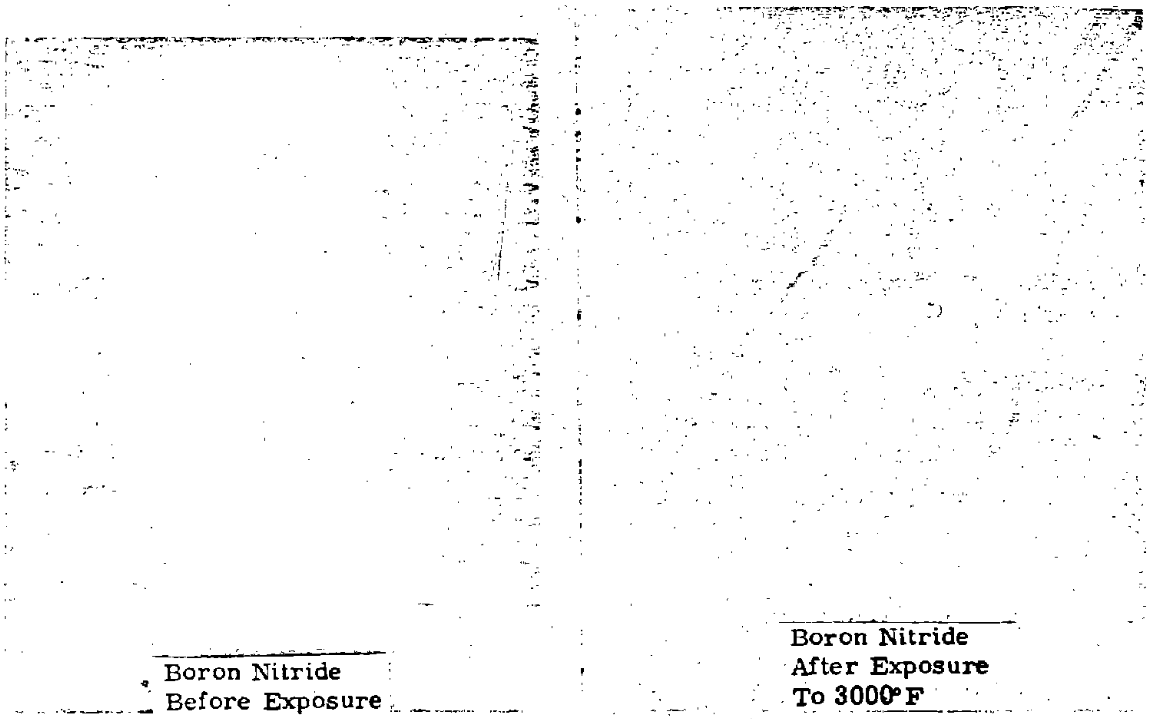

Boron Nitride Before Exposure

Boron Nitride After Exposure To 3000°F

(Top) Figure 24. Photomicrographs of Zirconium Carbide.

(Bottom) Figure 25. Photomicrographs of Boron Nitride.

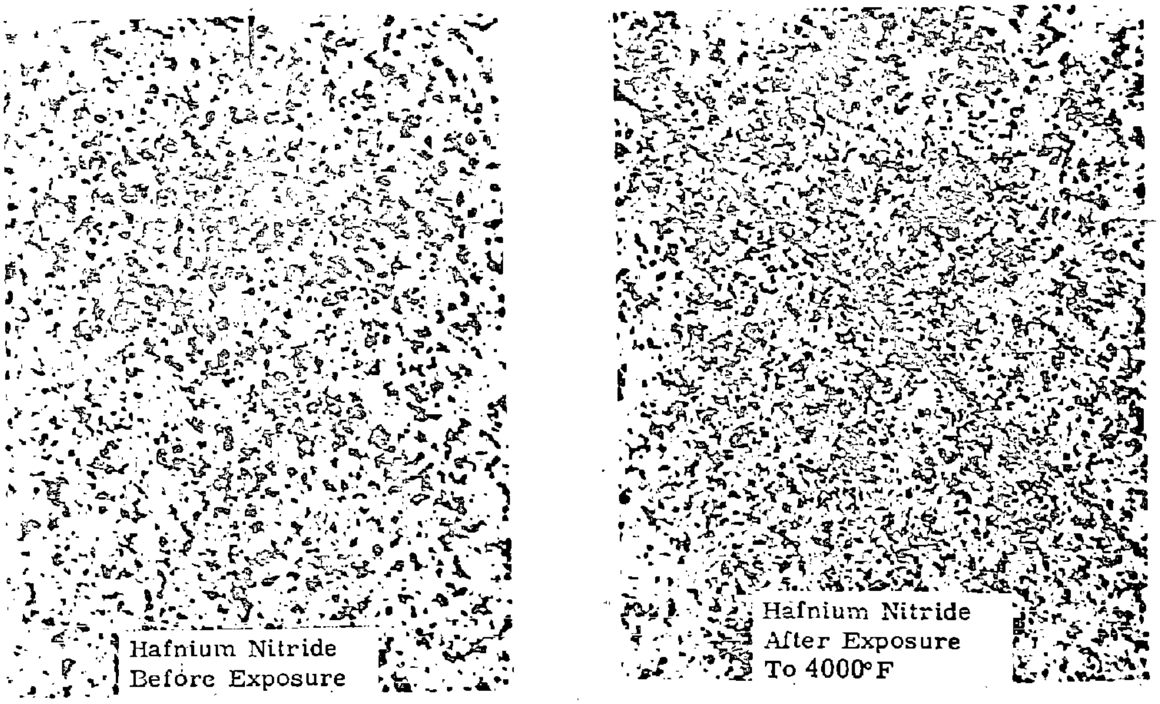

Hafnium Nitride
Before Exposure

Hafnium Nitride
After Exposure
To 4000°F

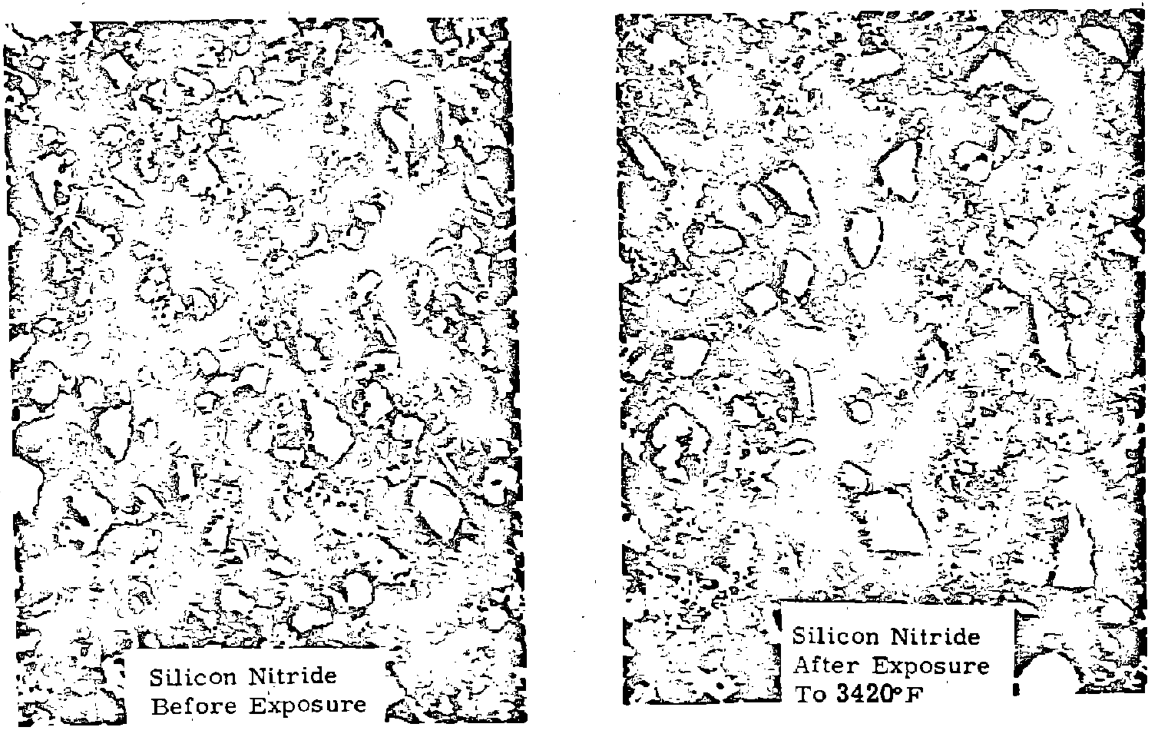

Silicon Nitride
Before Exposure

Silicon Nitride
After Exposure
To 3420°F

(Top) Figure 26. Photomicrographs of Hafnium Nitride.

(Bottom) Figure 27. Photomicrographs of Silicon Nitride.

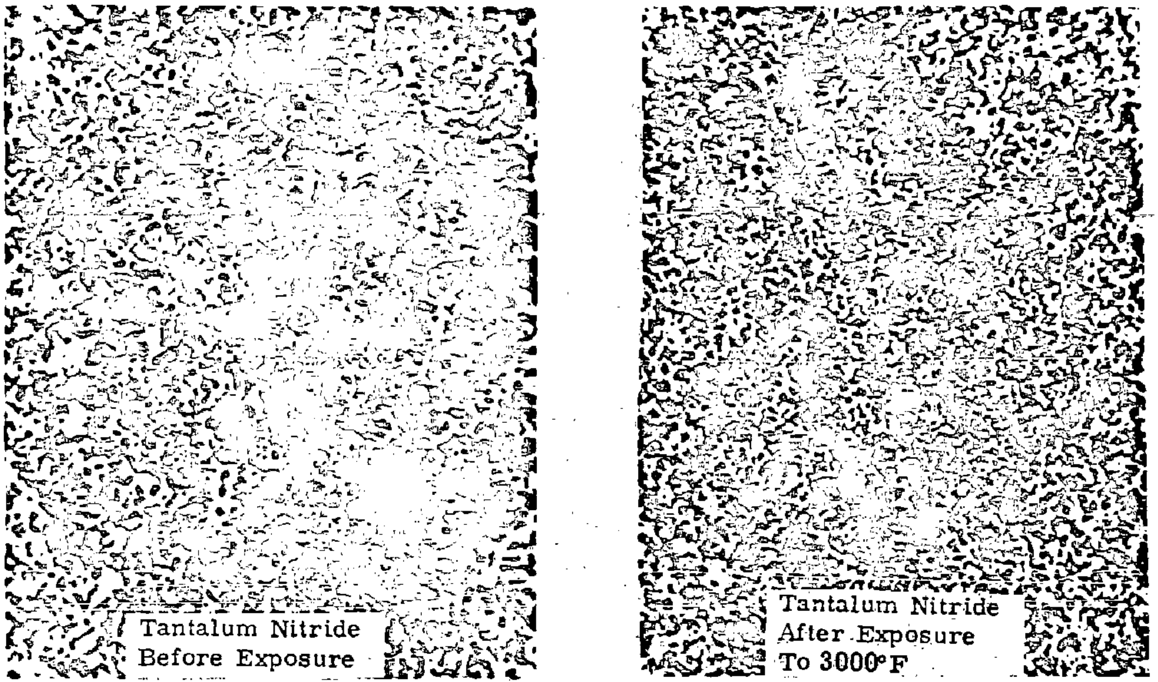

Tantalum Nitride Before Exposure

Tantalum Nitride After Exposure To 3000°F

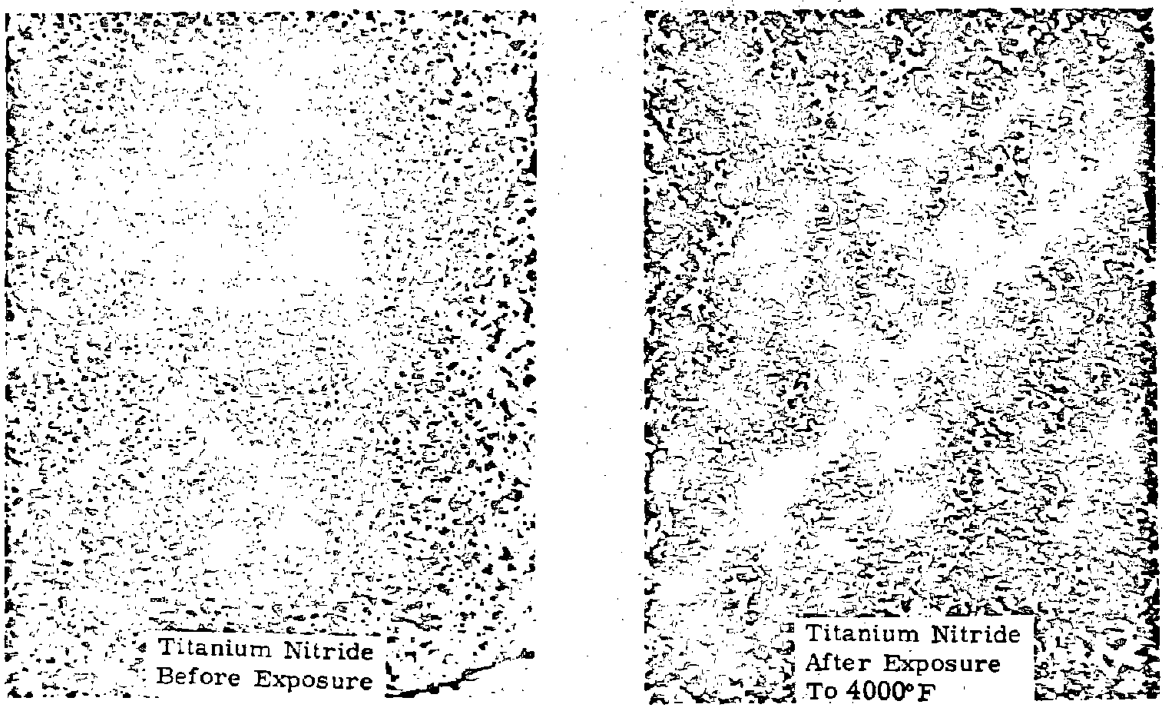

Titanium Nitride Before Exposure

Titanium Nitride After Exposure To 4000°F

(Top) Figure 28. Photomicrographs of Tantalum Nitride.

(Bottom) Figure 29. Photomicrographs of Titanium Nitride.

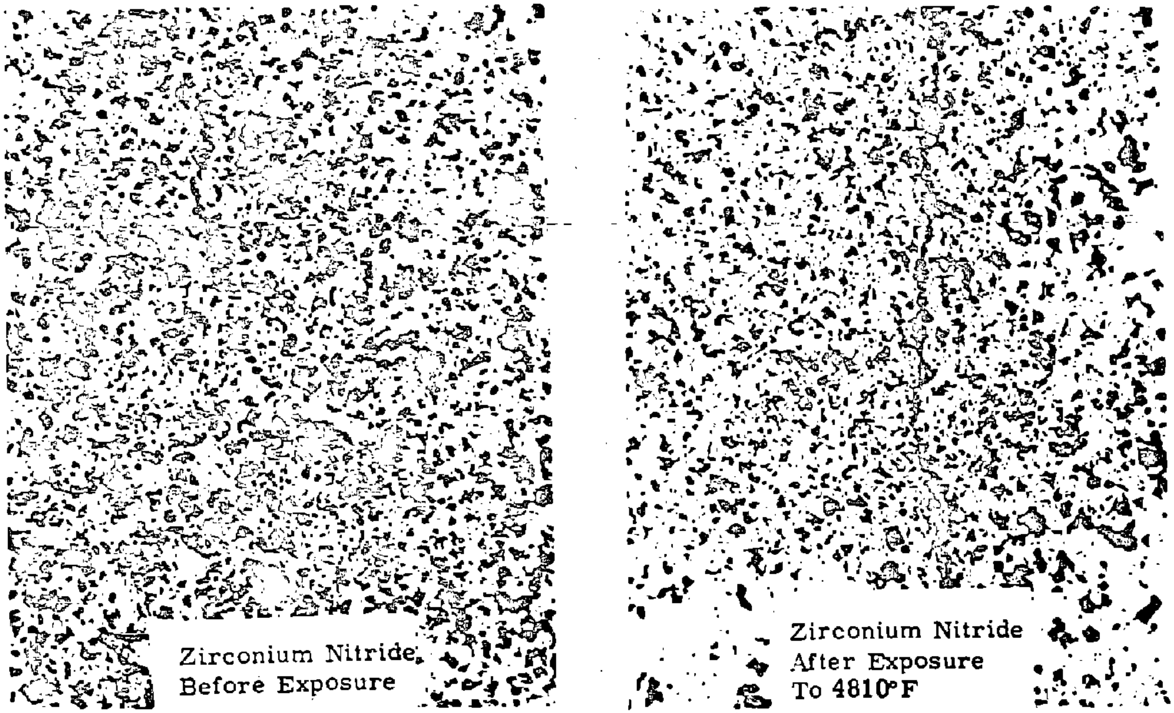
Zirconium Nitride Before Exposure

Zirconium Nitride After Exposure To 4810°F

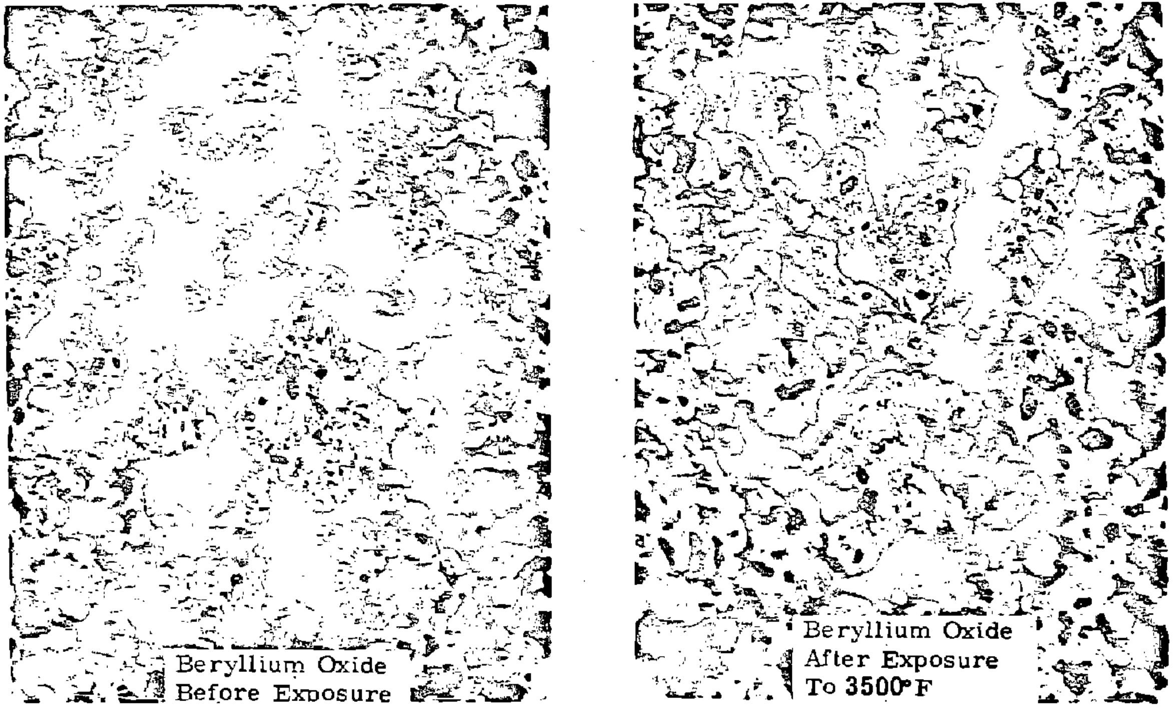
Beryllium Oxide Before Exposure

Beryllium Oxide After Exposure To 3500°F

(Top) Figure 30. Photomicrographs of Zirconium Nitride.

(Bottom) Figure 31. Photomicrographs of Beryllium Oxide.

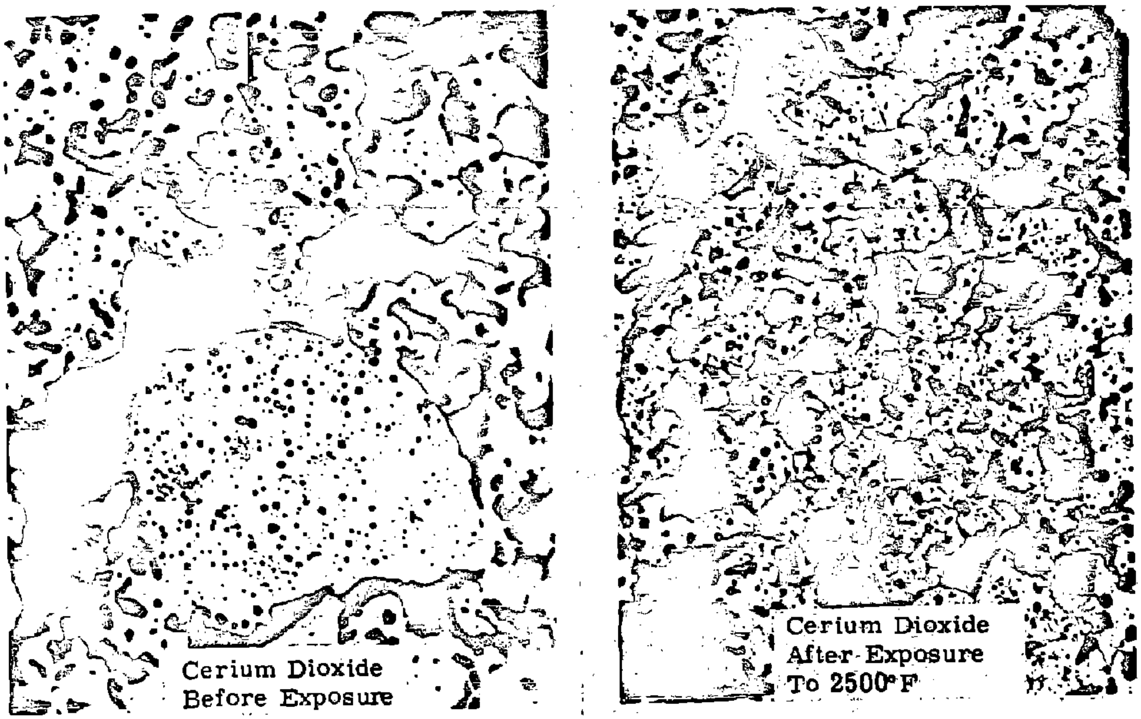

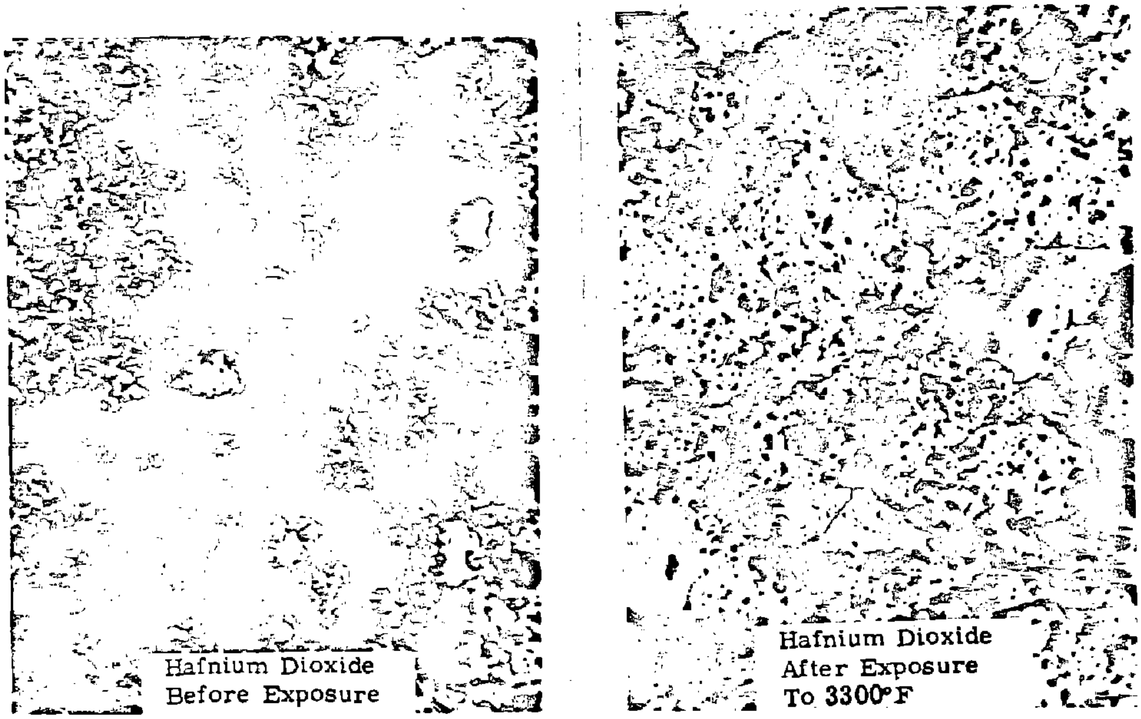

(Top) Figure 32. Photomicrographs of Cerium Dioxide.

(Bottom) Figure 33. Photomicrographs of Hafnium Dioxide.

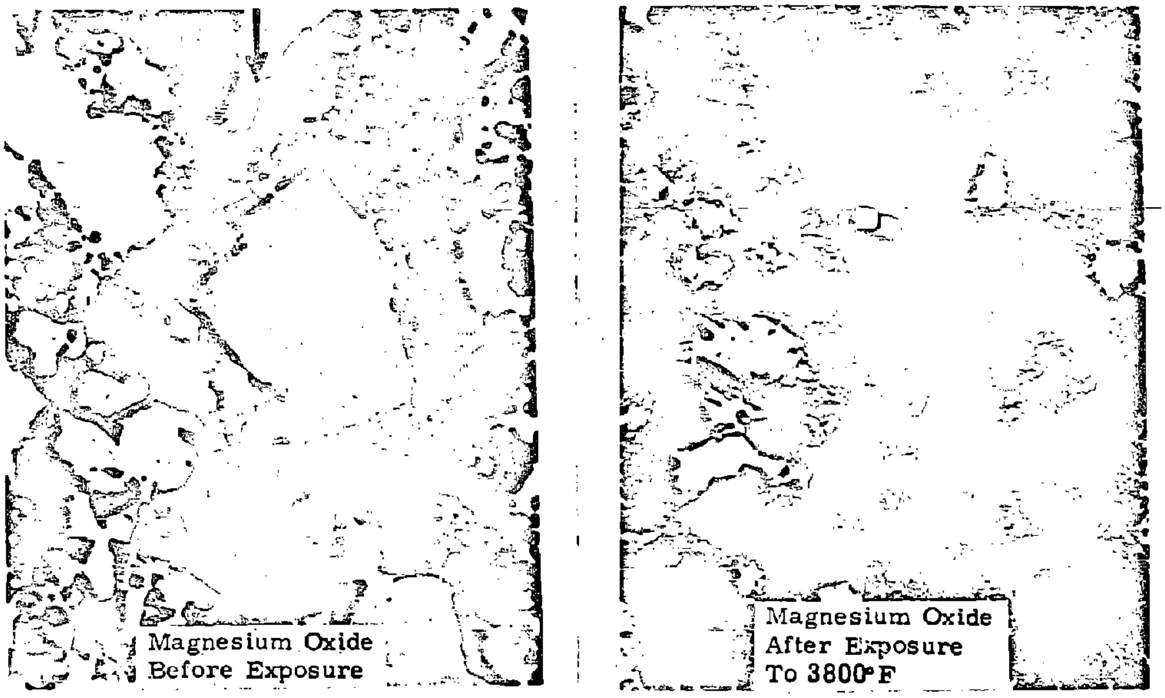

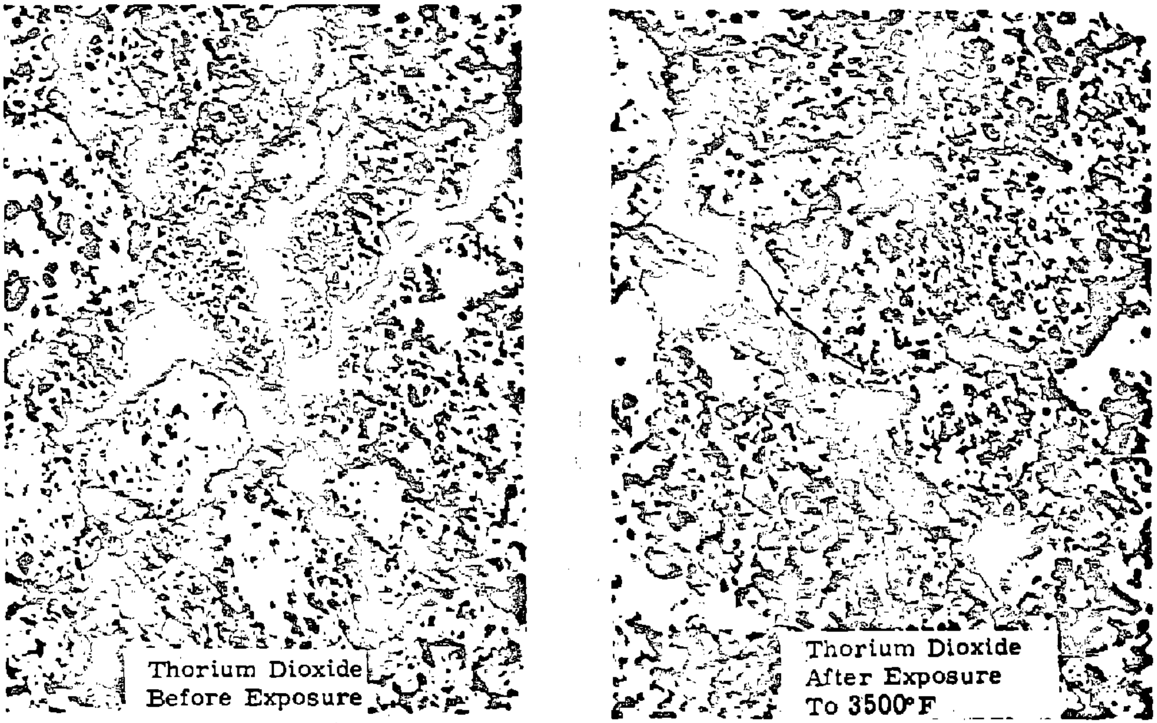

(Top) Figure 34. Photomicrographs of Magnesium Oxide.

(Bottom) Figure 35. Photomicrographs of Thorium Dioxide.

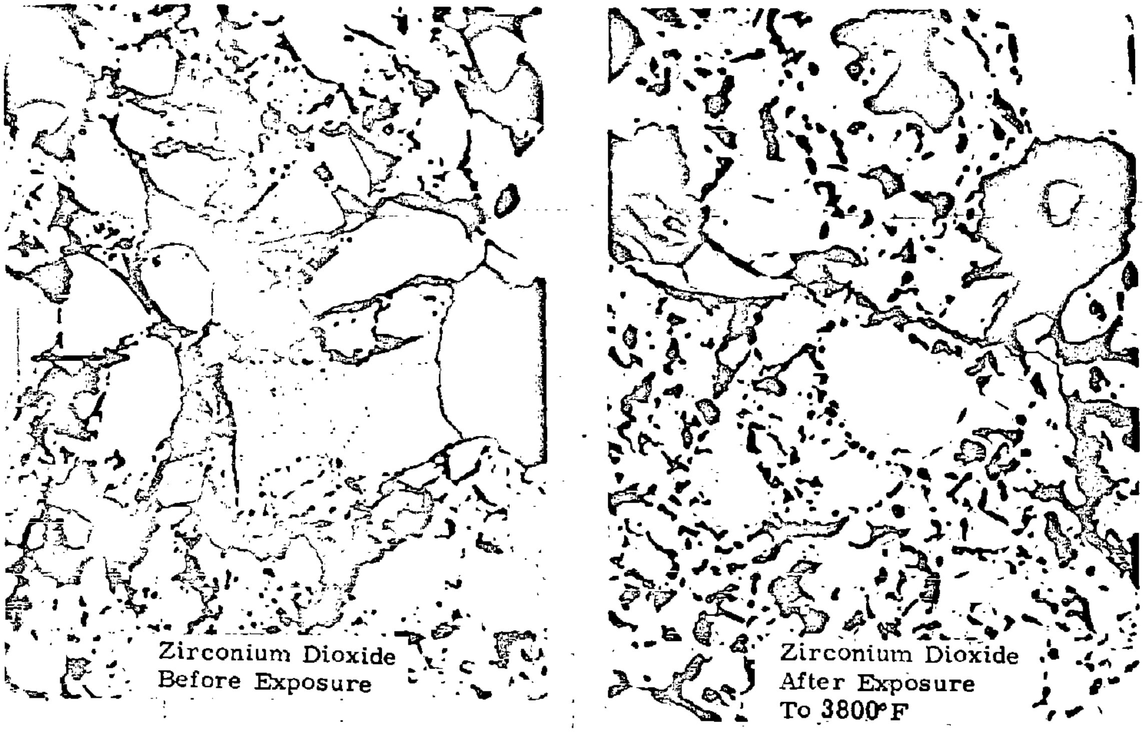
Zirconium Dioxide Before Exposure

Zirconium Dioxide After Exposure To 3800°F

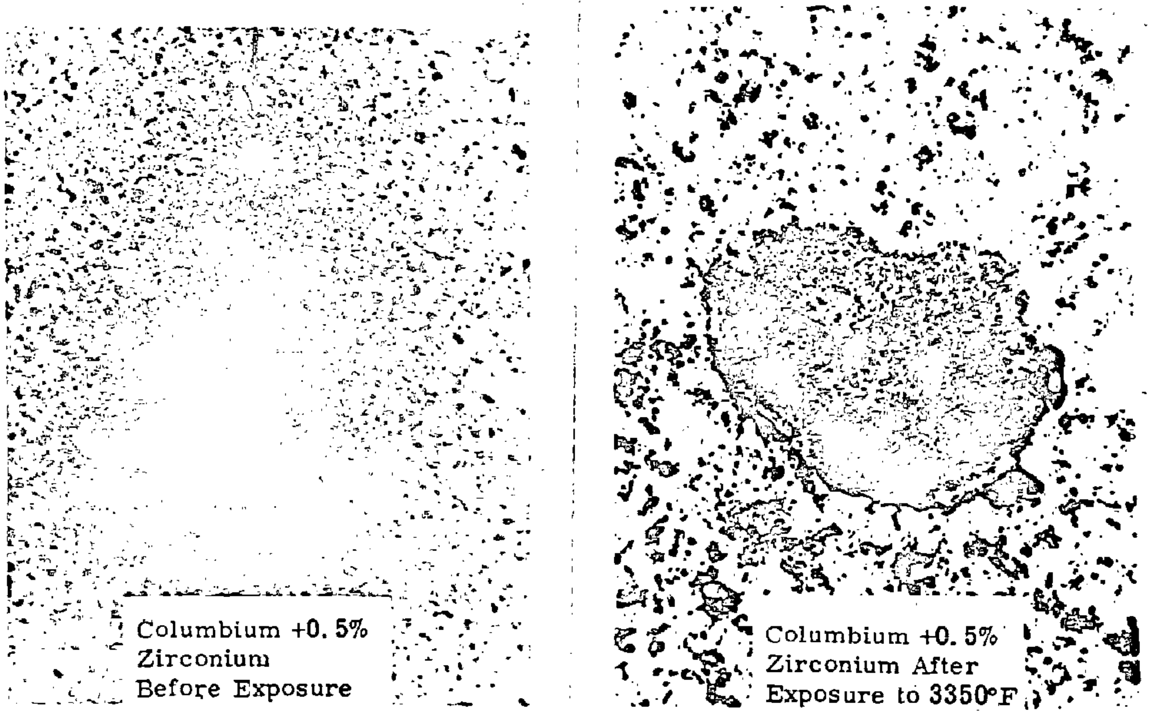
Columbium +0.5% Zirconium Before Exposure

Columbium +0.5% Zirconium After Exposure to 3350°F

(Top) Figure 36. Photomicrographs of Zirconium Dioxide.

(Bottom) Figure 37. Photomicrographs of Columbium +0.5% Zirconium.

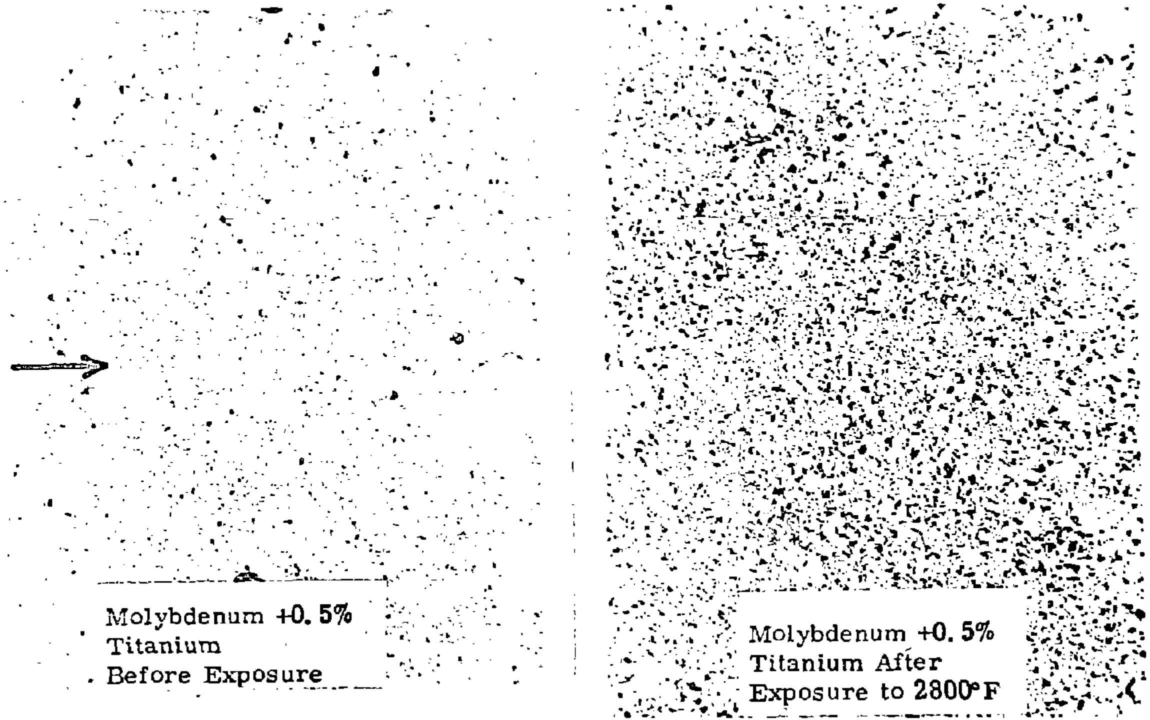

Molybdenum +0.5% Titanium Before Exposure

Molybdenum +0.5% Titanium After Exposure to 2800°F

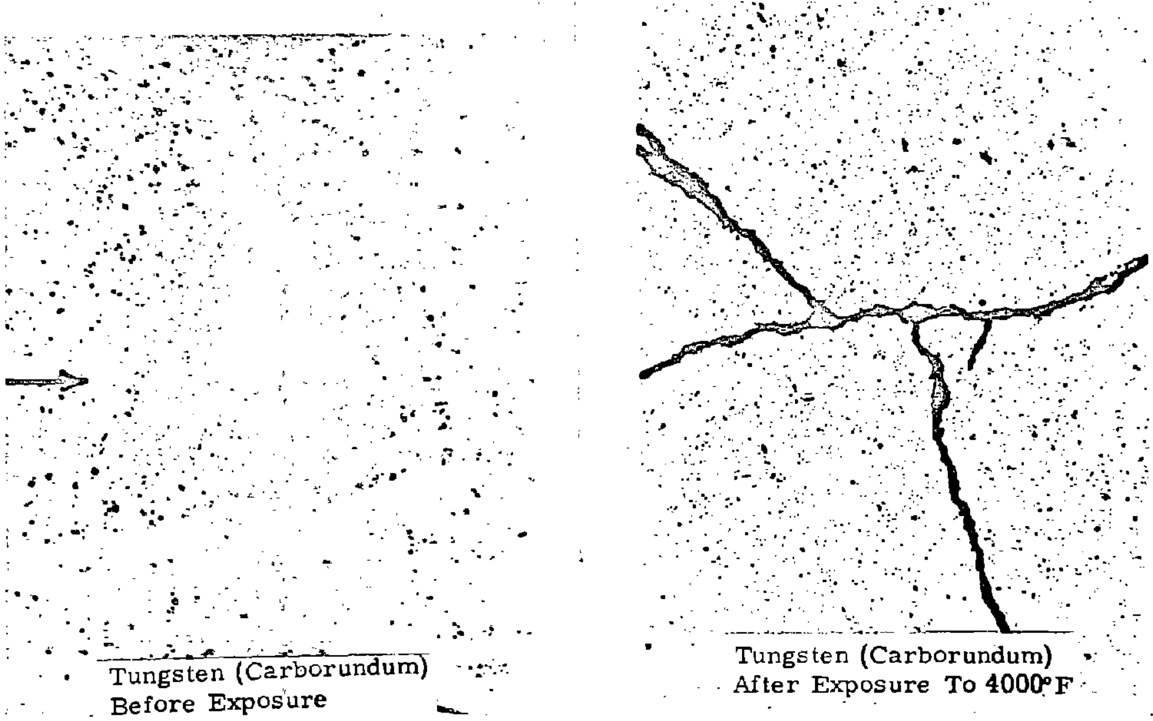

Tungsten (Carborundum) Before Exposure

Tungsten (Carborundum) After Exposure To 4000°F

(Top) Figure 38. Photomicrographs of Molybdenum + 0.5% Titanium.

(Bottom) Figure 39. Photomicrographs of Tungsten (Carborundum).

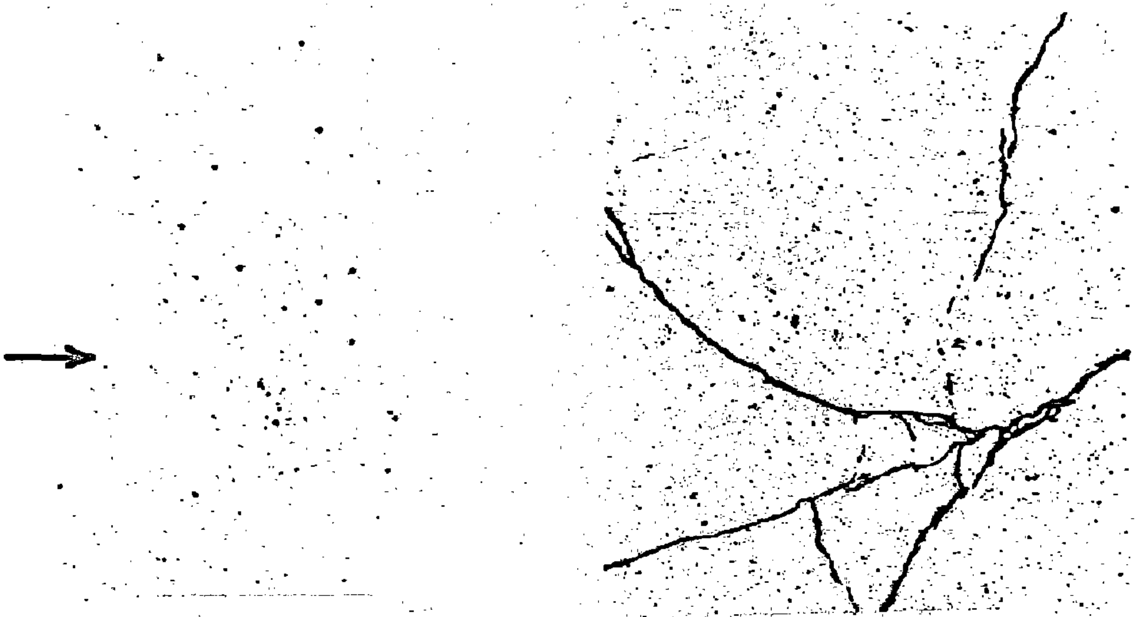

Tungsten (General Electric) Before Exposure

Tungsten (General Electric) After Exposure to 4000°F

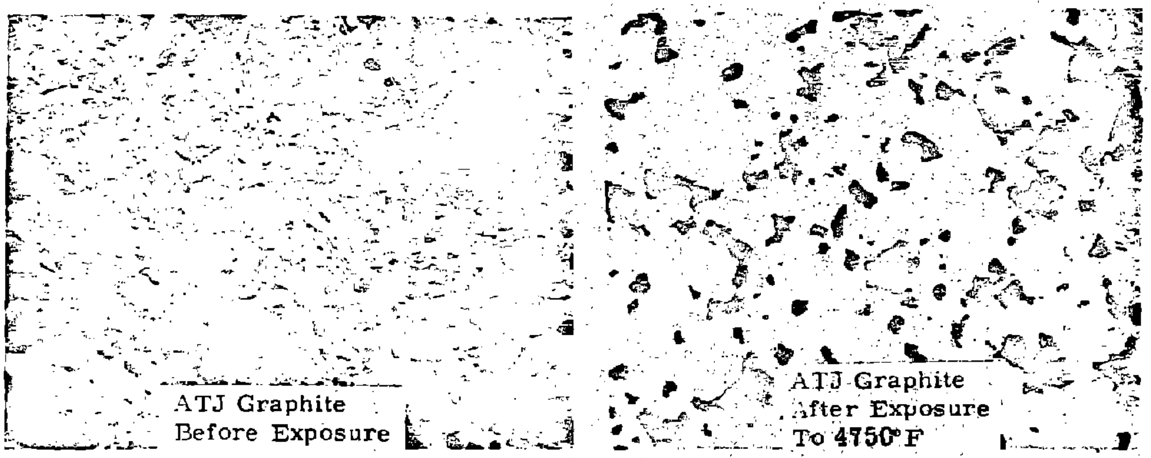

ATJ Graphite Before Exposure

ATJ Graphite After Exposure To 4750°F

(Top) Figure 40. Photomicrographs of Tungsten (General Electric).

(Bottom) Figure 41. Photomicrographs of ATJ Graphite.

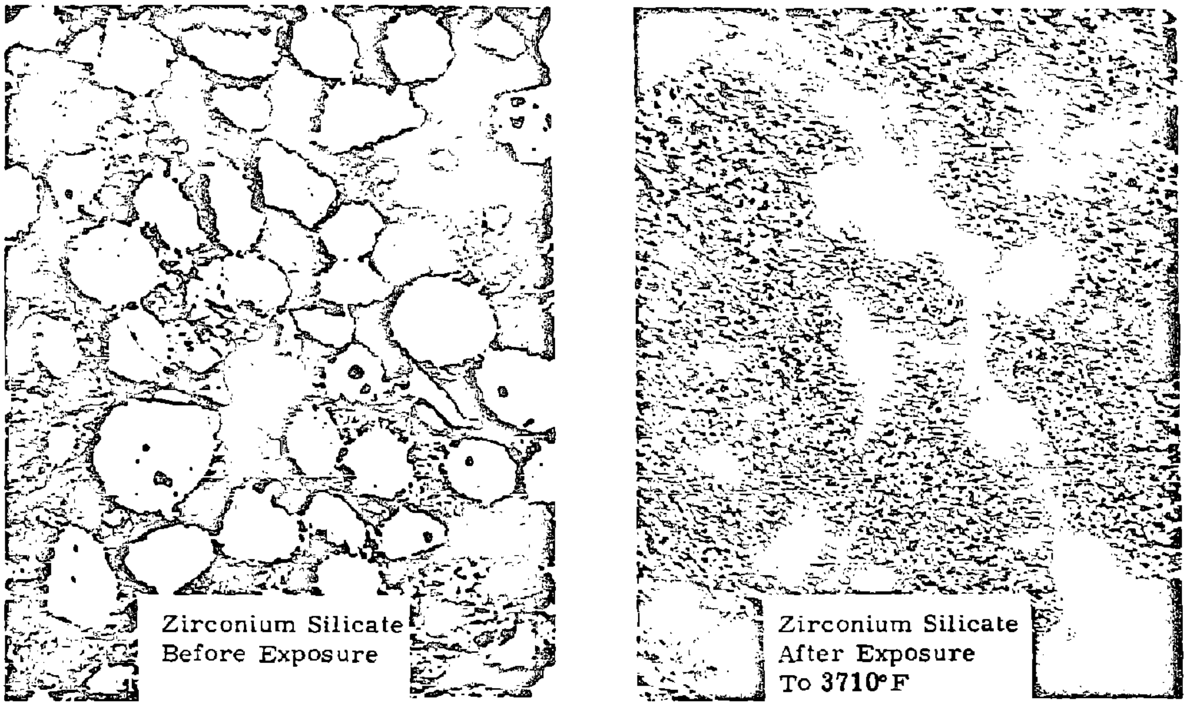

Zirconium Silicate Before Exposure

Zirconium Silicate After Exposure To 3710°F

Figure 42. Photomicrographs of Zirconium Silicate.

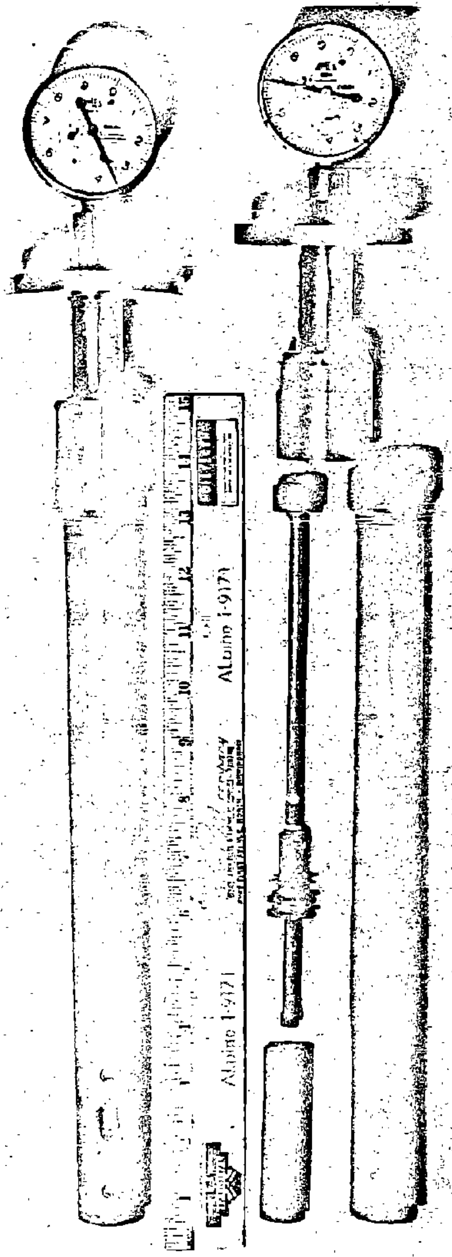

Figure 43. Picture of the Graphite Dilatometer Tubes for Measuring Thermal Expansion to 5000°F.

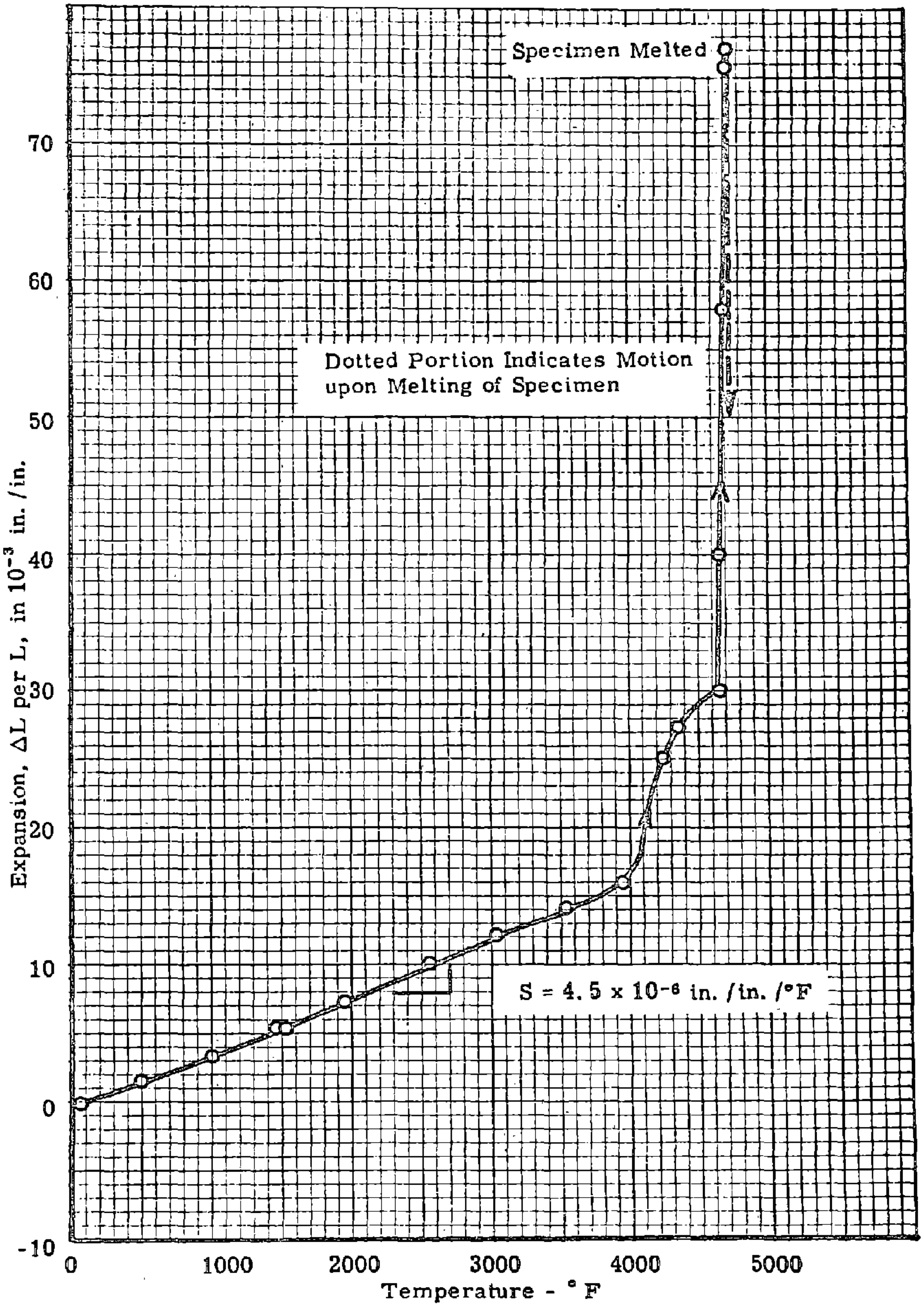

Figure 44. Thermal Expansion of Hafnium Diboride.

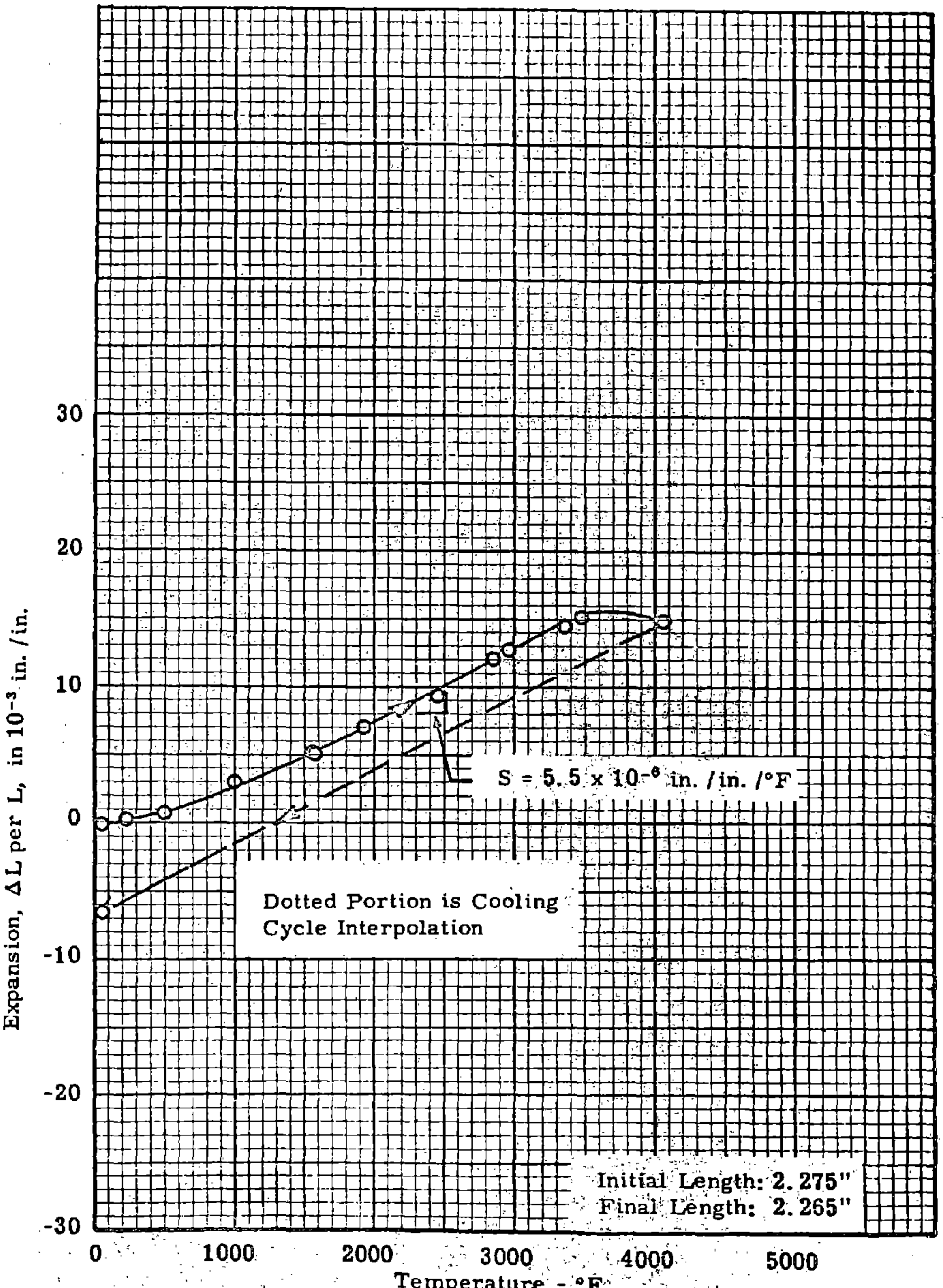

Figure 45. Thermal Expansion of Thorium Tetraboride.

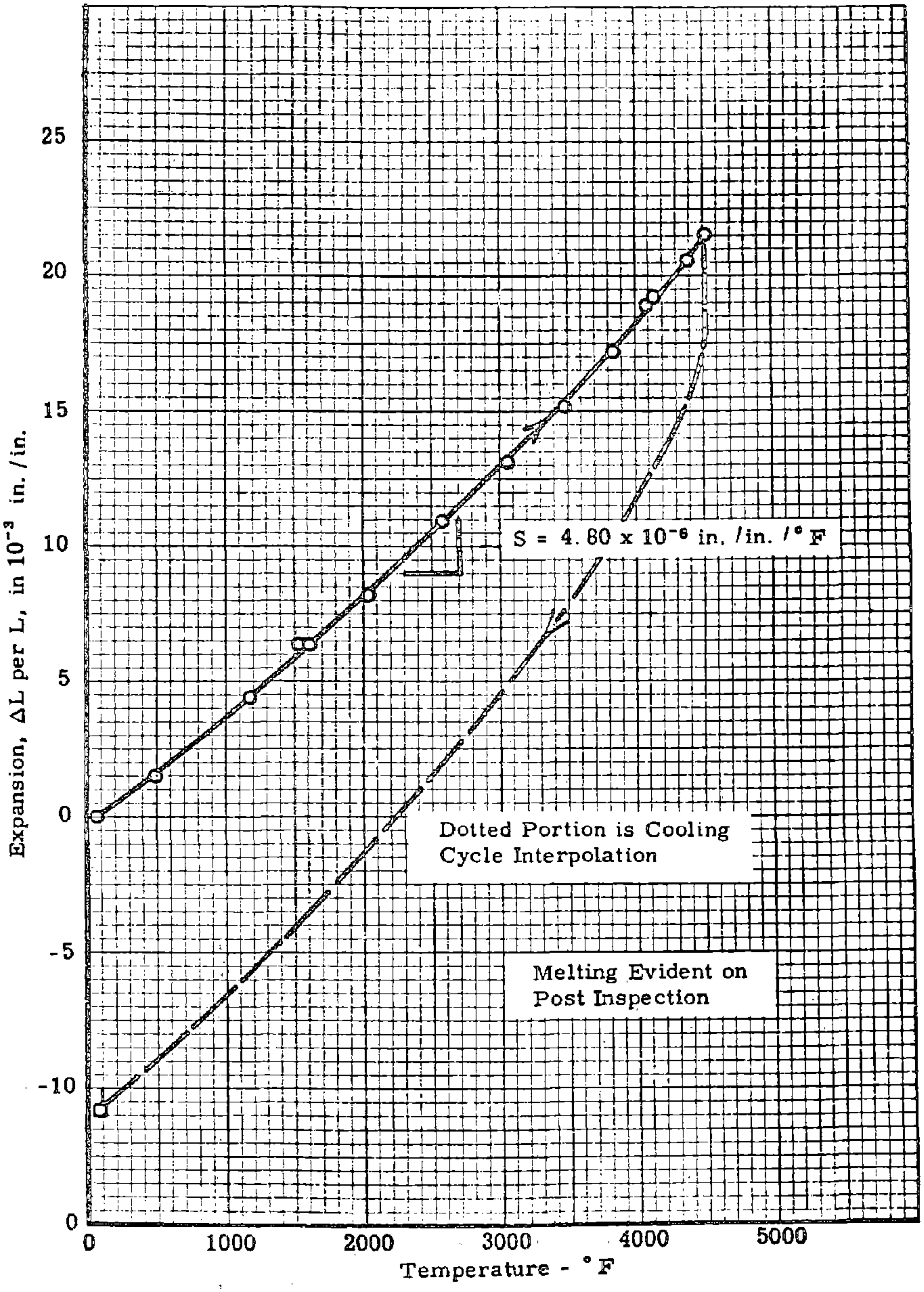

Figure 46. Thermal Expansion of Titanium Diboride.

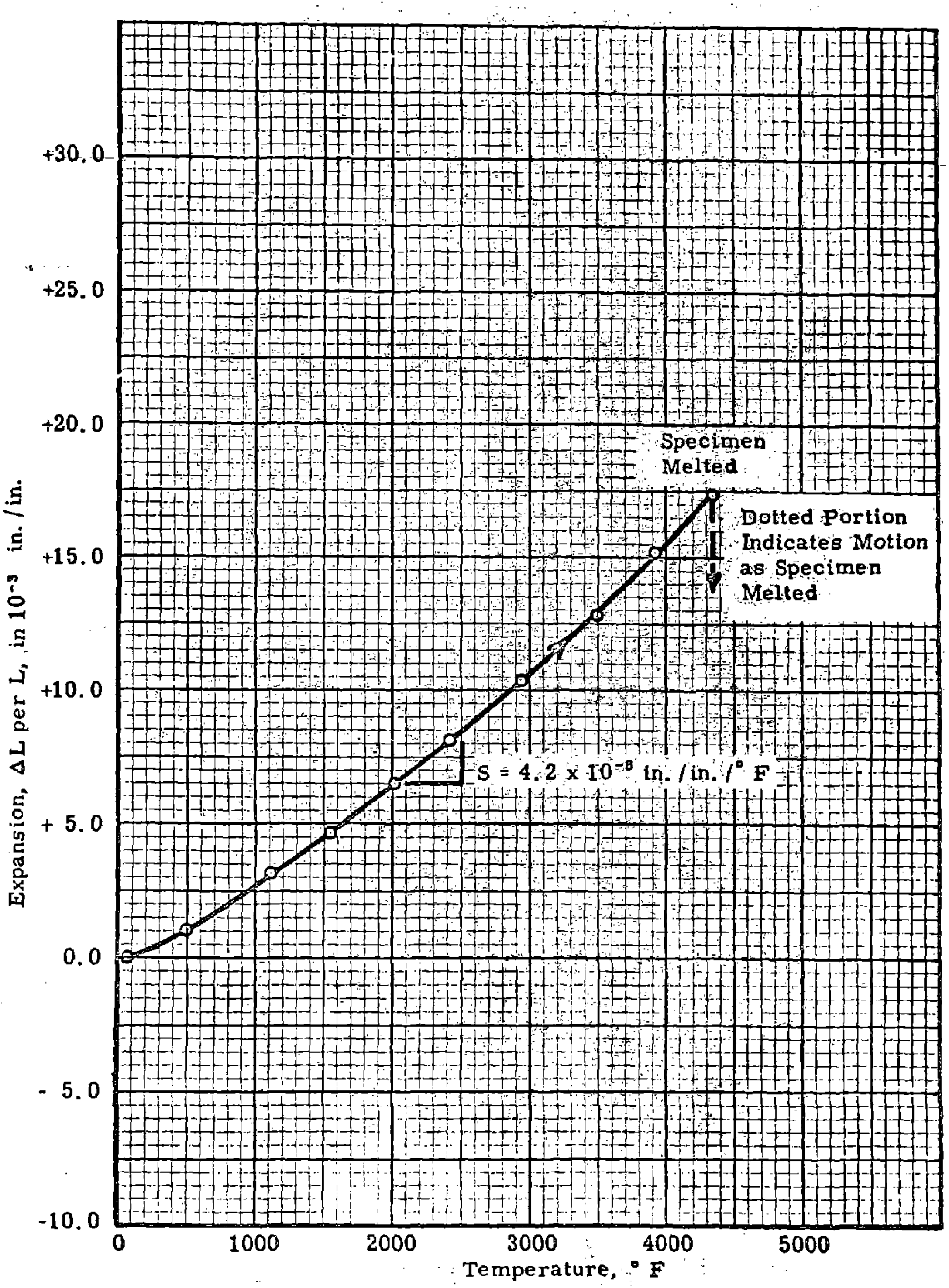

Figure 47. Thermal Expansion of Tungsten Boride.

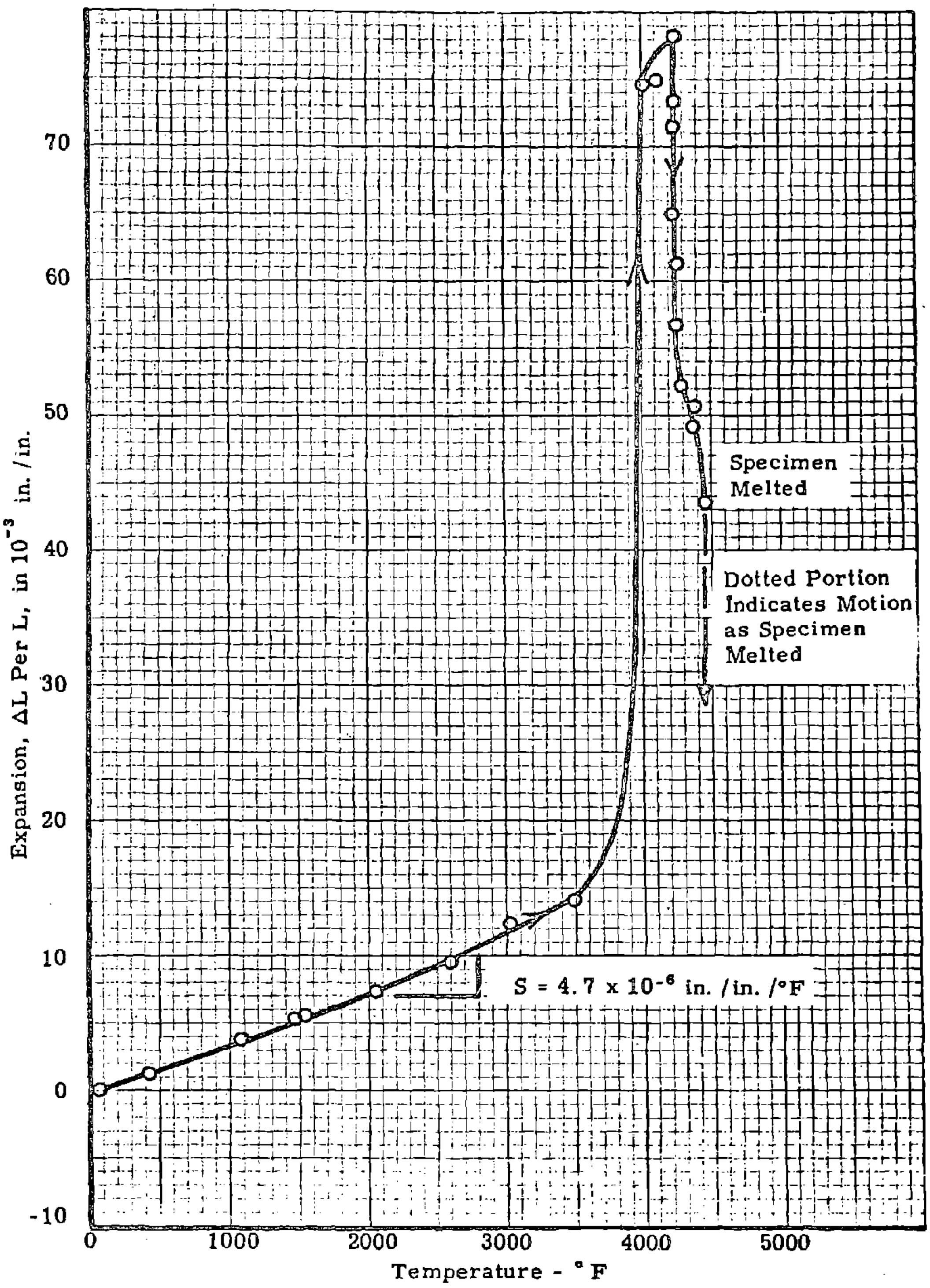

Figure 48. Thermal Expansion of Dimolybdenum Carbide.

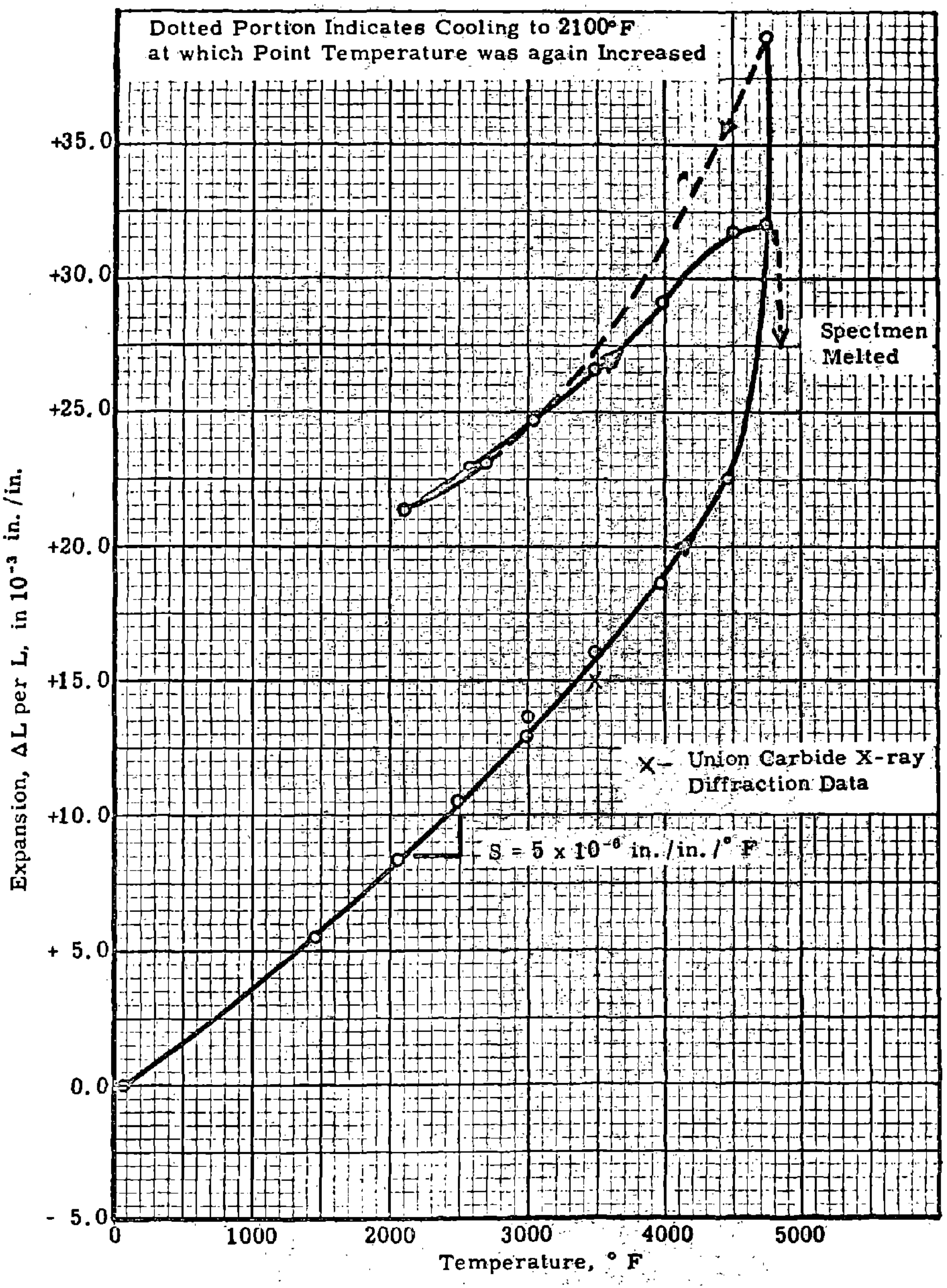

Figure 49. Thermal Expansion of Titanium Carbide.

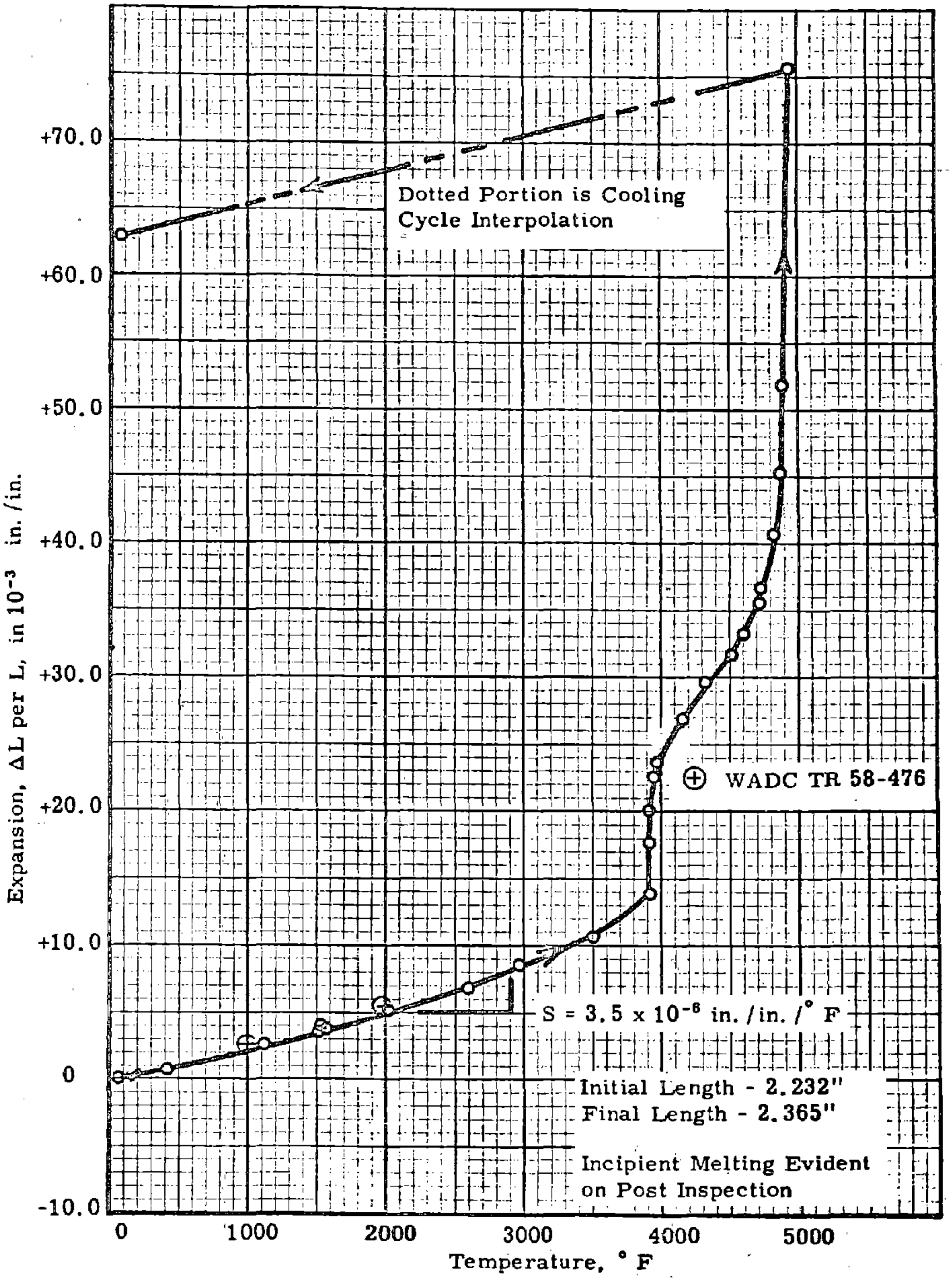

Figure 50. Thermal Expansion of Tungsten Carbide.

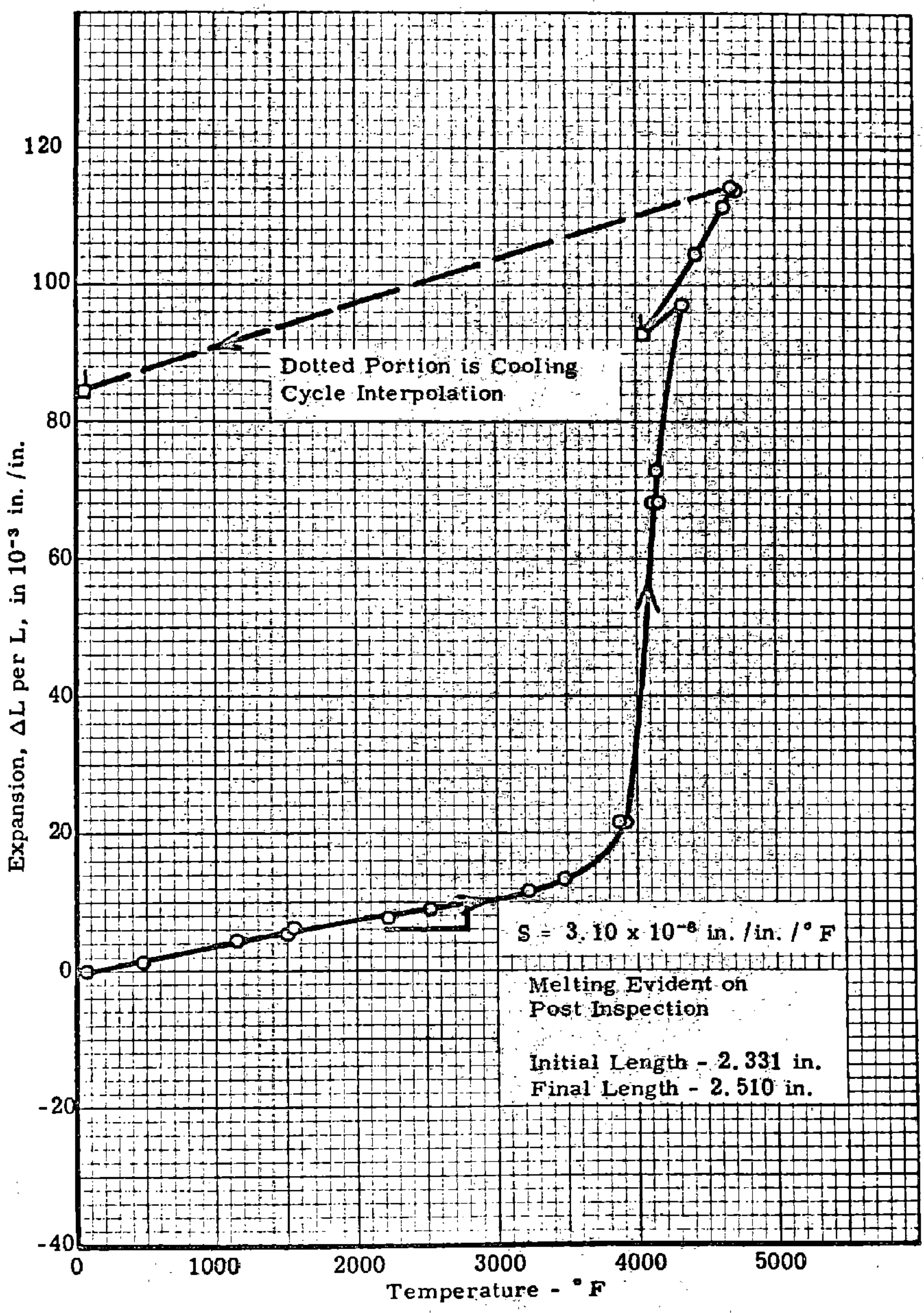

Figure 51. Thermal Expansion of Vanadium Carbide.

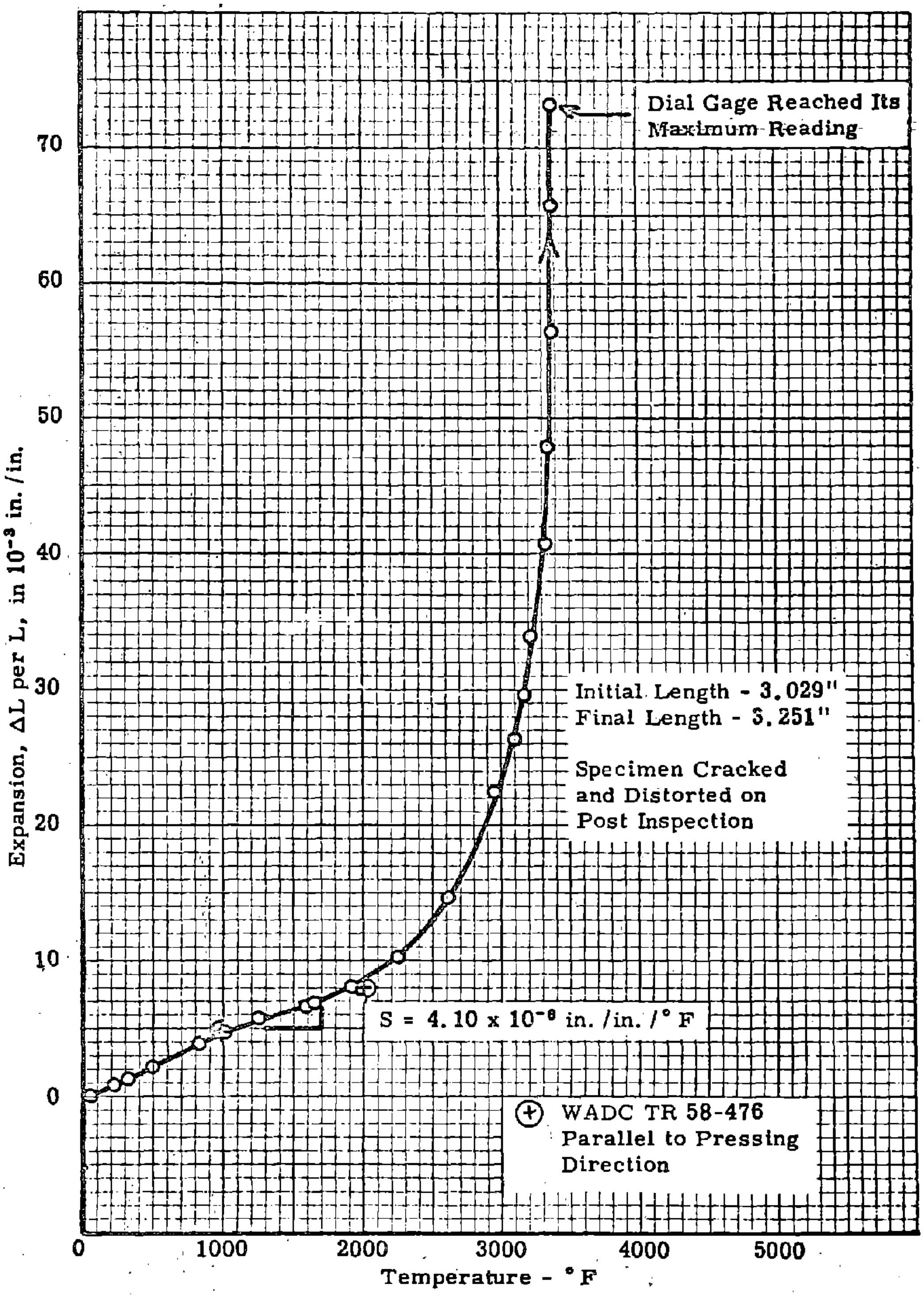

Figure 52. Thermal Expansion of Boron Nitride.

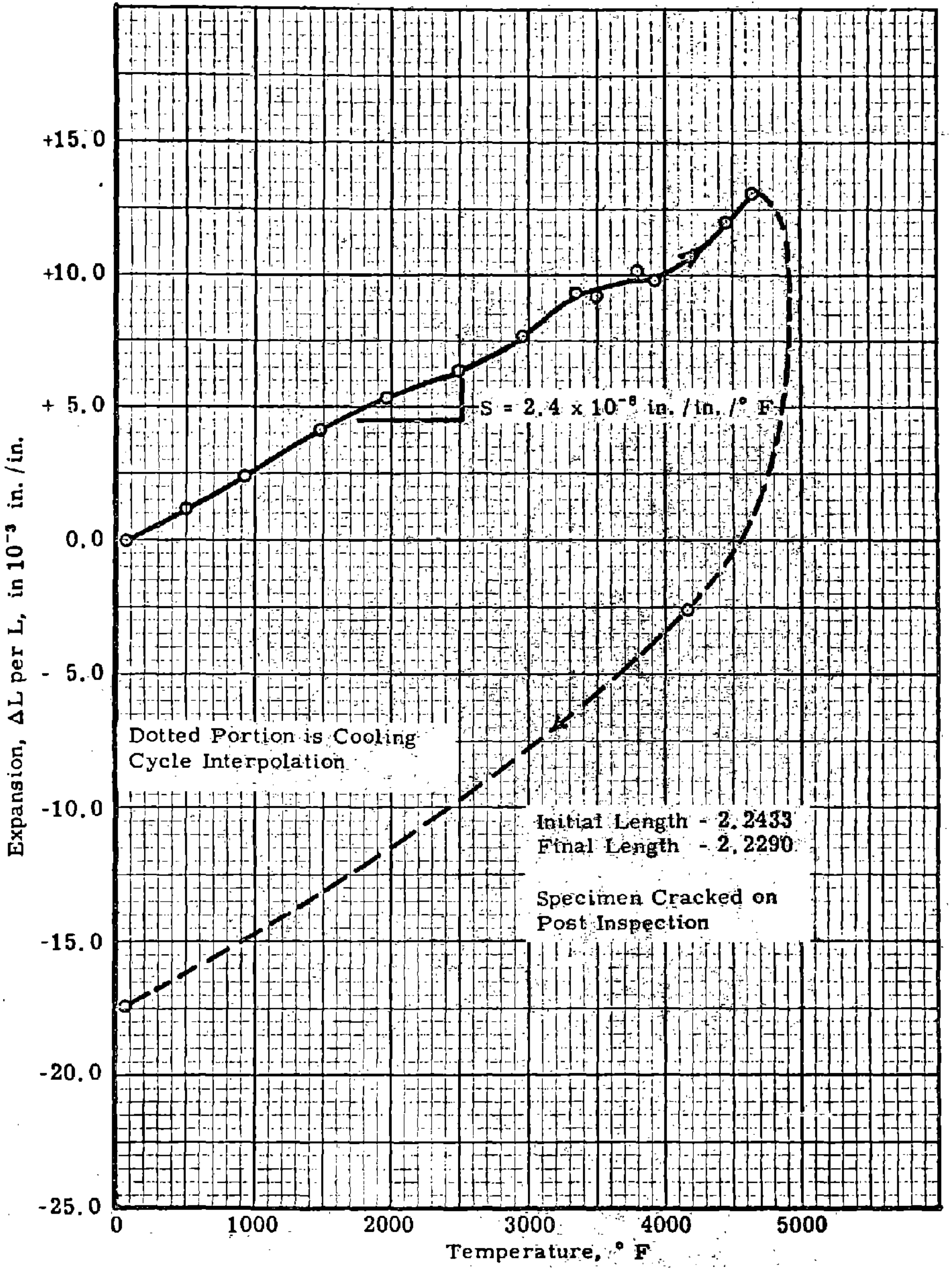

Figure 53. Thermal Expansion of Tantalum Nitride.

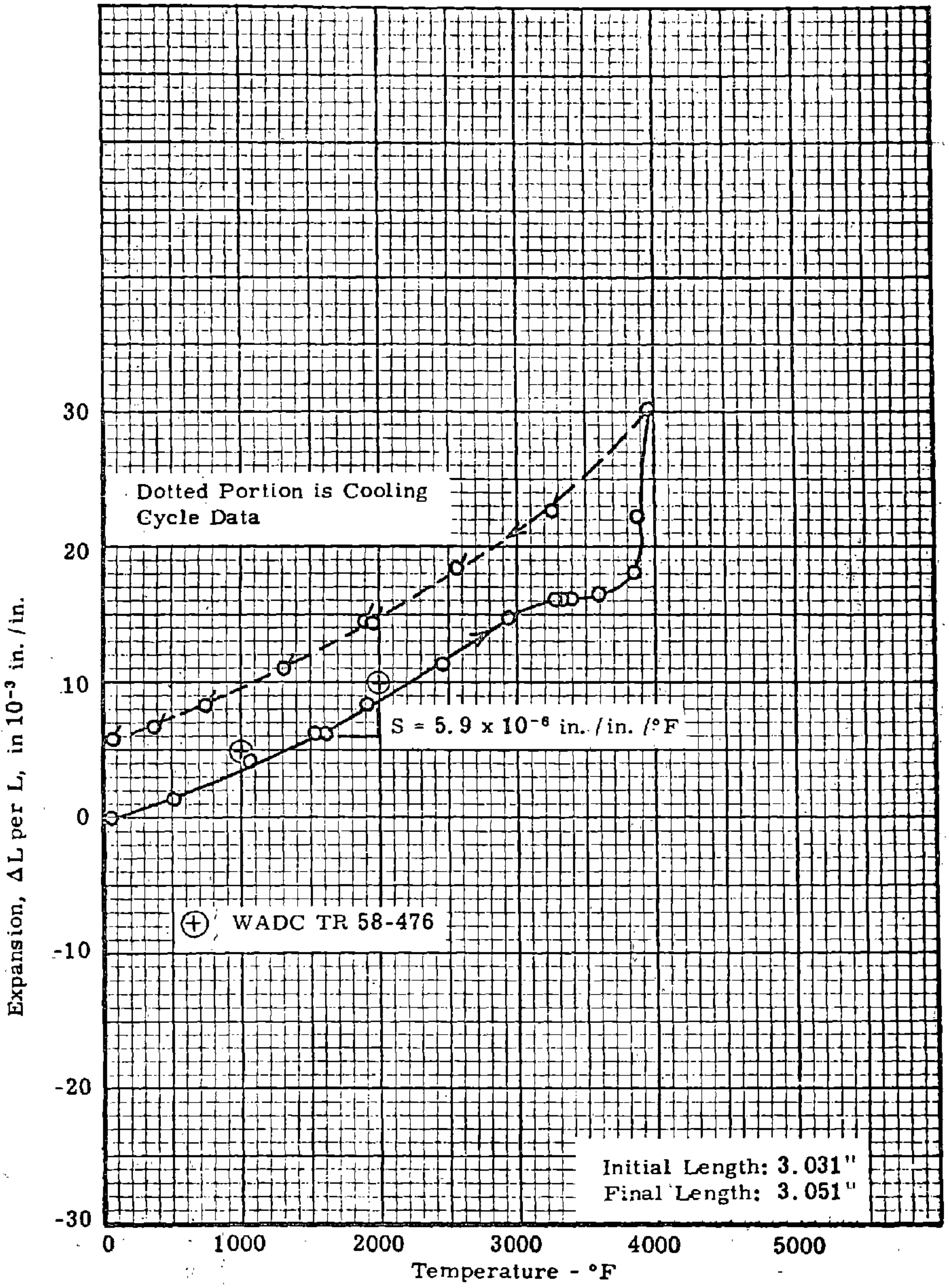

Figure 54. Thermal Expansion of Beryllium Oxide.

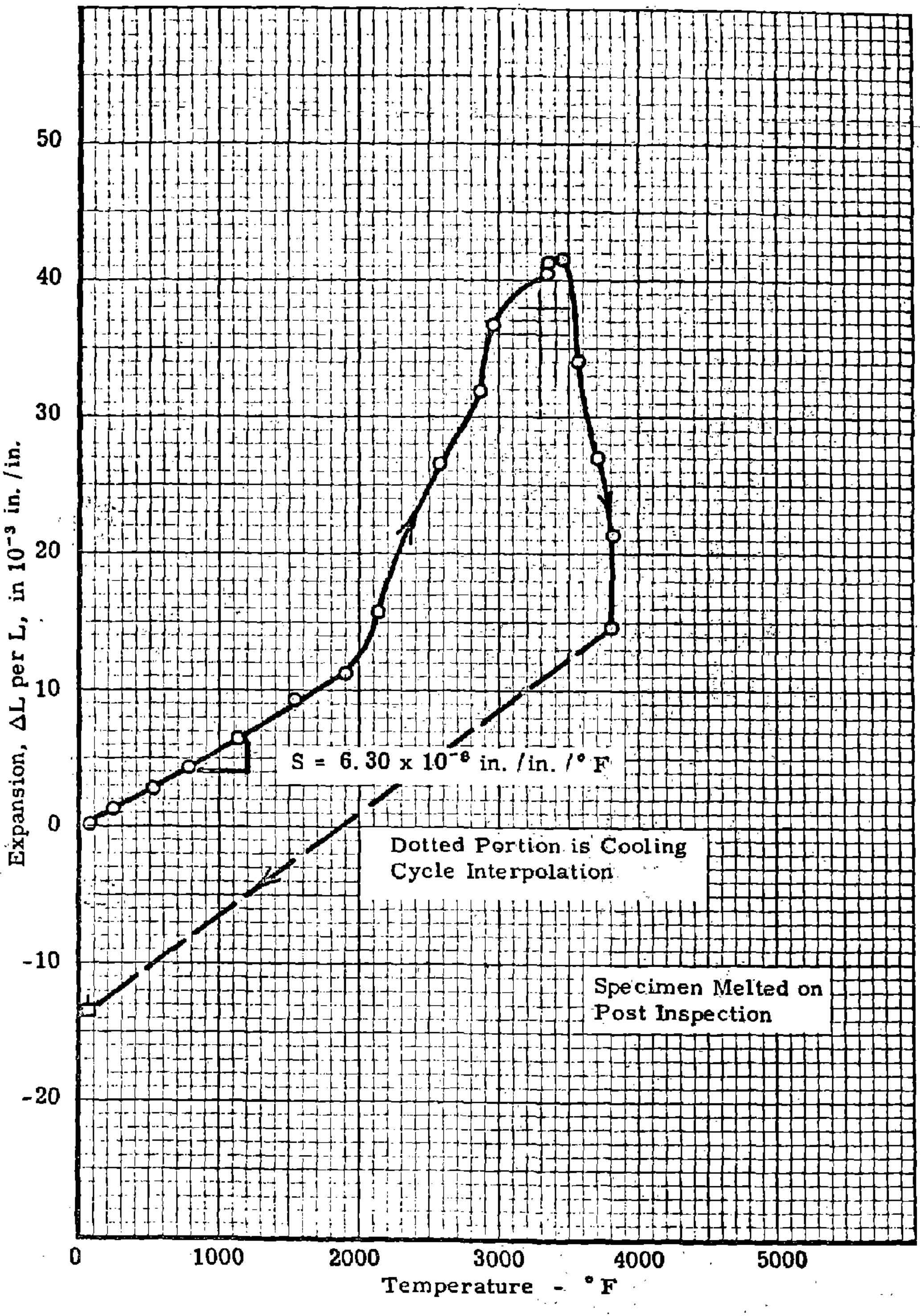

Figure 55. Thermal Expansion of Cerium Dioxide

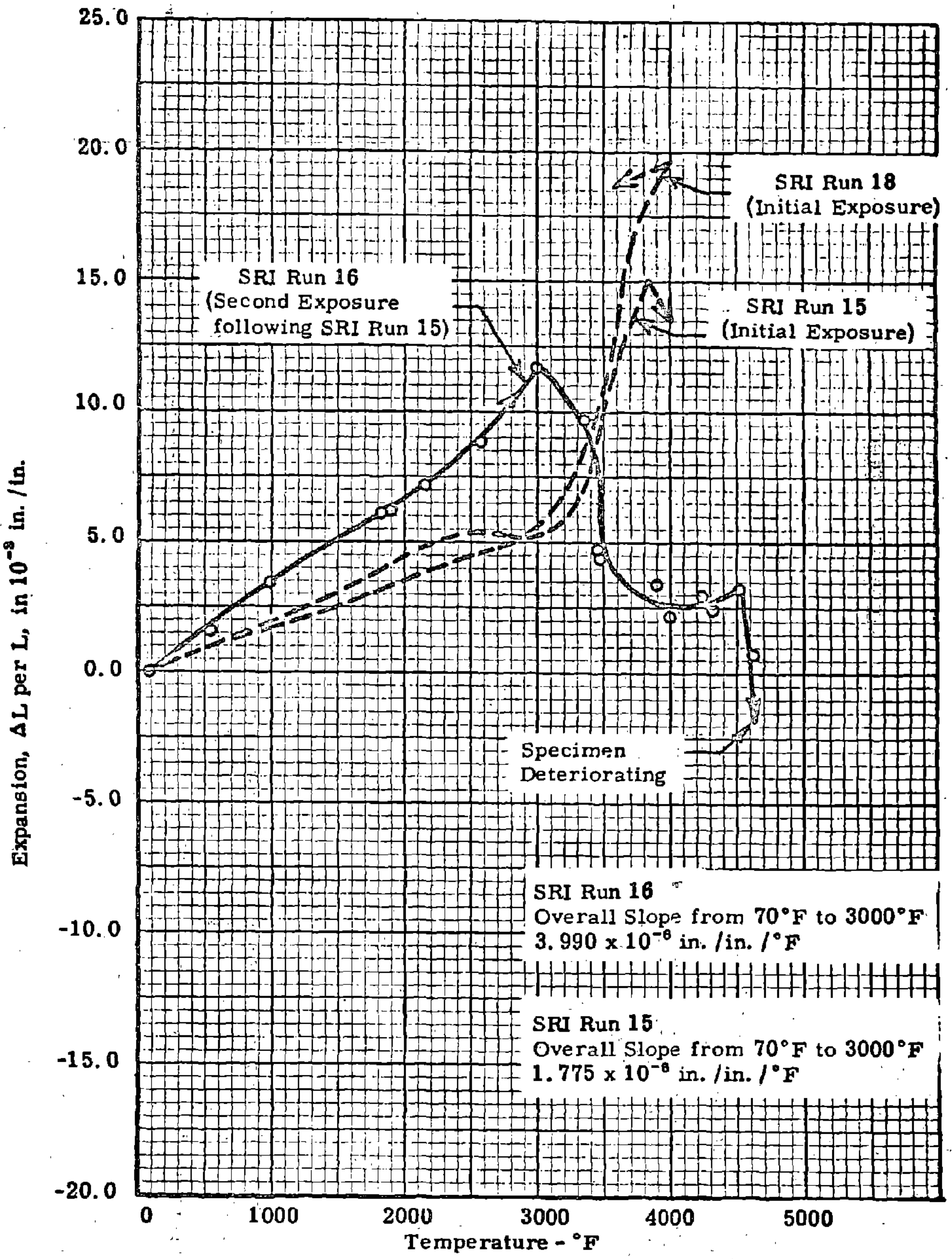

Figure 56. Thermal Expansion of Hafnium Dioxide

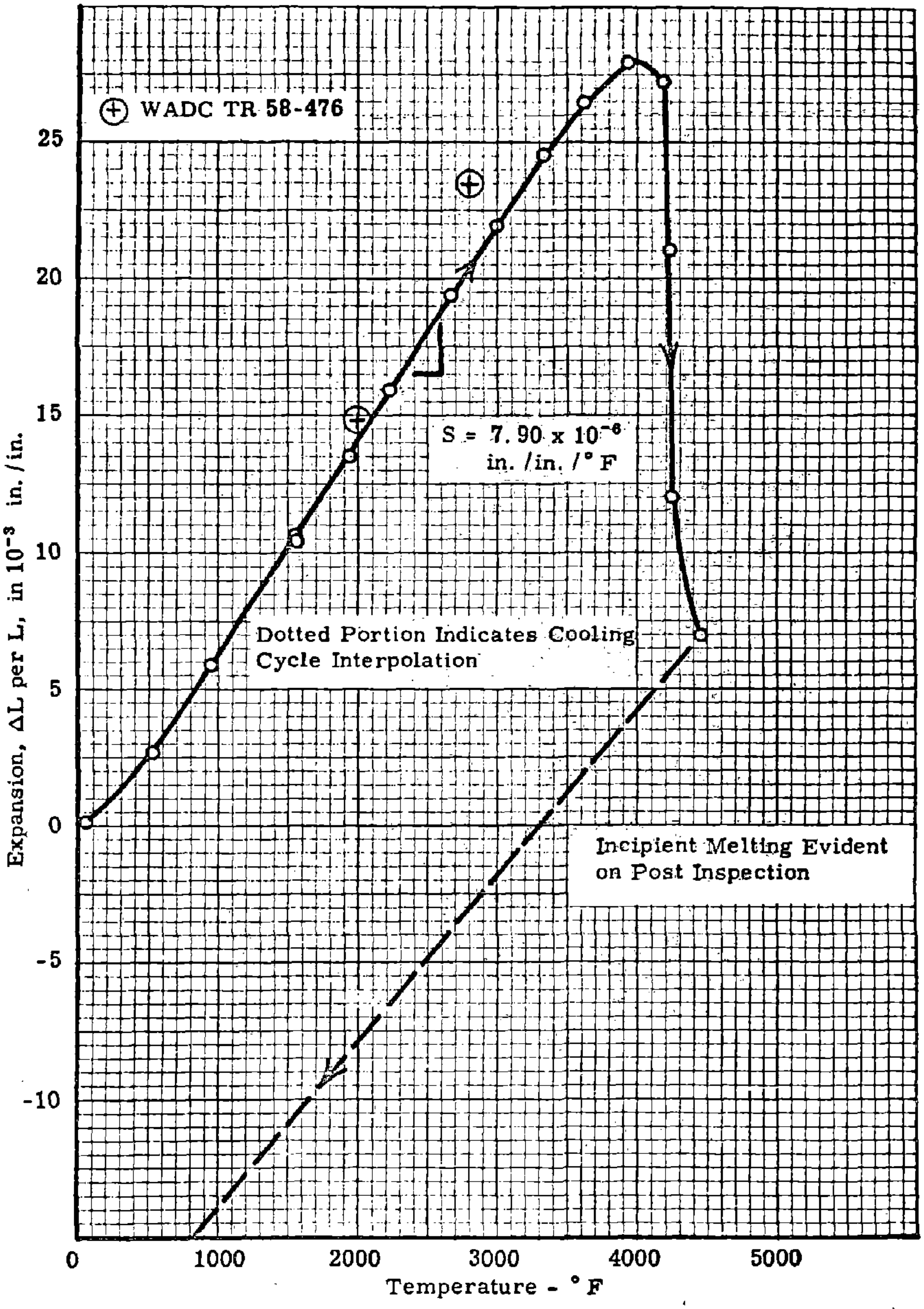

Figure 57. Thermal Expansion of Magnesium Oxide.

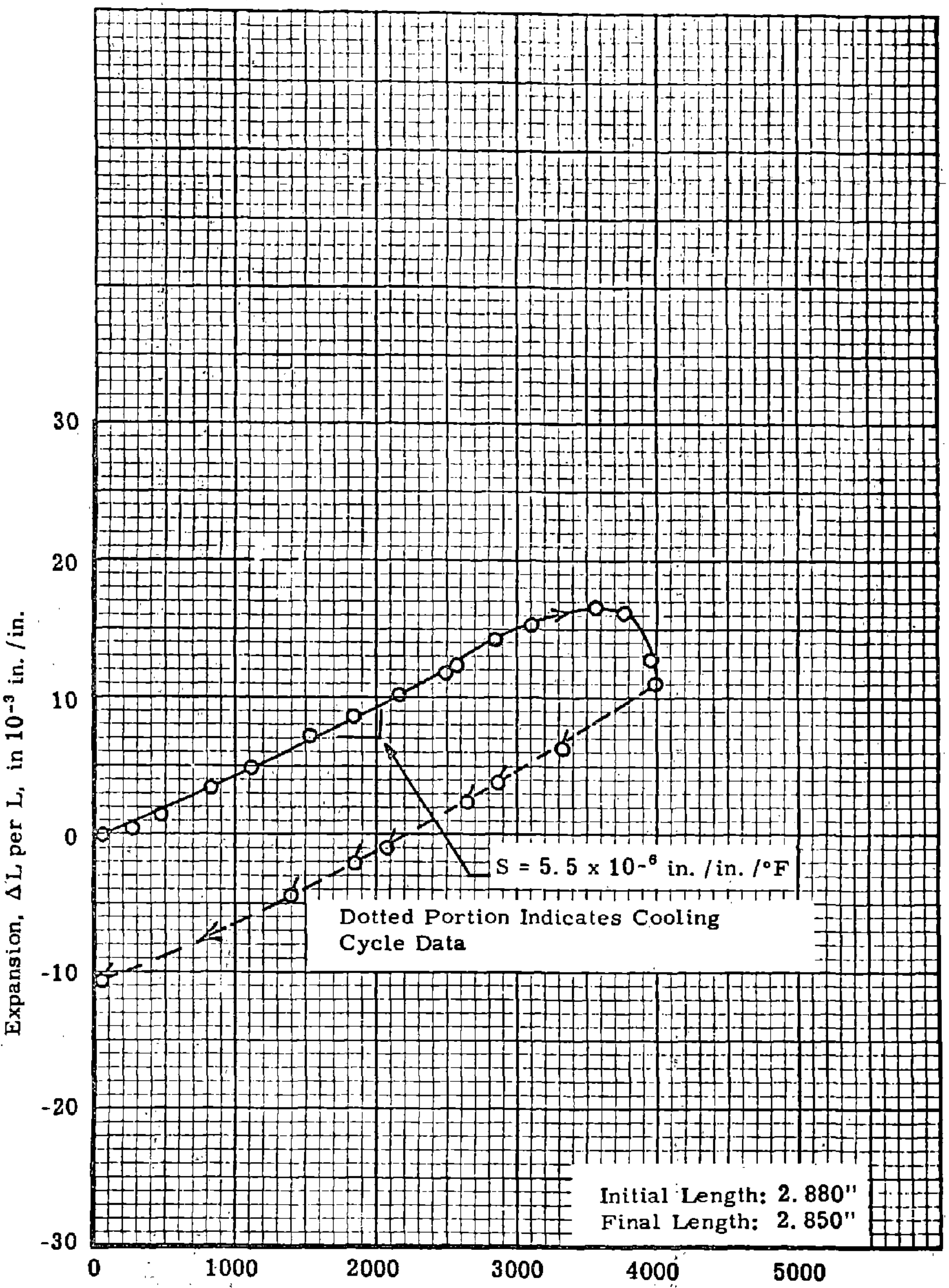

Figure 58. Thermal Expansion of Thorium Dioxide.

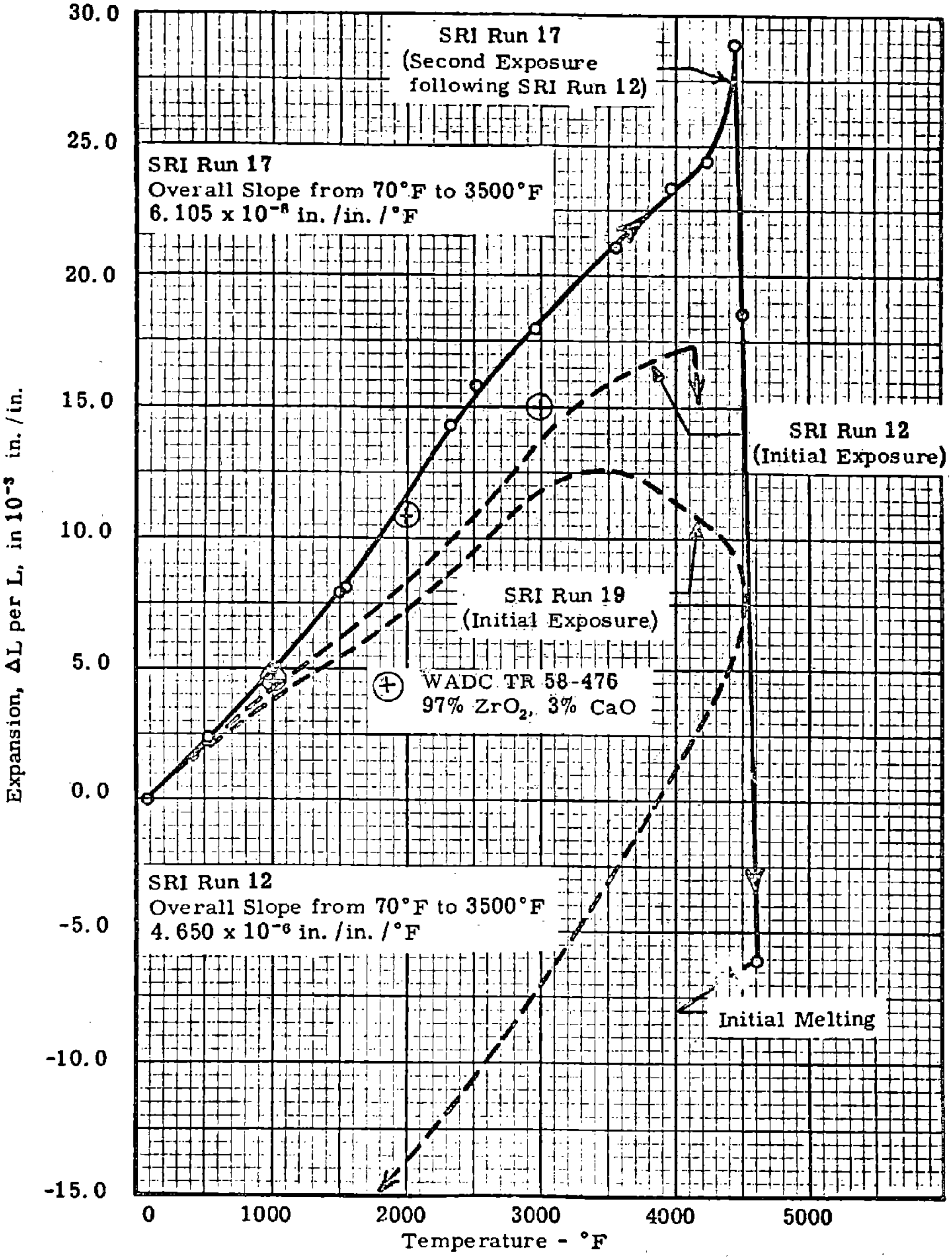

Figure 59. Thermal Expansion of Zirconium Dioxide

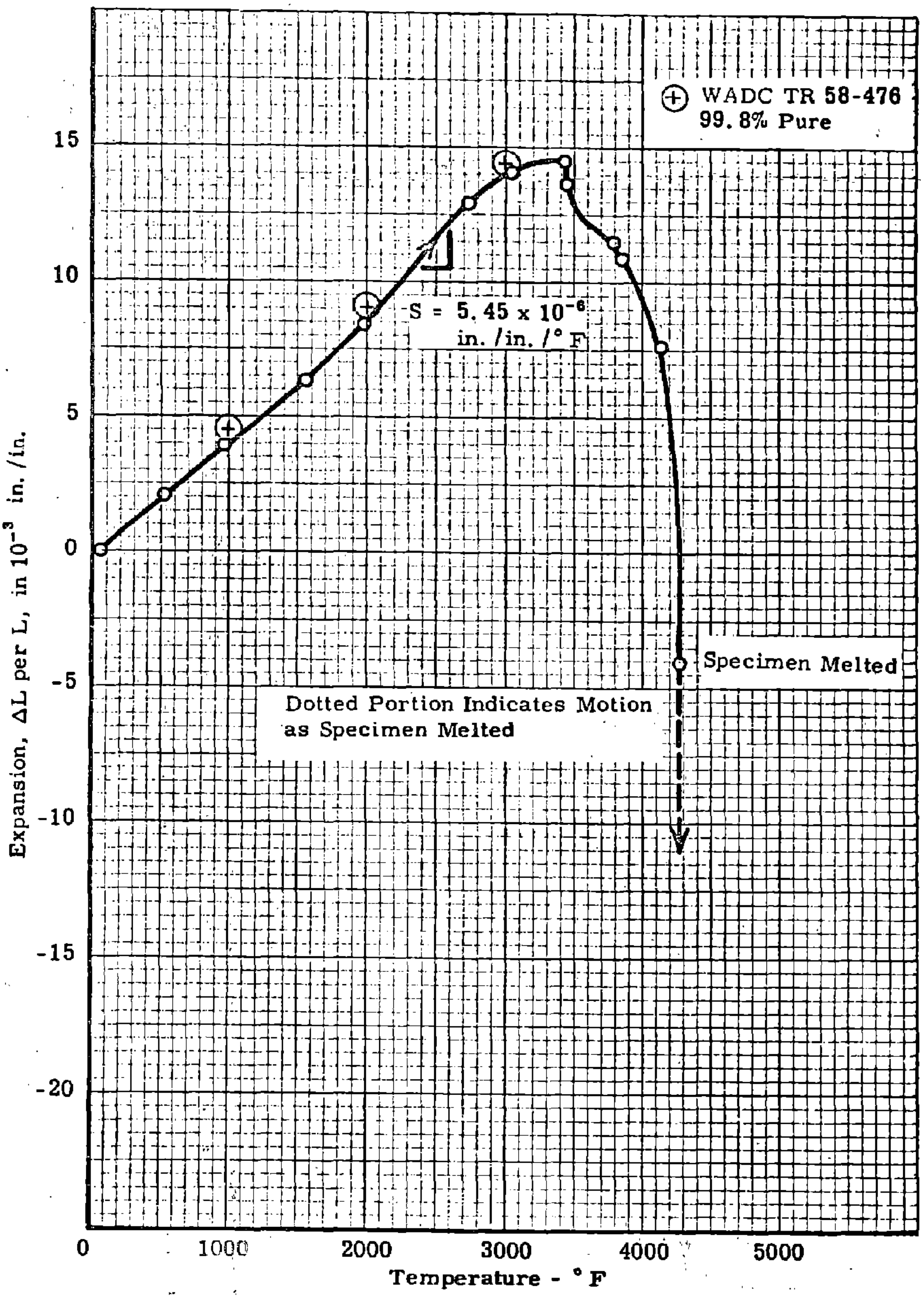

Figure 60. Thermal Expansion of Columbium +0.5% Zirconium.

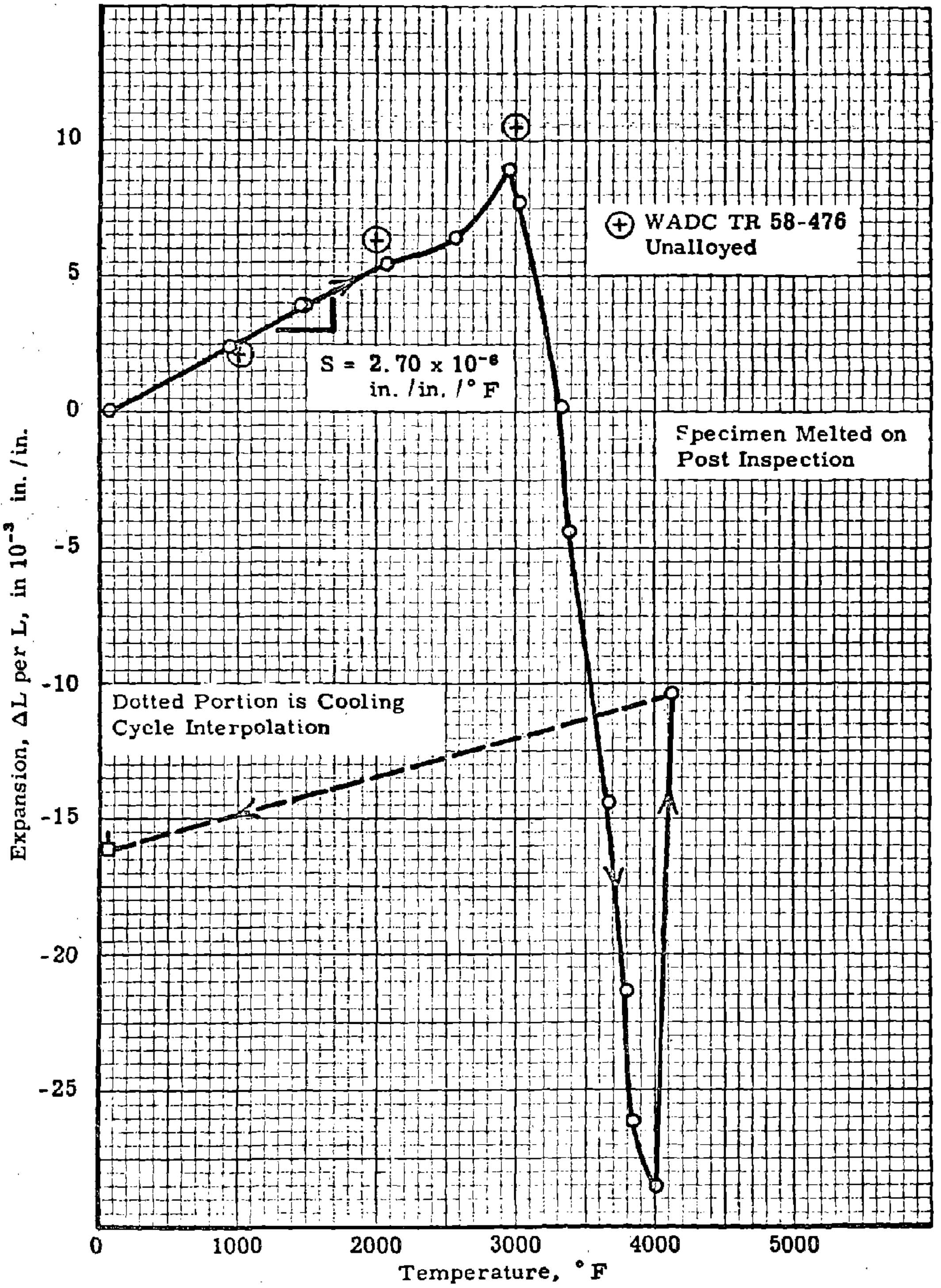

Figure 61. Thermal Expansion of Molybdenum + 0.5% Titanium.

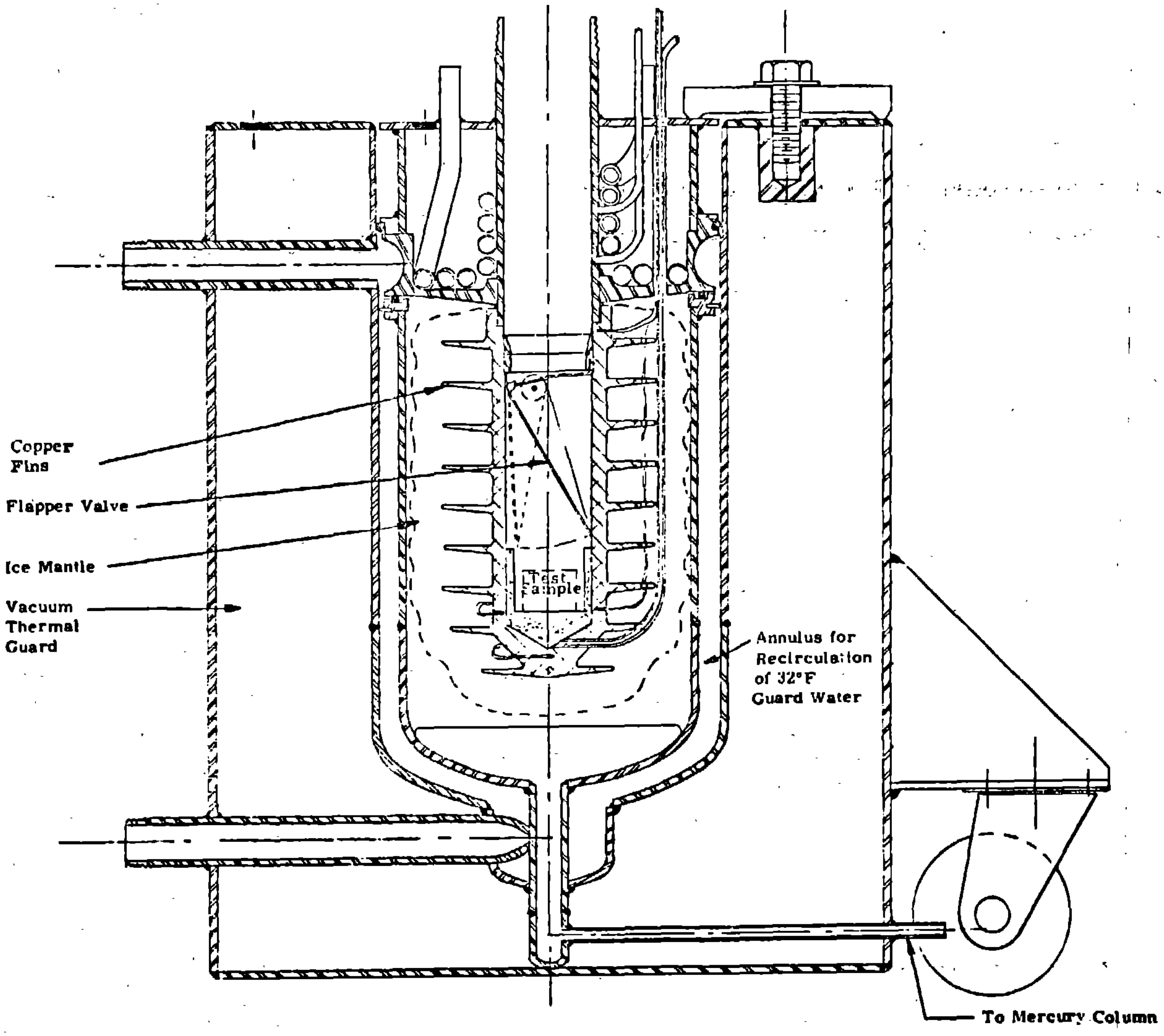

Figure 62. Ice Calorimeter, drop type - Specimen to 5000°F

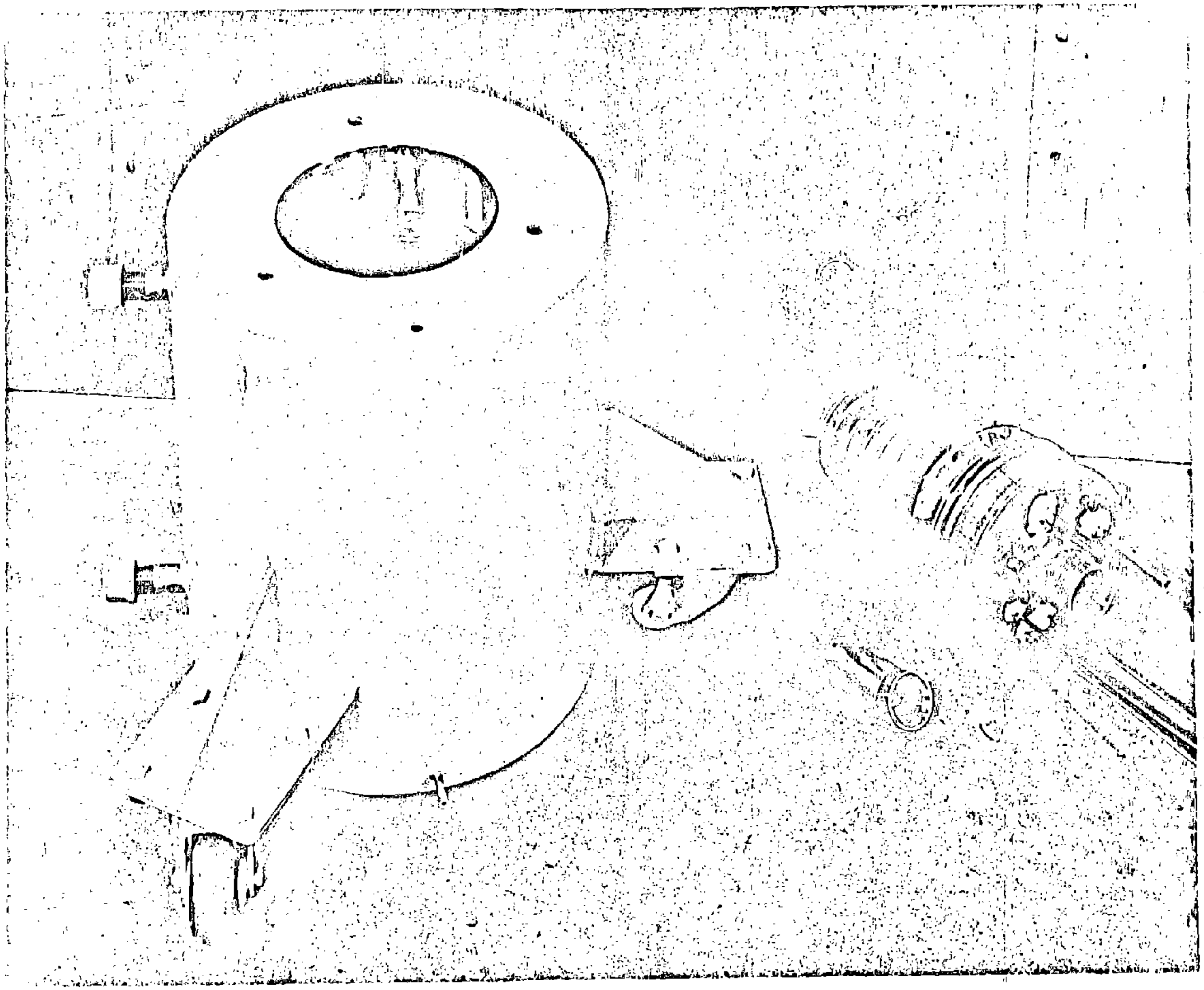

Figure 63. Picture of Ice Calorimeter Jacket and Drop Valve.

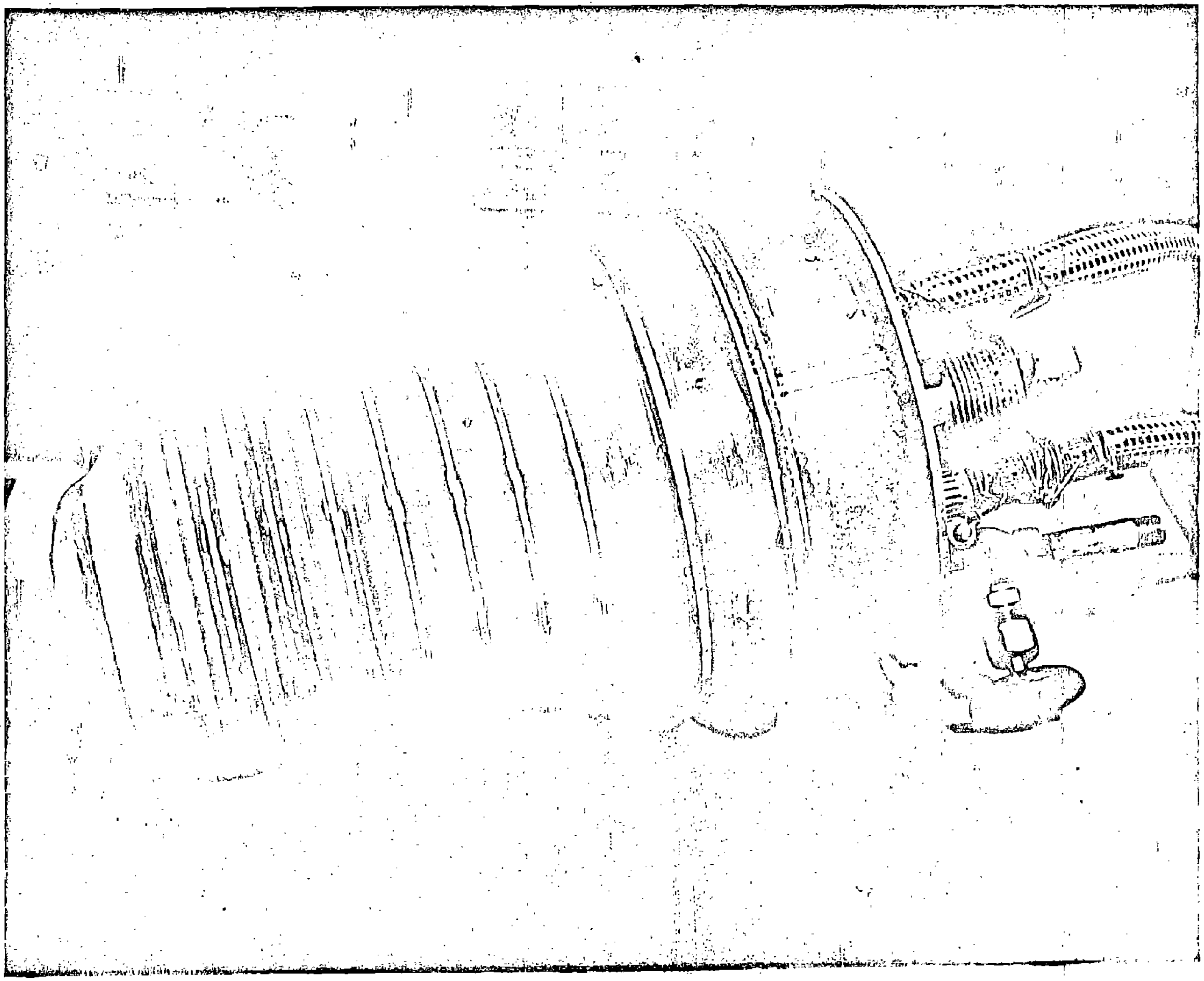

Figure 64. Picture of Ice Mantle.

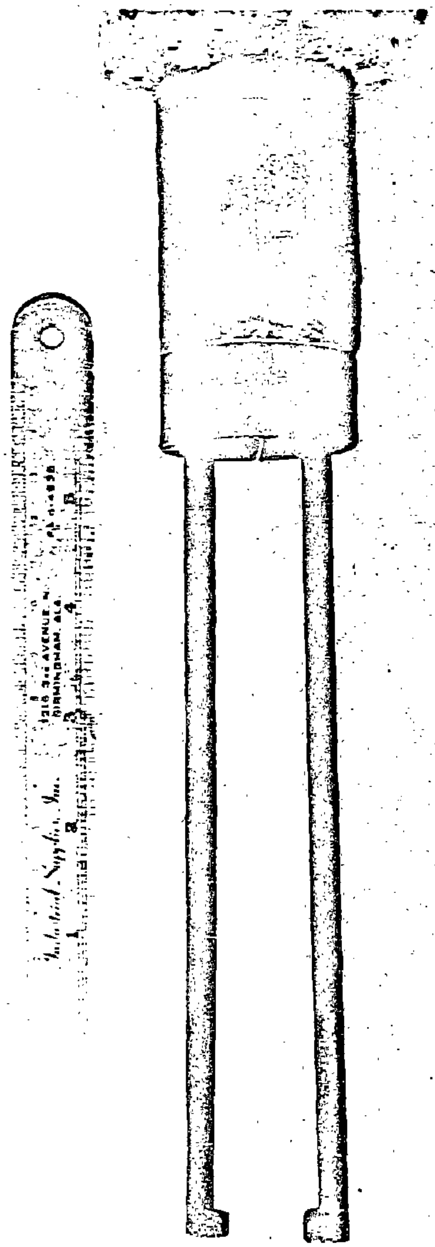

Figure 65. Specimen Holder and Drop Rig for Insertion into Top of Furnaces.

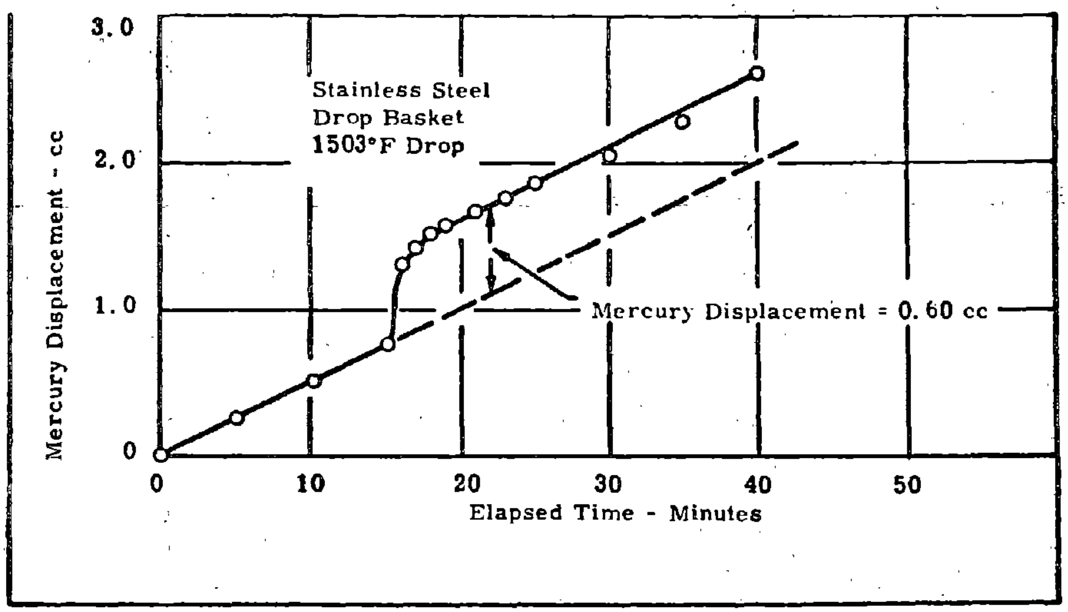

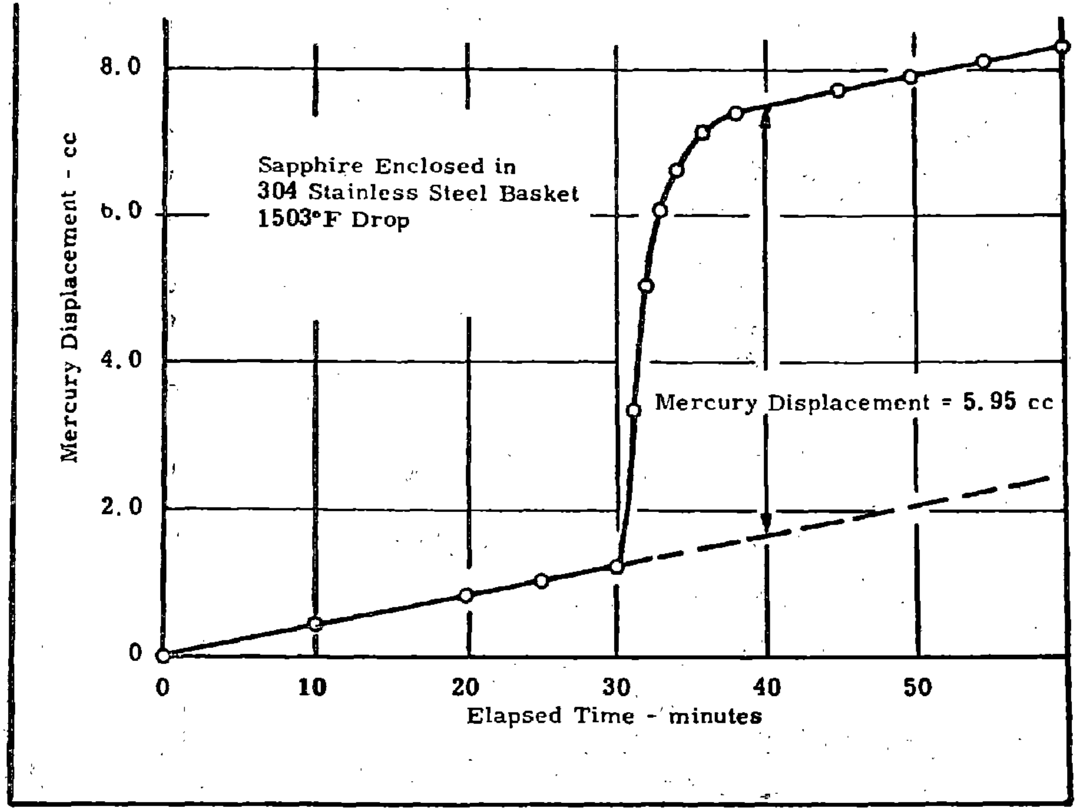

Figure 66. Mercury Displacement Due to Sapphire and 304 Stainless Steel Basket.

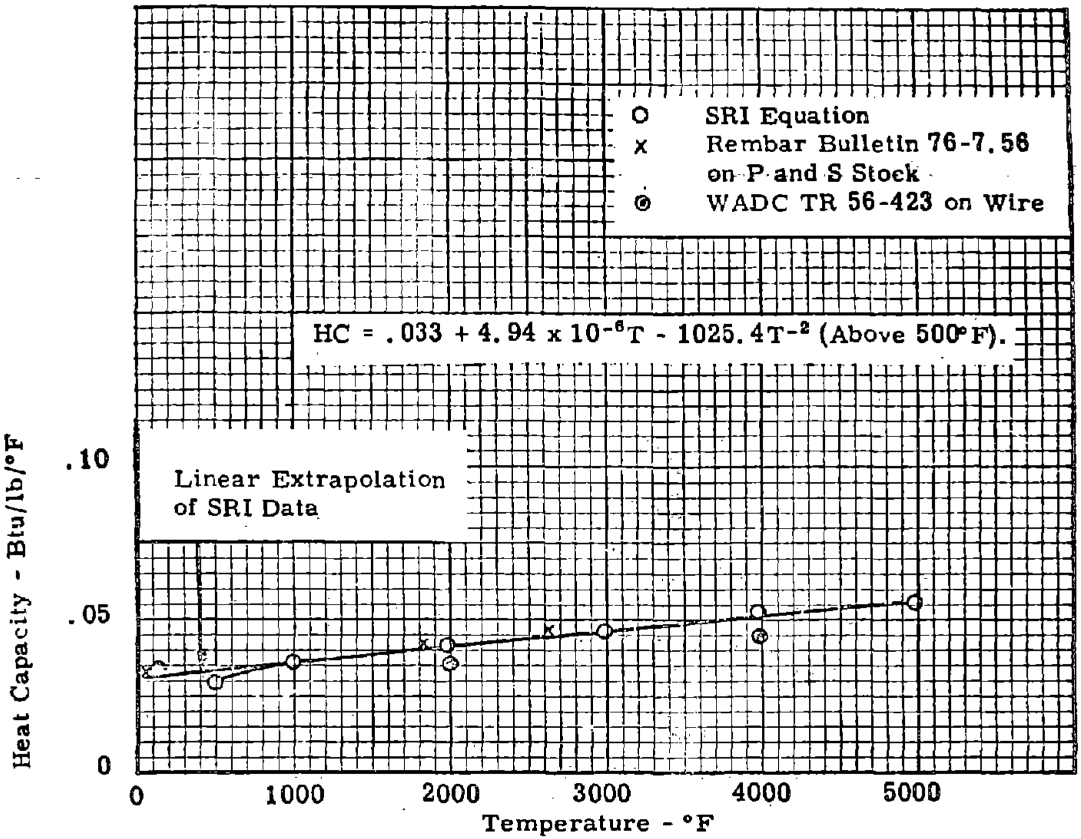

Heat Capacity of Tungsten from WADD TR 60-924.

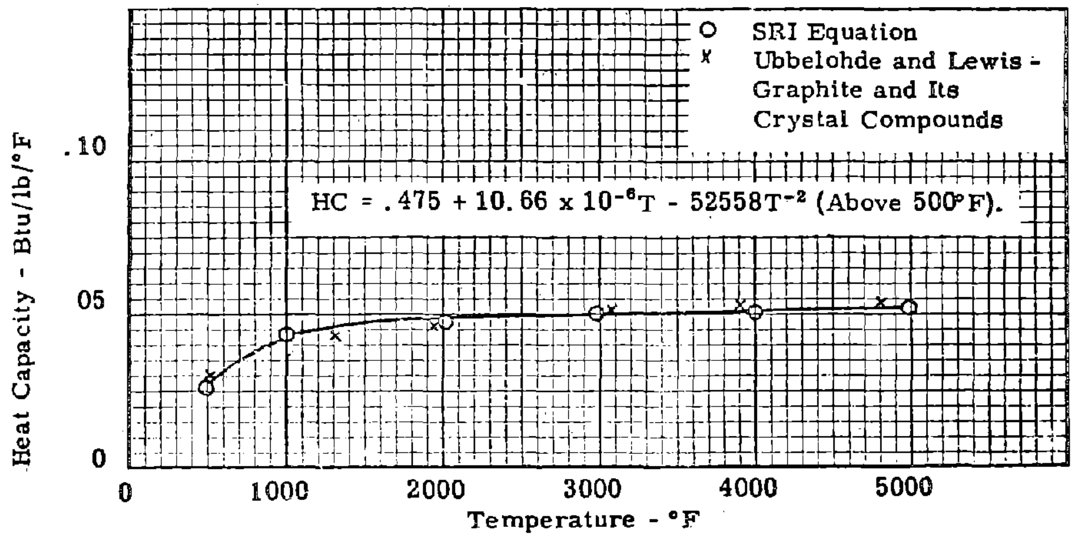

Heat Capacity of ATJ Graphite from WADD TR 60-924.

Figure 67. Heat Capacity of ATJ Graphite and Tungsten from WADD TR 60-924 by New Equations with Some Reference Values.

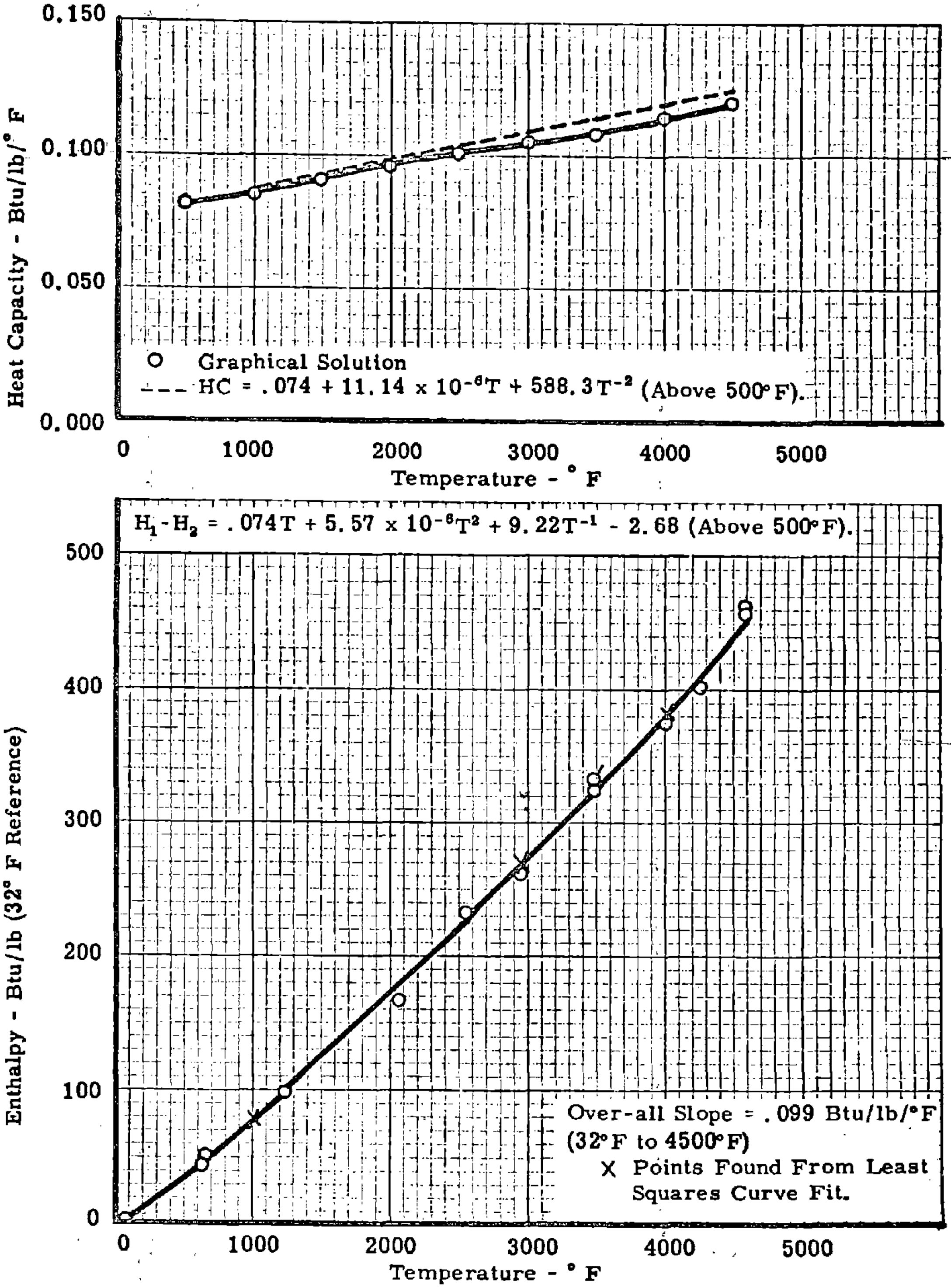

Figure 68. Enthalpy and Heat Capacity of Hafnium Diboride.

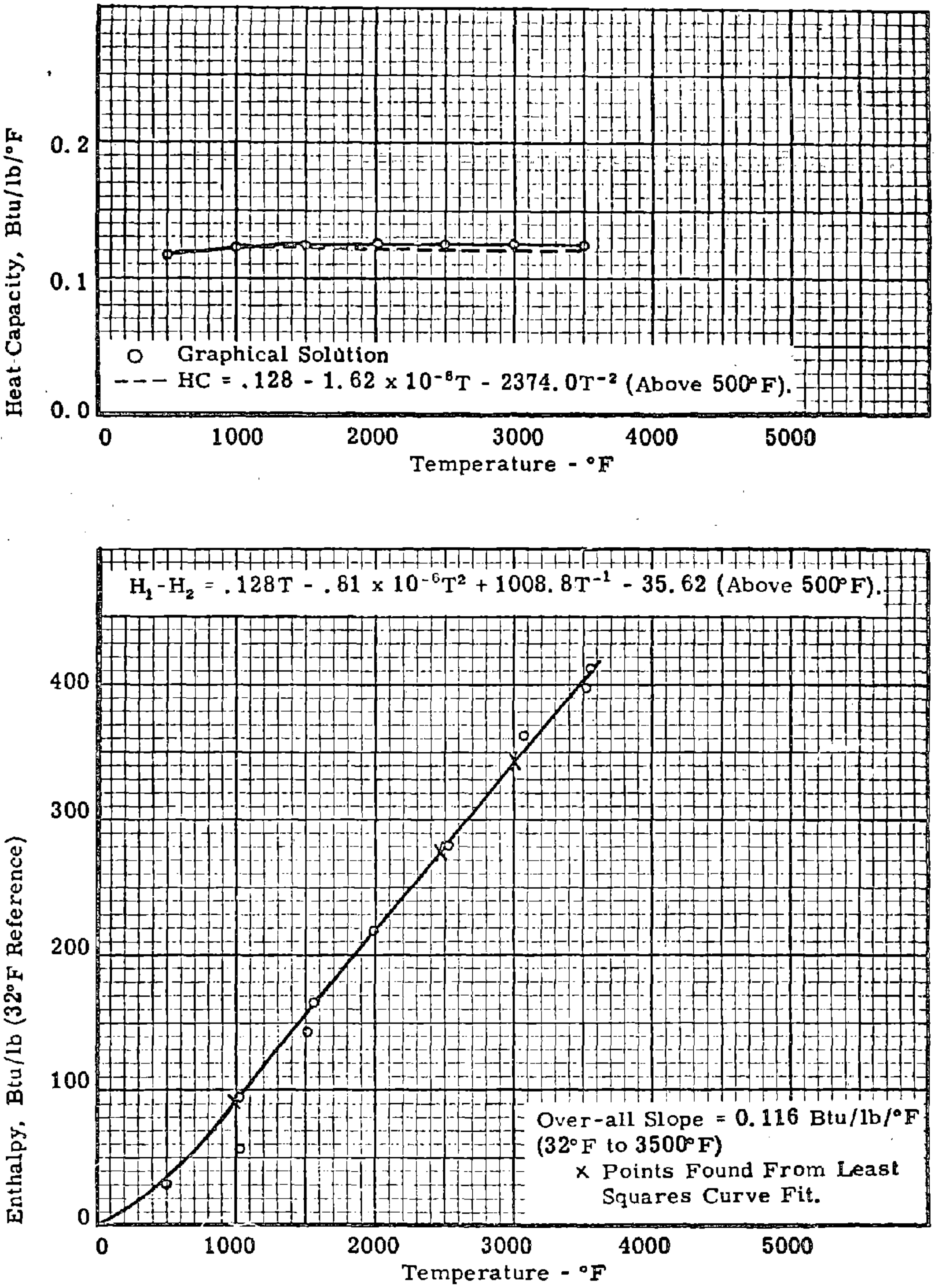

Figure 69. Enthalpy and Heat Capacity of Thorium Tetraboride.

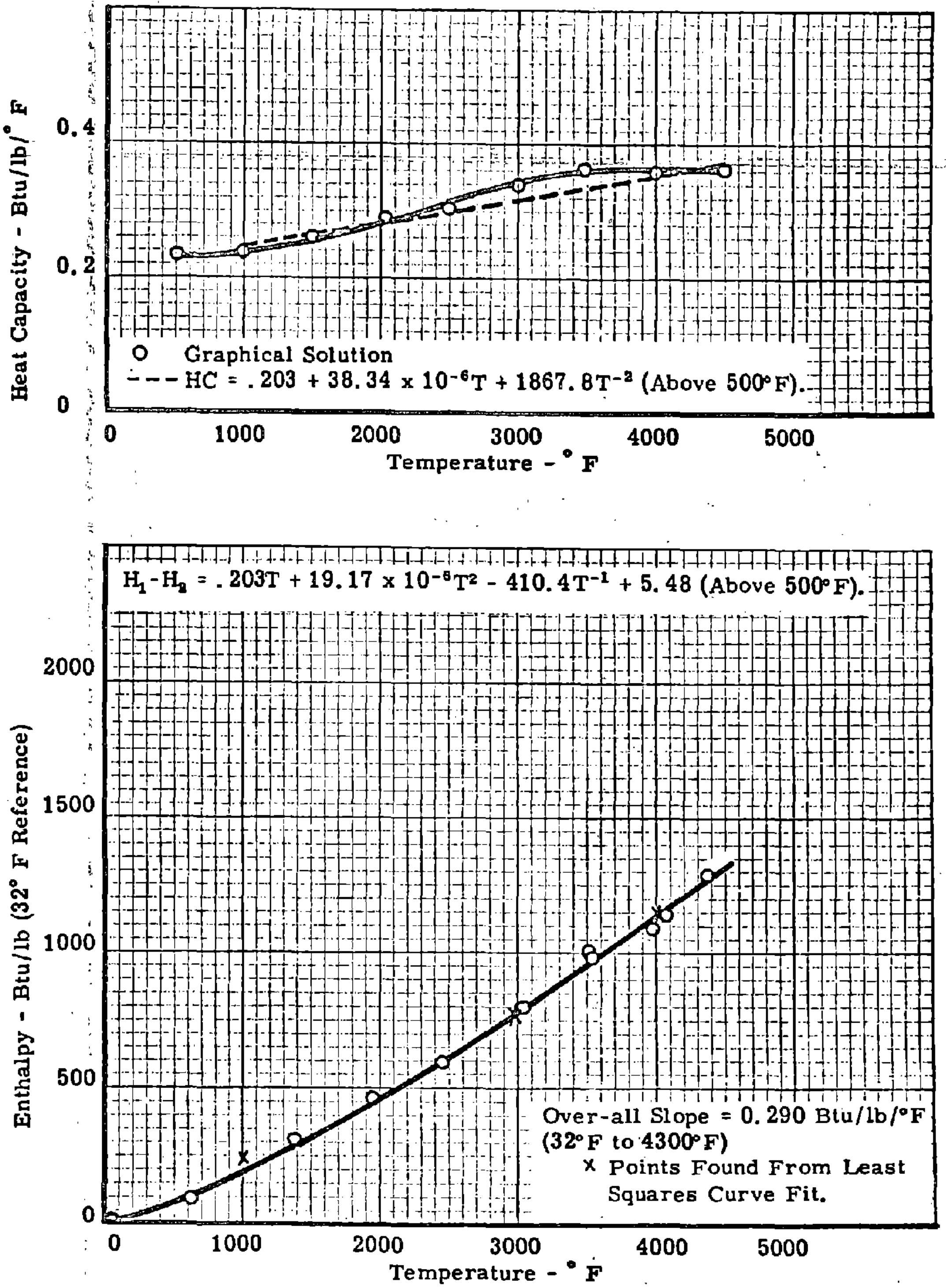

Figure 70. Enthalpy and Heat Capacity of Titanium Diboride.

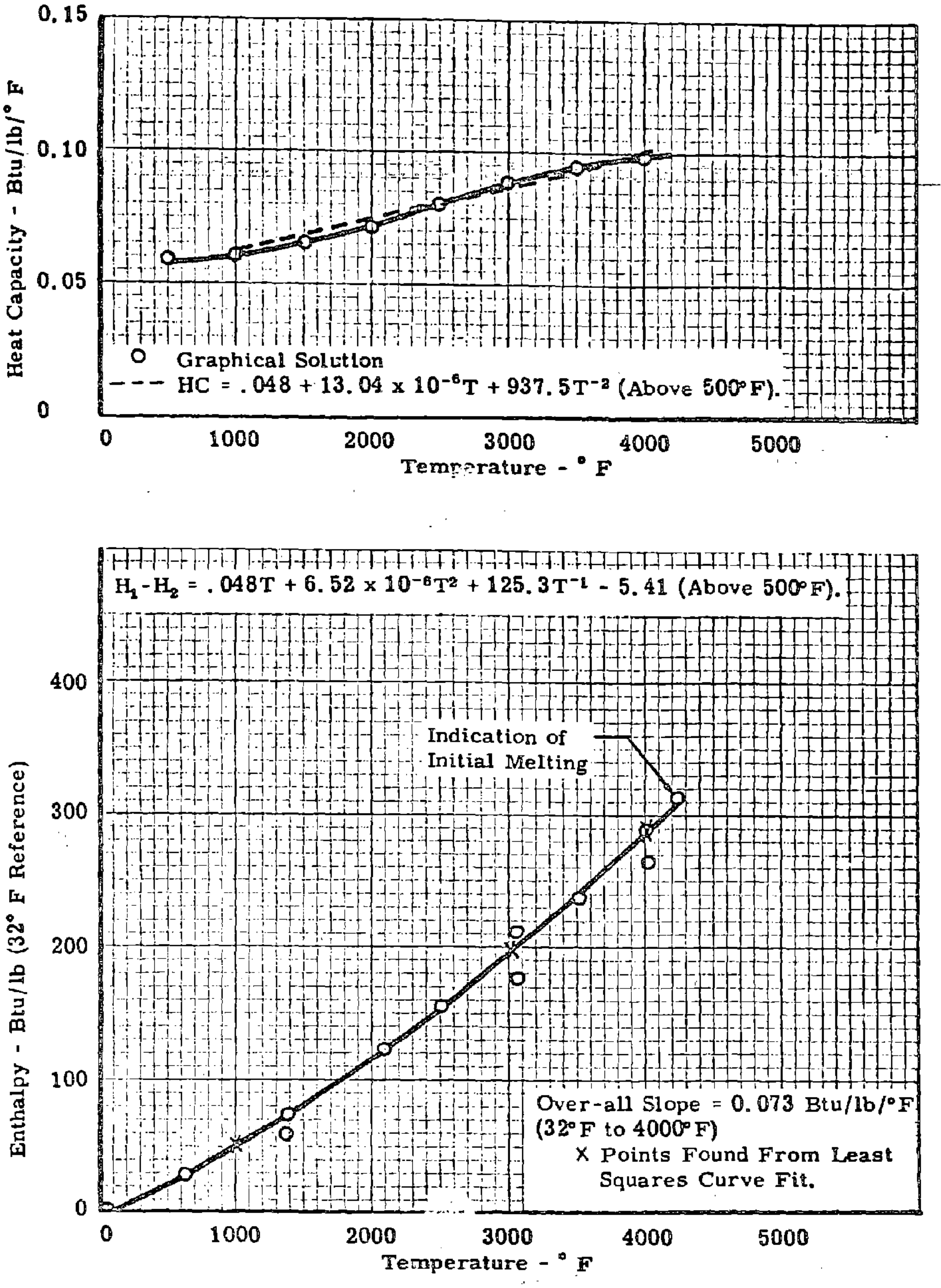

Figure 71. Enthalpy and Heat Capacity of Tungsten Boride.

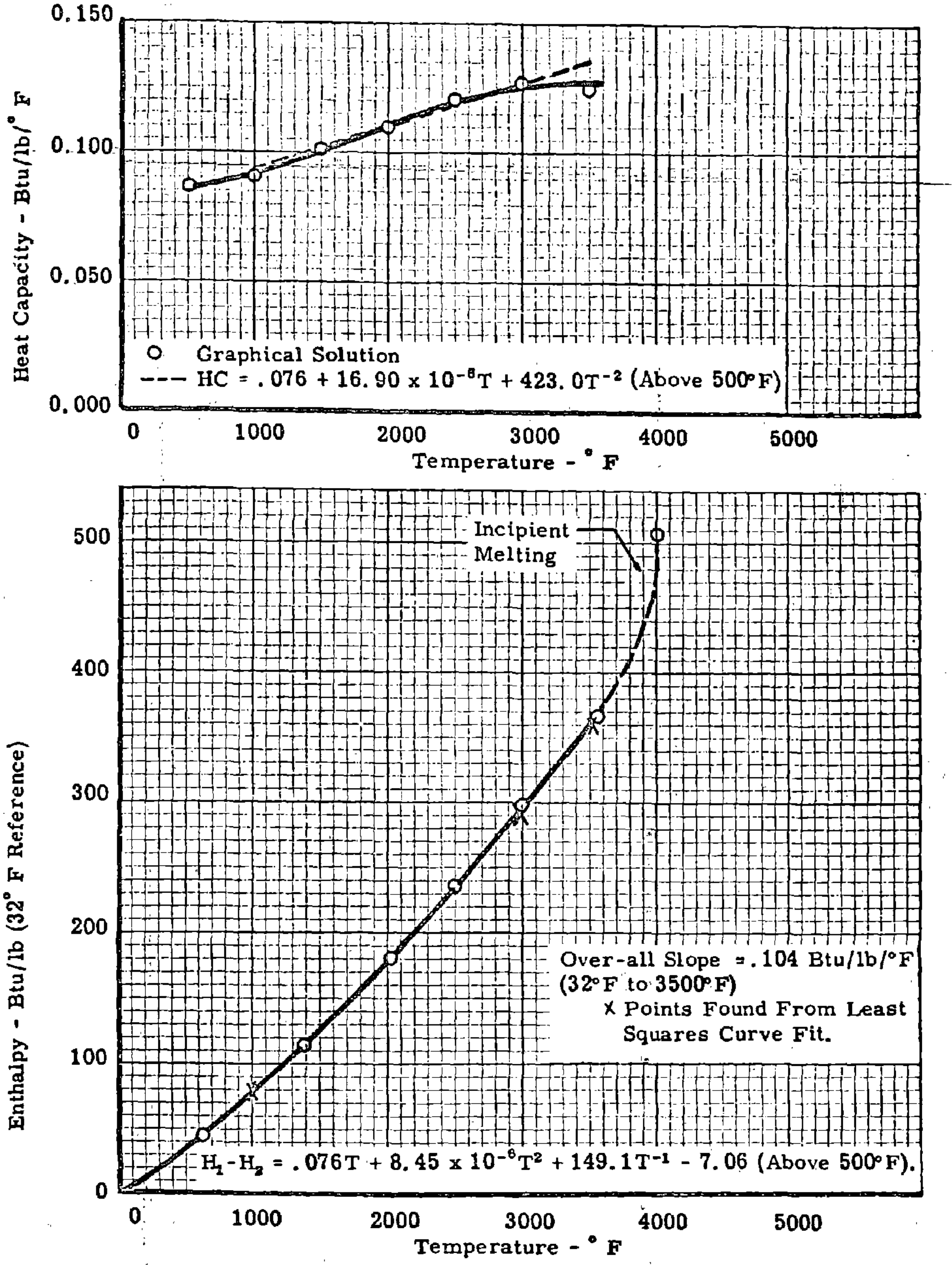

Figure 72. Enthalpy and Heat Capacity of Dimolybdenum Carbide.

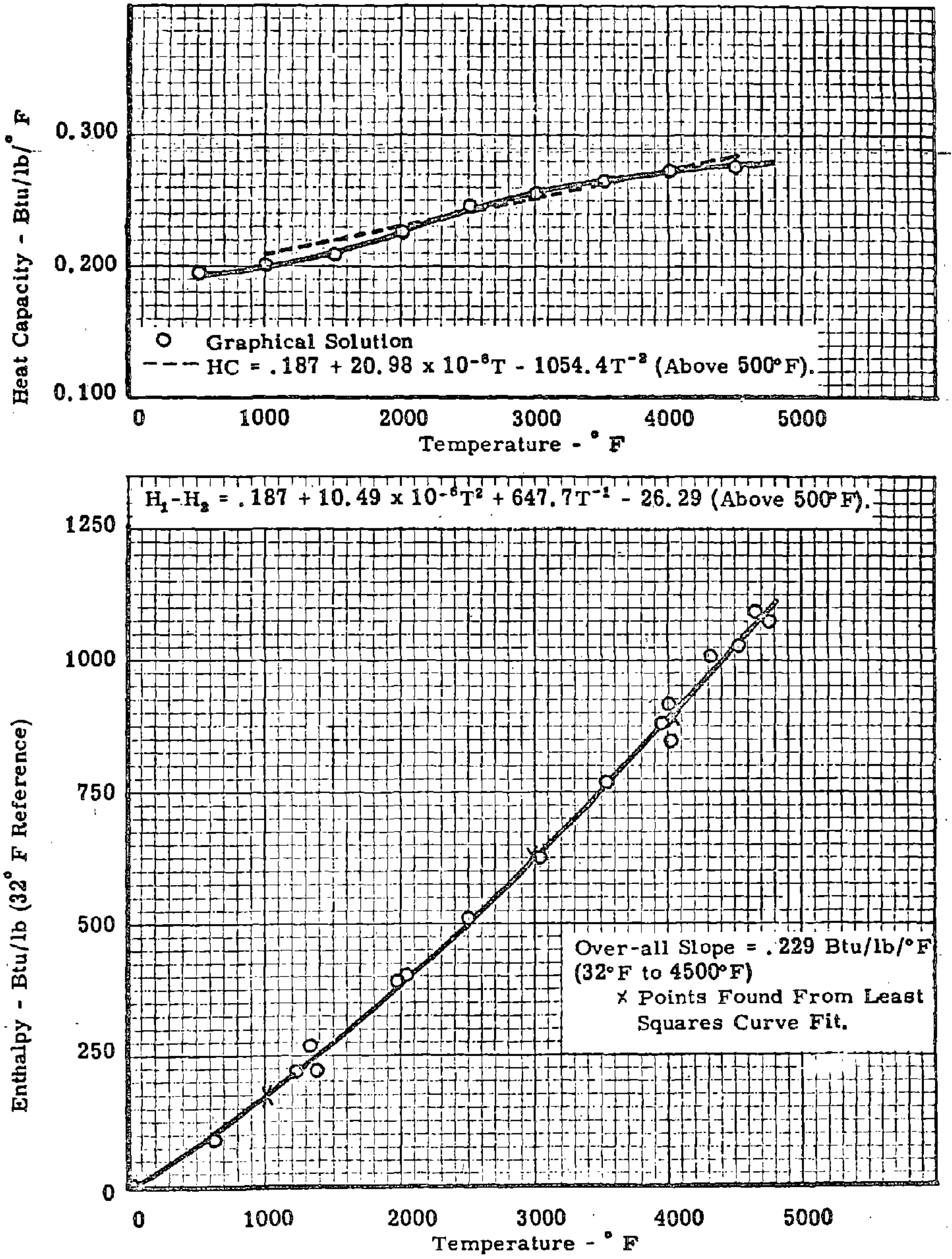

Figure 73. Enthalpy and Heat Capacity of Titanium Carbide.

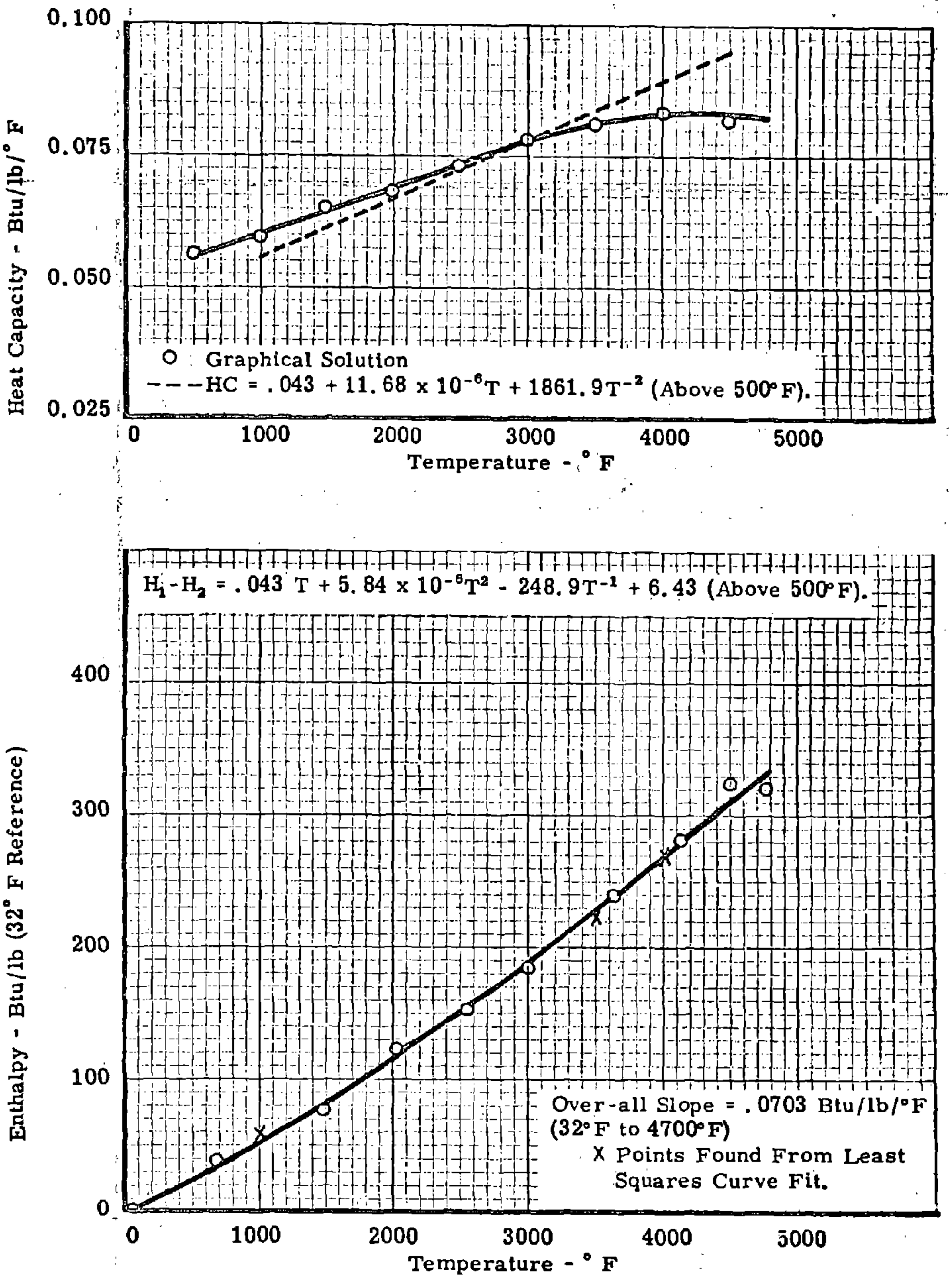

Figure 74. Enthalpy and Heat Capacity of Tungsten Carbide.

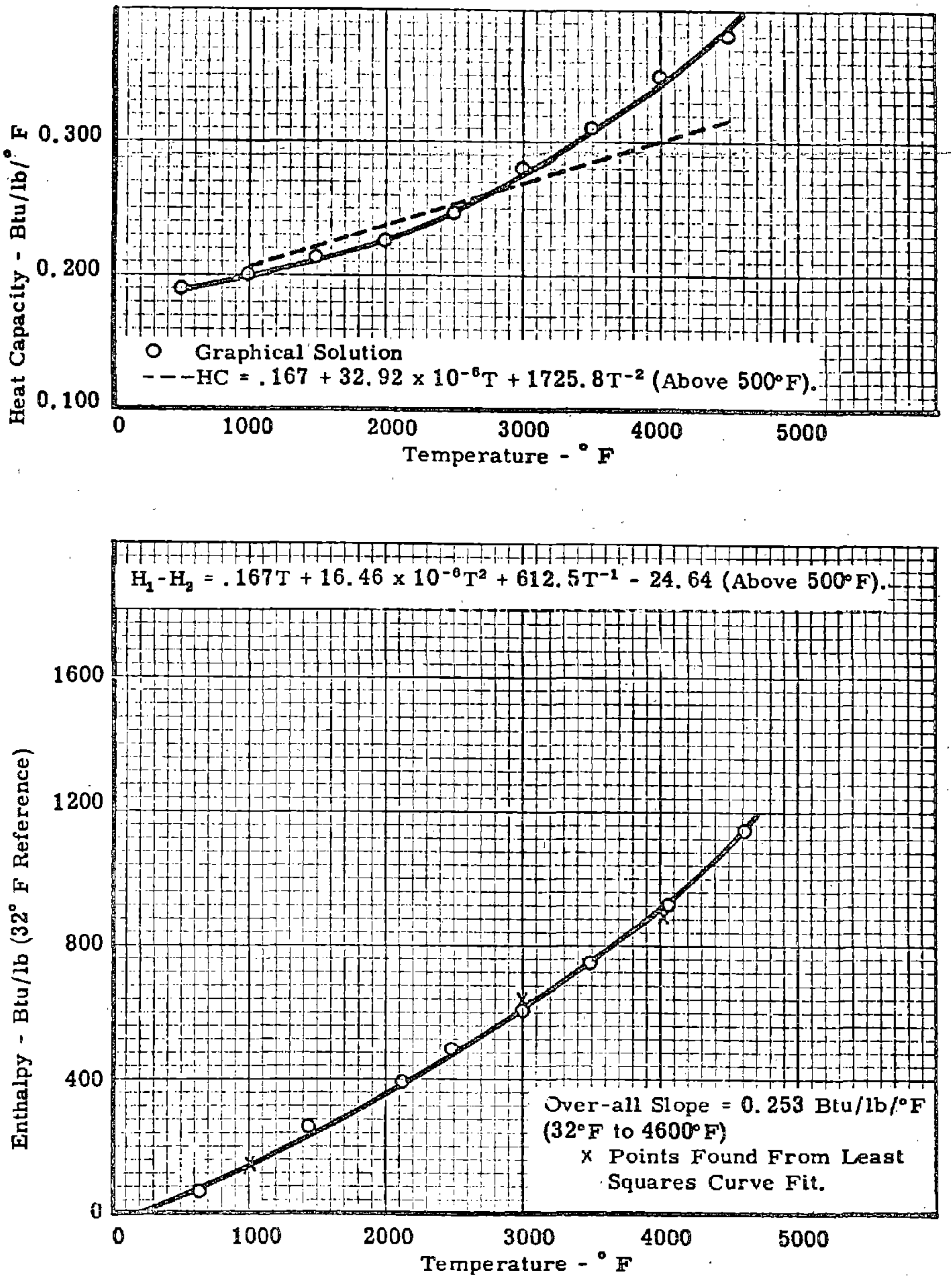

Figure 75. Enthalpy and Heat Capacity of Vanadium Carbide.

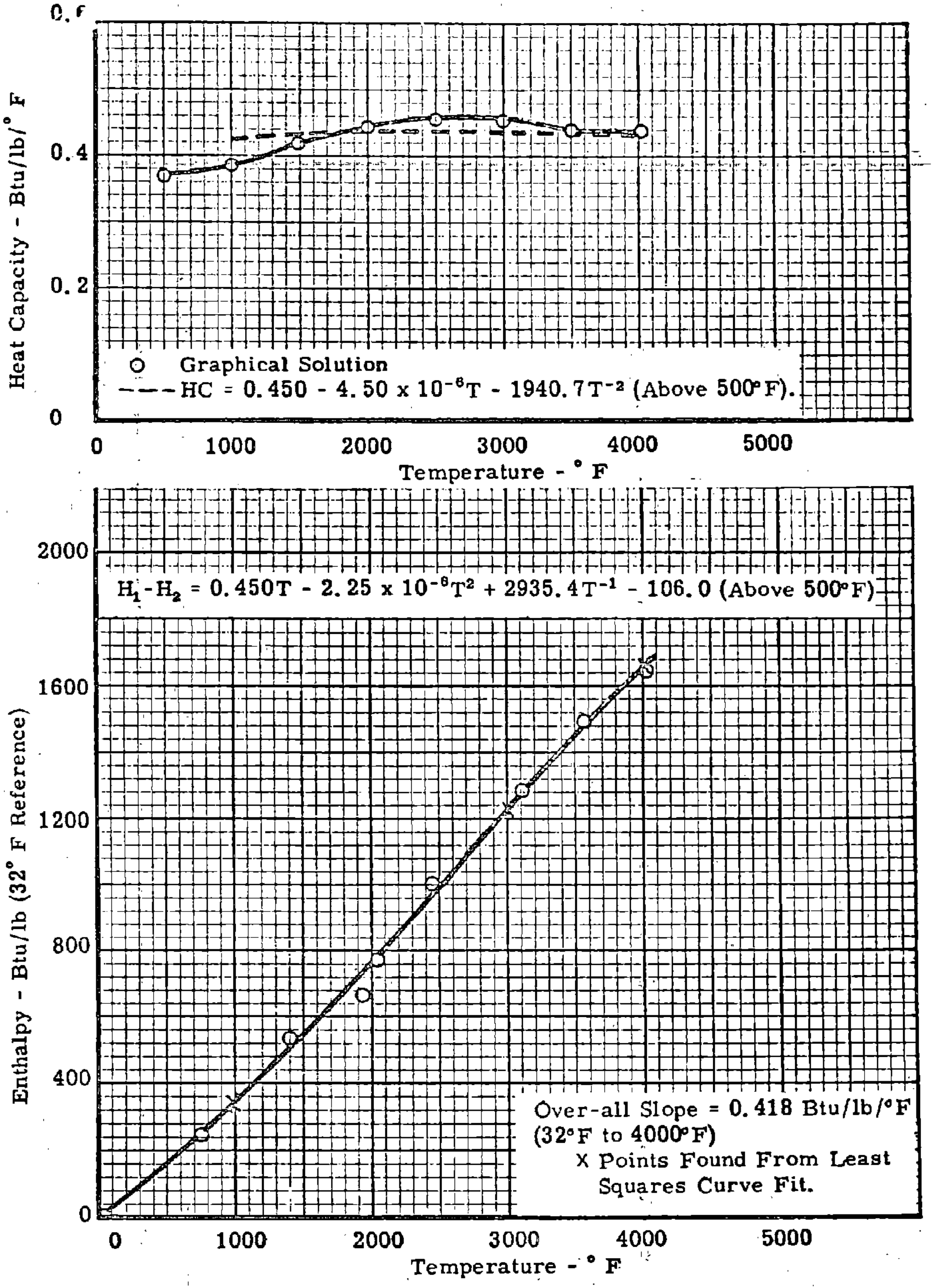

Figure 76. Enthalpy and Heat Capacity of Boron Nitride.

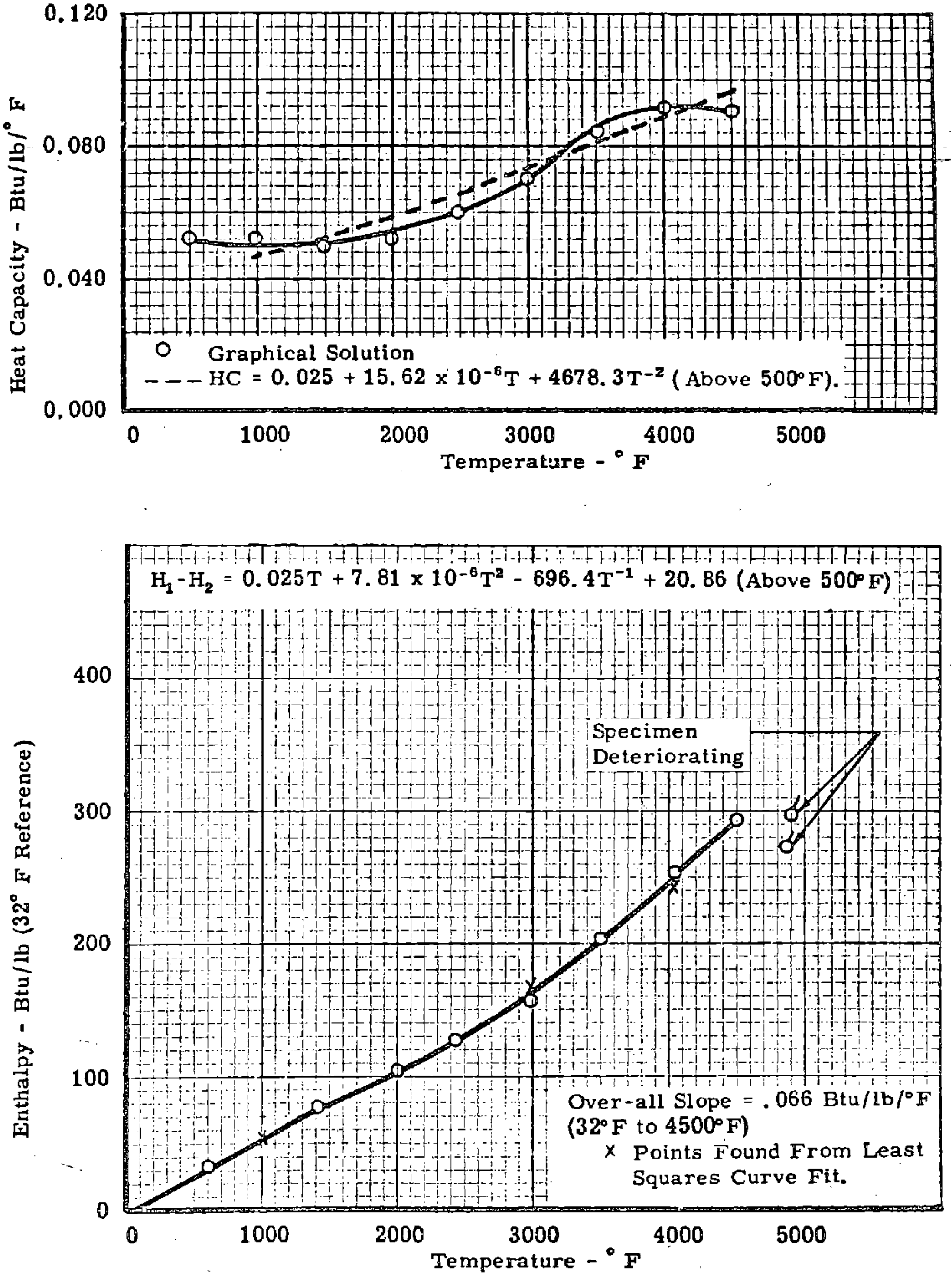

Figure 77. Enthalpy and Heat Capacity of Tantalum Nitride.

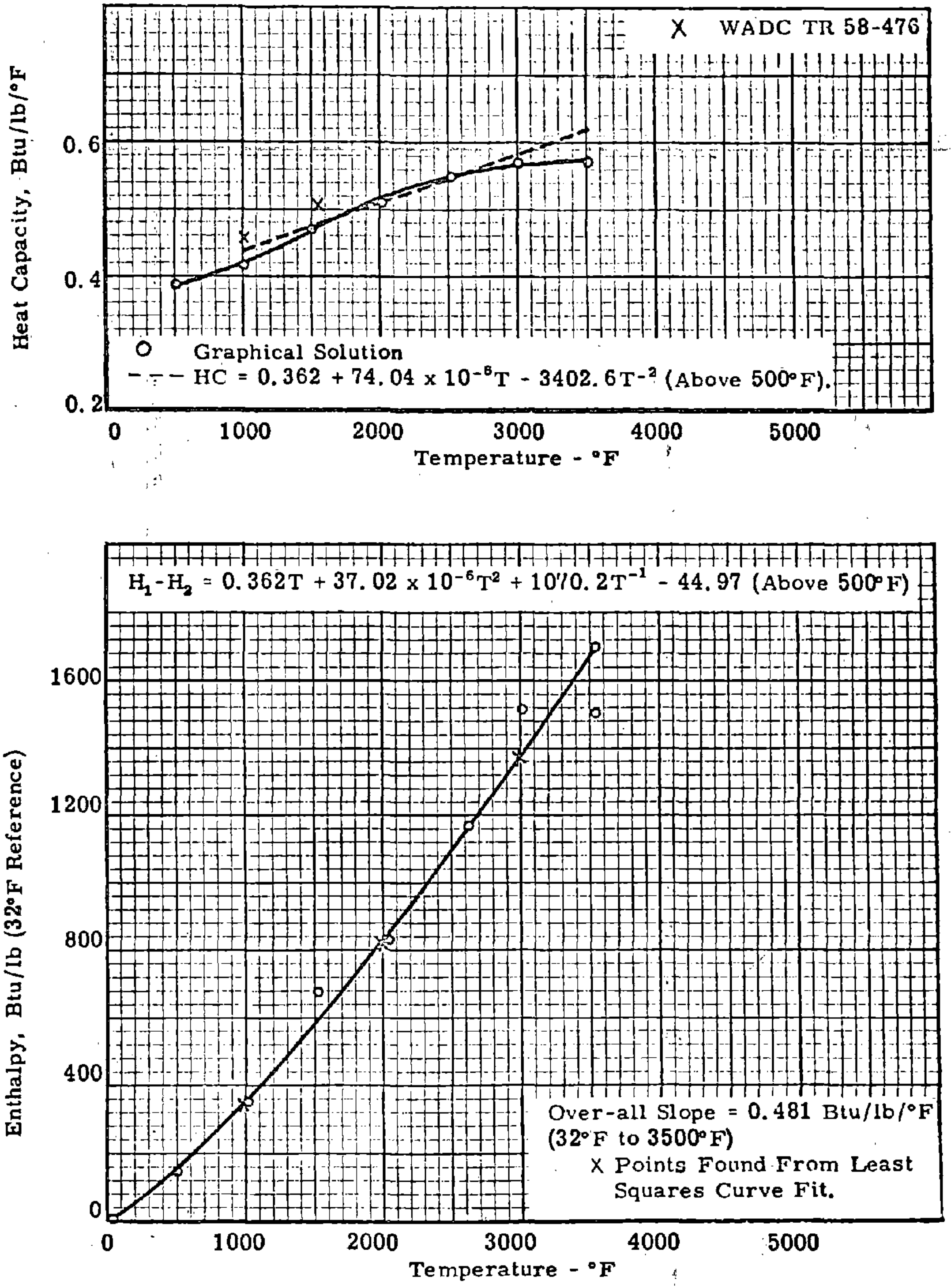

Figure 78. Enthalpy and Heat Capacity of Beryllium Oxide.

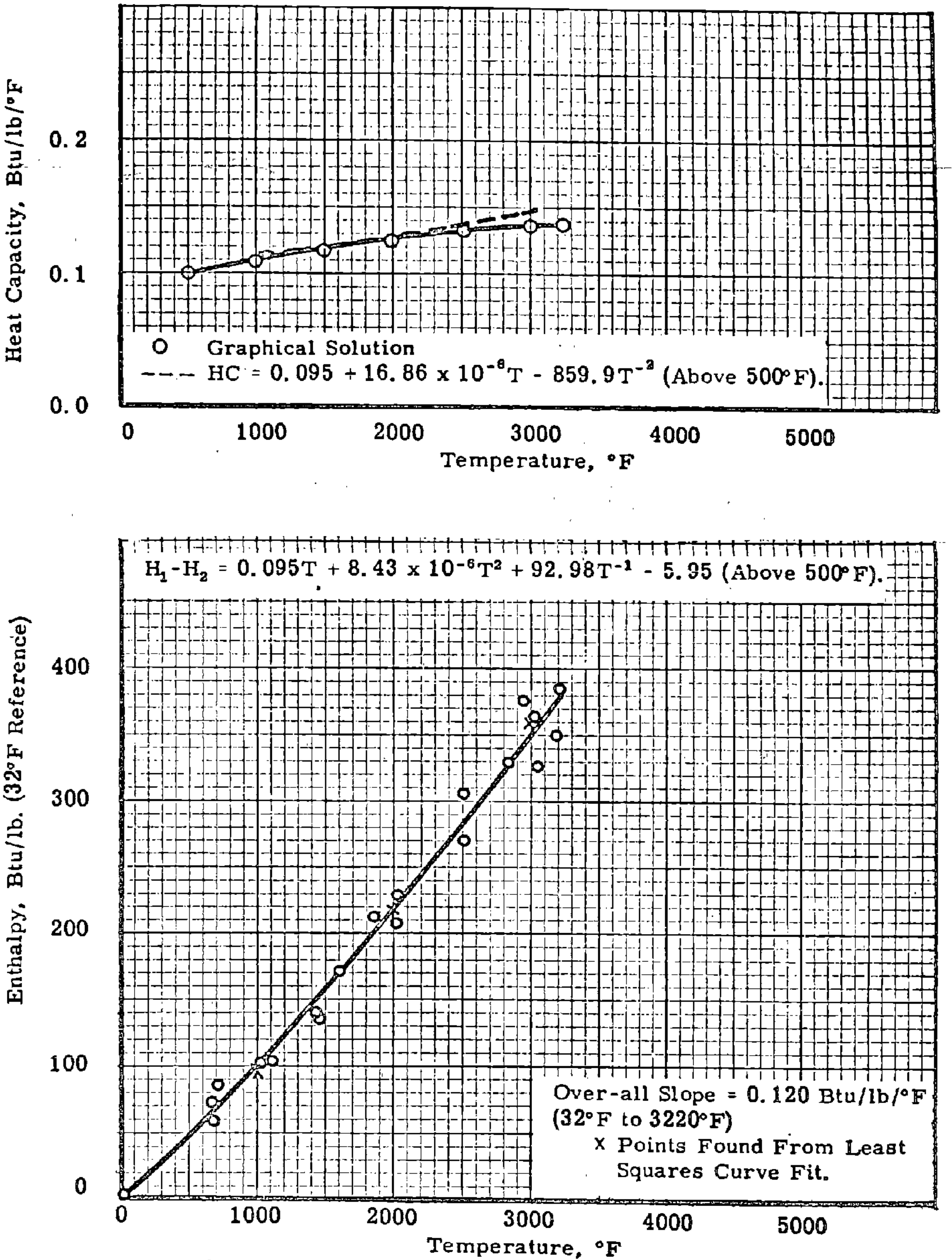

Figure 79. Enthalpy and Heat Capacity of Cerium Dioxide.

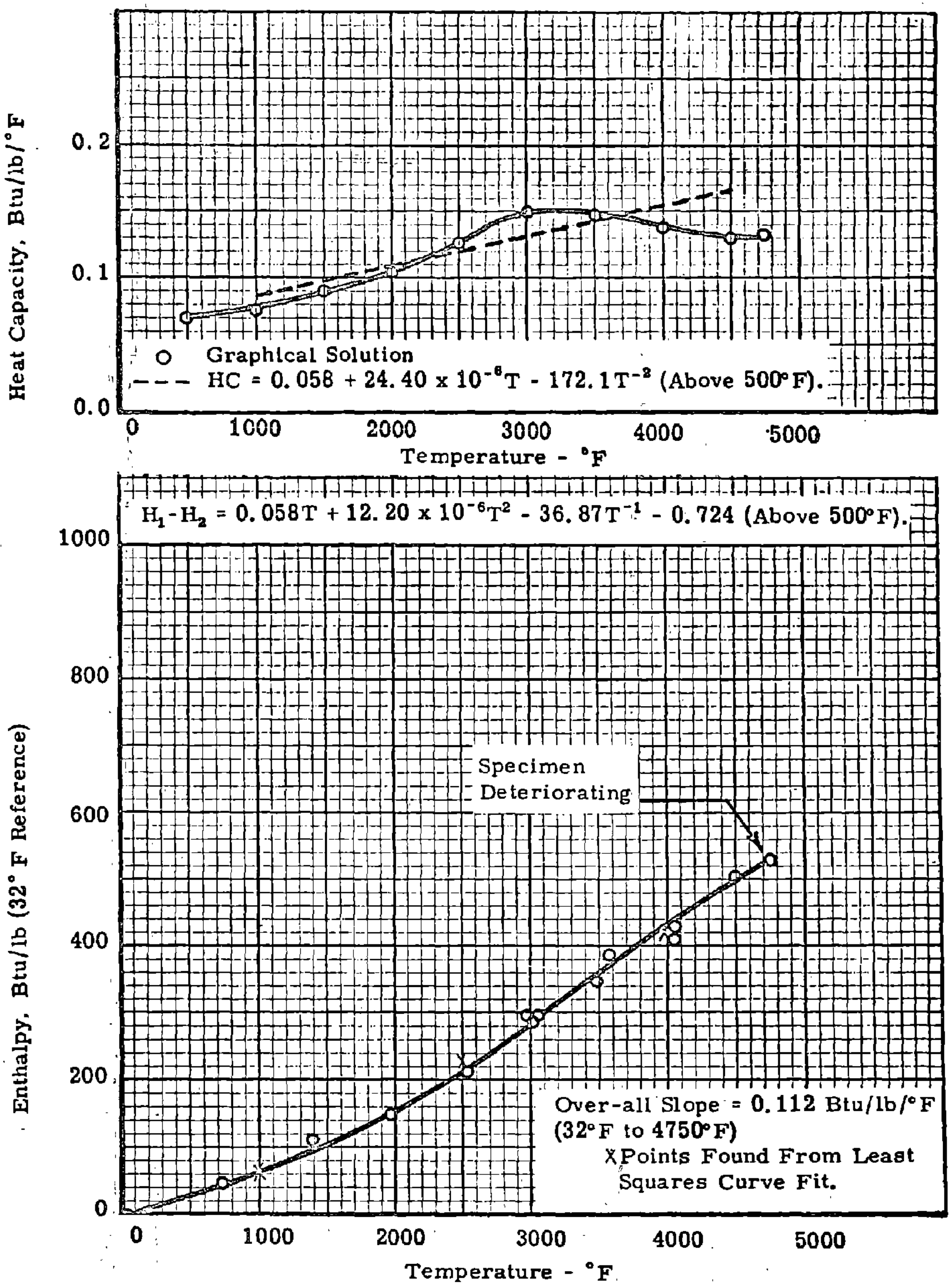

Figure 80. Enthalpy and Heat Capacity of Hafnium Dioxide.

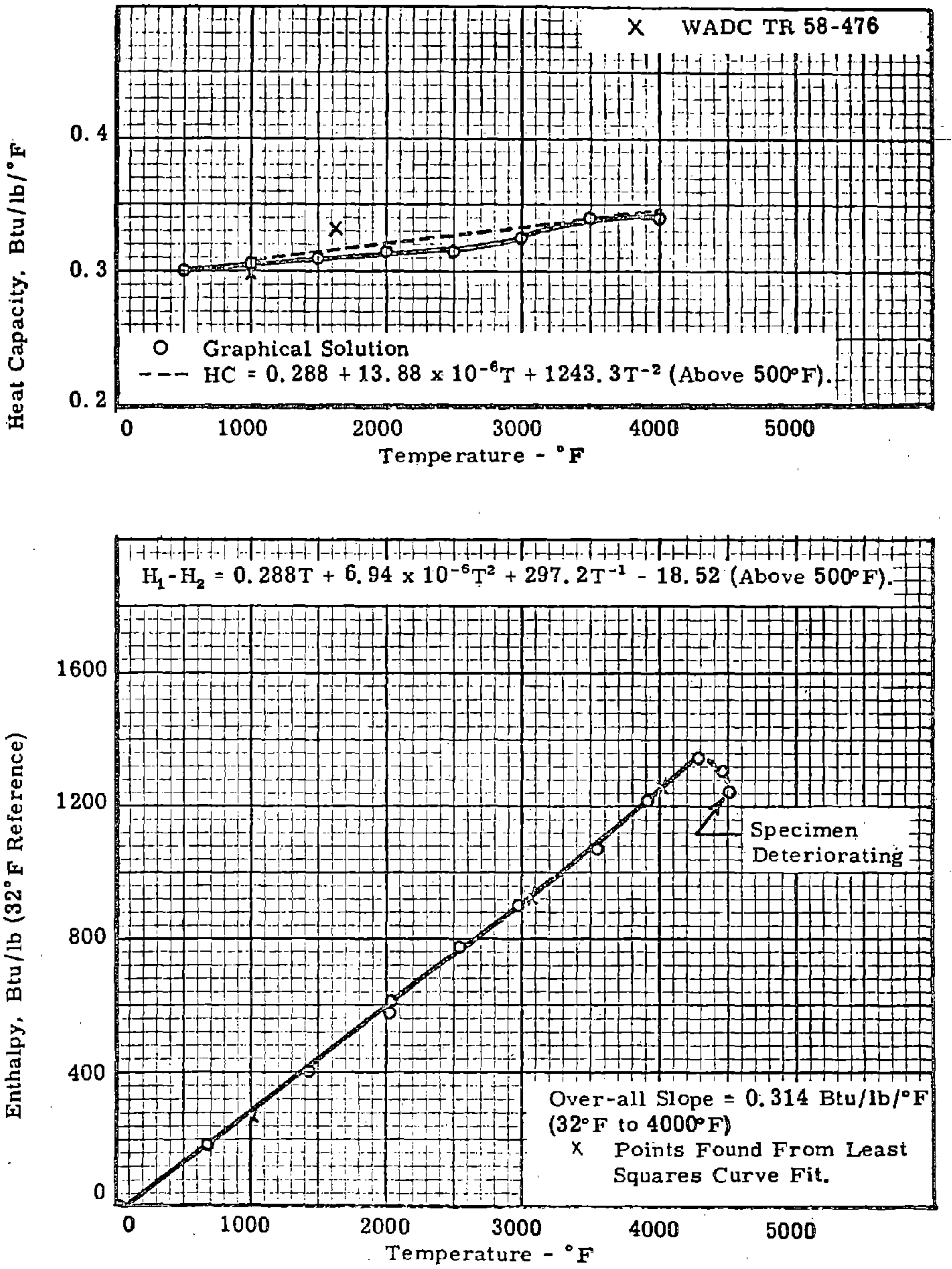

Figure 81. Enthalpy and Heat Capacity of Magnesium Oxide.

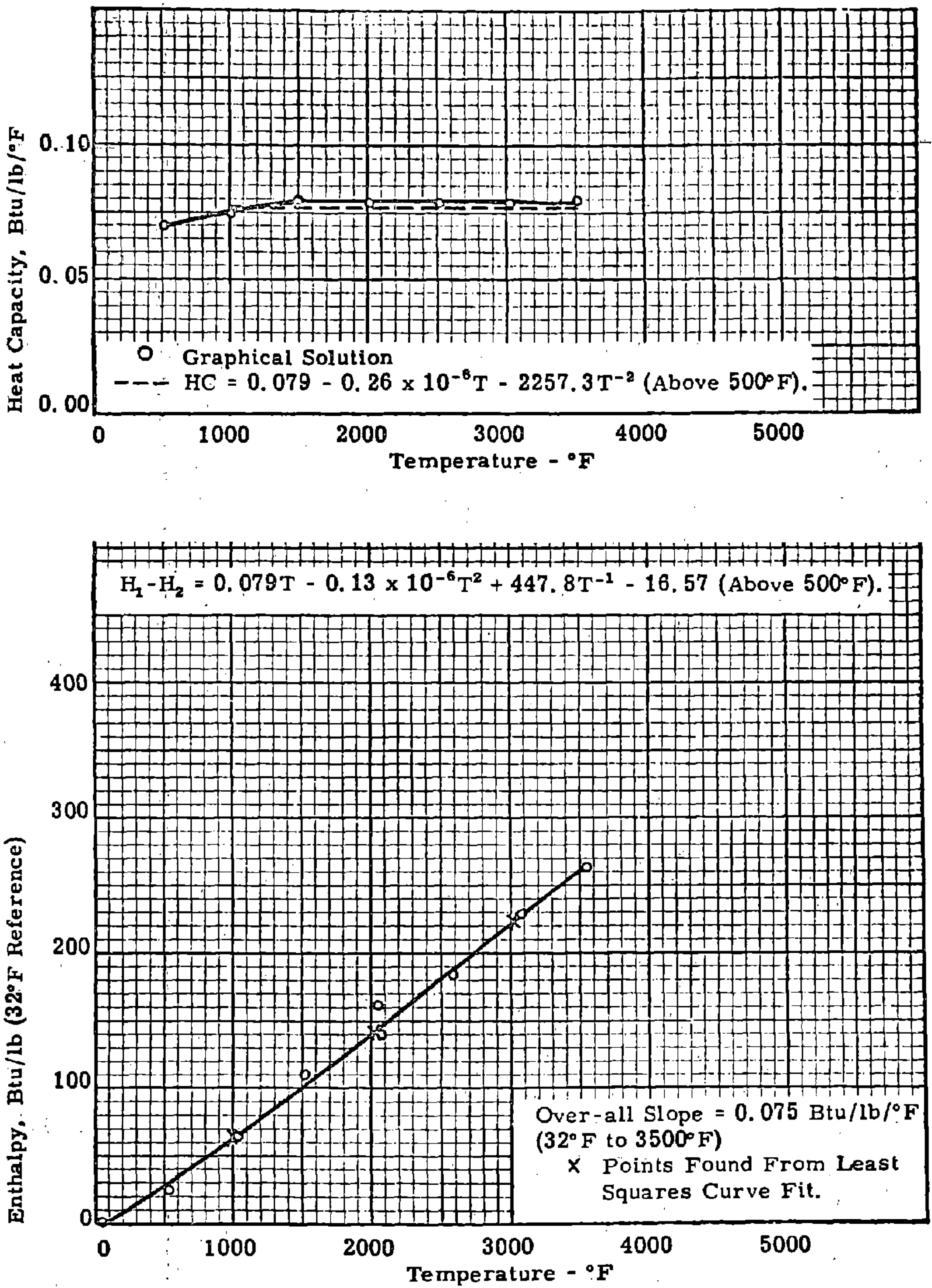

Figure 82. Enthalpy and Heat Capacity of Thorium Dioxide.

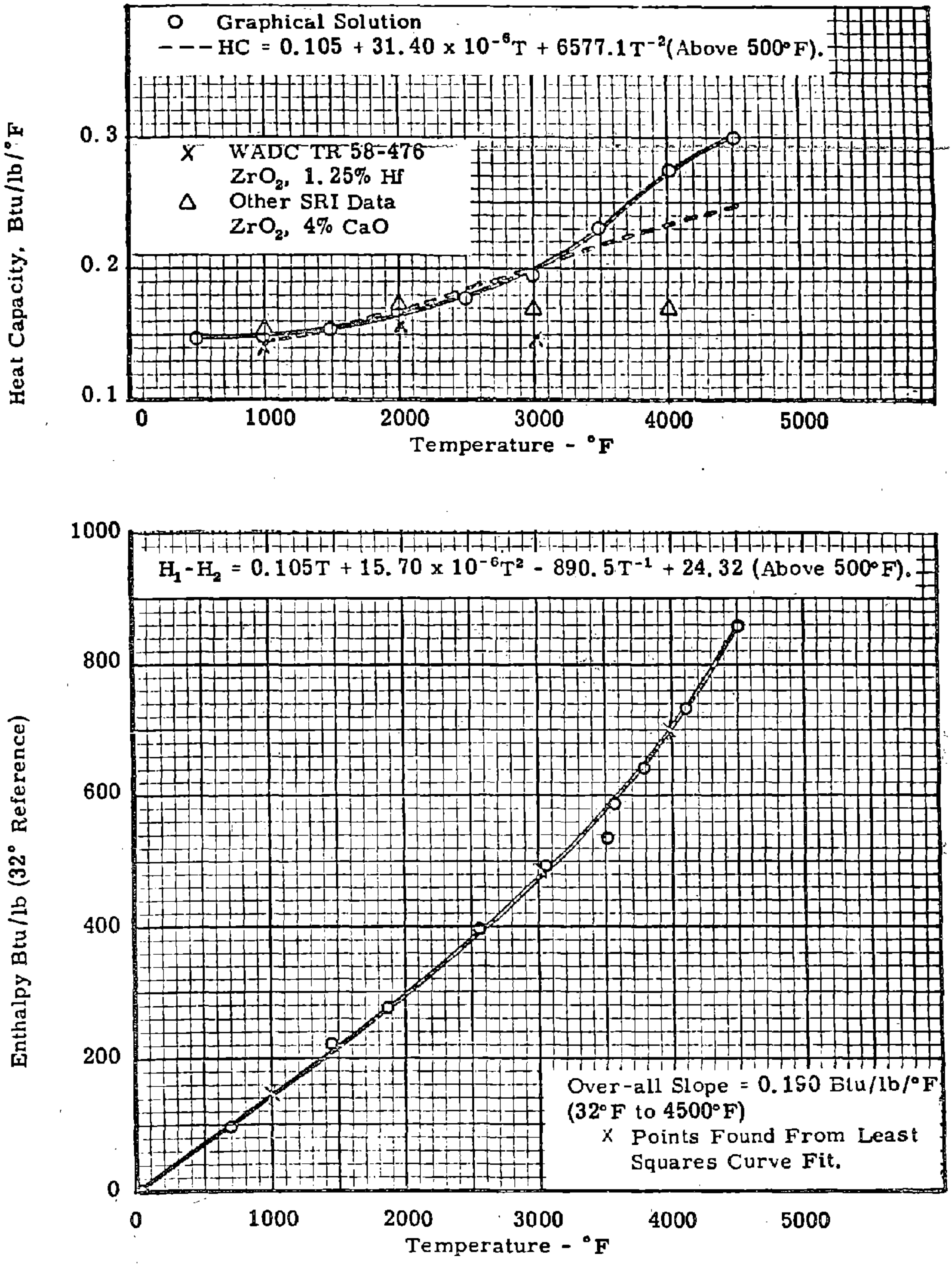

Figure 83. Enthalpy and Heat Capacity of Zirconium Dioxide.

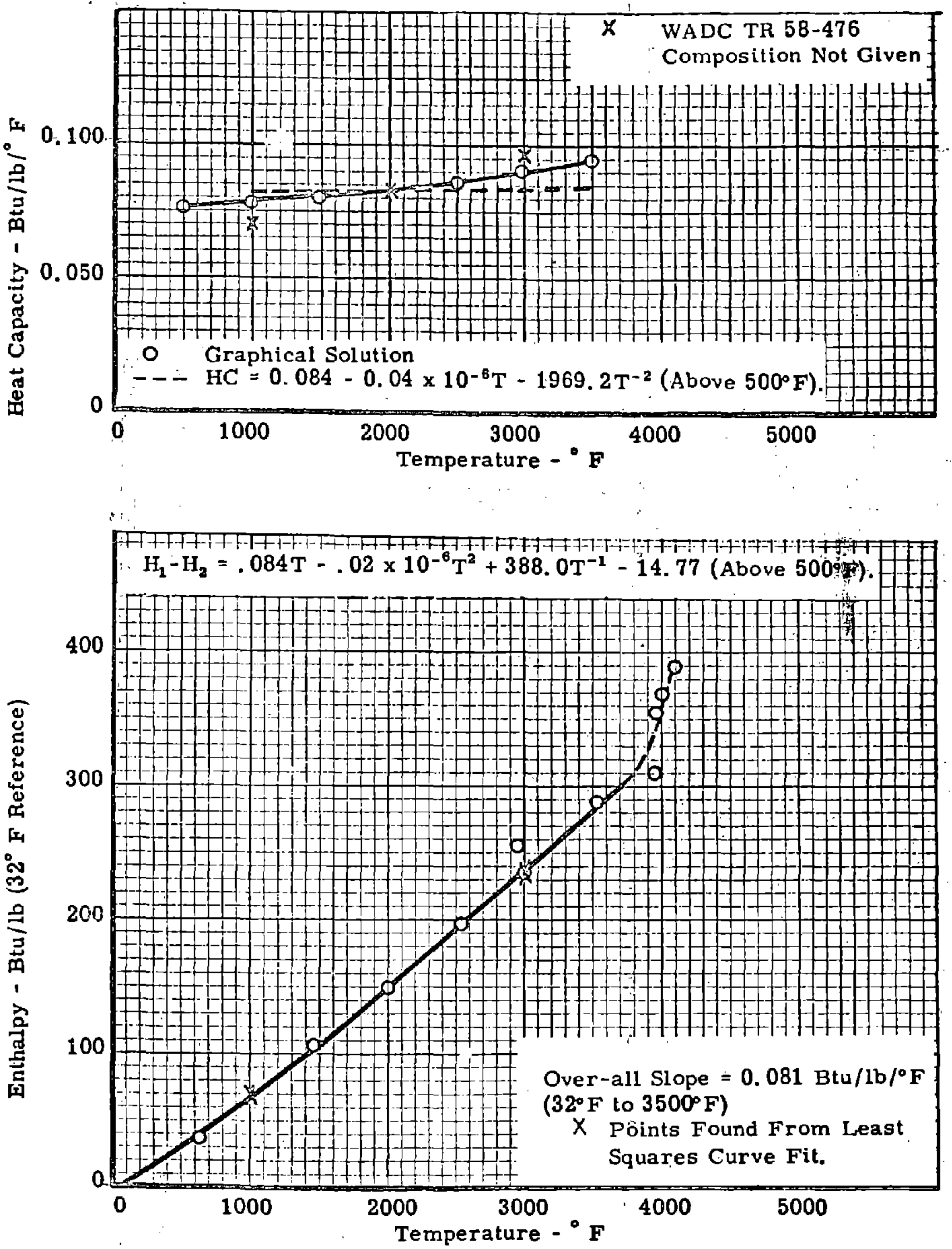

Figure 84. Enthalpy and Heat Capacity of Columbium + 0.5% Zirconium.

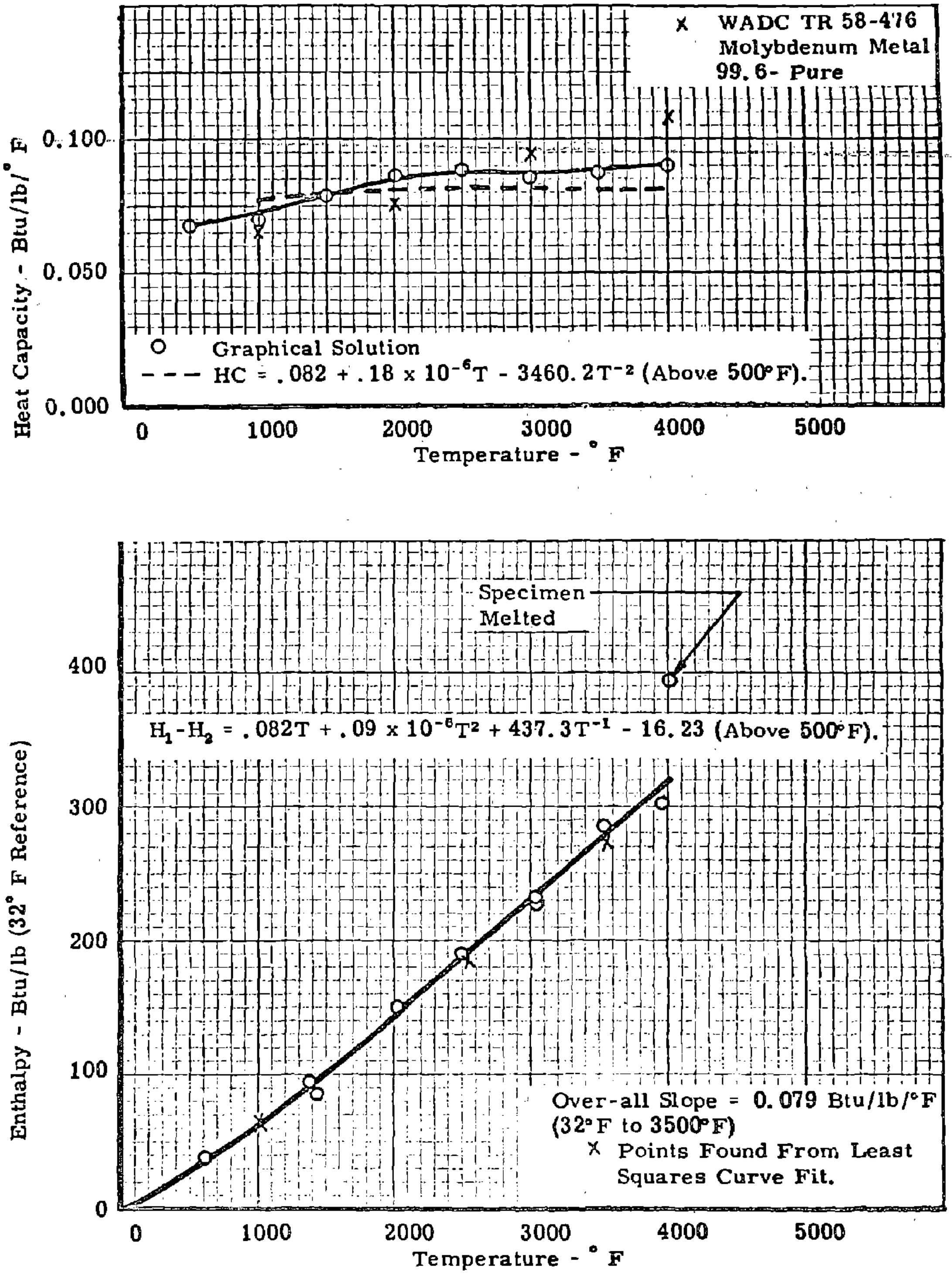

Figure 85. Enthalpy and Heat Capacity of Molybdenum + 0.5% Titanium.

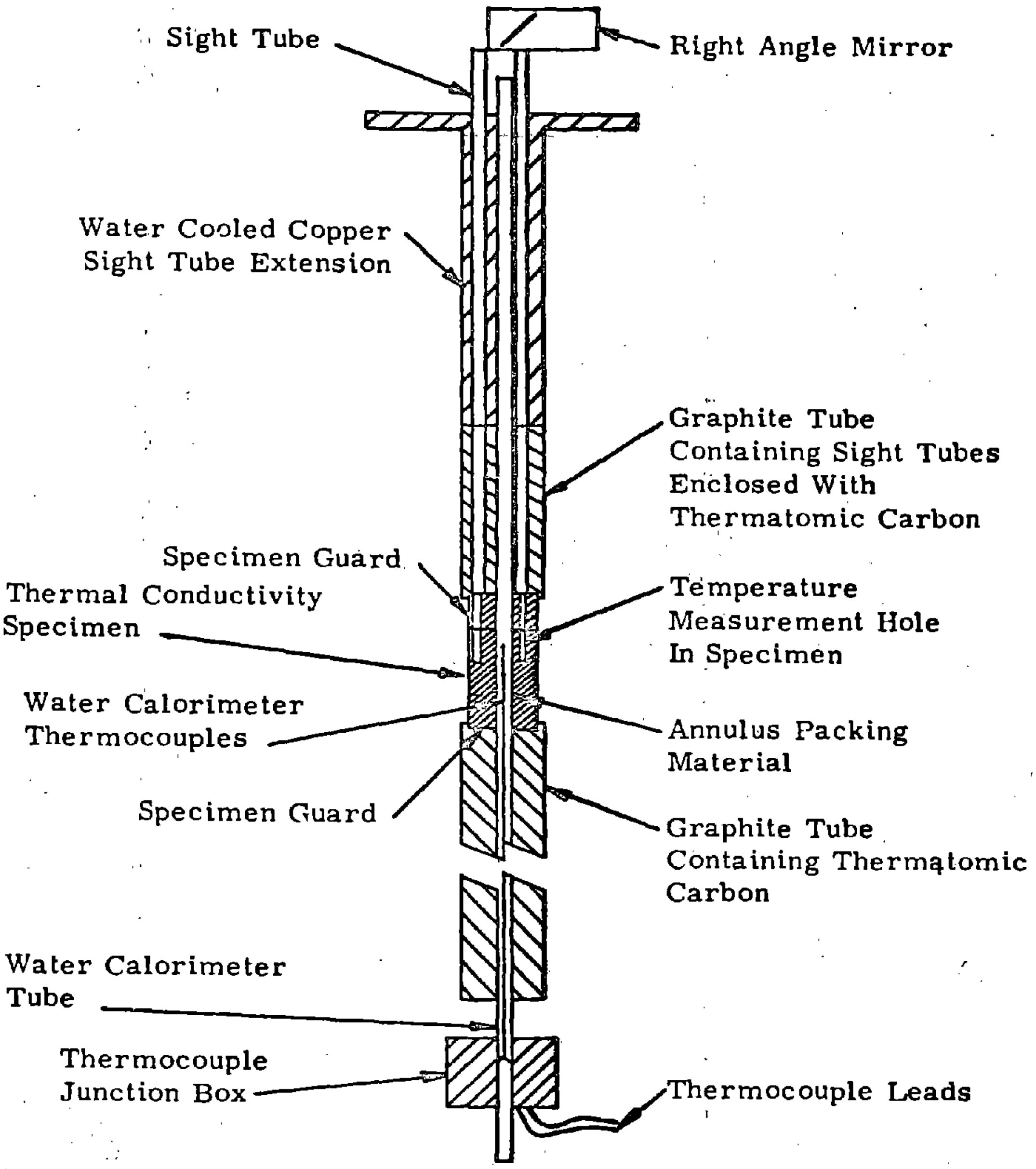
Sight Tube
Right Angle Mirror
Water Cooled Copper Sight Tube Extension
Graphite Tube Containing Sight Tubes Enclosed With Thermatomic Carbon
Specimen Guard
Thermal Conductivity Specimen
Temperature Measurement Hole In Specimen
Water Calorimeter Thermocouples
Annulus Packing Material
Specimen Guard
Graphite Tube Containing Thermatomic Carbon
Water Calorimeter Tube
Thermocouple Junction Box
Thermocouple Leads

Figure 86. Cross-section Schematic of the Thermal Conductivity Apparatus.

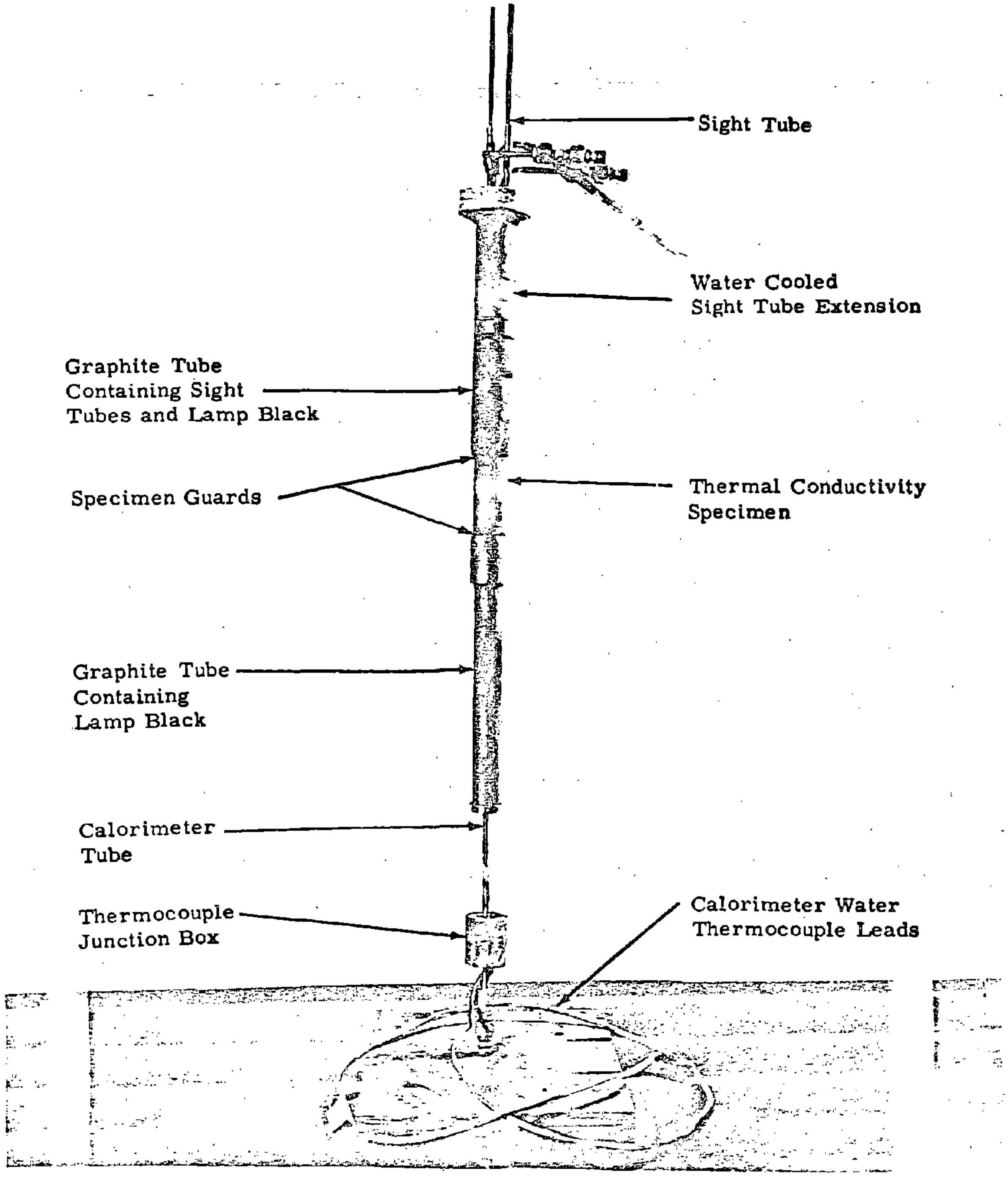
Sight Tube
Water Cooled Sight Tube Extension
Graphite Tube Containing Sight Tubes and Lamp Black
Specimen Guards
Thermal Conductivity Specimen
Graphite Tube Containing Lamp Black
Calorimeter Tube
Thermocouple Junction Box
Calorimeter Water Thermocouple Leads

Figure 87. Picture of the Radial Thermal Conductivity Apparatus.

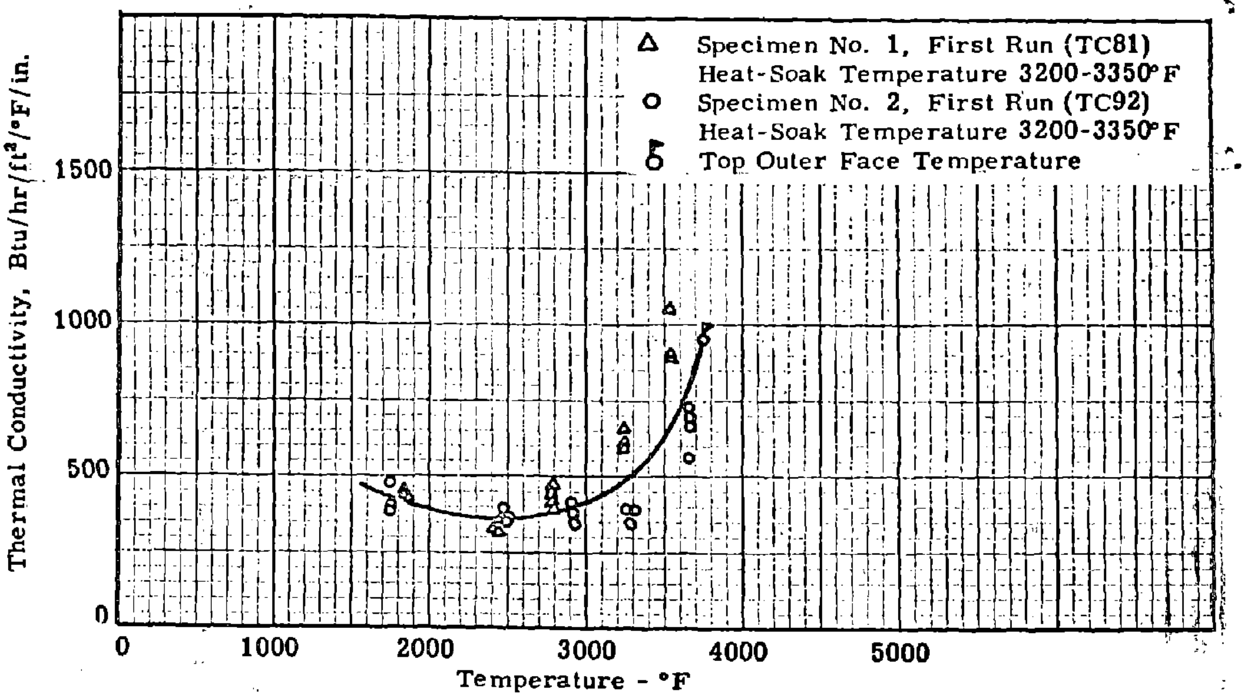

Figure 88. Thermal Conductivity of Hafnium Diboride

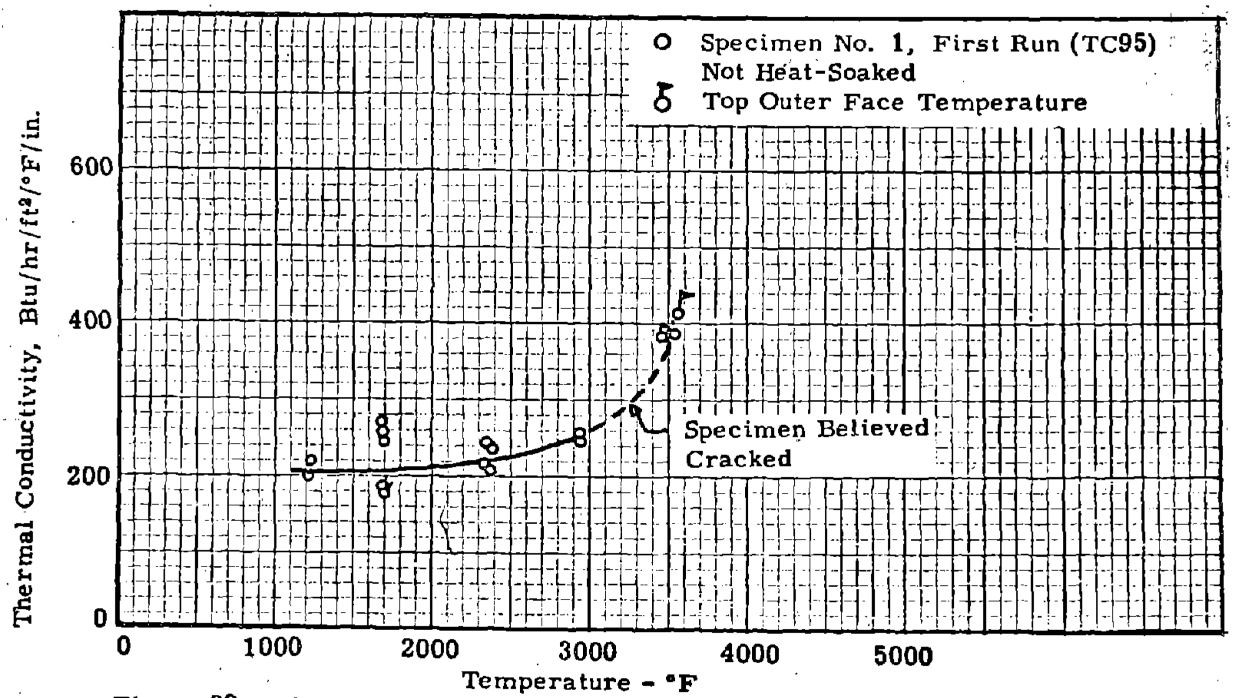

Figure 89. Thermal Conductivity of Thorium Tetraboride.

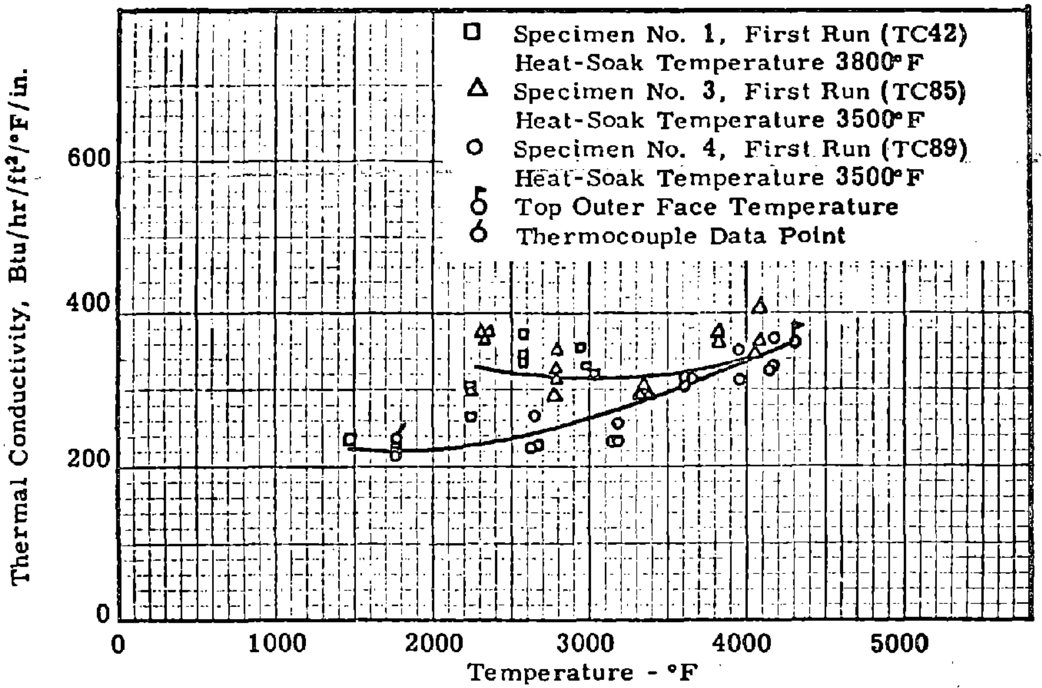

Figure 90. Thermal Conductivity of Titanium Diboride

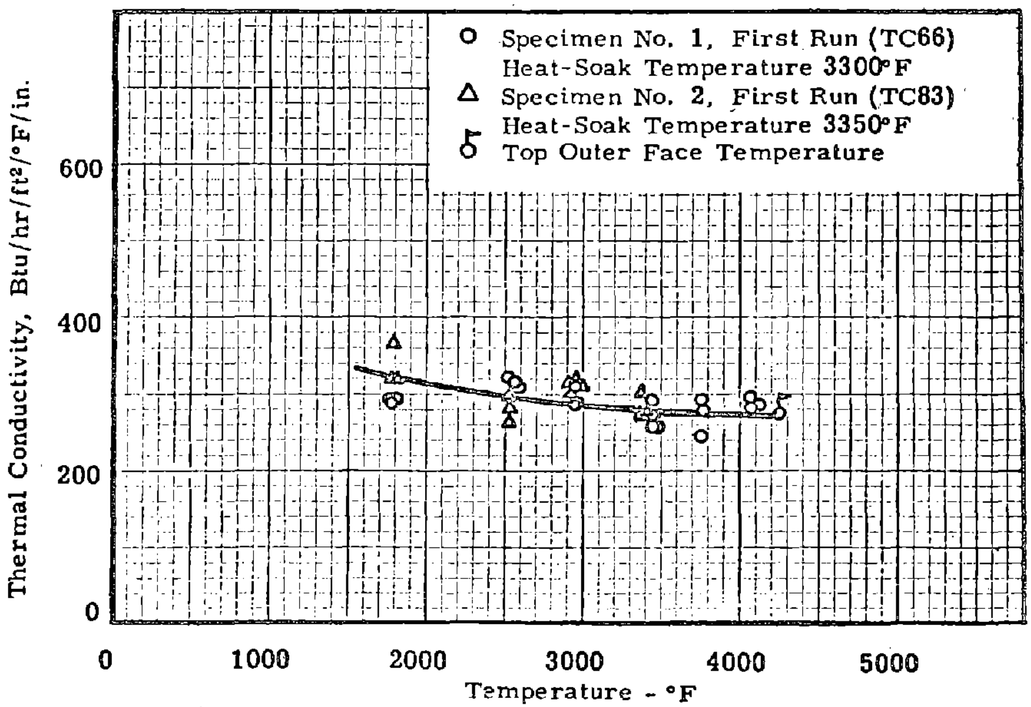

Figure 91. Thermal Conductivity of Tungsten Boride.

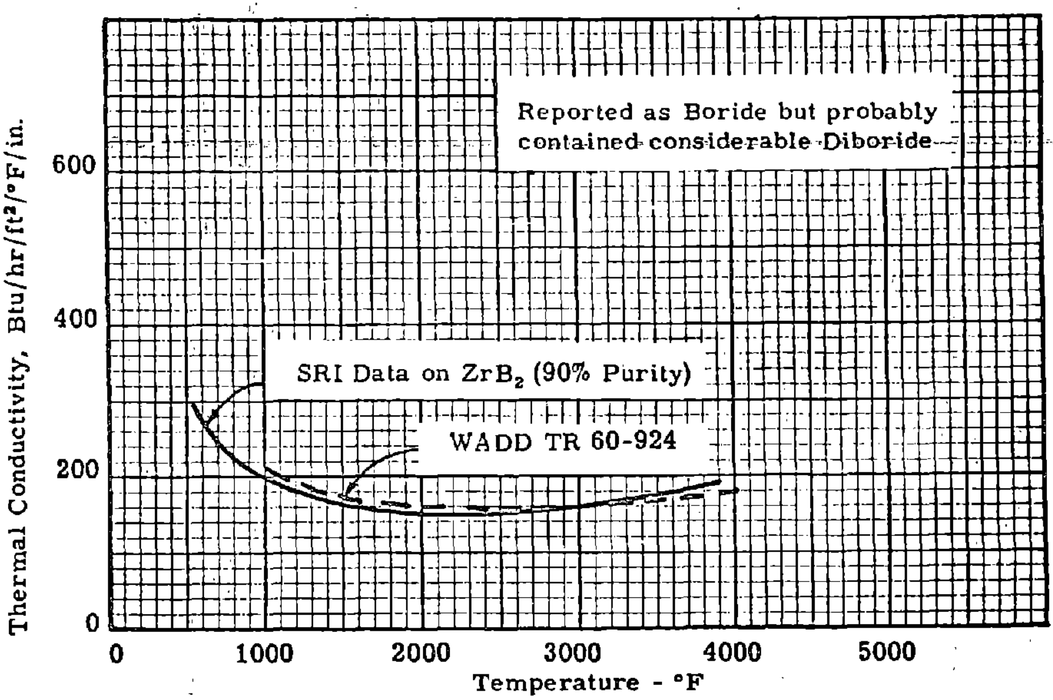

Figure 92. Thermal Conductivity of Zirconium Diboride.

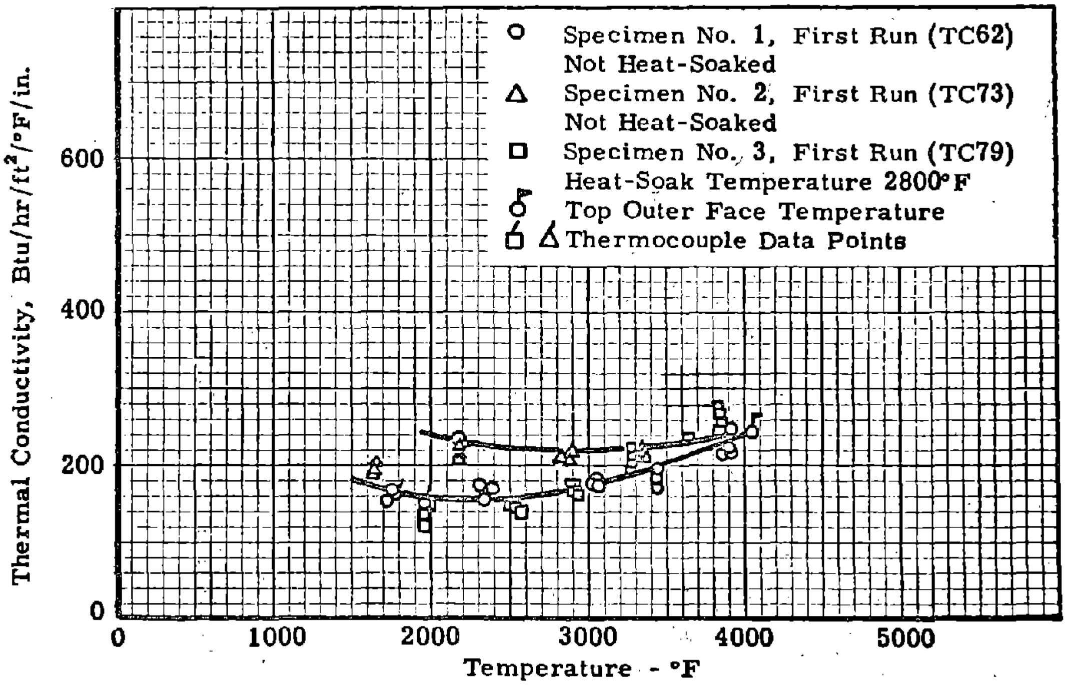

Figure 93. Thermal Conductivity of Dimolybdenum Carbide.

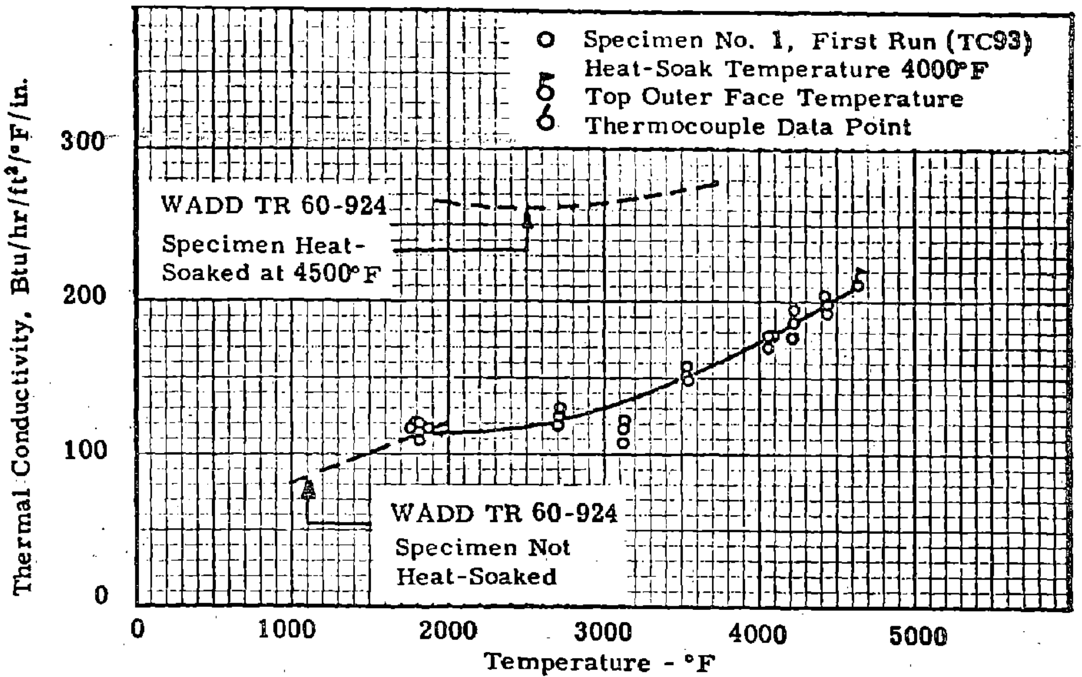

Figure 94. Thermal Conductivity of Hafnium Carbide.

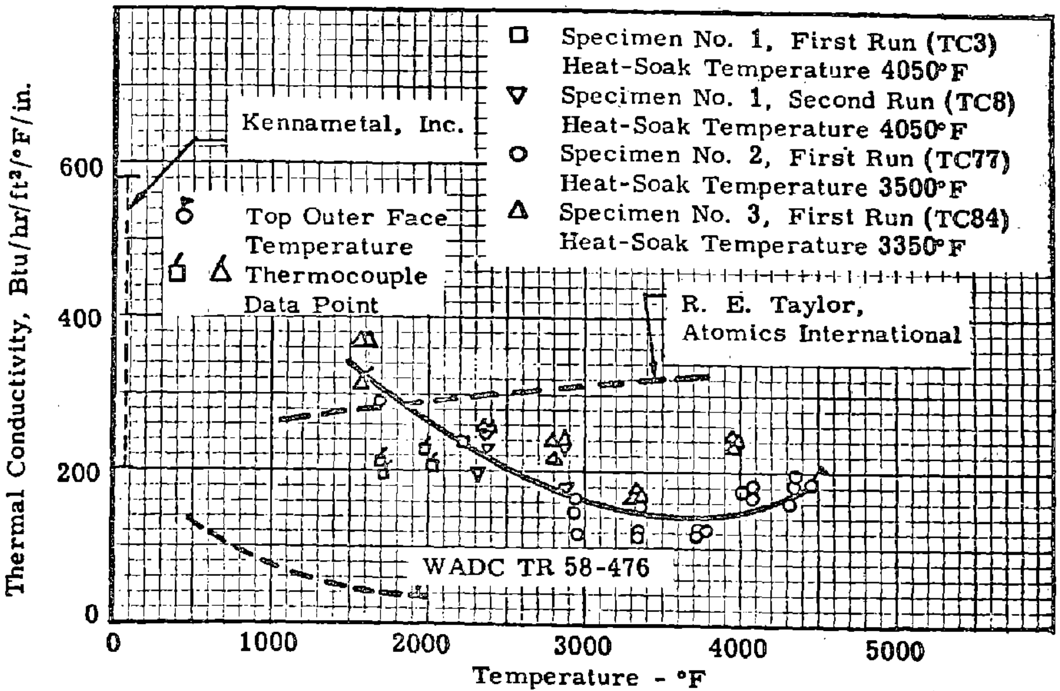

Figure 95. Thermal Conductivity of Titanium Carbide.

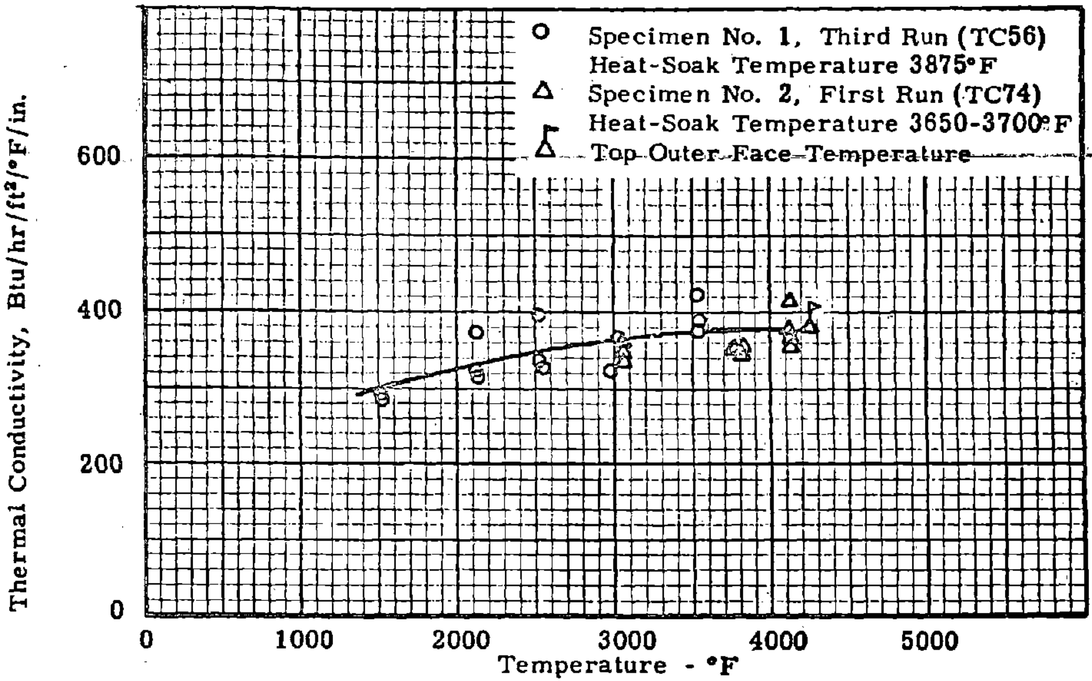

Figure 96. Thermal Conductivity of Tungsten Carbide

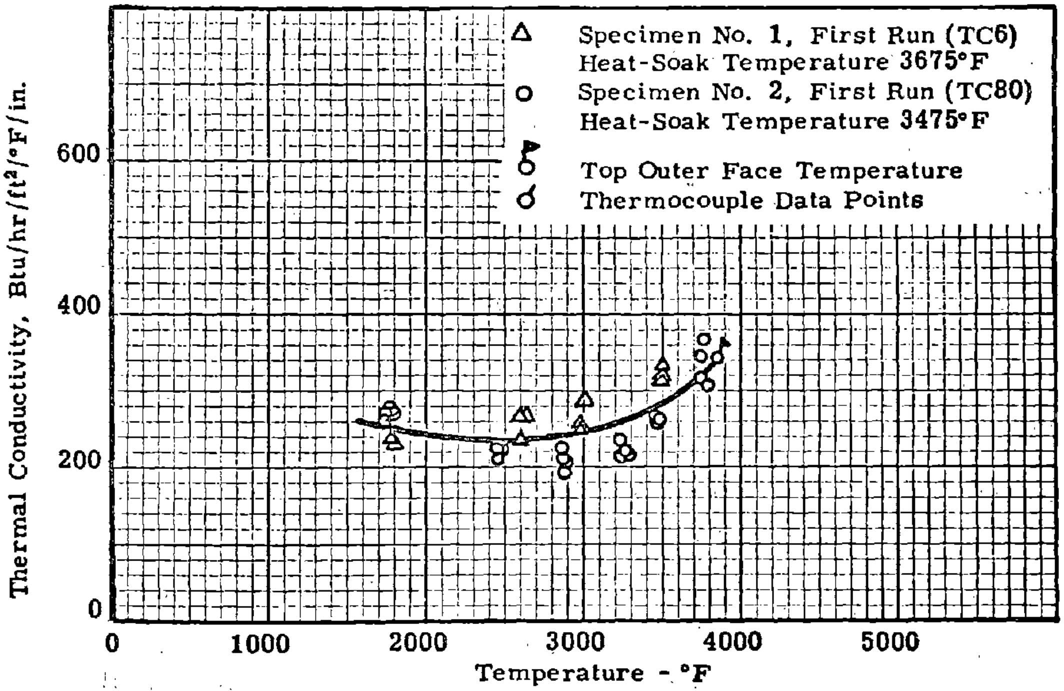

Figure 97. Thermal Conductivity of Vanadium Carbide.

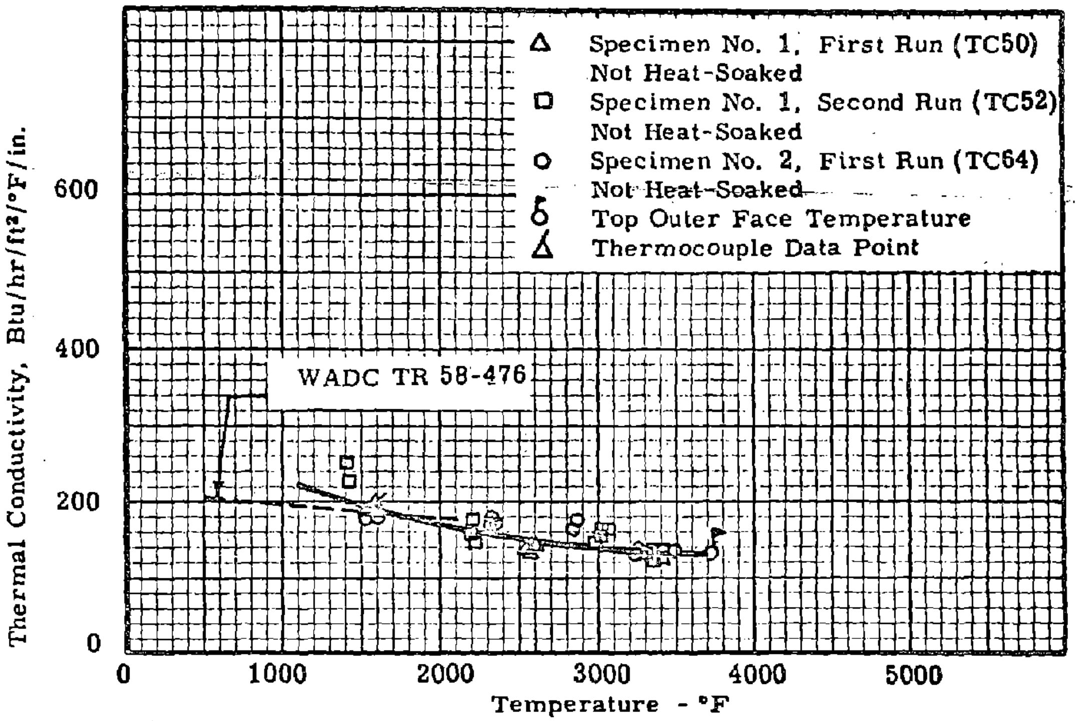

Figure 98. Thermal Conductivity of Boron Nitride.

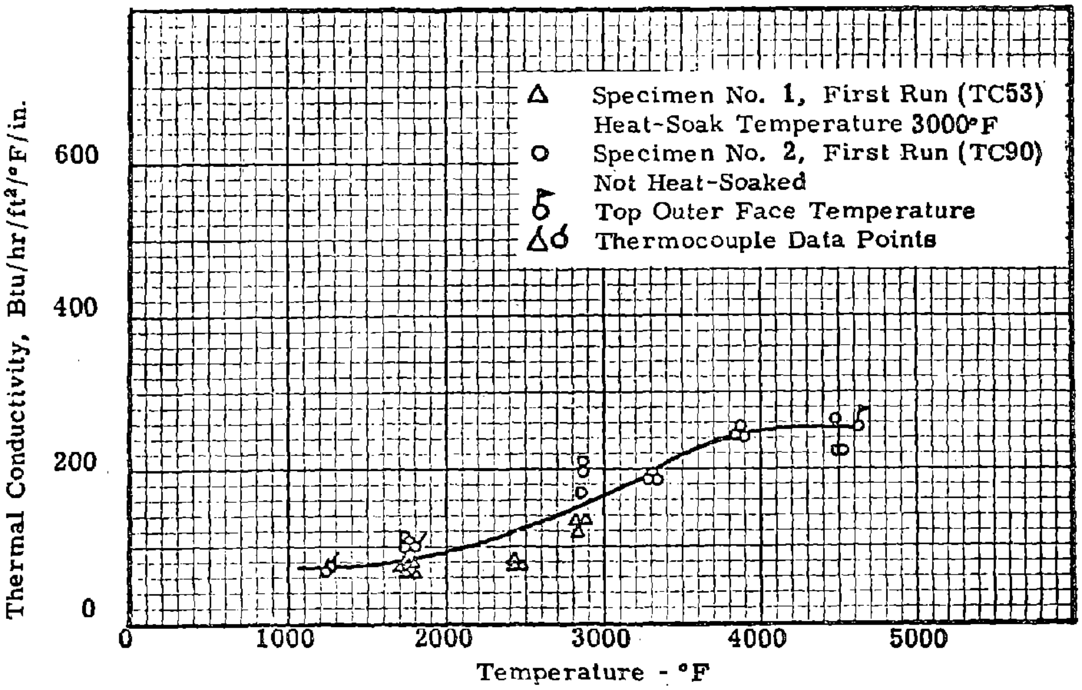

Figure 99. Thermal Conductivity of Tantalum Nitride

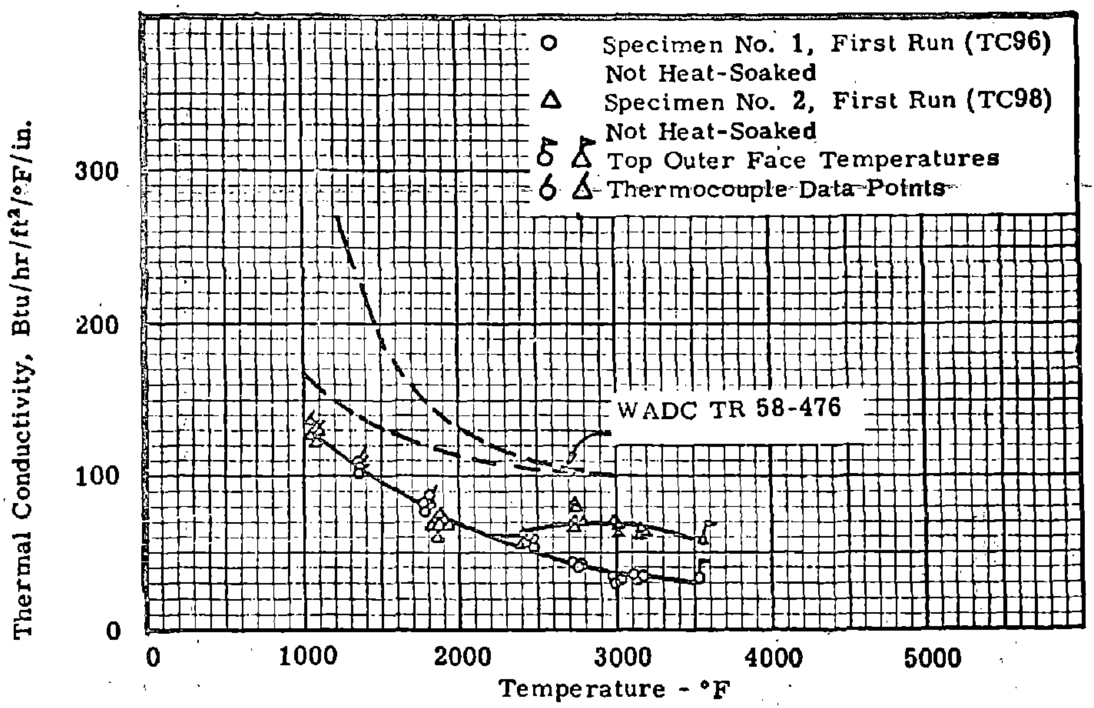

Figure 100. Thermal Conductivity of Beryllium Oxide.

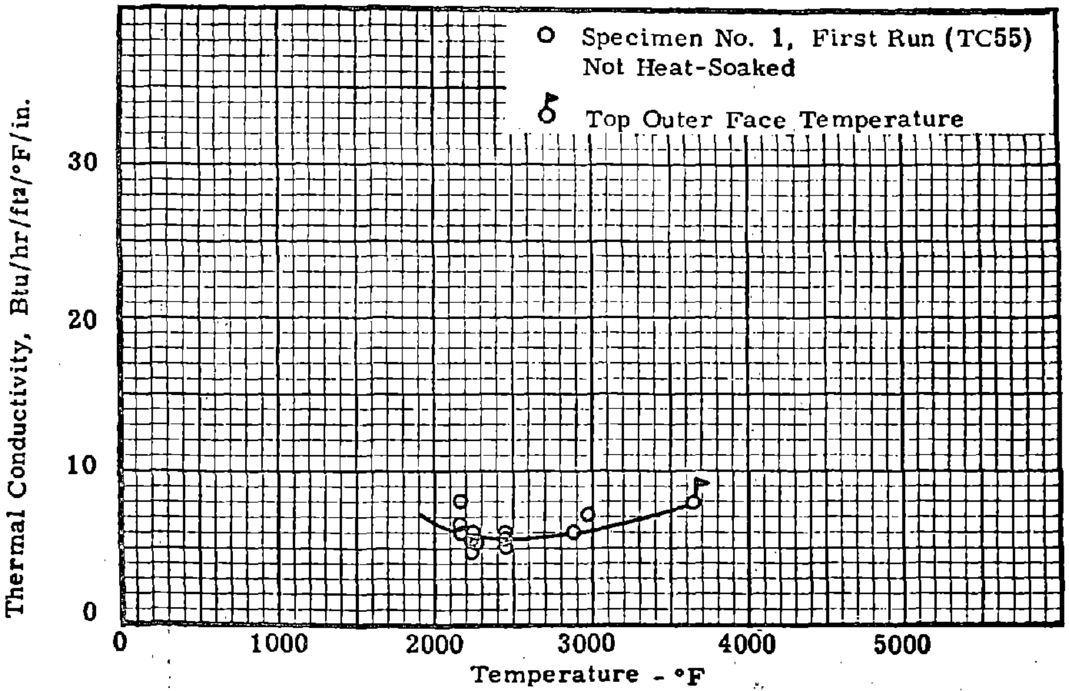

Figure 101. Thermal Conductivity of Cerium Dioxide.

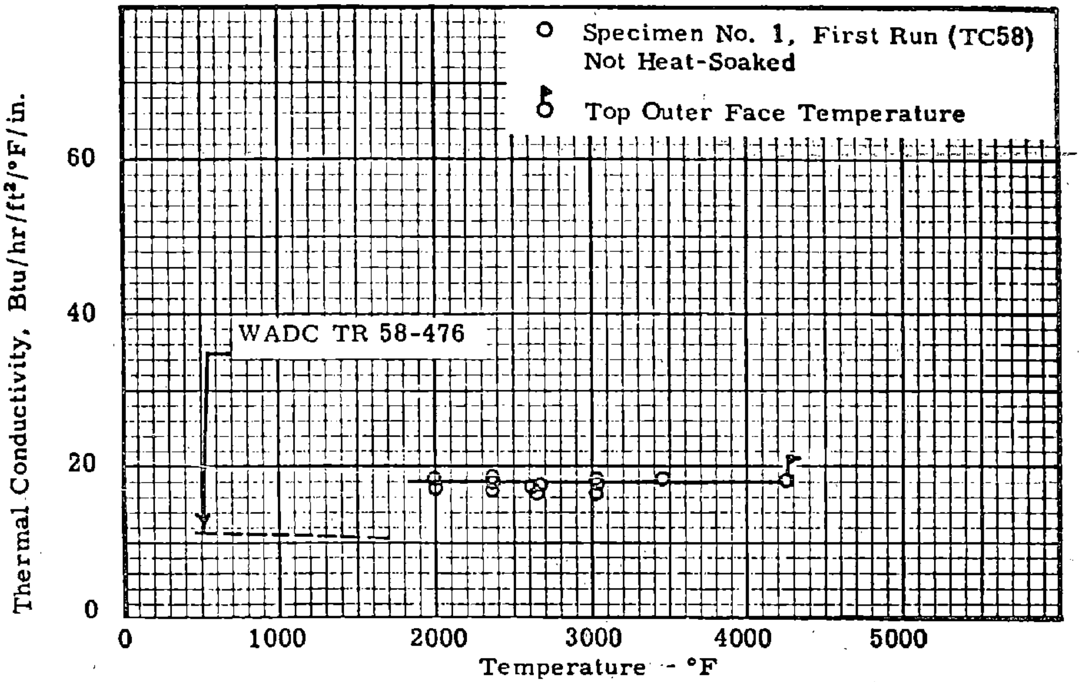

Figure 102. Thermal Conductivity of Hafnium Dioxide

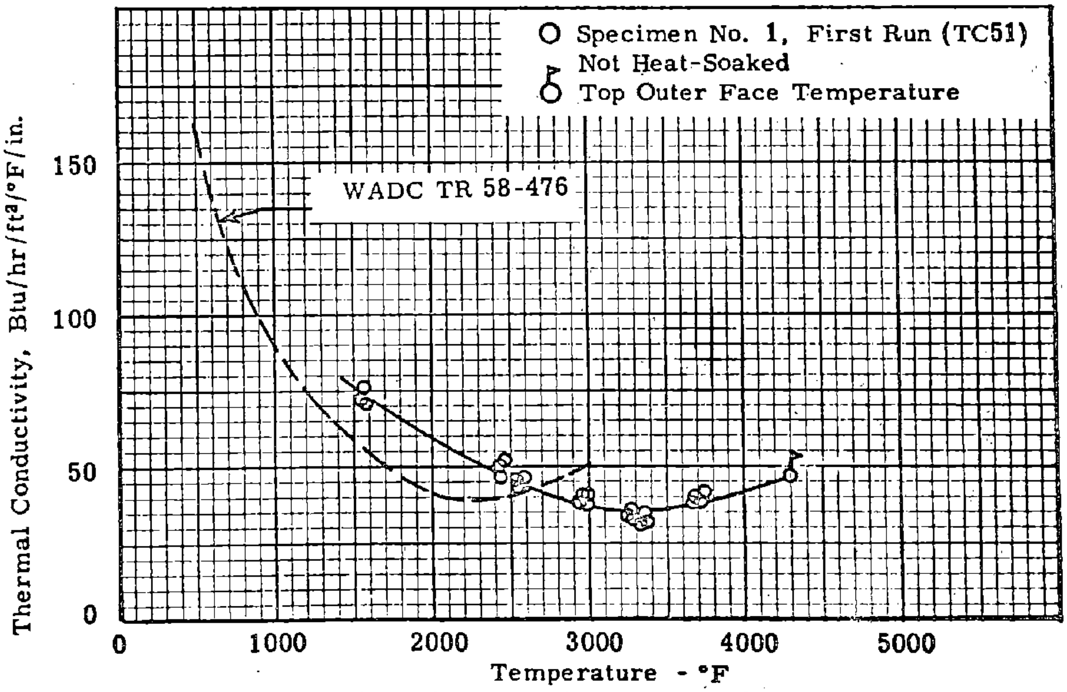

Figure 103. Thermal Conductivity of Magnesium Oxide

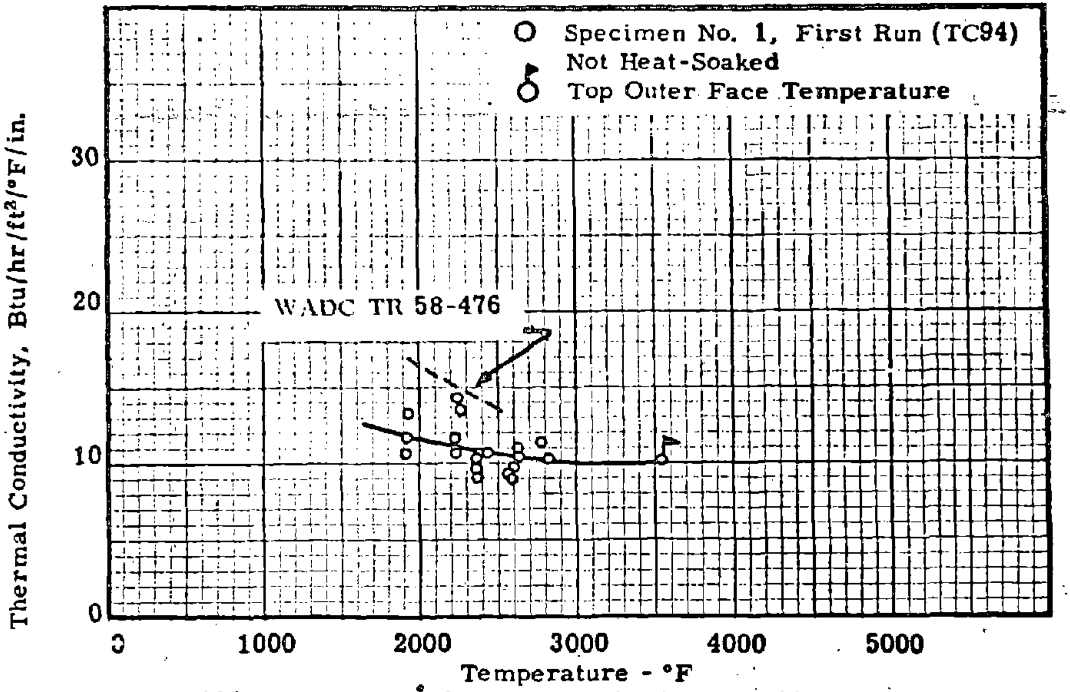

Figure 104. Thermal Conductivity of Thorium Dioxide.

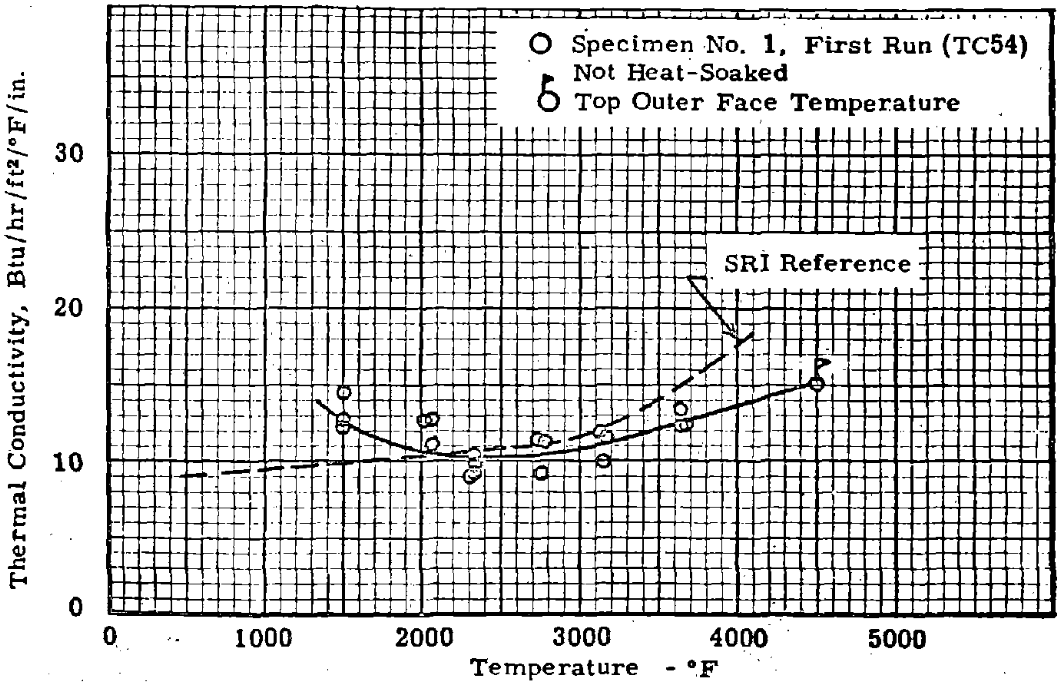

Figure 105. Thermal Conductivity of Zirconium Dioxide

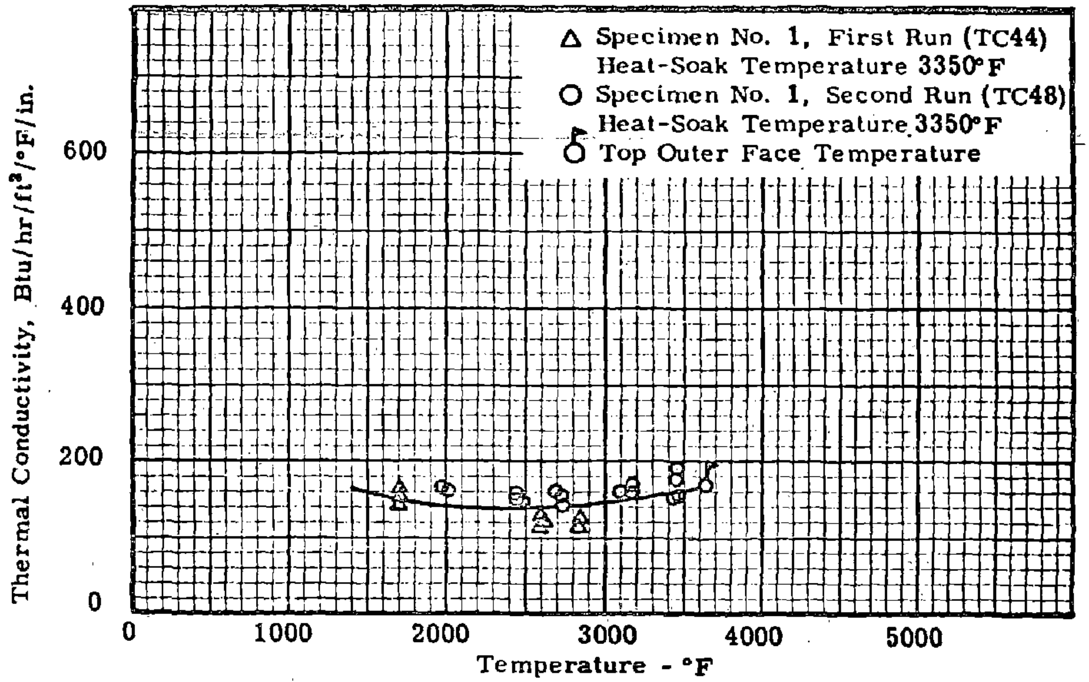

Figure 106. Thermal Conductivity of Columbium + 0.5% Zirconium

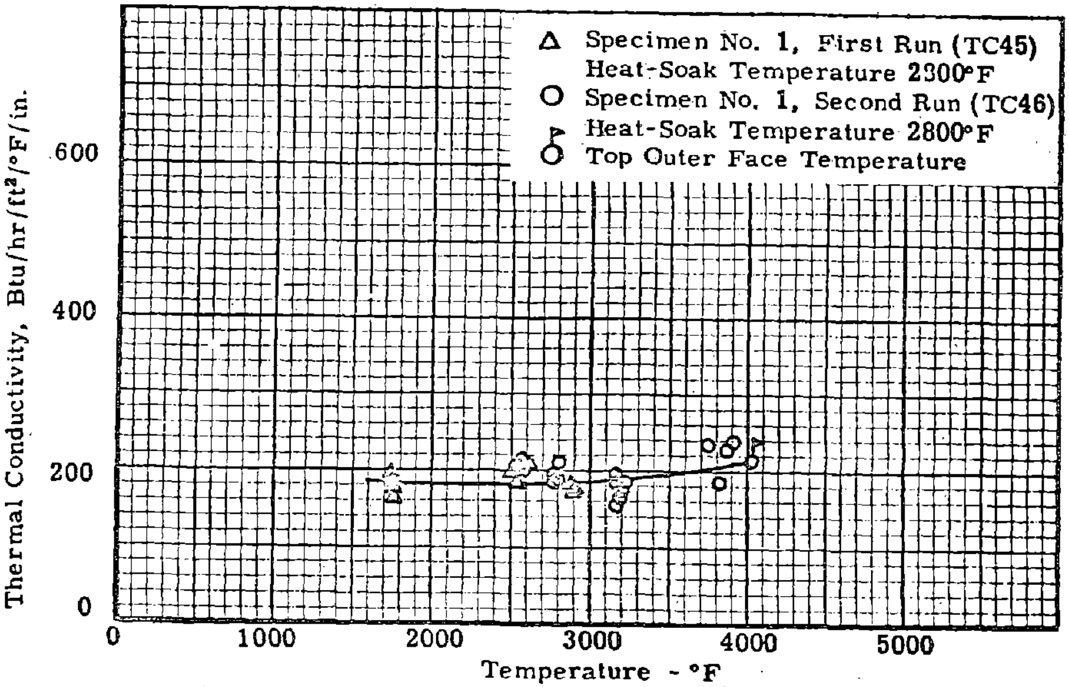

Figure 107. Thermal Conductivity of Molybdenum + 0.5% Titanium

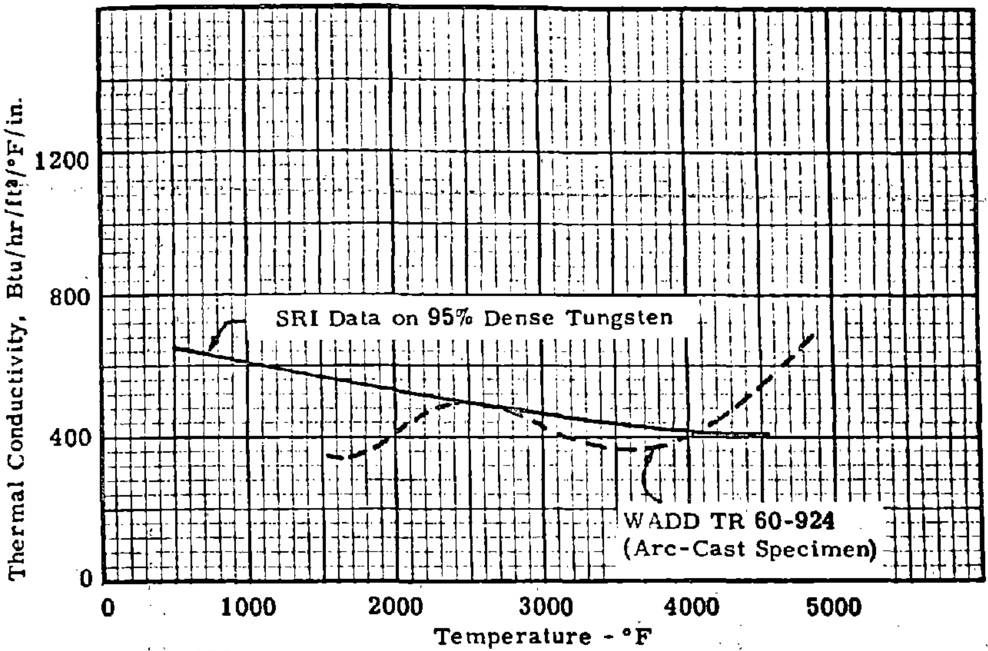

Figure 108. Thermal Conductivity of Tungsten.

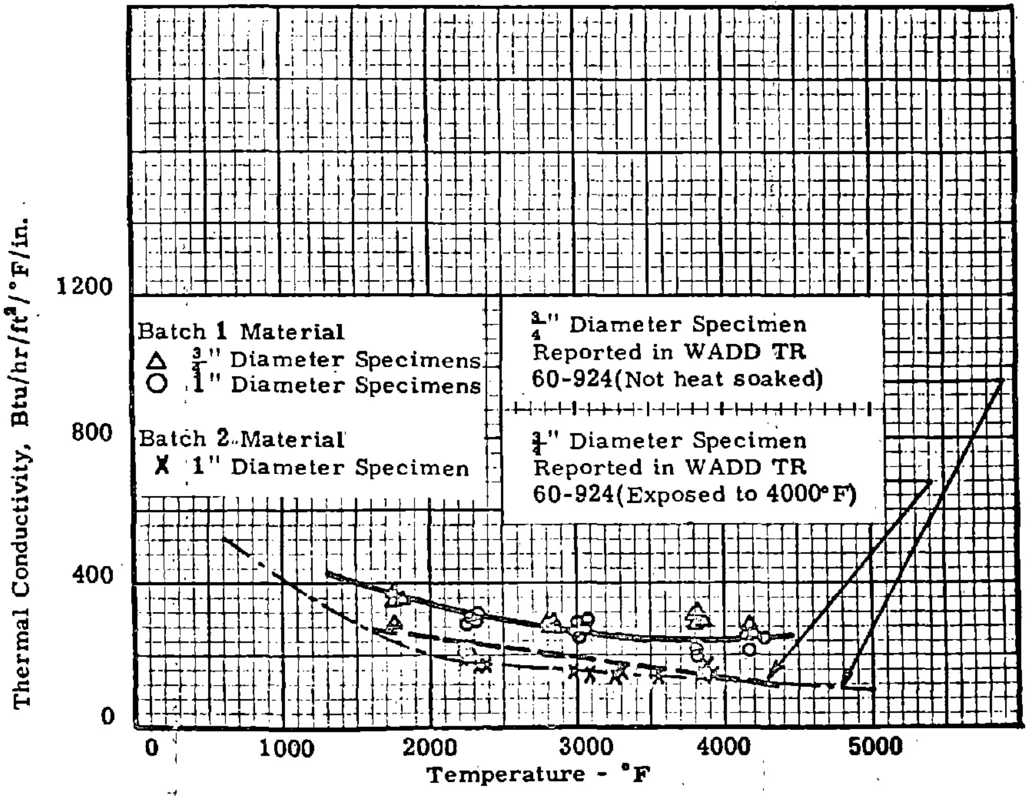

Figure 109. Thermal Conductivity of ATJ Graphite

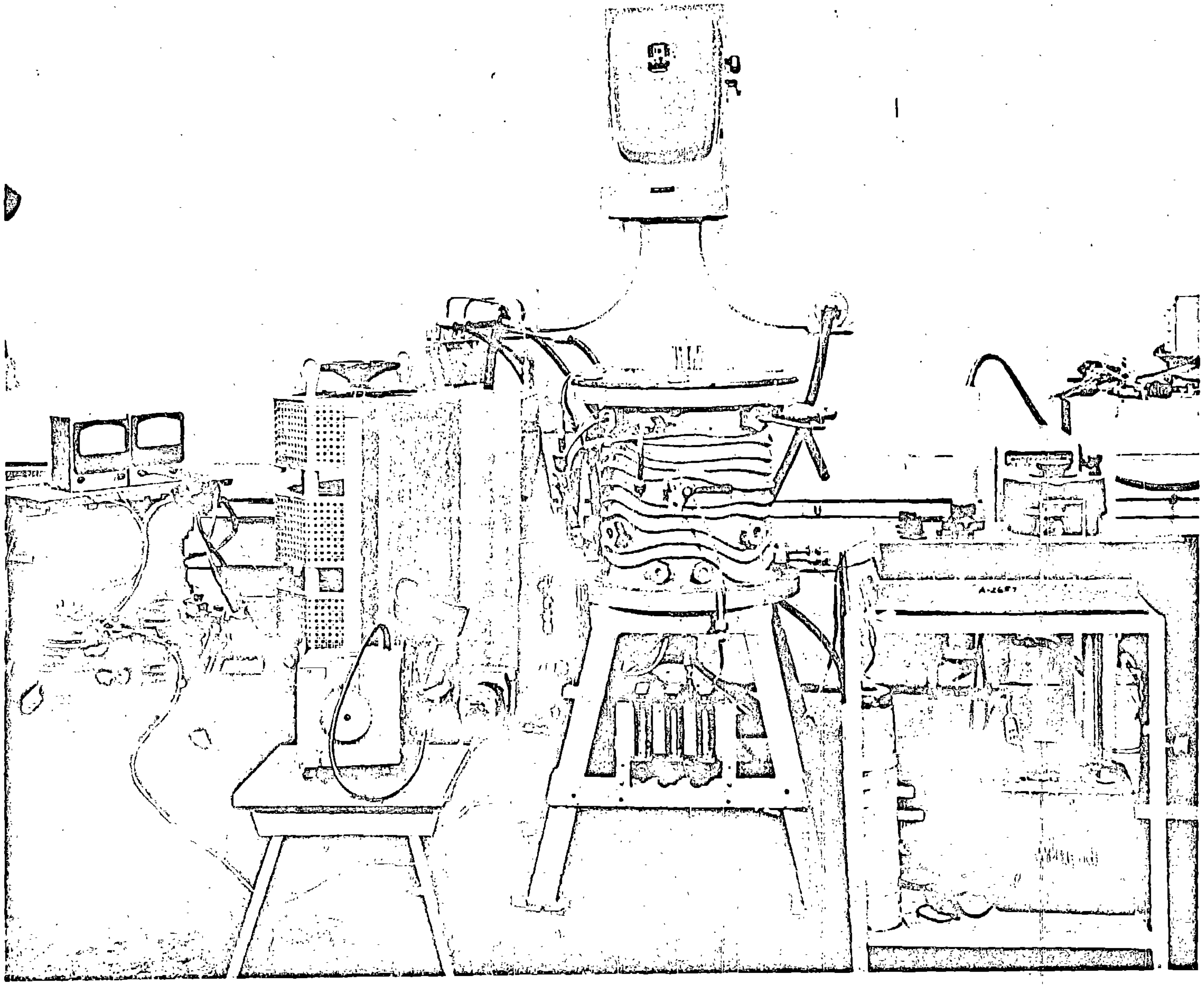

Figure 110. Picture of GFE Furnace with Thermal Conductivity Apparatus Installed.

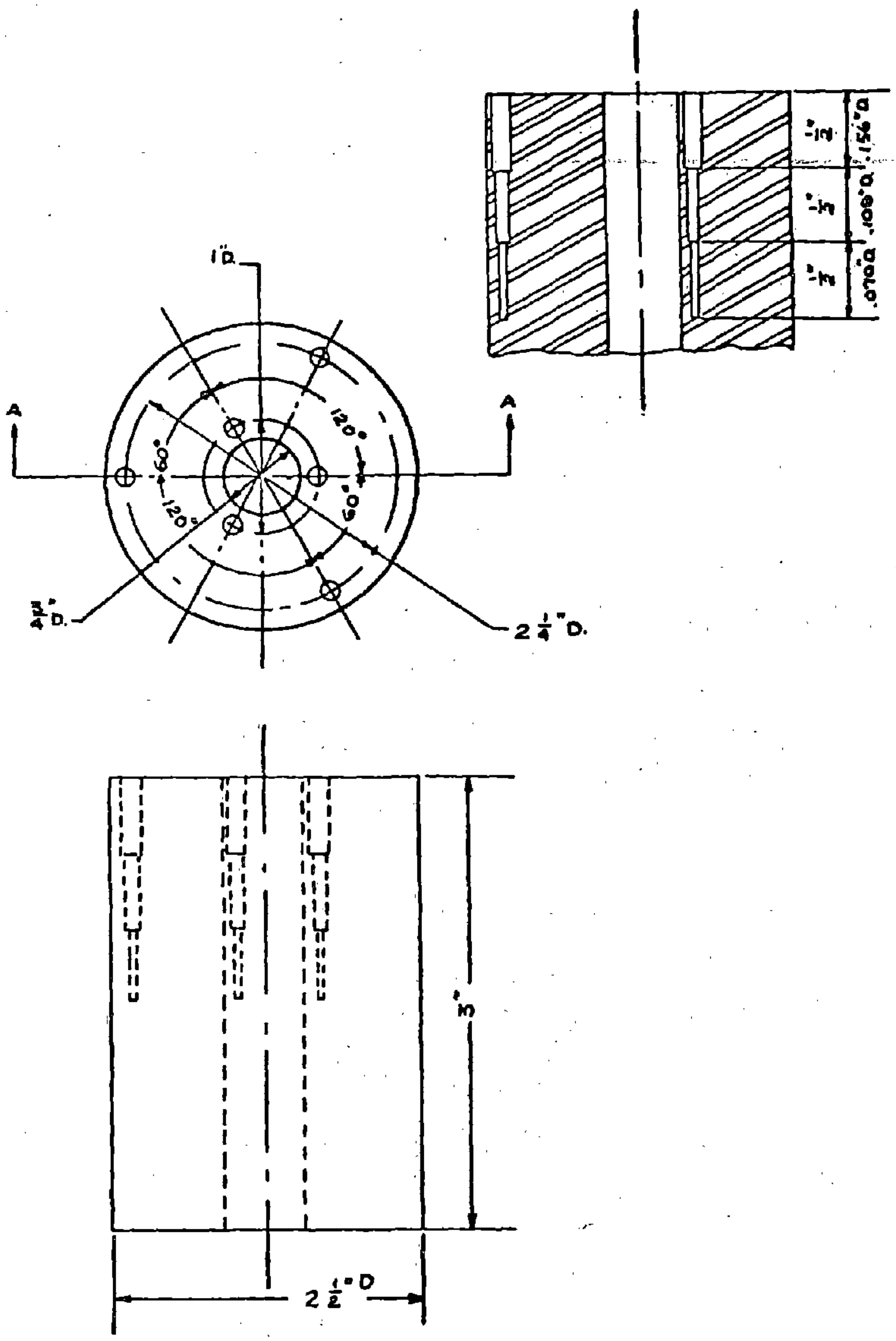

Figure 111. Thermal Conductivity Specimen for GFE.

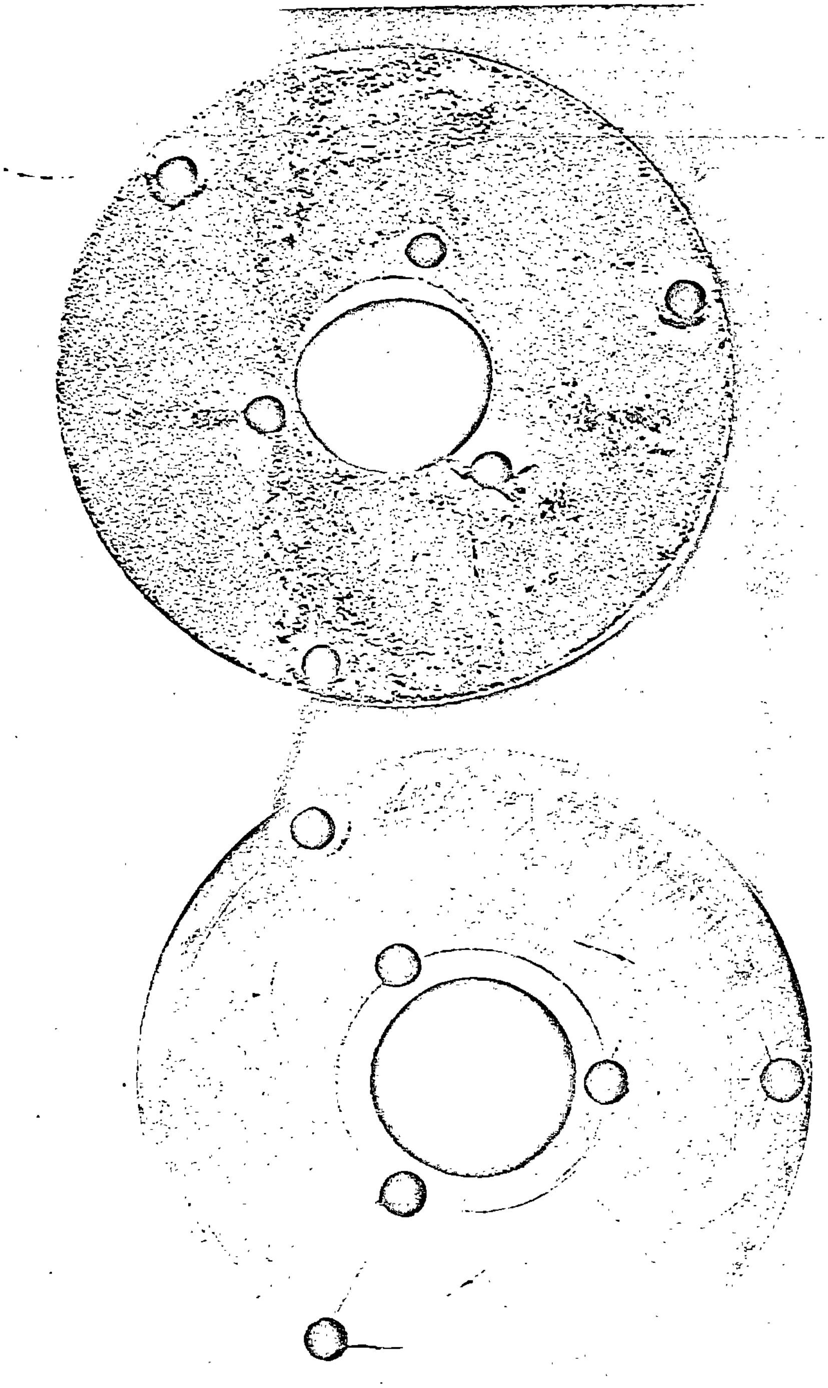

Figure 112. GFE Thermal Conductivity Specimens Showing Different Hole Configurations.

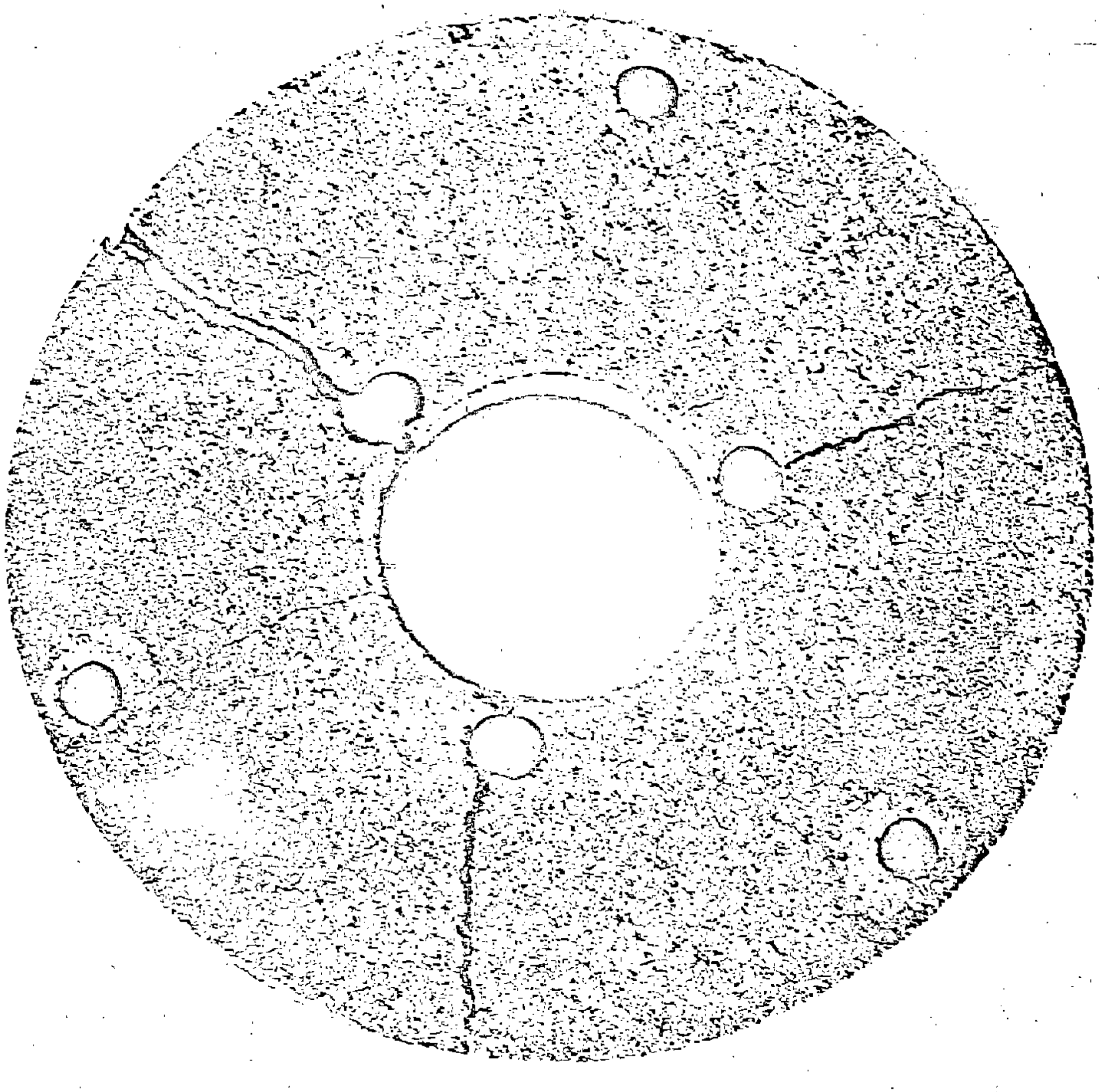

Figure 113. Exposed GFE Thermal Conductivity Specimen.

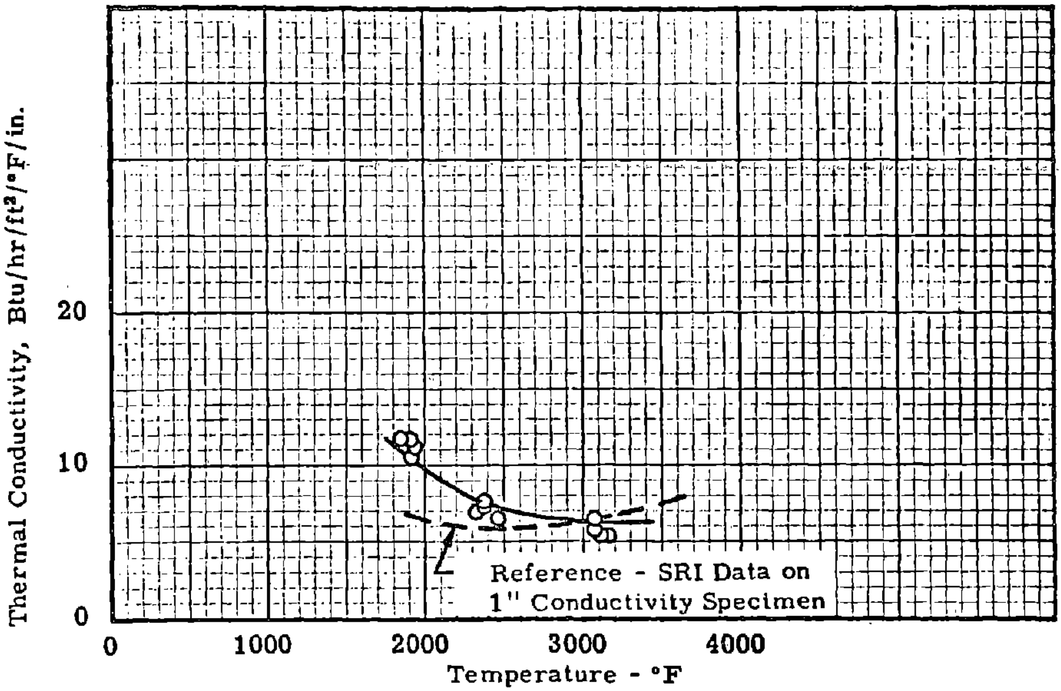

Figure 114. Thermal Conductivity of Cerium Dioxide with GFE Apparatus

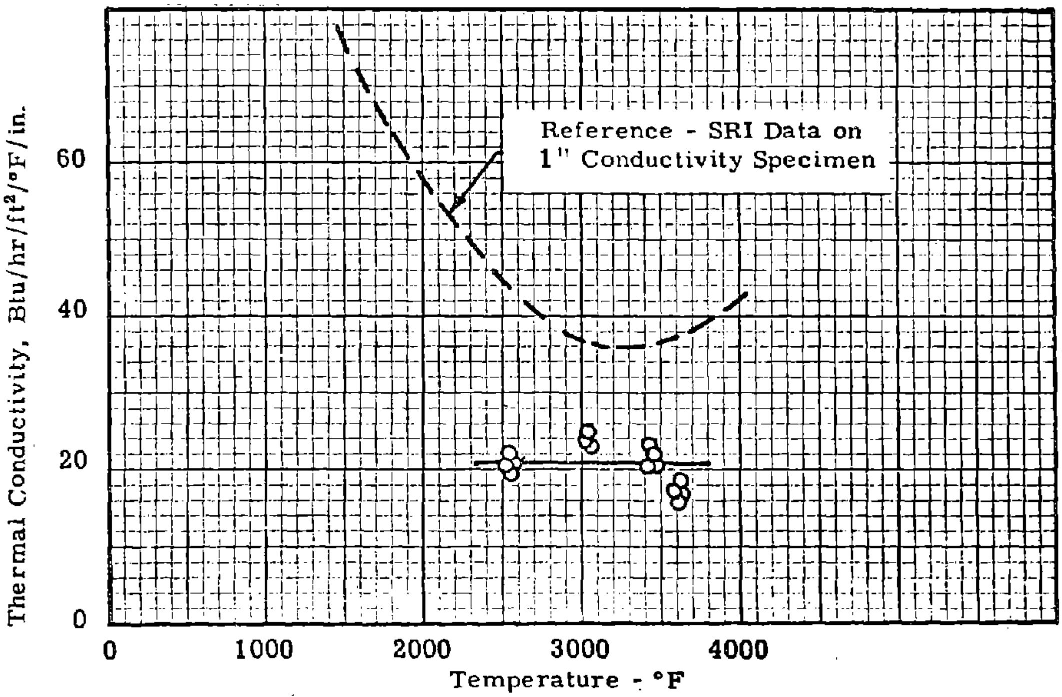

Figure 115. Thermal Conductivity of Magnesium Oxide with GFE Apparatus

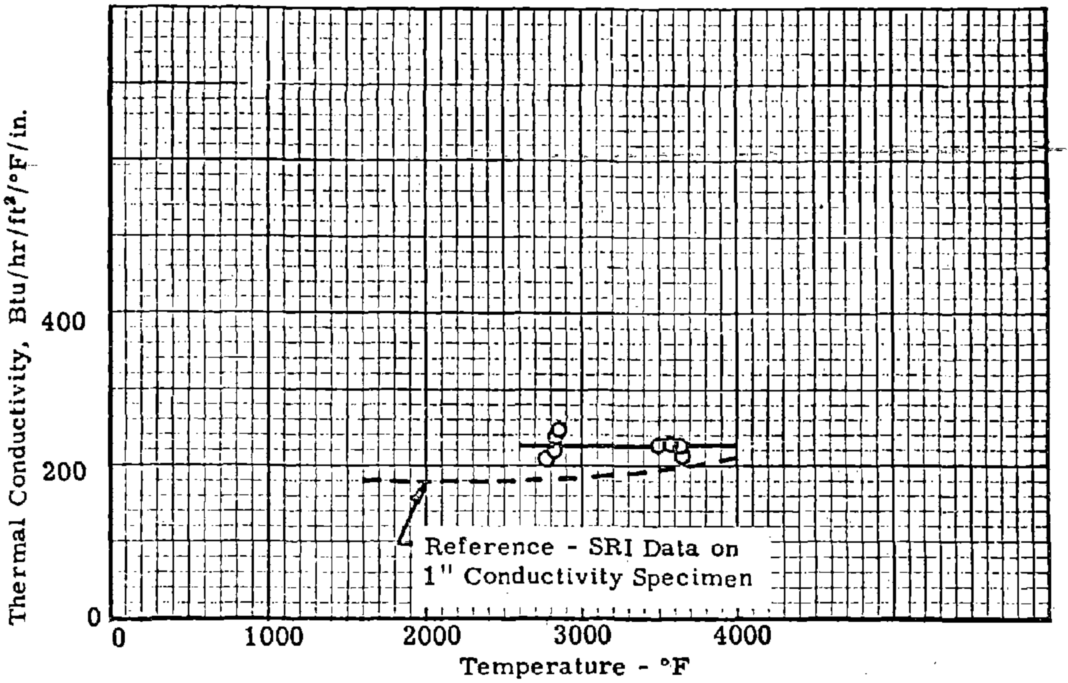

Figure 118. Thermal Conductivity of Molybdenum +0.5% Titanium with GFE Apparatus

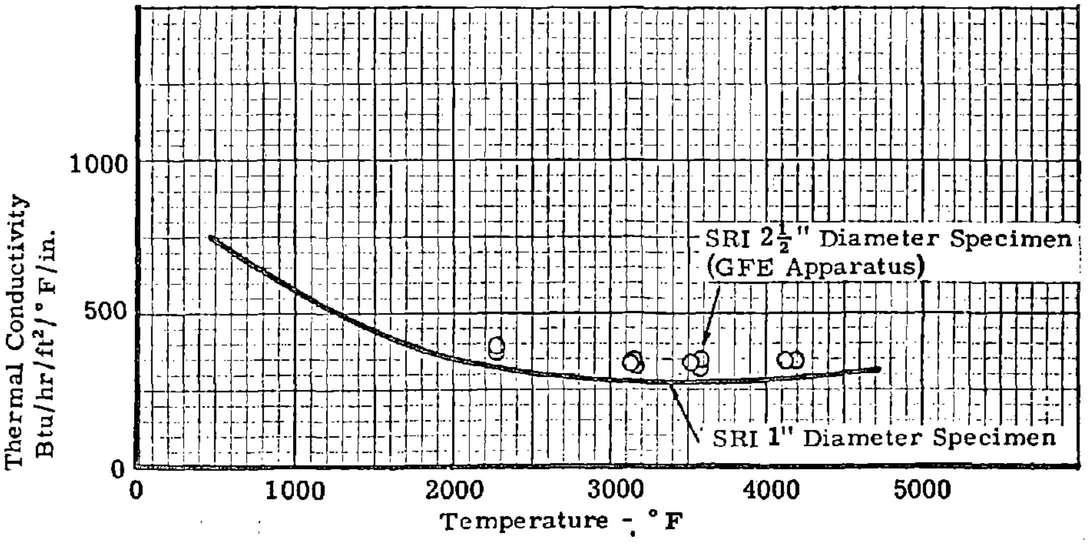

Figure 119. Thermal Conductivity of ATJ Graphite Using 1" and 2½" Diameter Specimens.

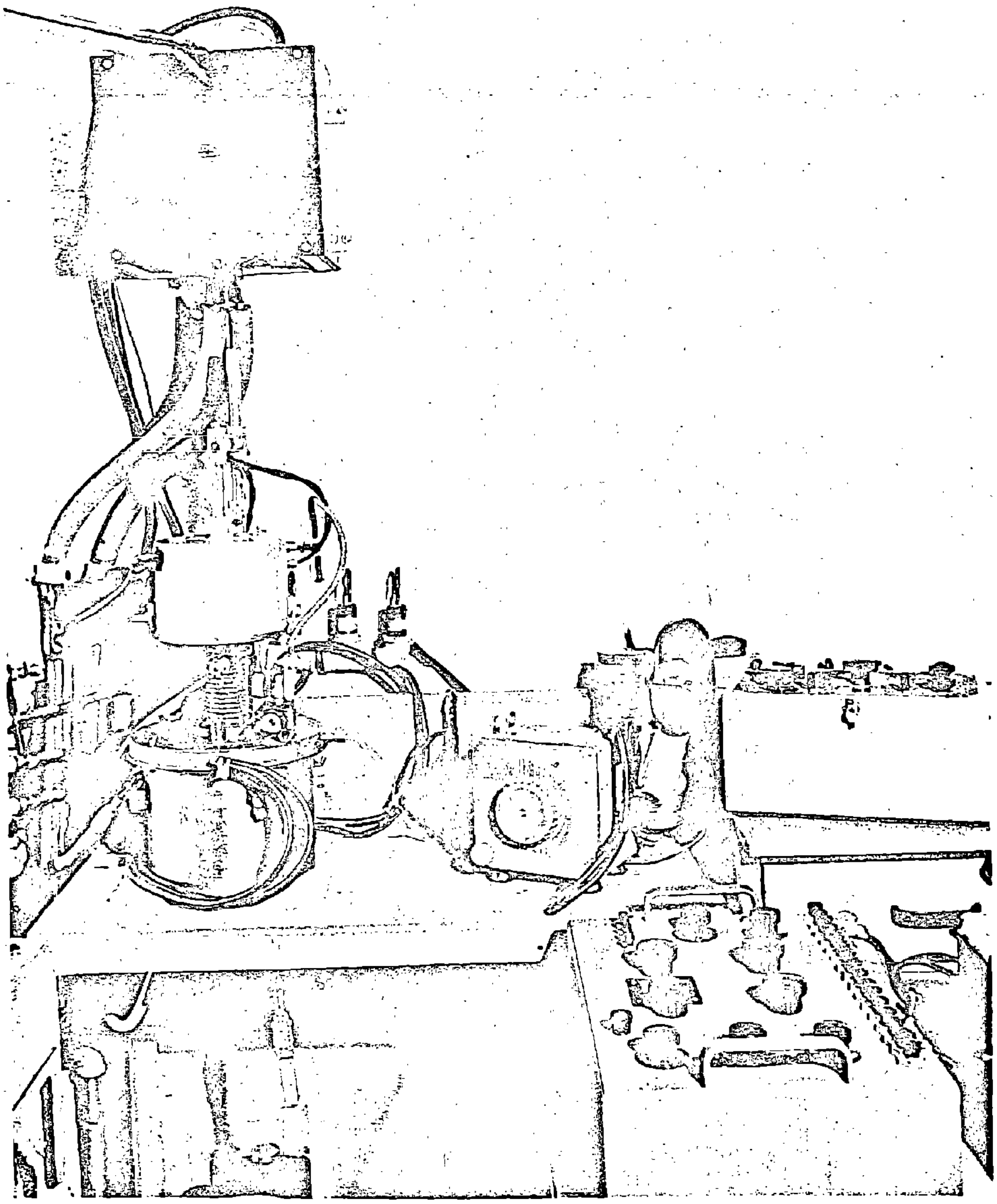

Figure 120. Picture of the Apparatus for Measuring Total Normal Emittance.

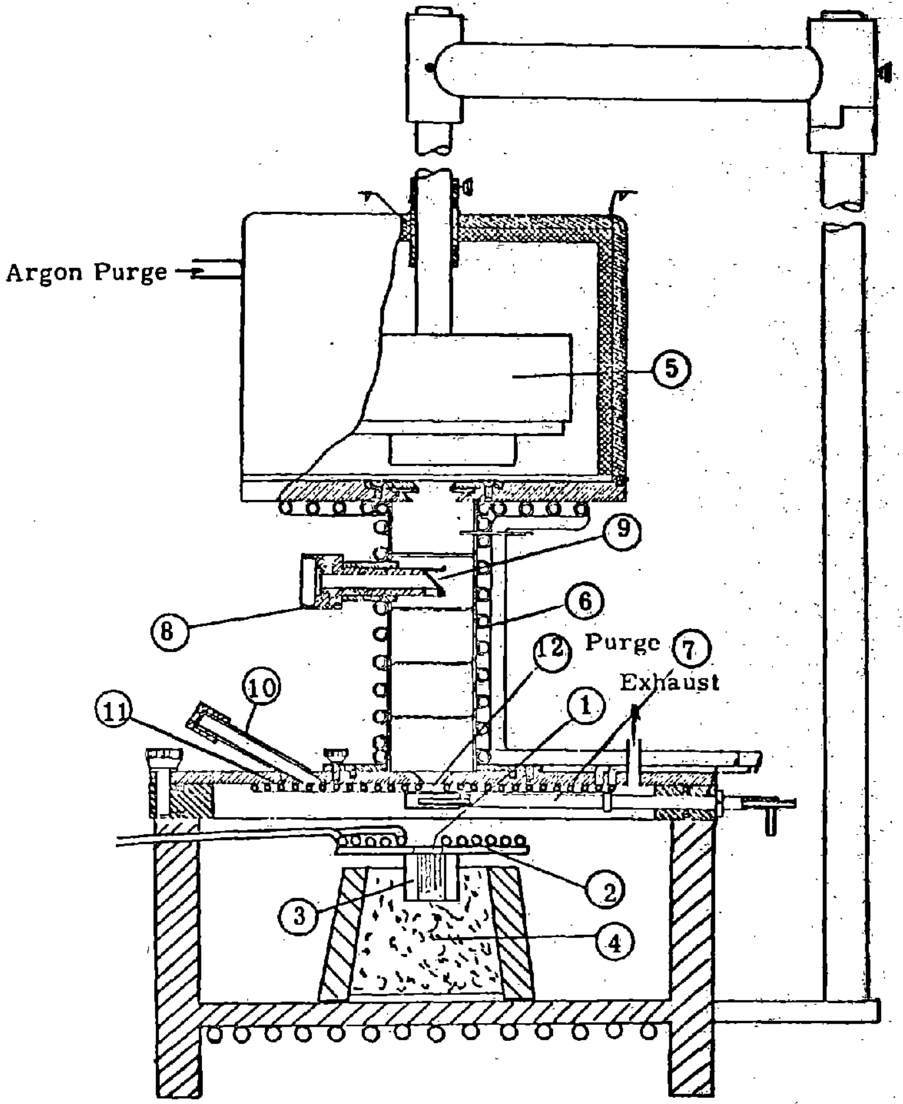

1. **Specimen**
2. **Induction Coil**
3. **Zirconia Cylinder Filled with Fine Zirconia Grog and Tungsten Wire**
4. **Crucible Filled with Coarse Zirconia Grog**
5. **Radiometer**
6. **Water-cooled Tube**
7. **Blank-off Valve**
8. **Main Optical Port**
9. **Right-angle Mirror for Viewing Target Area**
10. **Auxiliary Optical Port**
11. **Cooling Coils**
12. **$\frac{1}{4}$" Round Stop to Limit Receiver Field**

Figure 121. Cross Section of Emittance Apparatus with Flat Coil Furnace.

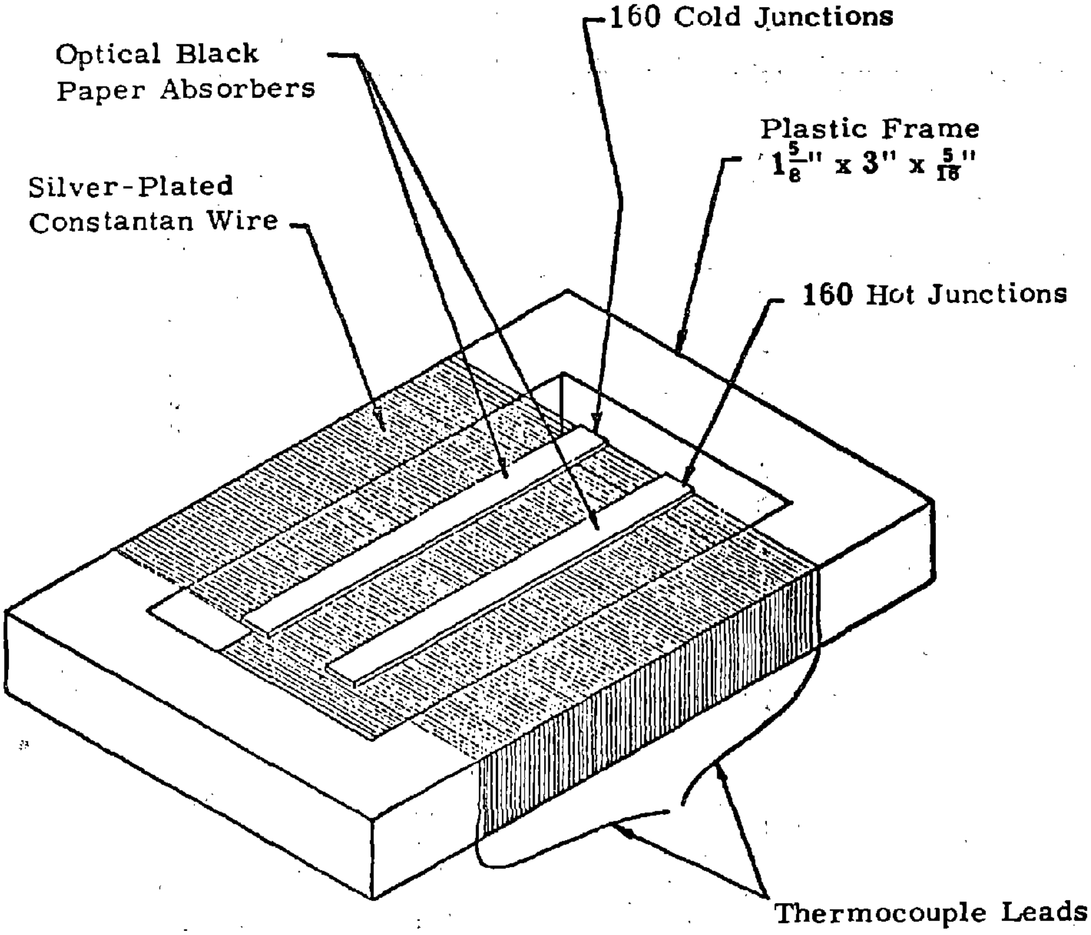
160 Cold Junctions
Optical Black Paper Absorbers
Plastic Frame
$1\frac{5}{8}" \times 3" \times \frac{5}{16}"$
Silver-Plated Constantan Wire
160 Hot Junctions
Thermocouple Leads

Figure 122. Schematic of 160-Junction Thermopile in Emissivity Equipment.

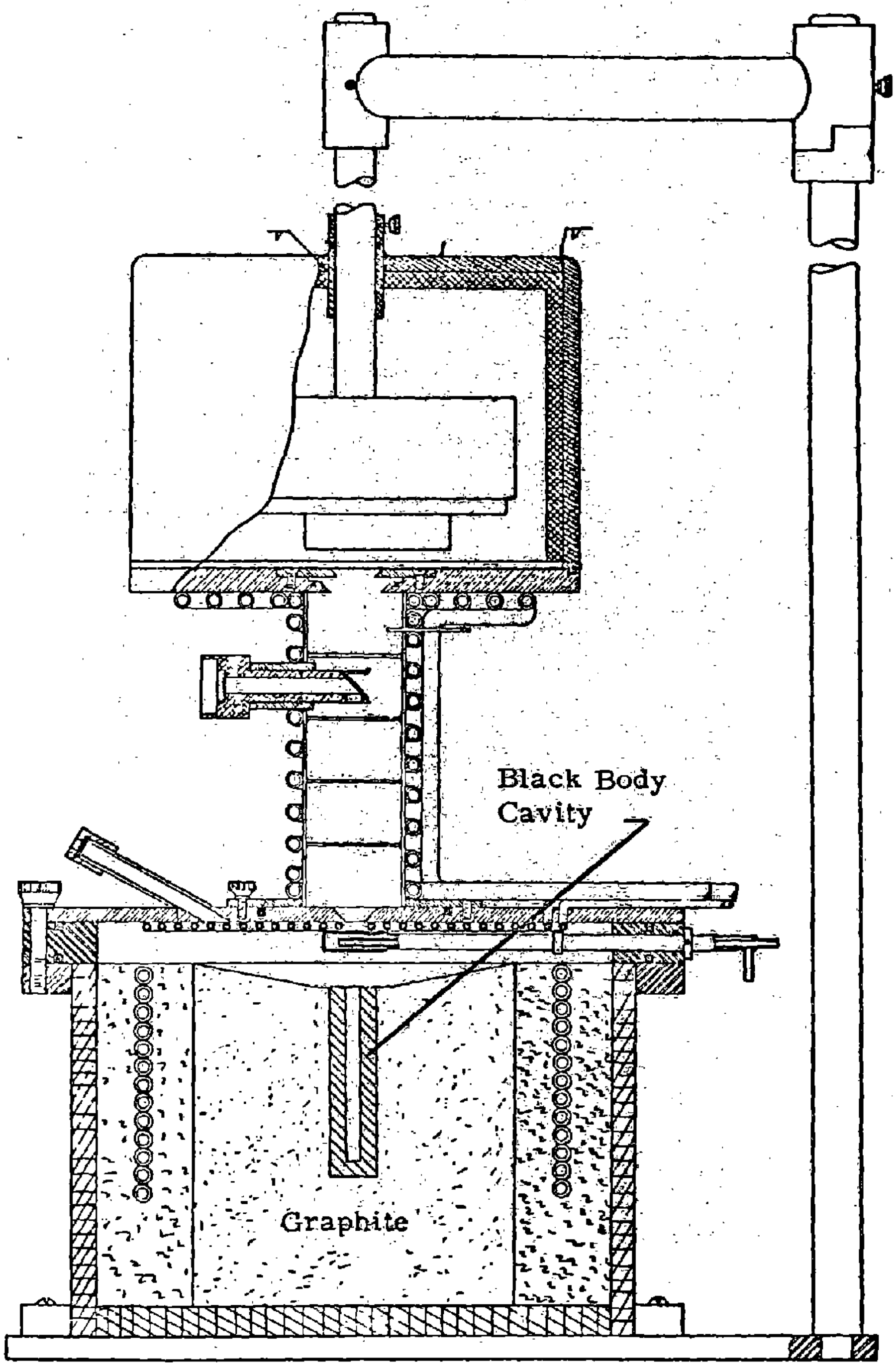

Figure 123. Cross Section of Emittance Apparatus with Black Body Furnace.

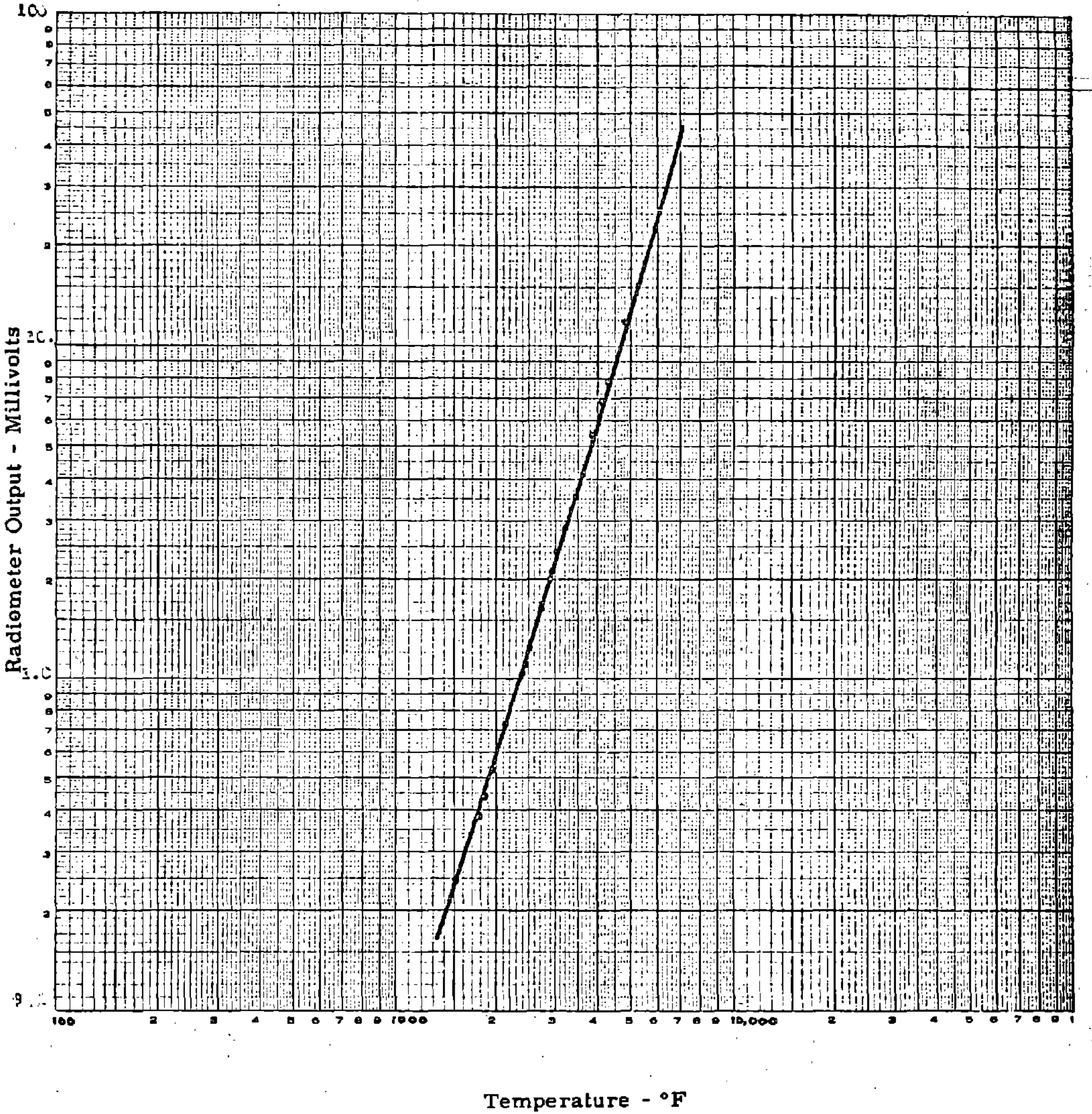

Figure 124. Black Body Calibration Curve.

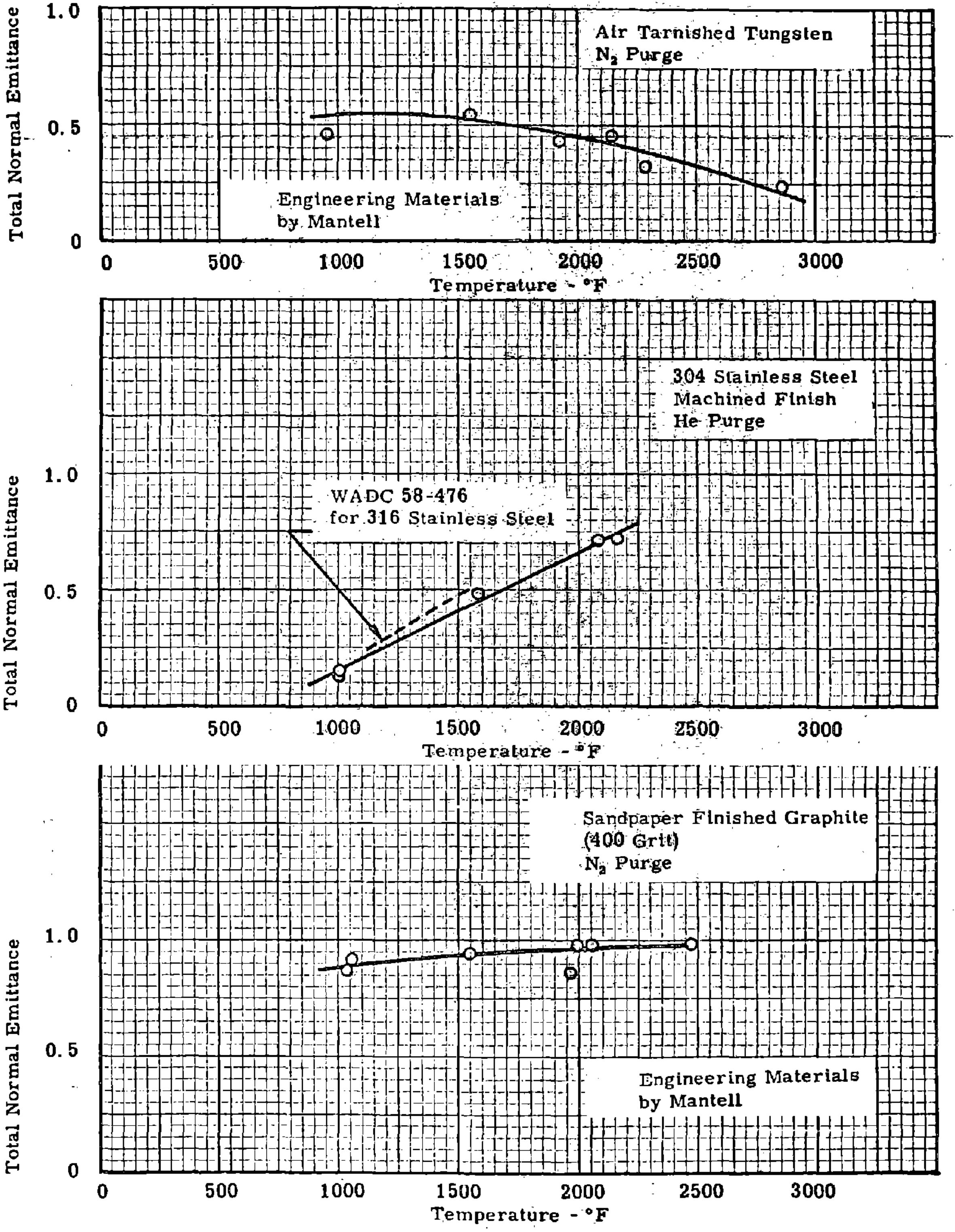

Figure 125. Calculation Standards for Total Normal Emittance.

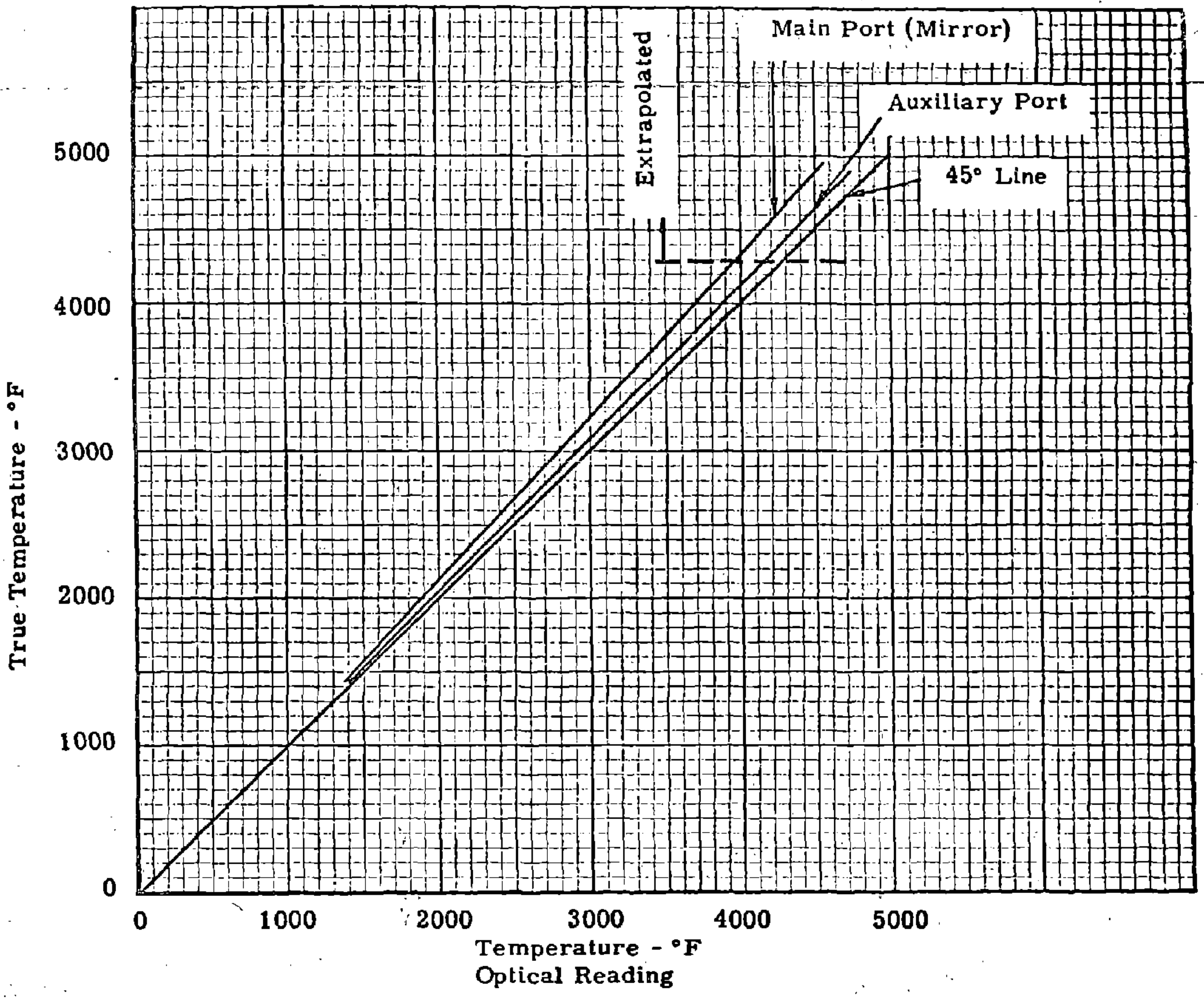

Figure 126. Correction for Mirror and Sapphire Window in Emittance Apparatus.

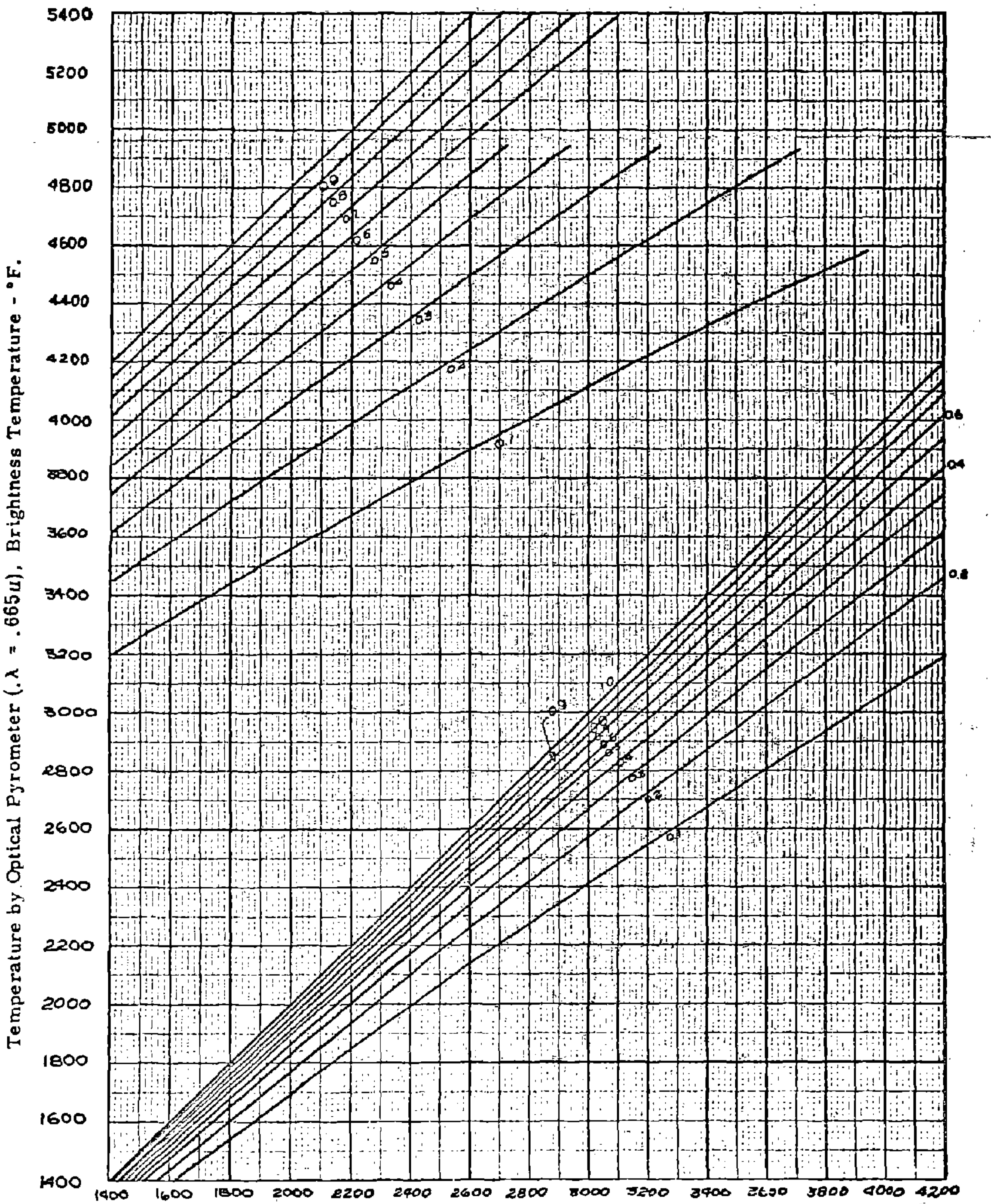

Figure 127. Correction for Brightness Temperature to True Temperature.

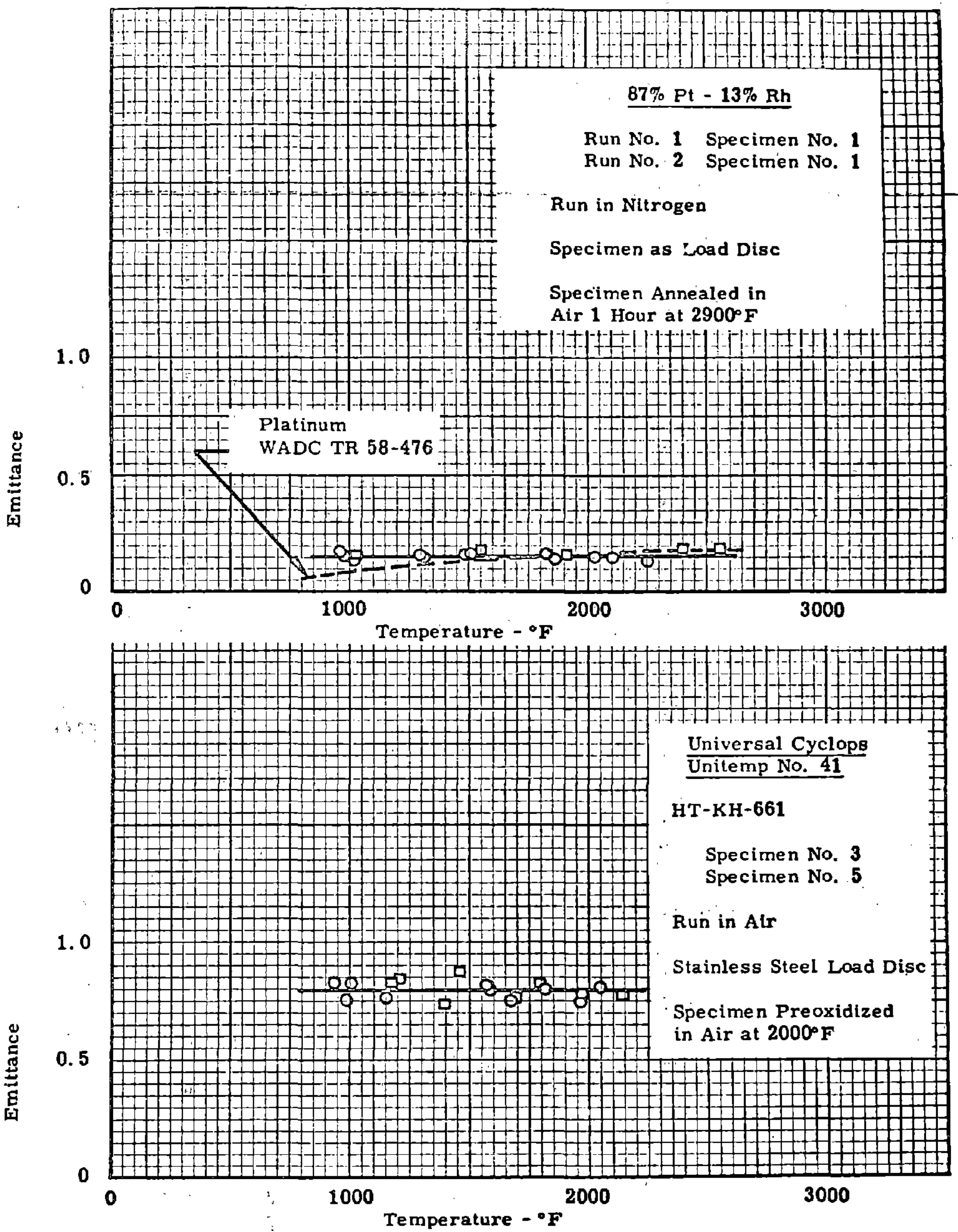

Figure 128. Calibration Standards for Total Normal Emittance.

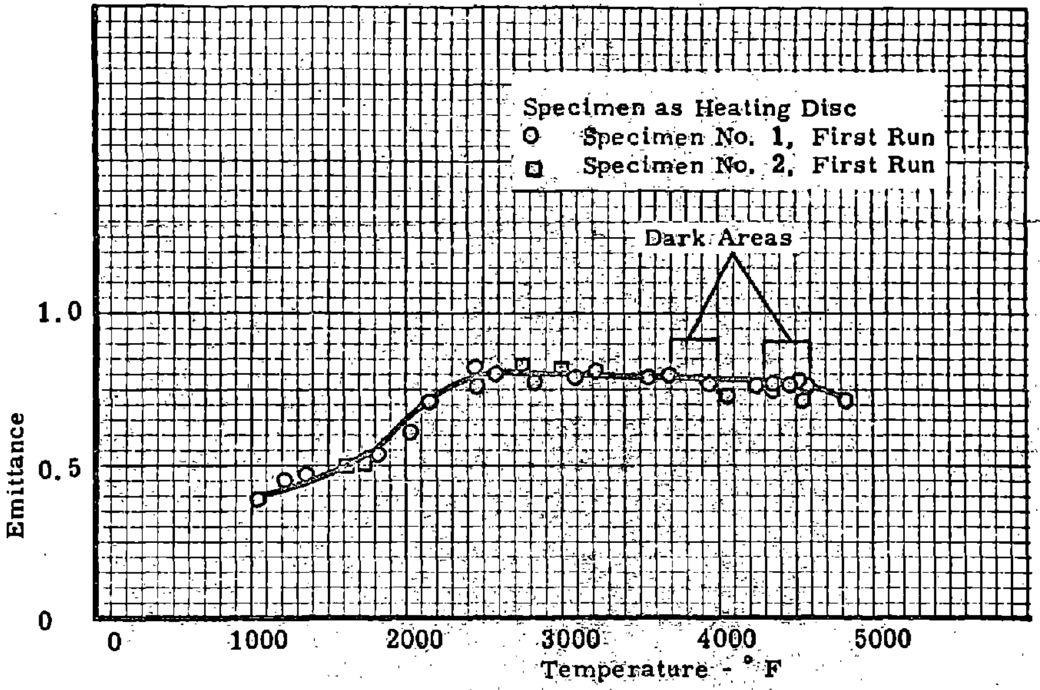

Figure 129. Total Normal Emittance of Hafnium Diboride.

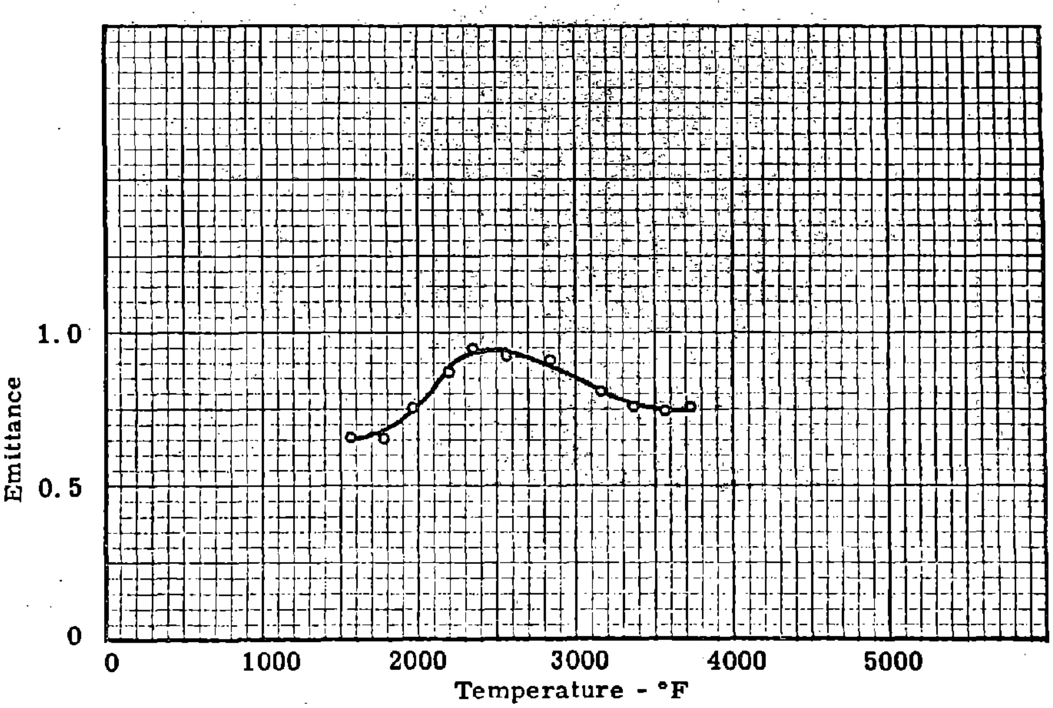

Figure 130. Total Normal Emittance of Thorium Tetraboride.

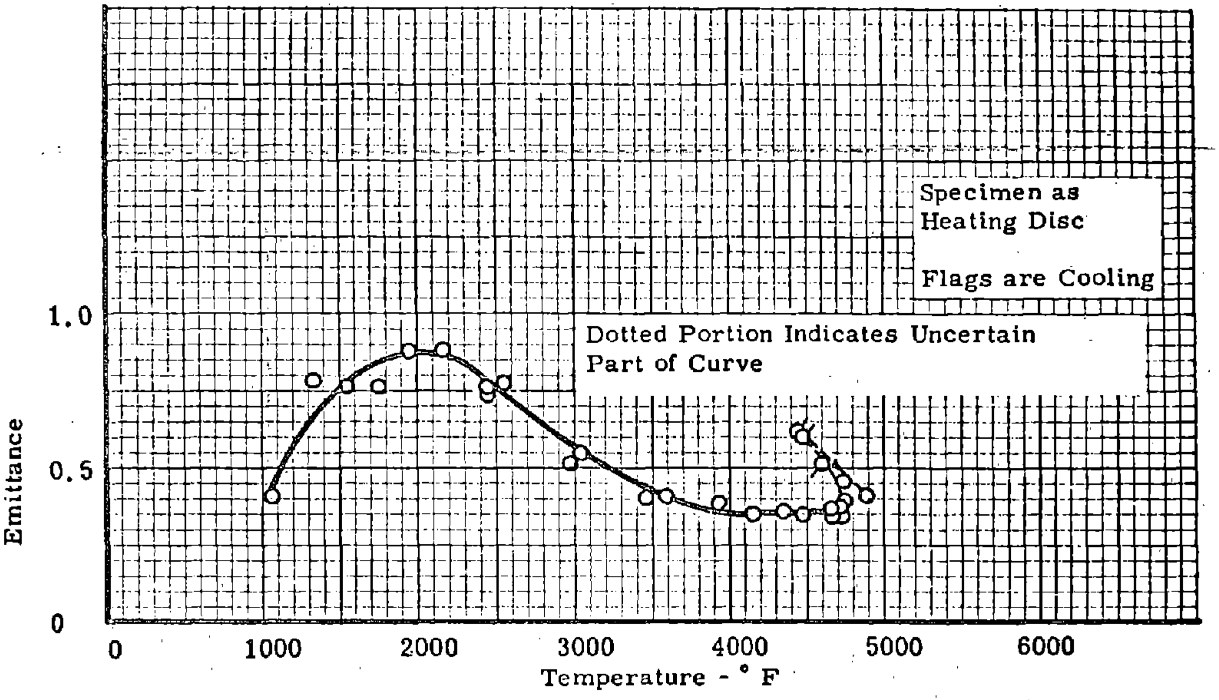

Figure 131. Total Normal Emittance of Titanium Diboride.

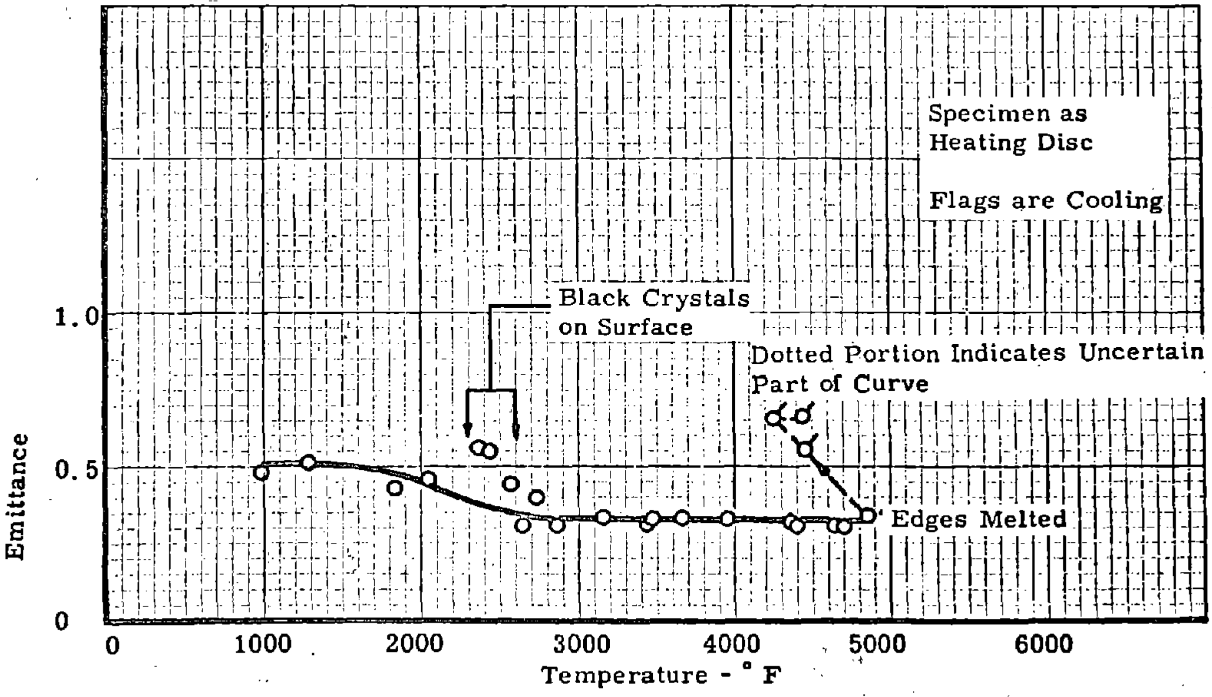

Figure 132. Total Normal Emittance of Tungsten Boride.

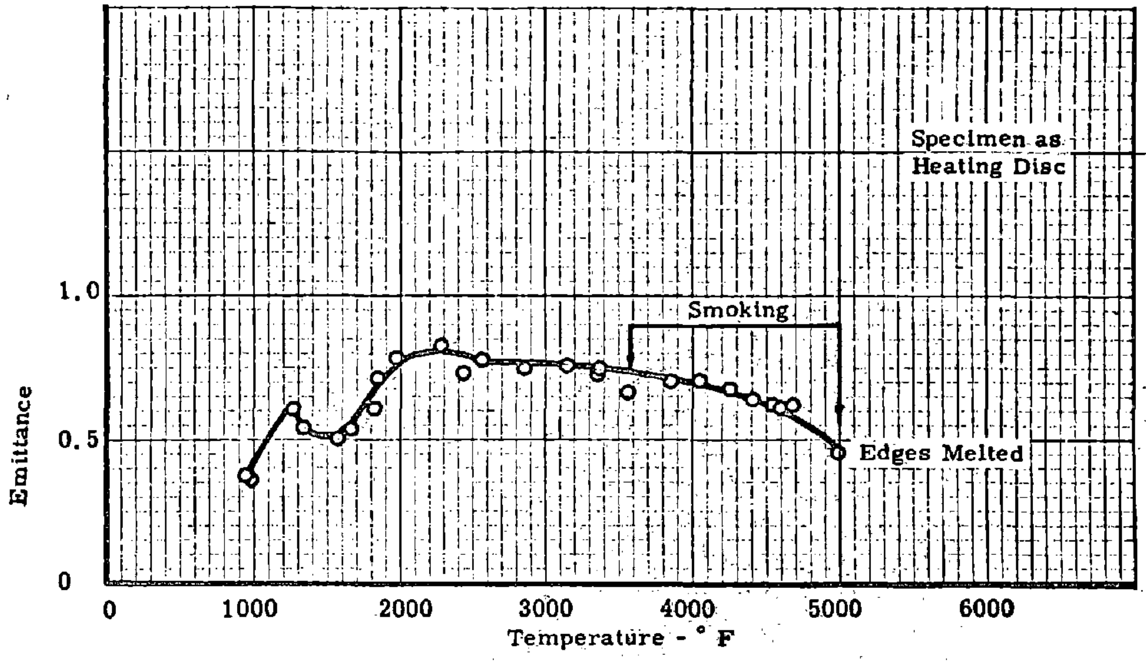

Figure 133. Total Normal Emittance of Zirconium Diboride.

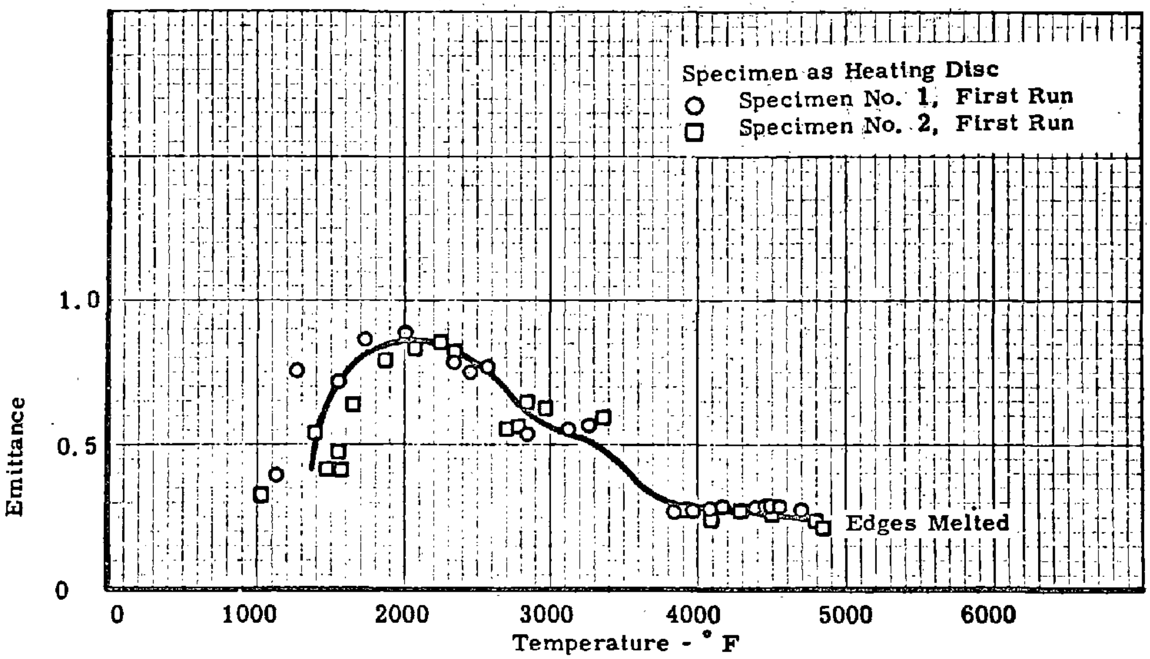

Figure 134. Total Normal Emittance of Columbium Carbide.

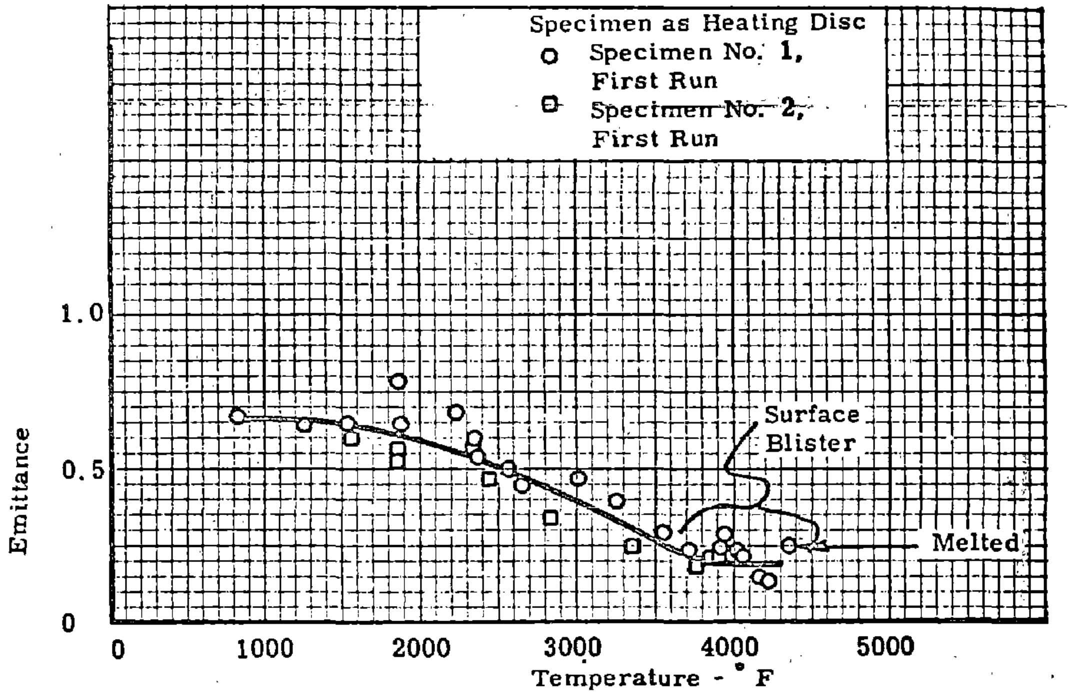

Figure 135. Total Normal Emittance of Dimolybdenum Carbide.

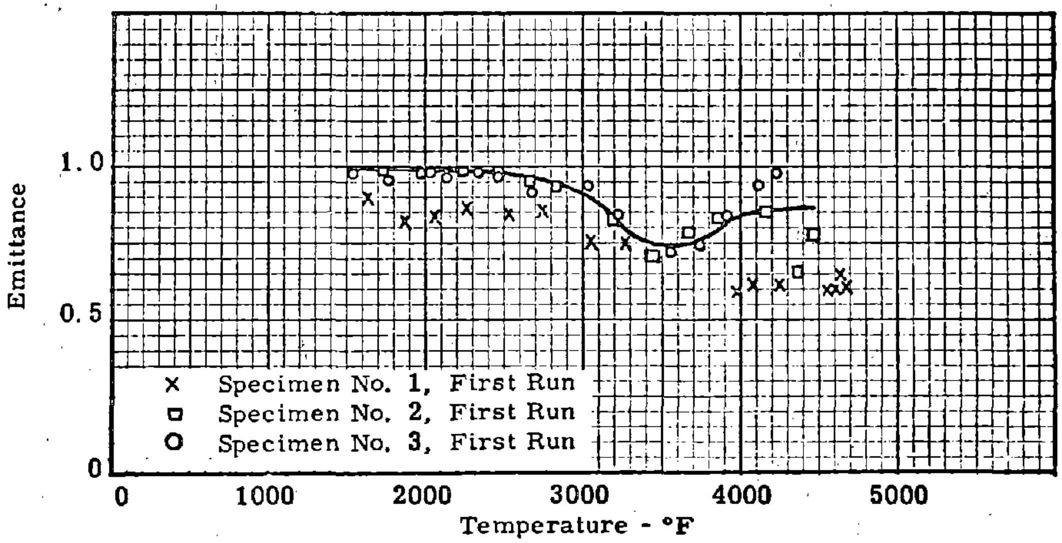

Figure 136. Total Normal Emittance of Hafnium Carbide.

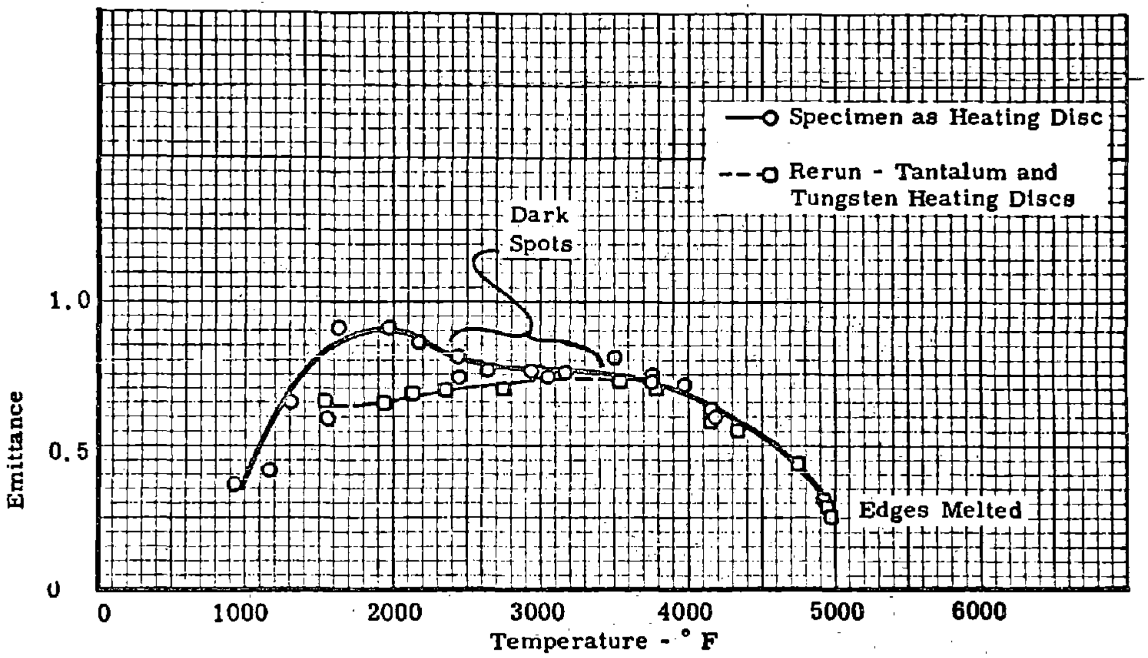

Figure 137. Total Normal Emittance of Tantalum Carbide.

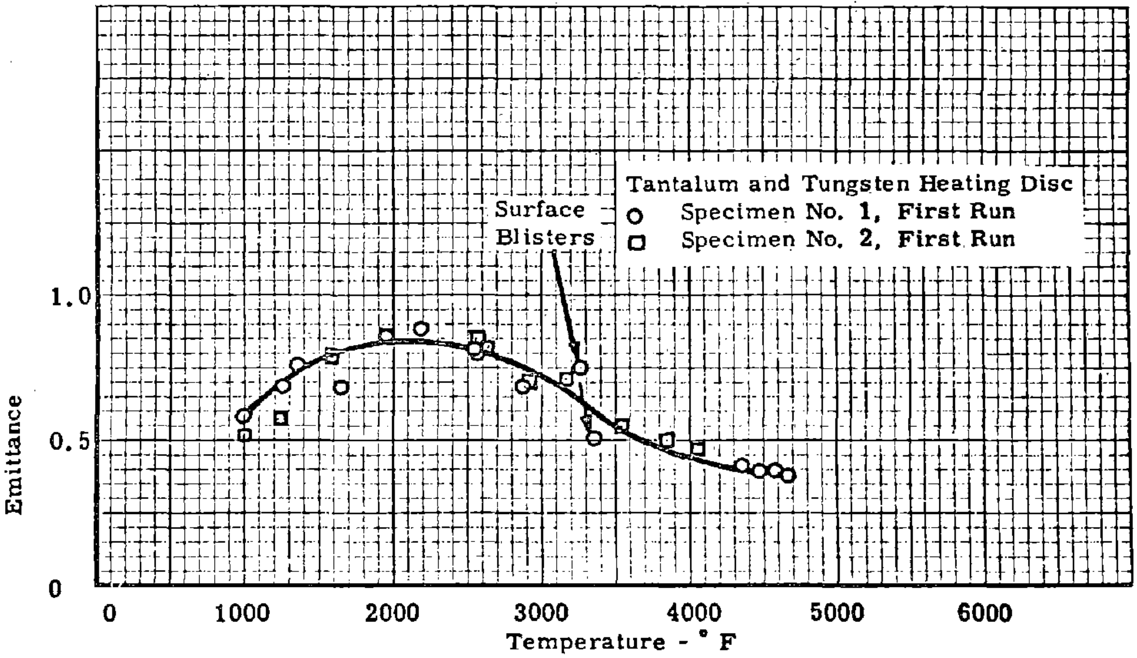

Figure 138. Total Normal Emittance of Titanium Carbide.

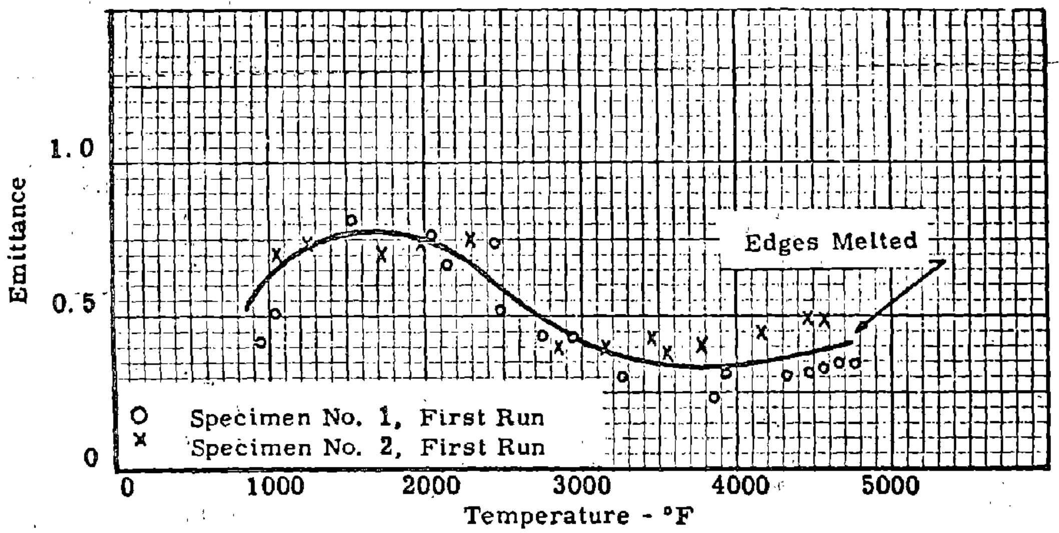

Figure 139. Total Normal Emittance of Tungsten Carbide.

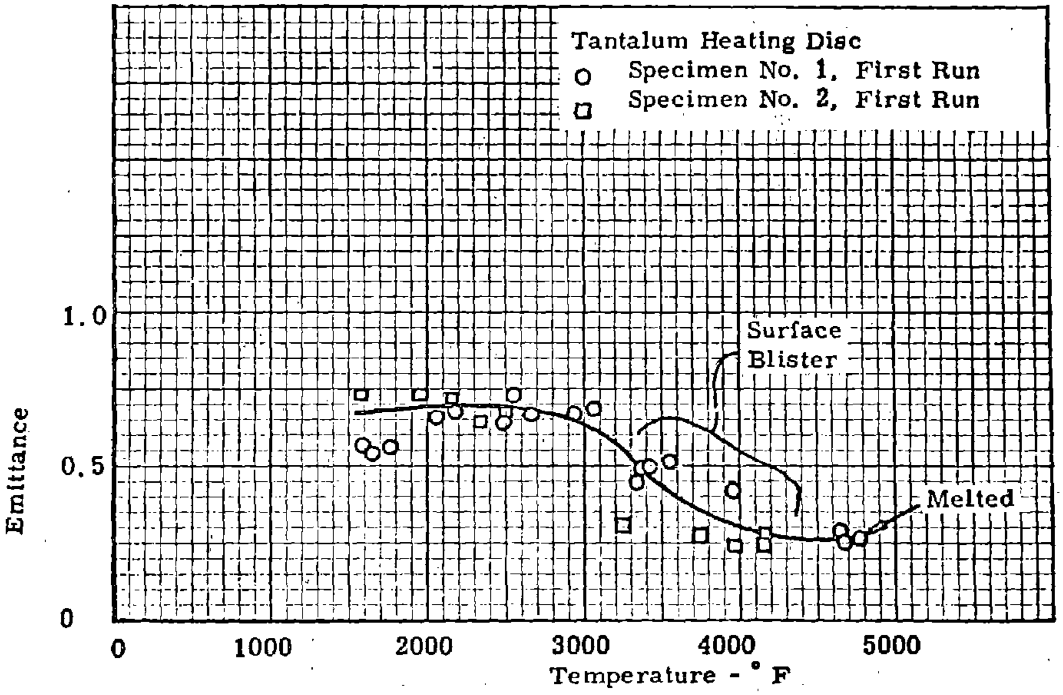

Figure 140. Total Normal Emittance of Vanadium Carbide.

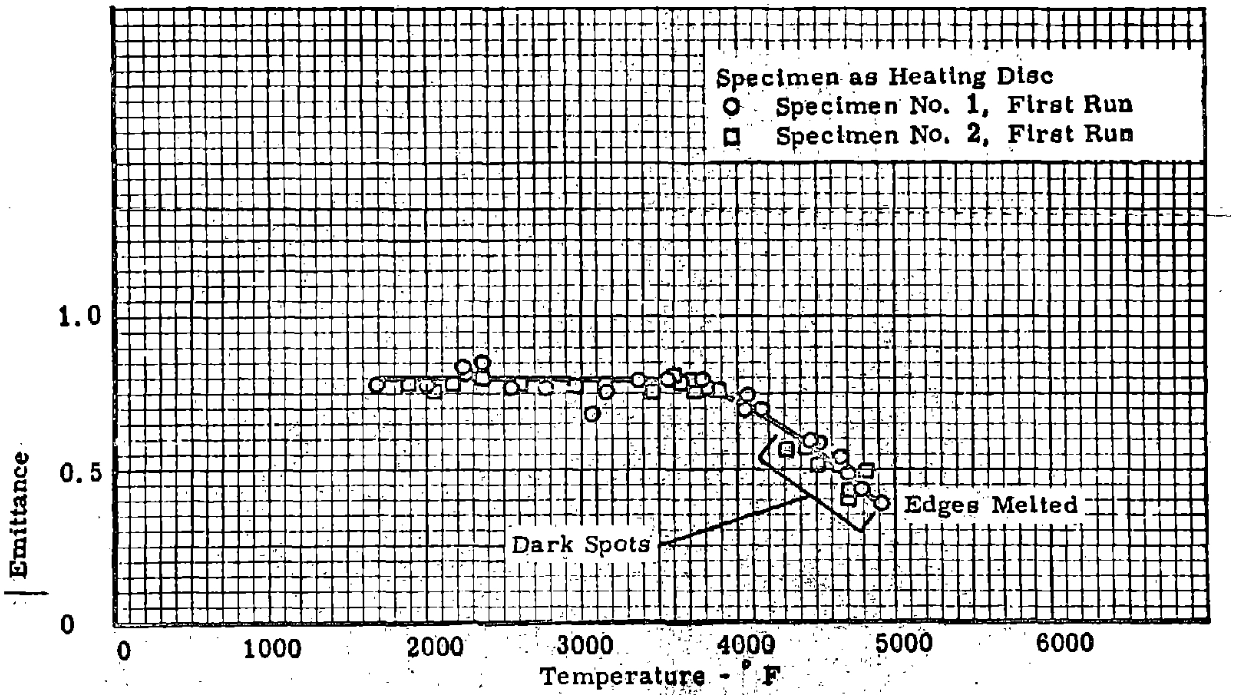

Figure 141. Total Normal Emittance of Zirconium Carbide.

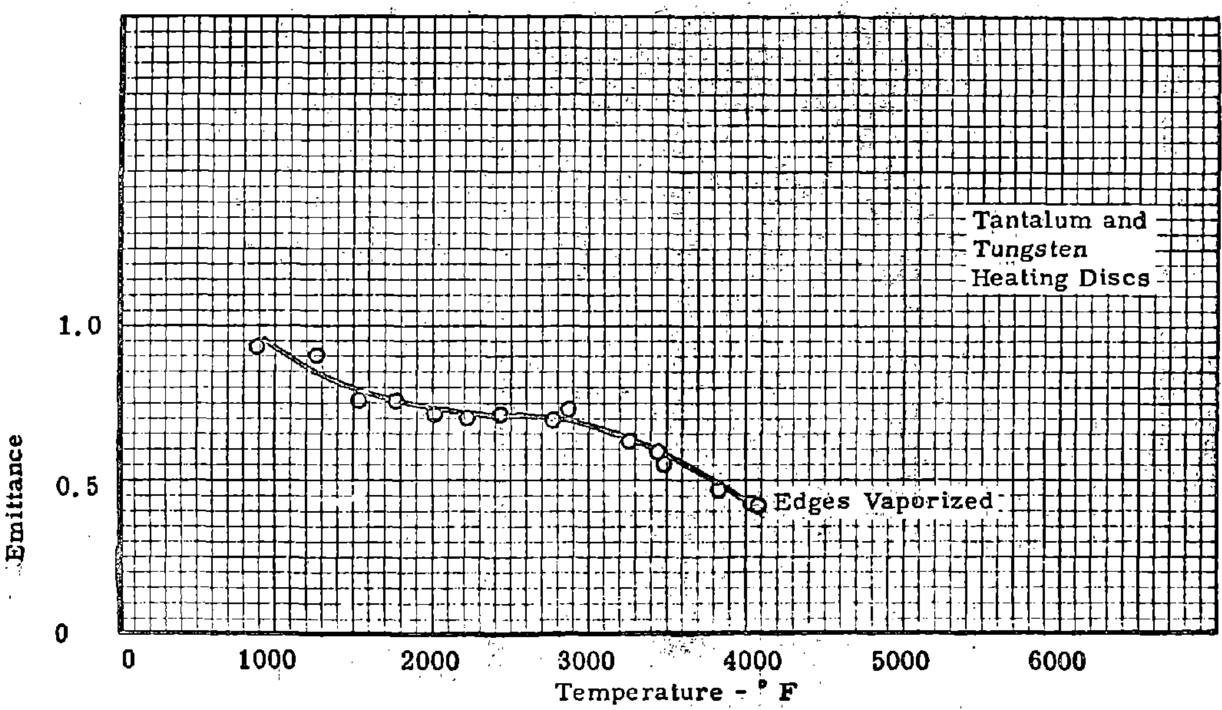

Figure 142. Total Normal Emittance of Boron Nitride.

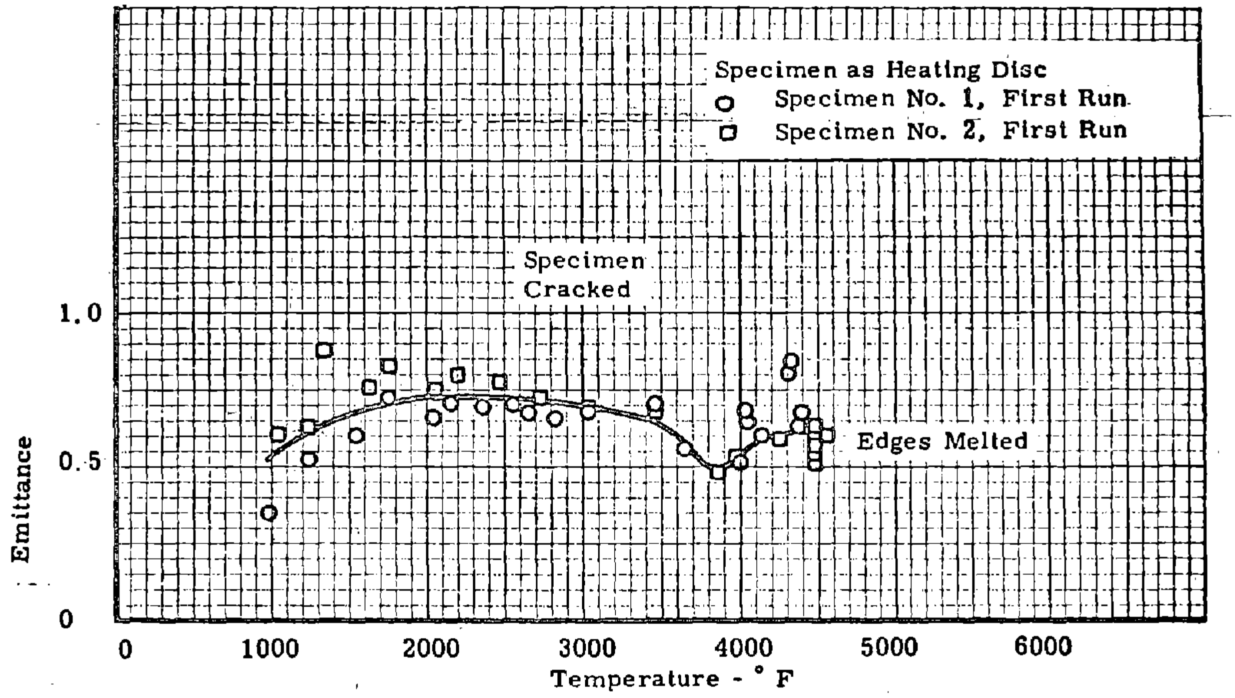

Figure 143. Total Normal Emittance of Hafnium Nitride.

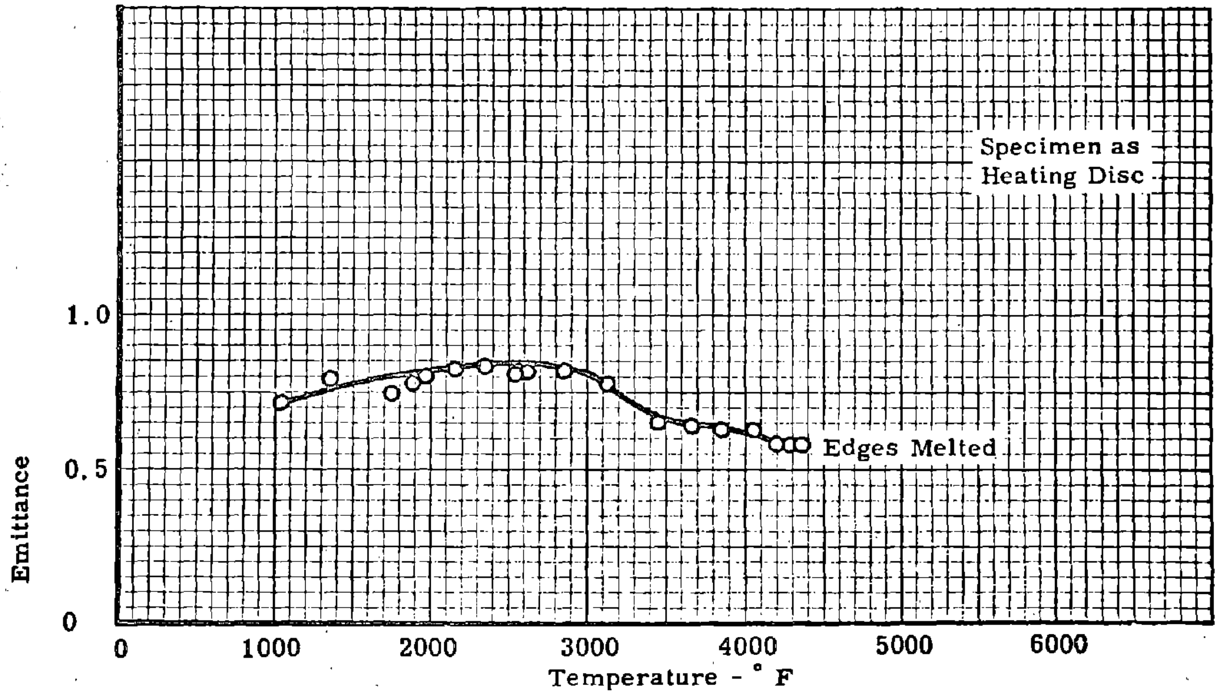

Figure 144. Total Normal Emittance of Tantalum Nitride.

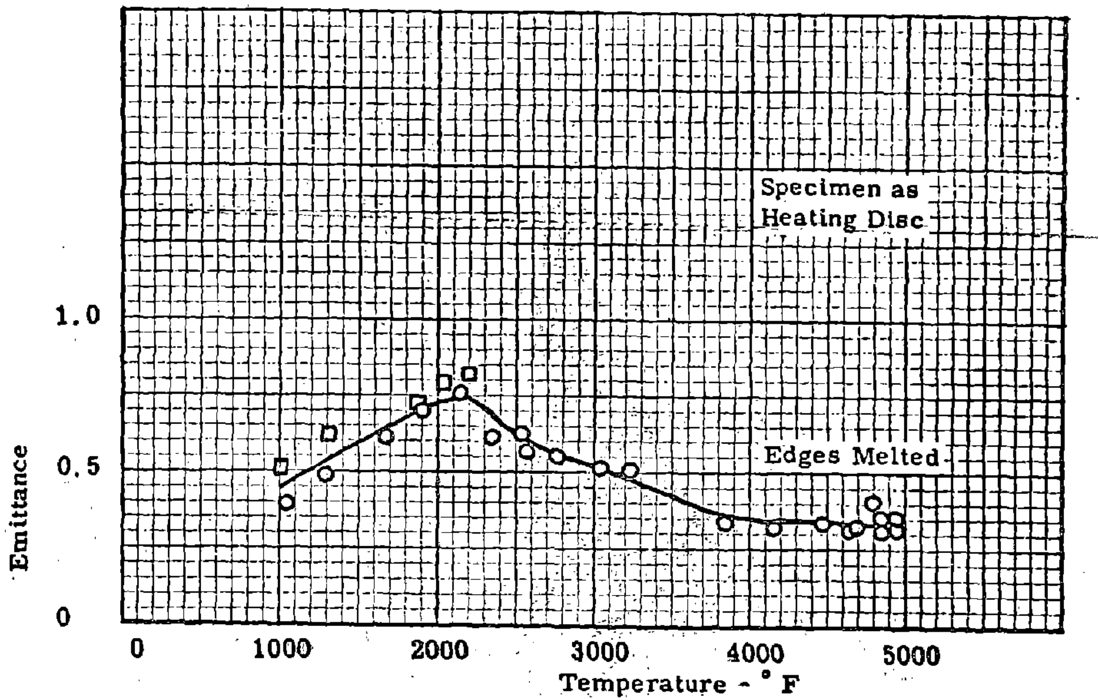

Figure 145. Total Normal Emittance of Titanium Nitride.

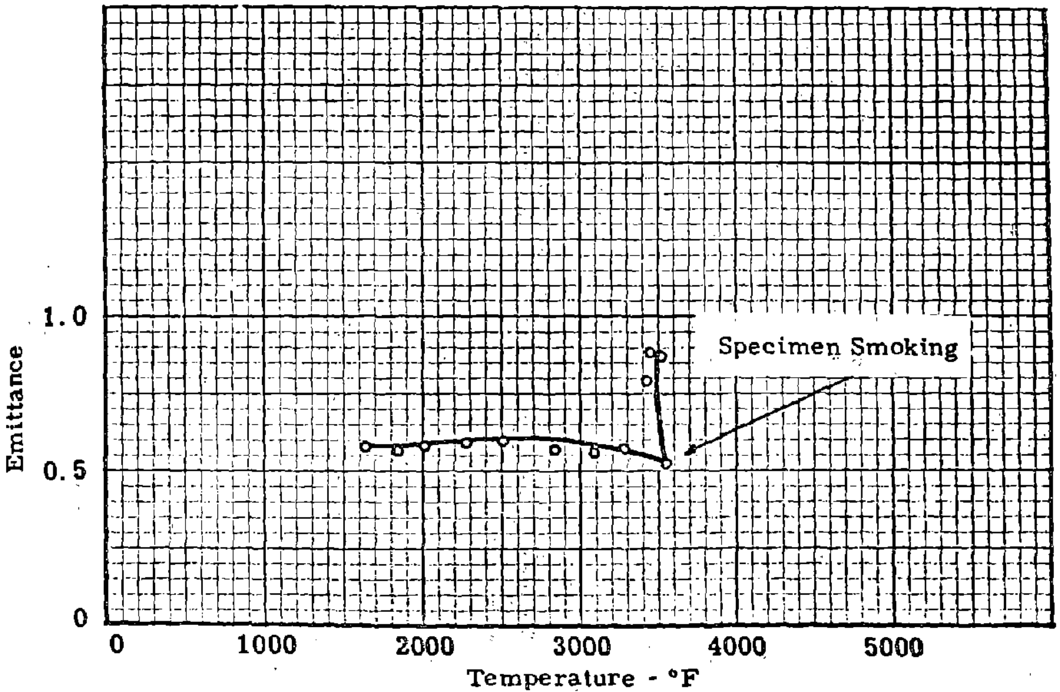

Figure 146. Total Normal Emittance of Beryllium Oxide.

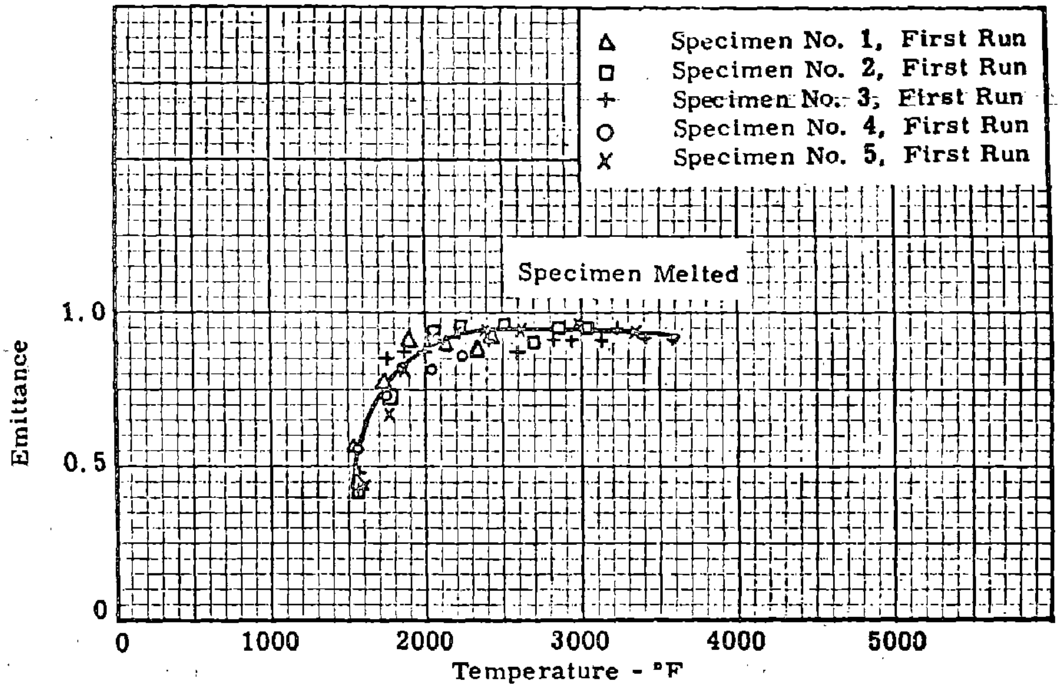

Figure 147. Total Normal Emittance of Cerium Dioxide

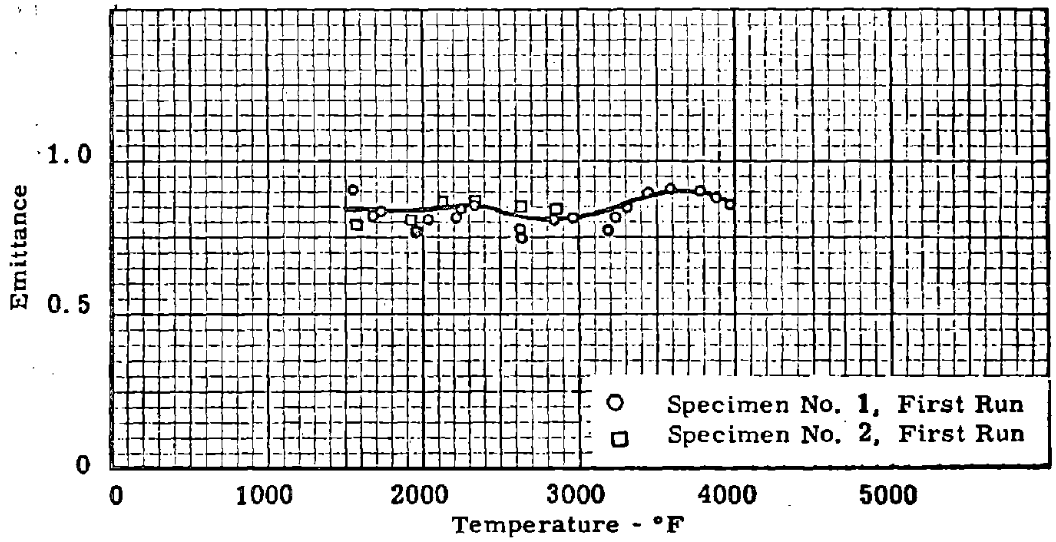

Figure 148. Total Normal Emittance of Hafnium Dioxide

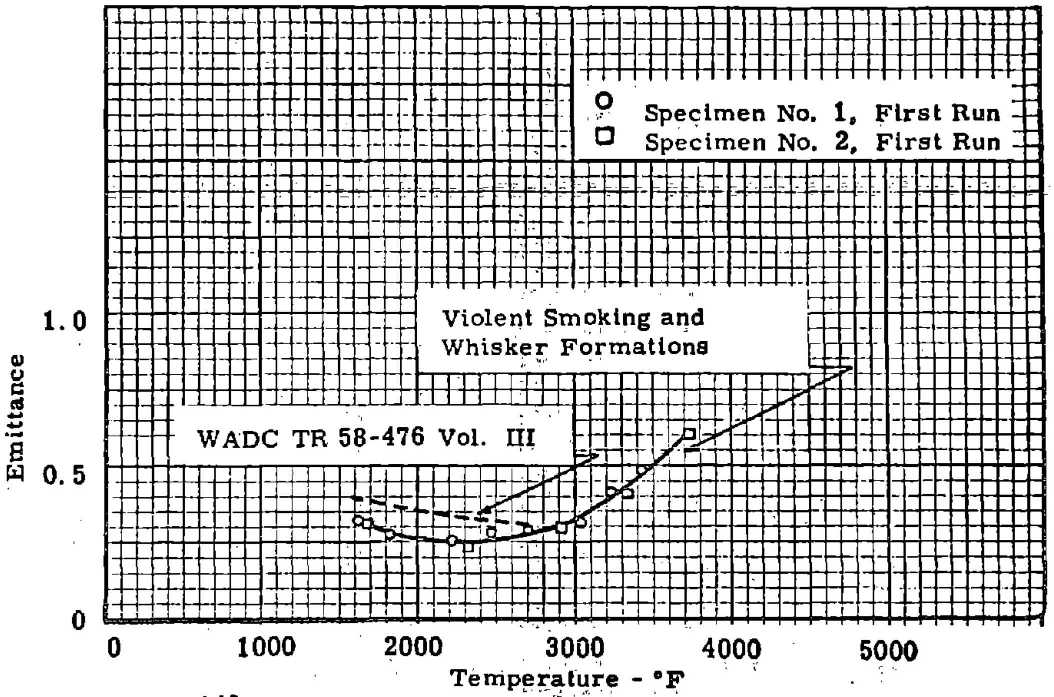

Figure 149. Total Normal Emittance of Magnesium Oxide.

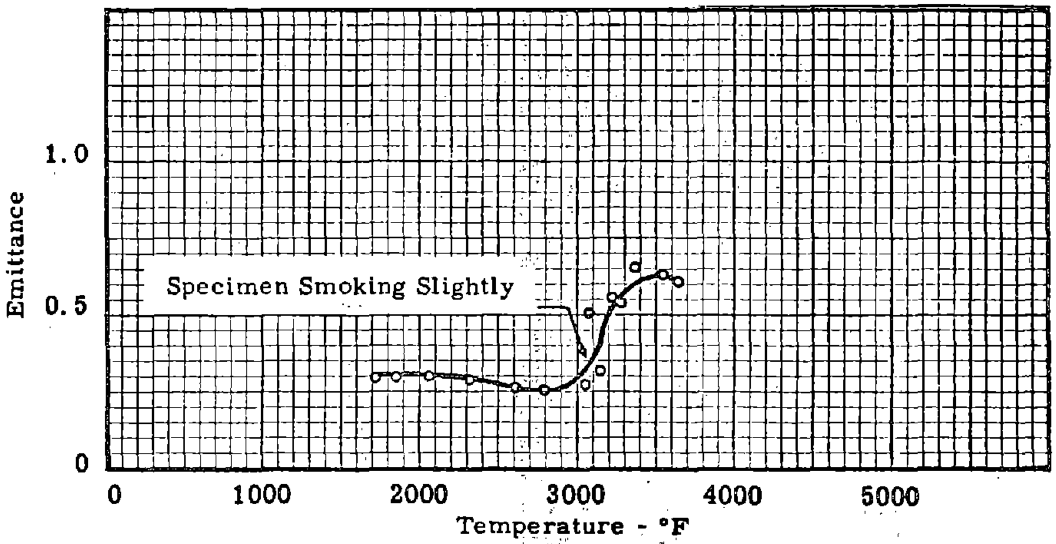

Figure 150. Total Normal Emittance of Thorium Dioxide

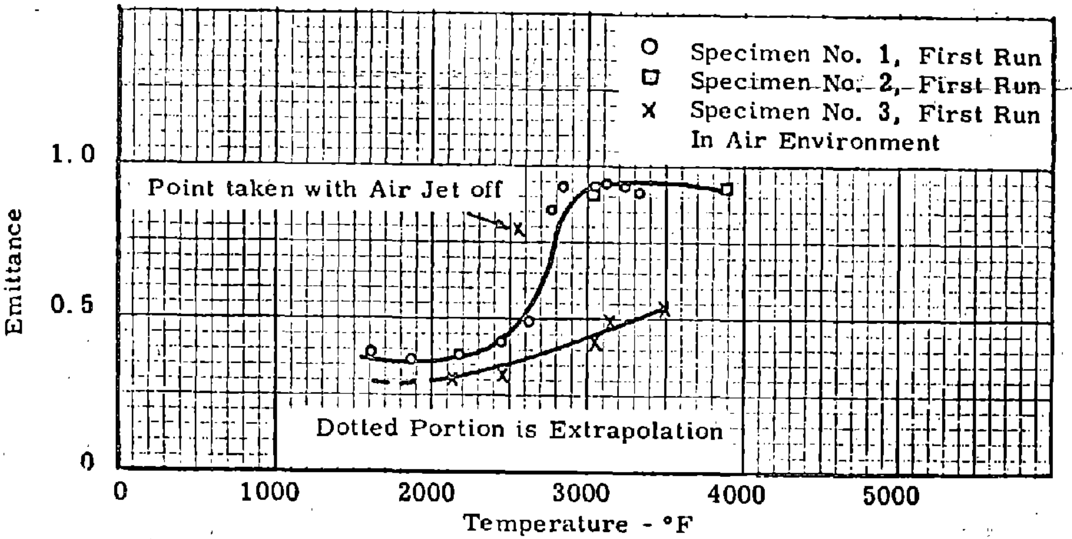

Figure 151. Total Normal Emittance of Zirconium Dioxide

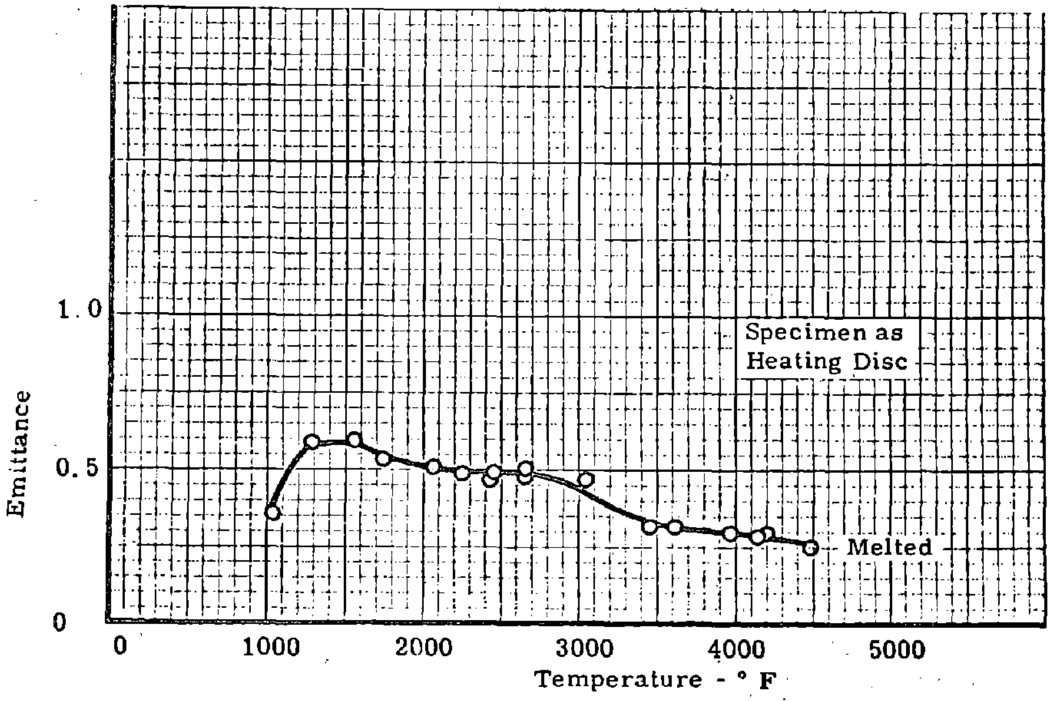

Figure 152. Total Normal Emittance of Columbium +0.5% Zirconium.

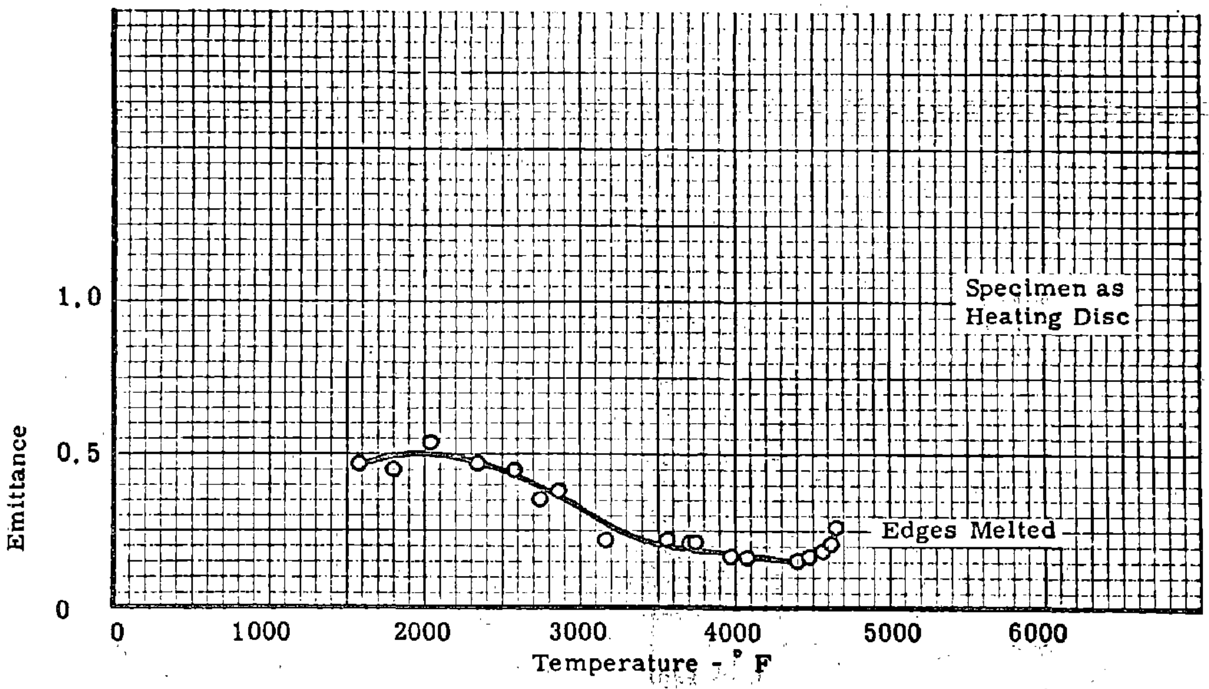

Figure 153. Total Normal Emittance of Molybdenum +0.5% Titanium.

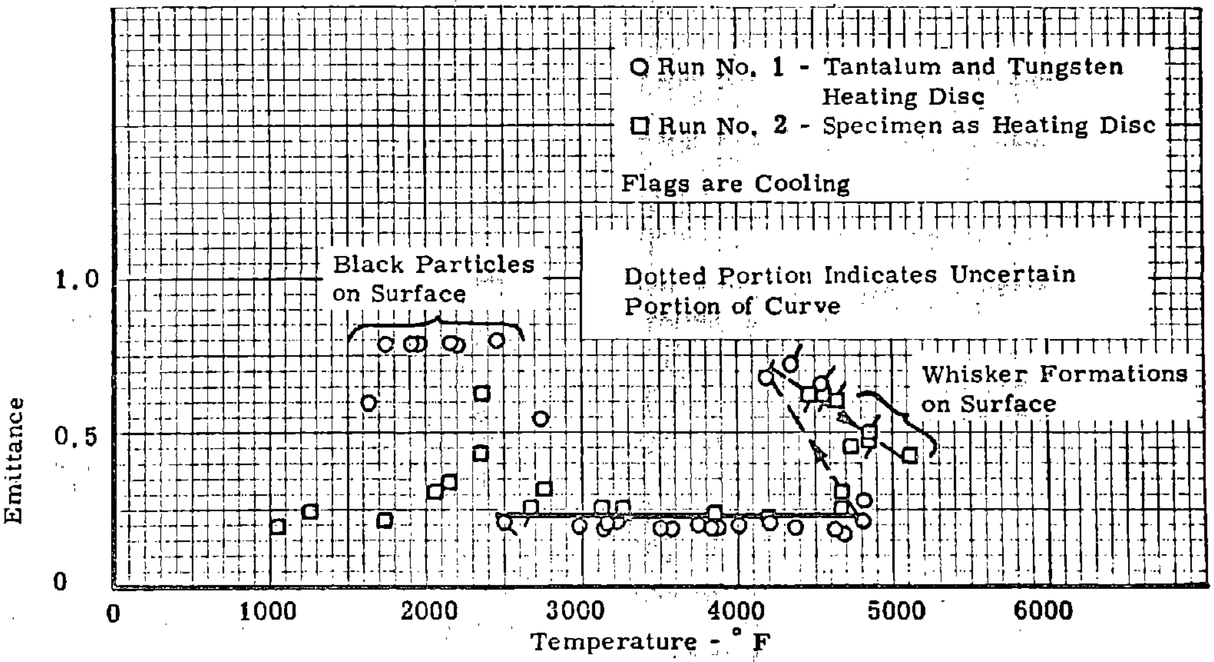

Figure 154. Total Normal Emittance of Tungsten (Carborundum) (Complete Data Including Dark Spots and Whiskers).

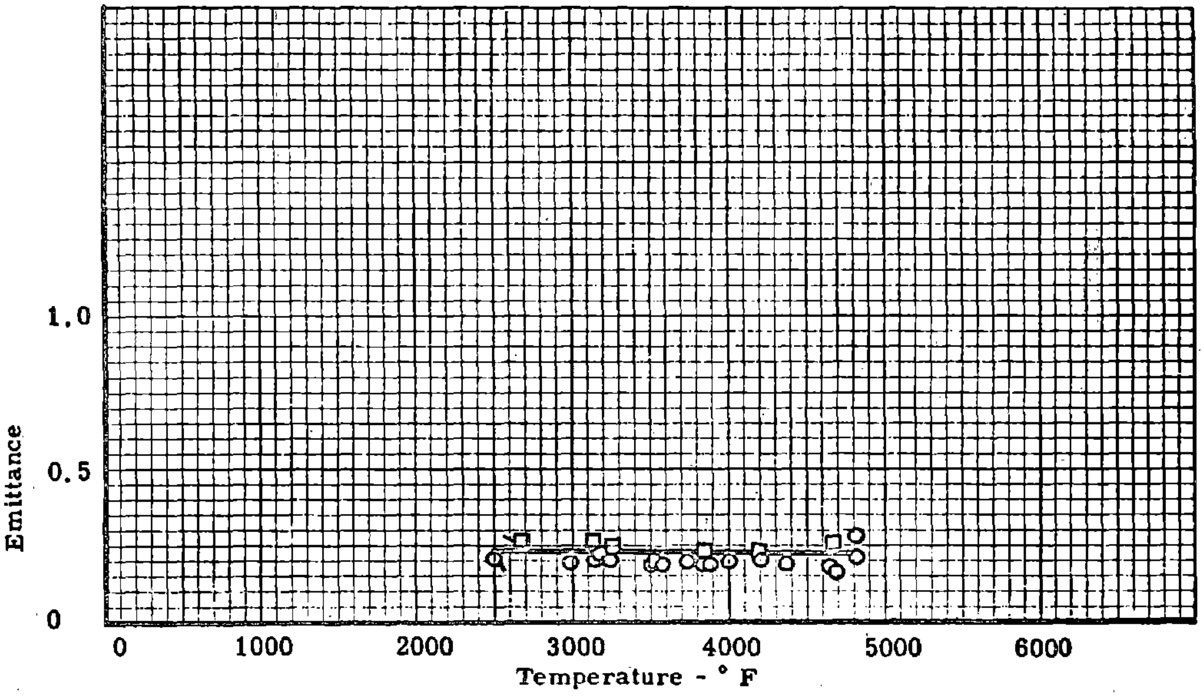

Figure 155. Total Normal Emittance of Tungsten (Reliable Data Unconfounded by Dark Spots or Whiskers).

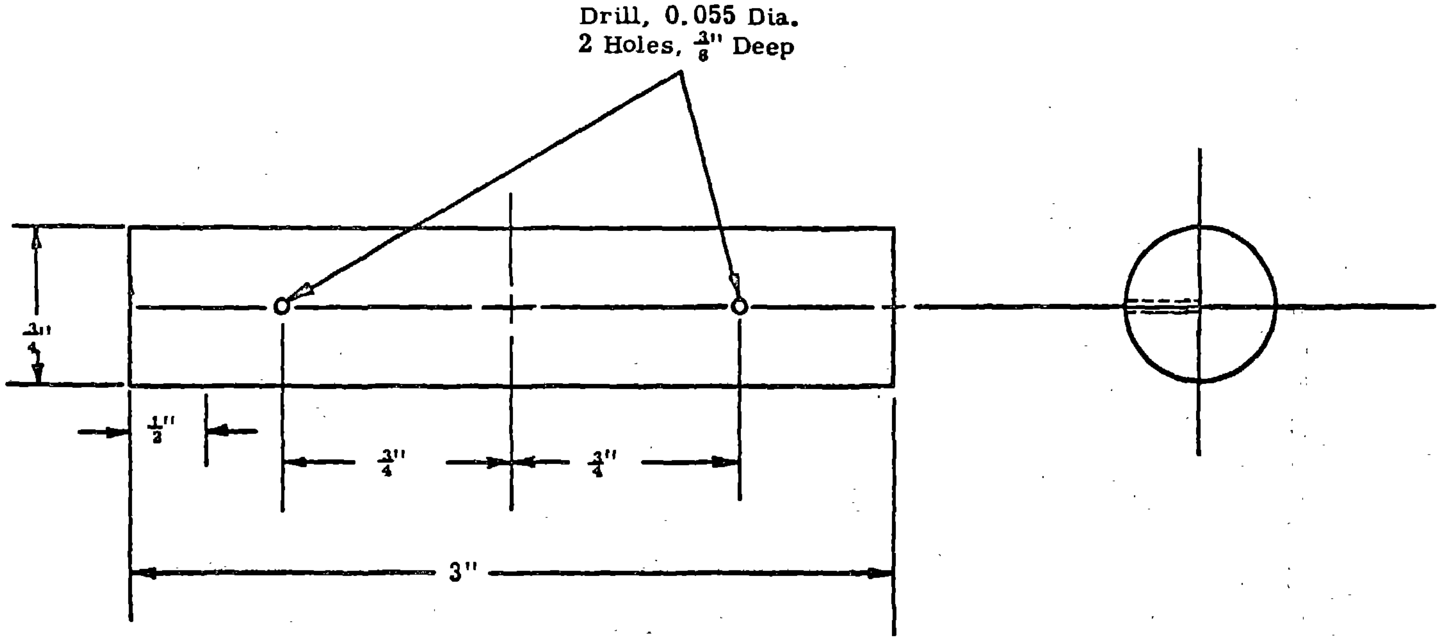

Figure 156. Standard Electrical Resistivity Specimen.

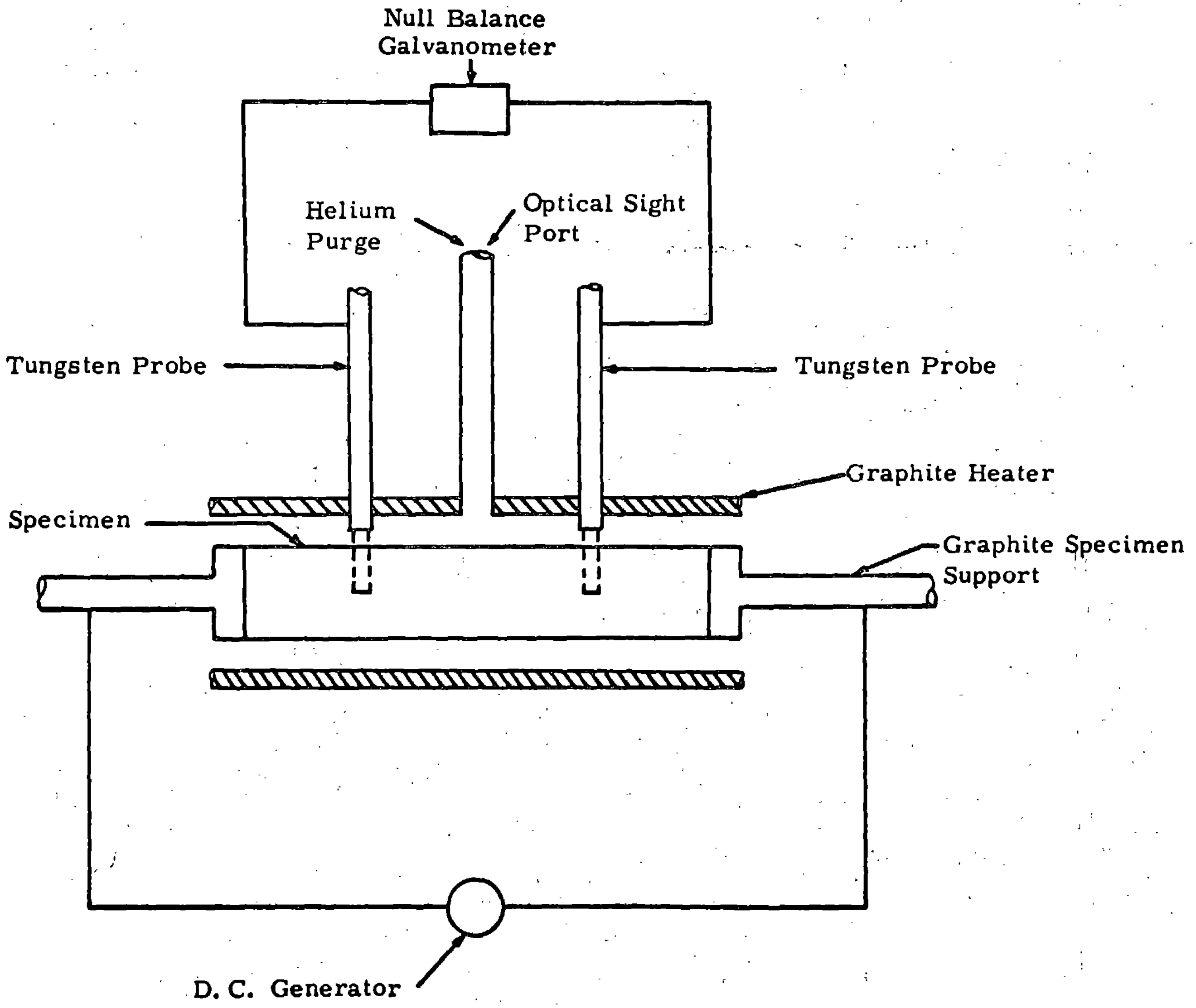

Figure 157. Apparatus for Measurement of Electrical Resistivity.

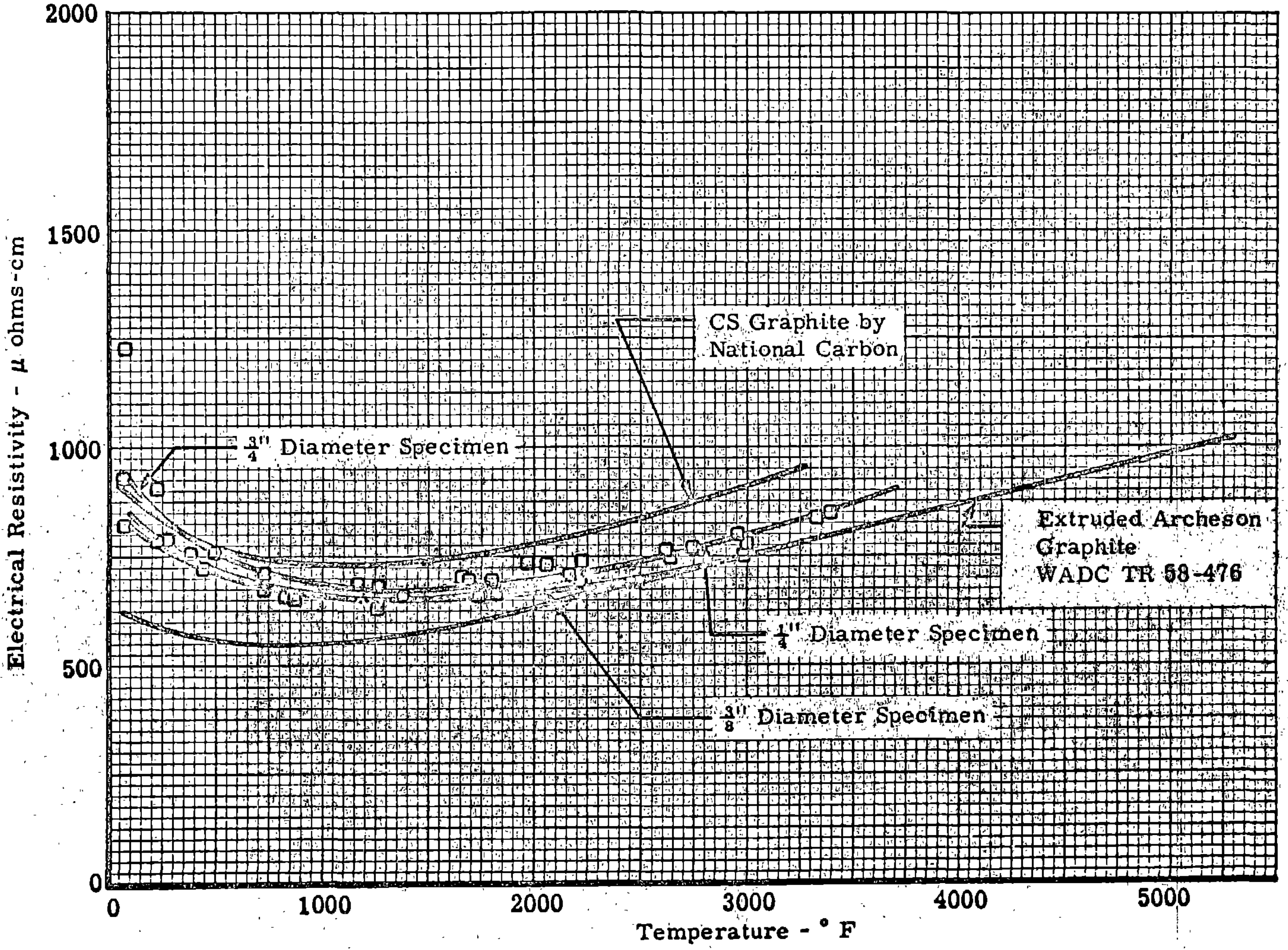

Figure 158. Electrical Resistivity of Graphite Illustrating the Effect of Specimen Size upon Resistivity.

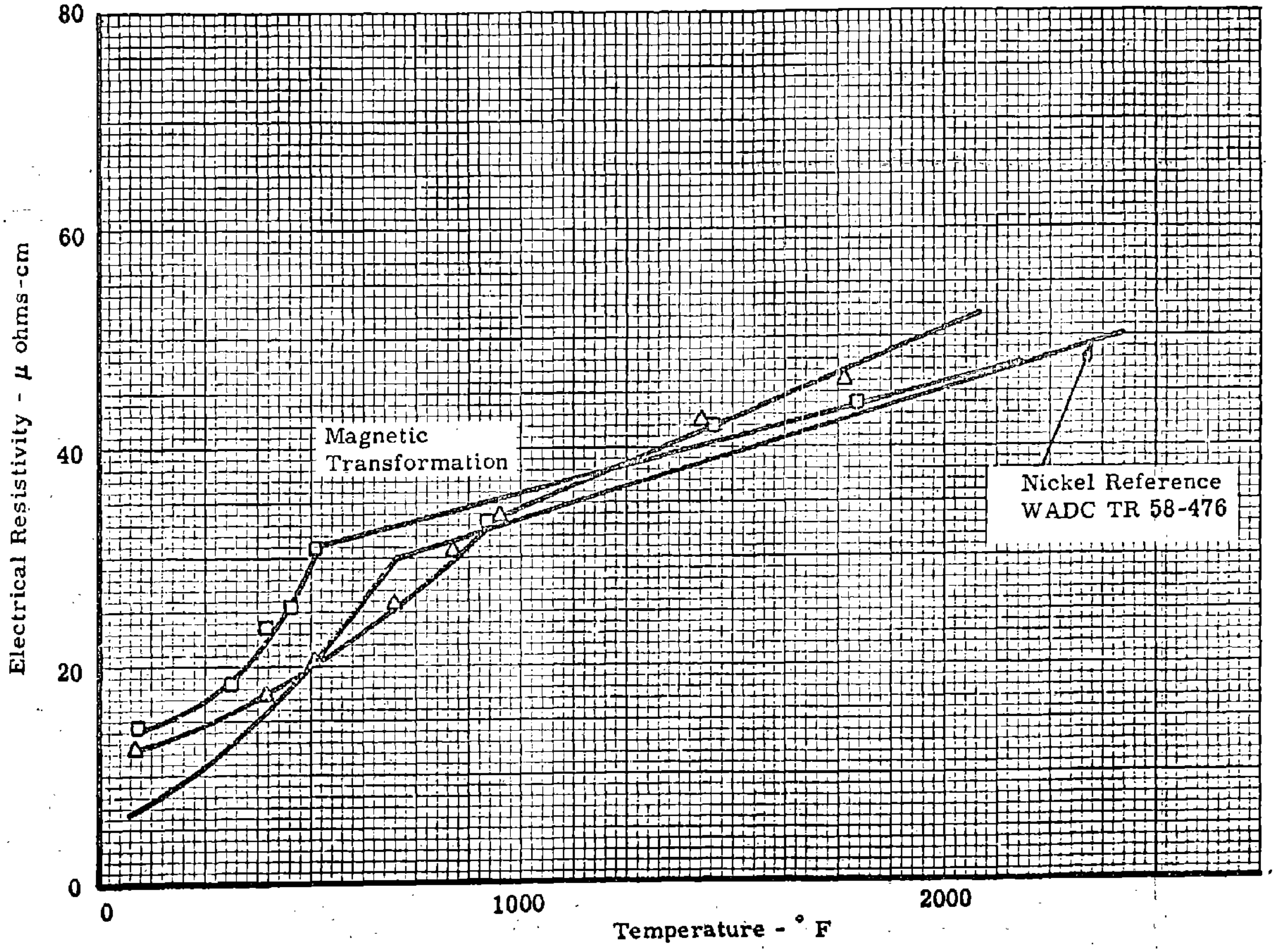

Figure 159. Electrical Resistivity of Nickel

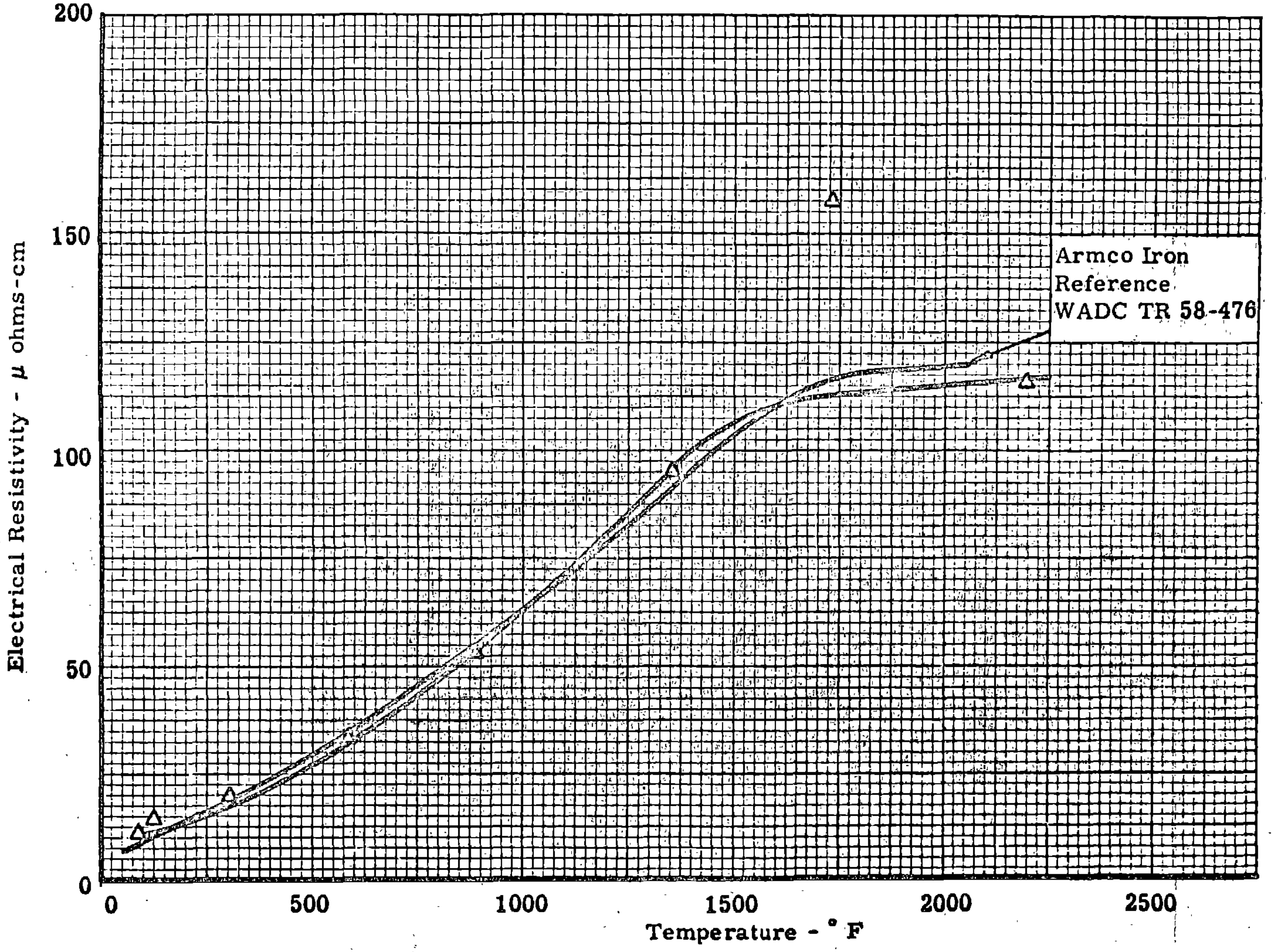

Figure 160. Electrical Resistivity of Armco Iron.

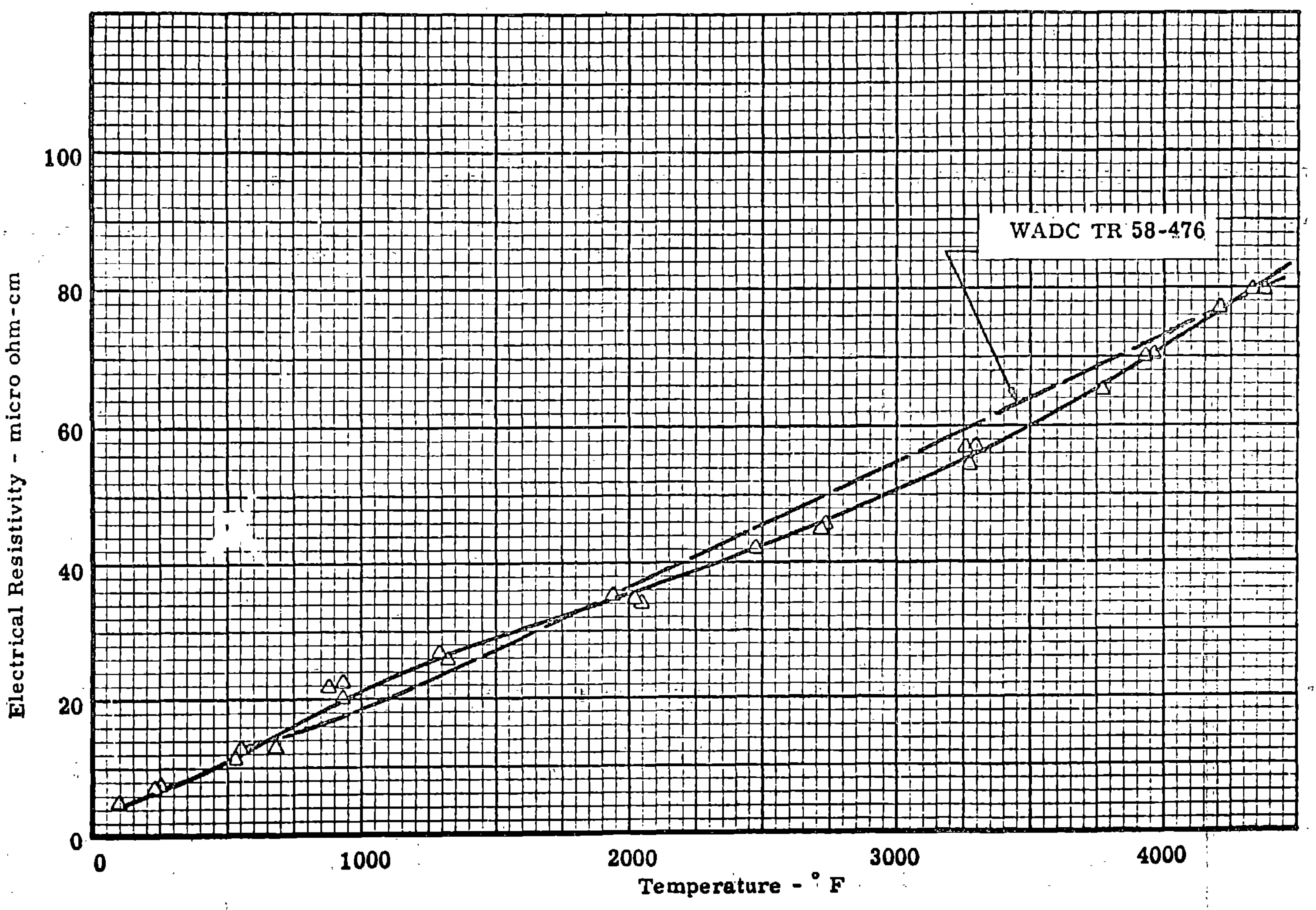

Figure 161. Electrical Resistivity of Tungsten.

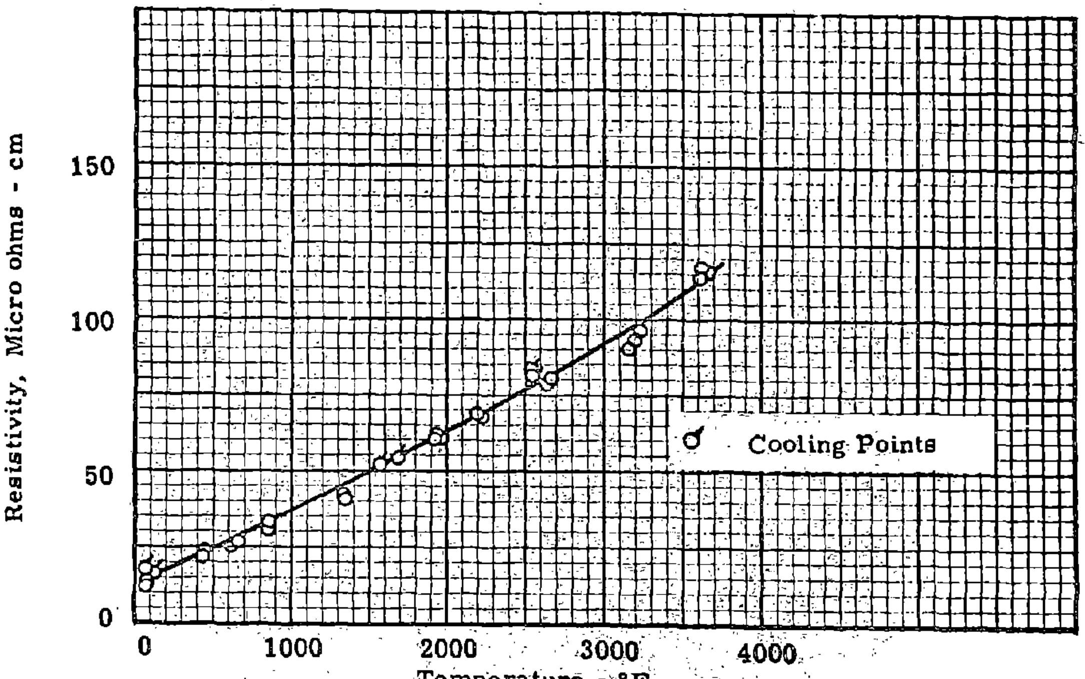

Figure 162. Electrical Resistivity of Hafnium Diboride.

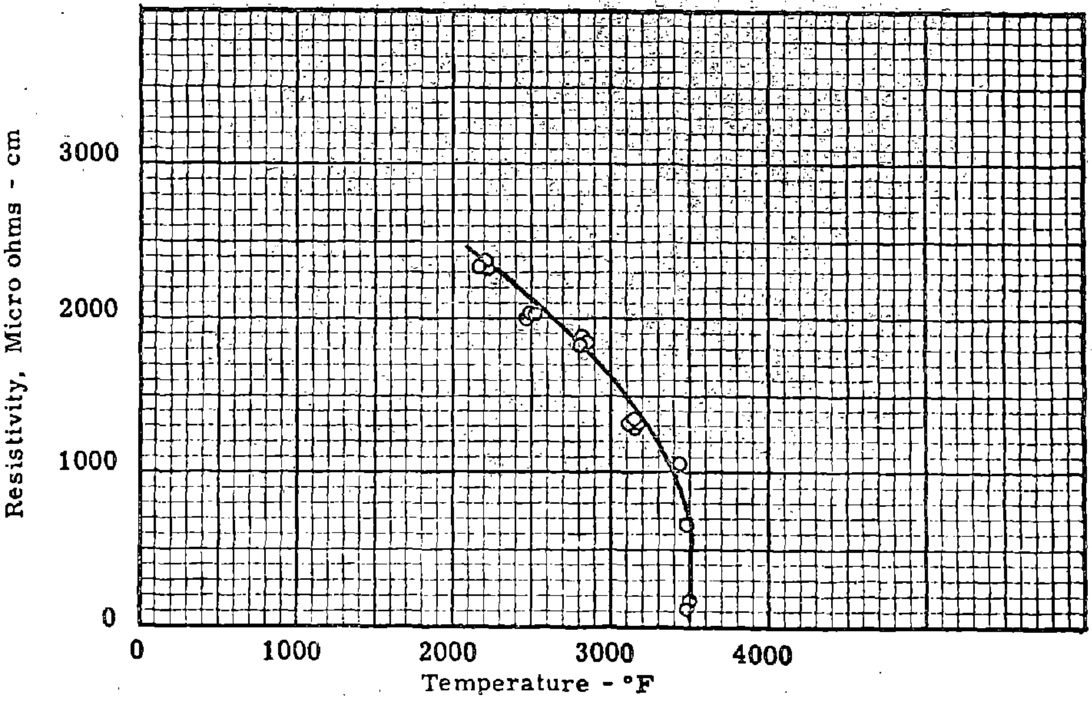

Figure 163. Electrical Resistivity of Thorium Tetraboride.

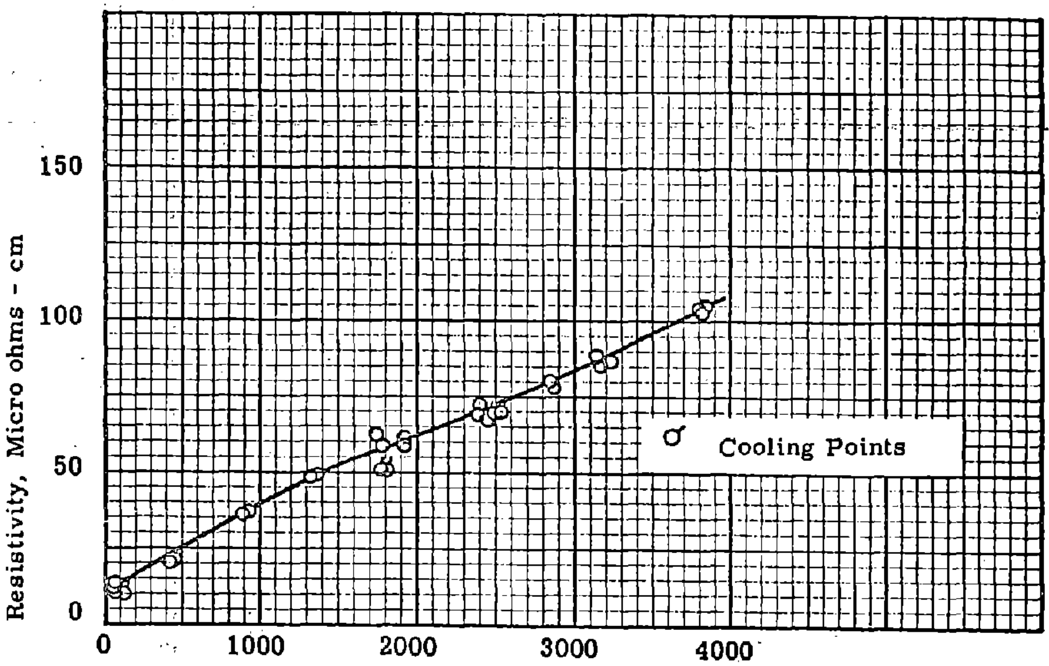

Figure 164. Electrical Resistivity of Titanium Diboride.

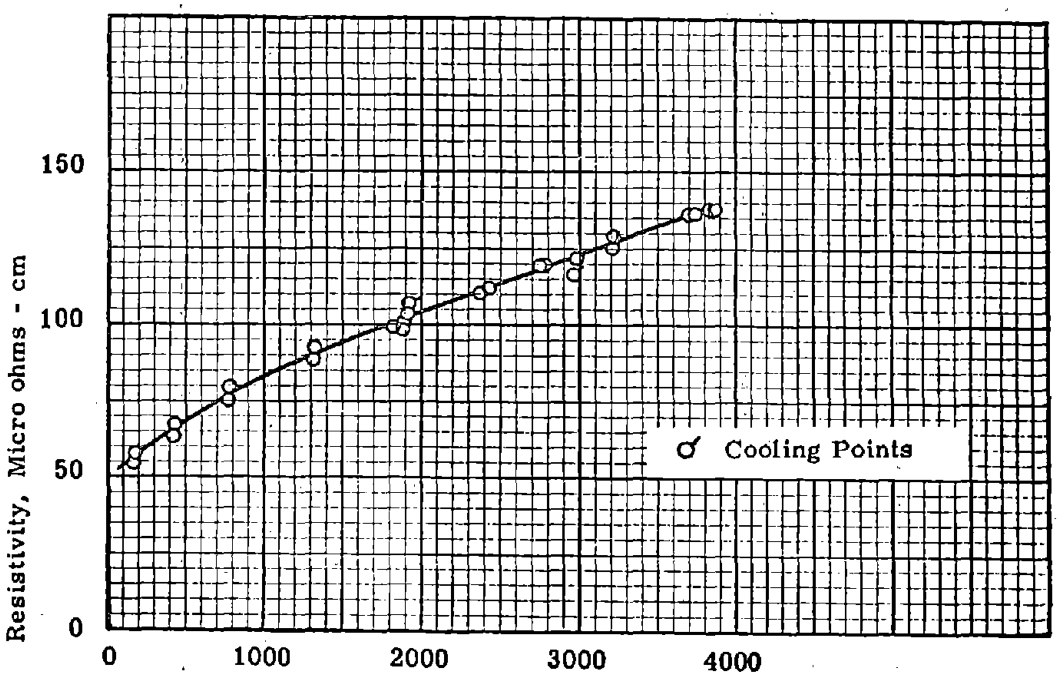

Figure 165. Electrical Resistivity of Tungsten Boride.

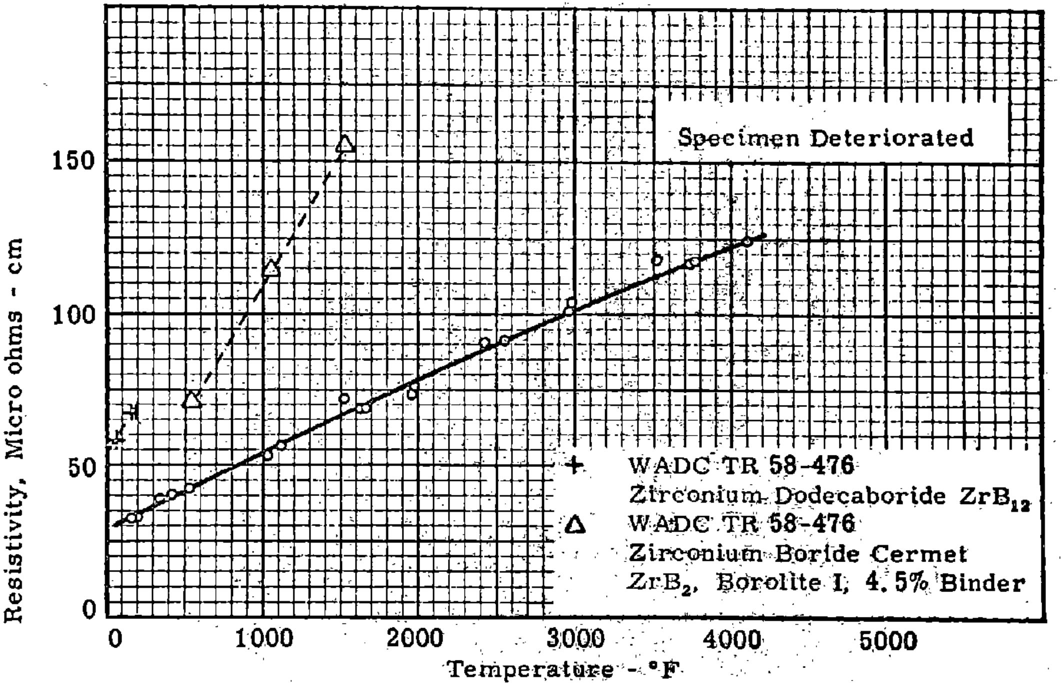

Figure 166. Electrical Resistivity of Zirconium Diboride

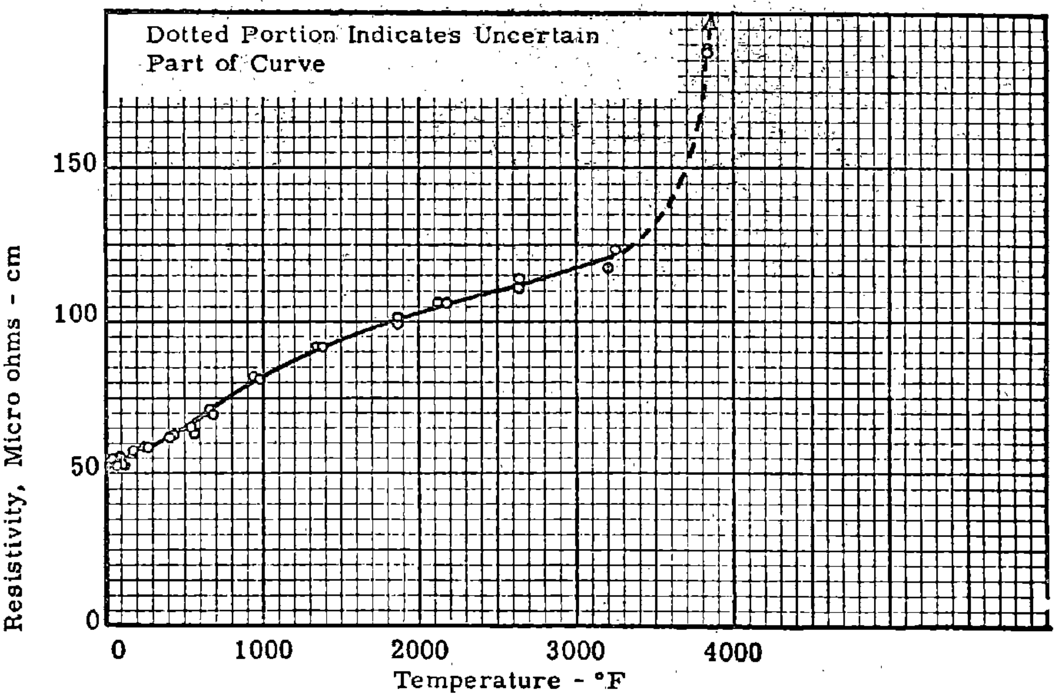

Figure 167. Electrical Resistivity of Columbium Carbide

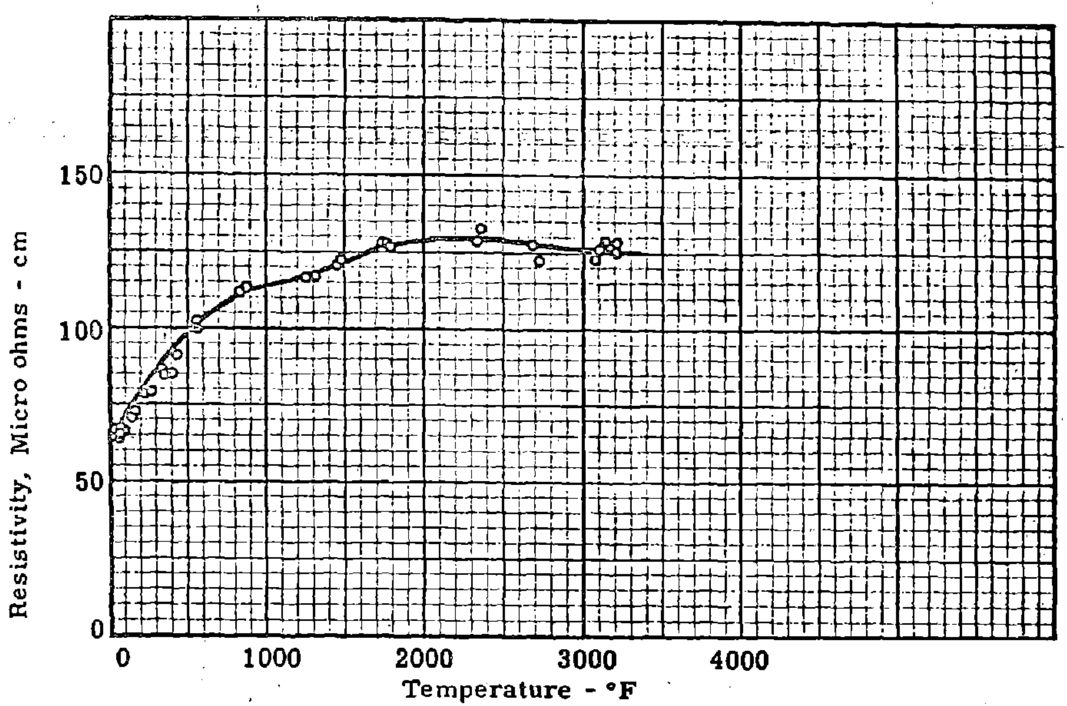

Figure 168. Electrical Resistivity of Dimolybdenum Carbide

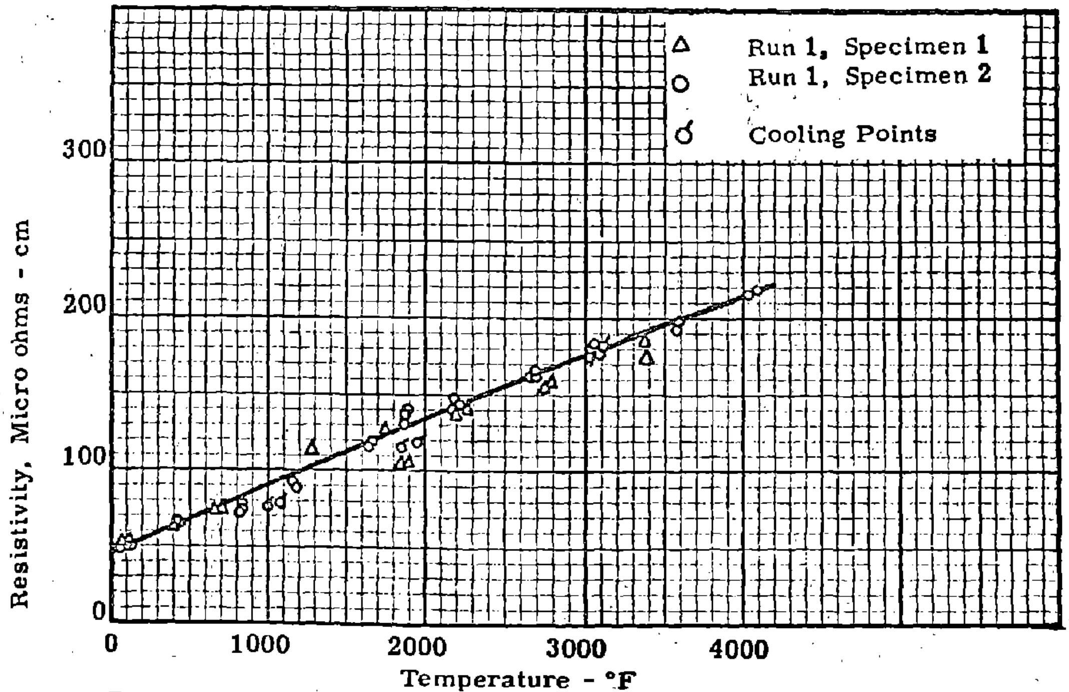

Figure 169. Electrical Resistivity Hafnium Carbide

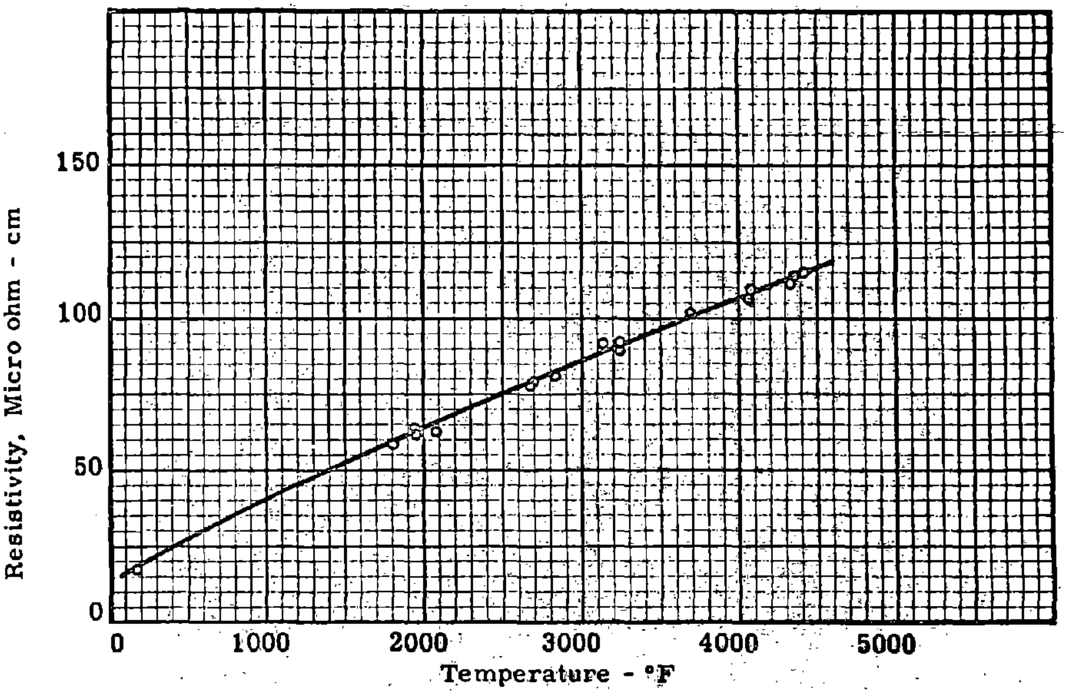

Figure 170. Electrical Resistivity of Tantalum Carbide

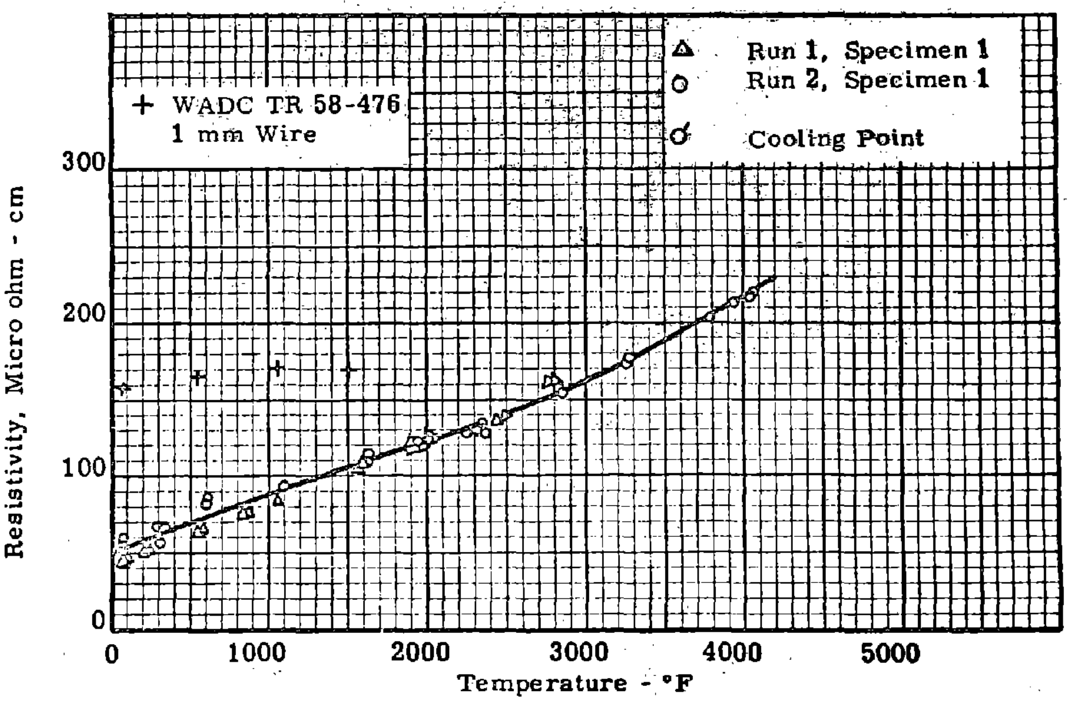

Figure 171. Electrical Resistivity of Titanium Carbide

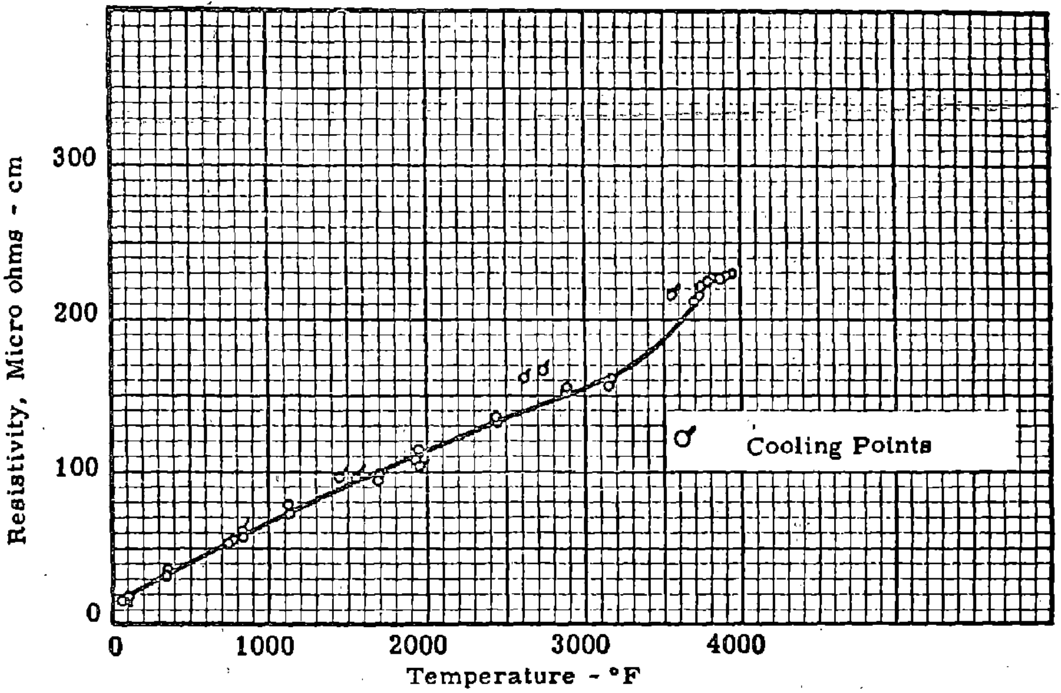

Figure 172. Electrical Resistivity of Tungsten Carbide

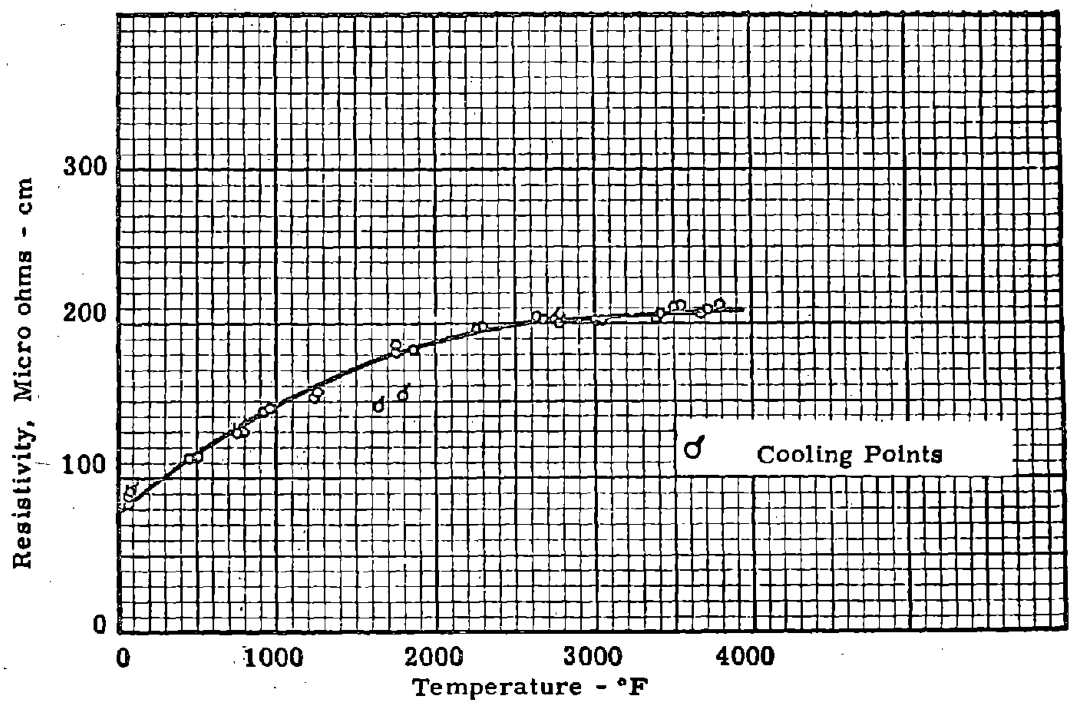

Figure 173. Electrical Resistivity of Vanadium Carbide

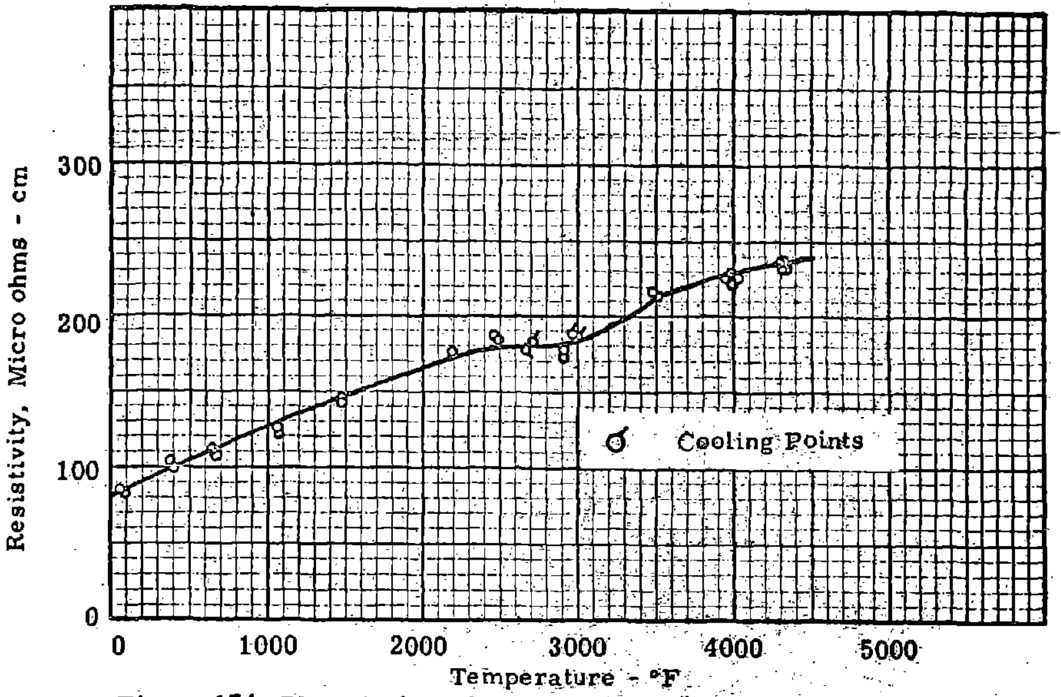

Figure 174. Electrical Resistivity of Zirconium Carbide

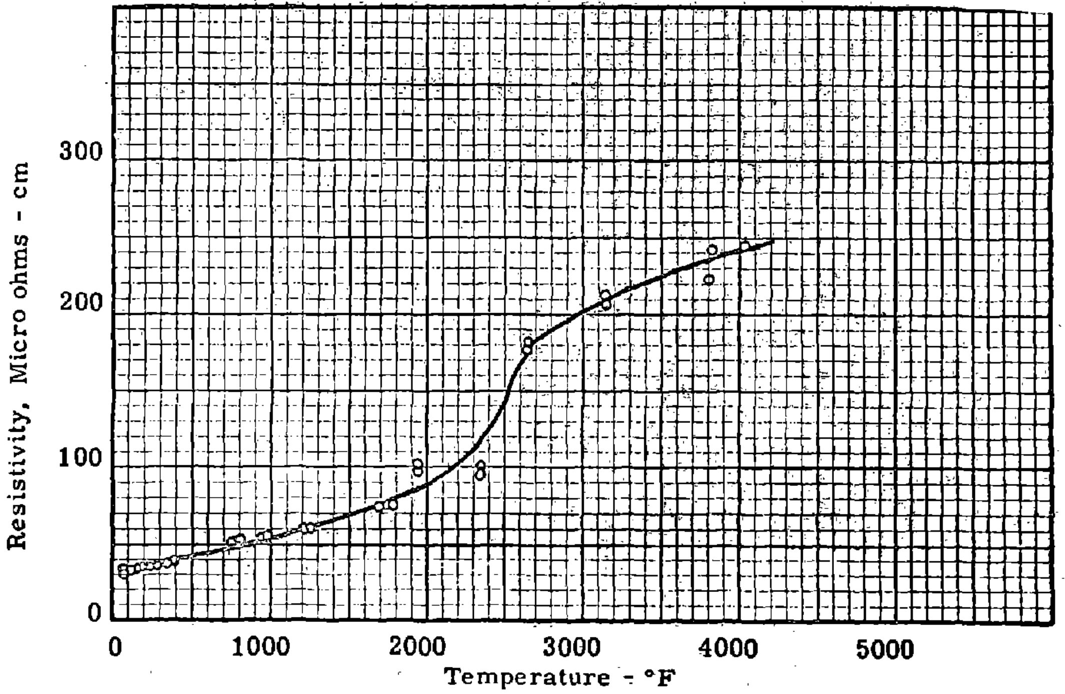

Figure 175. Electrical Resistivity of Hafnium Nitride

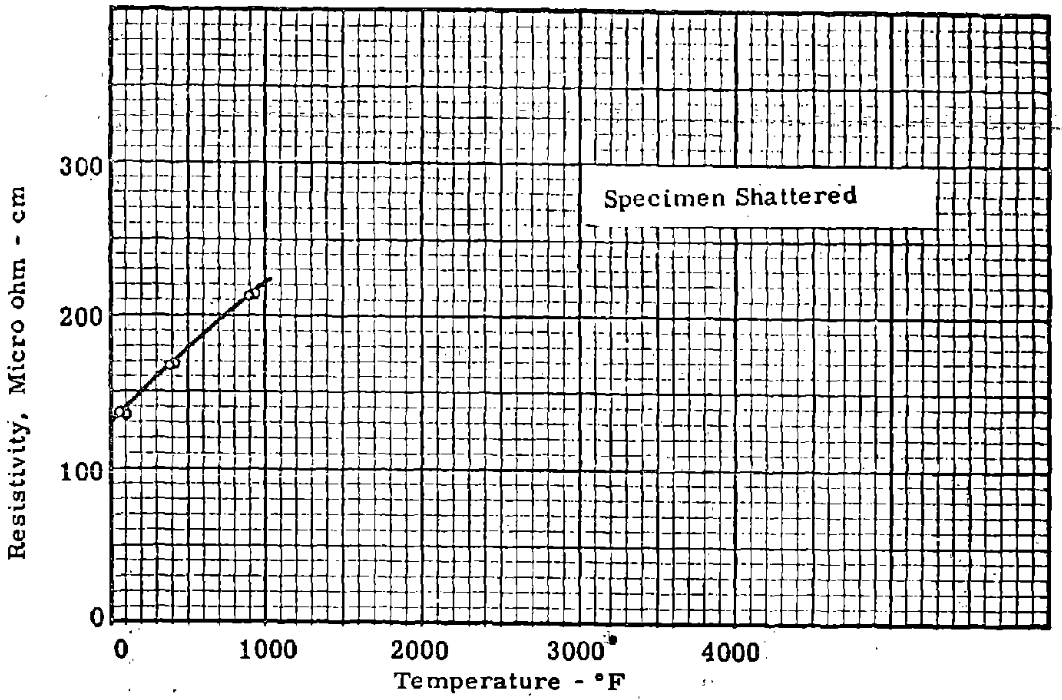

Figure 176. Electrical Resistivity of Tantalum Nitride

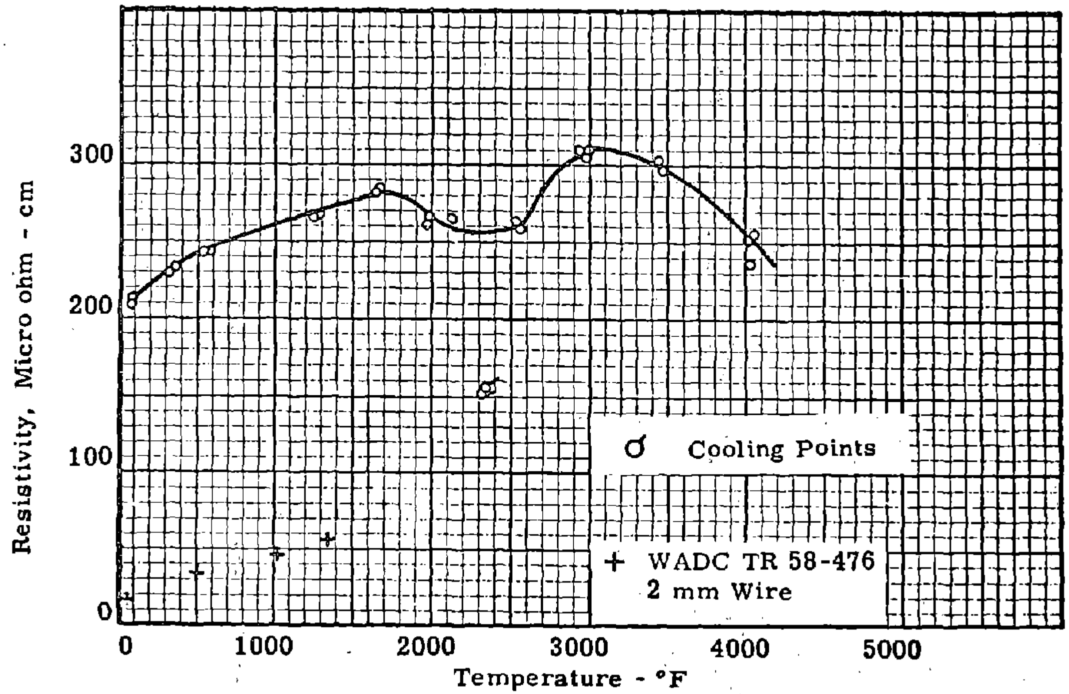

Figure 177. Electrical Resistivity of Titanium Nitride

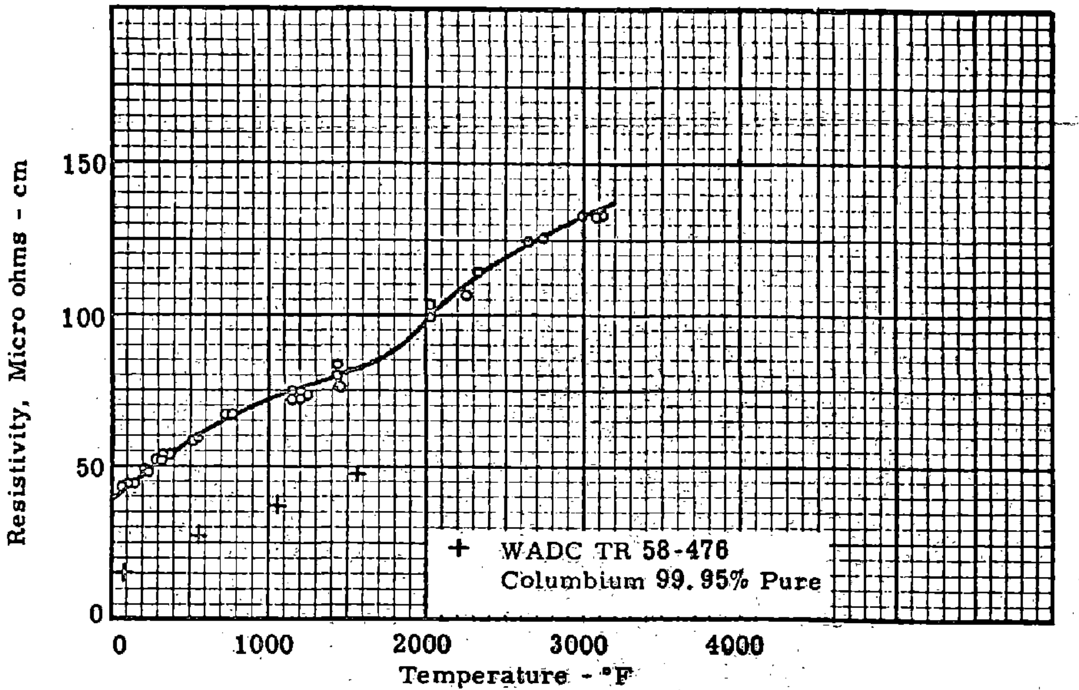

Figure 178. Electrical Resistivity of Columbium +0.5% Zirconium

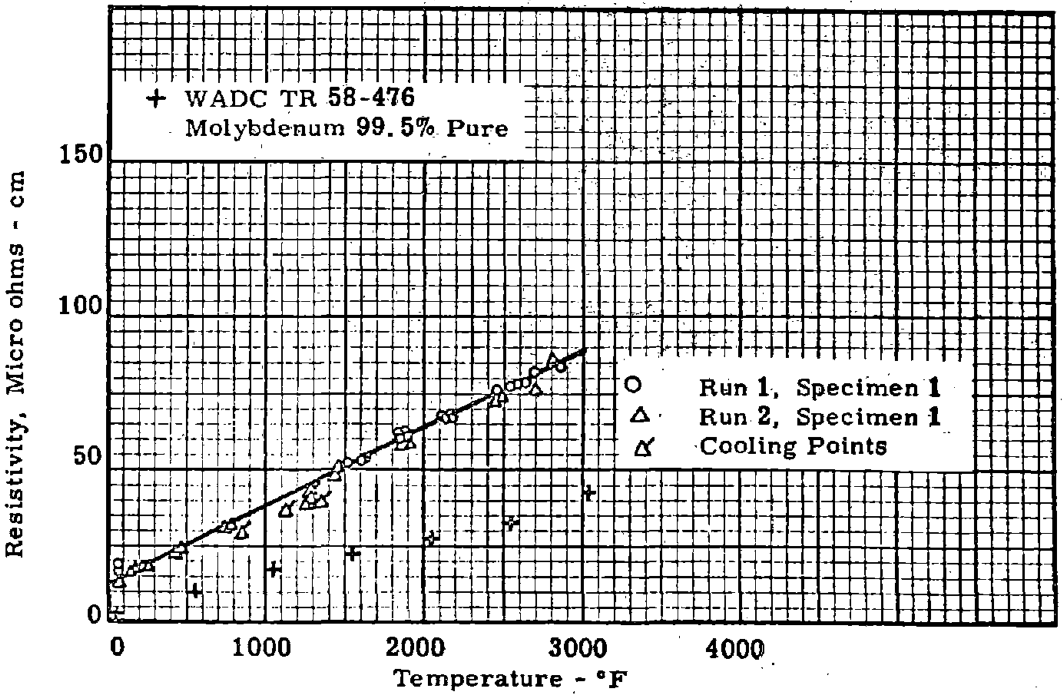

Figure 179. Electrical Resistivity of Molybdenum +0.5% Titanium

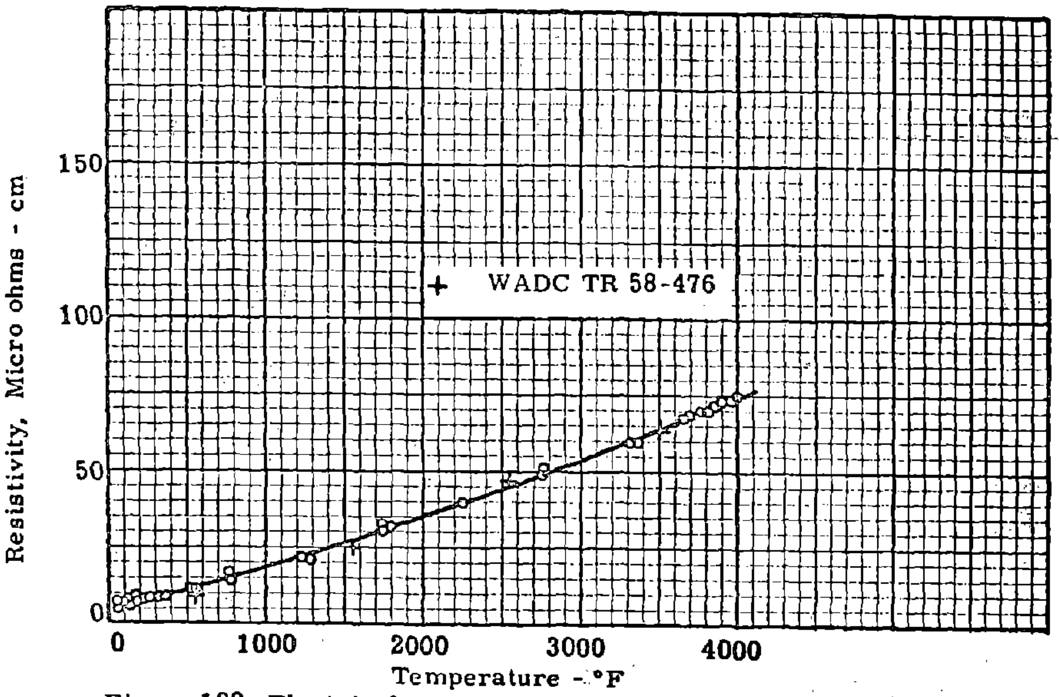

Figure 180. Electrical Resistivity of Tungsten (Supplied by Carborundum)

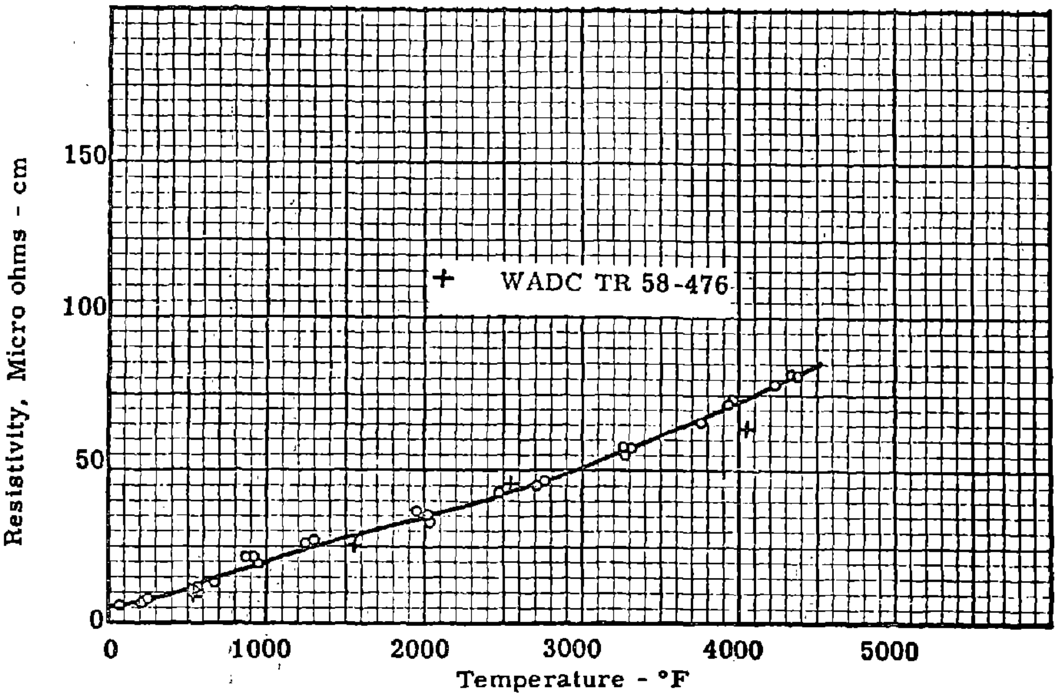

Figure 181. Electrical Resistivity of Tungsten (Supplied by General Electric)

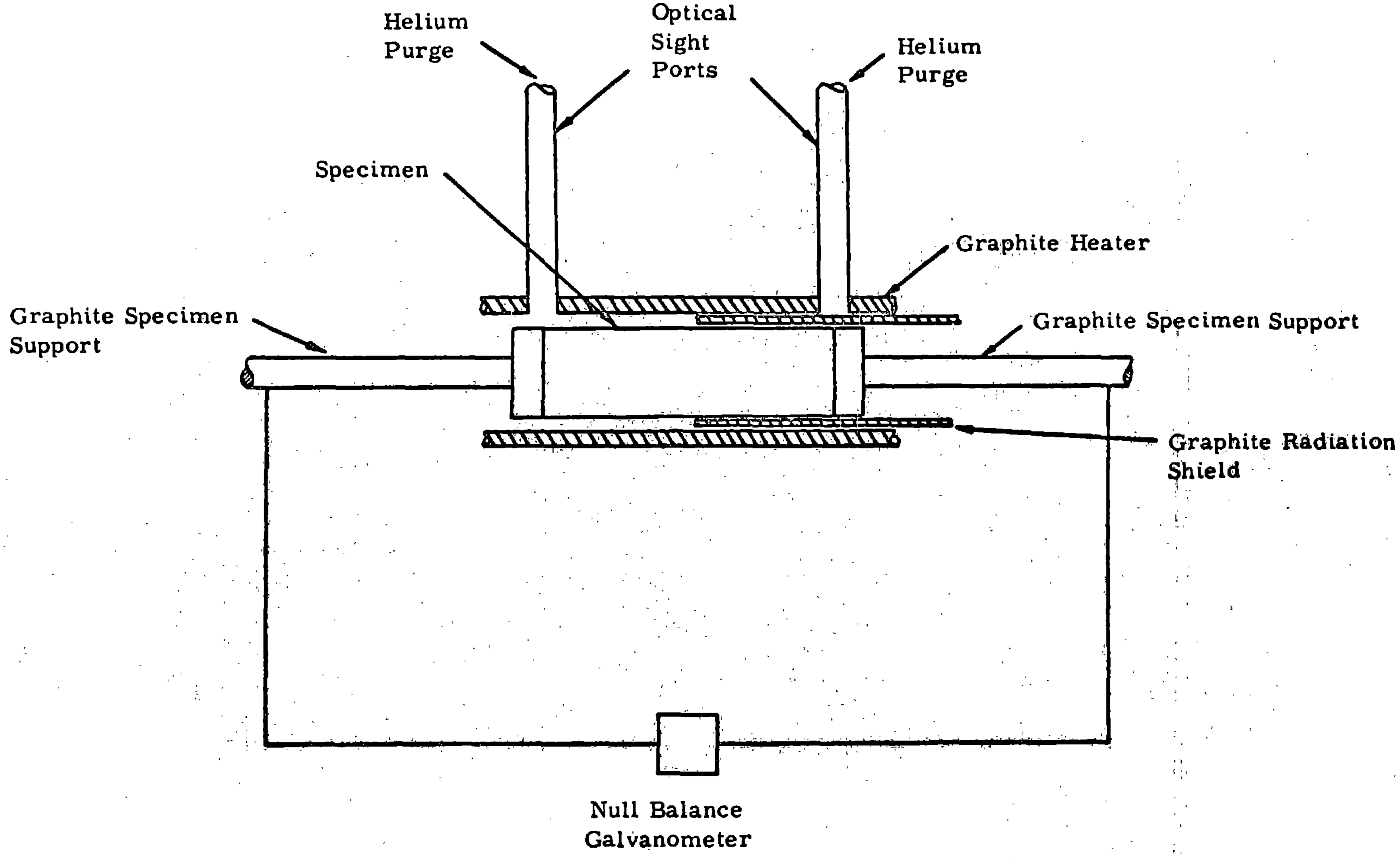
Helium Purge
Optical Sight Ports
Helium Purge
Specimen
Graphite Heater
Graphite Specimen Support
Graphite Specimen Support
Graphite Radiation Shield
Null Balance Galvanometer

Figure 182. Apparatus for Measurement of Thermoelectric Voltage.

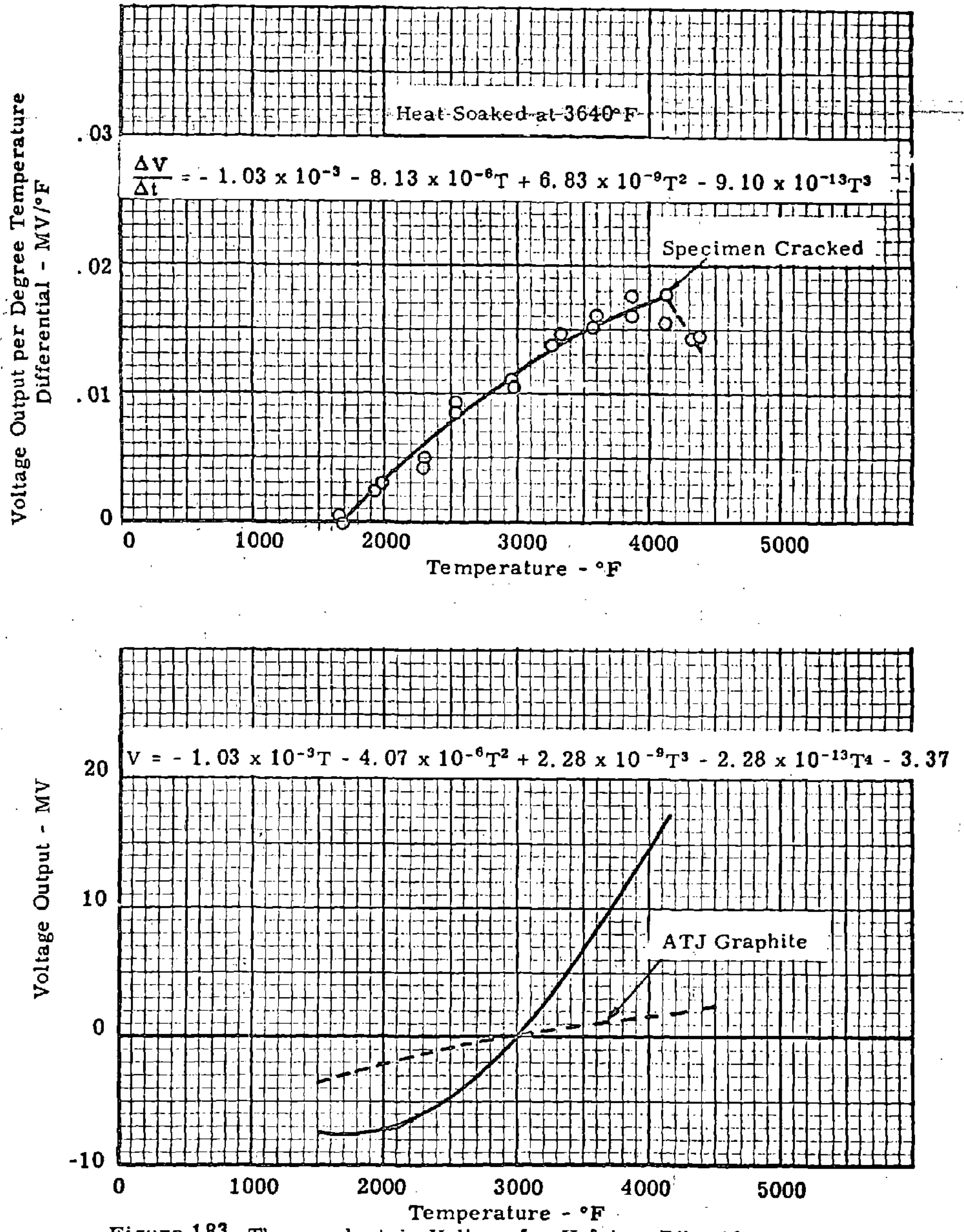

Figure 183. Thermoelectric Voltage for Hafnium Diboride (ATJ Graphite Reference, Density = 1.73 g/cc)

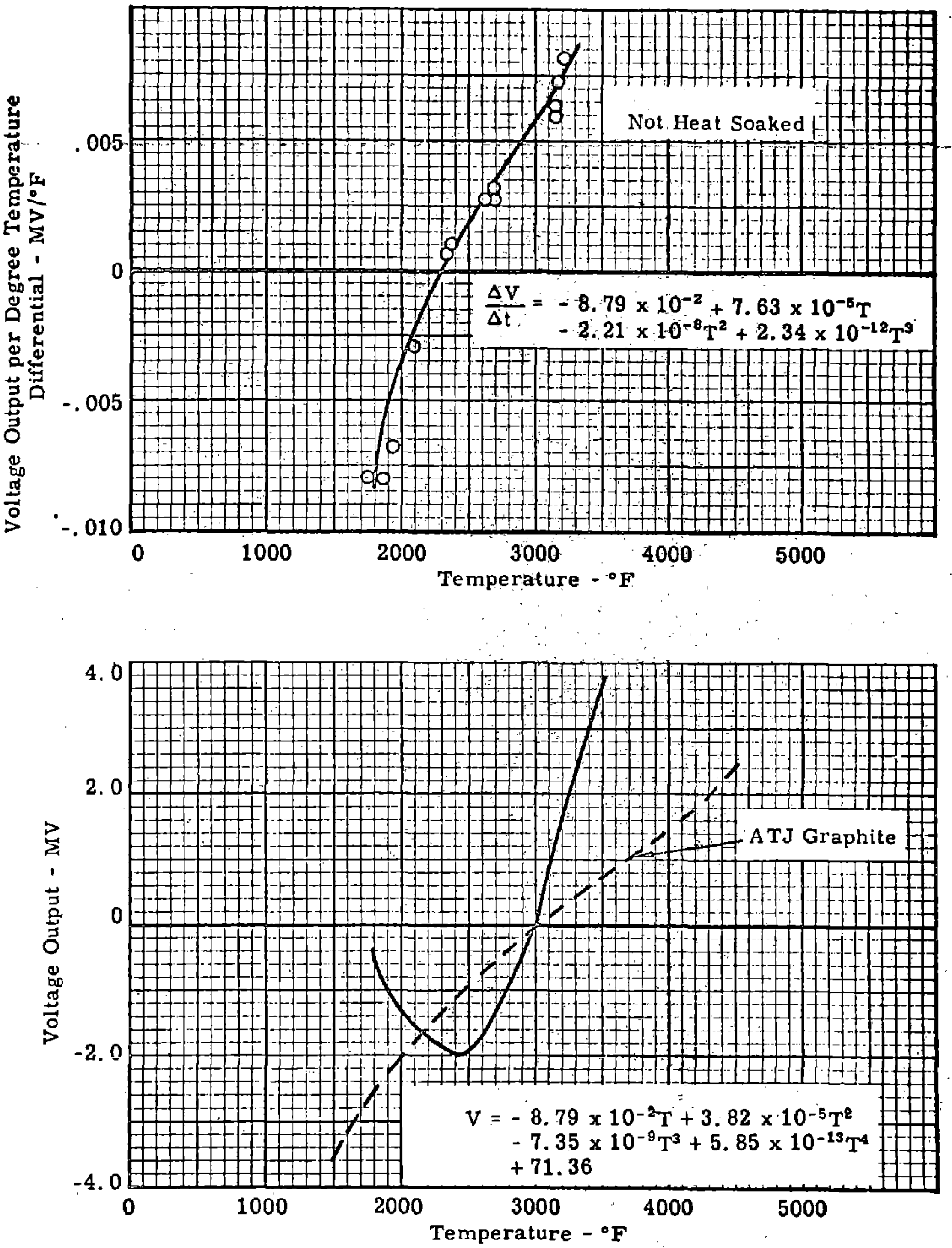

Figure 184. Thermoelectric Voltage for Thorium Tetraboride (ATJ Graphite Reference, Density = 1.73 g/cc)

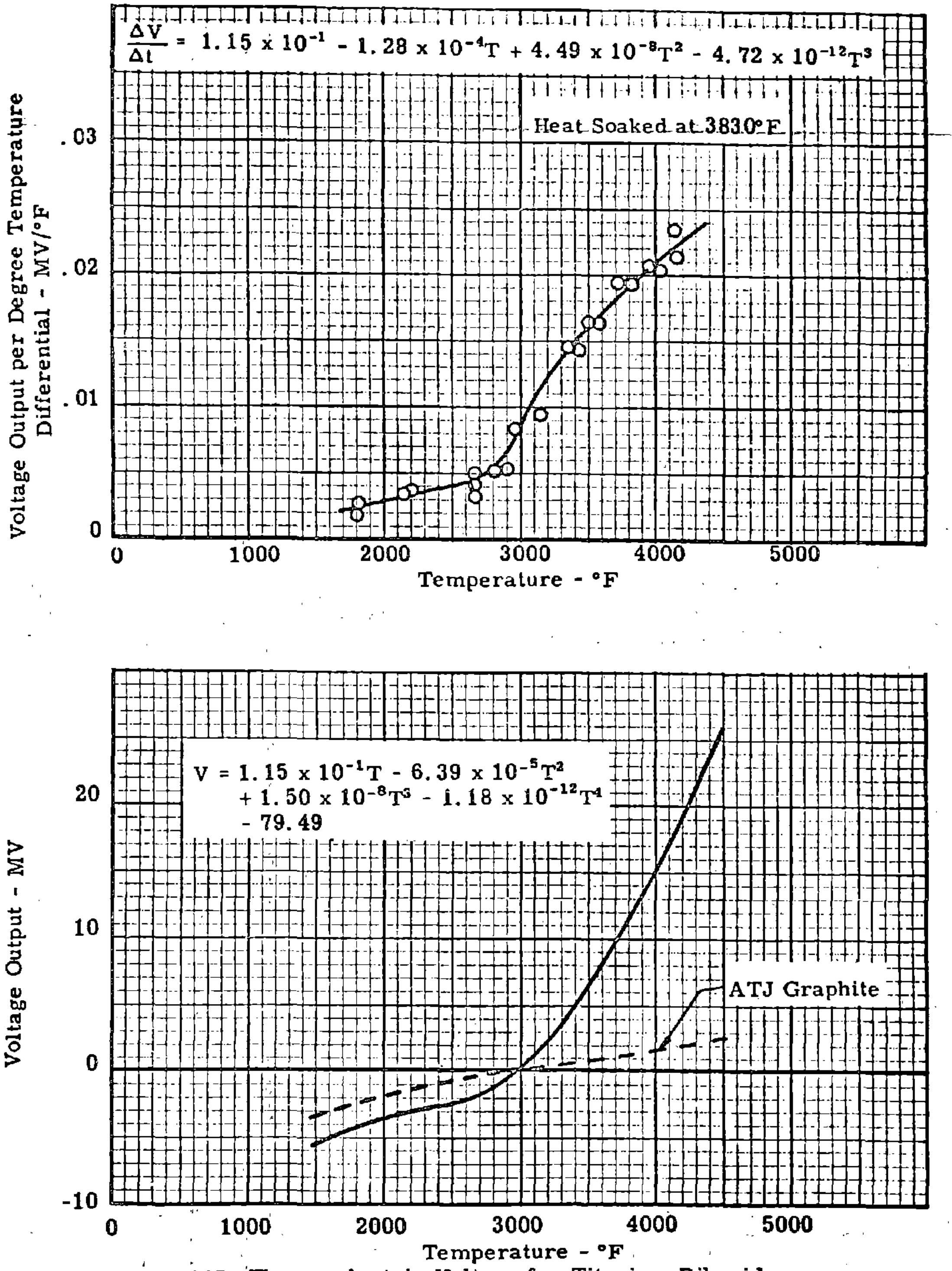

Figure 185. Thermoelectric Voltage for Titanium **Diboride** (ATJ Graphite Reference, Density = **1.73 g/cc)**

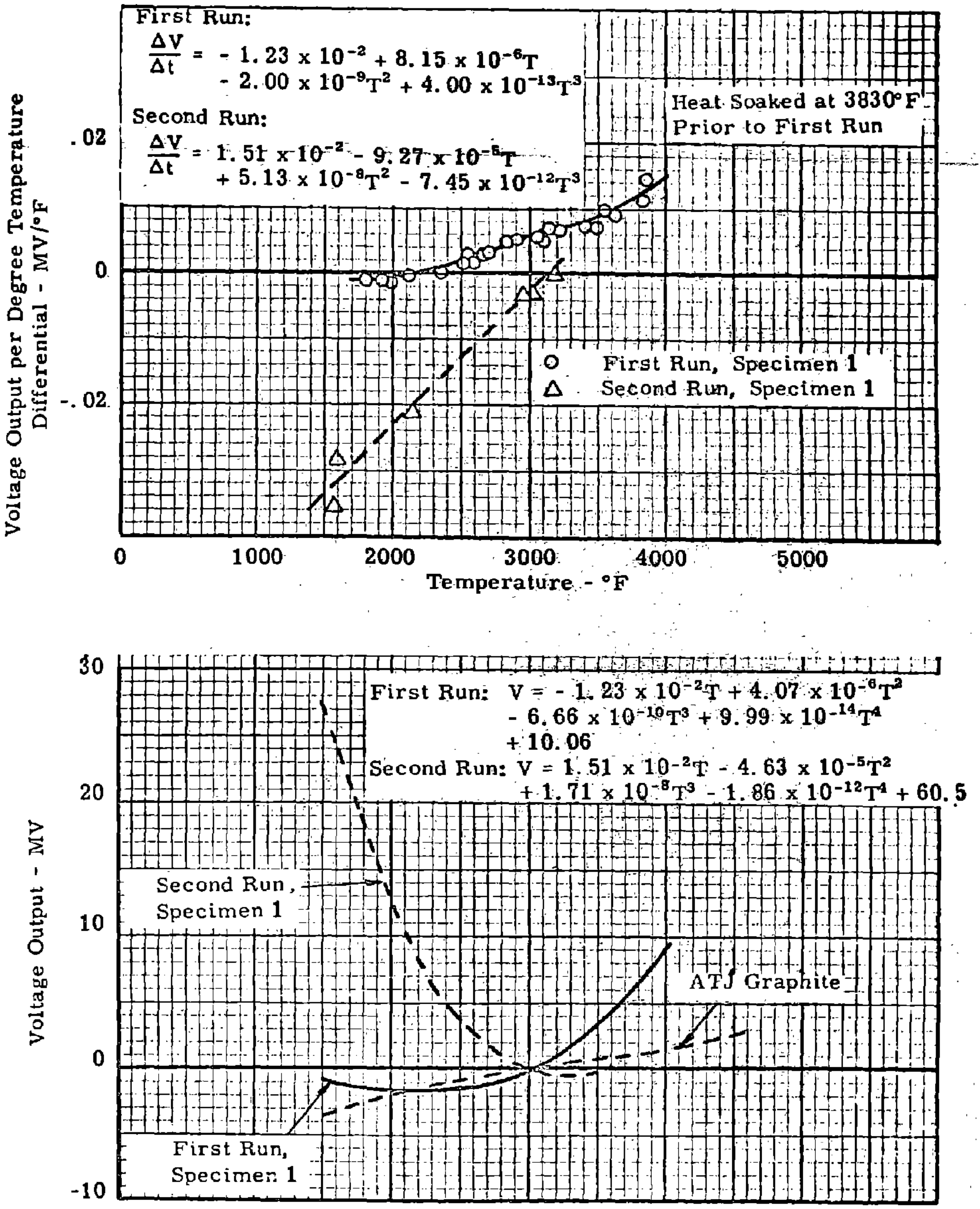

Figure 186. Thermoelectric Voltage for Tungsten Boride
(ATJ Graphite Reference, Density = 1.73 g/cc)

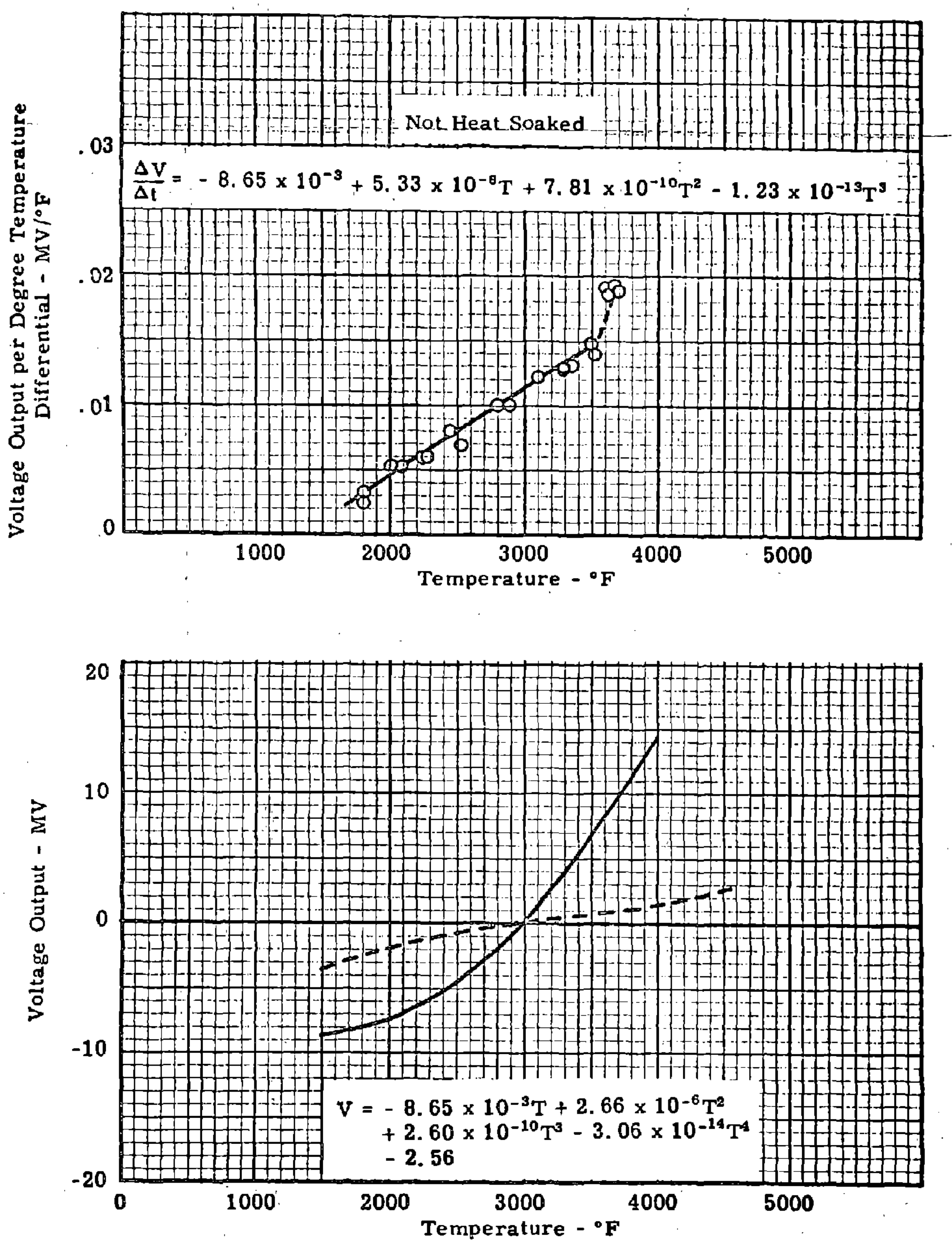

Figure 187. Thermoelectric Voltage for Zirconium Diboride (ATJ Graphite Reference, Density = 1.73 g/cc)

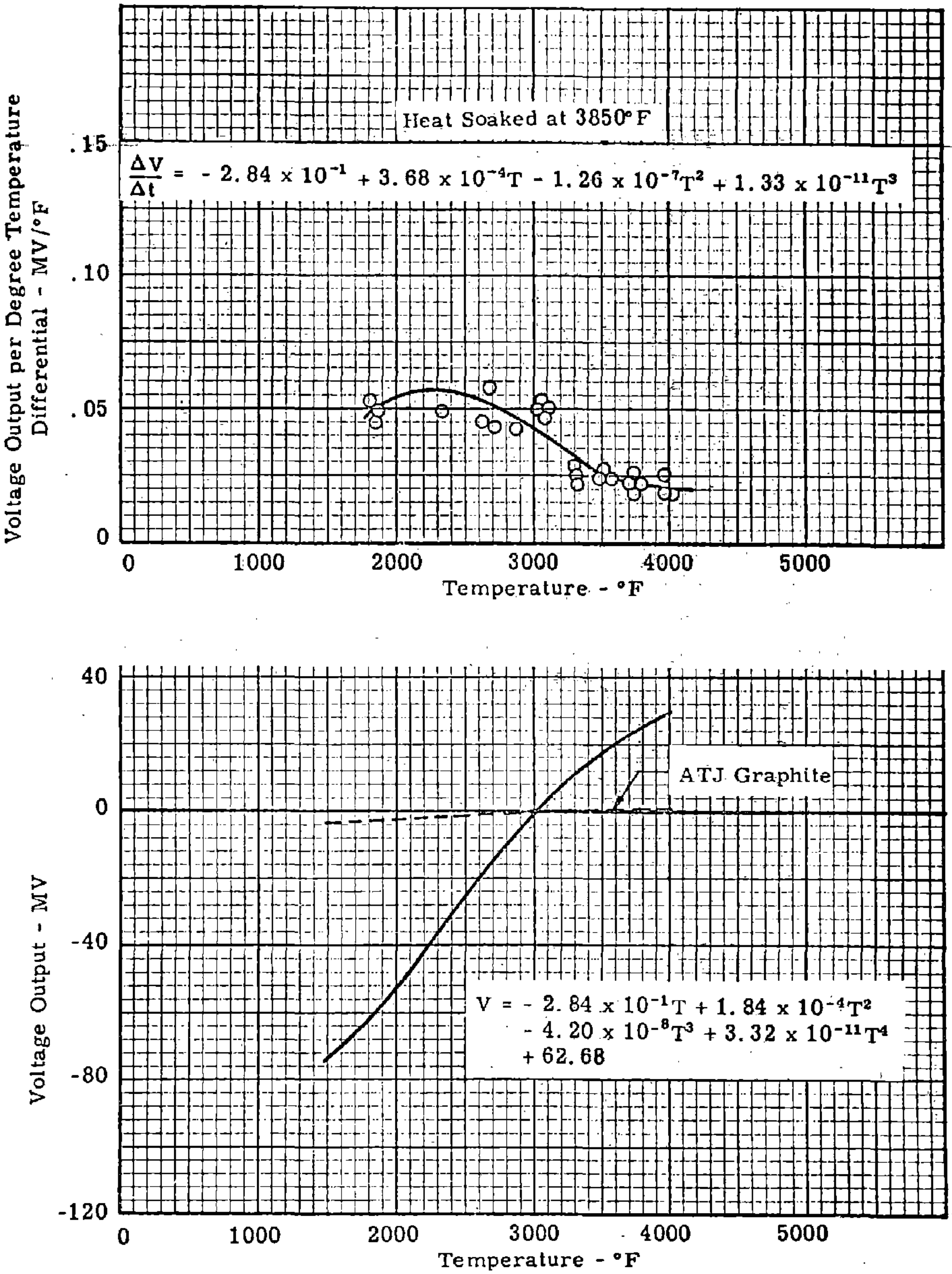

Figure 188. Thermoelectric Voltage for Columbium Carbide
(ATJ Graphite Reference, Density = 1.73 g/cc)

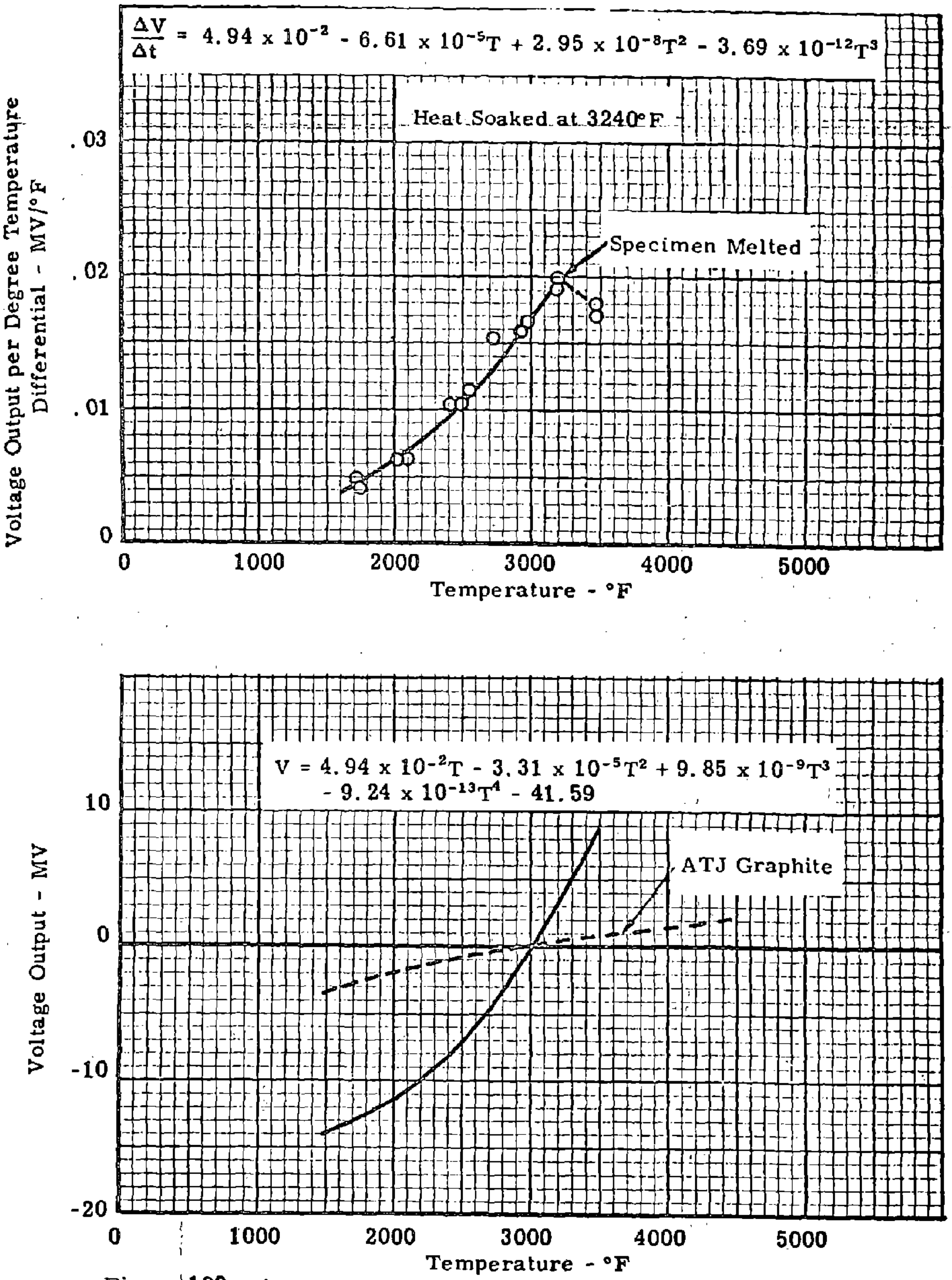

Figure 189. Thermoelectric Voltage for Dimolybdenum Carbide (ATJ Graphite Reference, Density = 1.73 g/cc)

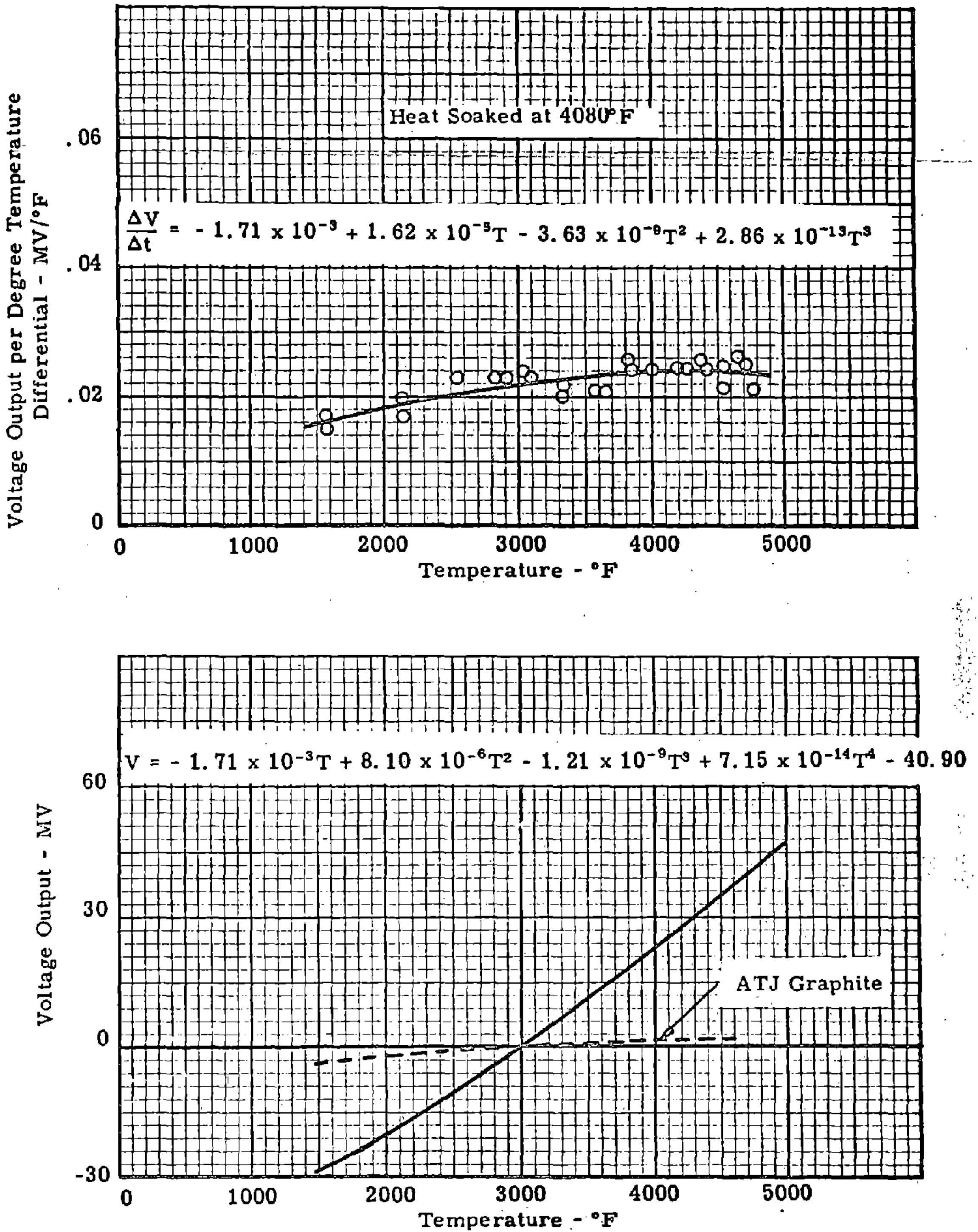

Figure 190. Thermoelectric Voltage for Hafnium Carbide (ATJ Graphite Reference, Density = 1.73 g/cc)

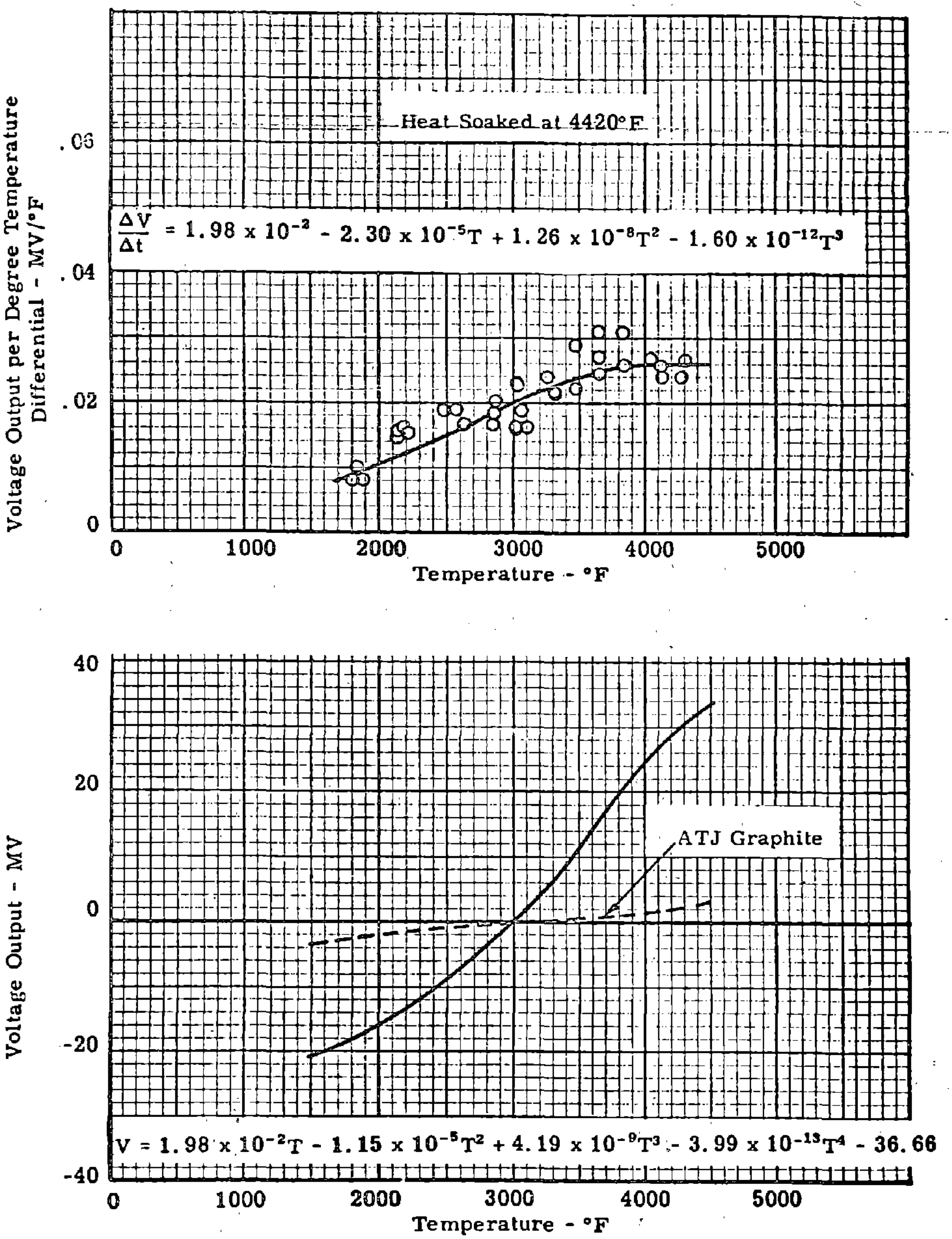

Figure 191. Thermoelectric Voltage for Tantalum Carbide
(ATJ Graphite Reference, Density = 1.73 g/cc)

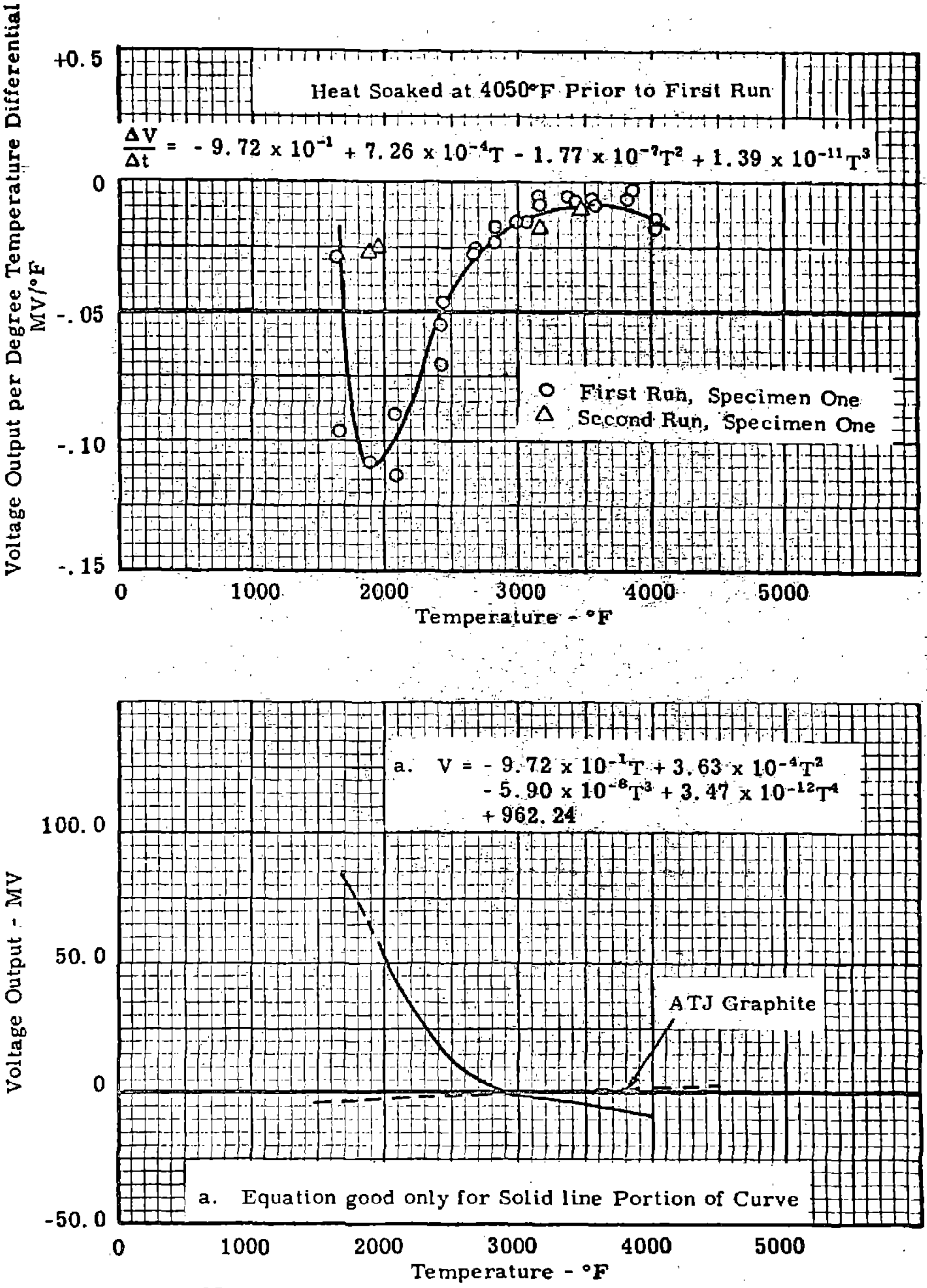

Figure 192. Thermoelectric Voltage for Titanium Carbide (ATJ Graphite Reference, Density = 1.73 g/cc)

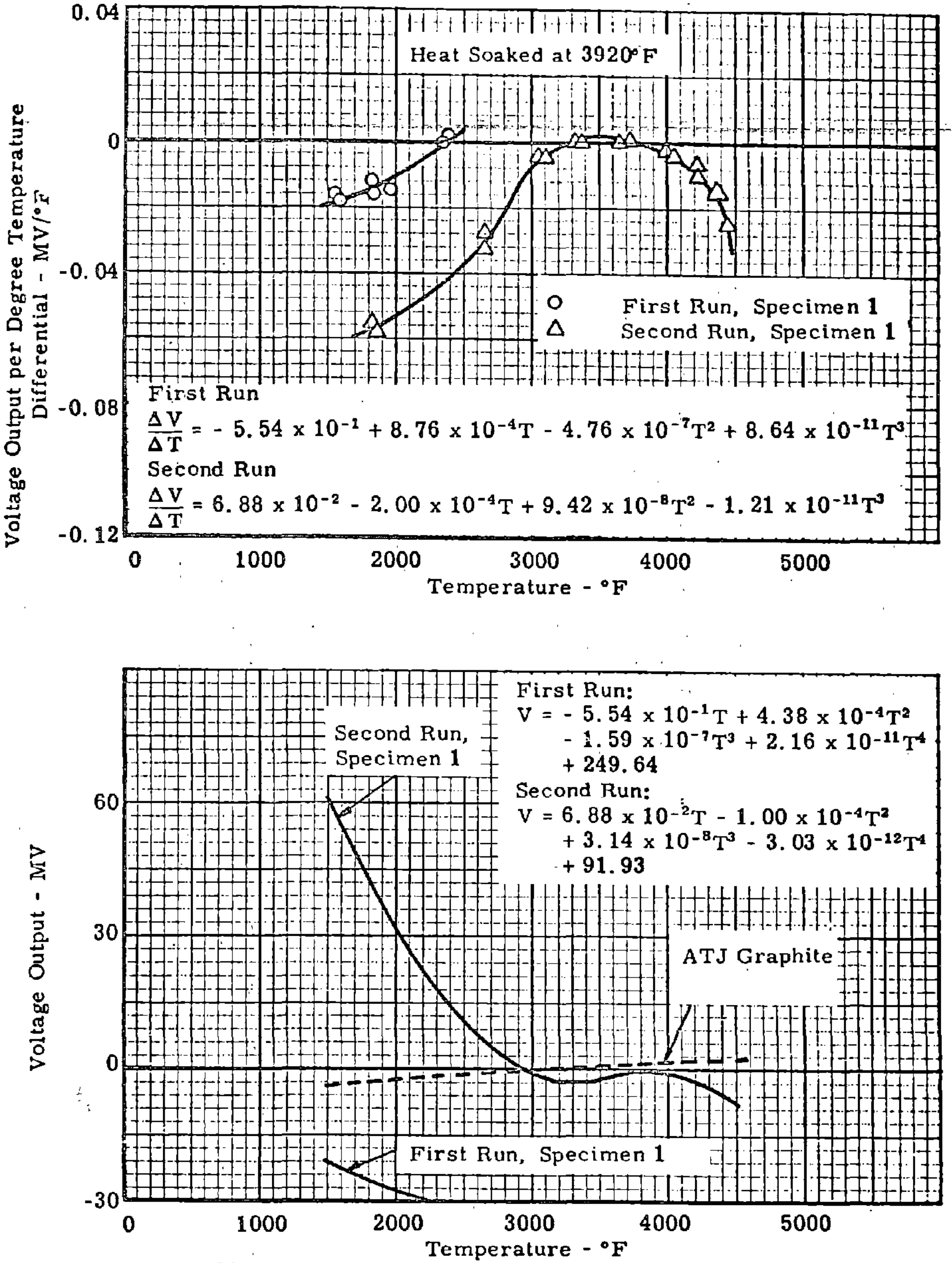

First Run

$$\frac{\Delta V}{\Delta T} = -5.54 \times 10^{-1} + 8.76 \times 10^{-4}T - 4.76 \times 10^{-7}T^2 + 8.64 \times 10^{-11}T^3$$

Second Run

$$\frac{\Delta V}{\Delta T} = 6.88 \times 10^{-2} - 2.00 \times 10^{-4}T + 9.42 \times 10^{-8}T^2 - 1.21 \times 10^{-11}T^3$$

First Run:

$$V = -5.54 \times 10^{-1}T + 4.38 \times 10^{-4}T^2 - 1.59 \times 10^{-7}T^3 + 2.16 \times 10^{-11}T^4 + 249.64$$

Second Run:

$$V = 6.88 \times 10^{-2}T - 1.00 \times 10^{-4}T^2 + 3.14 \times 10^{-8}T^3 - 3.03 \times 10^{-12}T^4 + 91.93$$

Figure 193. Thermoelectric Voltage for Tungsten Carbide (ATJ Graphite Reference, Density = 1.73 g/cc)

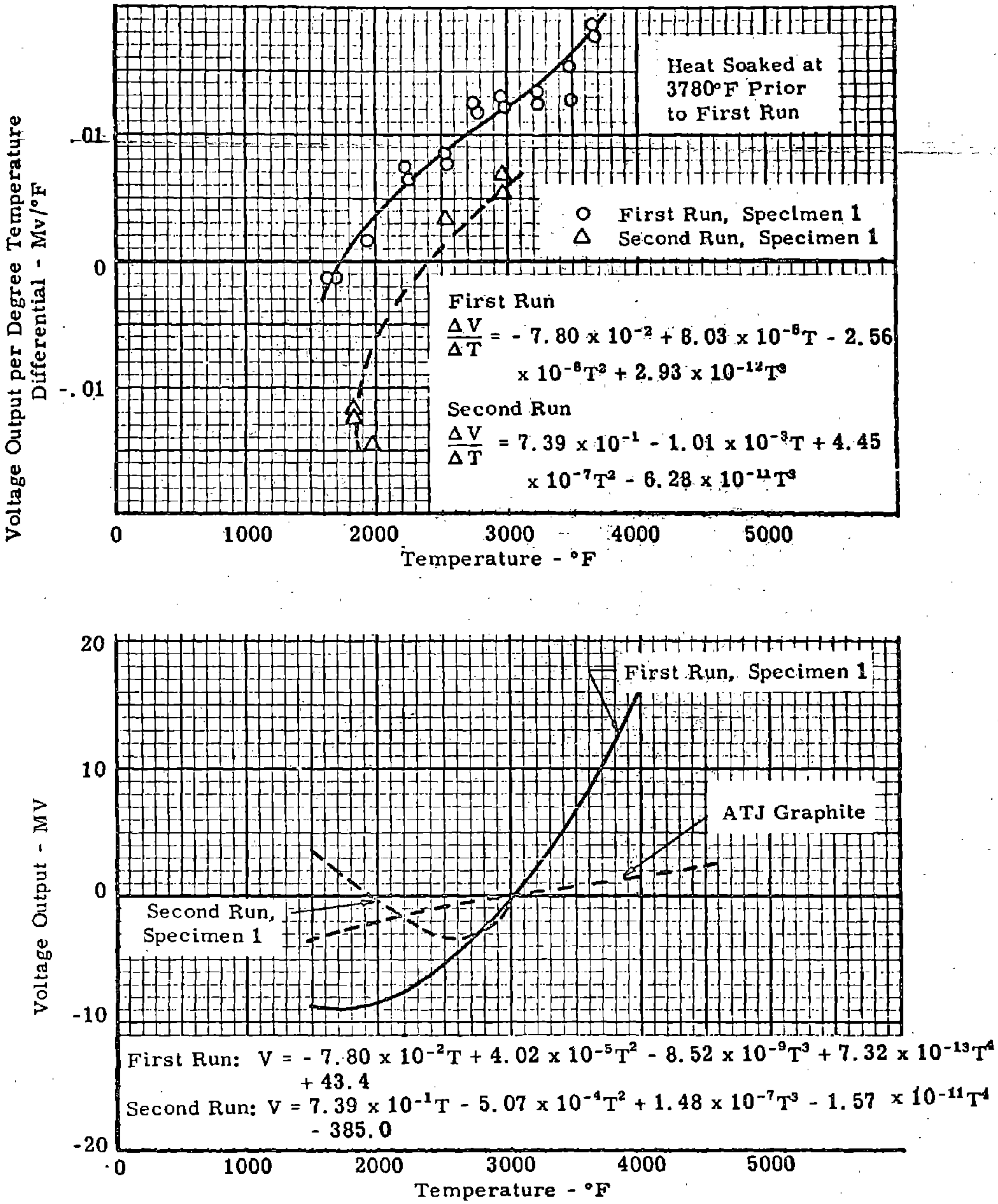

First Run

$$\frac{\Delta V}{\Delta T} = -7.80 \times 10^{-2} + 8.03 \times 10^{-5} T - 2.56 \times 10^{-8} T^2 + 2.93 \times 10^{-12} T^3$$

Second Run

$$\frac{\Delta V}{\Delta T} = 7.39 \times 10^{-1} - 1.01 \times 10^{-3} T + 4.45 \times 10^{-7} T^2 - 6.28 \times 10^{-11} T^3$$

First Run: $V = -7.80 \times 10^{-2} T + 4.02 \times 10^{-5} T^2 - 8.52 \times 10^{-9} T^3 + 7.32 \times 10^{-13} T^4 + 43.4$

Second Run: $V = 7.39 \times 10^{-1} T - 5.07 \times 10^{-4} T^2 + 1.48 \times 10^{-7} T^3 - 1.57 \times 10^{-11} T^4 - 385.0$

Figure 194. Thermoelectric Voltage for Vanadium Carbide (ATJ Graphite Reference, Density 1.73 g/cc)

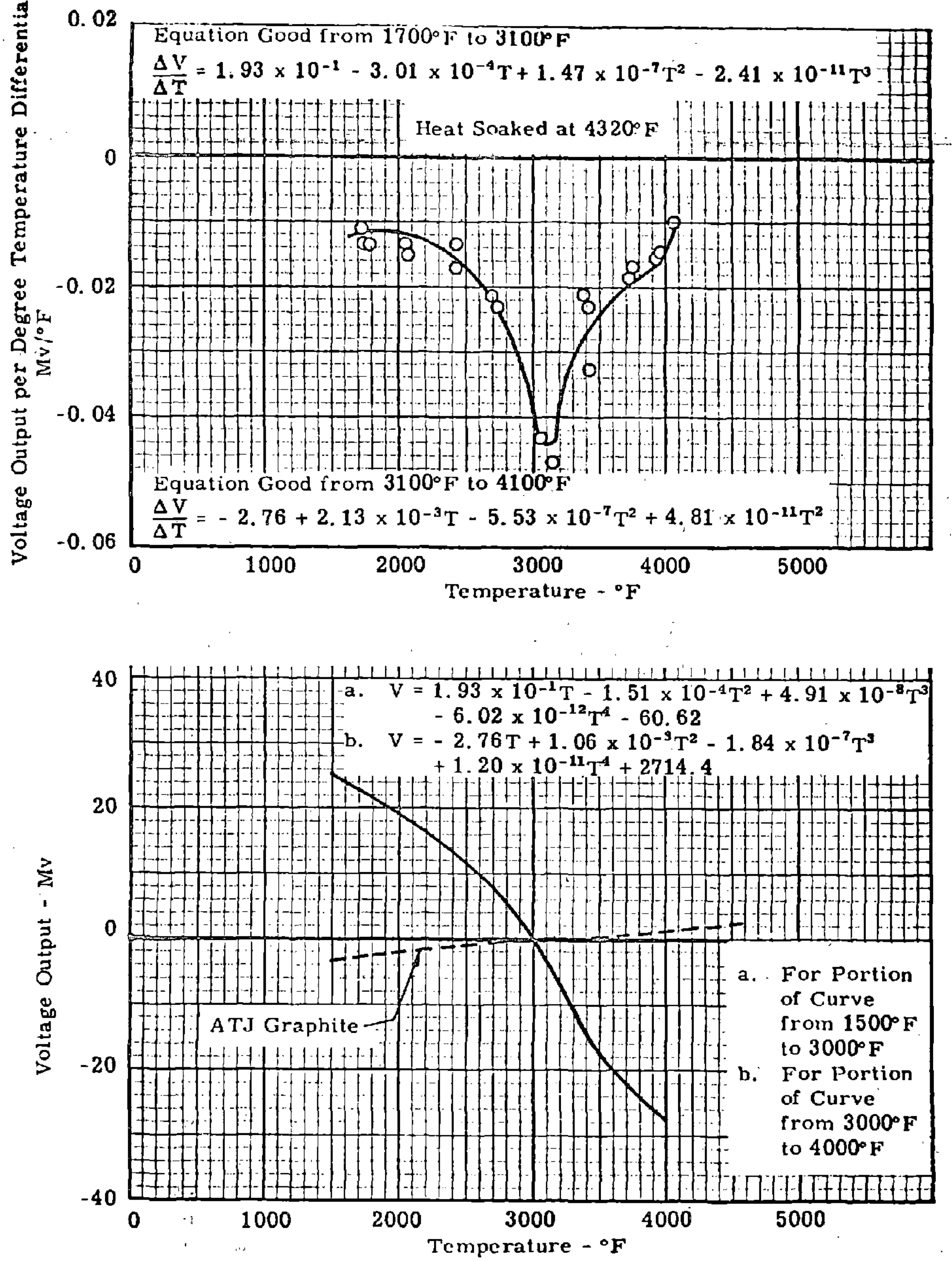

Figure 195. Thermoelectric Voltage for Zirconium Carbide (ATJ Graphite Reference, Density = 1.73 g/cc)

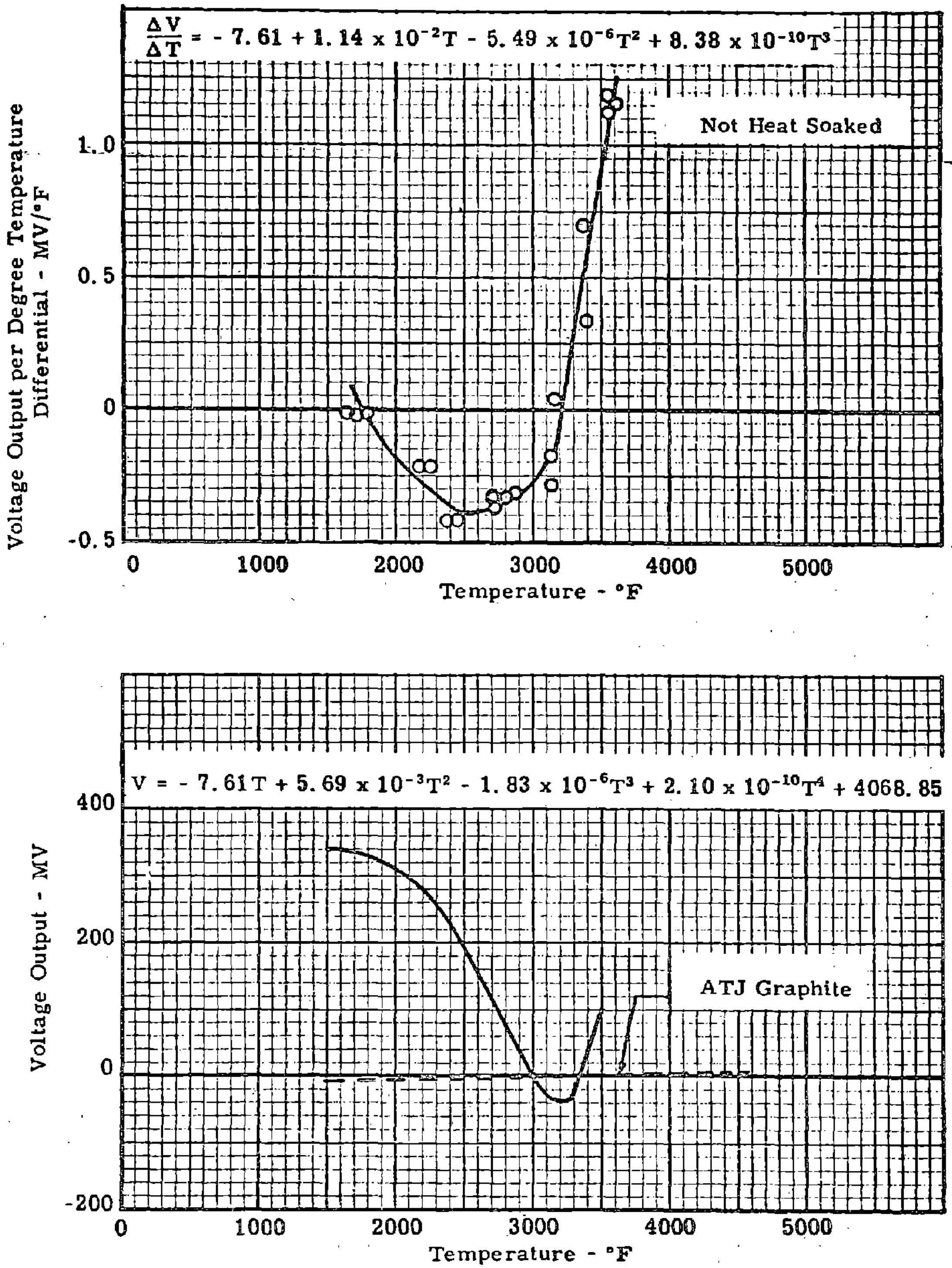

Figure 196. Thermoelectric Voltage for Boron Nitride (ATJ Graphite Reference, Density = 1.73 g/cc)

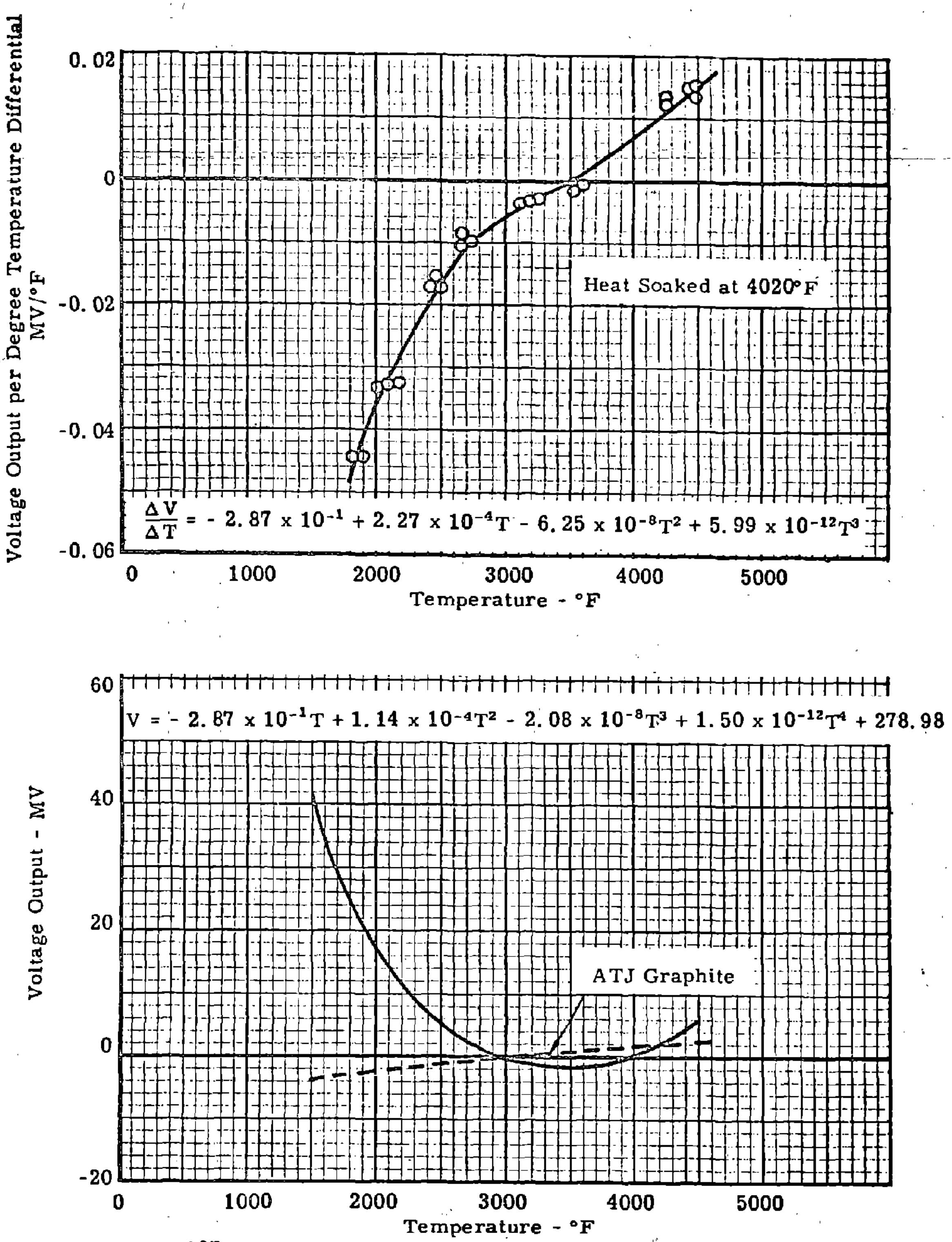

Figure 197. Thermoelectric Voltage for Hafnium Nitride (ATJ Graphite Reference, Density = 1.73 g/cc)

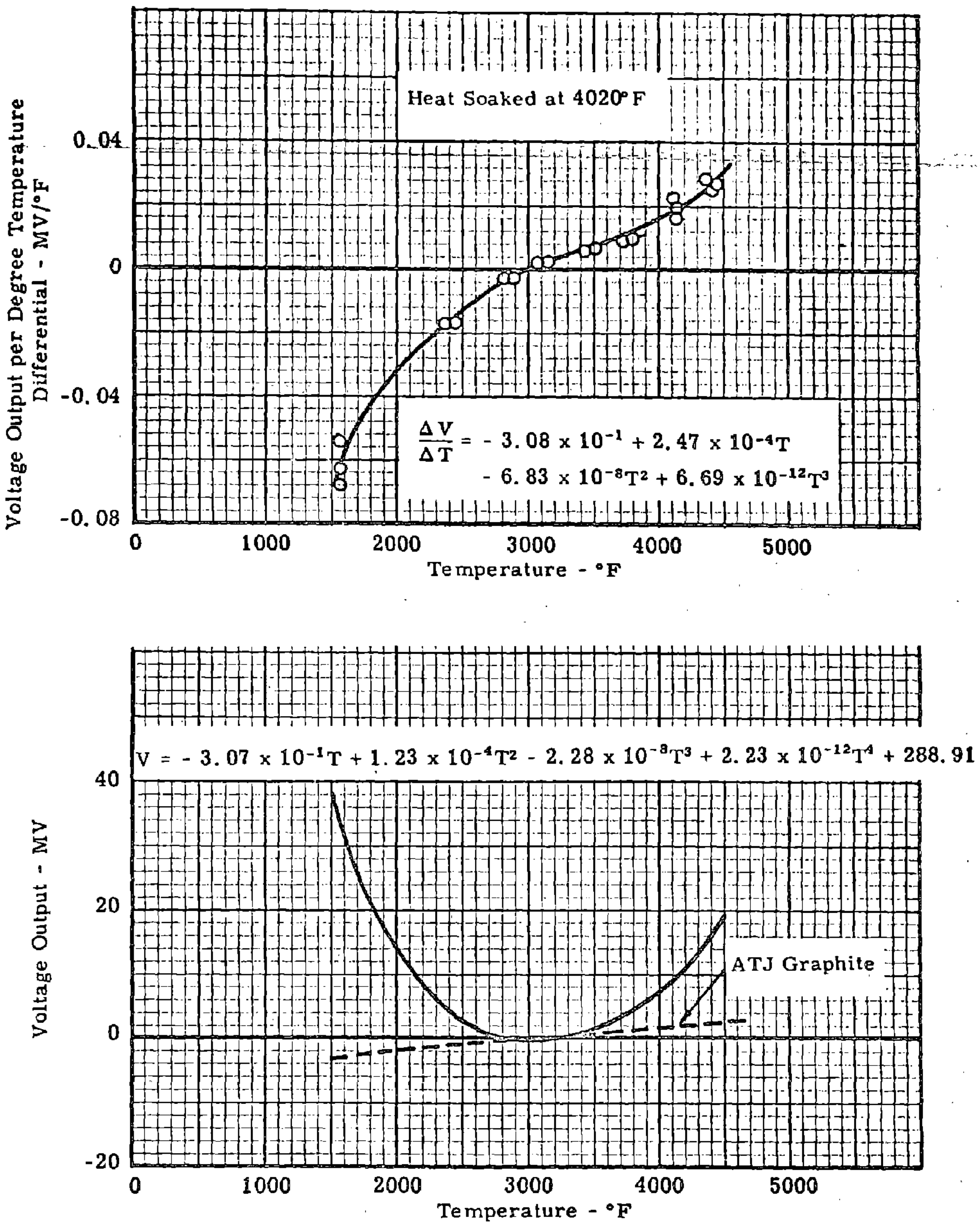

Figure 198. Thermoelectric Voltage for Titanium Nitride (ATJ Graphite Reference, Density = 1.73 g/cc)

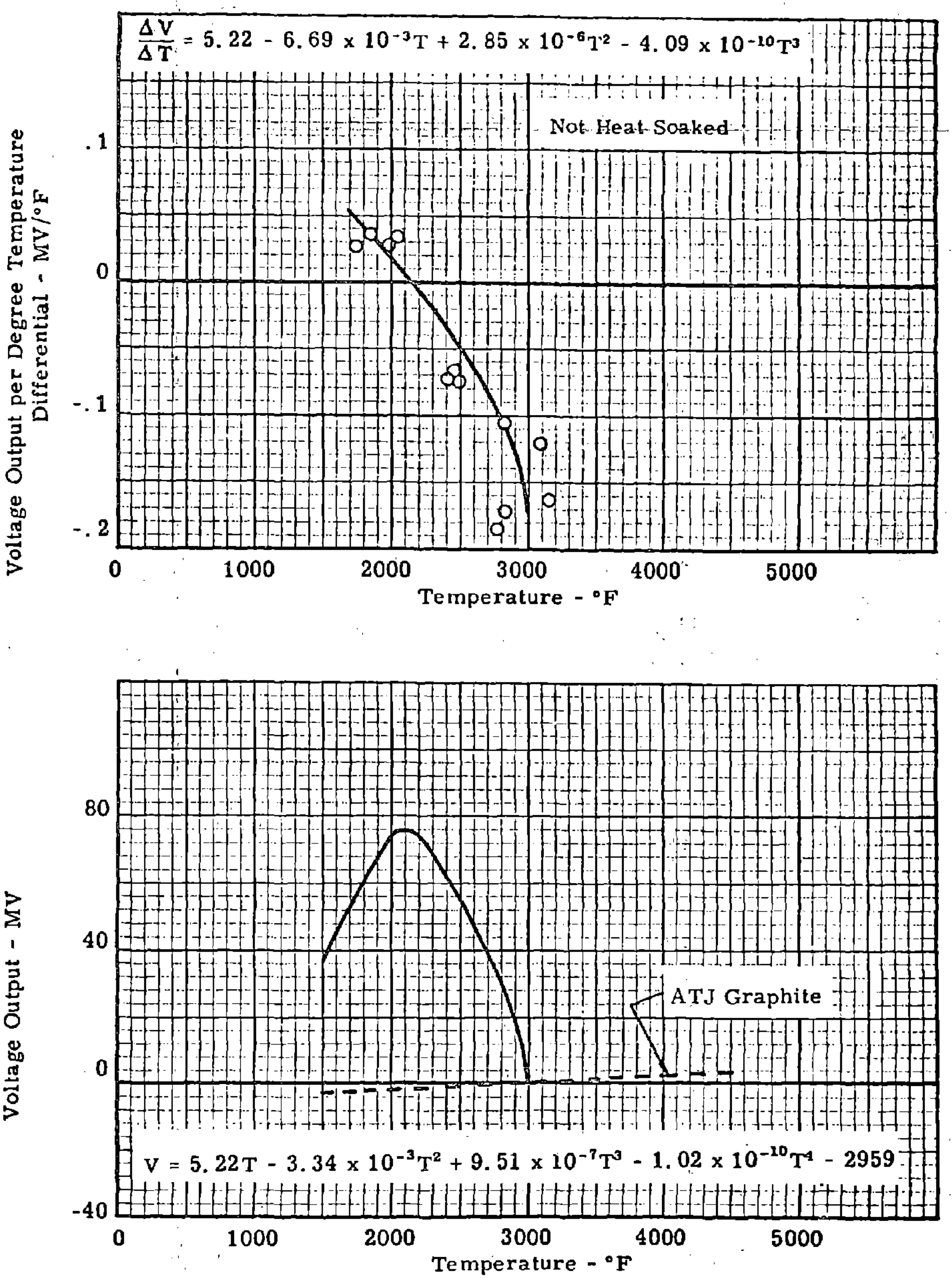

Figure 199. Thermoelectric Voltage for Beryllium Oxide
(ATJ Graphite Reference, Density = 1.73 g/cc)

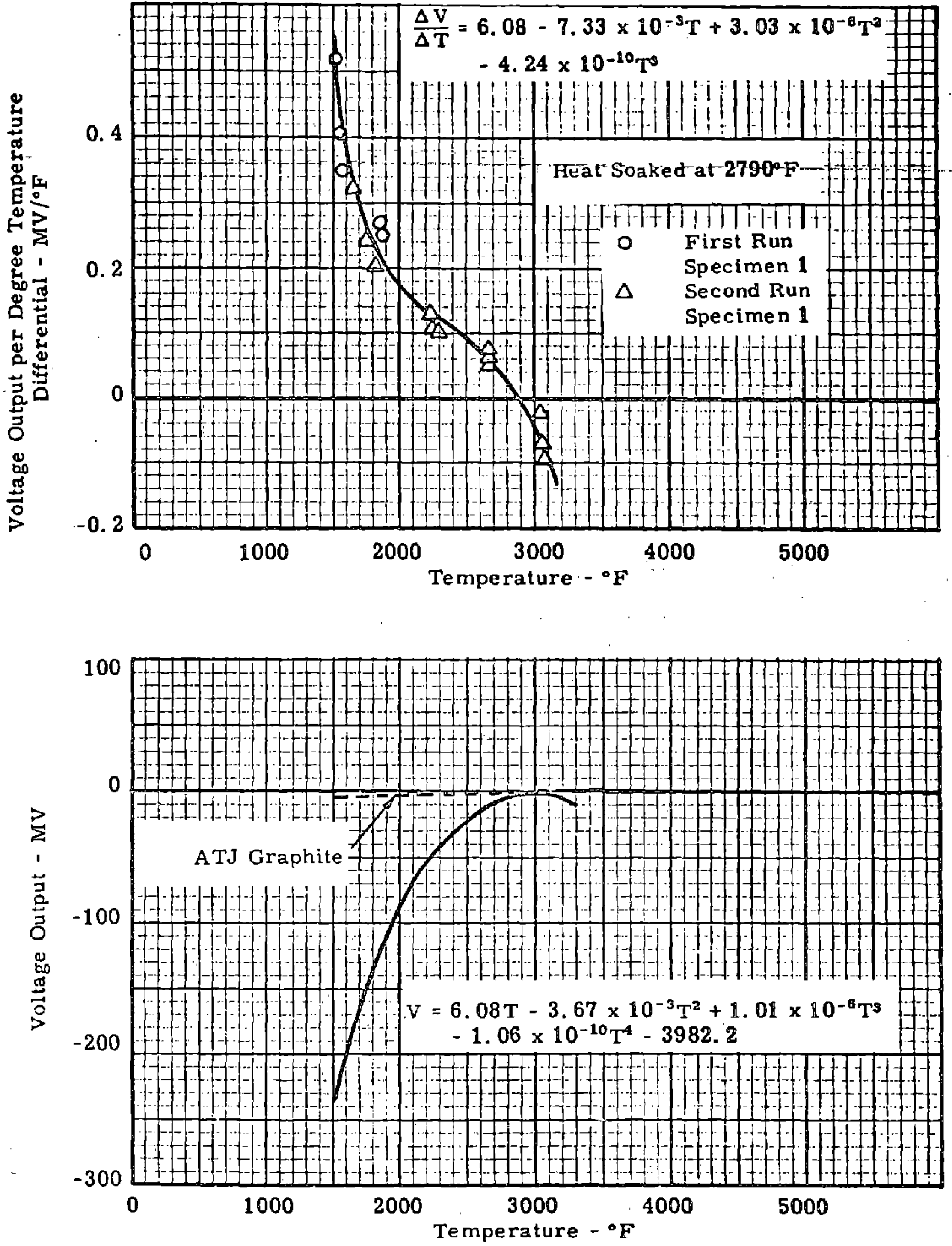

Figure 200. Thermoelectric Voltage for Cerium Dioxide (ATJ Graphite Reference, Density = 1.73 g/cc)

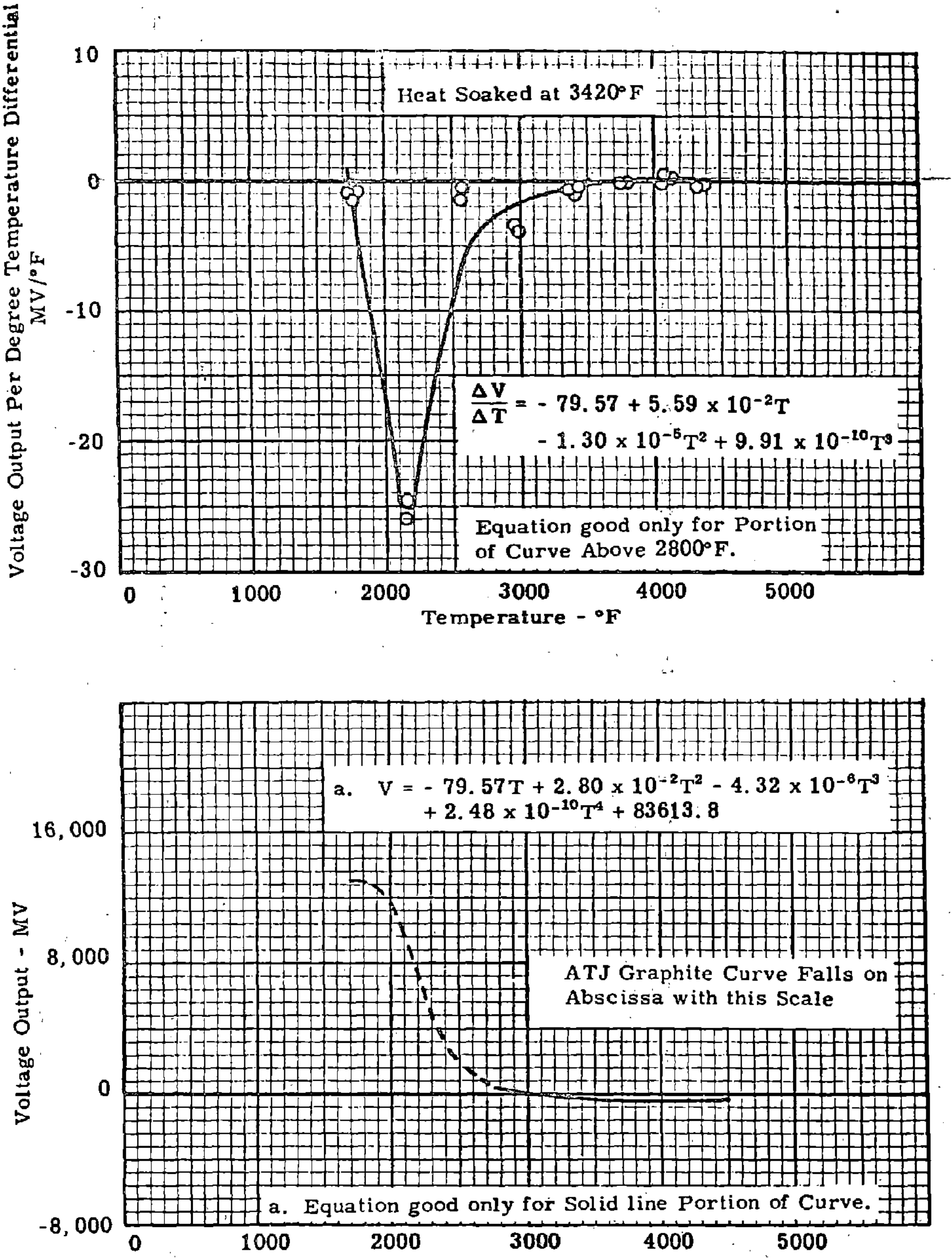

Figure 201. Thermoelectric Voltage for Hafnium Dioxide
(ATJ Graphite Reference, Density = 1.73 g/cc)

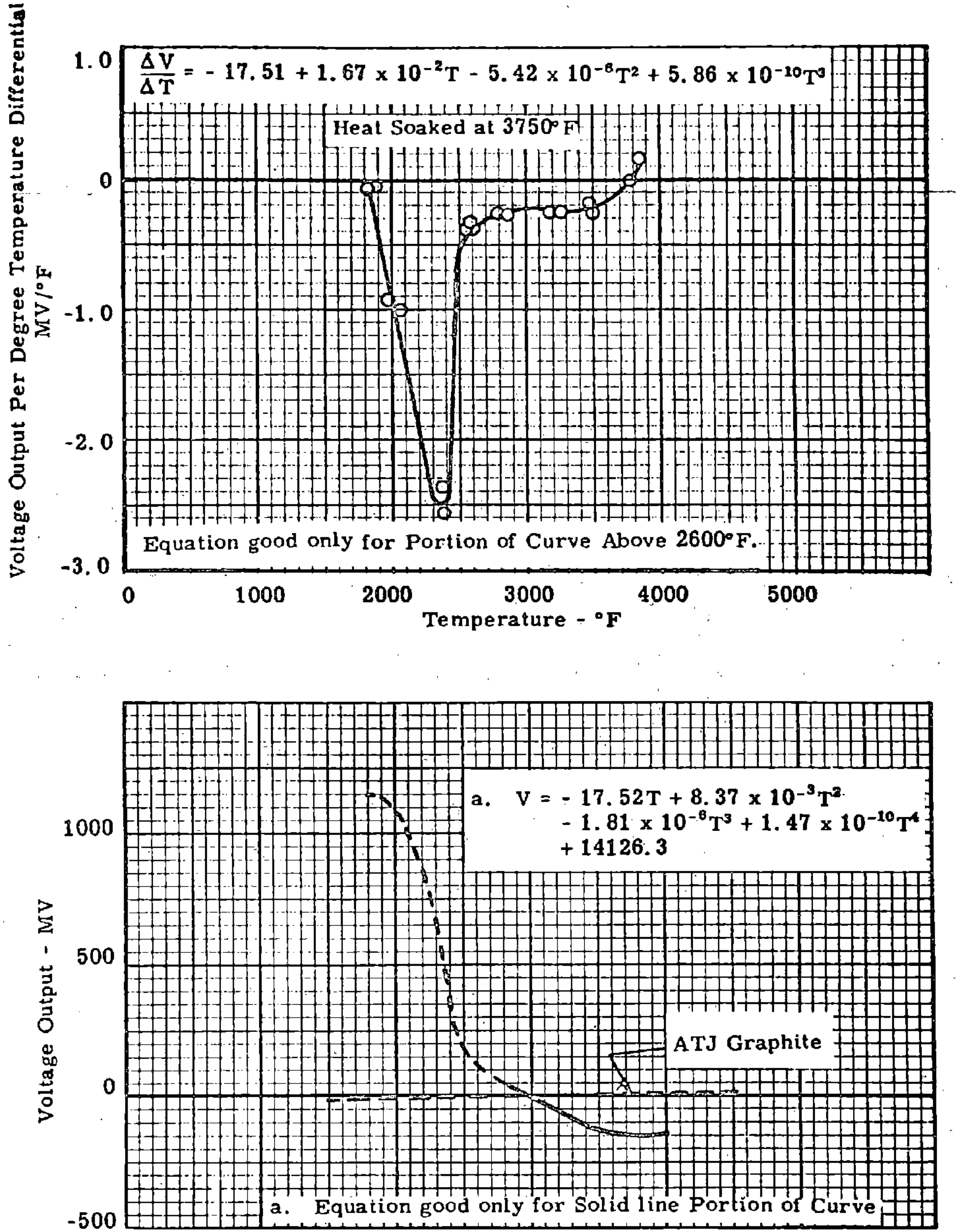

Figure 202. Thermoelectric Voltage for Magnesium Oxide (ATJ Graphite Reference, Density = 1.73 g/cc)

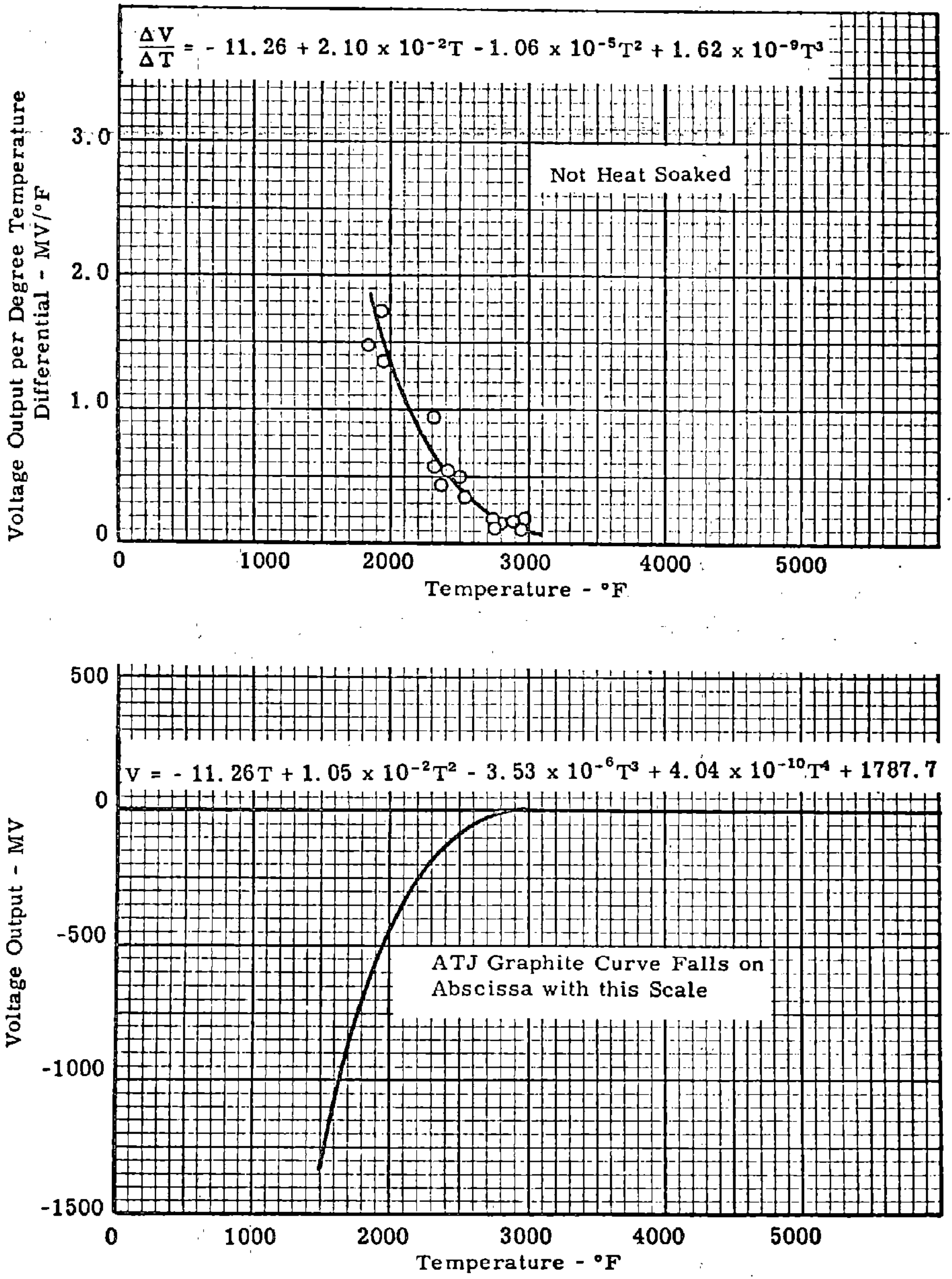

Figure 203. Thermoelectric Voltage for Thorium Dioxide (ATJ Graphite Reference, Density = 1.73 g/cc)

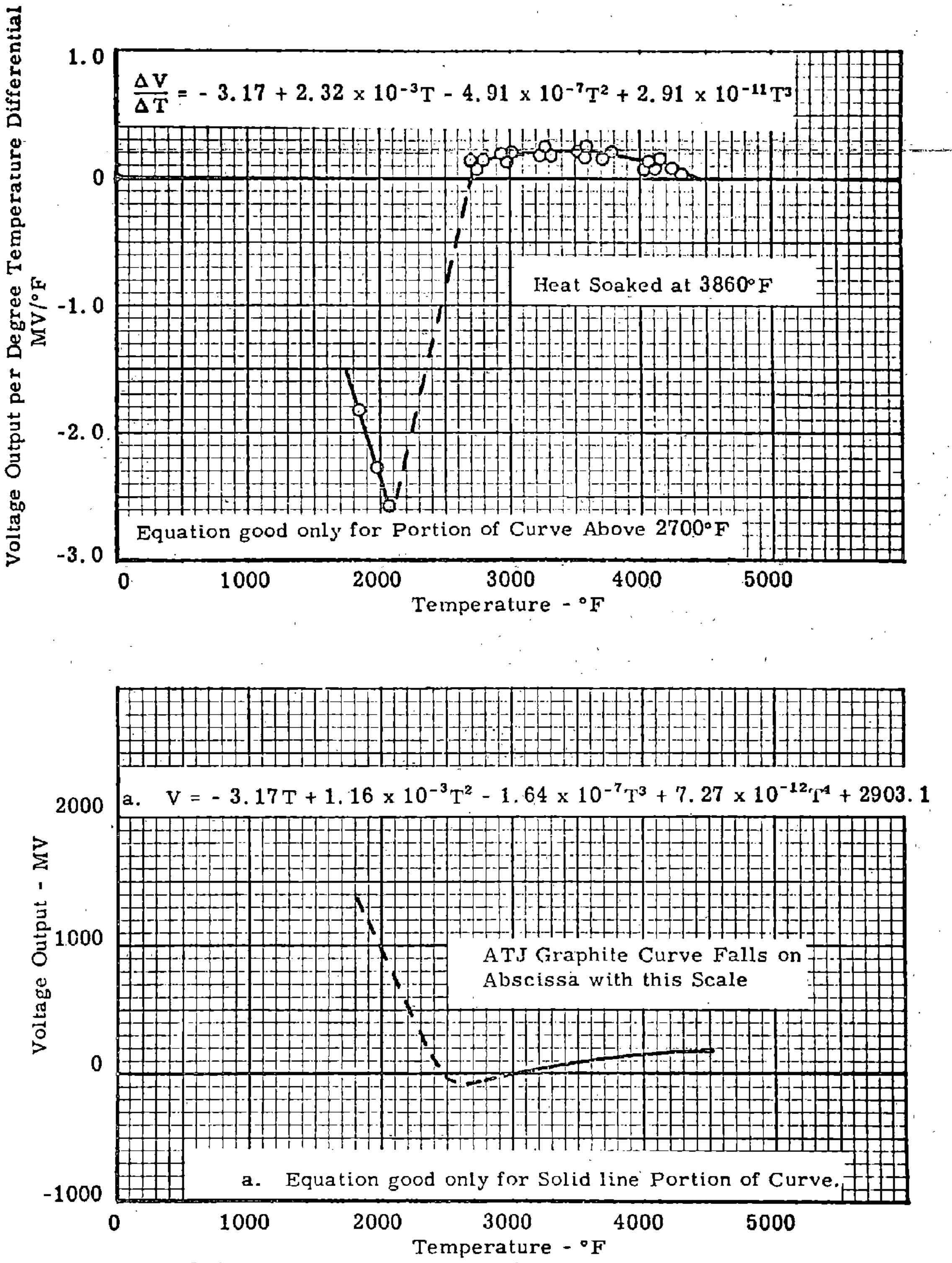

Figure 204. Thermoelectric Voltage for Zirconium Dioxide (ATJ Graphite Reference, Density = 1.73 g/cc)

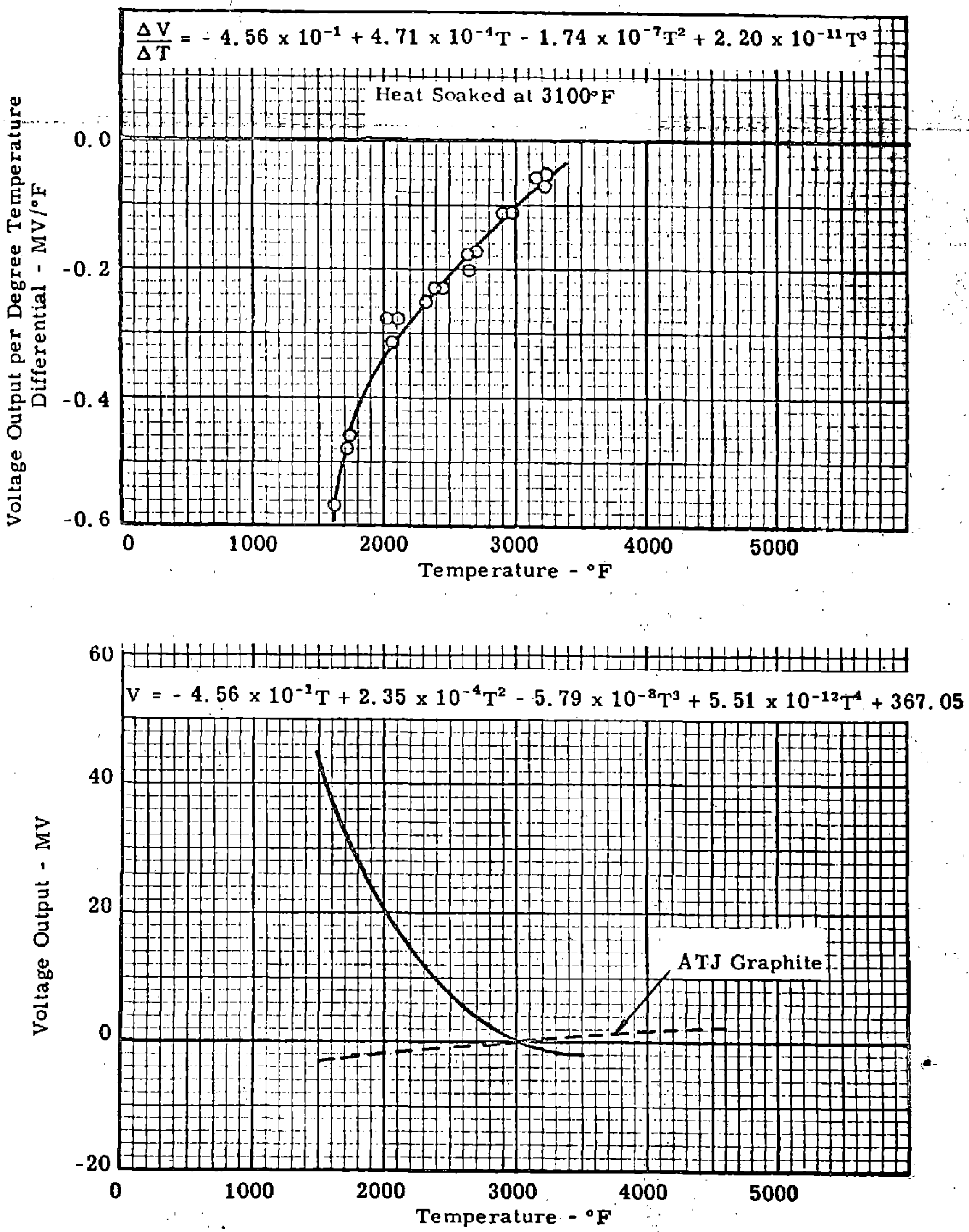

Figure 205. Thermoelectric Voltage for Columbium +0.5% Zirconium (ATJ Graphite Reference, Density = 1.73 g/cc)

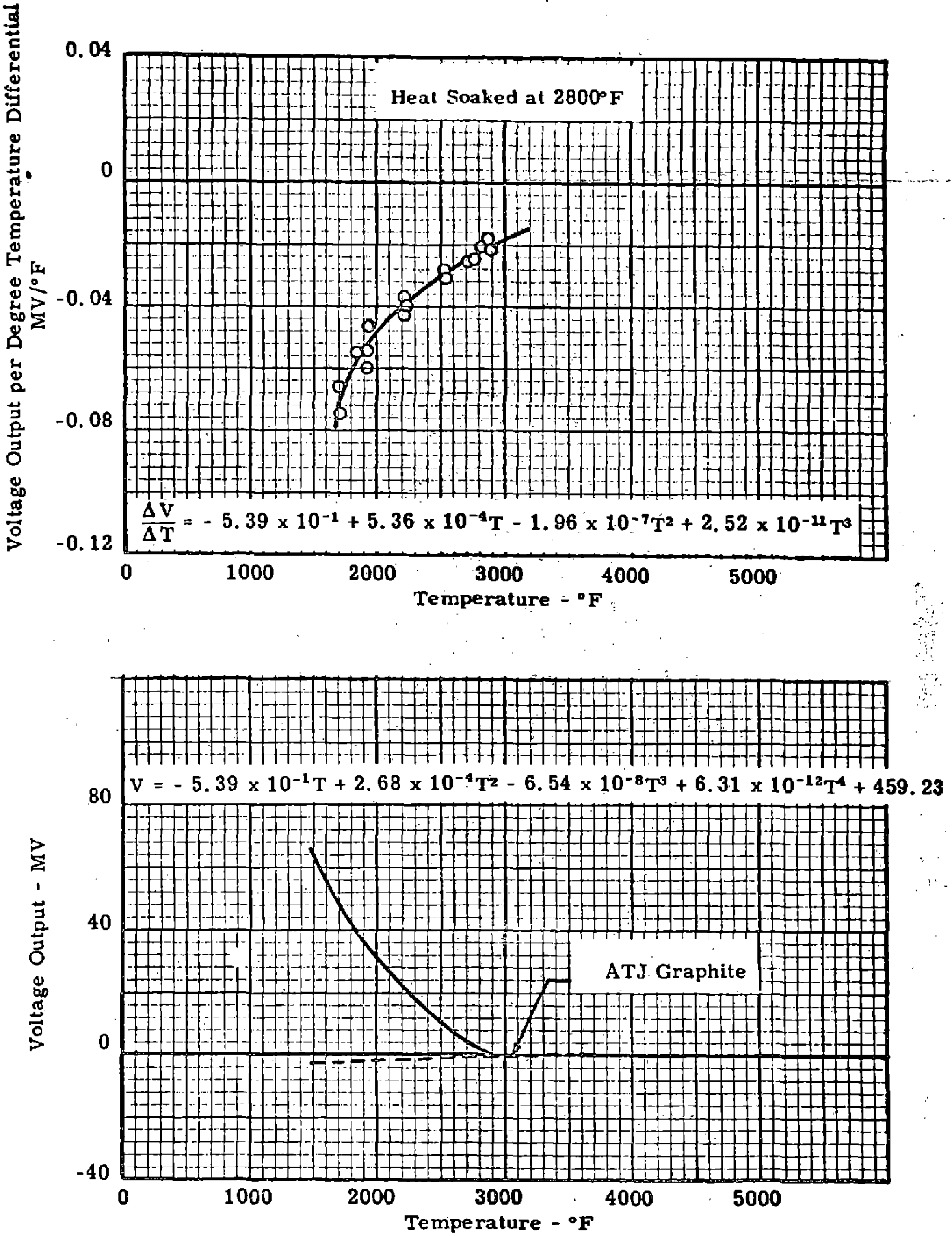

Figure 206. Thermoelectric Voltage for Molybdenum + 0.5% Titanium
(ATJ Graphite Reference, Density = 1.73 g/cc)

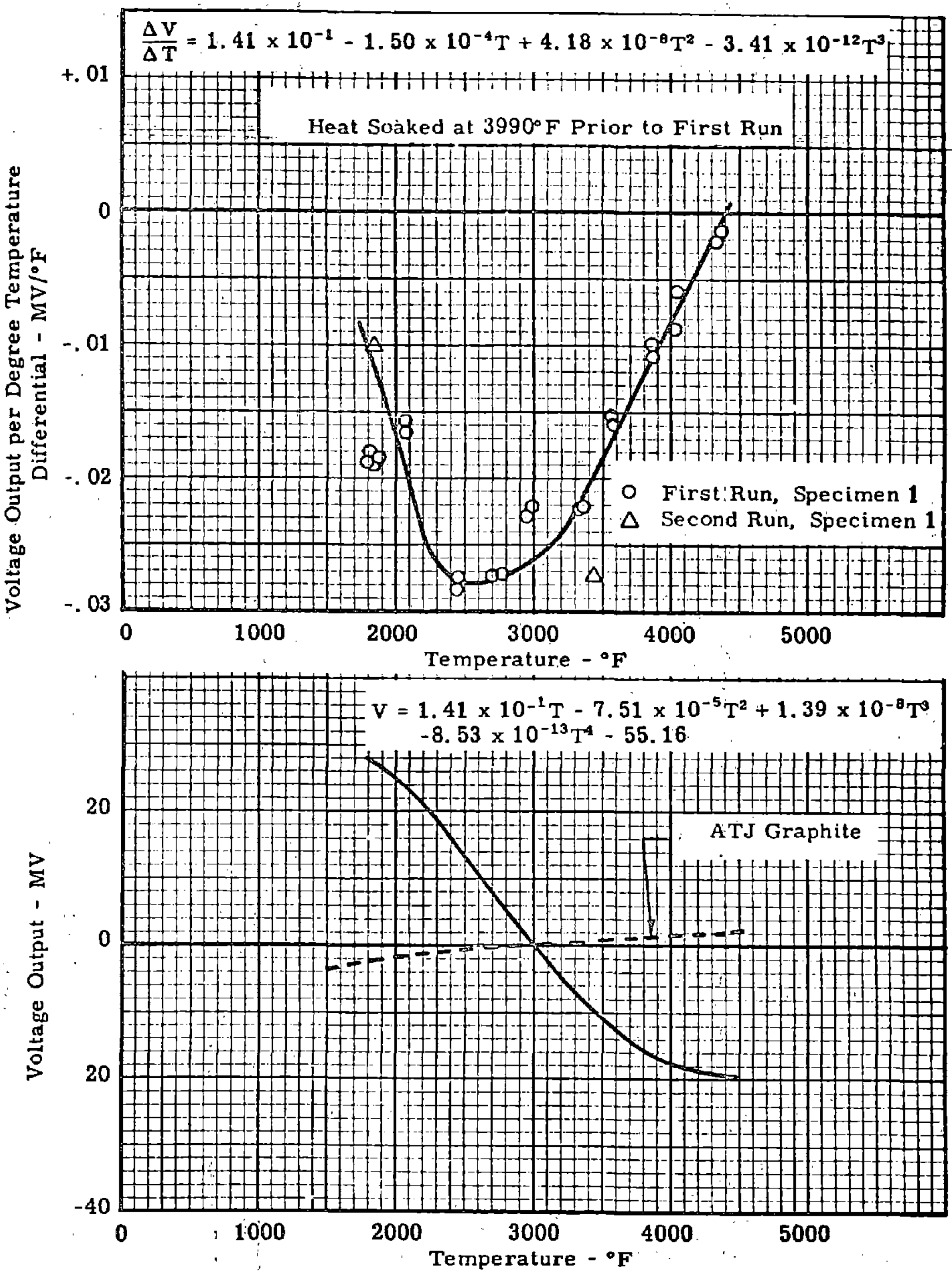

Figure 207. Thermoelectric Voltage for Tungsten (Carborundum) (ATJ Graphite Reference, Density = 1.73 g/cc)

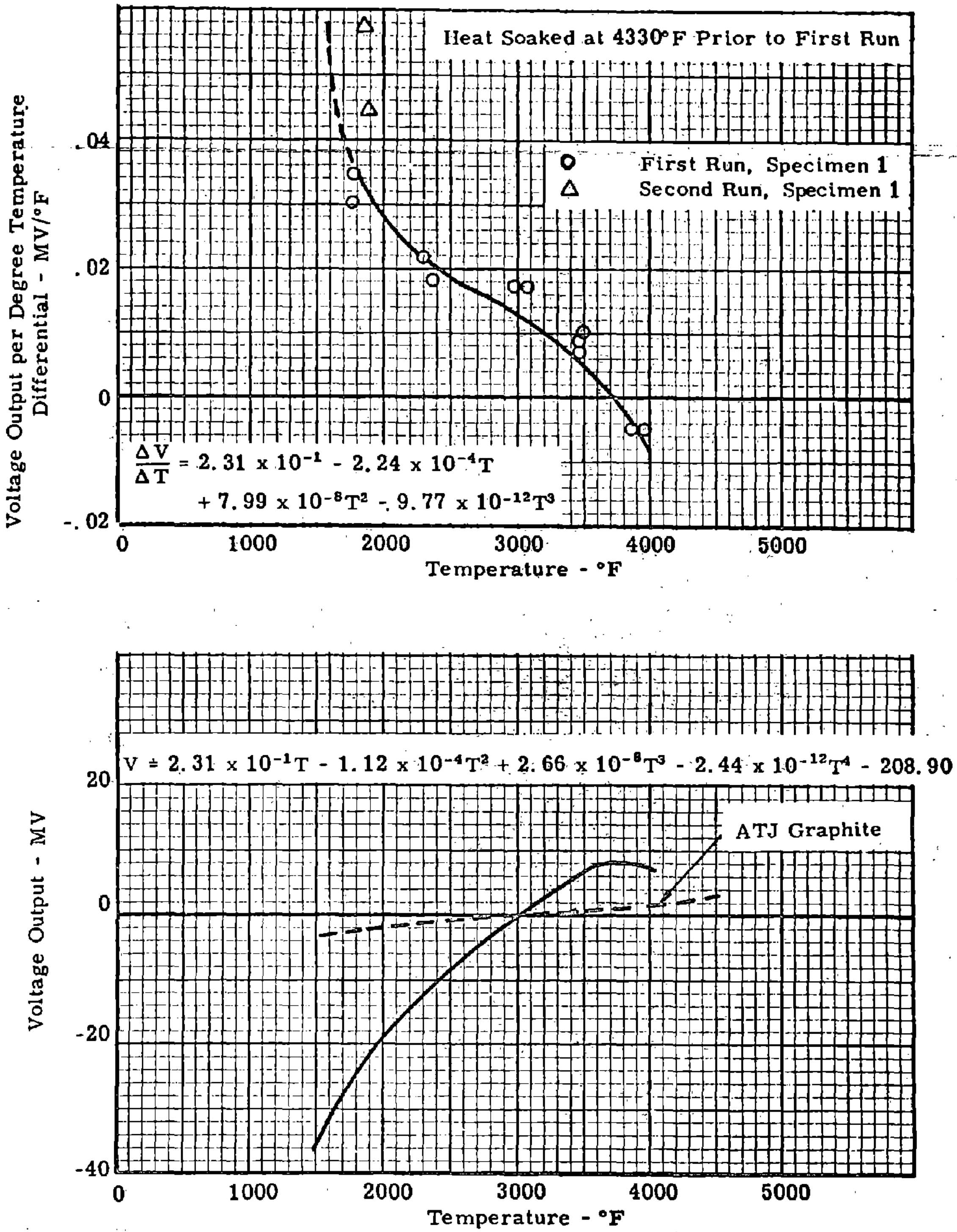

Figure 208. Thermoelectric Voltage for Tungsten (Supplied by General Electric) (ATJ Graphite Reference, Density 1.73 g/cc)

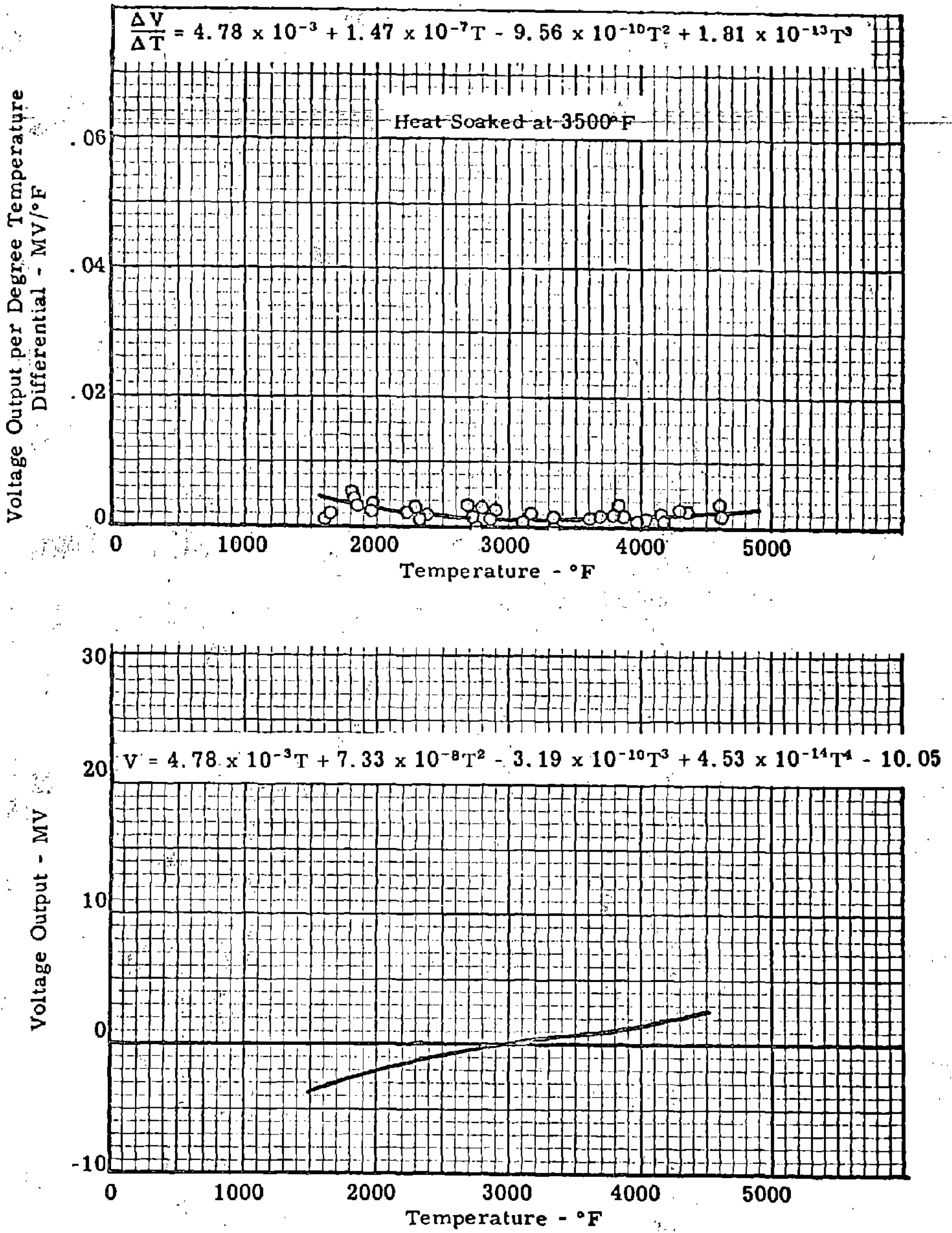

Figure 209. Thermoelectric Voltage for ATJ Graphite
(ATJ Graphite Reference, Density = 1.73 g/cc)

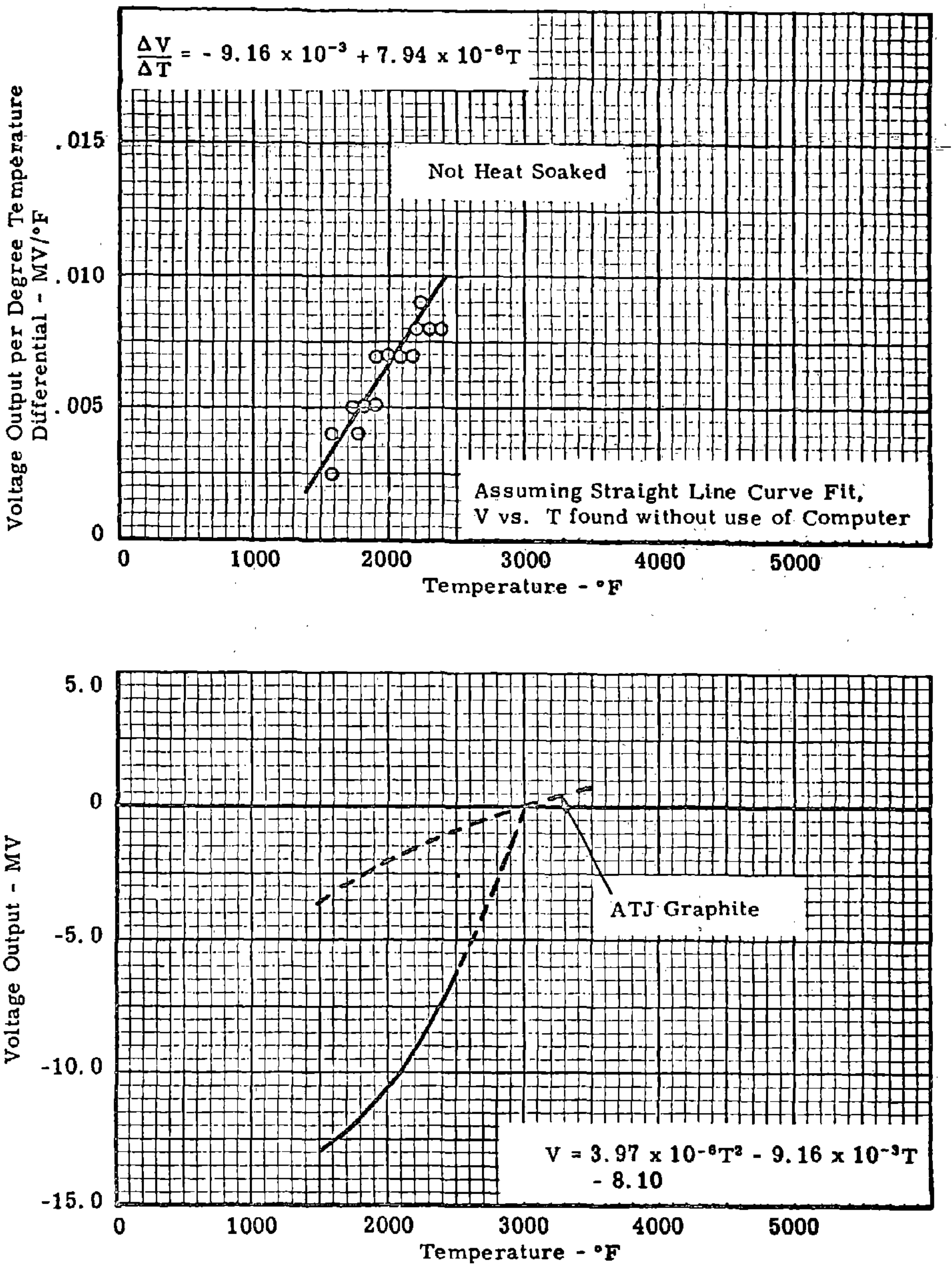

Figure 210. Thermoelectric Voltage for Platinum + 12.2% Rhodium (ATJ Graphite Reference, Density = 1.73 g/cc)

Table 1

Properties of the Materials Evaluated in the Work

| Material Name | Material Supplier | Chemical Symbol | Forming Method | Theoretical Melting or Destruction of Pure Material $^{\circ}F^{1}$ | Maximum Exposure Temperature $^{\circ}F^{2}$ | Remarks |
|---|---|---|---|---|---|---|
| Hafnium Diboride | The Carborundum Company | $HfB_2$ | Hot Pressed | 5530-5880 | 4810+ | Melted |
| Thorium Tetraboride | The Carborundum Company | $ThB_4$ | Hot Pressed | 4530 | 4065 | Fractured |
| Titanium Diboride | The Carborundum Company | $TiB_2$ | Hot Pressed | 5240-5400 | 4900 | Melted |
| Tungsten Boride | The Carborundum Company | WB | Hot Pressed | 5180 | 4430 | Melted |
| Zirconium Diboride | The Norton Company | $ZrB_2$ | Hot Pressed | 5500 | 5000 | Blistered and Cracked |
| Columbium Carbide | Kennametal, Inc. | CbC | Hot Pressed | 6330 | 4820 | Melted |
| Dimolybdenum Carbide | The Carborundum Company | $Mo_2C$ | Hot Pressed | 4870 | 4450+ | Melted |
| Hafnium Carbide | The Carborundum Company | HfC | Hot Pressed | 7030 | 5220 | Some Specimens Broke |
| Tantalum Carbide | Kennametal, Inc. | TaC | Hot Pressed | 6867 | 4800 | Pitted and Spalled |
| Titanium Carbide | The Carborundum Company | TiC | Hot Pressed | 5751 | 4850 | Melted |
| Tungsten Carbide | The Carborundum Company | WC | Hot Pressed | 4770 (Decomposes) | 4960 | Melted |
| Vanadium Carbide | The Carborundum Company | VaC | Hot Pressed | 5130 | 4675 | Melted |
| Zirconium Carbide | General Electric Company | ZrC | Pressed and Sintered | 5750-6390 | 4900 | Melted |
| Boron Nitride | The Carborundum Company | BN | Hot Pressed | 5427 | 4100 | Cracked and Blistered |
| Hafnium Nitride | The Carborundum Company | HfN | Hot Pressed | 5990 | 4750 | Fractured |
| Silicon Nitride | The Carborundum Company | $Si_3N_4$ | A Casting Method | 3500 (Sublimes) | 3420 | Melted |
| Tantalum Nitride | The Carborundum Company | TaN | Hot Pressed | 5590 | 4900 | Shattered |
| Titanium Nitride | General Astrometals Corp. | TiN | Hot Pressed | 5310 | 4930 | Melted |
| Zirconium Nitride | General Electric Company | ZrN | Pressed and Sintered | 5400 | 4810 | Fractured |

Table 1 (Continued)

Properties of the Materials Evaluated in the Work

| Material Name | Material Supplier | Chemical Symbol | Forming Method | Theoretical Melting or Destruction of Pure Material °F[1] | Maximum Exposure Temperature °F[2] | Remarks |
|---|---|---|---|---|---|---|
| Beryllium Oxide | Zirconium Corporation of America | BeO | Pressed and Sintered | 4585 | 3965 | Crumbled |
| Cerium Dioxide | Zirconium Corporation of America | $CeO_2$ | Pressed and Sintered | 3500 app (Decomposes) | 3800 | Melted |
| Hafnium Dioxide | Zirconium Corporation of America | $HfO_2$ | Pressed and Sintered | 4550 app (Decomposes) | 4625 | Blistered and Partially Melted |
| Magnesium Oxide | Zirconium Corporation of America | MgO | Pressed and Sintered | 5080 | 4450 | Softened |
| Thorium Dioxide | Zirconium Corporation of America | $ThO_2$ | Pressed and Sintered | 5520 | 4000 | Macro Cracked |
| Zirconium Dioxide | Zirconium Corporation of America | $ZrO_2$ | Pressed and Sintered | 4870 | 4600 | Melted |
| Columbium + 0.5% Zirconium | General Astrometals Corp. | Cb+0.5% Zr | Hot Pressed | | 4480 | Melted |
| Molybdenum + 0.5% Titanium | General Astrometals Corp. | Mo+0.5% Ti | Hot Pressed | | 4430 | Melted |
| Tungsten | The Carborundum Company | W | Hot Pressed | 6120-6170 | 5100 | Macro Cracked |
| Tungsten | General Electric Company | W | Arc Cast | 6120-6170 | 5100 | Macro Cracked |
| ATJ Graphite | National Carbon Company | C | Molded and Fired | 6600 (Sublimes) | 5150 | Not Deteriorated |
| Zirconium Silicate (Zirconium Orthosilicate) (Taylor Zircon CZ-5) | The Charles Taylor Sons Company | $ZrO_2 + SiO_2$ | Slip Cast and Sintered | 3250 (Disassociates) | 3710 | Softened (Incipient Melting) |

[1] Supplier and handbook information for crystals and pure materials.

[2] Maximum temperature exposure in Southern Research Institute, work limited by material failure — some failures occurred at lower temperatures.

## Table 2

### Data Interpreted from Photomicrographs of Non Toxic Refractory Materials

All Magnifications: 100X
All Specimens: As-Polished
Illumination: Bright Field

### I. Carbides

| Material | Exposure | |
|---|---|---|
| | Before | After |
| Ti C | Coarse meandering LD[1] | Fine LD |
| W C | Fine meandering LD | Severe intergranular C[3] |
| V C | Coarse RD[2] | Fine RD |
| Cb C | Coarse LD | Most severe interaggregate C intergranular C, and internal C bursts |
| Zr C | Coarse LD | Fine LD |
| Hf C | Coarse LD | Coarse RD |
| $Mo_2$ C | Coarse RD | Severe interaggregate C |
| Ta C | Minor RD | Very slight RD |

### II. Metals and Alloys

| Material | Exposure | |
|---|---|---|
| | Before | After |
| W (Carborundum) | LD | Transaggregate C |
| W (G. E.) | RD | Transaggregate C |
| Cb + 0.5% Zr | LD | Meandering LD |
| Mo + 0.5% Ti | Fine RD | RD |

### III. Diborides and Boride

| Material | Exposure | |
|---|---|---|
| | Before | After |
| Hf $B_2$ | Fine meandering LD | Fine RD |
| Ti $B_2$ | Coarse LD | Large interaggregate C, and small internal inter-aggregate C |
| Zr $B_2$ | Coarse meandering LD | Very Coarse RD with small transaggregate C |
| W B | LD | LD with trans-aggregate C |

### IV. Nitrides

| Material | Exposure | |
|---|---|---|
| | Before | After |
| B N | Very broad meandering LD | Extremely large trans-transaggregate C and small interaggregate C |
| Hf N | Coarse LD | Transgranular C and RD |
| Si N | RD and coarse, but short LD | Coarse RD |
| Ti N | Severe coarse LD | Large transaggregate C and coarse RD |
| Ta N | Pronounced and straight LD and RD | Meandering LD and RD |
| Zr N | Meandering LD and RD | Intergranular C, RD, mixed grain size |

### V. Dioxides and Oxide

| Material | Exposure | |
|---|---|---|
| | Before | After |
| Ce $O_2$ | Coarse LD and coarse aggregate size | Coarse LD and fine aggregate size with intergranular C |
| Hf $O_2$ | Coarse LD | Coarse LD with a few interaggregate C |
| Zr $O_2$ | Coarse LD with blocky aggregates | Coarse LD with interaggregate C |
| Mg O | Very coarse RD with blocky aggregates | Extremely coarse RD |

### VI. Silicate

| Material | Exposure | |
|---|---|---|
| | Before | After |
| $ZrSiO_4$ | Coarse inter-aggregate and transaggregate C, RD, and V[4] | Extremely large V connected by large C, small V, and fine RD |

---

[1] LD represents Line Discontinuities.
[2] RD represents Random Discontinuities.
[3] C represents Cracks.
[4] V represents Voids.

Table 3

Data Interpreted from Photomicrographs of Toxic Refractory Materials

All Magnifications: 100X
All Specimens: As-Polished
Illumination: Bright Field

I. Thorium Tetraboride

| Exposure | |
|---|---|
| Before | After |
| Fine RD,[1] distinct aggregate outline, and no fusion of aggregates. | Fine RD, distinct aggregate outline, and no fusion of aggregates. |

II. Beryllium Oxide

| Exposure | |
|---|---|
| Before | After |
| Very coarse RD and slight fusion of aggregates. | Very coarse RD and slight fusion of aggregates. |

III. Thorium Dioxide

| Exposure | |
|---|---|
| Before | After |
| Coarse RD and slight fusion of aggregates. | Transaggregate and interaggregate C[2], coarse RD, and slight fusion of aggregates. |

---

[1] RD represents random discontinuities.

[2] C represents Cracks.

Table 4

Chemical Analysis of Specimens Before and After Exposure

| | | Before Exposure | | | | After Exposure | | |
|---|---|---|---|---|---|---|---|---|
| Sample | | Assay Found, % | Assay Calculated, % | Elements Found by Semi-Quantitative Emission Spectrography, % | | | Found, % | Carbon, % |
| Hafnium Diboride | Hf | 89.5 | 89.2 | Mg | 0.1 | Hf | 89.4 | 0.77 |
| | B | 10.0 | 10.8 | Ti | 0.1 | B | 10.5 | |
| | C | 0.01 | | Fe | 3.5 | | | |
| | | | | Zr | 1.5 | | | |
| Titanium Diboride | Ti | 69.8 | 68.9 | V | 0.3 | Ti | 69.3 | 0.32 |
| | B | 29.5 | 31.1 | Fe | 0.4 | B | 28.7 | |
| | C | 0.2 | | | | $N_2$ | 0.3 | |
| | $N_2$ | 0.6 | | | | | | |
| Tungsten Boride | W | 95.3 | 94.5 | Si | 0.2 | W | 94.8 | 0.09 |
| | B | 4.7 | 5.5 | V | 0.2 | B | 5.2 | |
| | | | | Zr | 0.1 | | | |
| | | | | Fe | 0.2 | | | |
| | | | | Cb | 0.2 | | | |
| Zirconium Diboride | Zr | 78.0 | 80.8 | Ca | 0.1 | Zr | 78.6 | 0.57 |
| | B | 18.9 | 19.2 | Cr | 0.3 | B | 17.3 | |
| | C | 0.58 | | Fe | 0.8 | N | <0.1 | |
| | N | 0.1 | | Other | 0.1 | | | |
| Columbium Carbide | Cb | 88.9 | 88.6 | Fe | 0.1 | Cb | 89.1 | – |
| | C | 10.8 | 11.4 | Other | 0.1 | C | 10.7 | |
| | N | 0.2 | | | | N | 0.2 | |
| Dimolybdenum Carbide | Mo | 92.1 | 94.1 | Si | 2.0 | Mo | 92.4 | – |
| | C | 5.51 | 5.9 | Al | 0.2 | C | 5.39 | |
| | N | <0.1 | | Fe | 0.6 | N | <0.1 | |
| | | | | Ti | 0.3 | | | |
| Hafnium Carbide | Hf | 93.8 | 93.7 | Al | 0.2 | Hf | 93.9 | – |
| | C | 5.85 | 6.3 | Ti | 0.3 | C | 5.73 | |
| | N | 1.0 | | | | N | 0.9 | |
| Tantalum Carbide | Ta | 93.8 | 93.8 | Fe | 0.1 | Ta | 93.8 | – |
| | C | 6.77 | 6.2 | Si | 0.1 | C | 6.52 | |
| | N | <0.1 | | | | N | <0.1 | |
| Titanium Carbide | Ti | 79.8 | 80.0 | Zr | 0.5 | Ti | 79.2 | – |
| | C | 19.2 | 20.0 | Fe | 0.6 | C | 19.0 | |
| | N | 0.9 | | | | N | 0.6 | |
| Tungsten Carbide | W | 93.9 | 93.9 | Si | 0.3 | W | 94.1 | – |
| | C | 6.15 | 6.1 | Fe | 0.4 | C | 5.95 | |
| | N | <0.1 | | | | N | <0.1 | |
| Vanadium Carbide | V | 81.0 | 80.9 | Fe | 0.7 | V | 80.8 | – |
| | C | 18.6 | 19.1 | | | C | 18.4 | |
| | N | 0.5 | | | | N | 0.3 | |
| Zirconium Carbide | Zr | 88.5 | 88.4 | Total | 0.1 | Zr | 89.3 | – |
| | C | 11.0 | 11.6 | | | C | 10.8 | |
| | N | 0.5 | | | | N | 0.5 | |
| Boron Nitride | B | 42.9 | 43.6 | Si | 0.1 | B | 41.5 | 0.13 |
| | N | 52.4 | 56.4 | Ti | 0.2 | N | 55.0 | |
| | | | | Ca | 0.2 | | | |
| Hafnium Nitride | Hf | 93.6 | 92.7 | Mg | 0.2 | Hf | 93.6 | 0.07 |
| | N | 7.5 | 7.3 | Ca | 0.3 | N | 7.5 | |
| | | | | Zr | 3.4 | | | |
| Silicon Nitride | Si | | 60.08 | Mn | 0.1 | | | 0.49 |
| | N | | 39.91 | Mg | 0.1 | | | |
| | | | | Al | 0.3 | | | |
| | | | | Ca | 0.6 | | | |
| | | | | Zr | 0.1 | | | |
| | | | | Cr | 0.1 | | | |
| | | | | Fe | 0.7 | | | |
| | | | | Ti | Trace | | | |
| Tantalum Nitride | Ta | 95.7 | 92.8 | Si | 0.2 | Ta | 95.5 | 0.95 |
| | N | 3.5 | 7.2 | Mg | 0.1 | N | 3.1 | |
| | C | 0.13 | | Fe | 0.3 | | | |
| Titanium Nitride | Ti | 81.3 | 77.4 | Fe | 0.4 | Ti | 77.6 | 1.02 |
| | N | 17.0 | 22.6 | | | N | 18.9 | |
| | C | 0.87 | | | | | | |
| Zirconium Nitride | Zr | 86.9 | 86.69 | Fe | 0.1 | Zr | 86.5 | 1.19 |
| | $N_2$ | 12.8 | 13.31 | | | $N_2$ | 10.8 | |

## Table 4

### Chemical Analysis of Specimens Before and After Exposure (Continued)

| Sample | | Before Exposure: Assay, Found, % | Before Exposure: Assay, Calculated, % | Before Exposure: Elements Found by Semi-Quantitative Emission Spectrography, % | | After Exposure: Found, % | | After Exposure: Carbon, % |
|---|---|---|---|---|---|---|---|---|
| Cerium Dioxide | Ce | 82.2 | 81.1 | Ca | 0.1 | Ce | 81.5 | 0.10 |
| | O | – | | Zr | 0.2 | | | |
| Hafnium Dioxide | Hf | 82.0 | 84.8 | Mg | 0.3 | Hf | 84.0 | 0.51 |
| | O | – | | Ti | 0.1 | | | |
| | | | | Ca | 0.1 | | | |
| | | | | Fe | 2.5 | | | |
| Magnesium Oxide | Mg | 59.4 | 60.3 | Si | 0.3 | Mg | 60.1 | <0.05 |
| | O | – | | Al | 0.1 | | | |
| | | | | Ca | 0.2 | | | |
| | | | | Fe | 0.3 | | | |
| Zirconium Dioxide | Zr | 70.7 | 74.0 | Si | 0.1 | Zr | 71.2 | 0.15 |
| | O | – | | Mg | 0.1 | | | |
| | | | | Ca | 1.0 | | | |
| | | | | Ti | 0.1 | | | |
| | | | | Al | 0.1 | | | |
| Columbium +0.5% Zr | Cb | 99.2 | 99.5 | Less than 0.1 total | | Cb | 99.5 | 0.41 |
| | Zr | 0.5 | 0.5 | | | Zr | – | |
| Molybdenum +0.5% Ti | Mo | 98.6 | 99.5 | Ni | 0.2 | Mo | 98.3 | 0.20 |
| | Ti | 0.7 | 0.5 | Fe | 0.3 | Ti | – | |
| | | | | Si | 0.1 | | | |
| | | | | Al | 0.2 | | | |
| Tungsten (Carborundum Company) | W | 100.1 | 100.0 | Si | 0.2 | W | 100.0 | 0.15 |
| | | | | V | 0.2 | | | |
| | | | | Cu | 0.1 | | | |
| | | | | Cb | 0.2 | | | |
| Tungsten (General Electric) | W | 100.0 | 100.0 | Si | 0.2 | W | 100.1 | 0.49 |
| | | | | V | 0.2 | | | |
| | | | | Cb | 0.2 | | | |
| ATJ Graphite | C | 99.5 | 100.0 | Si | 0.2 | C | 99.5 | – |
| | | | | Fe | 0.1 | | | |
| | | | | Ca | Trace | | | |
| | | | | Mg | Trace | | | |
| Zirconium Silicate | Zr | | 49.75 | Al | 0.2 | | | 0.13 |
| | Si | | 15.33 | Ti | 0.1 | | | |
| | | | | Fe | 0.1 | | | |
| | | | | Mg | Trace | | | |
| | | | | Hf | Trace | | | |

Table 5. Densities of Specimens Before and After Exposure

Densities in g/cm³ at 25°C

| | Literature Values (From Various Sources) | Before Exposure | | | After Exposure | | |
|---|---|---|---|---|---|---|---|
| | | Apparent Density | | True Density (By Immersion in Xylene) | Apparent Density | | True Density (By Immersion in Xylene) |
| | | ASTM Method B311-58 | Wax-coated Specimen | | ASTM Method | Wax-coated Specimen | |
| Hafnium Diboride | 10.5 | 10.7 | 10.7 | 10.8 | 10.1 | 10.2 | 10.3 |
| Thorium Tetraboride | 7.5 | 7.78 | 7.82 | 8.17 | - | - | - |
| Titanium Diboride | 4.50-4.52 | 4.52 | 4.51 | 4.57 | 4.17 | 4.16 | 4.23 |
| Tungsten Boride | 15.3 | 15.2 | 15.0 | 15.3 | 14.7 | 14.7 | 14.8 |
| Zirconium Diboride | 5.7 | 5.62 | 5.75 | 5.69 | 5.44 | 5.46 | 5.60 |
| Columbium Carbide | 7.56; 7.82 | 7.68 | 7.74 | 7.75 | 7.51 | 7.51 | 7.53 |
| Dimolybdenum Carbide | 8.4; 8.9 | 8.86 | 8.92 | 8.96 | 8.56 | 8.59 | 8.69 |
| Hafnium Carbide | 12.2 | 11.2 | 11.5 | 12.0 | 11.2 | 11.1 | 11.8 |
| Tantalum Carbide | 14.0; 14.5 | 14.0 | 14.1 | 14.1 | 13.9 | 13.8 | 13.9 |
| Titanium Carbide | 4.25; 4.90 | 4.73 | 4.75 | 4.77 | 4.68 | 4.69 | 4.82 |
| Tungsten Carbide | 15.0; 15.5 | 15.0 | 15.1 | 15.1 | 13.1 | 13.2 | 14.7 |
| Vanadium Carbide | 5.36 | 5.42 | 5.45 | 5.47 | 5.0 | 5.0 | 5.1 |
| Zirconium Carbide | 6.70; 6.90 | 6.27 | 6.28 | 6.33 | 6.24 | 6.27 | 6.28 |
| Boron Nitride | 2.25; 2.34 | 2.14 | 2.15 | 2.16 | 1.96 | 1.99 | 2.17 |
| Hafnium Nitride | - | 12.7 | 12.7 | 12.8 | 12.4 | 12.4 | 12.4 |
| Silicon Nitride | - | 2.5 | 2.4 | 2.8 | 2.8 | 2.5 | 2.9 |
| Tantalum Nitride | 14.1 | 13.4 | 13.3 | 13.7 | 13.4 | 13.6 | 14.6 |
| Titanium Nitride | 4.57-5.21; 5.48 | 4.78 | 4.89 | 4.90 | 4.59 | 4.59 | 5.14 |
| Zirconium Nitride | - | 7.2 | 7.2 | 7.2 | 6.8 | 6.7 | 7.0 |
| Beryllium Oxide | 3.02 | 2.93 | 2.66 | 3.00 | - | - | - |
| Cerium Dioxide | 7.13 | 6.60 | 6.73 | 6.87 | 6.57 | 6.56 | 6.76 |
| Hafnium Dioxide | 9.68 | 9.00 | 9.14 | 9.55 | 8.93 | 9.02 | 9.64 |
| Magnesium Oxide | 3.58 | 3.30 | 3.30 | 3.51 | 3.50 | 3.35 | 3.60 |
| Thorium Dioxide | 9.67 | 9.10 | 8.90 | 9.69 | - | - | - |
| Zirconium Dioxide | 5.56; 5.8 | 5.36 | 5.49 | 5.63 | 5.35 | 5.44 | 5.72 |
| Columbium +0.5% Zr | - | 7.88 | 7.66 | 8.09 | 8.32 | 8.24 | 8.47 |
| Molybdenum +0.5% Ti | - | | 9.49 | 9.39 | 8.64 | 8.68 | 9.05 |
| Tungsten (Carborundum) | 19.3 | 18.9 | 18.4 | 19.1 | 18.8 | 18.7 | 18.8 |
| Tungsten (General Electric) | 19.3 | 18.9 | 18.8 | 19.1 | 18.7 | 18.7 | 18.7 |
| ATJ Graphite | - | 1.8 | 1.8 | 1.9 | 1.7 | 1.8 | 2.1 |
| Zirconium Silicate | - | 4.3 | 3.9 | 4.4 | 3.3 | 3.1 | 3.4 |

## Table 6.

### Thermal Expansion of Hafnium Diboride

Run No. E 8

| Temperature °F | Observed Total Elongation $10^{-3}$ inches | Observed Unit Elongation $10^{-3}$ inches/inch | Unit Elongation Correction for Dilatometer Motion $10^{-3}$ inches/inch | Corrected Specimen Unit Elongation $10^{-3}$ inches/inch |
|---|---|---|---|---|
| 70 | 0.0 | 0.0 | 0.0 | 0.0 |
| 504 | 2.8 | 1.3 | 0.3 | 1.6 |
| 1002 | 6.0 | 2.7 | 0.8 | 3.5 |
| 1487 | 9.4 | 4.2 | 1.2 | 5.4 |
| 1525 | 9.1 | 4.1 | 1.3 | 5.4 |
| 1950 | 12.2 | 5.5 | 1.8 | 7.3 |
| 2570 | 16.7 | 7.5 | 2.6 | 10.1 |
| 3030 | 20.7 | 9.3 | 3.1 | 12.4 |
| 3525 | 22.8 | 10.3 | 3.9 | 14.2 |
| 3950 | 25.3 | 11.4 | 4.7 | 16.1 |
| 4240 | 44.9 | 20.2 | 5.1 | 25.3 |
| 4350 | 49.5 | 22.3 | 5.3 | 27.6 |
| 4620 | 54.2 | 24.4 | 5.8 | 30.2 |
| 4650 | 76.5 | 34.5 | 5.8 | 40.3 |
| 4700 | 116.0 | 52.3 | 6.0 | 58.3 |
| 4710 | 155.5 | 70.0 | 6.0 | 76.0 |
| 4710 | 158.4 | 71.4 | 6.0 | 77.4 |
| 4710+ | Specimen Melted | - | - | - |
| 70 | -101.2 | -45.6 | 0.0 | -45.6 |

Initial Length = 2.222"
Final Length = Melted

Table 7.

Thermal Expansion of Thorium Tetraboride

Run No. E 20

| Temperature °F | Observed Total Elongation $10^{-3}$ inches | Observed Unit Elongation $10^{-3}$ inches/inch | Unit Elongation Correction for Dilatometer Motion $10^{-3}$ inches/inch | Corrected Specimen Unit Elongation $10^{-3}$ inches/inch |
|---|---|---|---|---|
| 70 | 0.0 | 0.0 | 0.0 | 0.0 |
| 218 | 0.0 | 0.0 | 0.2 | 0.2 |
| 501 | 1.2 | 0.5 | 0.3 | 0.8 |
| 1000 | 5.0 | 2.2 | 0.8 | 3.0 |
| 1532 | 8.8 | 3.9 | 1.3 | 5.2 |
| 1548 | 8.9 | 3.9 | 1.3 | 5.2 |
| 1940 | 12.3 | 5.4 | 1.7 | 7.1 |
| 2455 | 16.9 | 7.4 | 2.3 | 9.7 |
| 2870 | 21.0 | 9.2 | 2.9 | 12.1 |
| 2980 | 21.8 | 9.6 | 3.0 | 12.6 |
| 3355 | 25.2 | 11.1 | 3.6 | 14.7 |
| 3480 | 25.7 | 11.3 | 3.8 | 15.1 |
| 4065 | 23.2 | 10.2 | 4.8 | 15.0 |
| 70 | -14.5 | -6.4 | 0.0 | -6.4 |

Initial Length = 2.275"
Final Length = 2.265"

Table 8.

Thermal Expansion of Titanium Diboride

Run No. E 7

| Temperature °F | Observed Total Elongation $10^{-3}$ inches | Observed Unit Elongation $10^{-3}$ inches/inch | Unit Elongation Correction for Dilatometer Motion $10^{-3}$ inches/inch | Corrected Specimen Unit Elongation $10^{-3}$ inches/inch |
|---|---|---|---|---|
| 70 | 0.0 | 0.0 | 0.0 | 0.0 |
| 497 | 2.7 | 1.2 | 0.3 | 1.5 |
| 1171 | 7.8 | 3.4 | 1.0 | 4.4 |
| 1591 | 11.4 | 5.0 | 1.3 | 6.3 |
| 1580 | 11.3 | 5.0 | 1.3 | 6.3 |
| 2025 | 14.5 | 6.4 | 1.8 | 8.2 |
| 2570 | 19.0 | 8.4 | 2.5 | 10.9 |
| 3050 | 22.7 | 10.0 | 3.2 | 13.2 |
| 3480 | 25.7 | 11.3 | 3.8 | 15.1 |
| 3810 | 28.8 | 12.7 | 4.4 | 17.1 |
| 4070 | 31.8 | 14.0 | 4.8 | 18.8 |
| 4115 | 32.2 | 14.2 | 5.0 | 19.2 |
| 4380 | 34.4 | 15.2 | 5.3 | 20.5 |
| 4500 | 36.0 | 15.9 | 5.6 | 21.5 |
| 4500+ | Specimen Melted | - | - | - |
| 70 | -24.4 | -10.8 | 0.0 | -10.8 |

Initial Length = 2.271"
Final Length = Melted

Table 9.

Thermal Expansion of Tungsten Boride

Run No. E 3

| Temperature °F | Observed Total Elongation $10^{-3}$ inches | Observed Unit Elongation $10^{-3}$ inches/inch | Unit Elongation Correction for Dilatometer Motion $10^{-3}$ inches/inch | Corrected Specimen Unit Elongation $10^{-3}$ inches/inch |
|---|---|---|---|---|
| 70 | 0.0 | 0.0 | 0.0 | 0.0 |
| 502 | 1.4 | 0.6 | 0.4 | 1.0 |
| 1108 | 5.4 | 2.3 | 0.9 | 3.2 |
| 1550 | 8.0 | 3.4 | 1.3 | 4.7 |
| 2010 | 11.0 | 4.7 | 1.8 | 6.5 |
| 2420 | 13.6 | 5.8 | 2.3 | 8.1 |
| 2950 | 17.2 | 7.4 | 3.0 | 10.4 |
| 3500 | 20.7 | 8.9 | 3.9 | 12.8 |
| 3925 | 24.7 | 10.6 | 4.6 | 15.2 |
| 4350 | 28.2 | 12.1 | 5.3 | 17.4 |
| 4350+ | Specimen Melted | - | - | - |

Initial Length = 2.332"
Final Length = Melted

## Table 10.

## Thermal Expansion of Dimolybdenum Carbide

Run No. E 5

| Temperature °F | Observed Total Elongation $10^{-3}$ inches | Observed Unit Elongation $10^{-3}$ inches/inch | Unit Elongation Correction for Dilatometer Motion $10^{-3}$ inches/inch | Corrected Specimen Unit Elongation $10^{-3}$ inches/inch |
|---|---|---|---|---|
| 70 | 0.0 | 0.0 | 0.0 | 0.0 |
| 431 | 2.2 | 1.0 | 0.3 | 1.3 |
| 1084 | 6.4 | 2.9 | 0.8 | 3.7 |
| 1479 | 8.8 | 3.9 | 1.2 | 5.1 |
| 1525 | 9.0 | 4.0 | 1.3 | 5.3 |
| 2060 | 12.5 | 5.6 | 1.9 | 7.5 |
| 2600 | 15.9 | 7.1 | 2.6 | 9.7 |
| 3030 | 20.5 | 9.2 | 3.2 | 12.4 |
| 3490 | 23.2 | 10.4 | 3.8 | 14.2 |
| 4010 | 155.8 | 69.8 | 4.8 | 74.6 |
| 4100 | 155.9 | 69.8 | 5.0 | 74.8 |
| 4230 | 163.0 | 73.1 | 5.1 | 78.2 |
| 4230 | 152.0 | 68.1 | 5.1 | 73.2 |
| 4230 | 148.0 | 66.4 | 5.1 | 71.5 |
| 4230 | 133.5 | 59.9 | 5.1 | 65.0 |
| 4240 | 125.0 | 56.0 | 5.2 | 61.2 |
| 4240 | 115.0 | 51.6 | 5.2 | 56.8 |
| 4280 | 105.0 | 47.0 | 5.2 | 52.2 |
| 4360 | 101.3 | 45.5 | 5.3 | 50.8 |
| 4360 | 97.8 | 43.8 | 5.3 | 49.1 |
| 4450 | 85.0 | 38.1 | 5.5 | 43.6 |
| 4450+ | Specimen Melted | - | - | - |

Initial Length = 2.230
Final Length = Melted

## Table 11.

### Thermal Expansion of Titanium Carbide

Run No. E 1

| Temperature °F | Observed Total Elongation $10^{-3}$ inches | Observed Unit Elongation $10^{-3}$ inches/inch | Unit Elongation Correction for Dilatometer Motion $10^{-3}$ inches/inch | Corrected Specimen Unit Elongation $10^{-3}$ inches/inch |
|---|---|---|---|---|
| 70 | 0.0 | 0.0 | 0.0 | 0.0 |
| 1450 | 10.3 | 4.3 | 1.2 | 5.5 |
| 2050 | 15.7 | 6.5 | 1.9 | 8.4 |
| 2495 | 19.6 | 8.1 | 2.4 | 10.5 |
| 2975 | 23.9 | 9.9 | 3.0 | 12.9 |
| 3000 | 26.0 | 10.7 | 3.0 | 13.7 |
| 3475 | 29.5 | 12.2 | 3.8 | 16.0 |
| 3970 | 34.2 | 14.1 | 4.6 | 18.7 |
| 4460 | 41.5 | 17.1 | 5.5 | 22.6 |
| 4770 | 79.9 | 33.0 | 6.1 | 39.1 |
| 2700 | 49.4 | 20.4 | 2.7 | 23.1 |
| 2100 | 46.8 | 19.4 | 1.9 | 21.3 |
| 2570 | 49.4 | 20.4 | 2.5 | 22.9 |
| 3030 | 52.1 | 21.6 | 3.1 | 24.7 |
| 3475 | 55.0 | 22.7 | 3.9 | 26.6 |
| 3990 | 58.8 | 24.3 | 4.7 | 29.0 |
| 4500 | 63.4 | 26.2 | 5.5 | 31.7 |
| 4770 | 62.8 | 25.9 | 6.1 | 32.0 |
| 4850 | Specimen Melted | - | - | - |

Initial Length = 2.420"
Final Length = Melted

## Table 12.

## Thermal Expansion of Tungsten Carbide

Run No. E 4

| Temperature °F | Observed Total Elongation $10^{-3}$ inches | Observed Unit Elongation $10^{-3}$ inches/inch | Unit Elongation Correction for Dilatometer Motion $10^{-3}$ inches/inch | Corrected Specimen Unit Elongation $10^{-3}$ inches/inch |
|---|---|---|---|---|
| 70 | 0.0 | 0.0 | 0.0 | 0.0 |
| 417 | 1.3 | 0.6 | 0.3 | 0.9 |
| 1118 | 4.1 | 1.8 | 0.9 | 2.7 |
| 1507 | 5.4 | 2.4 | 1.3 | 3.7 |
| 1540 | 5.7 | 2.6 | 1.3 | 3.9 |
| 1565 | 5.7 | 2.6 | 1.3 | 3.9 |
| 2030 | 7.4 | 3.3 | 1.8 | 5.1 |
| 2600 | 9.8 | 4.4 | 2.5 | 6.9 |
| 2975 | 12.4 | 5.6 | 3.0 | 8.6 |
| 3510 | 14.9 | 6.7 | 4.0 | 10.7 |
| 3910 | 21.0 | 9.4 | 4.5 | 13.9 |
| 3910 | 29.5 | 13.2 | 4.5 | 17.7 |
| 3910 | 34.6 | 15.5 | 4.5 | 20.0 |
| 3970 | 40.2 | 18.0 | 4.6 | 22.6 |
| 3990 | 42.7 | 19.1 | 4.7 | 23.8 |
| 4180 | 49.1 | 22.0 | 5.0 | 27.0 |
| 4330 | 54.1 | 24.3 | 5.3 | 29.6 |
| 4525 | 58.5 | 26.2 | 5.6 | 31.8 |
| 4620 | 61.3 | 27.5 | 5.8 | 33.3 |

Table 12 (Continued).

Thermal Expansion of Tungsten Carbide

Run No. E 4 (continued)

| Temperature °F | Observed Total Elongation $10^{-3}$ inches | Observed Unit Elongation $10^{-3}$ inches/inch | Unit Elongation Correction for Dilatometer Motion $10^{-3}$ inches/inch | Corrected Specimen Unit Elongation $10^{-3}$ inches/inch |
|---|---|---|---|---|
| 4735 | 65.8 | 29.5 | 6.0 | 35.5 |
| 4745 | 68.5 | 30.7 | 6.0 | 36.7 |
| 4835 | 77.2 | 34.6 | 6.2 | 40.8 |
| 4890 | 86.7 | 38.9 | 6.3 | 45.2 |
| 4900 | 101.7 | 45.5 | 6.4 | 51.9 |
| 4960 | 154.1 | 69.1 | 6.5 | 75.6 |
| 70 | 140.5 | 63.0 | 0.0 | 63.0 |
|  | Specimen Melted |  |  |  |

Initial Length = 2.232"
Final Length = 2.365"

## Table 13.

### Thermal Expansion of Vanadium Carbide

Run No. E 6

| Temperature °F | Observed Total Elongation $10^{-3}$ inches | Observed Unit Elongation $10^{-3}$ inches/inch | Unit Elongation Correction for Dilatometer Motion $10^{-3}$ inches/inch | Corrected Specimen Unit Elongation $10^{-3}$ inches/inch |
|---|---|---|---|---|
| 70 | 0.0 | 0.0 | 0.0 | 0.0 |
| 490 | 2.5 | 1.1 | 0.3 | 1.4 |
| 1158 | 7.4 | 3.2 | 1.0 | 4.2 |
| 1534 | 10.0 | 4.3 | 1.3 | 5.6 |
| 1570 | 10.4 | 4.5 | 1.4 | 5.9 |
| 2210 | 13.0 | 5.6 | 2.0 | 7.6 |
| 2520 | 14.4 | 6.2 | 2.5 | 8.7 |
| 3225 | 19.2 | 8.2 | 3.5 | 11.7 |
| 3480 | 23.6 | 10.1 | 3.8 | 13.9 |
| 3475 | 23.6 | 10.1 | 3.8 | 13.9 |
| 3860 | 40.2 | 17.3 | 4.5 | 21.8 |
| 3870 | 40.2 | 17.3 | 4.5 | 21.8 |
| 4110 | 148.1 | 63.5 | 5.0 | 68.5 |
| 4120 | 148.1 | 63.5 | 5.0 | 68.5 |
| 4145 | 158.8 | 68.0 | 5.0 | 73.0 |
| 4310 | 214.0 | 91.7 | 5.2 | 96.9 |
| 4050 | 204.7 | 87.9 | 4.8 | 92.7 |
| 4425 | 230.7 | 99.0 | 5.5 | 104.5 |
| 4625 | 246.0 | 105.6 | 5.8 | 111.4 |
| 4675 | 253.0 | 108.6 | 5.9 | 114.5 |
| 4675 | 252.0 | 108.1 | 5.9 | 114.0 |
| 4675 | Specimen Melted | - | - | - |
| 70 | 196.2 | 84.1 | 0.0 | 84.1 |

Initial Length = 2.331"
Final Length = 2.510 (Melted)

## Table 14.

Thermal Expansion of Boron Nitride

Run No. E 11

| Temperature °F | Observed Total Elongation $10^{-3}$ inches | Observed Unit Elongation $10^{-3}$ inches/inch | Unit Elongation Correction for Dilatometer Motion $10^{-3}$ inches/inch | Corrected Specimen Unit Elongation $10^{-3}$ inches/inch |
|---|---|---|---|---|
| 70 | 0.0 | 0.0 | 0.0 | 0.0 |
| 230 | 1.7 | 0.6 | 0.2 | 0.8 |
| 323 | 2.8 | 0.9 | 0.2 | 1.1 |
| 500 | 5.0 | 1.7 | 0.3 | 2.0 |
| 829 | 10.0 | 3.3 | 0.6 | 3.9 |
| 1010 | 11.5 | 3.8 | 0.8 | 4.6 |
| 1258 | 13.8 | 4.6 | 1.0 | 5.6 |
| 1587 | 16.4 | 5.4 | 1.3 | 6.7 |
| 1650 | 16.4 | 5.4 | 1.4 | 6.8 |
| 1910 | 19.0 | 6.3 | 1.7 | 8.0 |
| 2260 | 24.3 | 8.0 | 2.1 | 10.1 |
| 2620 | 36.2 | 12.0 | 2.6 | 14.6 |
| 2960 | 59.1 | 19.5 | 3.0 | 22.5 |
| 3110 | 70.0 | 23.1 | 3.3 | 26.4 |
| 3180 | 80.0 | 26.4 | 3.3 | 29.7 |
| 3230 | 95.5 | 31.5 | 3.5 | 34.0 |
| 3330 | 112.2 | 37.1 | 3.6 | 40.7 |
| 3330 | 134.0 | 44.3 | 3.6 | 47.9 |

Table 14 (Continued).

Thermal Expansion of Boron Nitride

Run No. E 11 (continued)

| Temperature °F | Observed Total Elongation $10^{-3}$ inches | Observed Unit Elongation $10^{-3}$ inches/inch | Unit Elongation Correction for Dilatometer Motion $10^{-3}$ inches/inch | Corrected Specimen Unit Elongation $10^{-3}$ inches/inch |
|---|---|---|---|---|
| 3375 | 159.5 | 52.6 | 3.7 | 56.3 |
| 3375 | 187.5 | 61.9 | 3.7 | 65.6 |
| 3375 | 210.0 | 69.4 | 3.7 | 73.1 |
| 3375 | Dial Gage Reached Its Maximum Limit | | | |

Initial Length = 3.029"
Final Length = 3.251"

## Table 15.

### Thermal Expansion of Tantalum Nitride

Run No. E 2

| Temperature °F | Observed Total Elongation $10^{-3}$ inches | Observed Unit Elongation $10^{-3}$ inches/inch | Unit Elongation Correction for Dilatometer Motion $10^{-3}$ inches/inch | Corrected Specimen Unit Elongation $10^{-3}$ inches/inch |
|---|---|---|---|---|
| 70 | 0.0 | 0.0 | 0.0 | 0.0 |
| 500 | 1.9 | 0.8 | 0.4 | 1.2 |
| 937 | 3.9 | 1.7 | 0.7 | 2.4 |
| 1485 | 6.5 | 2.9 | 1.2 | 4.1 |
| 1980 | 8.0 | 3.6 | 1.7 | 5.3 |
| 2500 | 8.9 | 4.0 | 2.4 | 6.4 |
| 2960 | 10.5 | 4.7 | 3.0 | 7.7 |
| 3350 | 12.5 | 5.6 | 3.7 | 9.3 |
| 3500 | 12.0 | 5.3 | 3.9 | 9.2 |
| 3800 | 13.0 | 5.8 | 4.4 | 10.2 |
| 3925 | 11.7 | 5.2 | 4.6 | 9.8 |
| 4470 | 14.6 | 6.5 | 5.5 | 12.0 |
| 4650 | 16.2 | 7.2 | 5.9 | 13.1 |
| 4900 | Dial Gage Dropping Rapidly | - | - | - |
| 4160 | -17.0 | -7.6 | 5.0 | -2.6 |
| 70 | -39.1 | -17.4 | 0.0 | -17.4 |

Initial Length = 2.243"
Final Length = 2.229"

## Table 16.

### Thermal Expansion of Beryllium Oxide

Run No. E 21

| Temperature °F | Observed Total Elongation $10^{-3}$ inches | Observed Unit Elongation $10^{-3}$ inches/inch | Unit Elongation Correction for Dilatometer Motion $10^{-3}$ inches/inch | Corrected Specimen Unit Elongation $10^{-3}$ inches/inch |
|---|---|---|---|---|
| 70 | 0.0 | 0.0 | 0.0 | 0.0 |
| 510 | 3.4 | 1.1 | 0.4 | 1.5 |
| 1087 | 10.0 | 3.3 | 0.9 | 4.2 |
| 1538 | 15.5 | 5.1 | 1.3 | 6.4 |
| 1575 | 15.6 | 5.1 | 1.3 | 6.4 |
| 1915 | 20.3 | 6.7 | 1.7 | 8.4 |
| 2460 | 27.8 | 9.2 | 2.3 | 11.5 |
| 2940 | 36.0 | 11.9 | 3.0 | 14.9 |
| 3305 | 38.9 | 12.8 | 3.6 | 16.4 |
| 3340 | 38.8 | 12.8 | 3.6 | 16.4 |
| 3400 | 38.2 | 12.6 | 3.7 | 16.3 |
| 3600 | 37.6 | 12.4 | 4.1 | 16.5 |
| 3850 | 41.5 | 13.7 | 4.5 | 18.2 |
| 3875 | 53.0 | 17.9 | 4.5 | 22.4 |
| 3965 | 76.5 | 25.2 | 4.7 | 29.9 |
| 3965 | 76.9 | 25.4 | 4.7 | 30.1 |
| 3250 | 58.5 | 19.3 | 3.5 | 22.8 |
| 2555 | 48.1 | 15.9 | 2.5 | 18.4 |
| 1975 | 39.5 | 13.0 | 1.8 | 14.8 |
| 1947 | 39.4 | 13.0 | 1.8 | 14.8 |
| 1310 | 30.4 | 10.0 | 1.1 | 11.1 |
| 748 | 24.0 | 7.9 | 0.6 | 8.5 |
| 380 | 19.8 | 6.5 | 0.2 | 6.7 |
| 70 | 18.0 | 5.9 | 0.0 | 5.9 |

Initial Length = 3.031"
Final Length = 3.051"

## Table 17.

### Thermal Expansion of Cerium Dioxide

Run No. E 14

| Temperature °F | Observed Total Elongation $10^{-3}$ inches | Observed Unit Elongation $10^{-3}$ inches/inch | Unit Elongation Correction for Dilatometer Motion $10^{-3}$ inches/inch | Corrected Specimen Unit Elongation $10^{-3}$ inches/inch |
|---|---|---|---|---|
| 70 | 0.0 | 0.0 | 0.0 | 0.0 |
| 253 | 2.8 | 1.0 | 0.2 | 1.2 |
| 512 | 6.4 | 2.2 | 0.4 | 2.6 |
| 788 | 10.6 | 3.6 | 0.6 | 4.2 |
| 1124 | 15.7 | 5.4 | 1.0 | 6.4 |
| 1565 | 22.8 | 7.8 | 1.3 | 9.1 |
| 1550 | 23.0 | 7.8 | 1.3 | 9.1 |
| 1900 | 27.8 | 9.5 | 1.7 | 11.2 |
| 2130 | 40.0 | 13.6 | 2.0 | 15.6 |
| 2570 | 70.0 | 23.9 | 2.5 | 26.4 |
| 2880 | 84.7 | 28.9 | 3.0 | 31.9 |
| 2960 | 98.5 | 33.6 | 3.1 | 36.7 |
| 3330 | 108.0 | 36.8 | 3.6 | 40.4 |
| 3340 | 110.3 | 37.6 | 3.6 | 41.2 |
| 3460 | 110.3 | 37.6 | 3.8 | 41.4 |
| 3550 | 87.8 | 30.0 | 4.0 | 34.0 |
| 3700 | 67.0 | 22.8 | 4.2 | 27.0 |

Table 17 (Continued).

Thermal Expansion of Cerium Dioxide

Run No. E 14 (continued)

| Temperature °F | Observed Total Elongation $10^{-3}$ inches | Observed Unit Elongation $10^{-3}$ inches/inch | Unit Elongation Correction for Dilatometer Motion $10^{-3}$ inches/inch | Corrected Specimen Unit Elongation $10^{-3}$ inches/inch |
|---|---|---|---|---|
| 3800 | 50.0 | 17.0 | 4.4 | 21.4 |
| 3800 | 30.0 | 10.2 | 4.4 | 14.6 |
| 70 | -40.0 | -13.7 | 0.0 | -13.7 |
|  | Specimen Melted |  |  |  |

Initial Length = 2.934"
Final Length = Melted

## Table 18.

### Thermal Expansion of Hafnium Dioxide

Run No. E 15

| Temperature °F | Observed Total Elongation $10^{-3}$ inches | Observed Unit Elongation $10^{-3}$ inches/inch | Unit Elongation Correction for Dilatometer Motion $10^{-3}$ inches/inch | Corrected Specimen Unit Elongation $10^{-3}$ inches/inch |
|---|---|---|---|---|
| 70 | 0.0 | 0.0 | 0.0 | 0.0 |
| 234 | 0.4 | 0.2 | 0.2 | 0.4 |
| 495 | 1.3 | 0.6 | 0.3 | 0.9 |
| 786 | 2.1 | 0.9 | 0.6 | 1.5 |
| 1084 | 2.8 | 1.3 | 0.8 | 2.1 |
| 1459 | 3.6 | 1.6 | 1.2 | 2.8 |
| 1470 | 3.7 | 1.7 | 1.2 | 2.9 |
| 1750 | 4.7 | 2.1 | 1.5 | 3.6 |
| 2060 | 6.4 | 2.9 | 1.8 | 4.7 |
| 2420 | 7.2 | 3.2 | 2.3 | 5.5 |
| 2660 | 6.6 | 2.9 | 2.6 | 5.5 |
| 3025 | 4.5 | 2.0 | 3.2 | 5.2 |
| 3425 | 11.3 | 5.1 | 3.8 | 8.9 |
| 3820 | 23.5 | 10.5 | 4.5 | 15.0 |
| 4050 | 17.5 | 7.8 | 4.8 | 12.6 |
| 4075 | 3.4 | 1.5 | 4.8 | 6.3 |
| 4125 | -3.6 | -1.6 | 5.0 | 3.4 |
| 4170 | -9.5 | -4.2 | 5.0 | 0.8 |
| 3625 | -17.8 | -8.0 | 4.1 | -3.9 |

## Table 18 (Continued).

## Thermal Expansion of Hafnium Dioxide

Run No. E 15 (continued)

| Temperature °F | Observed Total Elongation $10^{-3}$ inches | Observed Unit Elongation $10^{-3}$ inches/inch | Unit Elongation Correction for Dilatometer Motion $10^{-3}$ inches/inch | Corrected Specimen Unit Elongation $10^{-3}$ inches/inch |
|---|---|---|---|---|
| 3200 | -22. 8 | -10. 2 | 3. 4 | -6. 8 |
| 3055 | -24. 5 | -10. 9 | 3. 2 | -7. 7 |
| 2660 | -27. 0 | -12. 1 | 2. 6 | -9. 5 |
| 2420 | -28. 1 | -12. 6 | 2. 3 | -10. 3 |
| 2065 | -26. 0 | -11. 7 | 1. 8 | -9. 9 |
| 1650 | -21. 4 | -9. 6 | 1. 4 | -8. 2 |
| 70 | -31. 3 | -14. 0 | 0. 0 | -14. 0 |

Initial Length = 2. 240"
Final Length = 2. 238"

Table 18 (Continued).

Thermal Expansion of Hafnium Dioxide

Run No. E 16

| Temperature °F | Observed Total Elongation $10^{-3}$ inches | Observed Unit Elongation $10^{-3}$ inches/inch | Unit Elongation Correction for Dilatometer Motion $10^{-3}$ inches/inch | Corrected Specimen Unit Elongation $10^{-3}$ inches/inch |
|---|---|---|---|---|
| 70 | 0.0 | 0.0 | 0.0 | 0.0 |
| 521 | 2.4 | 1.1 | 0.4 | 1.5 |
| 983 | 5.7 | 2.6 | 0.7 | 3.3 |
| 1852 | 10.1 | 4.5 | 1.6 | 6.1 |
| 1850 | 10.0 | 4.5 | 1.6 | 6.1 |
| 2170 | 11.4 | 5.1 | 2.0 | 7.1 |
| 2570 | 14.0 | 6.3 | 2.5 | 8.8 |
| 3000 | 19.2 | 8.6 | 3.1 | 11.7 |
| 3380 | 13.2 | 5.9 | 3.7 | 9.6 |
| 3440 | 2.0 | 0.9 | 3.8 | 4.7 |
| 3460 | 1.4 | 0.6 | 3.8 | 4.4 |
| 3900 | -2.5 | -1.1 | 4.5 | 3.4 |
| 4000 | -5.6 | -2.5 | 4.7 | 2.2 |
| 4240 | -5.2 | -2.3 | 5.2 | 2.9 |
| 4325 | -6.4 | -2.9 | 5.3 | 2.4 |
| 4525 | -5.4 | -2.4 | 5.7 | 3.3 |
| 4610 | -11.5 | -5.1 | 5.8 | 0.7 |
| 4610 | -28.0 | -12.5 | 5.8 | -6.7 |
| 4625 | -50.0 | -22.4 | 5.8 | -16.6 |
| 3400 | -51.9 | -23.2 | 3.7 | -19.5 |
| 3160 | -52.8 | -23.6 | 3.4 | -20.2 |
| 2640 | -58.3 | -26.1 | 2.6 | -23.5 |

Table 18 (Continued).

Thermal Expansion of Hafnium Dioxide

Run No. E 16 (continued)

| Temperature °F | Observed Total Elongation $10^{-3}$ inches | Observed Unit Elongation $10^{-3}$ inches/inch | Unit Elongation Correction for Dilatometer Motion $10^{-3}$ inches/inch | Corrected Specimen Unit Elongation $10^{-3}$ inches/inch |
|---|---|---|---|---|
| 1850 | -60.5 | -27.1 | 1.6 | -25.5 |
| 1740 | -61.0 | -27.3 | 1.5 | -25.8 |
| 936 | -66.0 | -29.6 | 0.7 | -28.9 |
| 70 | -70.2 | -31.4 | 0.0 | -31.4 |
|  | Specimen Deteriorated |  |  |  |

Initial Length = 2.238"
Final Length = 2.234"

Table 18 (Continued).

Thermal Expansion of Hafnium Dioxide

Run No. E 18

| Temperature °F | Observed Total Elongation $10^{-3}$ inches | Observed Unit Elongation $10^{-3}$ inches/inch | Unit Elongation Correction for Dilatometer Motion $10^{-3}$ inches/inch | Corrected Specimen Unit Elongation $10^{-3}$ inches/inch |
|---|---|---|---|---|
| 70 | 0.0 | 0.0 | 0.0 | 0.0 |
| 471 | 2.0 | 0.7 | 0.3 | 1.0 |
| 948 | 2.3 | 0.8 | 0.7 | 1.5 |
| 1687 | 3.3 | 1.2 | 1.4 | 2.6 |
| 1720 | 3.3 | 1.2 | 1.5 | 2.7 |
| 2175 | 5.5 | 1.9 | 2.0 | 3.9 |
| 2650 | 6.4 | 2.3 | 2.6 | 4.9 |
| 2945 | 6.1 | 2.2 | 3.0 | 5.2 |
| 3190 | 8.8 | 3.1 | 3.4 | 6.5 |
| 3455 | 15.7 | 5.5 | 3.8 | 9.3 |
| 3640 | 27.8 | 9.8 | 4.2 | 14.0 |
| 3740 | 37.8 | 13.3 | 4.3 | 17.6 |
| 4005 | 42.2 | 14.9 | 4.7 | 19.6 |
| 3850 | 39.2 | 13.8 | 4.5 | 18.3 |
| 3555 | 34.5 | 10.7 | 4.0 | 14.7 |
| 3320 | 30.6 | 10.8 | 3.6 | 14.4 |
| 3050 | 27.8 | 9.8 | 3.3 | 13.1 |
| 2750 | 29.4 | 10.4 | 2.7 | 13.1 |
| 2450 | 38.5 | 13.6 | 2.3 | 15.9 |
| 2050 | 38.7 | 13.6 | 1.8 | 15.4 |
| 1675 | 36.0 | 12.7 | 1.4 | 14.1 |

Table 18 (Continued).

Thermal Expansion of Hafnium Dioxide

Run No. E 18 (continued)

| Temperature °F | Observed Total Elongation $10^{-3}$ inches | Observed Unit Elongation $10^{-3}$ inches/inch | Unit Elongation Correction for Dilatometer Motion $10^{-3}$ inches/inch | Corrected Specimen Unit Elongation $10^{-3}$ inches/inch |
|---|---|---|---|---|
| 1538 | 35.0 | 12.3 | 1.3 | 13.6 |
| 1079 | 31.6 | 11.1 | 0.8 | 11.9 |
| 70 | 30.4 | 10.8 | 0.0 | 10.8 |

Initial Length = 2.837"
Final Length = 2.875"

## Table 19.

Thermal Expansion of Magnesium Oxide

Run No. E 13

| Temperature °F | Observed Total Elongation $10^{-3}$ inches | Observed Unit Elongation $10^{-3}$ inches/inch | Unit Elongation Correction for Dilatometer Motion $10^{-3}$ inches/inch | Corrected Specimen Unit Elongation $10^{-3}$ inches/inch |
|---|---|---|---|---|
| 70 | 0.0 | 0.0 | 0.0 | 0.0 |
| 515 | 6.5 | 2.2 | 0.4 | 2.6 |
| 956 | 14.6 | 5.0 | 0.8 | 5.8 |
| 1562 | 27.0 | 9.2 | 1.3 | 10.5 |
| 1560 | 26.9 | 9.1 | 1.3 | 10.4 |
| 1950 | 34.9 | 11.8 | 1.7 | 13.5 |
| 2240 | 40.7 | 13.8 | 2.1 | 15.9 |
| 2680 | 49.1 | 16.7 | 2.6 | 19.3 |
| 3000 | 55.2 | 18.7 | 3.1 | 21.8 |
| 3340 | 61.7 | 20.9 | 3.6 | 24.5 |
| 3610 | 65.7 | 22.3 | 4.1 | 26.4 |
| 3925 | 68.8 | 23.3 | 4.6 | 27.9 |
| 4180 | 65.5 | 22.2 | 5.0 | 27.2 |
| 4240 | 46.5 | 15.8 | 5.2 | 21.0 |
| 4240 | 20.0 | 6.8 | 5.2 | 12.0 |
| 4450 | 4.5 | 1.5 | 5.5 | 7.0 |
| 70 | -58.0<br>Specimen Softened | -19.7 | 0.0 | -19.7 |

Initial Length = 2.953"
Final Length = 2.887"

## Table 20.

### Thermal Expansion of Thorium Dioxide

Run No. E 19

| Temperature °F | Observed Total Elongation $10^{-3}$ inches | Observed Unit Elongation $10^{-3}$ inches/inch | Unit Elongation Correction for Dilatometer Motion $10^{-3}$ inches/inch | Corrected Specimen Unit Elongation $10^{-3}$ inches/inch |
|---|---|---|---|---|
| 70 | 0.0 | 0.0 | 0.0 | 0.0 |
| 258 | 1.4 | 0.5 | 0.2 | 0.7 |
| 486 | 4.1 | 1.4 | 0.3 | 1.7 |
| 832 | 8.1 | 2.8 | 0.6 | 3.4 |
| 1119 | 11.6 | 4.0 | 0.9 | 4.9 |
| 1557 | 16.7 | 5.8 | 1.3 | 7.1 |
| 1550 | 16.8 | 5.8 | 1.3 | 7.1 |
| 1865 | 20.3 | 7.0 | 1.7 | 8.7 |
| 2185 | 23.5 | 8.2 | 2.0 | 10.2 |
| 2500 | 27.3 | 9.5 | 2.4 | 11.9 |
| 2550 | 28.1 | 9.8 | 2.5 | 12.3 |
| 2870 | 32.7 | 11.4 | 2.9 | 14.3 |
| 3110 | 35.0 | 12.2 | 3.3 | 15.5 |
| 3560 | 36.9 | 12.8 | 4.0 | 16.8 |
| 3775 | 34.7 | 12.0 | 4.3 | 16.3 |
| 3950 | 23.7 | 8.2 | 4.7 | 12.9 |
| 4000 | 18.8 | 6.5 | 4.7 | 11.2 |
| 3320 | 8.3 | 2.9 | 3.6 | 6.5 |
| 2875 | 3.0 | 1.0 | 2.9 | 3.9 |
| 2645 | -0.4 | -0.1 | 2.5 | 2.4 |
| 2075 | -7.9 | -2.7 | 1.8 | -0.9 |
| 1850 | -10.9 | -3.8 | 1.7 | -2.1 |
| 1405 | -16.2 | -5.6 | 1.2 | -4.4 |
| 70 | -30.9 | -10.7 | 0.0 | -10.7 |

Initial Length = 2.880"

Final Length = 2.850"

## Table 21.

### Thermal Expansion of Zirconium Dioxide

Run No. E 12

| Temperature °F | Observed Total Elongation $10^{-3}$ inches | Observed Unit Elongation $10^{-3}$ inches/inch | Unit Elongation Correction for Dilatometer Motion $10^{-3}$ inches/inch | Corrected Specimen Unit Elongation $10^{-3}$ inches/inch |
|---|---|---|---|---|
| 70 | 0.0 | 0.0 | 0.0 | 0.0 |
| 486 | 4.5 | 1.5 | 0.3 | 1.8 |
| 908 | 9.9 | 3.3 | 0.7 | 4.0 |
| 1470 | 14.7 | 4.9 | 1.2 | 6.1 |
| 1530 | 14.8 | 4.9 | 1.3 | 6.2 |
| 1900 | 17.8 | 5.9 | 1.7 | 7.6 |
| 2510 | 25.5 | 8.5 | 2.5 | 11.0 |
| 2980 | 31.8 | 10.5 | 3.0 | 13.5 |
| 3480 | 36.5 | 12.1 | 3.8 | 15.9 |
| 3925 | 37.5 | 12.4 | 4.6 | 17.0 |
| 3925 | 36.8 | 12.2 | 4.6 | 16.8 |
| 4120 | 37.4 | 12.4 | 5.0 | 17.4 |
| 4200 | 20.0 | 6.6 | 5.1 | 11.7 |
| 4225 | 14.6 | 4.8 | 5.1 | 9.9 |
| 4440 | 0.5 | 0.2 | 5.5 | 5.7 |
| 4440 | -14.0 | -4.6 | 5.5 | 0.9 |
| 4530 | -60.0 | -19.9 | 5.7 | -14.2 |
| 70 | -117.5 | -38.9 | 0.0 | -38.9 |

Initial Length = 3.020"
Final Length = 2.942"

## Table 21 (Continued)

## Thermal Expansion of Zirconium Dioxide

### Run No. E 17

| Temperature °F | Observed Total Elongation $10^{-3}$ inches | Observed Unit Elongation $10^{-3}$ inches/inch | Unit Elongation Correction for Dilatometer Motion $10^{-3}$ inches/inch | Corrected Specimen Unit Elongation $10^{-3}$ inches/inch |
|---|---|---|---|---|
| 70 | 0.0 | 0.0 | 0.0 | 0.0 |
| 514 | 3.8 | 2.0 | 0.4 | 2.4 |
| 1004 | 8.2 | 4.2 | 0.8 | 5.0 |
| 1496 | 12.8 | 6.6 | 1.3 | 7.9 |
| 1550 | 13.1 | 6.8 | 1.3 | 8.1 |
| 2325 | 23.5 | 12.1 | 2.2 | 14.3 |
| 2520 | 25.7 | 13.3 | 2.5 | 15.8 |
| 2975 | 29.1 | 15.0 | 3.0 | 18.0 |
| 3560 | 33.0 | 17.1 | 4.0 | 21.1 |
| 3970 | 36.1 | 18.7 | 4.7 | 23.4 |
| 4240 | 37.2 | 19.2 | 5.2 | 24.4 |
| 4450 | 45.2 | 23.4 | 5.5 | 28.9 |
| 4500 | 25.0 | 12.9 | 5.6 | 18.5 |
| 4600 | -23.0 | -11.9 | 5.8 | -6.1 |
| 70 | -118.7<br>Specimen Melted | -60.8 | 0.0 | -60.8 |

Initial Length = 1.935"
Final Length = 1.775"

Table 21 (Continued).

Thermal Expansion of Zirconium Dioxide

Run No. E 19

| Temperature °F | Observed Total Elongation $10^{-3}$ inches | Observed Unit Elongation $10^{-3}$ inches/inch | Unit Elongation Correction for Dilatometer Motion $10^{-3}$ inches/inch | Corrected Specimen Unit Elongation $10^{-3}$ inches/inch |
|---|---|---|---|---|
| 70 | 0.0 | 0.0 | 0.0 | 0.0 |
| 475 | 4.3 | 1.4 | 0.3 | 1.7 |
| 863 | 8.0 | 2.7 | 0.7 | 3.4 |
| 1241 | 11.1 | 3.7 | 1.0 | 4.7 |
| 1521 | 13.0 | 4.3 | 1.3 | 5.6 |
| 1515 | 13.0 | 4.3 | 1.3 | 5.6 |
| 1900 | 14.8 | 4.9 | 1.7 | 6.6 |
| 2410 | 20.0 | 6.7 | 2.3 | 9.0 |
| 2945 | 25.7 | 8.6 | 3.0 | 11.6 |
| 3530 | 26.4 | 8.8 | 4.0 | 12.8 |
| 3970 | 19.2 | 6.4 | 4.7 | 11.1 |
| 4345 | 14.4 | 4.8 | 5.3 | 10.1 |
| 4505 | 2.1 | 0.7 | 5.6 | 6.3 |
| 4015 | -10.1 | -3.3 | 4.7 | 1.4 |
| 3565 | -19.3 | -6.4 | 4.0 | -2.4 |
| 3055 | -29.2 | -9.7 | 3.2 | -6.5 |
| 2550 | -38.0 | -12.7 | 2.5 | -10.2 |
| 2050 | -45.0 | -15.0 | 1.9 | -13.1 |
| 1570 | -52.4 | -17.5 | 1.3 | -16.2 |

Table 21 (Continued).

Thermal Expansion of Zirconium Dioxide

Run No. E 19 (continued)

| Temperature °F | Observed Total Elongation $10^{-3}$ inches | Observed Unit Elongation $10^{-3}$ inches/inch | Unit Elongation Correction for Dilatometer Motion $10^{-3}$ inches/inch | Corrected Specimen Unit Elongation $10^{-3}$ inches/inch |
|---|---|---|---|---|
| 1542 | -52.6 | -17.5 | 1.3 | -16.2 |
| 1051 | -58.5 | -19.5 | 0.8 | -18.7 |
| 441 | -64.9 | -21.6 | 0.3 | -21.3 |
| 70 | -67.0 | -22.3 | 0.0 | -22.3 |

Initial Length = 3.001"
Final Length = 2.956"

## Table 22.

Thermal Expansion of Columbium +0.5% Zirconium

Run No. E 9

| Temperature °F | Observed Total Elongation $10^{-3}$ inches | Observed Unit Elongation $10^{-3}$ inches/inch | Unit Elongation Correction for Dilatometer Motion $10^{-3}$ inches/inch | Corrected Specimen Unit Elongation $10^{-3}$ inches/inch |
|---|---|---|---|---|
| 70 | 0.0 | 0.0 | 0.0 | 0.0 |
| 530 | 4.7 | 1.6 | 0.4 | 2.0 |
| 974 | 9.6 | 3.2 | 0.7 | 3.9 |
| 1560 | 14.9 | 5.0 | 1.3 | 6.3 |
| 1560 | 15.0 | 5.0 | 1.3 | 6.3 |
| 1985 | 19.7 | 6.6 | 1.8 | 8.4 |
| 2725 | 30.0 | 10.1 | 2.7 | 12.8 |
| 3040 | 32.5 | 10.9 | 3.2 | 14.1 |
| 3425 | 32.0 | 10.7 | 3.8 | 14.5 |
| 3425 | 29.6 | 9.9 | 3.8 | 13.7 |
| 3770 | 21.5 | 7.2 | 4.3 | 11.5 |
| 3840 | 19.2 | 6.4 | 4.5 | 10.9 |
| 4120 | 8.3 | 2.8 | 4.9 | 7.7 |
| 4270 | -27.5 | -9.2 | 5.2 | -4.0 |
| 70 | -109.3 | -36.7 | 0.0 | -36.7 |
|  | Specimen Melted |  |  |  |

Initial Length = 2.982"
Final Length = Melted

## Table 23.

### Thermal Expansion of Molybdenum +0.5% Titanium

Run No. E 10

| Temperature °F | Observed Total Elongation $10^{-3}$ inches | Observed Unit Elongation $10^{-3}$ inches/inch | Unit Elongation Correction for Dilatometer Motion $10^{-3}$ inches/inch | Corrected Specimen Unit Elongation $10^{-3}$ inches/inch |
|---|---|---|---|---|
| 70 | 0.0 | 0.0 | 0.0 | 0.0 |
| 947 | 5.0 | 1.7 | 0.7 | 2.4 |
| 1481 | 8.0 | 2.7 | 1.2 | 3.9 |
| 1495 | 8.1 | 2.7 | 1.2 | 3.9 |
| 2080 | 10.6 | 3.6 | 1.8 | 5.4 |
| 2575 | 11.7 | 3.9 | 2.5 | 6.4 |
| 2960 | 17.5 | 5.9 | 3.0 | 8.9 |
| 3030 | 13.1 | 4.4 | 3.2 | 7.6 |
| 3330 | -10.0 | -3.4 | 3.6 | 0.2 |
| 3380 | -24.0 | -8.1 | 3.7 | -4.4 |
| 3670 | -55.0 | -18.5 | 4.1 | -14.4 |
| 3790 | -77.0 | -25.8 | 4.4 | -21.4 |
| 3830 | -91.0 | -30.6 | 4.5 | -26.1 |
| 4000 | -99.0 | -33.2 | 4.7 | -28.5 |
| 4110 | -46.0 | -15.4 | 5.0 | -10.4 |
| 70 | -48.2 | -16.2 | 0.0 | -16.2 |
|  | Specimen Melted |  |  |  |

Initial Length = 2.980"
Final Length = Melted

Table 24

Equations Expressing the Heat Capacity and Enthalpy as Functions of Temperature

| Material | Equation for Enthalpy of Material H in Btu/lb and T in °F (H is enthalpy above 32°F and T is °F) | Equation for Heat Capacity of Material HC in Btu/lb/°F and T in °F |
|---|---|---|
| ATJ Graphite | $H = .475T + 5.33 \times 10^{-6} T^2 + 5716.6T^{-1} - 191.9$ | $HC = .475 + 10.66 \times 10^{-6} T - 52558T^{-2}$ |
| Tungsten | $H = .033T + 2.47 \times 10^{-6} T^2 + 131.9T^{-1} - 5.16$ | $HC = .033 + 4.94 \times 10^{-6} T - 1025.4T^{-2}$ |
| Hafnium Nitride | $H = .083T - 1.99 \times 10^{-6} T^2 + 644.1T^{-1} - 22.65$ | $HC = .083 - 3.98 \times 10^{-6} T - 5309.8T^{-2}$ |
| Silicon Nitride | $H = .233T + 22.76 \times 10^{-6} T^2 + 1325.3T^{-1} - 48.94$ | $HC = .233 + 45.52 \times 10^{-6} T - 11428T^{-2}$ |
| Titanium Nitride | $H = .219T + 5.60 \times 10^{-6} T^2 + 1891.0T^{-1} - 65.29$ | $HC = .219 + 11.20 \times 10^{-6} T - 17429T^{-2}$ |
| Zirconium Nitride | $H = .096T + 6.88 \times 10^{-6} T^2 + 158.3T^{-1} - 8.00$ | $HC = .096 + 13.76 \times 10^{-6} T - 5449.4T^{-2}$ |
| Tantalum Boride | $H = .083T + 4.78 \times 10^{-6} T^2 + 605.6T^{-1} - 21.25$ | $HC = .083 + 9.56 \times 10^{-6} T - 6981.1T^{-2}$ |
| Zirconium Diboride | $H = .153T + 8.88 \times 10^{-6} T^2 + 868.6T^{-1} - 31.99$ | $HC = .153 + 17.76 \times 10^{-6} T - 9327.0T^{-2}$ |
| Zirconium Silicate | $H = .157T + 20.08 \times 10^{-6} T^2 + 881.6T^{-1} - 32.66$ | $HC = .157 + 40.16 \times 10^{-6} T - 10534T^{-2}$ |
| Columbium Carbide | $H = .107T + 4.46 \times 10^{-6} T^2 + 720.7T^{-1} - 25.94$ | $HC = .107 + 8.92 \times 10^{-6} T - 5429.6T^{-2}$ |
| Hafnium Carbide | $H = .067T + 1.08 \times 10^{-6} T^2 + 298.8T^{-1} - 11.43$ | $HC = .067 + 2.16 \times 10^{-6} T - 3155.1T^{-2}$ |
| Tantalum Carbide | $H = .068T + 1.89 \times 10^{-6} T^2 + 574.0T^{-1} - 19.95$ | $HC = .068 + 3.78 \times 10^{-6} T - 4883.5T^{-2}$ |
| Zirconium Carbide | $H = .116T + .135 \times 10^{-6} T^2 + 679.8T^{-1} - 24.89$ | $HC = .116 + 2.70 \times 10^{-6} T - 6575.9T^{-2}$ |
| Sapphire | $H = .268T + 12.34 \times 10^{-6} T^2 + 1104.7T^{-1} - 43.07$ | $HC = .268 + 24.68 \times 10^{-6} T - 10068T^{-2}$ |

Note: 1. Heat capacity - temperature equations obtained from derivative of enthalpy-temperature equation with "c" constant modified.

2. Equations are valid from 500°F to within 500°F of top exposure temperatures for enthalpy measurements.

## Table 25.

## Enthalpy and Heat Capacity Data for Hafnium Diboride

| SRI Run Number | Drop Temperature °F | Initial Weight Grams | Final Weight Grams | Enthalpy from Drop Temperature to 32°F Btu/lb | Mean Temperature for Heat Capacity by Slope Measurement °F | Heat Capacity by Slope Measurement Btu/lb/°F |
|---|---|---|---|---|---|---|
| HC-91 | 620 | 59.065 | 59.070 | 43.5 | 500 | 0.082 |
| HC-95 | 671 | 59.075 | 59.070 | 51.3 | 1000 | 0.086 |
| HC-93 | 1252 | 59.075 | 59.075 | 99.5 | 1500 | 0.091 |
| HC-97 | 2090 | 59.070 | 59.040 | 168.0 | 2000 | 0.096 |
| HC-98 | 2550 | 59.040 | 59.045 | 234.0 | 2500 | 0.101 |
| HC-100 | 2955 | 59.045 | 59.020 | 263.0 | 3000 | 0.105 |
| HC-102 | 3485 | 59.020 | 58.995 | 333.0 | 3500 | 0.109 |
| HC-116 | 3500 | 58.920 | 58.840 | 323.0 | 4000 | 0.113 |
| HC-107 | 4000 | 58.945 | 58.920 | 374.0 | 4500 | 0.120 |
| HC-118 | 4260 | 58.840 | 58.740 | 401.0 | | |
| HC-120 | 4600 | 58.740 | 58.520 | 465.0 | | |
| HC-127 | 4605 | 58.520 | 58.425 | 460.0 | | |

## Table 26.

## Enthalpy and Heat Capacity Data for Thorium Tetraboride

| SRI Run Number | Drop Temperature °F | Initial Weight Grams | Final Weight Grams | Enthalpy from Drop Temperature to 32°F Btu/lb | Mean Temperature for Heat Capacity by Slope Measurement °F | Heat Capacity by Slope Measurement Btu/lb/°F |
|---|---|---|---|---|---|---|
| HC 195 | 501 | 45.535 | 45.535 | 30.3 | 500 | 0.118 |
| HC 202 | 1015 | 45.320 | 45.315 | 56.4 | 1000 | 0.122 |
| HC 212 | 1015 | 44.170 | 44.170 | 96.7 | 1500 | 0.124 |
| HC 201 | 1512 | 45.315 | 45.320 | 144.0 | 2000 | 0.124 |
| HC 199 | 1593 | 45.505 | 45.315 | 165.4 | 2500 | 0.124 |
| HC 205 | 2000 | 45.315 | 45.320 | 217.2 | 3000 | 0.124 |
| HC 207 | 2520 | 45.320 | 45.320 | 280.6 | 3500 | 0.124 |
| HC 209 | 3090 | 45.320 | 45.315 | 361.6 | | |
| HC 213 | 3510 | 44.170 | 44.170 | 399.0 | | |
| HC 222 | 3555 | 44.170 | 44.165 | 412.0 | | |

## Table 27.

## Enthalpy and Heat Capacity Data for Titanium Diboride

| SRI Run Number | Drop Temperature °F | Initial Weight Grams | Final Weight Grams | Enthalpy from Drop Temperature to 32°F Btu/lb | Mean Temperature for Heat Capacity by Slope Measurement °F | Heat Capacity by Slope Measurement Btu/lb/°F |
|---|---|---|---|---|---|---|
| HC-65 | 595 | 23.270 | 23.270 | 93.7 | 500 | 0.230 |
| HC-73 | 1372 | 23.270 | 23.270 | 304.0 | 1000 | 0.240 |
| HC-75 | 1935 | 23.270 | 23.310 | 454.0 | 1500 | 0.260 |
| HC-77 | 2460 | 23.310 | 23.300 | 591.0 | 2000 | 0.280 |
| HC-79 | 3015 | 23.300 | 23.260 | 790.0 | 2500 | 0.305 |
| HC-82 | 3500 | 23.260 | 23.240 | 1005.0 | 3000 | 0.340 |
| HC-88 | 3530 | 23.185 | 23.180 | 970.0 | 3500 | 0.362 |
| HC-84 | 3975 | 23.240 | 23.200 | 1088.0 | 4000 | 0.360 |
| HC-128 | 4060 | 23.165 | 23.165 | 1146.0 | 4500 | 0.360 |
| HC-86 | 4380 | 23.200 | 23.185 | 1290.0 | | |

## Table 28.

## Enthalpy and Heat Capacity Data for Tungsten Boride

| SRI Run Number | Drop Temperature °F | Initial Weight Grams | Final Weight Grams | Enthalpy from Drop Temperature to 32°F Btu/lb | Mean Temperature for Heat Capacity by Slope Measurement °F | Heat Capacity by Slope Measurement Btu/lb/°F |
|---|---|---|---|---|---|---|
| HC-64 | 605 | 81.115 | 81.115 | 27.6 | 500 | 0.058 |
| HC-76 | 1349 | 81.115 | 81.115 | 58.8 | 1000 | 0.060 |
| HC-89 | 1370 | 80.755 | 80.750 | 70.7 | 1500 | 0.065 |
| HC-74 | 2093 | 81.115 | 81.120 | 121.0 | 2000 | 0.071 |
| HC-78 | 2500 | 81.115 | 81.105 | 152.0 | 2500 | 0.080 |
| HC-81 | 3045 | 81.105 | 80.860 | 210.0 | 3000 | 0.088 |
| HC-117 | 3060 | 80.750 | 80.745 | 176.0 | 3500 | 0.093 |
| HC-83 | 3500 | 80.860 | 80.835 | 238.0 | 4000 | 0.098 |
| HC-119 | 4000 | 80.745 | 80.725 | 289.0 | | |
| HC-85 | 4005 | 80.835 | 80.830 | 264.0 | | |
| HC-87 | 4225 | 80.830 | 80.755 | 312.0 | | |

Table 29.

Enthalpy and Heat Capacity Data for Dimolybdenum Carbide

| SRI Run Number | Drop Temperature °F | Initial Weight Grams | Final Weight Grams | Enthalpy from Drop Temperature to 32°F Btu/lb | Mean Temperature for Heat Capacity by Slope Measurement °F | Heat Capacity by Slope Measurement Btu/lb/°F |
|---|---|---|---|---|---|---|
| HC-30 | 604 | 48.190 | 48.190 | 43.6 | 500 | 0.086 |
| HC-34 | 1392 | 48.190 | 48.190 | 111.8 | 1000 | 0.090 |
| HC-38 | 2010 | 48.190 | 48.180 | 179.8 | 1500 | 0.101 |
| HC-42 | 2505 | 48.180 | 48.175 | 237.0 | 2000 | 0.110 |
| HC-46 | 3000 | 48.175 | 48.175 | 299.0 | 2500 | 0.120 |
| * HC-57 | 3550 | 34.105 | 34.085 | 367.0 | 3000 | 0.126 |
| HC-52 | 4005 | 48.175 | 48.110 | 508.0 | 3500 | 0.124 |

* Different Specimen

## Table 30.

## Enthalpy and Heat Capacity Data for Titanium Carbide

| SRI Run Number | Drop Temperature °F | Initial Weight Grams | Final Weight Grams | Enthalpy from Drop Temperature to 32°F Btu/lb | Mean Temperature for Heat Capacity by Slope Measurement °F | Heat Capacity by Slope Measurement Btu/lb/°F |
|---|---|---|---|---|---|---|
| HC-27 | 603 | 24.035 | 24.035 | 87.4 | 500 | 0.193 |
| HC-90 | 1220 | 23.990 | 24.000 | 226.0 | 1000 | 0.200 |
| HC-94 | 1333 | 24.000 | 24.005 | 264.0 | 1500 | 0.208 |
| HC-31 | 1385 | 24.035 | 24.035 | 221.5 | 2000 | 0.225 |
| HC-35 | 1995 | 24.035 | 24.040 | 383.5 | 2500 | 0.244 |
| HC-96 | 2035 | 24.005 | 24.025 | 400.0 | 3000 | 0.255 |
| HC-39 | 2500 | 24.040 | 24.045 | 506.5 | 3500 | 0.264 |
| HC-43 | 3030 | 24.045 | 24.040 | 625.0 | 4000 | 0.272 |
| HC-47 | 3530 | 24.040 | 24.040 | 768.0 | 4500 | 0.276 |
| HC-101 | 3950 | 23.990 | 23.995 | 881.0 | | |
| HC-53 | 4000 | 24.040 | 24.025 | 848.0 | | |
| HC-99 | 4000 | 24.025 | 23.990 | 918.0 | | |
| HC-103 | 4310 | 23.995 | 24.000 | 1010.0 | | |
| HC-56 | 4525 | 24.025 | 24.005 | 1028.0 | | |
| HC-105 | 4655 | 24.000 | 23.865 | 1097.0 | | |
| HC-62 | 4750 | 24.005 | 23.985 | 1075.0 | | |

## Table 31.

## Enthalpy and Heat Capacity Data for Tungsten Carbide

| SRI Run Number | Drop Temperature °F | Initial Weight Grams | Final Weight Grams | Enthalpy from Drop Temperature to 32°F Btu/lb | Mean Temperature for Heat Capacity by Slope Measurement °F | Heat Capacity by Slope Measurement Btu/lb/°F |
|---|---|---|---|---|---|---|
| HC-1 | 683 | 86.085 | 86.090 | 39.8 | 500 | 0.056 |
| HC-2 | 1496 | 86.090 | 86.090 | 77.2 | 1000 | 0.060 |
| HC-3 | 2035 | 86.090 | 86.090 | 123.0 | 1500 | 0.065 |
| HC-61 | 2550 | 85.975 | 85.985 | 152.0 | 2000 | 0.068 |
| HC-4 | 3000 | 86.090 | 86.065 | 186.0 | 2500 | 0.073 |
| HC-5 | 3620 | 86.065 | 86.045 | 240.0 | 3000 | 0.078 |
| HC-6 | 4140 | 86.045 | 86.010 | 282.0 | 3500 | 0.081 |
| HC-63 | 4500 | 85.985 | 85.955 | 326.0 | 4000 | 0.083 |
| HC-7 | 4770 | 86.010 | 85.990 | 321.0 | 4500 | 0.082 |

## Table 32.

### Enthalpy and Heat Capacity Data for Vanadium Carbide

| SRI Run Number | Drop Temperature °F | Initial Weight Grams | Final Weight Grams | Enthalpy from Drop Temperature to 32°F Btu/lb | Mean Temperature for Heat Capacity by Slope Measurement °F | Heat Capacity by Slope Measurement Btu/lb/°F |
|---|---|---|---|---|---|---|
| HC-11 | 603 | 31. 755 | 31. 755 | 75. 7 | 500 | 0. 190 |
| HC-9 | 1414 | 31. 755 | 31. 755 | 258. 5 | 1000 | 0. 200 |
| HC-12 | 2100 | 31. 755 | 31. 765 | 390. 0 | 1500 | 0. 213 |
| HC-14 | 2480 | 31. 765 | 31. 765 | 502. 0 | 2000 | 0. 227 |
| HC-16 | 3000 | 31. 765 | 31. 765 | 608. 0 | 2500 | 0. 246 |
| HC-19 | 3480 | 31. 765 | 31. 730 | 752. 0 | 3000 | 0. 280 |
| HC-21 | 4050 | 31. 730 | 31. 710 | 927. 0 | 3500 | 0. 310 |
| HC-23 | 4600 | 31. 710 | 31. 630 | 1154. 0 | 4000 | 0. 350 |
|  |  |  |  |  | 4500 | 0. 380 |

## Table 33.

## Enthalpy and Heat Capacity Data for Boron Nitride

| SRI Run Number | Drop Temperature °F | Initial Weight Grams | Final Weight Grams | Enthalpy from Drop Temperature to 32°F Btu/lb | Mean Temperature for Heat Capacity by Slope Measurement °F | Heat Capacity by Slope Measurement Btu/lb/°F |
|---|---|---|---|---|---|---|
| HC-108 | 752 | 11.255 | 11.230 | 240.0 | 500 | 0.370 |
| HC-110 | 1404 | 11.230 | 11.230 | 531.0 | 1000 | 0.385 |
| HC-113 | 1935 | 11.230 | 11.230 | 663.0 | 1500 | 0.420 |
| HC-123 | 2050 | 11.225 | 11.255 | 767.0 | 2000 | 0.445 |
| HC-114 | 2445 | 11.230 | 11.225 | 998.0 | 2500 | 0.455 |
| HC-124 | 3100 | 11.225 | 11.085 | 1280.0 | 3000 | 0.455 |
| HC-131 | 3580 | 11.085 | 10.665 | 1494.0 | 3500 | 0.440 |
| HC-134 | 4022 | 10.665 | 10.455 | 1650.0 | 4000 | 0.439 |

## Table 34.

## Enthalpy and Heat Capacity Data for Tantalum Nitride

| SRI Run Number | Drop Temperature °F | Initial Weight Grams | Final Weight Grams | Enthalpy from Drop Temperature to 32°F Btu/lb | Mean Temperature for Heat Capacity by Slope Measurement °F | Heat Capacity by Slope Measurement Btu/lb/°F |
|---|---|---|---|---|---|---|
| HC-8 | 600 | 76.845 | 76.850 | 34.3 | 500 | 0.052 |
| HC-8A | 1403 | 76.850 | 76.855 | 78.2 | 1000 | 0.052 |
| HC-10 | 2000 | 76.855 | 76.860 | 103.3 | 1500 | 0.050 |
| HC-13 | 2450 | 76.860 | 76.900 | 129.3 | 2000 | 0.052 |
| HC-15 | 2970 | 76.900 | 76.955 | 158.7 | 2500 | 0.060 |
| HC-18 | 3480 | 76.955 | 76.910 | 205.0 | 3000 | 0.070 |
| HC-20 | 4050 | 76.910 | 76.585 | 255.0 | 3500 | 0.085 |
| HC-22 | 4500 | 76.585 | 75.575 | 293.0 | 4000 | 0.092 |
| HC-25 | 4850 | 74.175 | 73.695 | 273.0 | 4500 | 0.090 |
| HC-24 | 4900 | 75.005 | 74.475 | 299.0 | | |

## Table 35.

### Enthalpy and Heat Capacity Data for Beryllium Oxide

| SRI Run Number | Drop Temperature °F | Initial Weight Grams | Final Weight Grams | Enthalpy from Drop Temperature to 32°F Btu/lb | Mean Temperature for Heat Capacity by Slope Measurement °F | Heat Capacity by Slope Measurement Btu/lb/°F |
|---|---|---|---|---|---|---|
| HC 215 | 505 | 9.070 | 9.070 | 152.3 | 500 | 0.385 |
| HC 216 | 1013 | 9.070 | 9.070 | 357.1 | 1000 | 0.417 |
| HC 217 | 1521 | 9.070 | 9.075 | 680.5 | 1500 | 0.470 |
| HC 218 | 2035 | 9.075 | 9.075 | 838.0 | 2000 | 0.510 |
| HC 219 | 2620 | 9.075 | 9.075 | 1166.9 | 2500 | 0.550 |
| HC 220 | 3005 | 9.075 | 9.020 | 1513.7 | 3000 | 0.570 |
| HC 221 | 3550 | 9.020 | 8.950 | 1507.8 | 3500 | 0.570 |
| HC 223 | 3550 | 8.950 | 8.915 | 1702.5 | | |

## Table 36.

## Enthalpy and Heat Capacity Data for Cerium Dioxide

| SRI Run Number | Drop Temperature °F | Initial Weight Grams | Final Weight Grams | Enthalpy from Drop Temperature to 32°F Btu/lb | Mean Temperature for Heat Capacity by Slope Measurement °F | Heat Capacity by Slope Measurement Btu/lb/°F |
|---|---|---|---|---|---|---|
| HC-189 | 693 | 29.855 | 29.855 | 71.8 | 500 | 0.100 |
| HC-109 | 696 | 28.360 | 28.370 | 57.0 | 1000 | 0.109 |
| HC-111 | 724 | 28.370 | 28.365 | 85.1 | 1500 | 0.117 |
| HC-183 | 1021 | 31.175 | 31.145 | 101.4 | 2000 | 0.125 |
| HC-136 | 1104 | 28.355 | 28.340 | 105.0 | 2500 | 0.132 |
| HC-112 | 1442 | 28.365 | 28.365 | 142.0 | 3000 | 0.137 |
| HC-184 | 1485 | 31.145 | 31.145 | 136.6 | 3220 | 0.138 |
| HC-140 | 1612 | 28.265 | 28.295 | 171.2 | | |
| HC-138 | 1894 | 28.340 | 28.265 | 213.5 | | |
| HC-185 | 2010 | 31.145 | 31.140 | 209.0 | | |
| HC-115 | 2055 | 28.365 | 28.060 | 229.0 | | |
| HC-187 | 2510 | 30.610 | 30.610 | 305.5 | | |
| HC-190 | 2510 | 29.855 | 29.185 | 270.9 | | |
| HC-192 | 2840 | 28.860 | 28.360 | 329.5 | | |
| HC-153 | 2970 | 28.255 | 26.670 | 376.0 | | |
| HC-188 | 3030 | 30.610 | 30.160 | 363.7 | | |
| HC-160 | 3075 | 30.855 | 29.805 | 327.6 | | |
| HC-191 | 3200 | 29.185 | 28.860 | 350.4 | | |
| HC-193 | 3220 | 28.860 | 28.640 | 385.3 | | |

## Table 37.

## Enthalpy and Heat Capacity Data for Hafnium Dioxide

| SRI Run Number | Drop Temperature °F | Initial Weight Grams | Final Weight Grams | Enthalpy from Drop Temperature to 32°F Btu/lb | Mean Temperature for Heat Capacity by Slope Measurement °F | Heat Capacity by Slope Measurement Btu/lb/°F |
|---|---|---|---|---|---|---|
| HC-137 | 711 | 30.860 | 30.860 | 45.7 | 500 | 0.070 |
| HC-141 | 1386 | 30.860 | 30.860 | 113.0 | 1000 | 0.075 |
| HC-144 | 1979 | 30.860 | 30.830 | 157.3 | 1500 | 0.090 |
| HC-149 | 2525 | 30.830 | 30.820 | 210.7 | 2000 | 0.103 |
| HC-167 | 2975 | 30.685 | 30.685 | 297.5 | 2500 | 0.125 |
| HC-156 | 3015 | 30.800 | 30.755 | 286.0 | 3000 | 0.150 |
| HC-154 | 3050 | 30.820 | 30.800 | 293.0 | 3500 | 0.147 |
| HC-159 | 3475 | 30.755 | 30.685 | 345.1 | 4000 | 0.138 |
| HC-168 | 3555 | 30.685 | 30.665 | 386.2 | 4500 | 0.130 |
| HC-171 | 4040 | 30.665 | 30.585 | 408.5 | 4750 | 0.131 |
| HC-180 | 4045 | 30.215 | 30.225 | 429.7 | | |
| HC-178 | 4495 | 30.585 | 30.215 | 504.9 | | |
| HC-181 | 4740 | 30.225 | 28.930 | 524.6 | | |

## Table 38.

Enthalpy and Heat Capacity Data for Magnesium Oxide

| SRI Run Number | Drop Temperature °F | Initial Weight Grams | Final Weight Grams | Enthalpy from Drop Temperature to 32°F Btu/lb | Mean Temperature for Heat Capacity by Slope Measurement °F | Heat Capacity by Slope Measurement Btu/lb/°F |
|---|---|---|---|---|---|---|
| HC-130 | 689 | 14.990 | 14.990 | 184.2 | 500 | 0.300 |
| HC-133 | 1413 | 14.990 | 14.995 | 400.0 | 1000 | 0.305 |
| HC-142 | 2016 | 14.990 | 14.990 | 578.0 | 1500 | 0.310 |
| HC-139 | 2035 | 14.995 | 14.990 | 605.0 | 2000 | 0.313 |
| HC-148 | 2540 | 14.990 | 14.985 | 773.6 | 2500 | 0.315 |
| HC-151 | 2975 | 14.985 | 14.980 | 898.9 | 3000 | 0.325 |
| HC-158 | 3550 | 14.980 | 14.610 | 1078.0 | 3500 | 0.340 |
| HC-165 | 3910 | 14.610 | 14.480 | 1214.8 | 4000 | 0.340 |
| HC-175 | 4295 | 12.180 | 11.425 | 1352.1 | | |

Table 39.

Enthalpy and Heat Capacity Data for Thorium Dioxide

| SRI Run Number | Drop Temperature °F | Initial Weight Grams | Final Weight Grams | Enthalpy from Drop Temperature to 32°F Btu/lb | Mean Temperature for Heat Capacity by Slope Measurement °F | Heat Capacity by Slope Measurement Btu/lb/°F |
|---|---|---|---|---|---|---|
| HC 194 | 510 | 42.150 | 42.150 | 23.0 | 500 | 0.070 |
| HC 196 | 1007 | 42.150 | 42.150 | 63.3 | 1000 | 0.075 |
| HC 198 | 1509 | 42.150 | 42.150 | 110.0 | 1500 | 0.079 |
| HC 211 | 2050 | 41.980 | 42.010 | 162.9 | 2000 | 0.079 |
| HC 200 | 2075 | 42.150 | 42.150 | 141.2 | 2500 | 0.079 |
| HC 203 | 2575 | 42.150 | 42.150 | 185.3 | 3000 | 0.079 |
| HC 206 | 3080 | 42.150 | 42.110 | 228.1 | 3500 | 0.079 |
| HC 208 | 3545 | 42.110 | 41.980 | 262.5 | | |

## Table 40.

## Enthalpy and Heat Capacity Data for Zirconium Dioxide

| SRI Run Number | Drop Temperature °F | Initial Weight Grams | Final Weight Grams | Enthalpy from Drop Temperature to 32°F Btu/lb | Mean Temperature for Heat Capacity by Slope Measurement °F | Heat Capacity by Slope Measurement Btu/lb/°F |
|---|---|---|---|---|---|---|
| HC-140A | 690 | 26.860 | 26.870 | 95.2 | 500 | 0.147 |
| HC-143 | 1446 | 26.870 | 26.880 | 220.0 | 1000 | 0.147 |
| HC-145 | 1866 | 26.880 | 26.870 | 277.0 | 1500 | 0.152 |
| HC-150 | 2555 | 26.870 | 26.850 | 394.5 | 2000 | 0.167 |
| HC-152 | 3055 | 26.850 | 26.830 | 489.0 | 2500 | 0.177 |
| HC-157 | 3475 | 26.830 | 26.735 | 565.0 | 3000 | 0.195 |
| HC-170 | 3570 | 26.465 | 26.435 | 586.0 | 3500 | 0.230 |
| HC-169 | 3780 | 26.505 | 26.465 | 641.9 | 4000 | 0.275 |
| HC-166 | 4105 | 26.735 | 26.505 | 732.0 | 4500 | 0.300 |
| HC-173 | 4505 | 26.435 | 25.700 | 858.7 | | |

## Table 41.

## Enthalpy and Heat Capacity Data for Columbium +0.5% Zirconium

| SRI Run Number | Drop Temperature °F | Initial Weight Grams | Final Weight Grams | Enthalpy from Drop Temperature to 32°F Btu/lb | Mean Temperature for Heat Capacity by Slope Measurement °F | Heat Capacity by Slope Measurement Btu/lb/°F |
|---|---|---|---|---|---|---|
| HC-29 | 605 | 44.750 | 44.750 | 38.0 | 500 | 0.076 |
| HC-33 | 1440 | 44.750 | 44.750 | 106.1 | 1000 | 0.078 |
| HC-37 | 2000 | 44.750 | 44.780 | 148.9 | 1500 | 0.081 |
| HC-41 | 2515 | 44.780 | 44.815 | 196.8 | 2000 | 0.084 |
| HC-48 | 2975 | 44.815 | 44.815 | 255.0 | 2500 | 0.086 |
| HC-45 | 3000 | 44.815 | 44.815 | 236.0 | 3000 | 0.090 |
| HC-51 | 3520 | 44.815 | 44.820 | 290.0 | 3500 | 0.094 |
| HC-54 | 3950 | 44.825 | 44.810 | 310.0 | | |
| HC-59 | 3950 | 44.665 | 44.315 | 354.0 | | |
| HC-60 | 4000 | 44.300 | 44.260 | 370.5 | | |
| HC-58 | 4080 | 44.800 | 44.650 | 392.0 | | |

## Table 42.

## Enthalpy and Heat Capacity Data for Molybdenum + 0. 5% Titanium

| SRI Run Number | Drop Temperature °F | Initial Weight Grams | Final Weight Grams | Enthalpy from Drop Temperature to 32°F Btu/lb | Mean Temperature for Heat Capacity by Slope Measurement °F | Heat Capacity by Slope Measurement Btu/lb/°F |
|---|---|---|---|---|---|---|
| HC-28 | 601 | 47. 280 | 47. 280 | 36. 0 | 500 | 0. 068 |
| HC-125 | 1385 | 47. 320 | 47. 325 | 93. 3 | 1000 | 0. 071 |
| HC-32 | 1412 | 47. 280 | 47. 285 | 84. 6 | 1500 | 0. 078 |
| HC-36 | 1997 | 47. 285 | 47. 285 | 147. 7 | 2000 | 0. 086 |
| HC-40 | 2490 | 47. 285 | 47. 275 | 190. 0 | 2500 | 0. 089 |
| HC-44 | 3010 | 47. 275 | 47. 275 | 227. 0 | 3000 | 0. 087 |
| HC-49 | 3025 | 47. 275 | 47. 275 | 231. 0 | 3500 | 0. 089 |
| HC-50 | 3520 | 47. 275 | 47. 290 | 284. 0 | 4000 | 0. 091 |
| HC-55 | 3950 | 47. 275 | 47. 320 | 302. 0 | | |
| HC-126 | 4000 | 47. 325 | 45. 695 | 394. 0 | | |

## Table 43.

## Thermal Conductivity Data for Hafnium Diboride

| SRI Run No. Specimen No. Heat-Soak Temperature °F | Specimen Mean Temperature For $\frac{1}{8}$" Gage Length °F | Total Heat Flow Into $\frac{1}{4}$" Axial Calorimeter Gage Length Btu/hr | Specimen ΔT Across $\frac{1}{8}$" Gage Length °F | Specimen Thermal Conductivity Btu/hr/ft$^2$/°F/in. |
|---|---|---|---|---|
| Run TC 81 | 1820 | 307.7 | 33.5 | 430.3 |
| | 1820 | 296.6 | 32.5 | 427.5 |
| Specimen | 1820 | 300.1 | 32.5 | 432.7 |
| No. 1 | 2406 | 363.1 | 52.5 | 324.1 |
| | 2419 | 367.3 | 49.5 | 347.6 |
| 3200-3350°F | 2412 | 376.7 | 57.5 | 306.9 |
| | 2790 | 519.8 | 60.0 | 405.8 |
| | 2794 | 510.9 | 55.0 | 435.2 |
| | 2796 | 527.6 | 53.5 | 462.0 |
| | 2787 | 544.0 | 64.0 | 398.2 |
| | 3241 | 918.2 | 71.0 | 605.9 |
| | 3246 | 905.6 | 65.0 | 652.7 |
| | 3240 | 906.4 | 72.5 | 585.7 |
| | 3510 | 1361.6 | 72.5 | 879.9 |
| | 3512 | 1330.2 | 70.0 | 890.3 |
| | 3519 | 1383.0 | 61.5 | 1053.6 |
| Specimen Found Cracked on Post Inspection | | | | |
| Run TC 92 | 1760 | 467.8 | 57.5 | 381.1 |
| | 1760 | 460.3 | 56.0 | 385.1 |
| Specimen | 1760 | 489.7 | 49.0 | 468.2 |
| No. 2 | 2464 | 582.9 | 80.0 | 341.3 |
| | 2477 | 562.9 | 76.0 | 346.9 |
| 3200-3350°F | 2488 | 525.1 | 62.5 | 393.6 |
| | 2926 | 664.7 | 89.5 | 347.9 |
| | 2929 | 673.5 | 85.0 | 371.2 |

Table 43 (Continued)

Thermal Conductivity Data for Hafnium Diboride

| SRI Run No. Specimen No. Heat-Soak Temperature °F | Specimen Mean Temperature For $\frac{1}{8}$" Gage Length °F | Total Heat Flow Into $\frac{1}{4}$" Axial Calorimeter Gage Length Btu/hr | Specimen ΔT Across $\frac{1}{8}$" Gage Length °F | Specimen Thermal Conductivity Btu/hr/ft²/°F/in. |
|---|---|---|---|---|
| Run TC 92 | 2927 | 710.1 | 88.0 | 378.0 |
| (Continued) | 3288 | 989.6 | 135.0 | 343.4 |
| | 3299 | 998.4 | 121.5 | 385.0 |
| Specimen | 3297 | 1030.8 | 124.0 | 389.5 |
| No. 2 | 3655 | 1204.0 | 102.5 | 550.3 |
| | 3675 | 1184.3 | 78.5 | 706.8 |
| 3200-3350°F | 3674 | 1183.5 | 80.0 | 693.1 |
| | 3670 | 1188.4 | 84.0 | 662.8 |
| Specimen Found Broken on Post Inspection | | | | |

## Table 44.

### Thermal Conductivity Data for Thorium Tetraboride

| SRI Run No. Specimen No. Heat-Soak Temperature °F | Specimen Mean Temperature For $\frac{1}{8}$" Gage Length °F | Total Heat Flow Into $\frac{1}{4}$" Axial Calorimeter Gage Length Btu/hr | Specimen ΔT Across $\frac{1}{8}$" Gage Length °F | Specimen Thermal Conductivity Btu/hr/ft²/°F/in. |
|---|---|---|---|---|
| Run TC 95 | 1184 | 294.0 | 74.0 | 186.1 |
| | 1202 | 305.3 | 71.5 | 200.1 |
| Specimen No. 1 | 1700 | 384.3 | 101.0 | 178.3 |
| | 1700 | 358.7 | 92.5 | 181.7 |
| | 1700 | 385.4 | 68.5 | 263.6 |
| Not Heat-Soaked | 1700 | 391.8 | 75.0 | 244.7 |
| | 1700 | 410.2 | 76.0 | 252.9 |
| | 2348 | 486.9 | 105.0 | 217.2 |
| | 2373 | 475.3 | 92.5 | 240.7 |
| | 2375 | 464.9 | 102.5 | 212.5 |
| | 2403 | 472.6 | 93.0 | 238.1 |
| | 2921 | 562.2 | 106.5 | 247.3 |
| | 2924 | 594.6 | 292.4 | 253.2 |
| | 3456 | 632.7 | 77.5 | 382.5 |
| | 3456 | 641.1 | 77.5 | 387.6 |
| | 3477 | 632.7 | 76.0 | 390.0 |
| Specimen Found Broken on Post Inspection | | | | |

Table 45.

Thermal Conductivity Data for Titanium Diboride

| SRI Run No. Specimen No. Heat-Soak Temperature °F | Specimen Mean Temperature For $\frac{1}{8}$" Gage Length °F | Total Heat Flow Into $\frac{1}{4}$" Axial Calorimeter Gage Length Btu/hr | Specimen $\Delta T$ Across $\frac{1}{8}$" Gage Length °F | Specimen Thermal Conductivity Btu/hr/ft$^2$/°F/in. |
|---|---|---|---|---|
| Run TC 42 | 1475 | 272.9 | 54.0 | 236.7 |
| | 2252 | 324.2 | 57.5 | 264.2 |
| Specimen | 2252 | 367.8 | 57.5 | 299.6 |
| No. 1 | 2271 | 382.7 | 59.0 | 303.9 |
| | 2593 | 493.1 | 62.0 | 372.6 |
| 3800°F | 2590 | 478.8 | 66.5 | 337.3 |
| | 2606 | 480.7 | 65.0 | 346.5 |
| | 2943 | 613.2 | 81.0 | 354.6 |
| | 2980 | 596.1 | 84.0 | 332.5 |
| | 3027 | 599.3 | 87.5 | 320.9 |
| Specimen Found Cracked on Post Inspection | | | | |
| Run TC 85 | 2315 | 434.8 | 54.0 | 377.3 |
| | 2322 | 460.3 | 57.5 | 375.0 |
| Specimen | 2320 | 484.4 | 60.0 | 378.3 |
| No. 3 | 2787 | 521.3 | 69.5 | 351.4 |
| | 2778 | 543.2 | 81.0 | 314.2 |
| 3500°F | 2775 | 553.2 | 78.5 | 330.1 |
| | 2768 | 542.8 | 86.5 | 294.0 |
| | 3327 | 627.9 | 100.0 | 294.2 |
| | 3340 | 635.1 | 96.0 | 309.9 |
| | 3338 | 620.5 | 99.0 | 293.6 |
| | 3807 | 704.9 | 87.5 | 377.4 |
| | 3811 | 636.9 | 82.5 | 361.7 |
| | 4048 | 740.7 | 99.0 | 350.5 |
| | 4069 | 742.5 | 85.0 | 409.2 |
| | 4061 | 740.1 | 95.0 | 365.0 |
| Specimen Found Cracked on Post Inspection | | | | |

## Table 45 (Continued)

### Thermal Conductivity Data for Titanium Diboride

| SRI Run No. Specimen No. Heat-Soak Temperature °F | Specimen Mean Temperature For $\frac{1}{8}$" Gage Length °F | Total Heat Flow Into $\frac{1}{4}$" Axial Calorimeter Gage Length Btu/hr | Specimen $\Delta T$ Across $\frac{1}{8}$" Gage Length °F | Specimen Thermal Conductivity Btu/hr/ft²/°F/in. |
|---|---|---|---|---|
| Run TC 89 | 1770 | 362.6 | 80.0 | 212.4 |
| | 1770 | 350.7 | 75.0 | 219.1 |
| Specimen | 1770 | 373.3 | 79.0 | 221.4 |
| No. 4 | 1772 | 372.5 | 73.0 | 239.1 |
| | 2637 | 473.2 | 100.0 | 221.7 |
| 3500°F | 2637 | 471.5 | 99.5 | 222.0 |
| | 2644 | 509.0 | 91.0 | 262.1 |
| | 3184 | 694.2 | 140.0 | 232.3 |
| | 3175 | 754.3 | 150.0 | 235.6 |
| | 3184 | 764.4 | 140.0 | 255.8 |
| | 3612 | 941.2 | 142.5 | 309.4 |
| | 3614 | 928.1 | 140.0 | 310.6 |
| | 3612 | 955.2 | 142.5 | 314.1 |
| | 3962 | 860.3 | 130.0 | 310.0 |
| | 3962 | 969.9 | 130.0 | 349.5 |
| | 4167 | 1107.6 | 160.0 | 324.3 |
| | 4165 | 1121.5 | 162.5 | 323.3 |
| | 4180 | 1137.1 | 145.0 | 367.4 |
| Specimen Found Cracked on Post Inspection | | | | |

## Table 46.

### Thermal Conductivity Data for Tungsten Boride

| SRI Run No. Specimen No. Heat-Soak Temperature °F | Specimen Mean Temperature For $\frac{1}{8}$'' Gage Length °F | Total Heat Flow Into $\frac{1}{4}$'' Axial Calorimeter Gage Length Btu/hr | Specimen $\Delta T$ Across $\frac{1}{8}$'' Gage Length °F | Specimen Thermal Conductivity Btu/hr/ft$^2$/°F/in. |
|---|---|---|---|---|
| Run TC 66 | 1800 | 538.5 | 85.5 | 295.1 |
| | 1800 | 628.2 | 103.5 | 284.4 |
| Specimen | 1800 | 539.0 | 85.5 | 295.3 |
| No. 1 | 2519 | 663.6 | 97.5 | 318.9 |
| | 2555 | 756.5 | 114.0 | 310.9 |
| 3300°F | 2577 | 652.7 | 100.0 | 305.8 |
| | 2959 | 802.4 | 121.0 | 310.7 |
| | 2954 | 772.7 | 127.5 | 283.9 |
| | 2970 | 741.0 | 120.5 | 288.1 |
| | 3433 | 834.6 | 152.5 | 256.4 |
| | 3450 | 818.6 | 132.5 | 289.5 |
| | 3432 | 804.9 | 147.5 | 255.7 |
| | 3440 | 793.4 | 138.5 | 268.4 |
| | 3780 | 917.3 | 150.0 | 286.5 |
| | 3760 | 901.6 | 175.0 | 241.4 |
| | 3769 | 938.9 | 157.5 | 279.3 |
| | 4088 | 1026.7 | 165.0 | 291.5 |
| | 4093 | 1006.6 | 171.0 | 275.8 |
| | 4113 | 1005.3 | 165.0 | 285.4 |
| Specimen Found Broken on Post Inspection | | | | |

## Table 46 (Continued).

Thermal Conductivity Data for Tungsten Boride

| SRI Run No. Specimen No. Heat-Soak Temperature °F | Specimen Mean Temperature For $\frac{1}{8}$'' Gage Length °F | Total Heat Flow Into $\frac{1}{4}$'' Axial Calorimeter Gage Length Btu/hr | Specimen $\Delta$T Across $\frac{1}{8}$'' Gage Length °F | Specimen Thermal Conductivity Btu/hr/ft$^2$/°F/in. |
|---|---|---|---|---|
| Run TC 83 | 1795 | 222.1 | 28.5 | 365.0 |
| | 1795 | 218.5 | 32.0 | 319.9 |
| Specimen No. 2 | 1795 | 222.1 | 32.5 | 320.2 |
| | 2530 | 307.7 | 48.0 | 300.4 |
| | 2526 | 313.1 | 53.5 | 274.2 |
| 3350°F | 2527 | 312.4 | 51.5 | 284.1 |
| | 2940 | 400.4 | 60.0 | 312.6 |
| | 2940 | 402.5 | 60.0 | 314.3 |
| | 2937 | 418.6 | 64.0 | 306.5 |
| | 2938 | 424.0 | 62.5 | 317.8 |
| | 3379 | 566.7 | 97.5 | 272.3 |
| | 3387 | 564.5 | 87.5 | 302.2 |
| | 3411 | 547.1 | 95.0 | 269.8 |
| Specimen Found Cracked on Post Inspection | | | | |

## Table 47.

### Thermal Conductivity Data for Dimolybdenum Carbide

| SRI Run No. Specimen No. Heat-Soak Temperature °F | Specimen Mean Temperature For $\frac{1}{8}$" Gage Length °F | Total Heat Flow Into $\frac{1}{4}$" Axial Calorimeter Gage Length Btu/hr | Specimen ΔT Across $\frac{1}{8}$" Gage Length °F | Specimen Thermal Conductivity Btu/hr/ft$^2$/°F/in. |
|---|---|---|---|---|
| Run TC 62 | 1740 | 473.0 | 146.0 | 151.8 |
| | 1740 | 465.3 | 137.0 | 159.1 |
| Specimen | 1740 | 487.6 | 140.0 | 163.2 |
| No. 1 | 1743 | 448.6 | 130.0 | 161.7 |
| | 2321 | 555.1 | 155.0 | 167.8 |
| Not Heat- | 2326 | 595.5 | 167.5 | 166.6 |
| Soaked | 2333 | 551.0 | 165.0 | 156.4 |
| | 3009 | 650.9 | 176.0 | 173.3 |
| | 3016 | 642.0 | 167.5 | 179.6 |
| | 3018 | 602.6 | 165.0 | 171.1 |
| | 3422 | 652.3 | 166.5 | 183.5 |
| | 3416 | 688.8 | 185.0 | 174.4 |
| | 3441 | 645.0 | 155.0 | 195.0 |
| | 3885 | 772.3 | 150.0 | 241.2 |
| | 3864 | 781.6 | 170.0 | 215.4 |
| | 3886 | 797.0 | 167.5 | 222.9 |
| | 3885 | 753.9 | 162.5 | 217.4 |
| Specimen Found Broken and Partially Melted on Post Inspection | | | | |

Table 47 (Continued).

Thermal Conductivity Data for Dimolybdenum Carbide

| SRI Run No. Specimen No. Heat-Soak Temperature °F | Specimen Mean Temperature For $\frac{1}{3}$" Gage Length °F | Total Heat Flow Into $\frac{1}{4}$" Axial Calorimeter Gage Length Btu/hr | Specimen ΔT Across $\frac{1}{8}$" Gage Length °F | Specimen Thermal Conductivity Btu/hr/ft$^2$/°F/in. |
|---|---|---|---|---|
| Run TC 73 | 1650 | 514.9 | 130.0 | 185.5 |
| | 1650 | 585.7 | 136.0 | 201.7 |
| Specimen | 1650 | 555.9 | 139.0 | 187.4 |
| No. 2 | 2185 | 671.2 | 138.5 | 227.1 |
| | 2196 | 639.0 | 125.0 | 239.5 |
| Not Heat- | 2196 | 617.4 | 125.0 | 231.4 |
| Soaked | 2192 | 587.1 | 130.0 | 211.6 |
| | 2190 | 589.6 | 132.5 | 208.5 |
| | 2857 | 705.2 | 159.5 | 207.1 |
| | 2860 | 749.1 | 162.5 | 215.9 |
| | 2865 | 744.9 | 162.5 | 214.8 |
| | 3345 | 853.7 | 186.0 | 215.0 |
| | 3332 | 856.9 | 190.5 | 210.7 |
| | 3330 | 844.3 | 180.0 | 219.8 |
| Specimen Found Broken on Post Inspection | | | | |

## Table 47 (Continued).

### Thermal Conductivity Data for Dimolybdenum Carbide

| SRI Run No. Specimen No. Heat-Soak Temperature °F | Specimen Mean Temperature For $\frac{1}{8}$'' Gage Length °F | Total Heat Flow Into $\frac{1}{4}$'' Axial Calorimeter Gage Length Btu/hr | Specimen ΔT Across $\frac{1}{8}$'' Gage Length °F | Specimen Thermal Conductivity Btu/hr/$ft^2$/°F/in. |
|---|---|---|---|---|
| Run TC 79 | 1960 | 203.3 | 66.5 | 143.2 |
| | 1960 | 208.3 | 65.5 | 149.0 |
| Specimen | 1960 | 209.2 | 73.5 | 133.3 |
| No. 3 | 1960 | 206.0 | 64.5 | 149.6 |
| | 2496 | 249.9 | 82.5 | 141.7 |
| 2800°F | 2503 | 252.4 | 81.0 | 146.0 |
| | 2503 | 262.1 | 86.5 | 142.0 |
| | 2883 | 353.2 | 92.5 | 178.9 |
| | 2893 | 361.3 | 104.5 | 162.0 |
| | 2898 | 375.6 | 99.0 | 177.8 |
| | 2911 | 351.4 | 95.5 | 172.4 |
| | 3267 | 428.6 | 99.5 | 201.8 |
| | 3258 | 464.9 | 111.0 | 196.2 |
| | 3266 | 461.5 | 101.0 | 214.1 |
| | 3263 | 494.5 | 104.5 | 221.7 |
| | 3621 | 637.5 | 125.0 | 238.9 |
| | 3832 | 734.7 | 130.0 | 264.8 |
| | 3812 | 762.3 | 142.5 | 250.6 |
| | 3818 | 748.0 | 135.0 | 259.6 |
| | 3811 | 745.7 | 125.0 | 279.5 |
| Specimen Found Broken on Post Inspection | | | | |

## Table 48.

### Thermal Conductivity Data for Hafnium Carbide

| SRI Run No. Specimen No. Heat-Soak Temperature °F | Specimen Mean Temperature For $\frac{1}{8}$" Gage Length °F | Total Heat Flow Into $\frac{1}{4}$" Axial Calorimeter Gage Length Btu/hr | Specimen $\Delta T$ Across $\frac{1}{8}$" Gage Length °F | Specimen Thermal Conductivity Btu/hr/ft$^2$/°F/in. |
|---|---|---|---|---|
| Run TC 93 | 1810 | 401.9 | 168.0 | 112.1 |
| | 1810 | 439.4 | 178.5 | 115.3 |
| Specimen | 1810 | 444.2 | 182.0 | 114.3 |
| No. 1 | 1813 | 459.3 | 184.0 | 117.0 |
| | 2705 | 464.0 | 175.0 | 124.2 |
| 4000°F | 2700 | 491.0 | 181.0 | 127.1 |
| | 2685 | 502.2 | 198.0 | 118.8 |
| | 3125 | 526.1 | 210.0 | 117.4 |
| | 3124 | 550.8 | 211.5 | 122.0 |
| | 3110 | 529.4 | 228.5 | 108.5 |
| | 3538 | 627.8 | 195.5 | 150.4 |
| | 3534 | 648.2 | 200.0 | 151.8 |
| | 3534 | 677.2 | 200.0 | 158.6 |
| | 4054 | 793.4 | 217.5 | 170.9 |
| | 4058 | 811.6 | 212.5 | 178.9 |
| | 4067 | 775.5 | 202.5 | 179.4 |
| | 4201 | 905.1 | 240.0 | 176.7 |
| | 4217 | 924.1 | 220.0 | 196.8 |
| | 4213 | 899.8 | 225.0 | 187.4 |
| | 4433 | 1000.7 | 237.5 | 197.4 |
| | 4416 | 1018.5 | 245.0 | 194.8 |
| | 4415 | 1005.3 | 235.0 | 200.4 |
| Specimen Found Broken on Post Inspection | | | | |

## Table 49.

Thermal Conductivity Data for Titanium Carbide

| SRI Run No. Specimen No. Heat-Soak Temperature °F | Specimen Mean Temperature For $\frac{1}{8}$" Gage Length °F | Total Heat Flow Into $\frac{1}{4}$" Axial Calorimeter Gage Length Btu/hr | Specimen $\Delta T$ Across $\frac{1}{8}$" Gage Length °F | Specimen Thermal Conductivity Btu/hr/ft²/°F/in. |
|---|---|---|---|---|
| Run TC 3<br>Specimen No. 1<br>4050°F | 1698 | 492.0 | 111.0 | 207.0 |
| | 1723 | 483.0 | 115.0 | 197.0 |
| | 1992 | 520.0 | 110.0 | 222.0 |
| | 2035 | 548.0 | 124.0 | 207.0 |
| | 2240 | 553.0 | 110.0 | 236.0 |
| Specimen Found in Good Condition on Post Inspection | | | | |
| Run TC 8<br>Specimen No. 1<br>4050°F | 2317 | 118.0 | 28.0 | 198.0 |
| | 2378 | 138.0 | 26.5 | 244.0 |
| | 2389 | 121.0 | 25.0 | 227.0 |
| | 2889 | 184.0 | 37.5 | 230.0 |
| | 2885 | 158.0 | 42.5 | 175.0 |
| Specimen Found Cracked on Post Inspection | | | | |
| Run TC 77<br>Specimen No. 2<br>3500°F | 2946 | 166.4 | 65.0 | 119.9 |
| | 2958 | 193.0 | 56.0 | 161.5 |
| | 2963 | 179.5 | 57.0 | 147.5 |
| | 3356 | 252.7 | 101.5 | 116.6 |
| | 3369 | 277.5 | 85.0 | 152.9 |
| | 3363 | 249.7 | 92.5 | 126.5 |
| | 3721 | 233.5 | 95.0 | 115.2 |
| | 3715 | 261.7 | 102.5 | 119.6 |

## Table 49 (Continued).

## Thermal Conductivity Data for Titanium Carbide

| SRI Run No. Specimen No. Heat-Soak Temperature °F | Specimen Mean Temperature For $\frac{1}{8}$" Gage Length °F | Total Heat Flow Into $\frac{1}{4}$" Axial Calorimeter Gage Length Btu/hr | Specimen $\Delta T$ Across $\frac{1}{8}$" Gage Length °F | Specimen Thermal Conductivity Btu/hr/ft²/°F/in. |
|---|---|---|---|---|
| Run TC 77 | 3719 | 253.1 | 97.5 | 121.6 |
| (Continued) | 4063 | 369.5 | 105.0 | 164.9 |
| | 4055 | 386.9 | 102.5 | 176.8 |
| Specimen | 4049 | 396.4 | 110.0 | 168.8 |
| No. 2 | 4340 | 457.2 | 120.0 | 178.5 |
| | 4342 | 457.4 | 117.5 | 182.4 |
| 3500°F | 4308 | 454.2 | 134.5 | 158.2 |
| Specimen Found Cracked on Post Inspection | | | | |
| Run TC 84 | 1560 | 426.1 | 54.5 | 366.3 |
| | 1560 | 442.7 | 56.0 | 370.3 |
| Specimen | 1558 | 452.6 | 67.0 | 316.5 |
| No. 3 | 2349 | 467.8 | 85.5 | 256.3 |
| | 2365 | 487.3 | 90.5 | 252.3 |
| 3350°F | 2766 | 514.7 | 101.5 | 237.6 |
| | 2796 | 524.3 | 113.5 | 216.4 |
| | 2815 | 516.4 | 102.5 | 236.0 |
| | 3300 | 584.5 | 169.0 | 162.0 |
| | 3335 | 613.6 | 162.5 | 176.9 |
| | 3347 | 578.9 | 160.0 | 169.5 |
| | 3942 | 711.7 | 142.5 | 234.0 |
| | 3968 | 706.7 | 135.0 | 245.2 |
| | 3957 | 755.8 | 147.5 | 240.1 |
| Specimen Found Cracked on Post Inspection | | | | |

## Table 50.

### Thermal Conductivity Data for Tungsten Carbide

| SRI Run No. Specimen No. Heat-Soak Temperature °F | Specimen Mean Temperature For $\frac{1}{8}$" Gage Length °F | Total Heat Flow Into $\frac{1}{4}$" Axial Calorimeter Gage Length Btu/hr | Specimen $\Delta$T Across $\frac{1}{8}$" Gage Length °F | Specimen Thermal Conductivity Btu/hr/ft$^2$/°F/in. |
|---|---|---|---|---|
| Run TC 56 | 1525 | 541.3 | 86.5 | 293.2 |
| | 1525 | 601.8 | 98.5 | 286.3 |
| Specimen | 2123 | 735.6 | 92.5 | 372.6 |
| No. 1 | 2117 | 691.6 | 100.0 | 324.0 |
| | 2117 | 673.7 | 100.0 | 315.6 |
| 3875°F | 2519 | 829.5 | 97.5 | 398.6 |
| | 2527 | 715.8 | 100.0 | 335.4 |
| | 2527 | 700.8 | 100.0 | 328.3 |
| | 2987 | 802.3 | 117.5 | 319.9 |
| | 3013 | 817.3 | 105.0 | 364.7 |
| | 3542 | 799.0 | 100.0 | 374.3 |
| | 3546 | 855.0 | 95.0 | 421.6 |
| | 3548 | 764.1 | 92.5 | 387.0 |
| Specimen Found Cracked on Post Inspection | | | | |
| Run TC 74 | 3048 | 924.0 | 122.5 | 353.4 |
| | 3046 | 919.3 | 125.0 | 344.6 |
| Specimen | 3057 | 947.2 | 123.5 | 359.3 |
| No. 2 | 3784 | 1043.5 | 140.0 | 349.2 |
| | 3816 | 1013.1 | 137.5 | 345.2 |
| 3650-3700°F | 3818 | 992.5 | 135.0 | 344.4 |
| | 4113 | 1108.5 | 141.0 | 368.3 |
| | 4124 | 1134.3 | 127.5 | 416.8 |
| | 4107 | 1124.2 | 147.5 | 357.1 |
| | 4116 | 1101.8 | 137.5 | 375.4 |
| Specimen Found Broken on Post Inspection | | | | |

## Table 51.

## Thermal Conductivity Data for Vanadium Carbide

| SRI Run No. Specimen No. Heat-Soak Temperature °F | Specimen Mean Temperature For $\frac{1}{8}$" Gage Length °F | Total Heat Flow Into $\frac{1}{4}$" Axial Calorimeter Gage Length Btu/hr | Specimen $\Delta T$ Across $\frac{1}{8}$" Gage Length °F | Specimen Thermal Conductivity Btu/hr/ft$^2$/°F/in. |
|---|---|---|---|---|
| Run TC 6 | 1775 | 545.0 | 107.5 | 238.0 |
| | 1775 | 549.0 | 110.0 | 233.0 |
| Specimen | 2590 | 695.0 | 121.5 | 268.0 |
| No. 1 | 2590 | 707.0 | 123.0 | 269.0 |
| | 2590 | 665.0 | 131.0 | 238.0 |
| 3675°F | 2985 | 835.0 | 137.5 | 284.0 |
| | 2975 | 805.0 | 145.5 | 259.0 |
| | 2970 | 838.0 | 155.0 | 253.0 |
| | 3480 | 965.0 | 142.5 | 317.0 |
| | 3480 | 981.0 | 137.5 | 334.0 |
| | 3480 | 1036.0 | 150.0 | 323.0 |
| Specimen Found Cracked on Post Inspection | | | | |
| Run TC 80 | 1754 | 265.7 | 46.0 | 270.6 |
| | 1754 | 265.3 | 45.0 | 276.2 |
| Specimen | 1754 | 256.3 | 46.5 | 258.2 |
| No. 2 | 1754 | 257.6 | 44.5 | 271.2 |
| | 2457 | 318.0 | 70.0 | 212.8 |
| 3475°F | 2457 | 330.2 | 69.5 | 222.6 |
| | 2459 | 320.8 | 67.5 | 222.7 |
| | 2860 | 429.5 | 96.5 | 208.5 |
| | 2868 | 426.9 | 98.5 | 203.1 |
| | 2874 | 428.1 | 104.0 | 192.8 |
| | 2876 | 420.5 | 89.0 | 221.4 |
| | 3225 | 506.2 | 102.0 | 232.5 |
| | 3233 | 525.1 | 117.0 | 210.3 |

## Table 51 (Continued).

## Thermal Conductivity Data for Vanadium Carbide

| SRI Run No. Specimen No. Heat-Soak Temperature °F | Specimen Mean Temperature For $\frac{1}{8}$" Gage Length °F | Total Heat Flow Into $\frac{1}{4}$" Axial Calorimeter Gage Length Btu/hr | Specimen $\Delta T$ Across $\frac{1}{8}$" Gage Length °F | Specimen Thermal Conductivity Btu/hr/ft²/°F/in. |
|---|---|---|---|---|
| Run TC 80 | 3259 | 515.2 | 110.0 | 219.4 |
| (Continued) | 3259 | 510.2 | 110.0 | 217.3 |
| | 3454 | 658.0 | 116.0 | 265.7 |
| Specimen | 3457 | 673.5 | 124.0 | 254.5 |
| No. 2 | 3472 | 659.3 | 118.5 | 260.7 |
| | 3742 | 798.3 | 117.5 | 318.3 |
| 3475°F | 3753 | 772.2 | 105.0 | 344.5 |
| | 3755 | 801.1 | 102.5 | 366.1 |
| | 3740 | 806.5 | 120.0 | 314.9 |
| Specimen Found Cracked on Post Inspection | | | | |

## Table 52.

Thermal Conductivity Data for Boron Nitride

| SRI Run No. Specimen No. Heat-Soak Temperature °F | Specimen Mean Temperature For $\frac{1}{8}$" Gage Length °F | Total Heat Flow Into $\frac{1}{4}$" Axial Calorimeter Gage Length Btu/hr | Specimen ΔT Across $\frac{1}{8}$" Gage Length °F | Specimen Thermal Conductivity Btu/hr/ft²/°F/in. |
|---|---|---|---|---|
| Run TC 50 | 1542 | 442.8 | 111.0 | 186.9 |
| | 1575 | 436.1 | 109.0 | 187.4 |
| Specimen No. 1 | 1575 | 541.2 | 131.0 | 193.5 |
| | 2548 | 579.3 | 195.0 | 139.2 |
| | 2563 | 594.1 | 207.5 | 134.1 |
| Not Heat-Soaked | 2594 | 561.5 | 187.5 | 140.3 |
| Specimen Found in Good Condition on Post Inspection | | | | |
| Run TC 52 | 1425 | 629.3 | 117.5 | 250.9 |
| | 1425 | 591.6 | 121.5 | 228.1 |
| Specimen No. 1 | 2220 | 563.8 | 181.0 | 145.9 |
| | 2195 | 703.8 | 186.0 | 177.3 |
| | 2196 | 621.2 | 185.0 | 157.3 |
| Not Heat-Soaked | 3011 | 776.4 | 239.5 | 151.9 |
| | 3020 | 830.5 | 241.0 | 161.4 |
| | 2991 | 829.2 | 240.0 | 161.9 |
| | 2979 | 794.8 | 253.5 | 146.9 |
| | 3365 | 915.3 | 342.5 | 125.2 |
| | 3336 | 1057.3 | 390.0 | 127.0 |
| | 3342 | 1076.1 | 395.0 | 127.6 |
| | 3340 | 1090.3 | 397.5 | 128.5 |
| | 3346 | 1070.6 | 390.0 | 128.6 |
| Specimen Found in Good Condition on Post Inspection | | | | |

Table 52 (Continued).

Thermal Conductivity Data for Boron Nitride

| SRI Run No. Specimen No. Heat-Soak Temperature °F | Specimen Mean Temperature For $\frac{1}{8}$" Gage Length °F | Total Heat Flow Into $\frac{1}{4}$" Axial Calorimeter Gage Length Btu/hr | Specimen $\Delta T$ Across $\frac{1}{8}$" Gage Length °F | Specimen Thermal Conductivity Btu/hr/ft$^2$/°F/in. |
|---|---|---|---|---|
| Run TC 64 | 1525 | 765.1 | 197.5 | 181.5 |
| | 1525 | 735.8 | 191.5 | 180.0 |
| Specimen No. 2 | 2329 | 902.9 | 236.0 | 179.2 |
| | 2313 | 920.2 | 242.5 | 177.8 |
| | 2317 | 894.9 | 238.5 | 175.8 |
| Not Heat-Soaked | 2871 | 1052.3 | 287.5 | 171.5 |
| | 2842 | 1070.1 | 310.0 | 161.7 |
| | 3357 | 1222.9 | 425.0 | 134.8 |
| | 3373 | 1225.3 | 417.5 | 137.5 |
| | 3367 | 1220.5 | 425.0 | 134.5 |
| Specimen Found in Good Condition on Post Inspection | | | | |

## Table 53.

## Thermal Conductivity Data for Tantalum Nitride

| SRI Run No. Specimen No. Heat-Soak Temperature °F | Specimen Mean Temperature For $\frac{1}{8}$" Gage Length °F | Total Heat Flow Into $\frac{1}{4}$" Axial Calorimeter Gage Length Btu/hr | Specimen $\Delta T$ Across $\frac{1}{8}$" Gage Length °F | Specimen Thermal Conductivity Btu/hr/ft$^2$/°F/in. |
|---|---|---|---|---|
| Run TC 53 | 1770 | 388.5 | 237.0 | 76.8 |
| | 1770 | 383.6 | 230.5 | 77.9 |
| Specimen | 1767 | 371.2 | 221.0 | 78.7 |
| No. 1 | 1770 | 363.6 | 230.5 | 73.9 |
| | 1770 | 333.6 | 213.5 | 73.2 |
| 3000°F | 2443 | 418.2 | 237.5 | 82.5 |
| | 2440 | 395.0 | 241.0 | 76.8 |
| | 2440 | 395.8 | 240.0 | 77.3 |
| | 2845 | 540.5 | 186.5 | 135.8 |
| | 2838 | 526.6 | 182.5 | 135.2 |
| | 2818 | 490.2 | 195.0 | 117.8 |
| Specimen Found Broken on Post Inspection | | | | |
| Run TC 90 | 1247 | 251.8 | 178.0 | 66.3 |
| | 1273 | 258.6 | 170.0 | 71.3 |
| Specimen | 1745 | 356.0 | 167.5 | 99.6 |
| No. 2 | 1745 | 366.0 | 162.5 | 105.5 |
| | 1745 | 381.9 | 171.0 | 104.6 |
| Not Heat- | 1743 | 388.2 | 175.5 | 103.6 |
| Soaked | 2847 | 445.9 | 124.0 | 168.5 |
| | 2856 | 477.3 | 113.0 | 197.9 |
| | 2859 | 477.1 | 109.0 | 205.1 |
| | 3280 | 521.7 | 132.5 | 184.5 |
| | 3290 | 568.3 | 145.0 | 183.6 |
| | 3302 | 605.5 | 142.5 | 199.1 |

Table 53 (Continued).

Thermal Conductivity Data for Tantalum Nitride

| SRI Run No. Specimen No. Heat-Soak Temperature °F | Specimen Mean Temperature Into $\frac{1}{8}$" Gage Length °F | Total Heat Flow Into $\frac{1}{4}$" Axial Calorimeter Gage Length Btu/hr | Specimen $\Delta T$ Across $\frac{1}{8}$" Gage Length °F | Specimen Thermal Conductivity Btu/hr/ft$^2$/°F/in. |
|---|---|---|---|---|
| Run TC 90 | 3886 | 757.2 | 137.5 | 258.0 |
| (Continued) | 3875 | 790.2 | 150.0 | 246.8 |
| | 3869 | 829.4 | 157.5 | 246.7 |
| Specimen | 4518 | 594.4 | 122.5 | 227.3 |
| No. 2 | 4492 | 633.9 | 130.0 | 228.4 |
| Not Heat- | 4471 | 706.4 | 125.0 | 264.7 |
| Soaked | | | | |
| Specimen Found Broken on Post Inspection | | | | |

## Table 54.

### Thermal Conductivity Data for Beryllium Oxide

| SRI Run No. Specimen No. Heat-Soak Temperature °F | Specimen Mean Temperature For $\frac{1}{8}$" Gage Length °F | Total Heat Flow Into $\frac{1}{4}$" Axial Calorimeter Gage Length Btu/hr | Specimen ΔT Across $\frac{1}{8}$" Gage Length °F | Specimen Thermal Conductivity Btu/hr/ft²/°F/in. |
|---|---|---|---|---|
| Run TC 96 | 1351 | 286.3 | 126.0 | 106.4 |
| | 1357 | 305.0 | 132.0 | 108.3 |
| Specimen No. 1 | 1381 | 250.6 | 112.0 | 104.8 |
| | 1785 | 326.1 | 183.0 | 83.5 |
| | 1800 | 293.5 | 157.0 | 87.6 |
| Not Heat-Soaked | 1800 | 264.4 | 161.0 | 76.9 |
| | 1800 | 261.3 | 158.0 | 77.5 |
| | 2439 | 324.4 | 266.5 | 57.0 |
| | 2448 | 305.9 | 242.5 | 59.1 |
| | 2434 | 305.1 | 259.5 | 55.1 |
| | 2442 | 309.5 | 250.0 | 58.0 |
| | 2754 | 267.8 | 295.5 | 42.5 |
| | 2756 | 268.1 | 293.5 | 42.8 |
| | 2712 | 297.7 | 335.0 | 41.6 |
| | 2998 | 268.5 | 363.5 | 34.6 |
| | 2978 | 267.2 | 387.5 | 32.3 |
| | 2978 | 282.6 | 387.5 | 34.2 |
| | 2983 | 286.6 | 381.0 | 35.2 |
| | 3143 | 301.6 | 430.0 | 32.9 |
| | 3133 | 301.8 | 441.5 | 32.0 |
| | 3157 | 312.1 | 425.0 | 34.4 |
| | 3135 | 336.3 | 451.0 | 34.9 |
| Specimen Found Broken on Post Inspection | | | | |

Table 54 (Continued).

Thermal Conductivity Data for Beryllium Oxide

| SRI Run No. Specimen No. Heat-Soak Temperature °F | Specimen Mean Temperature For $\frac{1}{8}$" Gage Length °F | Total Heat Flow Into $\frac{1}{4}$" Axial Calorimeter Gage Length Btu/hr | Specimen $\Delta T$ Across $\frac{1}{8}$" Gage Length °F | Specimen Thermal Conductivity Btu/hr/ft$^2$/°F/in. |
|---|---|---|---|---|
| Run TC 98 | 1012 | 277.5 | 101.5 | 128.1 |
| | 1038 | 281.1 | 101.0 | 130.4 |
| Specimen | 1042 | 273.4 | 93.5 | 137.0 |
| No. 2 | 1057 | 276.4 | 104.5 | 123.9 |
| | 1860 | 344.8 | 231.5 | 69.8 |
| Not Heat- | 1860 | 355.1 | 226.5 | 73.5 |
| Soaked | 1860 | 345.7 | 231.5 | 70.0 |
| | 1857 | 347.0 | 269.0 | 60.4 |
| | 2402 | 382.3 | 286.0 | 62.6 |
| | 2403 | 353.5 | 285.0 | 58.1 |
| | 2414 | 366.6 | 272.5 | 63.0 |
| | 2405 | 335.9 | 282.5 | 55.7 |
| | 2727 | 402.2 | 280.0 | 67.3 |
| | 2713 | 459.4 | 297.5 | 72.4 |
| | 2729 | 501.4 | 277.5 | 84.6 |
| | 2750 | 467.3 | 265.0 | 82.6 |
| | 2729 | 441.0 | 290.0 | 71.2 |
| | 2986 | 540.4 | 347.5 | 72.9 |
| | 3002 | 543.0 | 358.5 | 70.9 |
| | 2992 | 522.8 | 370.5 | 66.1 |
| | 3145 | 562.9 | 427.0 | 61.8 |
| | 3151 | 578.9 | 420.0 | 64.6 |
| | 3172 | 560.8 | 406.5 | 64.6 |
| | 3169 | 556.7 | 410.0 | 63.6 |
| Specimen Found Cracked on Post Inspection | | | | |

## Table 55.

### Thermal Conductivity Data for Cerium Dioxide

| SRI Run No. Specimen No. Heat-Soak Temperature °F | Specimen Mean Temperature For $\frac{1}{8}$" Gage Length °F | Total Heat Flow Into $\frac{1}{4}$" Axial Calorimeter Gage Length Btu/hr | Specimen $\Delta$T Across $\frac{1}{8}$" Gage Length °F | Specimen Thermal Conductivity Btu/hr/ft²/°F/in. |
|---|---|---|---|---|
| Run TC 55 | 2162 | 90.2 | 707.5 | 6.0 |
| | 2133 | 125.3 | 730.0 | 8.0 |
| Specimen No. 1 | 2079 | 113.7 | 807.5 | 6.6 |
| | 2234 | 120.5 | 982.5 | 5.7 |
| | 2227 | 122.1 | 990.0 | 5.8 |
| Not Heat-Soaked | 2223 | 97.4 | 995.0 | 4.6 |
| | 2240 | 111.6 | 975.0 | 5.4 |
| | 2439 | 132.8 | 1030.0 | 6.0 |
| | 2469 | 124.4 | 1012.5 | 5.8 |
| | 2515 | 109.9 | 992.5 | 5.2 |
| | 2888 | 101.3 | 785.0 | 6.0 |
| | 2987 | 115.4 | 737.5 | 7.3 |
| Specimen Found Broken on Post Inspection | | | | |

## Table 56.

Thermal Conductivity Data for Hafnium Dioxide

| SRI Run No. Specimen No. Heat-Soak Temperature °F | Specimen Mean Temperature For $\frac{1}{8}$" Gage Length °F | Total Heat Flow Into $\frac{1}{4}$" Axial Calorimeter Gage Length Btu/hr | Specimen $\Delta T$ Across $\frac{1}{8}$" Gage Length °F | Specimen Thermal Conductivity Btu/hr/ft$^2$/°F/in. |
|---|---|---|---|---|
| Run TC 58 | 1997 | 187.6 | 463.5 | 18.9 |
| | 1997 | 163.5 | 450.0 | 17.0 |
| Specimen | 2358 | 210.7 | 592.5 | 16.7 |
| No. 1 | 2337 | 233.7 | 617.5 | 17.7 |
| | 2358 | 236.3 | 592.5 | 18.7 |
| Not Heat- | 2666 | 262.1 | 702.5 | 17.5 |
| Soaked | 2629 | 281.4 | 747.5 | 17.6 |
| | 2650 | 278.8 | 752.5 | 17.4 |
| | 3020 | 284.3 | 830.0 | 16.1 |
| | 3027 | 320.5 | 810.0 | 18.5 |
| | 3014 | 313.4 | 825.0 | 17.8 |
| | 3452 | 374.1 | 960.0 | 18.3 |
| Specimen Found Deteriorated on Post Inspection | | | | |

## Table 57.

## Thermal Conductivity Data for Magnesium Oxide

| SRI Run No. Specimen No. Heat-Soak Temperature °F | Specimen Mean Temperature For $\frac{1}{8}$'' Gage Length °F | Total Heat Flow Into $\frac{1}{4}$'' Axial Calorimeter Gage Length Btu/hr | Specimen $\Delta T$ Across $\frac{1}{8}$'' Gage Length °F | Specimen Thermal Conductivity Btu/hr/ft²/°F/in. |
|---|---|---|---|---|
| Run TC 51 | 1580 | 277.7 | 170.0 | 76.5 |
| | 1580 | 266.3 | 171.0 | 72.9 |
| Specimen No. 1 | 1580 | 269.7 | 175.0 | 72.2 |
| | 2430 | 290.4 | 288.5 | 47.2 |
| | 2441 | 294.9 | 275.0 | 50.2 |
| Not Heat-Soaked | 2449 | 297.5 | 272.5 | 51.1 |
| | 2553 | 303.0 | 309.0 | 45.9 |
| | 2567 | 287.3 | 292.5 | 46.0 |
| | 2568 | 277.4 | 291.0 | 44.7 |
| | 2928 | 306.6 | 387.5 | 37.1 |
| | 2967 | 352.0 | 412.5 | 40.0 |
| | 2984 | 334.2 | 391.5 | 40.0 |
| | 2986 | 318.8 | 390.0 | 38.3 |
| | 3253 | 397.0 | 550.0 | 33.8 |
| | 3269 | 428.0 | 555.0 | 36.1 |
| | 3265 | 410.0 | 560.0 | 34.3 |
| | 3378 | 516.0 | 700.0 | 34.5 |
| | 3365 | 512.0 | 715.0 | 33.6 |
| | 3375 | 513.0 | 715.0 | 33.6 |
| | 3720 | 575.0 | 710.0 | 37.8 |
| | 3700 | 615.0 | 722.5 | 39.8 |
| | 3700 | 610.0 | 722.5 | 39.6 |
| | 3700 | 598.0 | 722.5 | 38.7 |
| Specimen Found Broken and Partially Melted on Post Inspection | | | | |

## Table 58.

### Thermal Conductivity Data for Thorium Dioxide

| SRI Run No. Specimen No. Heat-Soak Temperature °F | Specimen Mean Temperature For $\frac{1}{8}$" Gage Length °F | Total Heat Flow Into $\frac{1}{4}$" Axial Calorimeter Gage Length Btu/hr | Specimen $\Delta T$ Across $\frac{1}{8}$" Gage Length °F | Specimen Thermal Conductivity Btu/hr/ft$^2$/°F/in. |
|---|---|---|---|---|
| Run TC 94 | 1936 | 108.7 | 468.5 | 10.9 |
| | 1936 | 120.8 | 475.0 | 11.9 |
| Specimen No. 1 | 1936 | 137.5 | 476.0 | 13.5 |
| | 2224 | 164.7 | 656.5 | 11.8 |
| | 2237 | 147.8 | 641.5 | 10.8 |
| Not Heat-Socked | 2244 | 199.5 | 645.5 | 14.5 |
| | 2257 | 184.1 | 629.0 | 13.7 |
| | 2387 | 175.0 | 755.5 | 10.9 |
| | 2378 | 157.0 | 767.0 | 9.6 |
| | 2398 | 163.1 | 742.5 | 10.3 |
| | 2386 | 149.6 | 763.5 | 9.2 |
| | 2416 | 166.8 | 726.5 | 10.8 |
| | 2553 | 169.4 | 839.0 | 9.5 |
| | 2578 | 158.8 | 808.5 | 9.2 |
| | 2585 | 168.0 | 800.0 | 9.8 |
| | 2611 | 173.5 | 792.5 | 10.3 |
| | 2616 | 185.7 | 786.5 | 11.1 |
| | 2783 | 212.0 | 874.5 | 11.4 |
| | 2818 | 182.2 | 832.5 | 10.3 |
| Specimen Found Broken on Post Inspection | | | | |

## Table 59.

### Thermal Conductivity Data for Zirconium Dioxide

| SRI Run No. Specimen No. Heat-Soak Temperature °F | Specimen Mean Temperature For $\frac{1}{8}$" Gage Length °F | Total Heat Flow Into $\frac{1}{4}$" Axial Calorimeter Gage Length Btu/hr | Specimen ΔT Across $\frac{1}{8}$" Gage Length °F | Specimen Thermal Conductivity Btu/hr/ft²/°F/in. |
|---|---|---|---|---|
| Run TC 54 | 1500 | 92.7 | 360.0 | 12.1 |
| | 1500 | 118.0 | 385.0 | 14.4 |
| Specimen No. 1 | 1500 | 106.9 | 397.5 | 12.6 |
| | 2078 | 158.6 | 580.0 | 12.8 |
| | 2068 | 162.1 | 592.5 | 12.8 |
| Not Heat-Soaked | 2080 | 138.2 | 590.0 | 11.0 |
| | 2337 | 140.1 | 797.5 | 9.9 |
| | 2331 | 177.6 | 805.0 | 10.3 |
| | 2317 | 165.7 | 822.5 | 9.4 |
| | 2300 | 161.4 | 842.5 | 9.0 |
| | 2744 | 241.2 | 987.5 | 11.4 |
| | 2783 | 221.7 | 922.5 | 11.3 |
| | 2777 | 180.1 | 930.0 | 9.1 |
| | 3139 | 258.6 | 1012.5 | 12.0 |
| | 3176 | 245.4 | 980.0 | 11.7 |
| | 3163 | 211.7 | 995.0 | 10.0 |
| | 3646 | 266.6 | 1027.5 | 12.2 |
| | 3628 | 296.7 | 1037.5 | 13.4 |
| | 3642 | 269.1 | 1032.5 | 12.2 |
| Specimen Found Broken on Post Inspection | | | | |

Table 60.

Thermal Conductivity Data for Columbium +0.5% Zirconium

| SRI Run No. Specimen No. Heat-Soak Temperature °F | Specimen Mean Temperature For $\frac{1}{8}$" Gage Length °F | Total Heat Flow Into $\frac{1}{4}$" Axial Calorimeter Gage Length Btu/hr | Specimen $\Delta$T Across $\frac{1}{8}$" Gage Length °F | Specimen Thermal Conductivity Btu/hr/ft$^2$/°F/in. |
|---|---|---|---|---|
| Run TC 44 | 1700 | 345.7 | 104.0 | 155.7 |
| | 1700 | 338.9 | 106.5 | 149.1 |
| Specimen | 1700 | 349.1 | 101.1 | 161.9 |
| No. 1 | 2595 | 321.0 | 126.0 | 119.3 |
| | 2589 | 376.0 | 146.0 | 120.7 |
| 3350°F | 2595 | 378.1 | 138.5 | 127.9 |
| | 2844 | 373.7 | 140.0 | 125.1 |
| | 2841 | 382.2 | 155.0 | 115.5 |
| Specimen Found in Good Condition on Post Inspection | | | | |
| Run TC 48 | 1974 | 452.9 | 127.5 | 166.4 |
| | 2008 | 452.4 | 129.0 | 164.3 |
| Specimen | 2454 | 412.5 | 127.0 | 152.2 |
| No. 1 | 2440 | 489.9 | 150.0 | 153.0 |
| | 2441 | 471.6 | 149.0 | 148.3 |
| 3350°F | 2709 | 538.3 | 157.5 | 160.1 |
| | 2739 | 470.9 | 157.5 | 140.1 |
| | 2733 | 485.3 | 152.5 | 149.1 |
| | 3098 | 625.0 | 182.5 | 160.5 |
| | 3167 | 630.5 | 177.5 | 166.4 |
| | 3167 | 588.1 | 177.5 | 155.2 |
| | 3425 | 692.1 | 210.0 | 154.4 |
| | 3457 | 650.1 | 172.5 | 176.6 |
| | 3454 | 667.4 | 200.0 | 156.3 |
| | 3461 | 683.6 | 167.5 | 191.2 |
| Specimen Found Partially Melted on Post Inspection | | | | |

Table 61.

Thermal Conductivity Data for Molybdenum +0.5% Titanium

| SRI Run No. Specimen No. Heat-Soak Temperature °F | Specimen Mean Temperature For $\frac{1}{8}$" Gage Length °F | Total Heat Flow Into $\frac{1}{4}$" Axial Calorimeter Gage Length Btu/hr | Specimen ΔT Across $\frac{1}{8}$" Gage Length °F | Specimen Thermal Conductivity Btu/hr/ft$^2$/°F/in. |
|---|---|---|---|---|
| Run TC 45 | 1775 | 343.6 | 89.0 | 180.9 |
| | 1775 | 372.1 | 105.5 | 165.2 |
| Specimen | 1760 | 380.6 | 91.5 | 194.9 |
| No. 1 | 1760 | 396.7 | 94.5 | 196.7 |
| | 2503 | 446.9 | 105.0 | 199.4 |
| 2800°F | 2544 | 446.9 | 104.0 | 201.3 |
| | 2514 | 454.6 | 115.0 | 185.2 |
| | 2887 | 392.9 | 100.0 | 184.1 |
| | 2889 | 428.7 | 110.0 | 181.6 |
| | 2894 | 442.2 | 116.0 | 178.6 |
| Specimen Found in Good Condition on Post Inspection | | | | |
| Run TC 46 | 2528 | 593.2 | 135.0 | 205.8 |
| | 2528 | 586.1 | 135.0 | 203.4 |
| Specimen | 2528 | 589.8 | 135.0 | 204.7 |
| No. 1 | 2777 | 589.2 | 147.5 | 187.1 |
| | 2780 | 571.6 | 145.0 | 184.7 |
| 2800°F | 2782 | 593.6 | 142.5 | 195.2 |
| | 2807 | 609.6 | 135.5 | 210.8 |
| | 3187 | 568.7 | 136.0 | 195.9 |
| | 3155 | 580.3 | 175.0 | 155.4 |
| | 3177 | 569.9 | 147.5 | 181.0 |
| | 3195 | 619.3 | 162.5 | 178.6 |
| | 3205 | 631.7 | 162.5 | 182.1 |
| | 3199 | 589.5 | 170.0 | 162.5 |
| | 3732 | 592.2 | 117.5 | 236.1 |
| | 3824 | 551.4 | 140.0 | 184.5 |
| | 3871 | 530.0 | 107.5 | 231.0 |
| | 3917 | 510.8 | 100.0 | 239.3 |
| Specimen Found Partially Melted on Post Inspection | | | | |

## Table 63.

Thermal Conductivity Data for
Magnesium Oxide with GFE Apparatus

| SRI Run Number | Specimen Mean Temperature For $\frac{5}{8}$" Gage Length °F | Total Heat Flow Into $\frac{1}{4}$" Axial Calorimeter Gage Length Btu/hr | Specimen $\Delta T$ Across $\frac{5}{8}$" Gage Length °F | Specimen Thermal Conductivity Btu/hr/ft²/°F/in. |
|---|---|---|---|---|
| Run GFE 6 | 2575 | 107.5 | 356.0 | 22.3 |
| | 2542 | 101.3 | 384.0 | 19.5 |
| | 2576 | 103.7 | 377.0 | 20.3 |
| | 2562 | 99.4 | 366.0 | 20.1 |
| | 3032 | 129.2 | 400.0 | 23.9 |
| | 3050 | 131.8 | 403.0 | 24.2 |
| | 3058 | 130.1 | 390.0 | 24.7 |
| | 3077 | 122.0 | 392.0 | 23.0 |
| | 3416 | 128.7 | 477.0 | 20.0 |
| | 3444 | 121.9 | 447.0 | 20.2 |
| | 3466 | 137.5 | 443.0 | 23.0 |
| | 3482 | 132.8 | 450.0 | 21.8 |
| | 3625 | 152.7 | 613.0 | 18.4 |
| | 3599 | 153.3 | 657.0 | 17.3 |
| | 3609 | 154.5 | 674.0 | 17.0 |
| | 3606 | 148.3 | 713.0 | 15.4 |

Specimen Found Cracked on Post Inspection and Color Change.

## Table 62.

## Thermal Conductivity Data for Cerium Dioxide With GFE Apparatus

| SRI Run Number | Specimen Mean Temperature For $\frac{5}{8}$" Gage Length °F | Total Heat Flow Into $\frac{1}{4}$" Axial Calorimeter Gage Length Btu/hr | Specimen $\Delta T$ Across $\frac{5}{8}$" Gage Length °F | Specimen Thermal Conductivity Btu/hr/ft$^2$/°F/in. |
|---|---|---|---|---|
| Run GFE 7 | 1866 | 77.9 | 488.0 | 11.8 |
| | 1905 | 72.6 | 450.5 | 11.9 |
| | 1920 | 64.7 | 448.0 | 10.7 |
| | 1929 | 69.8 | 449.0 | 11.5 |
| | 2341 | 63.9 | 688.0 | 6.9 |
| | 2394 | 62.5 | 617.0 | 7.5 |
| | 2399 | 66.7 | 640.0 | 7.7 |
| | 2471 | 54.2 | 620.0 | 6.5 |
| | 3099 | 53.9 | 623.0 | 6.4 |
| | 3101 | 45.2 | 603.0 | 5.5 |
| | 3085 | 54.4 | 680.0 | 5.9 |
| | 3151 | 43.1 | 603.0 | 5.3 |
| Specimen Found Cracked on Post Inspection | | | | |

## Table 64.

### Thermal Conductivity Data for Zirconium Dioxide With GFE Apparatus

| SRI Run Number | Specimen Mean Temperature For $\frac{5}{8}$" Gage Length °F | Total Heat Flow Into $\frac{1}{4}$" Axial Calorimeter Gage Length Btu/hr | Specimen $\Delta T$ Across $\frac{5}{8}$" Gage Length °F | Specimen Thermal Conductivity Btu/hr/ft²/°F/in. |
|---|---|---|---|---|
| Run GFE 5 | 2412 | 77.4 | 720.0 | 8.0 |
| | 2426 | 87.7 | 713.0 | 9.1 |
| | 2406 | 83.8 | 730.0 | 8.5 |
| | 2420 | 85.2 | 741.0 | 8.5 |
| | 2982 | 110.7 | 803.0 | 10.2 |
| | 3010 | 101.5 | 790.0 | 9.5 |
| | 3026 | 108.8 | 763.0 | 10.5 |
| | 3014 | 120.4 | 783.0 | 11.4 |
| | 3302 | 113.9 | 853.0 | 9.9 |
| | 3320 | 131.9 | 857.0 | 11.4 |
| | 3306 | 150.3 | 880.0 | 12.6 |
| | 3700 | 136.4 | 1006.0 | 10.0 |
| | 3755 | 131.0 | 1000.0 | 9.7 |
| | 3813 | 122.5 | 987.0 | 9.2 |
| Specimen Found Cracked on Post Inspection With Discoloration | | | | |

## Table 65.

Thermal Conductivity Data for Columbium +0.5% Zirconium With GFE Apparatus

| SRI Run Number | Specimen Mean Temperature For $\frac{5}{8}$" Gage Length °F | Total Heat Flow Into $\frac{1}{4}$" Axial Calorimeter Gage Length Btu/hr | Specimen ΔT Across $\frac{5}{8}$" Gage Length °F | Specimen Thermal Conductivity Btu/hr/ft$^2$/°F/in. |
|---|---|---|---|---|
| Run GFE 9 | 1931 | 111.2 | 47.0 | 175.0 |
| | 1919 | 120.6 | 45.7 | 195.0 |
| | 2450 | 146.5 | 84.0 | 129.0 |
| | 2493 | 135.3 | 79.0 | 127.0 |
| | 2495 | 136.2 | 76.0 | 133.0 |
| | 2505 | 138.5 | 93.0 | 110.0 |
| | 2879 | 176.9 | 103.0 | 127.0 |
| | 2882 | 163.6 | 97.0 | 125.0 |
| | 2908 | 164.5 | 104.0 | 117.0 |
| | 3479 | 228.3 | 120.0 | 141.0 |
| | 3497 | 232.2 | 106.0 | 162.0 |
| | 3546 | 226.3 | 107.0 | 156.0 |
| Specimen Found Uncracked with Color Change on Post Inspection | | | | |

## Table 66.

### Thermal Conductivity Data for Molybdenum +0.5% Titanium With GFE Apparatus

| SRI Run Number | Specimen Mean Temperature For $\frac{5}{8}$" Gage Length °F | Total Heat Flow Into $\frac{1}{4}$" Axial Calorimeter Gage Length Btu/hr | Specimen $\Delta T$ Across $\frac{5}{8}$" Gage Length °F | Specimen Thermal Conductivity Btu/hr/ft$^2$/°F/in. |
|---|---|---|---|---|
| Run GFE 8 | 2780 | 238.5 | 83.0 | 213.0 |
| | 2827 | 238.7 | 73.0 | 242.0 |
| | 2832 | 240.7 | 80.0 | 223.0 |
| | 2847 | 243.8 | 73.0 | 247.0 |
| | 3510 | 310.6 | 100.0 | 230.0 |
| | 3580 | 316.7 | 100.0 | 234.0 |
| | 3640 | 306.1 | 100.0 | 227.0 |
| | 3656 | 312.4 | 107.0 | 216.0 |

Specimen Found Uncracked with Color Change on Post Inspection

## Table 67.

### Total Normal Emittance of Hafnium Diboride

Run No. 1

| Observed Temperature °F | Radiometer Output Millivolts | True Temperature °F | Emittance | Remarks |
|---|---|---|---|---|
| $1045^T$ | 0.029 | 1045 | .39 | |
| $1205^T$ | 0.051 | 1205 | .45 | |
| $1380^T$ | 0.110 | 1380 | .47 | |
| 1650 | 0.212 | 1810 | .54 | |
| 1850 | 0.348 | 2030 | .61 | |
| 2000 | 0.502 | 2170 | .72 | |
| 2260 | 0.820 | 2460 | .77 | |
| 2400 | 1.016 | 2590 | .80 | |
| 2270 | 0.870 | 2450 | .83 | |
| 2580 | 1.346 | 2820 | .77 | |
| 2830 | 1.891 | 3100 | .79 | |
| 2960 | 2.314 | 3220 | .83 | |
| 3250 | 3.113 | 3580 | .78 | Small Dark Spots on Surface |
| 3370 | 3.698 | 3700 | .80 | |
| 3530 | 4.359 | 3930 | .77 | Spots Disappeared |
| 3620 | 4.675 | 4060 | .73 | |
| 3820 | 5.760 | 4280 | .76 | |
| 3900 | 6.301 | 4360 | .77 | |
| 4020 | 6.712 | 4530 | .71 | Large Dark Areas on Surface |
| 4060 | 6.251 | 4390 | .75 | Dark Areas Disappeared With Evolution of Smoke |
| 4100 | 6.920 | 4480 | .77 | |

### Table 67 (Continued).

### Total Normal Emittance of Hafnium Diboride

Run No. 1 (Continued)

| Observed Temperature °F | Radiometer Output Millivolts | True Temperature °F | Emittance | Remarks |
|---|---|---|---|---|
| 4100 | 7.500 | 4600 | .77 | Dark Areas Again on Surface |
| 4050 | 7.515 | 4530 | .78 | |
| 4220 | 8.180 | 4810 | .71 | |
| Run No. 2 | | | | |
| 1490 | 0.1523 | 1630 | .50 | |
| 1555 | 0.1784 | 1720 | .50 | |
| 1690 | 0.2700 | 1840 | .67 | |
| 2530 | 1.4180 | 2750 | .83 | |
| 2760 | 1.9100 | 3000 | .83 | |

## Table 68.

## Total Normal Emittance of Thorium Tetraboride

| Observed Temperature °F | Radiometer Output Millivolts | True Temperature °F | Emittance | Remarks |
|---|---|---|---|---|
| 1475 | 0.175 | 1571 | .65 | |
| 1670 | 0.267 | 1794 | .66 | |
| 1825 | 0.402 | 1957 | .75 | |
| 2050 | 0.678 | 2192 | .87 | |
| 2185 | 0.905 | 2330 | .94 | |
| 2405 | 1.259 | 2579 | .92 | |
| 2635 | 1.748 | 2837 | .91 | |
| 2900 | 2.270 | 3172 | .80 | |
| 3060 | 2.680 | 3373 | .76 | |
| 3230 | 3.226 | 3580 | .74 | |
| 3370 | 3.814 | 3739 | .75 | |

Table 69.

Total Normal Emittance of Titanium Diboride

| Observed Temperature °F | Radiometer Output Millivolts | True Temperature °F | Emittance | Remarks |
|---|---|---|---|---|
| $1065^{T}$ | 0.032 | 1065 | .41 | |
| $1315^{T}$ | 0.117 | 1315 | .79 | |
| 1450 | 0.174 | 1530 | .77 | |
| 1660 | 0.281 | 1790 | .77 | |
| 1830 | 0.418 | 1950 | .87 | |
| 2040 | 0.590 | 2180 | .87 | |
| 2240 | 0.801 | 2450 | .76 | |
| 2350 | 0.951 | 2560 | .78 | |
| 2270 | 0.799 | 2460 | .76 | |
| 2690 | 1.238 | 3050 | .55 | |
| 2610 | 1.035 | 2990 | .50 | |
| 2940 | 1.438 | 3470 | .40 | |
| 3030 | 1.669 | 3600 | .41 | |
| 3280 | 2.220 | 3920 | .39 | |
| 3410 | 2.435 | 4180 | .35 | |
| 3520 | 2.965 | 4350 | .36 | |
| 3610 | 3.150 | 4480 | .35 | |
| 3730 | 3.555 | 4660 | .35 | |
| 3800 | 4.110 | 4730 | .37 | |
| 3740 | 3.850 | 4660 | .37 | |
| 3870 | 4.500 | 4730 | .40 | |
| 3880 | 4.620 | 4740 | .40 | |
| 3920 | 5.110 | 4730 | .46 | |
| 3880 | 5.070 | 4600 | .51 | |
| 3840 | 5.480 | 4410 | .63 | Specimen Smoking |
| 3840 | 5.430 | 4440 | .61 | |
| 4000 | 5.21 | 4900 | .42 | |

## Table 70.

### Total Normal Emittance of Tungsten Boride

| Observed Temperature °F | Radiometer Output Millivolts | True Temperature °F | Emittance | Remarks |
|---|---|---|---|---|
| 975$^T$ | 0.030 | 975 | .48 | |
| 1290$^T$ | 0.071 | 1290 | .52 | |
| 1620 | 0.166 | 1810 | .43 | |
| 1810 | 0.262 | 2030 | .47 | |
| 2200 | 0.353 | 2630 | .26 | |
| 2360 | 0.465 | 2850 | .26 | Black Crystals Formed on Surface |
| 2360 | 0.610 | 2720 | .40 | Crystals Disappeared |
| 2650 | 0.864 | 3150 | .34 | |
| 2810 | 1.048 | 3410 | .30 | |
| 2850 | 1.152 | 3440 | .33 | |
| 3050 | 1.496 | 3670 | .34 | |
| 3220 | 1.898 | 3950 | .33 | |
| 3460 | 2.516 | 4320 | .32 | |
| 3490 | 2.541 | 4370 | .31 | |
| 3640 | 3.100 | 4610 | .31 | |
| 3710 | 3.368 | 4700 | .31 | Edges Melting |
| 3860 | 4.150 | 4840 | .35 | |
| 3800 | 5.130 | 4440 | .57 | |
| 3710 | 4.955 | 4230 | .66 | Specimen Bubbling |
| 3880 | 5.732 | 4430 | .66 | |

## Table 71.

### Total Normal Emittance of Zirconium Diboride

| Observed Temperature °F | Radiometer Output Millivolts | True Temperature °F | Emittance | Remarks |
|---|---|---|---|---|
| $990^{T}$ | 0.023 | 990 | .35 | |
| $1325^{T}$ | 0.082 | 1325 | .55 | |
| 1470 | 0.127 | 1590 | .51 | |
| 1720 | 0.285 | 1850 | .72 | |
| 1530 | 0.156 | 1670 | .54 | |
| 1680 | 0.244 | 1820 | .61 | |
| 1830 | 0.401 | 1990 | .79 | |
| 2130 | 0.643 | 2290 | .83 | |
| 2230 | 0.774 | 2420 | .73 | |
| 2300 | 0.995 | 2540 | .79 | |
| 2610 | 1.359 | 2860 | .75 | |
| 2850 | 1.932 | 3140 | .76 | |
| 3060 | 2.425 | 3370 | .75 | |
| 3030 | 2.333 | 3360 | .73 | |
| 3280 | 2.956 | 3580 | .67 | Dark area on Surface |
| 3360 | 3.827 | 3850 | .72 | Specimen Smoking |
| 3600 | 4.475 | 4050 | .71 | |
| 3740 | 5.145 | 4240 | .68 | |
| 3840 | 5.420 | 4400 | .65 | Large Dark Spot on Surface |
| 3940 | 6.040 | 4540 | .63 | |
| 3990 | 6.340 | 4590 | .63 | |
| 4060 | 6.730 | 4670 | .64 | |
| 4120 | 6.070 | 5000 | .46 | Specimen Smoking |

## Table 72.

### Total Normal Emittance of Columbium Carbide

Run No. 1

| Observed Temperature °F | Radiometer Output Millivolts | True Temperature °F | Emittance | Remarks |
|---|---|---|---|---|
| 1115$^{T}$ | 0.034 | 1115 | .38 | |
| 1270$^{T}$ | 0.098 | 1270 | .75 | |
| 1450 | 0.166 | 1540 | .72 | |
| 1610 | 0.277 | 1710 | .87 | |
| 1880 | 0.463 | 2000 | .89 | |
| 2100 | 0.707 | 2350 | .78 | |
| 2210 | 0.782 | 2440 | .75 | |
| 2050 | 0.628 | 2220 | .84 | |
| 2350 | 0.959 | 2580 | .77 | |
| 2490 | 0.957 | 2850 | .54 | |
| 2730 | 1.377 | 3130 | .55 | |
| 2860 | 1.678 | 3290 | .57 | |
| 3020 | 1.372 | 3860 | .26 | |
| 3110 | 1.577 | 3980 | .27 | Specimen Cracked |
| 3210 | 1.814 | 4080 | .28 | |
| 3290 | 2.005 | 4150 | .28 | |
| 3420 | 2.317 | 4380 | .28 | |
| 3470 | 2.498 | 4440 | .28 | |
| 3490 | 2.595 | 4470 | .28 | |
| 3550 | 2.740 | 4550 | .28 | |
| 3630 | 2.940 | 4700 | .27 | |

Table 72 (Continued).

Total Normal Emittance of Columbium Carbide

Run No. 2

| Observed Temperature °F | Radiometer Output Millivolts | True Temperature °F | Emittance | Remarks |
|---|---|---|---|---|
| 1010 $^{T}$ | 0.0231 | 1010 | .33 | |
| 1380 $^{T}$ | 0.0883 | 1380 | .54 | |
| 1430 | 0.1026 | 1590 | .41 | |
| 1405 | 0.1079 | 1550 | .47 | |
| 1410 | 0.1105 | 1550 | .47 | |
| 1528 | 0.1750 | 1650 | .63 | |
| 1740 | 0.3260 | 1870 | .78 | |
| 1935 | 0.4810 | 2060 | .83 | |
| 2163 | 0.7240 | 2320 | .82 | |
| 2100 | 0.6670 | 2250 | .85 | |
| 2405 | 0.8160 | 2700 | .55 | |
| 2475 | 0.9390 | 2770 | .57 | |
| 2570 | 1.1990 | 2860 | .65 | |
| 2640 | 1.2880 | 2970 | .63 | |
| 2970 | 1.9000 | 3380 | .58 | |
| 3120 | 1.4330 | 3900 | .27 | |
| 3230 | 1.4510 | 4100 | .23 | |
| 3340 | 1.6330 | 4300 | .26 | |
| 3490 | 2.0990 | 4500 | .25 | |
| 3670 | 2.5590 | 4800 | .23 | |
| 3640 | 2.5090 | 4820 | .22 | Edges Bubbling |

Table 73.

Total Normal Emittance of Dimolybdenum Carbide

Run No. 1

| Observed Temperature °F | Radiometer Output Millivolts | True Temperature °F | Emittance | Remarks |
|---|---|---|---|---|
| 825$^{T}$ | 0.027 | 825 | .67 | |
| 1270$^{T}$ | 0.083 | 1270 | .64 | |
| 1440 | 0.153 | 1550 | .65 | |
| 1720 | 0.328 | 1860 | .80 | |
| 2010 | 0.527 | 2220 | .72 | |
| 2120 | 0.520 | 2390 | .65 | |
| 2290 | 0.625 | 2630 | .45 | |
| 1740 | 0.294 | 1910 | .68 | |
| 2100 | 0.528 | 2350 | .59 | |
| 2250 | 0.632 | 2570 | .50 | |
| 2580 | 0.993 | 3000 | .47 | |
| 2750 | 1.131 | 3240 | .40 | |
| 2860 | 1.117 | 3530 | .29 | |
| 3050 | 1.326 | 3900 | .24 | Large Surface Blister in Center of Specimen |
| 2900 | 1.029 | 3700 | .23 | |
| 3120 | 1.353 | 4040 | .22 | |
| 3120 | 1.439 | 4000 | .24 | |
| 3020 | 0.948 | 4220 | .13 | |
| 3030 | 1.051 | 4150 | .15 | |
| 3120 | 1.642 | 3930 | .29 | Blister Collapsed |
| 3330 | 2.058 | 4330 | .25 | |

Table 73 (Continued).

Total Normal Emittance of Dimolybdenum Carbide

Run No. 2

| Observed Temperature °F | Radiometer Output Millivolts | True Temperature °F | Emittance | Remarks |
|---|---|---|---|---|
| 1720 | 0. 246 | 1890 | . 52 | Dark Area in Center of Specimen |
| 1470 | 0. 144 | 1570 | . 60 | |
| 1720 | 0. 258 | 1880 | . 57 | |
| 2110 | 0. 509 | 2360 | . 55 | |
| 2390 | 0. 658 | 2720 | . 42 | |
| 2400 | 0. 571 | 2820 | . 33 | |
| 2710 | 0. 798 | 3370 | . 25 | |
| 2900 | 0. 854 | 3730 | . 18 | |
| 2990 | 1. 146 | 3810 | . 22 | Large Surface Blister |
| 3060 | 1. 198 | 3930 | . 21 | |

## Table 74.

## Total Normal Emittance of Hafnium Carbide

Run No. 1

| Observed Temperature °F | Radiometer Output Millivolts | True Temperature °F | Emittance | Remarks |
|---|---|---|---|---|
| 1530 | 0.238 | 1620 | .88 | |
| 1750 | 0.354 | 1880 | .82 | |
| 1940 | 0.507 | 2070 | .83 | |
| 2110 | 0.690 | 2260 | .86 | |
| 2350 | 1.017 | 2540 | .84 | |
| 2550 | 1.352 | 2750 | .85 | |
| 2270 | 0.857 | 2430 | .82 | |
| 2550 | 1.277 | 2770 | .79 | |
| 2760 | 1.672 | 3050 | .75 | |
| 2970 | 2.144 | 3280 | .74 | |
| 3450 | 3.450 | 3970 | .59 | |
| 3570 | 4.040 | 4080 | .62 | |
| 3690 | 4.685 | 4240 | .62 | |
| 3780 | 5.226 | 4340 | .64 | |
| 3930 | 5.635 | 4560 | .59 | |
| 3970 | 5.960 | 4600 | .60 | |
| 4000 | 6.287 | 4610 | .62 | |
| 4050 | 6.514 | 4670 | .62 | |
| 4020 | 6.621 | 4630 | .64 | |

## Table 74 (Continued).

## Total Normal Emittance of Hafnium Carbide

Run No. 2

| Observed Temperature °F | Radiometer Output Millivolts | True Temperature °F | Emittance | Remarks |
|---|---|---|---|---|
| 1485 | 0.235 | 1550 | .98 | |
| 1640 | 0.320 | 1720 | .96 | |
| 1900 | 0.531 | 2000 | .98 | |
| 2095 | 0.764 | 2220 | .98 | |
| 2320 | 1.075 | 2470 | .98 | |
| 2490 | 1.303 | 2660 | .95 | |
| 2610 | 1.545 | 2810 | .93 | |
| 2960 | 2.112 | 3200 | .77 | |
| 3080 | 2.410 | 3430 | .70 | |
| 3200 | 2.789 | 3570 | .72 | |
| 3320 | 3.394 | 3660 | .79 | |
| 3520 | 4.417 | 3870 | .83 | |
| 3750 | 5.247 | 4160 | .80 | |
| 3820 | 5.060 | 4350 | .64 | |
| 3980 | 6.962 | 4470 | .77 | |
| | | Run No. 3 | | |
| 1482 | 0.251 | 1546 | .98 | |
| 1690 | 0.377 | 1778 | .96 | |
| 1875 | 0.550 | 1976 | .98 | |
| 1940 | 0.613 | 2050 | .98 | |
| 2015 | 0.687 | 2139 | .96 | |
| 2190 | 0.940 | 2325 | .98 | |
| 2305 | 1.115 | 2459 | .96 | |
| 2500 | 1.443 | 2686 | .91 | |
| 2830 | 2.308 | 3048 | .94 | |
| 2970 | 2.564 | 3237 | .84 | |
| 3210 | 3.101 | 3567 | .72 | |
| 3390 | 3.890 | 3764 | .74 | |
| 3560 | 5.028 | 3909 | .84 | |
| 3780 | 6.700 | 4107 | .93 | |
| 3890 | 7.573 | 4215 | .96 | |

## Table 75.

## Total Normal Emittance of Tantalum Carbide

Run No. 1

| Observed Temperature °F | Radiometer Output Millivolts | True Temperature °F | Emittance | Remarks |
|---|---|---|---|---|
| 920$^{T}$ | 0.019 | 920 | .37 | |
| 1140$^{T}$ | 0.039 | 1140 | .41 | |
| 1300$^{T}$ | 0.092 | 1300 | .66 | |
| 1450 | 0.143 | 1550 | .61 | |
| 1570 | 0.251 | 1620 | .91 | |
| 1880 | 0.463 | 1990 | .92 | |
| 2040 | 0.608 | 2190 | .87 | |
| 2240 | 0.861 | 2440 | .82 | Small Dark Spots on Surface |
| 2230 | 0.804 | 2460 | .74 | |
| 2390 | 1.042 | 2620 | .77 | |
| 2660 | 1.534 | 2940 | .76 | |
| 2730 | 1.670 | 3050 | .74 | Size of Spots Increasing |
| 2840 | 1.626 | 3240 | .58 | Spots Moving About |
| 3010 | 1.964 | 3160 | .76 | Spots Disappeared |
| 3180 | 3.055 | 3500 | .82 | |
| 3330 | 3.536 | 3740 | .74 | |
| 3490 | 4.016 | 3960 | .71 | |
| 3470 | 3.400 | 3730 | .70 | |
| 3570 | 4.100 | 4180 | .58 | |

Table 75 (Continued).

Total Normal Emittance of Tantalum Carbide

Run No. 2

| Observed Temperature °F | Radiometer Output Millivolts | True Temperature °F | Emittance | Remarks |
|---|---|---|---|---|
| 1470 | 0.1580 | 1580 | .65 | |
| 1770 | 0.2941 | 1950 | .64 | |
| 1990 | 0.4650 | 2170 | .67 | |
| 2150 | 0.6270 | 2380 | .67 | |
| 2450 | 1.048 | 2730 | .68 | |
| 2690 | 1.545 | 2990 | .75 | Uneven Temperature on Surface |
| 3150 | 2.699 | 3550 | .71 | Surface Temperature Fairly Uniform |
| 3330 | 3.355 | 3790 | .69 | |
| 3550 | 4.002 | 4140 | .58 | |
| 3570 | 4.117 | 4150 | .60 | |
| 3670 | 4.391 | 4320 | .55 | Slight Temperature Gradient on Surface |
| 3750 | 3.261 | 4980 | .25 | |
| 3770 | 3.607 | 4950 | .27 | |
| 3830 | 4.105 | 4920 | .32 | |
| 3860 | 4.900 | 4730 | .44 | Edges of Specimen Melted |

## Table 76.

### Total Normal Emittance of Titanium Carbide

Run No. 1

| Observed Temperature °F | Radiometer Output Millivolts | True Temperature °F | Emittance | Remarks |
|---|---|---|---|---|
| $1220^{T}$ | 0.0808 | 1220 | .68 | |
| $980^{T}$ | 0.0369 | 980 | .58 | |
| $1315^{T}$ | 0.1113 | 1315 | .76 | |
| 1510 | 0.1864 | 1630 | .68 | |
| 1810 | 0.4110 | 1940 | .86 | |
| 2020 | 0.6150 | 2170 | .89 | |
| 2360 | 0.9860 | 2580 | .80 | |
| 2350 | 1.0010 | 2550 | .82 | |
| 2570 | 1.2440 | 2870 | .69 | Several Dark Spots on Surface |
| 2870 | 1.5480 | 3320 | .50 | Blisters on Surface |
| 2910 | 2.1500 | 3250 | .75 | |
| 3550 | 3.2540 | 4310 | .42 | |
| 3600 | 3.410 | 4440 | .39 | |
| 3710 | 3.847 | 4560 | .40 | |
| 3740 | 3.778 | 4650 | .38 | |

Table 76 (Continued).

Total Normal Emittance of Titanium Carbide

Run No. 2

| Observed Temperature °F | Radiometer Output Millivolts | True Temperature °F | Emittance | Remarks |
|---|---|---|---|---|
| 1005$^T$ | 0.0336 | 1005 | .51 | |
| 1240$^T$ | 0.0684 | 1240 | .57 | |
| 1490 | 0.1909 | 1590 | .79 | |
| 1810 | 0.4110 | 1940 | .86 | |
| 2390 | 1.0280 | 2550 | .85 | Black Scale on Surface |
| 2380 | 1.0080 | 2560 | .83 | |
| 2620 | 1.2800 | 2900 | .69 | Dark Spots (Scale) Disappeared |
| 2880 | 1.8800 | 3170 | .74 | |
| 3070 | 1.9780 | 3520 | .54 | Dark Spots Formed and Disappeared |
| 3350 | 2.7160 | 3860 | .52 | |
| 3430 | 2.9830 | 4040 | .48 | Specimen Surface Melted |

## Table 77.

### Total Normal Emittance of Tungsten Carbide

Run No. 1

| Observed Temperature °F | Radiometer Output Millivolts | True Temperature °F | Emittance | Remarks |
|---|---|---|---|---|
| 965T | 0.0246 | 965 | .41 | |
| 1010T | 0.0352 | 1010 | .50 | |
| 1460 | 0.1877 | 1530 | .81 | |
| 1940 | 0.4400 | 2120 | .67 | |
| 2200 | 0.5460 | 2470 | .51 | |
| 2380 | 0.7010 | 2740 | .44 | |
| 1870 | 0.4330 | 2040 | .76 | |
| 2240 | 0.7950 | 2460 | .73 | |
| 2540 | 0.8910 | 2970 | .43 | |
| 2700 | 0.8640 | 3290 | .30 | |
| 3010 | 1.2160 | 3880 | .23 | |
| 3170 | 1.7720 | 3940 | .31 | |
| 3450 | 2.4930 | 4350 | .31 | |
| 3560 | 2.9360 | 4480 | .33 | |
| 3640 | 3.1960 | 4600 | .33 | |
| 3710 | 3.4800 | 4690 | .35 | |
| 3800 | 3.7900 | 4780 | .34 | |
| 3700 | 3.4420 | 4660 | .34 | Melted Around Edges |

Table 77 (Continued).

Total Normal Emittance of Tungsten Carbide

Run No. 2

| Observed Temperature °F | Radiometer Output Millivolts | True Temperature °F | Emittance | Remarks |
|---|---|---|---|---|
| 1050$^T$ | 0.0534 | 1050 | .71 | |
| 1270$^T$ | 0.0938 | 1270 | .74 | |
| 1840 | 0.3713 | 1990 | .75 | |
| 1600 | 0.2300 | 1730 | .70 | |
| 2110 | 0.6340 | 2280 | .78 | |
| 2970 | 1.5160 | 3460 | .43 | |
| 2710 | 1.0000 | 3140 | .41 | |
| 2480 | 0.7000 | 2860 | .40 | |
| 2990 | 1.4270 | 3560 | .38 | |
| 3170 | 1.9310 | 3790 | .40 | |
| 3500 | 3.1270 | 4160 | .45 | |
| 3760 | 4.5450 | 4470 | .51 | |
| 3840 | 4.6600 | 4570 | .49 | |

## Table 78.

## Total Normal Emittance of Vanadium Carbide

Run No. 1

| Observed Temperature °F | Radiometer Output Millivolts | True Temperature °F | Emittance | Remarks |
|---|---|---|---|---|
| 1100 | 0.059 | 1100 | .68 | |
| 1335 | 0.114 | 1335 | .76 | |
| 1460 | 0.138 | 1590 | .56 | |
| 1500 | 0.151 | 1650 | .53 | |
| 1620 | 0.201 | 1780 | .56 | |
| 1860 | 0.370 | 2050 | .65 | |
| 2240 | 0.710 | 2490 | .65 | |
| 2380 | 0.900 | 2660 | .64 | |
| 1990 | 0.470 | 2180 | .67 | |
| 2400 | 0.949 | 2670 | .67 | |
| 2710 | 1.373 | 3320 | .44 | Blisters on Surface |
| 2300 | 0.888 | 2540 | .73 | |
| 2610 | 1.347 | 2930 | .67 | |
| 2730 | 1.597 | 3060 | .69 | Crust on Surface |
| 2860 | 1.534 | 3340 | .48 | |
| 2910 | 1.690 | 3409 | .50 | |
| 3030 | 1.995 | 3540 | .51 | |
| 3240 | 2.370 | 3950 | .41 | |
| 3580 | 2.770 | 4620 | .28 | Specimen Melted |

Table 78 (Continued).

Total Normal Emittance of Vanadium Carbide

Run No. 2

| Observed Temperature °F | Radiometer Output Millivolts | True Temperature °F | Emittance | Remarks |
|---|---|---|---|---|
| 1500 | 0.181 | 1590 | .74 | |
| 1810 | 0.343 | 1950 | .73 | |
| 2000 | 0.493 | 2170 | .72 | |
| 2275 | 0.735 | 2500 | .67 | |
| 2130 | 0.539 | 2320 | .64 | |
| 2200 | 0.597 | 2410 | .63 | |
| 2680 | 1.341 | 2960 | .67 | Blisters on Surface |
| 2710 | 0.788 | 3240 | .29 | Blisters Disappeared |
| 2990 | 1.220 | 3750 | .26 | |
| 3140 | 1.297 | 3980 | .23 | |
| 3240 | 1.546 | 4150 | .23 | |
| 3280 | 1.699 | 4170 | .27 | Specimen Bubbling at Edges |

## Table 79.

### Total Normal Emittance of Zirconium Carbide

Run No. 1

| Observed Temperature °F | Radiometer Output Millivolts | True Temperature °F | Emittance | Remarks |
|---|---|---|---|---|
| 1590 | 0.244 | 1680 | .79 | |
| 1850 | 0.412 | 2000 | .78 | |
| 2080 | 0.632 | 2220 | .83 | |
| 2090 | 0.619 | 2230 | .82 | |
| 2190 | 0.762 | 2330 | .85 | |
| 2320 | 0.910 | 2510 | .77 | |
| 2530 | 1.227 | 2770 | .76 | |
| 2770 | 1.595 | 3090 | .69 | |
| 2880 | 1.970 | 3170 | .77 | |
| 3070 | 2.592 | 3360 | .80 | |
| 3220 | 3.169 | 3550 | .80 | |
| 3420 | 3.839 | 3790 | .80 | |
| 3600 | 4.385 | 4060 | .70 | |
| 3680 | 4.900 | 4150 | .70 | |
| 3630 | 4.840 | 4070 | .75 | Black Spots on Surface |
| 3800 | 4.700 | 4470 | .53 | Specimen Smoking |
| 3850 | 5.310 | 4450 | .60 | |
| 3880 | 5.330 | 4500 | .59 | |
| 3930 | 5.490 | 4620 | .54 | |
| 3930 | 4.940 | 4700 | .48 | |
| 3940 | 4.820 | 3800 | .43 | |
| 4020 | 5.400 | 4900 | .38 | Edges of Specimen Melted |

Table 79 (Continued).

Total Normal Emittance of Zirconium Carbide

Run No. 2

| Observed Temperature °F | Radiometer Output Millivolts | True Temperature °F | Emittance | Remarks |
|---|---|---|---|---|
| 1760 | 0.336 | 1890 | .78 | |
| 1860 | 0.409 | 2010 | .76 | |
| 2010 | 0.534 | 2170 | .78 | |
| 2190 | 0.730 | 2340 | .81 | |
| 2410 | 1.063 | 2620 | .79 | |
| 2690 | 1.567 | 2930 | .78 | |
| 2900 | 2.009 | 3180 | .77 | |
| 3130 | 2.654 | 3440 | .76 | |
| 3280 | 3.216 | 3600 | .80 | |
| 3420 | 3.787 | 3800 | .76 | |
| 3310 | 3.626 | 3680 | .77 | |
| 3220 | 3.431 | 3700 | .78 | |
| 3470 | 4.074 | 3750 | .77 | |

## Table 80.

### Total Normal Emittance of Boron Nitride

| Observed Temperature °F | Radiometer Output Millivolts | True Temperature °F | Emittance | Remarks |
|---|---|---|---|---|
| 895$^T$ | 0.046 | 895 | .93 | |
| 1250$^T$ | 0.112 | 1250 | .90 | |
| 1420 | 0.168 | 1510 | .76 | |
| 1650 | 0.271 | 1760 | .77 | |
| 1850 | 0.381 | 2000 | .72 | |
| 2020 | 0.510 | 2200 | .70 | |
| 2230 | 0.743 | 2410 | .72 | |
| 2500 | 1.106 | 2760 | .69 | Small Bright Spots on Surface |
| 2630 | 1.316 | 2880 | .73 | |
| 2930 | 1.832 | 3280 | .63 | |
| 3020 | 2.031 | 3420 | .58 | |
| 3040 | 1.947 | 3470 | .55 | Specimen Smoking |
| 3280 | 2.458 | 3830 | .47 | |
| 3400 | 2.704 | 4070 | .42 | Dark Spots on Surface |
| 3380 | 2.754 | 4040 | .43 | Specimen Smoking Violently |

## Table 81.

### Total Normal Emittance of Hafnium Nitride

Run No. 1

| Observed Temperature °F | Radiometer Output Millivolts | True Temperature °F | Emittance | Remarks |
|---|---|---|---|---|
| $995^{T}$ | 0.025 | 995 | .37 | |
| $1250^{T}$ | 0.067 | 1250 | .54 | |
| 1440 | 0.146 | 1550 | .62 | |
| 1630 | 0.253 | 1740 | .74 | |
| 1860 | 0.367 | 2030 | .66 | |
| 2000 | 0.489 | 2160 | .73 | |
| 2190 | 0.672 | 2370 | .70 | |
| 2370 | 0.975 | 2580 | .72 | |
| 2540 | 1.155 | 2820 | .66 | |
| 2420 | 0.952 | 2660 | .68 | |
| 2730 | 1.558 | 3020 | .69 | |
| Run No. 2 | | | | |
| $1015^{T}$ | 0.042 | 1015 | .60 | |
| $1205^{T}$ | 0.073 | 1205 | .64 | |
| 1325 | 0.134 | 1325 | .89 | |
| 1510 | 0.207 | 1620 | .77 | |
| 1690 | 0.311 | 1790 | .84 | |
| 1900 | 0.438 | 2050 | .77 | |
| 2050 | 0.595 | 2200 | .81 | |
| 2290 | 0.865 | 2480 | .79 | |
| 2500 | 1.173 | 2740 | .74 | |
| 2380 | 0.920 | 2630 | .68 | |
| 2780 | 1.661 | 3060 | .72 | |
| 3090 | 2.392 | 3450 | .68 | |
| 3300 | 2.523 | 3870 | .48 | |
| 3430 | 3.163 | 3980 | .55 | |

Table 81 (Continued).

Total Normal Emittance of Hafnium Nitride

Run No. 2 (Continued)

| Observed Temperature °F | Radiometer Output Millivolts | True Temperature °F | Emittance | Remarks |
|---|---|---|---|---|
| 3740 | 4.532 | 4240 | .60 | |
| 3850 | 5.196 | 4480 | .57 | |
| 3900 | 5.648 | 4480 | .62 | |
| 3900 | 5.543 | 4490 | .61 | |
| 3980 | 6.078 | 4570 | .63 | |
| 3920 | 5.869 | 4480 | .64 | Specimen Cracked, Edges Melted |

## Table 82.

### Total Normal Emittance of Tantalum Nitride

| Observed Temperature °F | Radiometer Output Millivolts | True Temperature °F | Emittance | Remarks |
|---|---|---|---|---|
| 1035$^T$ | 0.052 | 1035 | .72 | |
| 1335$^T$ | 0.121 | 1335 | .80 | |
| 1550 | 0.218 | 1650 | .75 | |
| 1670 | 0.287 | 1790 | .78 | |
| 1850 | 0.421 | 1990 | .81 | |
| 1990 | 0.551 | 2130 | .83 | |
| 2180 | 0.762 | 2340 | .84 | |
| 2350 | 0.982 | 2550 | .81 | |
| 2410 | 1.119 | 2610 | .82 | |
| 2640 | 1.510 | 2870 | .83 | |
| 2850 | 1.990 | 3130 | .79 | |
| 3100 | 2.345 | 3460 | .66 | |
| 3260 | 2.857 | 3670 | .65 | |
| 3400 | 3.372 | 3850 | .64 | |
| 3590 | 4.025 | 4070 | .64 | |
| 3700 | 4.463 | 4300 | .58 | |
| 3750 | 4.725 | 4350 | .58 | |
| 3610 | 4.207 | 4200 | .58 | |

### Table 83.

### Total Normal Emittance of Titanium Nitride

Run No. 1

| Observed Temperature °F | Radiometer Output Millivolts | True Temperature °F | Emittance | Remarks |
|---|---|---|---|---|
| 1055$^{T}$ | 0.030 | 1055 | .39 | |
| 1300$^{T}$ | 0.068 | 1300 | .48 | |
| 1550 | 0.182 | 1680 | .62 | |
| 1760 | 0.315 | 1900 | .70 | |
| 1970 | 0.510 | 2130 | .75 | |
| 2120 | 0.556 | 2320 | .63 | |
| 2300 | 0.700 | 2570 | .57 | |
| 2460 | 0.889 | 2770 | .55 | |
| 2280 | 0.757 | 2510 | .64 | |
| 2650 | 1.161 | 3020 | .52 | |
| 2830 | 1.492 | 3240 | .52 | |
| 3150 | 1.804 | 3830 | .34 | |
| 3350 | 2.286 | 4140 | .33 | |
| 3580 | 3.032 | 4460 | .34 | |
| 3660 | 3.130 | 4630 | .31 | |
| 3720 | 3.354 | 4690 | .32 | |
| 3820 | 3.761 | 4840 | .31 | |
| 3880 | 3.992 | 4930 | .32 | |
| 3900 | 4.195 | 4860 | .35 | |
| 3930 | 4.480 | 4780 | .40 | Specimen Smoking |
| 3930 | 4.321 | 4930 | .35 | Edges Melted |

Table 83 (Continued).

Total Normal Emittance of Titanium Nitride

Run No. 2

| Observed Temperature °F | Radiometer Output Millivolts | True Temperature °F | Emittance | Remarks |
|---|---|---|---|---|
| 1000$^T$ | 0.033 | 1000 | .50 | |
| 1300$^T$ | 0.087 | 1300 | .62 | |
| 1480 | 0.145 | 1610 | .57 | |
| 1750 | 0.313 | 1880 | .72 | |
| 1870 | 0.439 | 2010 | .80 | |
| 2060 | 0.619 | 2200 | .84 | |

## Table 84.

## Total Normal Emittance of Beryllium Oxide

| Observed Temperature °F | Radiometer Output Millivolts | True Temperature °F | Emittance | Remarks |
|---|---|---|---|---|
| 1532 | | 1648 | .58 | |
| 1700 | | 1846 | .56 | |
| 1840 | | 2008 | .57 | |
| 2094 | | 2302 | .60 | |
| 2275 | | 2514 | .60 | |
| 2550 | | 2857 | .56 | |
| 2740 | | 3091 | .55 | |
| 2915 | | 3295 | .57 | |
| 3100 | | 3556 | .52 | Specimen Smoking |
| 3114 | | 3423 | .79 | |
| 3180 | | 3461 | .88 | |
| 3230 | | 3518 | .88 | |

Table 85.

Total Normal Emittance of Cerium Dioxide

Run No. 1

| Observed Temperature °F | Radiometer Output Millivolts | True Temperature °F | Emittance | Remarks |
|---|---|---|---|---|
| 1420 | 0. 1376 | 1560 | . 57 | |
| 1610 | 0. 2582 | 1730 | . 78 | Specimen Cracked |
| 1795 | 0. 4020 | 1900 | . 91 | |
| 2010 | 0. 5920 | 2140 | . 90 | |
| 2190 | 0. 7930 | 2350 | . 88 | |
| 2280 | 0. 9500 | 2420 | . 92 | |
| | | Run No. 2 | | |
| 1425 | 0. 101 | 1570 | . 42 | |
| 1645 | 0. 255 | 1760 | . 74 | |
| 1775 | 0. 400 | 1880 | . 93 | |
| 1960 | 0. 566 | 2070 | . 94 | |
| 2125 | 0. 757 | 2250 | . 96 | |
| 2360 | 1. 104 | 2510 | . 96 | |
| 2210 | 0. 844 | 2240 | . 94 | Specimen Cracked |
| 2125 | 0. 708 | 2230 | . 93 | |
| 2320 | 0. 975 | 2510 | . 84 | |
| 2495 | 1. 294 | 2700 | . 90 | |
| 2640 | 1. 700 | 2820 | . 96 | |
| 2800 | 2. 105 | 3020 | . 96 | |

Table 85 (Continued).

Total Normal Emittance of Cerium Dioxide

Run No. 3

| Observed Temperature °F | Radiometer Output Millivolts | True Temperature °F | Emittance | Remarks |
|---|---|---|---|---|
| 1415 | 0.0998 | 1570 | .42 | |
| 1410 | 0.1244 | 1560 | .47 | |
| 1465 | 0.1829 | 1560 | .78 | |
| 1670 | 0.2913 | 1710 | .85 | |
| 1765 | 0.3570 | 1860 | .87 | |
| 1765 | 0.3680 | 1860 | .88 | Specimen Cracked |
| 1880 | 0.4680 | 2000 | .87 | |
| 2250 | 0.9590 | 2420 | .92 | |
| 2420 | 1.1440 | 2600 | .87 | |
| 2650 | 1.6800 | 2840 | .96 | |
| 2740 | 1.8430 | 2960 | .90 | |
| 2900 | 2.3220 | 3130 | .92 | |
| 3000 | 2.5530 | 3230 | .94 | |
| 3150 | 3.0290 | 3400 | .92 | |
| 3180 | 3.2240 | 3440 | .92 | |
| 3330 | 3.6330 | 3600 | .91 | Specimen Melting |
| Run No. 4 | | | | |
| 1465 | 0.149 | 1580 | .57 | |
| 1645 | 0.276 | 1760 | .73 | |
| 1750 | 0.373 | 1850 | .82 | |
| 1925 | 0.517 | 2050 | .82 | |
| 2100 | 0.738 | 2240 | .87 | Specimen Cracked |

Table 85 (Continued).

Total Normal Emittance of Cerium Dioxide

Run No. 5

| Observed Temperature °F | Radiometer Output Millivolts | True Temperature °F | Emittance | Remarks |
|---|---|---|---|---|
| 1472 | 0.127 | 1599 | .45 | |
| 1660 | 0.268 | 1782 | .66 | |
| 1755 | 0.375 | 1868 | .82 | |
| 1940 | 0.583 | 2061 | .92 | |
| 2090 | 0.767 | 2226 | .93 | |
| 2250 | 1.002 | 2403 | .94 | |
| 2465 | 1.402 | 2640 | .94 | |
| 2790 | 2.245 | 2994 | .97 | |
| 3125 | 3.300 | 3380 | .93 | |

## Table 86.

## Total Normal Emittance of Hafnium Dioxide

Run No. 1

| Observed Temperature °F | Radiometer Output Millivolts | True Temperature °F | Emittance | Remarks |
|---|---|---|---|---|
| 1490 | 0.2115 | 1560 | .90 | |
| 1595 | 0.2530 | 1700 | .82 | |
| 1835 | 0.3970 | 1940 | .76 | |
| 1925 | 0.4740 | 2060 | .80 | |
| 2070 | 0.6100 | 2220 | .81 | |
| 2165 | 0.7560 | 2340 | .85 | |
| 2425 | 1.0430 | 2630 | .77 | |
| 2600 | 1.4160 | 2840 | .81 | |
| 2110 | 0.6550 | 2260 | .85 | |
| 1645 | 0.2820 | 1750 | .83 | |
| 2430 | 0.9760 | 2650 | .73 | |
| 2740 | 1.6740 | 2990 | .82 | |
| 2940 | 2.0720 | 3200 | .77 | |
| 2990 | 2.3030 | 3250 | .81 | |
| 3030 | 2.5140 | 3310 | .84 | |
| 3180 | 3.1150 | 3460 | .89 | |
| 3320 | 3.7320 | 3600 | .90 | |
| 3490 | 4.4620 | 3800 | .89 | |
| 3580 | 4.7500 | 3900 | .87 | |
| Run No. 2 | | | | |
| 1505 | 0.201 | 1590 | .78 | |
| 1820 | 0.404 | 1943 | .80 | |
| 2015 | 0.621 | 2153 | .87 | |
| 2194 | 0.843 | 2356 | .86 | |
| 2445 | 1.252 | 2639 | .85 | |
| 2635 | 1.629 | 2859 | .83 | |

## Table 87.

## Total Normal Emittance of Magnesium Oxide

Run No. 1

| Observed Temperature °F | Radiometer Output Millivolts | True Temperature °F | Emittance | Remarks |
|---|---|---|---|---|
| 1482 | 0.097 | 1642 | .32 | |
| 1645 | 0.123 | 1860 | .27 | |
| 1925 | 0.209 | 2229 | .25 | |
| 2140 | 0.330 | 2500 | .27 | |
| 2325 | 0.468 | 2738 | .28 | |
| 2595 | 0.790 | 3065 | .31 | |
| 2800 | 1.272 | 3256 | .41 | |
| 2990 | 1.814 | 3448 | .48 | |
| Run No. 2 | | | | |
| 1525 | 0.105 | 1697 | .31 | |
| 1980 | 0.217 | 2316 | .23 | |
| 2475 | 0.618 | 2928 | .29 | |
| 2870 | 1.387 | 3351 | .40 | |
| 3310 | 1.105 | 3759 | .60 | |

## Table 88.

### Total Normal Emittance of Thorium Dioxide

| Observed Temperature °F | Radiometer Output Millivolts | True Temperature °F | Emittance | Remarks |
|---|---|---|---|---|
| 1540 | | 1723 | .29 | |
| 1645 | | 1851 | .29 | |
| 1828 | | 2083 | .29 | |
| 2007 | | 2318 | .28 | |
| 2220 | | 2610 | .26 | |
| 2350 | | 2786 | .26 | |
| 2560 | | 3055 | .28 | |
| 2645 | | 3128 | .32 | |
| 2725 | | 3096 | .51 | |
| 2850 | | 3221 | .56 | |
| 2875 | | 3257 | .55 | |
| 3019 | | 3371 | .66 | |
| 3150 | | 3544 | .63 | |
| 3200 | | 3619 | .61 | |

Table 89.

Total Normal Emittance of Zirconium Dioxide

Run No. 1

| Observed Temperature °F | Radiometer Output Millivolts | True Temperature °F | Emittance | Remarks |
|---|---|---|---|---|
| 1475 | 0.113 | 1615 | .39 | This run made, as usual, in an argon environment |
| 1690 | 0.173 | 1882 | .37 | |
| 1945 | 0.301 | 2189 | .39 | |
| 2170 | 0.493 | 2449 | .43 | |
| 2340 | 0.722 | 2632 | .49 | |
| 2565 | 1.516 | 2773 | .86 | |
| 2645 | 1.789 | 2845 | .93 | |
| 2805 | 2.225 | 3022 | .93 | |
| 2910 | 2.647 | 3122 | .98 | |
| 3000 | 2.841 | 3240 | .93 | |
| 3080 | 3.080 | 3337 | .91 | |
| Run No. 2 | | | | |
| 2805 | 2.181 | 3029 | .90 | This run made, as usual, in an argon environment |
| 3570 | 5.400 | 3876 | .93 | |

Table 89 (Continued).

Total Normal Emittance of Zirconium Dioxide

Run No. 3

| Observed Temperature °F | Radiometer Output Millivolts | True Temperature °F | Emittance | Remarks |
|---|---|---|---|---|
| 1870 | 0.208 | 2138 | .29 | This run made with air jets directed at specimen surface |
| 2135 | 0.360 | 2466 | .31 | |
| 2345 | 1.033 | 2540 | .80 | Air Jets Cut Off To Obtain This Point |
| 2640 | 1.035 | 3040 | .42 | Air Jets On |
| 2750 | 1.335 | 3138 | .49 | |

Table 90.

Total Normal Emittance of Columbium + 0.5% Zirconium

| Observed Temperature °F | Radiometer Output Millivolts | True Temperature °F | Emittance | Remarks |
|---|---|---|---|---|
| $1020^{T}$ | 0.025 | 1020 | .36 | |
| $1280^{T}$ | 0.076 | 1280 | .58 | |
| 1420 | 0.136 | 1540 | .59 | |
| 1590 | 0.183 | 1740 | .53 | |
| 1850 | 0.295 | 1950 | .51 | |
| 1980 | 0.366 | 2220 | .48 | |
| 2170 | 0.505 | 2450 | .48 | |
| 2340 | 0.657 | 2660 | .47 | |
| 2370 | 0.714 | 2670 | .50 | |
| 2150 | 0.479 | 2420 | .47 | |
| 2640 | 1.041 | 3030 | .47 | |
| 2850 | 1.086 | 3450 | .31 | |
| 2970 | 1.286 | 3600 | .31 | |
| 3210 | 1.759 | 3980 | .30 | |
| 3300 | 1.942 | 4110 | .29 | |
| 3380 | 2.085 | 4200 | .31 | |
| 3460 | 2.290 | 4480 | .25 | Specimen Melting at Edges |

## Table 91.

### Total Normal Emittance of Molybdenum +0.5% Titanium

| Observed Temperature °F | Radiometer Output Millivolts | True Temperature °F | Emittance | Remarks |
|---|---|---|---|---|
| 2270 | 0.575 | 2580 | .45 | |
| 1440 | 0.117 | 1590 | .47 | |
| 1630 | 0.170 | 1800 | .45 | |
| 1830 | 0.301 | 2020 | .54 | |
| 2070 | 0.416 | 2320 | .47 | |
| 2330 | 0.535 | 2730 | .35 | |
| 2440 | 0.690 | 2860 | .38 | Uneven Surface Temperature |
| 2550 | 0.553 | 3160 | .21 | |
| 2820 | 0.845 | 3530 | .22 | |
| 2940 | 1.055 | 3720 | .22 | |
| 2910 | 0.826 | 3700 | .21 | |
| 3010 | 0.906 | 3980 | .16 | |
| 3070 | 0.999 | 4080 | .16 | |
| 3220 | 1.263 | 4400 | .15 | |
| 3290 | 1.468 | 4460 | .16 | |
| 3360 | 1.685 | 4570 | .17 | |
| 3480 | 2.210 | 4600 | .22 | |
| 3570 | 2.582 | 4630 | .26 | |
| 3560 | 2.896 | 4430 | .33 | Edges Melted |

## Table 92.

### Total Normal Emittance of Tungsten

Run No. 1

| Observed Temperature °F | Radiometer Output Millivolts | True Temperature °F | Emittance | Remarks |
|---|---|---|---|---|
| 1520 | 0.1710 | 1650 | .60 | |
| 1770 | 0.3668 | 1910 | .79 | |
| 2030 | 0.5602 | 2190 | .80 | |
| 2250 | 0.8492 | 2460 | .80 | |
| 1610 | 0.2640 | 1740 | .78 | |
| 2020 | 0.5703 | 2200 | .79 | |
| 2420 | 0.8750 | 2750 | .55 | Spots on Surface of Specimen, Smoking |
| 2550 | 0.5660 | 3170 | .22 | Surface Clear, Smoking Stopped |
| 2560 | 0.5710 | 3210 | .21 | |
| 2060 | 0.2360 | 2500 | .21 | |
| 2390 | 0.3920 | 2980 | .19 | |
| 2520 | 0.5150 | 3160 | .20 | |
| 2720 | 0.6960 | 3500 | .19 | |
| 2770 | 0.7460 | 3570 | .19 | |
| 2900 | 0.9630 | 3750 | .20 | |
| 2960 | 0.9910 | 3850 | .19 | |
| 2970 | 1.0320 | 3870 | .19 | |
| 3060 | 1.2310 | 4000 | .20 | |
| 3200 | 1.5510 | 4200 | .22 | |
| 3280 | 1.5840 | 4370 | .19 | |
| 3400 | 1.7350 | 4690 | .17 | |
| 3430 | 1.9170 | 4630 | .19 | |
| 3560 | 2.5260 | 4800 | .21 | |
| 3560 | 2.5260 | 4800 | .21 | |
| 3710 | 3.4040 | 4800 | .29 | |
| 3780 | 5.0410 | 4200 | .68 | |
| 3820 | 5.8800 | 4350 | .73 | |
| 3950 | 6.5250 | 4560 | .67 | |

## Table 92 (Continued).

Total Normal Emittance of Tungsten

Run No. 2

| Observed Temperature °F | Radiometer Output Millivolts | True Temperature °F | Emittance | Remarks |
|---|---|---|---|---|
| $1030^{T}$ | 0.013 | 1030 | .18 | |
| $1265^{T}$ | 0.030 | 1265 | .24 | |
| 1490 | 0.073 | 1710 | .22 | |
| 1740 | 0.178 | 2010 | .32 | Whisker Growth Around Edges |
| 1880 | 0.235 | 2160 | .34 | |
| 2030 | 0.389 | 2350 | .44 | |
| 2410 | 0.504 | 2720 | .33 | |
| 2150 | 0.591 | 2360 | .64 | Spots on Surface, Spots Disappearing |
| 2580 | 0.667 | 3150 | .26 | |
| 2240 | 0.373 | 2690 | .26 | |
| 2650 | 0.705 | 3260 | .25 | |
| 2770 | 0.780 | 3540 | .20 | |
| 2990 | 1.185 | 3760 | .24 | |
| 3050 | 1.292 | 3860 | .24 | |
| 3280 | 1.687 | 4200 | .32 | |
| 3270 | 1.790 | 4170 | .25 | |
| 3490 | 2.252 | 4480 | .25 | |
| 3580 | 2.516 | 4640 | .25 | |
| 3600 | 2.918 | 4680 | .27 | |
| 3700 | 3.400 | 4670 | .32 | |
| 3890 | 4.605 | 4720 | .46 | |
| 3920 | 5.860 | 4490 | .64 | |
| 3980 | 6.284 | 4590 | .64 | |
| 3980 | 6.080 | 4600 | .61 | |
| 4080 | 6.150 | 4850 | .51 | |
| 4080 | 6.100 | 4850 | .51 | |
| 4160 | 6.270 | 5100 | .43 | |

## Table 93.

The Probable Error that can be Anticipated in the Electrical Resistivity Data. Basic Data is the Electrical Resistivity at Temperature Ordinates

| Curve Value | Data Point | Deviation of Data Point from Curve | Per cent Deviation from Curve | Per cent Deviation Squared |
|---|---|---|---|---|
| 6.0 | 5.89 | -0.11 | -1.8 | 3.24 |
| 7.2 | 7.12 | -0.08 | -1.1 | 1.21 |
| 7.5 | 7.26 | -0.24 | -3.2 | 10.24 |
| 11.5 | 11.47 | -0.03 | -0.3 | 0.09 |
| 12.5 | 12.38 | -0.12 | -1.0 | 1.00 |
| 14.0 | 13.15 | -0.85 | -6.1 | 37.21 |
| 18.0 | 22.04 | +4.04 | 22.4 | 501.76 |
| 19.0 | 22.64 | +3.64 | 19.2 | 368.64 |
| 19.0 | 20.36 | +1.36 | 7.2 | 51.84 |
| 24.5 | 27.43 | +2.93 | 12.0 | 144.00 |
| 25.0 | 27.13 | +2.13 | 8.5 | 72.25 |
| 34.0 | 35.79 | +1.79 | 5.3 | 28.09 |
| 35.0 | 34.65 | -0.35 | -1.0 | 1.00 |
| 35.0 | 34.12 | -0.88 | -2.5 | 6.25 |
| 42.5 | 42.78 | +0.28 | 0.7 | 0.49 |
| 46.5 | 45.29 | -1.21 | -2.6 | 6.76 |
| 46.5 | 46.20 | -0.30 | -0.6 | 0.36 |
| 57.0 | 54.86 | -2.14 | -3.8 | 14.44 |
| 57.0 | 57.52 | +0.52 | 0.9 | 0.81 |
| 57.5 | 57.75 | +0.25 | 0.4 | 0.16 |
| 66.0 | 65.95 | -0.05 | -0.1 | 0.01 |
| 70.5 | 70.89 | +0.39 | 0.6 | 0.36 |
| 72.0 | 71.42 | -0.58 | -0.8 | 0.64 |
| 78.0 | 78.26 | +0.26 | 0.3 | 0.09 |

Table 93 (Continued).

The Probable Error that can be Anticipated in the Electrical Resistivity Data. Basic Data is the Electrical Resistivity at Temperature Ordinates

| Curve Value | Data Point | Deviation of Data Point from Curve | Per cent Deviation from Curve | Per cent Deviation Squared |
|---|---|---|---|---|
| 80.5 | 80.16 | -0.34 | -0.4 | 0.16 |
| 81.0 | 80.54 | -0.46 | -0.6 | 0.36 |

$$\Sigma X^2 = 1251.5$$

Standard Deviation $= \sqrt{\frac{\Sigma X^2}{n - 2}}$

$= \sqrt{\frac{1251.5}{26 - 2}}$

$= 7.2$

Probable Error = 0.6745 Standard Deviation

= 4.86%

Therefore, 50% of all values of the electrical resistivity deviate from the curve by no more than 4.86%. This includes the reading variation in picking values off the curve.

Table 94.

Electrical Resistivity Data for Hafnium Diboride

| Temperature °F | Specimen Circuit | | Open Circuit Gage Length Potential Millivolts | Closed Circuit Gage Length Potential Millivolts | Resistivity Micro Ohms Centimeter |
|---|---|---|---|---|---|
| | Amps | Millivolts | | | |
| 75 | 5.75 | 0.109 | -0.001 | 0.110 | 14.34 |
| 75 | 5.79 | 0.111 | 0.001 | 0.110 | 14.27 |
| 445 | 5.80 | 0.165 | -0.011 | 0.176 | 22.75 |
| 450 | 5.81 | 0.166 | -0.013 | 0.179 | 23.13 |
| 845 | 5.81 | 0.771 | 0.526 | 0.245 | 31.69 |
| 847 | 5.83 | 0.768 | 0.517 | 0.251 | 32.36 |
| 1325 | 5.83 | 0.520 | 0.194 | 0.326 | 41.98 |
| 1330 | 5.87 | 0.386 | 0.065 | 0.321 | 41.08 |
| 1925 | 5.87 | 2.161 | 1.681 | 0.480 | 61.43 |
| 1930 | 5.89 | 2.166 | 1.675 | 0.491 | 62.63 |
| 1930 | 5.91 | 2.160 | 1.669 | 0.491 | 62.40 |
| 2200 | 5.89 | 2.460 | 1.916 | 0.544 | 69.39 |
| 2210 | 5.90 | 2.445 | 1.901 | 0.544 | 69.23 |
| 2630 | 5.90 | 2.202 | 1.579 | 0.623 | 79.30 |
| 2650 | 5.90 | 2.051 | 1.420 | 0.631 | 80.27 |
| 3170 | 5.90 | 1.533 | 0.815 | 0.718 | 91.39 |
| 3190 | 5.91 | 1.425 | 0.686 | 0.739 | 93.87 |
| 3220 | 5.92 | 1.294 | 0.540 | 0.754 | 95.67 |
| 3640 | 5.99 | 0.166 | -0.764 | 0.930 | 116.62 |
| 3645 | 5.99 | 0.165 | -0.758 | 0.923 | 115.72 |
| 3640 | 5.98 | 0.155 | -0.764 | 0.919 | 115.42 |

Table 94 (Continued).

Electrical Resistivity Data for
Hafnium Diboride

| Temperature °F | Specimen Circuit | | Open Circuit Gage Length Potential Millivolts | Closed Circuit Gage Length Potential Millivolts | Resistivity Micro Ohms Centimeter |
|---|---|---|---|---|---|
| | Amps | Millivolts | | | |
| 2570 | 5. 91 | 1. 250 | 0. 600 | 0. 650 | 82. 60 |
| 2570 | 5. 92 | 1. 273 | 0. 620 | 0. 653 | 82. 83 |
| 1670 | 5. 92 | 0. 662 | 0. 229 | 0. 433 | 54. 89 |
| 1570 | 5. 92 | 0. 578 | 0. 165 | 0. 413 | 52. 41 |
| 660 | 5. 90 | -0. 092 | -0. 300 | 0. 208 | 26. 51 |
| 635 | 5. 90 | -0. 104 | -0. 310 | 0. 206 | 26. 21 |
| 75 | 5. 82 | 0. 133 | -0. 001 | 0. 134 | 17. 27 |
| 75 | 5. 82 | 0. 132 | -0. 001 | 0. 133 | 17. 20 |

## Table 95.

### Electrical Resistivity Data for Thorium Tetraboride

| Temperature °F | Specimen Circuit | | Open Circuit Gage Length Potential Millivolts | Closed Circuit Gage Length Potential Millivolts | Resistivity Micro Ohms Centimeter |
|---|---|---|---|---|---|
| | Amps | Millivolts | | | |
| 2200 | 5.89 | 40.850 | 22.408 | 18.442 | 2348.6 |
| 2220 | 5.90 | 41.250 | 22.771 | 18.479 | 2349.3 |
| 2230 | 5.91 | 41.505 | 22.971 | 18.534 | 2352.3 |
| 2495 | 5.85 | 38.262 | 22.165 | 16.097 | 2064.3 |
| 2500 | 5.90 | 38.184 | 22.130 | 16.054 | 2041.0 |
| 2505 | 5.91 | 38.520 | 22.256 | 16.264 | 2063.5 |
| 2830 | 5.90 | 36.745 | 22.410 | 14.335 | 1822.7 |
| 2840 | 5.91 | 36.384 | 21.708 | 14.676 | 1862.4 |
| 2855 | 5.94 | 36.192 | 21.490 | 14.702 | 1856.5 |
| 3160 | 5.90 | 26.479 | 15.989 | 10.490 | 1333.7 |
| 3185 | 5.93 | 25.961 | 15.644 | 10.317 | 1305.2 |
| 3185 | 5.95 | 25.237 | 15.049 | 10.188 | 1284.2 |
| 3440 | 5.90 | 20.979 | 12.553 | 8.426 | 1071.1 |
| 3470 | 5.95 | 8.202 | 2.830 | 5.372 | 677.3 |
| 3500 | 5.90 | 0.415 | -0.824 | 1.239 | 157.5 |
| 3500 | 5.90 | -0.08 | -1.23 | 1.150 | 146.3 |

Table 96.

Electrical Resistivity Data for
Titanium Diboride

| Temperature °F | Specimen Circuit |  | Open Circuit Gage Length Potential Millivolts | Closed Circuit Gage Length Potential Millivolts | Resistivity Micro Ohms Centimeter |
|---|---|---|---|---|---|
|  | Amps | Millivolts |  |  |  |
| 74 | 5.75 | 0.091 | 0.001 | 0.090 | 11.75 |
| 74 | 5.80 | 0.090 | -0.005 | 0.095 | 12.27 |
| 430 | 5.85 | -0.260 | -0.425 | 0.165 | 21.10 |
| 430 | 5.85 | -0.261 | -0.426 | 0.165 | 21.10 |
| 895 | 5.85 | -1.635 | -1.913 | 0.278 | 35.55 |
| 900 | 5.89 | -1.605 | -1.884 | 0.279 | 35.47 |
| 905 | 5.90 | -1.576 | -1.855 | 0.279 | 35.40 |
| 1315 | 5.92 | -2.552 | -2.943 | 0.391 | 49.39 |
| 1320 | 5.95 | -2.435 | -2.828 | 0.393 | 49.46 |
| 1765 | 5.92 | -4.348 | -4.832 | 0.484 | 61.21 |
| 1775 | 5.93 | -4.256 | -4.715 | 0.459 | 57.92 |
| 1785 | 5.95 | -4.184 | -4.642 | 0.458 | 57.62 |
| 1900 | 5.95 | -4.380 | -4.877 | 0.497 | 62.48 |
| 1920 | 5.92 | -3.456 | -3.903 | 0.447 | 57.99 |
| 2400 | 5.91 | -3.052 | -3.605 | 0.553 | 70.04 |
| 2400 | 5.92 | -2.975 | -3.526 | 0.551 | 69.67 |

Table 96 (Continued).

Electrical Resistivity Data for
Titanium Diboride

| Temperature °F | Specimen Circuit Amps | Specimen Circuit Millivolts | Open Circuit Gage Length Potential Millivolts | Closed Circuit Gage Length Potential Millivolts | Resistivity Micro Ohms Centimeter |
|---|---|---|---|---|---|
| 2875 | 5.90 | -2.430 | -3.070 | 0.630 | 79.92 |
| 2880 | 5.93 | -2.390 | -3.005 | 0.615 | 77.60 |
| 3150 | 5.92 | -2.345 | -3.046 | 0.701 | 88.60 |
| 3160 | 5.95 | -2.385 | -3.073 | 0.688 | 86.51 |
| 3170 | 5.96 | -2.503 | -3.191 | 0.688 | 86.36 |
| 3810 | 5.91 | -2.530 | -3.350 | 0.820 | 103.79 |
| 3800 | 5.93 | -2.492 | -3.320 | 0.828 | 104.47 |
| 3830 | 5.94 | -2.443 | -3.285 | 0.842 | 106.11 |
| 2510 | 5.97 | -2.534 | -3.092 | 0.558 | 69.97 |
| 2480 | 6.00 | -2.552 | -3.113 | 0.561 | 69.97 |
| 2475 | 6.00 | -2.577 | -3.137 | 0.560 | 69.82 |
| 1800 | 5.93 | -2.532 | -2.940 | 0.408 | 51.48 |
| 1770 | 5.93 | -2.614 | -3.020 | 0.406 | 51.26 |
| 85 | 5.93 | 0.095 | 0.006 | 0.089 | 11.22 |
| 80 | 5.86 | 0.090 | 0.004 | 0.086 | 11.00 |

## Table 97.

### Electrical Resistivity Data for Tungsten Boride

| Temperature ° F | Specimen Circuit | | Open Circuit Gage Length Potential Millivolts | Closed Circuit Gage Length Potential Millivolts | Resistivity Micro Ohms Centimeter |
|---|---|---|---|---|---|
| | Amps | Millivolts | | | |
| 75 | 5.71 | 0.425 | -0.001 | 0.426 | 55.94 |
| 75 | 5.75 | 0.431 | 0.001 | 0.430 | 56.09 |
| 415 | 5.80 | 0.804 | 0.295 | 0.509 | 65.84 |
| 420 | 5.81 | 0.812 | 0.301 | 0.511 | 65.99 |
| 775 | 5.82 | 1.723 | 1.135 | 0.588 | 75.74 |
| 780 | 5.82 | 1.734 | 1.144 | 0.590 | 76.04 |
| 1305 | 5.84 | 3.029 | 2.330 | 0.699 | 89.77 |
| 1308 | 5.86 | 3.039 | 2.325 | 0.714 | 91.34 |
| 1855 | 5.85 | 3.318 | 2.544 | 0.774 | 99.21 |
| 1900 | 5.90 | 3.136 | 2.334 | 0.802 | 101.91 |
| 1900 | 5.90 | 3.089 | 2.284 | 0.805 | 102.29 |
| 2375 | 5.89 | 3.395 | 2.516 | 0.879 | 111.89 |
| 2410 | 5.90 | 3.362 | 2.480 | 0.882 | 112.11 |
| 2750 | 5.85 | 2.751 | 1.819 | 0.932 | 119.46 |
| 2760 | 5.89 | 2.667 | 1.727 | 0.940 | 119.69 |
| 3205 | 5.89 | 1.995 | 1.000 | 0.995 | 126.66 |
| 3205 | 5.90 | 1.971 | 0.971 | 1.000 | 127.11 |
| 3725 | 5.88 | 2.011 | 0.948 | 1.063 | 135.59 |
| 3740 | 5.90 | 2.025 | 0.960 | 1.065 | 135.36 |
| 3810 | 5.89 | 2.050 | 0.974 | 1.076 | 137.01 |
| 3830 | 5.90 | 2.059 | 0.984 | 1.075 | 136.64 |
| 2970 | 5.89 | 2.372 | 1.410 | 0.962 | 122.46 |
| 2955 | 5.90 | 2.345 | 1.434 | 0.911 | 115.79 |
| 1910 | 5.88 | 1.825 | 1.040 | 0.825 | 105.21 |
| 1820 | 5.89 | 2.113 | 1.328 | 0.785 | 99.96 |

Table 98.

Electrical Resistivity Data for Zirconium Diboride

| Temperature °F | Specimen Circuit | | Open Circuit Gage Length Potential Millivolts | Closed Circuit Gage Length Potential Millivolts | Resistivity Micro Ohms Centimeter |
|---|---|---|---|---|---|
| | Amps | Millivolts | | | |
| 95 | 28.2 | 1.188 | 0.000 | 1.188 | 32.9 |
| 95 | 28.2 | 1.186 | 0.000 | 1.186 | 32.9 |
| 348 | 28.6 | 1.135 | -0.266 | 1.401 | 38.4 |
| 418 | 29.0 | 1.004 | -0.481 | 1.485 | 40.2 |
| 510 | 29.0 | 0.901 | -0.659 | 1.560 | 42.2 |
| 1027 | 29.3 | -0.865 | -2.870 | 2.005 | 53.6 |
| 1103 | 29.5 | -1.138 | -3.290 | 2.152 | 57.0 |
| 1515 | 30.0 | 2.160 | -0.584 | 2.744 | 71.5 |
| 1625 | 30.2 | 1.807 | -0.875 | 2.682 | 69.6 |
| 1640 | 30.0 | 3.500 | 0.848 | 2.652 | 69.1 |
| 1940 | 30.0 | 2.830 | -0.010 | 2.840 | 74.0 |
| 1980 | 30.8 | 4.175 | 1.191 | 2.984 | 75.8 |
| 2430 | 30.5 | 4.005 | 0.477 | 3.528 | 90.3 |
| 2560 | 30.6 | 3.783 | 0.204 | 3.579 | 91.5 |
| 2970 | 30.6 | 4.635 | 0.690 | 3.945 | 100.9 |
| 3100 | 30.5 | 5.925 | 1.845 | 4.070 | 104.0 |
| 3500 | 30.1 | 6.605 | 2.065 | 4.540 | 118.1 |
| 3780 | 30.1 | 6.296 | 1.757 | 4.539 | 118.1 |
| 3750 | 30.5 | 6.215 | 1.644 | 4.571 | 116.9 |
| 4110 | 30.7 | 7.582 | 2.677 | 4.905 | 125.1 |

Specimen had begun to deteriorate.

### Table 99.

### Electrical Resistivity Data for Columbium Carbide

| Temperature °F | Specimen Circuit |  | Open Circuit Gage Length Potential Millivolts | Closed Circuit Gage Length Potential Millivolts | Resistivity Micro Ohms Centimeter |
|---|---|---|---|---|---|
|  | Amps | Millivolts |  |  |  |
| 74 | 5.90 | 0.366 | 0.001 | 0.365 | 53.82 |
| 74 | 5.90 | 0.366 | 0.001 | 0.365 | 53.82 |
| 75 | 5.90 | 0.362 | -0.001 | 0.363 | 53.47 |
| 75 | 5.90 | 0.363 | -0.001 | 0.364 | 53.64 |
| 110 | 5.90 | 0.361 | -0.006 | 0.367 | 54.08 |
| 111 | 5.90 | 0.365 | -0.005 | 0.370 | 54.51 |
| 170 | 5.90 | 0.378 | -0.001 | 0.379 | 55.82 |
| 180 | 5.90 | 0.384 | 0.002 | 0.382 | 56.25 |
| 250 | 5.90 | 0.400 | 0.005 | 0.395 | 58.16 |
| 255 | 5.92 | 0.405 | 0.008 | 0.397 | 58.34 |
| 415 | 5.92 | 0.446 | 0.020 | 0.426 | 62.60 |
| 420 | 5.95 | 0.460 | 0.030 | 0.430 | 62.86 |
| 530 | 5.95 | 0.550 | 0.112 | 0.438 | 63.99 |
| 530 | 5.98 | 0.537 | 0.086 | 0.451 | 65.55 |
| 680 | 5.95 | 0.557 | 0.072 | 0.485 | 70.86 |

Table 99 (Continued).

Electrical Resistivity Data for
Columbium Carbide

| Temperature °F | Specimen Circuit |  | Open Circuit Gage Length Potential Millivolts | Closed Circuit Gage Length Potential Millivolts | Resistivity Micro Ohms Centimeter |
|---|---|---|---|---|---|
|  | Amps | Millivolts |  |  |  |
| 685 | 5.99 | 0.556 | 0.078 | 0.478 | 69.38 |
| 975 | 5.90 | 0.500 | -0.047 | 0.547 | 80.59 |
| 980 | 5.92 | 0.504 | -0.044 | 0.548 | 80.51 |
| 1355 | 5.85 | 0.243 | -0.376 | 0.619 | 91.98 |
| 1365 | 5.89 | 0.259 | -0.364 | 0.623 | 91.98 |
| 1865 | 6.00 | 0.675 | -0.015 | 0.690 | 99.98 |
| 1867 | 6.05 | 0.660 | -0.038 | 0.698 | 100.33 |
| 2130 | 6.01 | 1.040 | 0.306 | 0.734 | 106.15 |
| 2150 | 6.05 | 1.035 | 0.295 | 0.740 | 106.33 |
| 2640 | 6.05 | -0.455 | -1.225 | 0.770 | 110.67 |
| 2640 | 6.09 | -0.520 | -1.310 | 0.790 | 112.76 |
| 3200 | 6.09 | -0.680 | -1.506 | 0.826 | 117.89 |
| 3250 | 6.09 | -0.665 | -1.540 | 0.875 | 124.93 |
| 3840 | 6.05 | 561.20 | 559.88 | 1.320 | 189.70 |
| 3850 | 6.05 | 597.20 | 557.25 | 39.95 | 5741.0 |

Table 100.

Electrical Resistivity Data for
Dimolybdenum Carbide

| Temperature °F | Specimen Circuit | | Open Circuit Gage Length Potential Millivolts | Closed Circuit Gage Length Potential Millivolts | Resistivity Micro Ohms Centimeter |
|---|---|---|---|---|---|
| | Amps | Millivolts | | | |
| 70 | 6.05 | 0.524 | -0.001 | 0.525 | 64.88 |
| 67 | 6.20 | 0.540 | -0.001 | 0.541 | 65.25 |
| 85 | 6.10 | 0.544 | -0.001 | 0.545 | 66.81 |
| 35 | 6.19 | 0.551 | -0.001 | 0.552 | 66.68 |
| 125 | 6.15 | 0.581 | 0.001 | 0.580 | 70.51 |
| 130 | 6.20 | 0.589 | 0.001 | 0.588 | 70.92 |
| 235 | 6.15 | 0.660 | 0.006 | 0.654 | 79.49 |
| 240 | 6.15 | 0.665 | 0.007 | 0.658 | 80.00 |
| 320 | 6.15 | 0.726 | 0.019 | 0.707 | 85.96 |
| 330 | 6.15 | 0.731 | 0.020 | 0.711 | 86.44 |
| 415 | 6.20 | 0.748 | 0.040 | 0.708 | 85.39 |
| 425 | 6.20 | 0.802 | 0.040 | 0.762 | 91.90 |
| 570 | 6.15 | 0.925 | 0.100 | 0.825 | 100.28 |
| 585 | 6.15 | 0.940 | 0.107 | 0.833 | 101.25 |
| 870 | 6.11 | 1.235 | 0.322 | 0.913 | 111.72 |
| 895 | 6.20 | 1.274 | 0.344 | 0.930 | 112.17 |

## Table 100 (Continued).

Electrical Resistivity Data for
Dimolybdenum Carbide

| Temperature °F | Specimen Circuit | | Open Circuit Gage Length Potential Millivolts | Closed Circuit Gage Length Potential Millivolts | Resistivity Micro Ohms Centimeter |
|---|---|---|---|---|---|
| | Amps | Millivolts | | | |
| 1265 | 6.20 | 1.800 | 0.841 | 0.959 | 115.68 |
| 1300 | 6.15 | 1.840 | 0.885 | 0.955 | 116.13 |
| 1480 | 6.15 | 1.950 | 0.954 | 0.996 | 121.10 |
| 1490 | 6.20 | 1.910 | 0.904 | 1.006 | 121.33 |
| 1705 | 6.16 | 2.741 | 1.673 | 1.068 | 129.66 |
| 1750 | 6.19 | 2.897 | 1.832 | 1.065 | 128.69 |
| 1790 | 6.19 | 3.045 | 1.987 | 1.058 | 127.81 |
| 2340 | 6.10 | 4.706 | 3.650 | 1.056 | 129.44 |
| 2380 | 6.20 | 4.782 | 3.679 | 1.103 | 133.03 |
| 2700 | 6.11 | 5.136 | 4.093 | 1.043 | 127.64 |
| 2730 | 6.20 | 5.106 | 4.080 | 1.026 | 123.76 |
| 3060 | 6.15 | 4.920 | 3.904 | 1.016 | 123.53 |
| 3110 | 6.15 | 4.860 | 3.824 | 1.036 | 126.00 |
| 3160 | 6.20 | 4.851 | 3.789 | 1.062 | 128.09 |
| 3220 | 6.21 | 4.826 | 3.786 | 1.040 | 125.25 |
| 3240 | 6.21 | 4.844 | 3.768 | 1.076 | 129.59 |

## Table 101.

Electrical Resistivity Data for Hafnium Carbide

| Temperature °F | Specimen Circuit | | Open Circuit Gage Length Potential Millivolts | Closed Circuit Gage Length Potential Millivolts | Resistivity Micro Ohms Centimeter |
|---|---|---|---|---|---|
| | Amps | Millivolts | | | |
| | | First Run, Specimen 1 | | | |
| 74 | 5.60 | 0.361 | 0.000 | 0.361 | 48.33 |
| 74 | 5.61 | 0.364 | -0.003 | 0.367 | 48.93 |
| 410 | 5.65 | 0.557 | 0.096 | 0.461 | 61.14 |
| 408 | 5.65 | 0.638 | 0.180 | 0.458 | 60.77 |
| 682 | 5.70 | 1.462 | 0.915 | 0.547 | 71.93 |
| 687 | 5.70 | 1.489 | 0.943 | 0.546 | 71.78 |
| 1295 | 5.80 | 7.601 | 6.735 | 0.866 | 111.87 |
| 1705 | 5.85 | 14.333 | 13.334 | 0.999 | 127.98 |
| 1840 | 5.90 | 8.571 | 7.744 | 0.827 | 105.05 |
| 1820 | 5.90 | 8.070 | 7.225 | 0.845 | 107.30 |
| 2160 | 5.91 | 6.425 | 5.324 | 1.101 | 139.60 |
| 2200 | 5.91 | 6.401 | 5.272 | 1.129 | 143.12 |
| 2720 | 5.91 | 5.106 | 3.873 | 1.233 | 156.31 |
| 2740 | 5.95 | 5.150 | 3.895 | 1.255 | 158.03 |
| 3350 | 5.91 | 5.180 | 3.691 | 1.489 | 188.75 |
| 3380 | 5.95 | 5.020 | 3.660 | 1.360 | 171.29 |

Specimen surface found to be flaked off.

| | | | | | |
|---|---|---|---|---|---|
| | | Second Run, Specimen 2 | | | |
| 75 | 5.70 | 0.371 | 0.000 | 0.371 | 48.78 |
| 75 | 5.70 | 0.372 | 0.000 | 0.372 | 48.93 |
| 420 | 5.80 | 0.924 | 0.445 | 0.479 | 61.89 |

Table 101 (Continued).

Electrical Resistivity Data for
Hafnium Carbide

| Temperature °F | Specimen Circuit | | Open Circuit Gage Length Potential Millivolts | Closed Circuit Gage Length Potential Millivolts | Resistivity Micro Ohms Centimeter |
|---|---|---|---|---|---|
| | Amps | Millivolts | | | |
| 425 | 5.80 | 0.929 | 0.450 | 0.479 | 61.89 |
| 817 | 5.86 | 1.726 | 1.160 | 0.566 | 72.38 |
| 820 | 5.89 | 1.782 | 1.165 | 0.617 | 78.53 |
| 818 | 5.90 | 1.763 | 1.149 | 0.614 | 78.00 |
| 1170 | 5.88 | 2.770 | 2.033 | 0.737 | 93.89 |
| 1172 | 5.90 | 2.777 | 2.039 | 0.738 | 93.74 |
| 1630 | 5.89 | 3.540 | 2.614 | 0.926 | 117.79 |
| 1635 | 5.90 | 3.545 | 2.612 | 0.933 | 118.47 |
| 1895 | 5.90 | 3.830 | 2.801 | 1.029 | 130.68 |
| 1897 | 5.90 | 3.826 | 2.797 | 1.029 | 130.68 |
| 1870 | 5.90 | 3.771 | 2.745 | 1.026 | 130.31 |
| 2170 | 5.90 | 4.277 | 3.132 | 1.145 | 145.44 |
| 2175 | 5.92 | 4.284 | 3.145 | 1.139 | 144.17 |
| 2650 | 5.90 | 4.184 | 2.896 | 1.288 | 163.58 |
| 2680 | 5.93 | 4.069 | 2.780 | 1.289 | 162.90 |
| 3000 | 5.91 | 3.256 | 1.861 | 1.395 | 176.84 |
| 3040 | 5.93 | 3.568 | 2.110 | 1.458 | 184.26 |
| 3070 | 5.95 | 3.506 | 2.112 | 1.394 | 175.57 |
| 3570 | 5.93 | 3.006 | 1.470 | 1.536 | 194.07 |
| 3580 | 5.95 | 2.950 | 1.404 | 1.546 | 194.67 |
| 4040 | 5.93 | 2.950 | 1.237 | 1.713 | 216.49 |
| 4080 | 5.94 | 2.905 | 1.184 | 1.721 | 217.08 |
| 3100 | 5.91 | 4.180 | 2.741 | 1.439 | 182.46 |
| 3025 | 5.91 | 5.060 | 3.660 | 1.400 | 177.51 |

Table 101 (Continued).

Electrical Resistivity Data for
Hafnium Carbide

| Temperature ° F | Specimen Circuit | | Open Circuit Gage Length Potential Millivolts | Closed Circuit Gage Length Potential Millivolts | Resistivity Micro Ohms Centimeter |
|---|---|---|---|---|---|
| | Amps | Millivolts | | | |
| 1950 | 5.91 | 3.097 | 2.159 | 0.938 | 118.92 |
| 1820 | 5.92 | 3.026 | 2.111 | 0.915 | 115.84 |
| 1070 | 5.92 | 1.336 | 0.712 | 0.624 | 78.98 |
| 995 | 5.92 | 1.236 | 0.637 | 0.599 | 75.83 |
| 75 | 5.82 | 0.376 | 0.000 | 0.376 | 48.41 |
| 75 | 5.86 | 0.377 | 0.000 | 0.377 | 48.18 |

Table 102.

Electrical Resistivity Data for Tantalum Carbide

| Temperature ° F | Specimen Circuit Amps | Specimen Circuit Millivolts | Open Circuit Gage Length Potential Millivolts | Closed Circuit Gage Length Potential Millivolts | Resistivity Micro Ohms Centimeter |
|---|---|---|---|---|---|
| 70 | 25.0 | 0.618 | 0.000 | 0.618 | 18.5 |
| 1800 | 28.5 | -0.495 | -2.75 | 2.255 | 59.1 |
| 1950 | 28.5 | 3.62 | 1.26 | 2.360 | 62.2 |
| 1955 | 28.6 | 4.28 | 1.81 | 2.47 | 64.6 |
| 2070 | 28.4 | 3.29 | 0.92 | 2.37 | 62.5 |
| 2670 | 28.9 | 3.37 | 0.37 | 3.00 | 77.7 |
| 2700 | 28.7 | 3.31 | 0.27 | 3.04 | 79.4 |
| 2810 | 29.2 | 3.25 | 0.13 | 3.12 | 80.2 |
| 3120 | 30.8 | 4.21 | 0.47 | 3.74 | 91.1 |
| 3220 | 30.2 | 4.43 | 0.78 | 3.65 | 90.6 |
| 3220 | 30.4 | 4.30 | 0.60 | 3.70 | 91.3 |
| 3690 | 30.6 | 5.55 | 1.38 | 4.17 | 102 |
| 4070 | 31.1 | 5.55 | 1.10 | 4.45 | 107 |
| 4090 | 31.0 | 5.72 | 1.21 | 4.51 | 109 |
| 4320 | 30.9 | 5.55 | 0.94 | 4.61 | 112 |
| 4360 | 30.8 | 5.60 | 0.91 | 4.69 | 114 |
| 4420 | 30.8 | 5.66 | 0.98 | 4.68 | 115 |

## Table 103.

### Electrical Resistivity Data for Titanium Carbide

| Temperature ° F | Specimen Circuit Amps | Specimen Circuit Millivolts | Open Circuit Gage Length Potential Millivolts | Closed Circuit Gage Length Potential Millivolts | Resistivity Micro Ohms Centimeter |
|---|---|---|---|---|---|
| | | First Run, Specimen 1 | | | |
| 75 | 5.82 | 0.380 | 0.000 | 0.380 | 47.84 |
| 75 | 5.83 | 0.381 | -0.001 | 0.382 | 47.99 |
| 215 | 5.89 | 0.416 | -0.007 | 0.423 | 52.60 |
| 220 | 5.90 | 0.420 | -0.009 | 0.429 | 53.26 |
| 555 | 5.91 | 0.544 | 0.023 | 0.521 | 64.62 |
| 560 | 5.92 | 0.545 | 0.020 | 0.525 | 64.99 |
| 860 | 5.95 | 0.845 | 0.223 | 0.622 | 76.56 |
| 870 | 5.99 | 0.861 | 0.237 | 0.624 | 76.34 |
| 1080 | 5.95 | 1.157 | 0.460 | 0.697 | 85.79 |
| 1085 | 5.95 | 1.175 | 0.480 | 0.695 | 85.57 |
| 1575 | 6.00 | 2.128 | 1.249 | 0.879 | 107.33 |
| 1595 | 6.00 | 2.145 | 1.255 | 0.890 | 108.65 |
| 1900 | 6.00 | 2.375 | 1.400 | 0.975 | 119.05 |
| 1910 | 6.00 | 2.378 | 1.390 | 0.988 | 120.67 |
| 2000 | 6.00 | 0.693 | -0.350 | 1.043 | 127.33 |
| 2440 | 6.00 | 2.695 | 1.564 | 1.131 | 138.10 |
| 2475 | 6.00 | 2.727 | 1.590 | 1.137 | 138.84 |
| 2850 | 6.00 | 2.905 | 1.592 | 1.313 | 160.30 |
| 2900 | 6.00 | 2.899 | 1.575 | 1.324 | 161.69 |

## Table 103 (Continued).

Electrical Resistivity Data for
Titanium Carbide

| Temperature °F | Specimen Circuit |  | Open Circuit Gage Length Potential Millivolts | Closed Circuit Gage Length Potential Millivolts | Resistivity Micro Ohms Centimeter |
|---|---|---|---|---|---|
|  | Amps | Millivolts |  |  |  |
|  |  | Second Run, Specimen 1 |  |  |  |
| 85 | 5.90 | 0.481 | 0.010 | 0.471 | 58.46 |
| 70 | 5.81 | 0.465 | -0.001 | 0.466 | 58.76 |
| 70 | 5.85 | 0.466 | -0.001 | 0.467 | 58.61 |
| 315 | 5.85 | 0.422 | -0.132 | 0.554 | 69.38 |
| 320 | 5.87 | 0.425 | -0.131 | 0.556 | 69.38 |
| 615 | 5.90 | 0.287 | -0.359 | 0.646 | 80.22 |
| 617 | 5.91 | 0.330 | -0.337 | 0.667 | 82.72 |
| 1070 | 5.85 | 1.192 | 0.478 | 0.714 | 89.46 |
| 1090 | 5.85 | 1.056 | 0.321 | 0.735 | 92.02 |
| 1620 | 5.95 | -0.626 | -1.550 | 0.924 | 113.78 |
| 1630 | 5.95 | -0.576 | -1.520 | 0.944 | 116.27 |
| 1955 | 5.92 | -0.246 | -1.246 | 1.000 | 123.74 |
| 1955 | 5.95 | -0.288 | -1.280 | 0.992 | 122.13 |
| 2055 | 5.95 | -0.392 | -1.370 | 0.978 | 120.45 |
| 2370 | 5.95 | -2.584 | -3.690 | 1.106 | 136.20 |
| 2380 | 5.95 | -2.576 | -3.617 | 1.041 | 128.21 |
| 2830 | 5.95 | -1.000 | -2.270 | 1.270 | 156.35 |
| 2840 | 5.96 | -0.941 | -2.205 | 1.264 | 155.39 |
| 3250 | 5.95 | -0.147 | -1.570 | 1.423 | 175.25 |
| 3270 | 5.95 | -0.097 | -1.573 | 1.476 | 181.77 |
| 3790 | 5.95 | 0.325 | -1.330 | 1.655 | 203.82 |
| 3910 | 5.95 | 0.478 | -1.230 | 1.708 | 210.34 |
| 4025 | 5.96 | 1.050 | -0.736 | 1.786 | 219.57 |
| 4050 | 6.00 | 1.209 | -0.596 | 1.805 | 220.38 |
| 2240 | 5.95 | 0.921 | -0.120 | 1.041 | 128.21 |

## Table 104.

### Electrical Resistivity Data for Tungsten Carbide

| Temperature °F | Specimen Circuit |  | Open Circuit Gage Length Potential Millivolts | Closed Circuit Gage Length Potential Millivolts | Resistivity Micro Ohms Centimeter |
|---|---|---|---|---|---|
|  | Amps | Millivolts |  |  |  |
| 75 | 5.85 | 0.151 | 0.000 | 0.151 | 19.40 |
| 75 | 5.85 | 0.151 | 0.000 | 0.151 | 19.40 |
| 365 | 5.85 | 0.391 | 0.138 | 0.253 | 32.48 |
| 365 | 5.89 | 0.392 | 0.138 | 0.254 | 32.41 |
| 755 | 5.85 | 1.065 | 0.646 | 0.419 | 53.84 |
| 760 | 5.89 | 1.068 | 0.646 | 0.422 | 53.84 |
| 1130 | 5.88 | 1.836 | 1.263 | 0.573 | 73.24 |
| 1130 | 5.90 | 1.855 | 1.276 | 0.579 | 73.76 |
| 1585 | 5.89 | 3.303 | 2.562 | 0.741 | 94.59 |
| 1590 | 5.89 | 3.323 | 2.579 | 0.744 | 94.97 |
| 1910 | 5.90 | 4.744 | 3.895 | 0.849 | 108.20 |
| 1915 | 5.91 | 4.731 | 3.881 | 0.850 | 108.13 |
| 1920 | 5.91 | 4.644 | 3.742 | 0.902 | 114.74 |
| 1925 | 5.92 | 4.606 | 3.753 | 0.853 | 108.35 |
| 2420 | 5.90 | 4.843 | 3.817 | 1.026 | 130.76 |
| 2420 | 5.91 | 4.609 | 3.572 | 1.037 | 131.96 |
| 2880 | 5.91 | 4.300 | 3.110 | 1.190 | 151.44 |
| 2880 | 5.91 | 4.287 | 3.095 | 1.192 | 151.66 |

## Table 104 (Continued).

### Electrical Resistivity Data for Tungsten Carbide

| Temperature °F | Specimen Circuit | | Open Circuit Gage Length Potential Millivolts | Closed Circuit Gage Length Potential Millivolts | Resistivity Micro Ohms Centimeter |
|---|---|---|---|---|---|
| | Amps | Millivolts | | | |
| 3170 | 5.90 | 4.120 | 2.860 | 1.260 | 160.61 |
| 3170 | 5.90 | 4.128 | 2.864 | 1.264 | 161.06 |
| 3700 | 5.90 | 3.929 | 2.275 | 1.654 | 210.76 |
| 3720 | 5.91 | 3.989 | 2.306 | 1.683 | 214.15 |
| 3740 | 5.91 | 4.121 | 2.386 | 1.735 | 220.76 |
| 3780 | 5.91 | 4.196 | 2.432 | 1.764 | 224.45 |
| 3830 | 5.90 | 4.218 | 2.450 | 1.768 | 225.35 |
| 3880 | 5.90 | 4.200 | 2.428 | 1.772 | 225.80 |
| 3900 | 5.90 | 4.169 | 2.380 | 1.789 | 227.98 |
| 3920 | 5.91 | 4.147 | 2.357 | 1.790 | 227.76 |
| 3540 | 5.90 | 4.841 | 3.151 | 1.690 | 215.35 |
| 2710 | 5.91 | 4.162 | 2.850 | 1.312 | 166.93 |
| 2600 | 5.91 | 3.829 | 2.550 | 1.279 | 162.72 |
| 1550 | 5.90 | 1.619 | 0.840 | 0.779 | 99.25 |
| 1440 | 5.90 | 1.155 | 0.388 | 0.762 | 97.75 |
| 805 | 5.90 | 0.295 | -0.169 | 0.464 | 59.10 |
| 70 | 5.85 | 0.148 | 0.001 | 0.147 | 18.87 |

## Table 105.

### Electrical Resistivity Data for Vanadium Carbide

| Temperature °F | Specimen Circuit | | Open Circuit Gage Length Potential Millivolts | Closed Circuit Gage Length Potential Millivolts | Resistivity Micro Ohms Centimeter |
|---|---|---|---|---|---|
| | Amps | Millivolts | | | |
| 75 | 5.81 | 0.641 | 0.000 | 0.641 | 82.85 |
| 75 | 5.82 | 0.644 | 0.000 | 0.644 | 83.15 |
| 470 | 5.82 | 1.096 | 0.211 | 0.885 | 114.25 |
| 475 | 5.85 | 1.104 | 0.215 | 0.889 | 114.17 |
| 930 | 5.89 | 2.715 | 1.610 | 1.105 | 140.91 |
| 935 | 5.89 | 2.751 | 1.645 | 1.106 | 141.06 |
| 1225 | 5.87 | 3.779 | 2.589 | 1.190 | 152.25 |
| 1230 | 5.89 | 3.784 | 2.587 | 1.197 | 152.63 |
| 1740 | 5.85 | 7.681 | 6.272 | 1.409 | 180.94 |
| 1745 | 5.89 | 7.841 | 6.415 | 1.426 | 181.85 |
| 1850 | 5.89 | 8.050 | 6.620 | 1.430 | 182.37 |
| 2260 | 5.90 | 11.955 | 10.391 | 1.564 | 199.12 |
| 2270 | 5.90 | 11.820 | 10.250 | 1.570 | 199.87 |
| 2640 | 5.90 | 12.662 | 11.075 | 1.587 | 202.05 |
| 2650 | 5.91 | 12.650 | 11.066 | 1.584 | 201.30 |
| 3000 | 5.90 | 13.211 | 11.617 | 1.594 | 202.95 |

Table 105 (Continued).

Electrical Resistivity Data for
Vanadium Carbide

| Temperature °F | Specimen Circuit | | Open Circuit Gage Length Potential Millivolts | Closed Circuit Gage Length Potential Millivolts | Resistivity Micro Ohms Centimeter |
|---|---|---|---|---|---|
| | Amps | Millivolts | | | |
| 3040 | 5.91 | 13.054 | 11.459 | 1.595 | 202.73 |
| 3390 | 5.90 | 9.993 | 8.405 | 1.588 | 202.20 |
| 3420 | 5.90 | 9.794 | 8.166 | 1.628 | 207.23 |
| 3500 | 5.91 | 9.633 | 7.971 | 1.662 | 211.21 |
| 3510 | 5.91 | 9.495 | 7.833 | 1.662 | 211.21 |
| 3680 | 5.92 | 9.091 | 7.450 | 1.641 | 208.21 |
| 3720 | 5.92 | 8.952 | 7.290 | 1.662 | 210.84 |
| 3780 | 5.95 | 8.832 | 7.146 | 1.686 | 212.87 |
| 2770 | 5.90 | 9.970 | 8.396 | 1.574 | 200.40 |
| 2750 | 5.90 | 10.045 | 8.459 | 1.586 | 201.90 |
| 1800 | 5.90 | 4.402 | 3.196 | 1.206 | 153.53 |
| 1640 | 5.90 | 3.812 | 2.636 | 1.176 | 149.70 |
| 740 | 5.89 | 1.063 | 0.056 | 1.007 | 128.44 |
| 750 | 5.90 | 1.053 | 0.047 | 1.011 | 128.74 |
| 75 | 5.81 | 0.674 | -0.006 | 0.680 | 87.88 |
| 75 | 5.83 | 0.679 | 0.000 | 0.679 | 87.51 |

Table 106.

Electrical Resistivity Data for Zirconium Carbide

| Temperature °F | Specimen Circuit | | Open Circuit Gage Length Potential Millivolts | Closed Circuit Gage Length Potential Millivolts | Resistivity Micro Ohms Centimeter |
|---|---|---|---|---|---|
| | Amps | Millivolts | | | |
| 80 | 5.72 | 0.643 | -0.005 | 0.648 | 84.83 |
| 80 | 5.75 | 0.645 | -0.005 | 0.650 | 84.61 |
| 385 | 5.81 | 0.701 | -0.098 | 0.799 | 102.95 |
| 387 | 5.85 | 0.710 | -0.094 | 0.804 | 102.87 |
| 640 | 5.87 | -0.231 | -1.094 | 0.863 | 110.06 |
| 650 | 5.88 | -0.220 | -1.072 | 0.852 | 108.49 |
| 1020 | 5.72 | -1.052 | -1.995 | 0.943 | 123.46 |
| 1030 | 5.73 | -1.056 | -1.996 | 0.940 | 122.79 |
| 1035 | 5.80 | -1.052 | -2.008 | 0.956 | 123.39 |
| 1435 | 5.90 | -0.695 | -1.858 | 1.163 | 147.57 |
| 1445 | 5.91 | -0.867 | -2.008 | 1.141 | 144.58 |
| 2180 | 5.89 | -3.105 | -4.492 | 1.387 | 176.32 |
| 2455 | 5.89 | -2.072 | -3.545 | 1.473 | 187.25 |
| 2490 | 5.90 | -2.012 | -3.484 | 1.472 | 186.81 |

## Table 106 (Continued).

Electrical Resistivity Data for
Zirconium Carbide

| Temperature °F | Specimen Circuit | | Open Circuit Gage Length Potential Millivolts | Open Circuit Gage Length Potential Millivolts | Resistivity Micro Ohms Centimeter |
|---|---|---|---|---|---|
| | Amps | Millivolts | | | |
| 2875 | 5.90 | -5.134 | -6.505 | 1.371 | 174.00 |
| 2900 | 5.90 | -5.826 | -7.240 | 1.414 | 179.47 |
| 3470 | 5.91 | -3.825 | -5.530 | 1.705 | 216.00 |
| 3490 | 5.92 | -3.550 | -5.255 | 1.705 | 215.63 |
| 3930 | 5.91 | -1.300 | -3.091 | 1.791 | 226.86 |
| 3955 | 5.99 | -1.085 | -2.887 | 1.802 | 225.21 |
| 3960 | 5.99 | -0.794 | -2.623 | 1.829 | 228.58 |
| 4310 | 5.98 | 0.251 | -1.650 | 1.901 | 238.02 |
| 4320 | 5.99 | 0.621 | -1.295 | 1.916 | 239.52 |
| 2960 | 5.95 | 0.156 | -1.341 | 1.497 | 188.38 |
| 2960 | 5.95 | 0.110 | -1.379 | 1.489 | 187.40 |
| 2650 | 5.95 | -0.492 | -1.904 | 1.412 | 177.67 |
| 2800 | 5.95 | -0.324 | -1.780 | 1.456 | 183.20 |

Table 107.

Electrical Resistivity Data for Boron Nitride

| Temperature °F | Specimen Circuit Amps | Specimen Circuit Millivolts | Open Circuit Gage Length Potential Millivolts | Closed Circuit Gage Length Potential Millivolts | Resistivity Micro Ohms Centimeter |
|---|---|---|---|---|---|
| 75 | 0.00 | 0.00 | 0.00 | 0.00 | |
| 250 | 0.00 | 0.00 | 0.00 | 0.00 | |
| 650 | 0.00 | 0.00 | 0.00 | 0.00 | |
| 1455 | 0.00 | 0.00 | 0.00 | 0.00 | |
| 1775 | 0.00 | 0.00 | 0.00 | 0.00 | |
| 3330 | 0.0007 | 466.14 | 367.94 | 98.20 | $1.05 \times 10^{10}$ |
| 3380 | 0.0007 | 481.31 | 391.25 | 90.06 | $0.94 \times 10^{10}$ |
| 3490 | 0.0002 | 778.10 | 672.08 | 106.02 | $0.45 \times 10^{10}$ |
| 4100 | 0.0060 | 697.45 | 692.24 | 5.21 | $6.52 \times 10^{5}$ |
| 4100 | 0.0064 | 680.42 | 665.56 | 14.86 | $1.74 \times 10^{6}$ |

Post inspection revealed specimen was blistered and split from outside to center line.

## Table 108.

### Electrical Resistivity Data for Hafnium Nitride

| Temperature °F | Specimen Circuit Amps | Specimen Circuit Millivolts | Open Circuit Gage Length Potential Millivolts | Closed Circuit Gage Length Potential Millivolts | Resistivity Micro Ohms Centimeter |
|---|---|---|---|---|---|
| 90 | 6.00 | 0.249 | 0.001 | 0.248 | 31.02 |
| 90 | 6.00 | 0.250 | 0.001 | 0.249 | 31.15 |
| 112 | 6.00 | 0.261 | 0.001 | 0.260 | 32.52 |
| 117 | 6.00 | 0.263 | 0.003 | 0.260 | 32.52 |
| 190 | 5.90 | 0.283 | 0.009 | 0.274 | 34.85 |
| 195 | 6.01 | 0.286 | 0.010 | 0.276 | 34.45 |
| 275 | 6.00 | 0.315 | 0.020 | 0.295 | 36.90 |
| 280 | 6.01 | 0.317 | 0.022 | 0.295 | 36.85 |
| 385 | 6.01 | 0.361 | 0.048 | 0.313 | 39.10 |
| 386 | 6.05 | 0.364 | 0.049 | 0.315 | 39.10 |
| 780 | 6.00 | 0.689 | 0.288 | 0.401 | 50.14 |
| 790 | 6.05 | 0.700 | 0.296 | 0.404 | 50.14 |
| 980 | 5.81 | 0.892 | 0.461 | 0.431 | 55.69 |
| 995 | 5.80 | 0.892 | 0.465 | 0.427 | 55.24 |
| 1210 | 5.04 | 0.949 | 0.544 | 0.405 | 60.34 |
| 1220 | 5.00 | 0.936 | 0.534 | 0.402 | 60.34 |
| 1680 | 5.20 | 1.824 | 1.290 | 0.534 | 77.08 |
| 1775 | 5.20 | 1.867 | 1.330 | 0.537 | 77.53 |
| 1940 | 5.40 | 2.510 | 1.793 | 0.717 | 99.67 |
| 1940 | 5.40 | 2.500 | 1.767 | 0.733 | 101.85 |
| 2330 | 5.40 | 3.871 | 3.141 | 0.730 | 101.47 |
| 2330 | 5.40 | 3.749 | 3.031 | 0.718 | 99.82 |
| 2660 | 5.85 | 5.030 | 3.644 | 1.386 | 177.80 |
| 2680 | 5.90 | 5.185 | 3.752 | 1.433 | 182.30 |
| 3140 | 6.00 | 6.251 | 4.530 | 1.721 | 215.25 |
| 3160 | 6.10 | 6.170 | 4.466 | 1.704 | 209.62 |
| 3800 | 6.00 | 6.181 | 4.382 | 1.799 | 225.01 |
| 3810 | 6.01 | 6.150 | 4.225 | 1.925 | 240.39 |
| 4020 | 6.02 | 6.185 | 4.228 | 1.957 | 244.00 |

## Table 109.

## Electrical Resistivity Data for Tantalum Nitride

| Temperature °F | Specimen Circuit | | Open Circuit Gage Length Potential Millivolts | Closed Circuit Gage Length Potential Millivolts | Resistivity Micro Ohms Centimeter |
|---|---|---|---|---|---|
| | Amps | Millivolts | | | |
| 75 | 5.70 | 1.022 | 0.001 | 1.021 | 134.45 |
| 75 | 5.70 | 1.022 | 0.001 | 1.021 | 134.45 |
| 385 | 5.77 | 1.349 | 0.069 | 1.280 | 166.51 |
| 386 | 5.80 | 1.357 | 0.071 | 1.286 | 166.43 |
| 900 | 5.80 | 2.446 | 0.724 | 1.722 | 222.89 |
| 905 | 5.82 | 2.470 | 0.731 | 1.739 | 224.32 |

Next reading gave resistivity of 4.87 x $10^4$ micro ohms-cm; the run was ended to inspect the specimen. Upon inspection the specimen was found to be shattered into several pieces.

### Table 110.

### Electrical Resistivity Data for Titanium Nitride

| Temperature °F | Specimen Circuit Amps | Specimen Circuit Millivolts | Open Circuit Gage Length Potential Millivolts | Closed Circuit Gage Length Potential Millivolts | Resistivity Micro Ohms Centimeter |
|---|---|---|---|---|---|
| 75 | 5.85 | 1.516 | 0.001 | 1.515 | 210.49 |
| 75 | 5.89 | 1.525 | 0.001 | 1.524 | 210.25 |
| 340 | 5.85 | 1.685 | 0.018 | 1.667 | 231.62 |
| 345 | 5.88 | 1.690 | 0.020 | 1.670 | 230.81 |
| 535 | 5.90 | 1.824 | 0.060 | 1.764 | 243.00 |
| 540 | 5.91 | 1.837 | 0.066 | 1.771 | 243.57 |
| 1245 | 5.91 | 2.295 | 0.347 | 1.948 | 267.87 |
| 1260 | 5.95 | 2.321 | 0.360 | 1.961 | 267.87 |
| 1645 | 5.91 | 3.046 | 0.999 | 2.047 | 281.52 |
| 1655 | 5.95 | 3.118 | 1.040 | 2.078 | 283.79 |
| 1940 | 5.95 | 2.090 | 0.177 | 1.913 | 261.28 |
| 1950 | 5.98 | 2.068 | 0.117 | 1.951 | 265.10 |
| 2120 | 5.98 | 2.050 | 0.099 | 1.951 | 265.10 |
| 2530 | 5.99 | 1.708 | -0.218 | 1.926 | 261.28 |
| 2540 | 6.00 | 1.680 | -0.249 | 1.929 | 261.28 |
| 2950 | 5.99 | 1.380 | -0.925 | 2.305 | 312.73 |
| 2960 | 6.00 | 1.362 | -0.947 | 2.309 | 312.73 |
| 2980 | 6.00 | 1.315 | -0.958 | 2.273 | 307.85 |
| 3450 | 6.00 | 0.715 | -1.507 | 2.222 | 300.94 |
| 3470 | 6.01 | 0.720 | -1.472 | 2.192 | 296.39 |
| 4000 | 5.99 | -1.925 | -3.772 | 1.847 | 250.56 |
| 4020 | 5.99 | -1.949 | -3.700 | 1.751 | 237.55 |
| 4020 | 6.00 | -1.795 | -3.664 | 1.869 | 253.16 |
| 2340 | 5.95 | 0.645 | -0.498 | 1.143 | 156.12 |
| 2320 | 5.95 | 0.641 | -0.495 | 1.136 | 155.14 |

Table 111.

Electrical Resistivity Data for
Beryllium Oxide

| Temperature °F | Specimen Circuit | | Open Circuit Gage Length Potential Millivolts | Closed Circuit Gage Length Potential Millivolts | Resistivity Micro Ohms Centimeter |
|---|---|---|---|---|---|
| | Amps | Millivolts | | | |
| 1800 | 0.00 | 0.00 | 0.00 | 0.00 | |
| 2460 | $2.54 \times 10^{-5}$ | 4.00 | 0.00 | 4.00 | $1.2 \times 10^{9}$ |
| 2650 | $1.45 \times 10^{-3}$ | 15.00 | -20.00 | 35.00 | $1.8 \times 10^{7}$ |

Specimen sheared along a 45° plane and became crumbly.

## Table 112.

### Electrical Resistivity Data for Cerium Dioxide

| Temperature °F | Specimen Circuit | | Open Circuit Gage Length Potential Millivolts | Closed Circuit Gage Length Potential Millivolts | Resistivity Micro Ohms Centimeter |
|---|---|---|---|---|---|
| | Amps | Millivolts | | | |
| 75 | 0.0 | 0.0 | 0.0 | 0.0 | |
| 442 | 0.0 | 0.0 | 0.0 | 0.0 | |
| 965 | $1.4 \times 10^{-5}$ | 740.94 | 0.0 | 740.94 | $4.0 \times 10^{10}$ |
| 1600 | $2.4 \times 10^{-5}$ | 22.20 | 21.15 | 1.04 | $3.3 \times 10^{8}$ |
| 1610 | $2.5 \times 10^{-5}$ | 20.80 | 20.55 | .25 | $.76 \times 10^{8}$ |
| 1605 | $2.6 \times 10^{-5}$ | 10.22 | 9.28 | .94 | $2.7 \times 10^{8}$ |
| 2050 | $2.4 \times 10^{-3}$ | 20.92 | 19.05 | 1.87 | $5.9 \times 10^{6}$ |
| 2110 | $2.3 \times 10^{-3}$ | 20.96 | 19.42 | 1.54 | $5.0 \times 10^{6}$ |
| 2590 | .79 | 263.33 | 21.61 | 241.72 | $2.3 \times 10^{5}$ |
| 2640 | .91 | 295.50 | 21.11 | 274.40 | $2.3 \times 10^{5}$ |
| 2680 | 1.28 | 381.70 | 17.48 | 364.22 | $2.1 \times 10^{5}$ |
| 2740 | 1.70 | 482.40 | 16.84 | 465.60 | $2.1 \times 10^{5}$ |
| 2790 | 1.75 | 482.05 | 16.31 | 465.70 | $1.99 \times 10^{5}$ |

## Table 113.

### Electrical Resistivity Data for Hafnium Dioxide

| Temperature °F | Specimen Circuit Amps | Specimen Circuit Millivolts | Open Circuit Gage Length Potential Millivolts | Closed Circuit Gage Length Potential Millivolts | Resistivity Micro Ohms Centimeter |
|---|---|---|---|---|---|
| 70 | 0.0 | 0.0 | 0.0 | 0.0 | |
| 163 | 0.0 | 0.0 | 0.0 | 0.0 | |
| 200 | 0.0 | 0.0 | 0.0 | 0.0 | |
| 310 | 0.0 | 0.0 | 0.0 | 0.0 | |
| 605 | 0.0 | 0.0 | 0.0 | 0.0 | |
| 1005 | 0.0 | 0.0 | 0.0 | 0.0 | |
| 1245 | 0.0 | 0.0 | 0.0 | 0.0 | |
| 2030 | $6.0 \times 10^{-4}$ | 3400.0 | 7.8 | 3392.0 | $4.3 \times 10^{9}$ |
| 1900 | $3.2 \times 10^{-3}$ | 3500.0 | 12.3 | 3488.0 | $8.2 \times 10^{9}$ |
| 1900 | $3.1 \times 10^{-3}$ | 3600.0 | 18.3 | 3582.0 | $9.0 \times 10^{8}$ |
| 2260 | $1.9 \times 10^{-3}$ | 440.0 | 14.0 | 436.0 | $1.7 \times 10^{8}$ |
| 2840 | $11.0 \times 10^{-3}$ | 547.0 | 80.0 | 467.0 | $3.1 \times 10^{7}$ |

### Table 114.

### Electrical Resistivity Data for Magnesium Oxide

| Temperature °F | Specimen Circuit | | Open Circuit Gage Length Potential Millivolts | Closed Circuit Gage Length Potential Millivolts | Resistivity Micro Ohms Centimeter |
|---|---|---|---|---|---|
| | Amps | Millivolts | | | |
| 75 | 0.0 | 0.0 | 0.0 | 0.0 | |
| 350 | 0.0 | 0.0 | 0.0 | 0.0 | |
| 803 | 0.0 | 0.0 | 0.0 | 0.0 | |
| 1205 | 0.0 | 0.0 | 0.0 | 0.0 | |
| 1752 | 0.0 | 0.0 | 0.0 | 0.0 | |
| 2070 | 0.0 | 0.0 | 0.0 | 0.0 | |
| 2370 | 0.0 | 0.0 | 0.0 | 0.0 | |
| 2700 | 0.0 | 0.0 | 0.0 | 0.0 | |
| 3110 | 0.0 | 0.0 | 0.0 | 0.0 | |
| 3250 | 0.0 | 0.0 | 0.0 | 0.0 | |
| 3320 | 0.0 | 0.0 | 0.0 | 0.0 | |
| 3570 | $3.0 \times 10^{-5}$ | 1100.0 | 1000.0 | 100.0 | $2.5 \times 10^{9}$ |
| 3750 | $2.0 \times 10^{-5}$ | 1525.0 | 1510.0 | 15.0 | $5.6 \times 10^{8}$ |

## Table 115.

### Electrical Resistivity Data for Thorium Dioxide

| Temperature °F | Specimen Circuit Amps | Specimen Circuit Millivolts | Open Circuit Gage Length Potential Millivolts | Closed Circuit Gage Length Potential Millivolts | Resistivity Micro Ohms Centimeter |
|---|---|---|---|---|---|
| 1605 | 0.00 | 0.00 | 0.00 | 0.00 | |
| 2060 | 0.00 | 0.00 | 0.00 | 0.00 | |
| 2570 | 0.00 | 0.00 | 0.00 | 0.00 | |
| 2870 | 0.00 | 0.00 | 0.00 | 0.00 | |
| 3130 | 0.01 | 461.62 | 353.57 | 108.05 | $8.11 \times 10^6$ |
| 3555 | 0.03 | 545.35 | 525.39 | 19.96 | $4.99 \times 10^5$ |

## Table 116.

### Electrical Resistivity Data for Zirconium Dioxide

| Temperature °F | Specimen Circuit Amps | Specimen Circuit Millivolts | Open Circuit Gage Length Potential Millivolts | Closed Circuit Gage Length Potential Millivolts | Resistivity Micro Ohms Centimeter |
|---|---|---|---|---|---|
| 74 | 0.0 | 0.0 | 0.0 | 0.0 | |
| 270 | 0.0 | 0.0 | 0.0 | 0.0 | |
| 585 | 0.0 | 0.0 | 0.0 | 0.0 | |
| 1075 | 0.0 | 0.0 | 0.0 | 0.0 | |
| 1555 | 0.0 | 0.0 | 0.0 | 0.0 | |
| 2050 | $4.9 \times 10^{-4}$ | 31.0 | 22.2 | 8.8 | $1.35 \times 10^{7}$ |
| 2270 | $9.8 \times 10^{-4}$ | 6.3 | -40.3 | 34.0 | $2.61 \times 10^{7}$ |
| 3040 | $2.7 \times 10^{-3}$ | 124.9 | 40.9 | 84.0 | $2.34 \times 10^{7}$ |
| 3055 | $2.8 \times 10^{-3}$ | 121.5 | 41.3 | 80.2 | $2.19 \times 10^{7}$ |
| 3330 | $7.6 \times 10^{-2}$ | 425.4 | 286.8 | 138.6 | $1.37 \times 10^{7}$ |
| 3360 | $7.2 \times 10^{-2}$ | 424.5 | 391.2 | 33.3 | $3.48 \times 10^{5}$ |
| 3800 | .54 | 539.4 | 378.7 | 160.7 | $2.23 \times 10^{5}$ |

## Table 117.

### Electrical Resistivity Data for Columbium + 0.5% Zirconium

| Temperature °F | Specimen Circuit Amps | Specimen Circuit Millivolts | Open Circuit Gage Length Potential Millivolts | Closed Circuit Gage Length Potential Millivolts | Resistivity Micro Ohms Centimeter |
|---|---|---|---|---|---|
| 76 | 5.75 | 0.294 | 0.000 | 0.294 | 43.08 |
| 81 | 5.79 | 0.296 | 0.001 | 0.295 | 42.92 |
| 125 | 5.80 | 0.320 | 0.011 | 0.309 | 44.89 |
| 130 | 5.85 | 0.328 | 0.015 | 0.313 | 45.07 |
| 205 | 5.90 | 0.328 | -0.006 | 0.334 | 47.69 |
| 215 | 5.90 | 0.325 | -0.012 | 0.337 | 48.12 |
| 300 | 5.95 | 0.346 | -0.014 | 0.360 | 50.97 |
| 305 | 5.95 | 0.353 | -0.010 | 0.363 | 51.39 |
| 375 | 6.00 | 0.378 | -0.005 | 0.383 | 53.78 |
| 385 | 6.05 | 0.385 | -0.003 | 0.388 | 53.96 |
| 515 | 6.05 | 0.467 | 0.045 | 0.422 | 58.76 |
| 530 | 6.09 | 0.482 | 0.054 | 0.428 | 59.21 |
| 745 | 6.05 | 0.664 | 0.183 | 0.481 | 66.98 |
| 780 | 6.10 | 0.685 | 0.198 | 0.487 | 67.26 |
| 1150 | 6.10 | 0.405 | -0.114 | 0.519 | 71.70 |
| 1150 | 6.15 | 0.274 | -0.274 | 0.548 | 75.07 |
| 1205 | 6.15 | -0.100 | -0.646 | 0.546 | 74.80 |
| 1225 | 6.10 | -0.589 | -1.117 | 0.528 | 72.93 |
| 1460 | 6.15 | -4.646 | -5.233 | 0.587 | 80.37 |
| 1480 | 6.11 | -4.614 | -5.224 | 0.610 | 84.08 |
| 1475 | 6.13 | -4.895 | -5.450 | 0.555 | 76.25 |
| 2030 | 6.15 | 2.177 | 1.450 | 0.727 | 99.58 |
| 2050 | 6.20 | 2.116 | 1.370 | 0.746 | 101.35 |
| 2280 | 6.20 | 2.396 | 1.540 | 0.856 | 116.31 |
| 2330 | 6.20 | 2.391 | 1.551 | 0.840 | 114.20 |

## Table 117 (Continued).

Electrical Resistivity Data for Columbium + 0. 5% Zirconium

| Temperature °F | Specimen Circuit | | Open Circuit Gage Length Potential Millivolts | Closed Circuit Gage Length Potential Millivolts | Resistivity Micro Ohms Centimeter |
|---|---|---|---|---|---|
| | Amps | Millivolts | | | |
| 2650 | 6. 20 | 2. 317 | 1. 407 | 0. 910 | 123. 65 |
| 2740 | 6. 25 | 2. 295 | 1. 363 | 0. 932 | 125. 63 |
| 3000 | 6. 21 | 2. 013 | 1. 030 | 0. 983 | 133. 36 |
| 3100 | 6. 25 | 1. 932 | 0. 946 | 0. 986 | 132. 91 |

## Table 118.

### Electrical Resistivity Data for Molydenum + 0.5% Titanium

| Temperature °F | Specimen Circuit Amps | Specimen Circuit Millivolts | Open Circuit Gage Length Potential Millivolts | Closed Circuit Gage Length Potential Millivolts | Resistivity Micro Ohms Centimeter |
|---|---|---|---|---|---|
| | | First Run Specimen 1 | | | |
| 75 | 6.20 | 0.119 | 0.000 | 0.119 | 15.79 |
| 75 | 6.20 | 0.118 | 0.000 | 0.118 | 15.62 |
| 1500 | 6.30 | 0.619 | 0.222 | 0.397 | 51.79 |
| 1595 | 6.31 | 0.759 | 0.353 | 0.403 | 52.87 |
| 1620 | 6.30 | 0.856 | 0.446 | 0.410 | 53.52 |
| 1820 | 6.25 | 0.640 | 0.165 | 0.475 | 62.49 |
| 1855 | 6.30 | 0.709 | 0.246 | 0.463 | 60.43 |
| 1865 | 6.30 | 0.740 | 0.278 | 0.462 | 60.29 |
| 1880 | 6.30 | 0.820 | 0.360 | 0.460 | 60.02 |
| 2110 | 6.25 | 1.190 | 0.678 | 0.512 | 67.34 |
| 2130 | 6.25 | 1.206 | 0.696 | 0.510 | 67.09 |
| 2130 | 6.29 | 1.210 | 0.695 | 0.515 | 67.34 |
| 2160 | 6.30 | 1.192 | 0.681 | 0.511 | 66.69 |
| 2450 | 6.29 | 1.540 | 0.961 | 0.579 | 75.72 |
| 2530 | 6.30 | 1.580 | 0.986 | 0.594 | 77.53 |
| 2550 | 6.30 | 1.602 | 1.006 | 0.596 | 77.78 |
| 2590 | 6.30 | 1.616 | 1.020 | 0.596 | 77.78 |
| 2640 | 6.30 | 1.634 | 1.032 | 0.602 | 78.76 |
| 2740 | 6.30 | 1.665 | 1.042 | 0.623 | 81.30 |
| 2790 | 6.30 | 1.673 | 1.036 | 0.637 | 83.13 |
| 2840 | 6.30 | 1.690 | 1.047 | 0.643 | 83.91 |

## Table 118 (Continued).

Electrical Resistivity Data for
Molydenum + 0.5% Titanium

| Temperature °F | Specimen Circuit Amps | Specimen Circuit Millivolts | Open Circuit Gage Length Potential Millivolts | Closed Circuit Gage Length Potential Millivolts | Resistivity Micro Ohms Centimeter |
|---|---|---|---|---|---|
| | | Second Run Specimen 1 | | | |
| 75 | 6.09 | 0.106 | -0.001 | 0.107 | 14.44 |
| 75 | 6.10 | 0.107 | -0.001 | 0.108 | 14.55 |
| 84 | 6.00 | 0.108 | -0.002 | 0.110 | 15.00 |
| 84 | 6.00 | 0.109 | -0.001 | 0.110 | 15.07 |
| 129 | 6.00 | 0.118 | 0.002 | 0.116 | 15.89 |
| 132 | 6.00 | 0.119 | 0.003 | 0.116 | 15.89 |
| 203 | 6.00 | 0.133 | 0.006 | 0.127 | 17.40 |
| 205 | 6.00 | 0.133 | 0.006 | 0.127 | 17.40 |
| 437 | 6.00 | 0.182 | 0.015 | 0.165 | 22.61 |
| 442 | 6.05 | 0.186 | 0.017 | 0.169 | 22.96 |
| 750 | 6.09 | 0.169 | -0.060 | 0.229 | 30.91 |
| 755 | 6.10 | 0.182 | -0.055 | 0.237 | 31.94 |
| 1425 | 6.20 | -0.535 | -0.890 | 0.365 | 48.40 |
| 1485 | 6.19 | -0.423 | -0.807 | 0.384 | 51.00 |
| 1850 | 6.10 | -0.146 | -0.585 | 0.439 | 59.17 |
| 1880 | 6.20 | -0.115 | -0.570 | 0.455 | 60.34 |
| 1900 | 6.20 | -0.012 | -0.470 | 0.458 | 60.73 |
| 1905 | 6.20 | 0.079 | 0.389 | 0.468 | 61.99 |
| 2430 | 6.20 | 1.113 | 0.560 | 0.553 | 73.33 |
| 2440 | 6.20 | 1.126 | 0.566 | 0.560 | 74.34 |
| 2700 | 6.20 | 1.154 | 0.583 | 0.571 | 75.72 |
| 2800 | 6.20 | 1.156 | 0.510 | 0.646 | 85.66 |
| 1350 | 6.19 | 0.504 | 0.204 | 0.300 | 39.88 |
| 1250 | 6.20 | 0.482 | 0.189 | 0.293 | 38.86 |
| 1110 | 6.19 | 0.511 | 0.237 | 0.274 | 36.39 |

## Table 118 (Continued).

Electrical Resistivity Data for
Molydenum + 0.5% Titanium

| Temperature °F | Specimen Circuit Amps | Specimen Circuit Millivolts | Open Circuit Gage Length Potential Millivolts | Closed Circuit Gage Length Potential Millivolts | Resistivity Micro Ohms Centimeter |
|---|---|---|---|---|---|
| | | Second Run Specimen 1 | | | |
| 860 | 6.10 | 1.026 | 0.808 | 0.218 | 29.38 |
| 1180 | 6.15 | 1.791 | 1.436 | 0.355 | 47.46 |
| 1280 | 6.12 | 1.634 | 1.316 | 0.318 | 42.72 |
| 1300 | 6.19 | 1.680 | 1.346 | 0.334 | 44.36 |

### Table 119.

### Electrical Resistivity Data for Tungsten (Supplied by Carborundum)

| Temperature °F | Specimen Circuit Amps | Specimen Circuit Millivolts | Open Circuit Gage Length Potential Millivolts | Closed Circuit Gage Length Potential Millivolts | Resistivity Micro Ohms Centimeter |
|---|---|---|---|---|---|
| 75 | 6.00 | 0.055 | 0.001 | 0.056 | 6.98 |
| 75 | 6.00 | 0.045 | 0.001 | 0.046 | 5.78 |
| 111 | 6.00 | 0.045 | -0.005 | 0.050 | 6.23 |
| 113 | 5.99 | 0.045 | -0.017 | 0.062 | 7.80 |
| 193 | 5.95 | 0.053 | -0.005 | 0.058 | 7.28 |
| 195 | 5.98 | 0.054 | -0.005 | 0.059 | 7.43 |
| 285 | 5.97 | 0.065 | -0.003 | 0.068 | 8.48 |
| 290 | 6.00 | 0.066 | -0.002 | 0.068 | 8.48 |
| 395 | 5.98 | 0.080 | 0.007 | 0.073 | 9.15 |
| 396 | 5.99 | 0.081 | 0.008 | 0.073 | 9.15 |
| 515 | 5.95 | 0.100 | 0.013 | 0.087 | 11.03 |
| 520 | 5.98 | 0.100 | 0.013 | 0.087 | 10.89 |
| 770 | 5.99 | 0.169 | 0.035 | 0.134 | 16.80 |
| 775 | 6.00 | 0.154 | 0.036 | 0.118 | 14.78 |
| 1235 | 5.99 | 0.260 | 0.077 | 0.183 | 22.95 |
| 1242 | 5.99 | 0.239 | 0.060 | 0.179 | 22.43 |
| 1770 | 5.99 | 0.494 | 0.245 | 0.249 | 31.21 |
| 1775 | 5.99 | 0.487 | 0.241 | 0.246 | 30.83 |
| 1750 | 6.00 | 0.466 | 0.215 | 0.251 | 31.36 |
| 2235 | 6.00 | 0.574 | 0.260 | 0.314 | 39.23 |
| 2745 | 6.00 | 0.808 | 0.411 | 0.397 | 49.66 |
| 2780 | 6.00 | 0.810 | 0.410 | 0.400 | 50.03 |
| 3320 | 6.00 | 0.875 | 0.406 | 0.469 | 58.66 |
| 3330 | 6.00 | 0.874 | 0.402 | 0.472 | 59.04 |

## Table 119 (Continued).

Electrical Resistivity Data for
Tungsten
(Supplied by Carborundum)

| Temperature °F | Specimen Circuit | | Open Circuit Gage Length Potential Millivolts | Closed Circuit Gage Length Potential Millivolts | Resistivity Micro Ohms Centimeter |
|---|---|---|---|---|---|
| | Amps | Millivolts | | | |
| 3675 | 6.00 | 0.983 | 0.446 | 0.537 | 67.14 |
| 3685 | 6.00 | 0.972 | 0.436 | 0.536 | 66.99 |
| 3790 | 6.00 | 0.963 | 0.407 | 0.556 | 69.54 |
| 3790 | 6.00 | 0.962 | 0.405 | 0.557 | 69.61 |
| 3890 | 6.00 | 1.035 | 0.455 | 0.580 | 72.54 |
| 3950 | 6.00 | 1.051 | 0.464 | 0.587 | 73.36 |
| 3990 | 6.00 | 1.055 | 0.458 | 0.597 | 74.64 |

## Table 120.

### Electrical Resistivity Data for Tungsten (Supplied by General Electric)

| Temperature °F | Specimen Circuit | | Open Circuit Gage Length Potential Millivolts | Closed Circuit Gage Length Potential Millivolts | Resistivity Micro Ohms Centimeter |
|---|---|---|---|---|---|
| | Amps | Millivolts | | | |
| 75 | 30. 7 | 0. 238 | 0. 000 | 0. 238 | 5. 89 |
| 215 | 31. 0 | 0. 246 | -0. 044 | 0. 290 | 7. 12 |
| 230 | 30. 8 | 0. 257 | -0. 037 | 0. 294 | 7. 26 |
| 536 | 30. 8 | 0. 588 | 0. 122 | 0. 466 | 11. 47 |
| 545 | 30. 7 | 0. 737 | 0. 235 | 0. 502 | 12. 38 |
| 679 | 30. 0 | 1. 498 | 0. 980 | 0. 518 | 13. 15 |
| 875 | 30. 5 | 2. 577 | 1. 693 | 0. 884 | 22. 04 |
| 917 | 30. 4 | 3. 355 | 2. 478 | 0. 877 | 22. 64 |
| 920 | 30. 4 | 3. 365 | 2. 531 | 0. 814 | 20. 36 |
| 1295 | 30. 5 | 7. 472 | 6. 370 | 1. 102 | 27. 43 |
| 1290 | 30. 5 | 7. 915 | 6. 825 | 1. 090 | 27. 13 |
| 1950 | 30. 4 | 1. 828 | 0. 398 | 1. 430 | 35. 79 |
| 2025 | 30. 8 | 1. 493 | 0. 095 | 1. 398 | 34. 65 |
| 2025 | 30. 8 | 1. 384 | 0. 000 | 1. 384 | 34. 12 |
| 2470 | 30. 7 | 1. 778 | 0. 048 | 1. 730 | 42. 78 |
| 2700 | 30. 9 | 1. 826 | -0. 015 | 1. 841 | 45. 29 |
| 2710 | 30. 8 | 1. 862 | -0. 010 | 1. 872 | 46. 20 |
| 3270 | 30. 5 | 1. 832 | -0. 388 | 2. 220 | 54. 86 |
| 3270 | 30. 7 | 1. 646 | -0. 677 | 2. 323 | 57. 52 |
| 3300 | 30. 7 | 1. 377 | -0. 954 | 2. 331 | 57. 75 |
| 3750 | 30. 5 | 1. 647 | -0. 995 | 2. 642 | 65. 95 |
| 3920 | 30. 7 | 1. 559 | -1. 303 | 2. 862 | 70. 89 |
| 3950 | 30. 5 | 1. 384 | -1. 483 | 2. 867 | 71. 42 |
| 4210 | 30. 6 | 1. 587 | -1. 557 | 3. 144 | 78. 26 |
| 4360 | 30. 5 | 1. 539 | -1. 683 | 3. 222 | 80. 16 |
| 4330 | 30. 8 | 1. 574 | -1. 687 | 3. 261 | 80. 54 |

## Table 121.

### The Probable Error that can be Anticipated in the Thermoelectric Voltage Data. Basic Data is the Voltage Output per Degree Temperature Differential at Temperature Ordinates

| Curve Value | Data Point | Deviation of Data Point from Curve | Per cent Deviation from Curve | Per cent Deviation Squared |
|---|---|---|---|---|
| -0.0570 | -0.055 | -0.0020 | -3.50 | 12.25 |
| -0.0530 | -0.055 | +0.0020 | 3.77 | 14.21 |
| -0.0525 | -0.061 | +0.0085 | 16.19 | 262.12 |
| -0.0530 | -0.047 | -0.0060 | -11.32 | 128.14 |
| -0.0410 | -0.042 | +0.0010 | 2.43 | 5.90 |
| -0.0410 | -0.038 | -0.0030 | -7.31 | 53.44 |
| -0.0400 | -0.042 | +0.0020 | 5.00 | 25.00 |
| -0.0300 | -0.029 | -0.0010 | -3.33 | 11.09 |
| -0.0290 | -0.030 | +0.0010 | 3.44 | 11.83 |
| -0.0250 | -0.025 | 0.0000 | 0.00 | 0.00 |
| -0.0240 | -0.025 | +0.0010 | 4.16 | 17.31 |
| -0.0210 | -0.021 | 0.0000 | 0.00 | 0.00 |
| -0.0205 | -0.020 | -0.0005 | -2.43 | 5.90 |
| -0.0210 | -0.020 | -0.0010 | -4.76 | 22.66 |
| -0.0700 | -0.076 | +0.0060 | 8.57 | 73.44 |
| -0.0720 | -0.066 | -0.0060 | -8.33 | 69.39 |

$$\Sigma X^2 = 712.68$$

$$\text{Standard Deviation} = \sqrt{\frac{\Sigma X^2}{n - 2}}$$

$$= \sqrt{\frac{712.68}{14}}$$

$$= 7.14$$

Probable Error = 0.6745 Standard Deviation
= 4.82%

Therefore, 50% of all values of the thermoelectric voltage deviate from the curve value by no more than 4.82%. This value includes the reading variation in picking values off the curve.

## Table 122.

### Thermoelectric Voltage Data for Hafnium Diboride

| Mean Temperature °F | Specimen ΔT °F | Resultant Voltage Output Millivolts | Voltage Output Per Degree Temperature Differential Mv/°F |
|---|---|---|---|
| 1670 | 120 | 0.05 | 0.000 |
| 1685 | 117 | 0.00 | 0.000 |
| 1945 | 160 | 0.40 | 0.003 |
| 1970 | 140 | 0.40 | 0.003 |
| 2290 | 160 | 0.80 | 0.005 |
| 2295 | 170 | 0.80 | 0.005 |
| 2635 | 170 | 1.50 | 0.009 |
| 2633 | 165 | 1.50 | 0.009 |
| 2978 | 245 | 2.60 | 0.011 |
| 2975 | 240 | 2.60 | 0.011 |
| 3298 | 245 | 3.40 | 0.014 |
| 3305 | 230 | 3.40 | 0.015 |
| 3578 | 255 | 4.05 | 0.016 |
| 3588 | 255 | 4.00 | 0.016 |
| 3858 | 275 | 4.40 | 0.016 |
| 3875 | 250 | 4.45 | 0.018 |
| 4113 | 195 | 3.50 | 0.018 |
| 4120 | 220 | 3.40 | 0.015 |
| 4333 | 255 | 3.65 | 0.014 |
| 4338 | 265 | 3.80 | 0.014 |
| Specimen Found Cracked on Post Inspection | | | |

## Table 124.

### Thermoelectric Voltage Data for Titanium Diboride

| Mean Temperature °F | Specimen ΔT °F | Resultant Voltage Output Millivolts | Voltage Output Per Degree Temperature Differential Mv/°F |
|---|---|---|---|
| 1815 | 130 | 0.25 | 0.002 |
| 1825 | 130 | 0.30 | 0.002 |
| 2155 | 190 | 0.65 | 0.003 |
| 2170 | 180 | 0.60 | 0.003 |
| 2685 | 210 | 0.90 | 0.004 |
| 2683 | 235 | 0.80 | 0.003 |
| 2665 | 210 | 0.85 | 0.004 |
| 2808 | 275 | 1.40 | 0.005 |
| 2813 | 275 | 1.40 | 0.005 |
| 2983 | 295 | 2.40 | 0.008 |
| 2978 | 285 | 2.45 | 0.009 |
| 3163 | 325 | 3.10 | 0.010 |
| 3363 | 325 | 4.80 | 0.015 |
| 3365 | 330 | 4.85 | 0.015 |
| 3525 | 350 | 5.80 | 0.017 |
| 3543 | 365 | 6.05 | 0.017 |
| 3745 | 370 | 7.20 | 0.019 |
| 3765 | 370 | 7.25 | 0.020 |
| 3948 | 385 | 8.00 | 0.021 |
| 3965 | 390 | 8.00 | 0.021 |
| 4135 | 350 | 8.50 | 0.024 |
| 4150 | 400 | 8.50 | 0.021 |

## Table 123.

### Thermoelectric Voltage Data for Thorium Tetraboride

| Mean Temperature °F | Specimen ΔT °F | Resultant Voltage Output Millivolts | Voltage Output Per Degree Temperature Differential Mv/°F |
|---|---|---|---|
| 1765 | 150 | -1.20 | -0.008 |
| 1845 | 150 | -1.20 | -0.008 |
| 1928 | 145 | -1.00 | -0.007 |
| 2100 | 140 | -0.40 | -0.003 |
| 2368 | 195 | 0.15 | 0.001 |
| 2375 | 200 | 0.20 | 0.001 |
| 2640 | 220 | 0.65 | 0.003 |
| 2653 | 205 | 0.60 | 0.003 |
| 2705 | 210 | 0.70 | 0.003 |
| 3160 | 320 | 2.10 | 0.007 |
| 3145 | 350 | 2.40 | 0.007 |
| 3210 | 360 | 2.40 | 0.007 |
| 3233 | 315 | 2.65 | 0.008 |
| 3190 | 340 | 2.50 | 0.007 |

Table 125.

Thermoelectric Voltage Data for Tungsten Boride

| Mean Temperature °F | Specimen ΔT °F | Resultant Voltage Output Millivolts | Voltage Output Per Degree Temperature Differential Mv/°F |
|---|---|---|---|
| | First Run, Specimen 1 | | |
| 1805 | 310 | -0.35 | -0.001 |
| 1925 | 330 | -0.35 | -0.001 |
| 1980 | 360 | -0.40 | -0.001 |
| 2135 | 470 | -0.15 | 0.000 |
| 2335 | 470 | 0.25 | 0.001 |
| 2325 | 450 | 0.15 | 0.000 |
| 2338 | 455 | 0.20 | 0.000 |
| 2528 | 445 | 1.05 | 0.002 |
| 2530 | 490 | 1.00 | 0.002 |
| 2525 | 500 | 1.00 | 0.002 |
| 2665 | 550 | 1.70 | 0.003 |
| 2675 | 550 | 1.65 | 0.003 |
| 2895 | 630 | 3.15 | 0.005 |
| 2855 | 650 | 3.00 | 0.005 |
| 3022 | 685 | 3.95 | 0.006 |
| 3017 | 695 | 3.85 | 0.006 |
| 3185 | 670 | 4.60 | 0.007 |
| 3180 | 680 | 4.50 | 0.007 |
| 3405 | 750 | 5.60 | 0.007 |
| 3435 | 770 | 5.65 | 0.007 |
| 3585 | 730 | 6.70 | 0.009 |
| 3565 | 710 | 6.75 | 0.010 |
| 3767 | 705 | 7.80 | 0.011 |
| 3802 | 715 | 8.30 | 0.012 |
| 3872 | 725 | 9.00 | 0.012 |
| 3880 | 660 | 9.40 | 0.014 |

## Table 125 (Continued).

### Thermoelectric Voltage Data for Tungsten Boride

| Mean Temperature °F | Specimen ΔT °F | Resultant Voltage Output Millivolts | Voltage Output Per Degree Temperature Differential Mv/°F |
|---|---|---|---|
| | Second Run, | Specimen 1 | |
| 1580 | 80 | -2.85 | -0.036 |
| 1600 | 100 | -2.90 | -0.029 |
| 2130 | 120 | -2.60 | -0.022 |
| 2885 | 170 | -0.60 | -0.004 |
| 3000 | 200 | -0.45 | -0.002 |
| 3188 | 175 | 0.00 | 0.000 |

## Table 126.

### Thermoelectric Voltage Data for Zirconium Diboride

| Mean Temperature °F | Specimen ΔT °F | Resultant Voltage Output Millivolts | Voltage Output Per Degree Temperature Differential Mv/°F |
|---|---|---|---|
| 1837 | 135 | 0.35 | 0.003 |
| 1820 | 100 | 0.30 | 0.003 |
| 2035 | 110 | 0.60 | 0.005 |
| 2043 | 115 | 0.59 | 0.005 |
| 2285 | 120 | 0.75 | 0.006 |
| 2283 | 125 | 0.75 | 0.006 |
| 2478 | 125 | 1.05 | 0.008 |
| 2513 | 135 | 1.00 | 0.007 |
| 2853 | 195 | 1.95 | 0.010 |
| 2893 | 205 | 2.00 | 0.010 |
| 3045 | 230 | 2.85 | 0.012 |
| 3045 | 230 | 2.85 | 0.012 |
| 3310 | 280 | 3.65 | 0.013 |
| 3315 | 270 | 3.60 | 0.013 |
| 3515 | 290 | 4.05 | 0.014 |
| 3495 | 270 | 4.20 | 0.015 |
| 3678 | 245 | 4.60 | 0.019 |
| 3675 | 250 | 4.65 | 0.019 |
| Specimen Found Melted on Post Inspection | | | |

## Table 127.

### Thermoelectric Voltage Data for Columbium Carbide

| Mean Temperature °F | Specimen ΔT °F | Resultant Voltage Output Millivolts | Voltage Output Per Degree Temperature Differential Mv/°F |
|---|---|---|---|
| 1805 | 30 | 1.60 | 0.053 |
| 1850 | 40 | 1.80 | 0.045 |
| 1890 | 40 | 2.00 | 0.050 |
| 2265 | 30 | 1.80 | 0.060 |
| 2316 | 35 | 1.75 | 0.050 |
| 2615 | 40 | 1.80 | 0.045 |
| 2680 | 30 | 1.75 | 0.058 |
| 2723 | 45 | 1.95 | 0.043 |
| 2863 | 45 | 2.00 | 0.044 |
| 3077 | 35 | 1.80 | 0.051 |
| 3087 | 35 | 1.80 | 0.051 |
| 3087 | 35 | 1.65 | 0.047 |
| 3085 | 30 | 1.60 | 0.053 |
| 3333 | 55 | 1.50 | 0.027 |
| 3330 | 60 | 1.50 | 0.025 |
| 3330 | 60 | 1.45 | 0.024 |
| 3502 | 55 | 1.40 | 0.025 |
| 3507 | 55 | 1.40 | 0.025 |
| 3525 | 50 | 1.40 | 0.028 |
| 3742 | 75 | 1.70 | 0.023 |
| 3760 | 60 | 1.60 | 0.027 |
| 3752 | 75 | 1.40 | 0.019 |
| 3752 | 65 | 1.35 | 0.021 |
| 3982 | 55 | 1.40 | 0.025 |
| 3962 | 65 | 1.25 | 0.019 |
| 3985 | 50 | 0.95 | 0.019 |

Table 128.

Thermoelectric Voltage Data for
Dimolybdenum Carbide

| Mean Temperature °F | Specimen ΔT °F | Resultant Voltage Output Millivolts | Voltage Output Per Degree Temperature Differential Mv/°F |
|---|---|---|---|
| 1728 | 291 | 1.25 | 0.004 |
| 1724 | 283 | 1.30 | 0.005 |
| 2025 | 350 | 2.15 | 0.006 |
| 2045 | 370 | 2.25 | 0.006 |
| 2418 | 405 | 4.20 | 0.010 |
| 2440 | 420 | 4.30 | 0.010 |
| 2588 | 555 | 6.20 | 0.011 |
| 2703 | 425 | 6.45 | 0.015 |
| 2915 | 490 | 7.80 | 0.016 |
| 2960 | 480 | 7.90 | 0.017 |
| 3170 | 480 | 9.20 | 0.019 |
| 3183 | 475 | 9.20 | 0.019 |
| 3468 | 475 | 6.00 | 0.013 |
| 3470 | 480 | 6.00 | 0.013 |
| Specimen Melted During Run | | | |

## Table 129.

### Thermoelectric Voltage Data for Hafnium Carbide

| Mean Temperature °F | Specimen ΔT °F | Resultant Voltage Output Millivolts | Voltage Output Per Degree Temperature Differential Mv/°F |
|---|---|---|---|
| 1585 | 100 | 1.70 | 0.017 |
| 1597 | 115 | 1.75 | 0.015 |
| 2140 | 140 | 2.75 | 0.020 |
| 2125 | 150 | 2.60 | 0.017 |
| 2537 | 175 | 4.10 | 0.023 |
| 2857 | 215 | 4.80 | 0.022 |
| 2860 | 220 | 4.80 | 0.022 |
| 3040 | 240 | 5.60 | 0.023 |
| 3035 | 240 | 5.55 | 0.023 |
| 3350 | 300 | 6.20 | 0.021 |
| 3337 | 315 | 6.20 | 0.020 |
| 3600 | 320 | 6.75 | 0.021 |
| 3607 | 315 | 6.75 | 0.021 |
| 3810 | 280 | 7.00 | 0.025 |
| 3830 | 300 | 7.15 | 0.024 |
| 4000 | 340 | 8.20 | 0.024 |
| 4205 | 330 | 7.80 | 0.024 |
| 4205 | 330 | 7.80 | 0.024 |
| 4365 | 310 | 7.60 | 0.025 |
| 4360 | 320 | 7.60 | 0.024 |
| 4525 | 410 | 8.80 | 0.021 |
| 4545 | 390 | 9.25 | 0.024 |
| 4700 | 360 | 8.90 | 0.025 |
| 4675 | 350 | 9.10 | 0.026 |
| 4775 | 390 | 8.00 | 0.021 |

## Table 130.

### Thermoelectric Voltage Data for Tantalum Carbide

| Mean Temperature °F | Specimen ΔT °F | Resultant Voltage Output Millivolts | Voltage Output Per Degree Temperature Differential Mv/°F |
|---|---|---|---|
| 1825 | 50 | 0.40 | 0.008 |
| 1830 | 60 | 0.50 | 0.008 |
| 1830 | 60 | 0.60 | 0.010 |
| 2190 | 80 | 1.25 | 0.016 |
| 2207 | 85 | 1.30 | 0.015 |
| 2215 | 80 | 1.20 | 0.015 |
| 2500 | 80 | 1.50 | 0.019 |
| 2525 | 80 | 1.50 | 0.019 |
| 2632 | 125 | 1.95 | 0.016 |
| 2885 | 130 | 2.60 | 0.020 |
| 2855 | 150 | 2.60 | 0.017 |
| 2850 | 150 | 2.65 | 0.018 |
| 3010 | 120 | 2.80 | 0.023 |
| 3022 | 155 | 2.55 | 0.016 |
| 3015 | 170 | 2.65 | 0.016 |
| 3070 | 160 | 3.00 | 0.019 |
| 3272 | 145 | 3.55 | 0.024 |
| 3270 | 180 | 4.00 | 0.022 |
| 3277 | 195 | 4.30 | 0.022 |
| 3445 | 170 | 4.85 | 0.029 |
| 3437 | 225 | 5.00 | 0.022 |
| 3685 | 130 | 4.00 | 0.031 |
| 3653 | 195 | 5.30 | 0.027 |
| 3640 | 220 | 5.50 | 0.025 |
| 3840 | 140 | 4.30 | 0.031 |
| 3830 | 220 | 5.80 | 0.026 |
| 3820 | 220 | 5.75 | 0.026 |
| 4110 | 180 | 4.60 | 0.026 |

Table 130 (Continued).

Thermoelectric Voltage Data for Tantalum Carbide

| Mean Temperature °F | Specimen ΔT °F | Resultant Voltage Output Millivolts | Voltage Output Per Degree Temperature Differential Mv/°F |
|---|---|---|---|
| 4110 | 180 | 4.40 | 0.024 |
| 4085 | 230 | 6.15 | 0.027 |
| 4310 | 180 | 4.90 | 0.027 |
| 4288 | 225 | 5.40 | 0.024 |

# Table 131.

## Thermoelectric Voltage Data for Titanium Carbide

| Mean Temperature °F | Specimen ΔT °F | Resultant Voltage Output Millivolts | Voltage Output Per Degree Temperature Differential Mv/°F |
|---|---|---|---|
| First Run, Specimen 1 | | | |
| 1649 | 38 | -1.05 | -0.028 |
| 1674 | 12 | -1.15 | -0.096 |
| 1858 | 15 | -1.60 | -0.107 |
| 1863 | 15 | -1.60 | -0.107 |
| 2088 | 15 | -1.70 | -0.113 |
| 2090 | 20 | -1.80 | -0.090 |
| 2403 | 25 | -1.75 | -0.070 |
| 2405 | 30 | -1.65 | -0.055 |
| 2428 | 35 | -1.60 | -0.046 |
| 2673 | 35 | -1.00 | -0.029 |
| 2678 | 35 | -0.90 | -0.026 |
| 2815 | 30 | -0.65 | -0.022 |
| 2816 | 45 | -0.75 | -0.017 |
| 3030 | 40 | -0.60 | -0.015 |
| 3020 | 40 | -0.60 | -0.015 |
| 3185 | 50 | -0.40 | -0.008 |
| 3185 | 70 | -0.45 | -0.006 |
| 3420 | 40 | -0.30 | -0.008 |
| 3378 | 35 | -0.20 | -0.006 |
| 3575 | 30 | -0.25 | -0.008 |
| 3573 | 35 | -0.25 | -0.007 |
| 3838 | 55 | -0.25 | -0.005 |
| 3845 | 30 | -0.20 | -0.007 |
| 4010 | 40 | -0.70 | -0.018 |
| 4010 | 40 | -0.60 | -0.015 |

Table 131 (Continued).

Thermoelectric Voltage Data for Titanium Carbide

| Mean Temperature °F | Specimen ΔT °F | Resultant Voltage Output Millivolts | Voltage Output Per Degree Temperature Differential Mv/°F |
|---|---|---|---|
| | Second Run, Specimen 1 | | |
| 1905 | 110 | -3.10 | -0.028 |
| 1910 | 120 | -3.10 | -0.026 |
| 3180 | 100 | -1.60 | -0.016 |
| 3478 | 145 | -1.00 | -0.007 |

## Table 132.

### Thermoelectric Voltage Data for Tungsten Carbide

| Mean Temperature °F | Specimen ΔT °F | Resultant Voltage Output Millivolts | Voltage Output Per Degree Temperature Differential Mv/°F |
|---|---|---|---|
| | First Run, Specimen 1 | | |
| 1555 | 130 | -2.05 | -0.016 |
| 1589 | 122 | -2.15 | -0.018 |
| 1825 | 170 | -2.00 | -0.012 |
| 1933 | 145 | -2.15 | -0.015 |
| 1975 | 150 | -2.15 | -0.014 |
| 2335 | 170 | 0.00 | 0.000 |
| 2388 | 175 | 0.20 | 0.001 |
| | Second Run, Specimen 1 | | |
| 1823 | 65 | -3.60 | -0.055 |
| 1833 | 65 | -3.65 | -0.056 |
| 2648 | 55 | -1.50 | -0.027 |
| 2648 | 45 | -1.45 | -0.032 |
| 3065 | 90 | -0.35 | -0.004 |
| 3075 | 70 | -0.25 | -0.004 |
| 3345 | 110 | 0.05 | 0.001 |
| 3360 | 100 | 0.10 | 0.001 |
| 3688 | 125 | 0.05 | 0.000 |
| 3705 | 130 | 0.10 | 0.001 |
| 4000 | 140 | -0.40 | -0.003 |
| 4035 | 130 | -0.55 | -0.004 |
| 4215 | 130 | -0.80 | -0.007 |
| 4215 | 110 | -1.00 | -0.009 |
| 4373 | 105 | -1.80 | -0.017 |
| 4415 | 90 | -2.20 | -0.024 |
| Specimen Found Partially Melted on Post Inspection | | | |

## Table 133.

### Thermoelectric Voltage Data for Vanadium Carbide

| Mean Temperature °F | Specimen ΔT °F | Resultant Voltage Output Millivolts | Voltage Output Per Degree Temperature Differential Mv/°F |
|---|---|---|---|
| First Run, Specimen 1 | | | |
| 1652 | 165 | -0.20 | -0.001 |
| 1670 | 160 | -0.20 | -0.001 |
| 1860 | 190 | 0.25 | 0.001 |
| 1940 | 180 | 0.30 | 0.002 |
| 2188 | 165 | 1.00 | 0.006 |
| 2205 | 150 | 1.10 | 0.007 |
| 2260 | 180 | 1.15 | 0.006 |
| 2527 | 225 | 1.95 | 0.009 |
| 2550 | 240 | 1.90 | 0.008 |
| 2780 | 280 | 3.40 | 0.012 |
| 2790 | 300 | 3.60 | 0.012 |
| 2982 | 355 | 4.50 | 0.013 |
| 2985 | 350 | 4.40 | 0.013 |
| 3252 | 405 | 5.10 | 0.013 |
| 3220 | 400 | 5.20 | 0.013 |
| 3462 | 475 | 6.15 | 0.013 |
| 3495 | 390 | 6.00 | 0.015 |
| 3680 | 360 | 6.45 | 0.018 |
| 3675 | 350 | 6.50 | 0.019 |
| Second Run, Specimen 1 | | | |
| 1833 | 185 | -2.15 | -0.012 |
| 1833 | 185 | -2.25 | -0.012 |
| 2505 | 170 | 0.60 | 0.004 |

## Table 133 (Continued).

### Thermoelectric Voltage Data for Vanadium Carbide

| Mean Temperature °F | Specimen ΔT °F | Resultant Voltage Output Millivolts | Voltage Output Per Degree Temperature Differential Mv/°F |
|---|---|---|---|
| 2905 | 310 | 1.65 | 0.005 |
| 2973 | 255 | 1.75 | 0.007 |
| 1970 | 160 | -2.15 | -0.013 |

## Table 134.

### Thermoelectric Voltage Data for Zirconium Carbide

| Mean Temperature °F | Specimen ΔT °F | Resultant Voltage Output Millivolts | Voltage Output Per Degree Temperature Differential Mv/°F |
|---|---|---|---|
| 1730 | 50 | -0.55 | -0.011 |
| 1748 | 45 | -0.60 | -0.013 |
| 1758 | 45 | -0.60 | -0.013 |
| 2063 | 75 | -1.00 | -0.013 |
| 2083 | 65 | -0.95 | -0.015 |
| 2415 | 70 | -1.15 | -0.016 |
| 2415 | 90 | -1.20 | -0.013 |
| 2700 | 120 | -2.60 | -0.022 |
| 2733 | 115 | -2.65 | -0.023 |
| 3080 | 140 | -6.00 | -0.043 |
| 3135 | 130 | -6.00 | -0.046 |
| 3415 | 90 | -2.90 | -0.032 |
| 3405 | 90 | -2.00 | -0.022 |
| 3395 | 90 | -1.90 | -0.021 |
| 3718 | 55 | -1.00 | -0.018 |
| 3720 | 60 | -1.05 | -0.018 |
| 3963 | 65 | -1.00 | -0.015 |
| 3965 | 70 | -1.05 | -0.015 |
| 4170 | 80 | -0.80 | -0.010 |

## Table 135

### Thermoelectric Voltage Data for Boron Nitride

| Mean Temperature °F | Specimen ΔT °F | Resultant Voltage Output Millivolts | Voltage Output Per Degree Temperature Differential Mv/°F |
|---|---|---|---|
| 1680 | 160 | -1.70 | -0.011 |
| 1713 | 155 | -2.60 | -0.017 |
| 1710 | 150 | -2.20 | -0.015 |
| 2198 | 335 | -69.50 | -0.208 |
| 2203 | 305 | -68.00 | -0.223 |
| 2378 | 295 | -120.00 | -0.407 |
| 2454 | 308 | -125.00 | -0.406 |
| 2415 | 330 | -125.00 | -0.379 |
| 2713 | 415 | -140.00 | -0.337 |
| 2718 | 425 | -155.00 | -0.365 |
| 2810 | 430 | -140.00 | -0.326 |
| 2818 | 435 | -140.00 | -0.322 |
| 3133 | 445 | -120.00 | -0.270 |
| 3120 | 360 | -60.00 | -0.167 |
| 3158 | 395 | 15.00 | 0.038 |
| 3390 | 480 | 165.00 | 0.344 |
| 3385 | 350 | 245.00 | 0.700 |
| 3545 | 250 | 300.00 | 1.200 |
| 3570 | 260 | 300.00 | 1.154 |
| 3575 | 260 | 295.00 | 1.135 |
| Specimen Found Cracked on Post Inspection | | | |

## Table 136.

### Thermoelectric Voltage Data for Hafnium Nitride

| Mean Temperature °F | Specimen ΔT °F | Resultant Voltage Output Millivolts | Voltage Output Per Degree Temperature Differential Mv/°F |
|---|---|---|---|
| 1832 | 73 | -3.25 | -0.045 |
| 1832 | 73 | -3.20 | -0.044 |
| 2045 | 90 | -2.95 | -0.033 |
| 2075 | 100 | -2.85 | -0.029 |
| 2105 | 90 | -2.60 | -0.029 |
| 2428 | 155 | -2.60 | -0.017 |
| 2448 | 145 | -2.60 | -0.018 |
| 2445 | 150 | -2.45 | -0.016 |
| 2770 | 180 | -1.80 | -0.010 |
| 2783 | 205 | -1.70 | -0.008 |
| 2823 | 175 | -1.65 | -0.009 |
| 3105 | 210 | -0.80 | -0.004 |
| 3213 | 205 | -0.70 | -0.003 |
| 3185 | 230 | -0.70 | -0.003 |
| 3570 | 220 | 0.05 | 0.000 |
| 3565 | 230 | 0.06 | 0.000 |
| 3555 | 250 | 0.06 | 0.000 |
| 4245 | 210 | 2.60 | 0.012 |
| 4245 | 210 | 2.80 | 0.013 |
| 4448 | 195 | 2.95 | 0.015 |
| 4478 | 195 | 3.00 | 0.015 |
| 4463 | 225 | 3.10 | 0.014 |

## Table 137.

### Thermoelectric Voltage Data for Titanium Nitride

| Mean Temperature °F | Specimen ΔT °F | Resultant Voltage Output Millivolts | Voltage Output Per Degree Temperature Differential Mv/°F |
|---|---|---|---|
| 1568 | 65 | -3.55 | -0.055 |
| 1565 | 60 | -3.80 | -0.063 |
| 1570 | 60 | -4.05 | -0.068 |
| 2398 | 145 | -2.40 | -0.017 |
| 2403 | 135 | -2.35 | -0.017 |
| 2820 | 200 | -0.55 | -0.003 |
| 2825 | 200 | -0.50 | -0.003 |
| 3103 | 255 | 0.80 | 0.003 |
| 3093 | 235 | 0.75 | 0.003 |
| 3448 | 255 | 1.50 | 0.006 |
| 3453 | 245 | 1.45 | 0.006 |
| 3760 | 280 | 2.70 | 0.010 |
| 3763 | 275 | 2.80 | 0.010 |
| 4135 | 290 | 4.90 | 0.017 |
| 4108 | 235 | 5.35 | 0.023 |
| 4148 | 305 | 5.85 | 0.019 |
| 4380 | 250 | 7.35 | 0.029 |
| 4410 | 280 | 7.30 | 0.026 |
| 4425 | 270 | 7.40 | 0.027 |

## Table 138.

## Thermoelectric Voltage Data for Beryllium Oxide

| Mean Temperature °F | Specimen ΔT °F | Resultant Voltage Output Millivolts | Voltage Output Per Degree Temperature Differential Mv/°F |
|---|---|---|---|
| 1720 | 300 | 7.50 | 0.025 |
| 1850 | 240 | 9.00 | 0.038 |
| 1993 | 265 | 7.50 | 0.028 |
| 2030 | 230 | 8.00 | 0.035 |
| 2473 | 335 | -25.00 | -0.075 |
| 2425 | 290 | -21.00 | -0.072 |
| 2460 | 320 | -22.00 | -0.069 |
| 2810 | 380 | -39.00 | -0.103 |
| 2815 | 380 | -65.00 | -0.171 |
| 2760 | 320 | -60.00 | -0.188 |
| 3100 | 500 | -60.00 | -0.120 |
| 3135 | 370 | -60.00 | -0.162 |
| Specimen Found Crumbled on Post Inspection | | | |

## Table 139.

### Thermoelectric Voltage Data for Cerium Dioxide

| Mean Temperature °F | Specimen ΔT °F | Resultant Voltage Output Millivolts | Voltage Output Per Degree Temperature Differential Mv/°F |
|---|---|---|---|
| | First Run, Specimen 1 | | |
| 1530 | 100 | 52.0 | 0.520 |
| 1558 | 115 | 47.0 | 0.409 |
| 1578 | 125 | 44.0 | 0.352 |
| 1863 | 145 | 42.0 | 0.270 |
| 1885 | 150 | 37.5 | 0.250 |
| | Second Run, Specimen 1 | | |
| 1655 | 160 | 51.5 | 0.322 |
| 1753 | 185 | 44.5 | 0.241 |
| 1815 | 210 | 42.5 | 0.202 |
| 2255 | 230 | 30.0 | 0.130 |
| 2275 | 250 | 26.0 | 0.104 |
| 2293 | 255 | 26.0 | 0.102 |
| 2685 | 280 | 18.0 | 0.064 |
| 2698 | 275 | 20.0 | 0.073 |
| 2685 | 310 | 21.5 | 0.069 |
| 3015 | 290 | -6.0 | -0.021 |
| 3040 | 260 | -20.0 | -0.077 |
| 3053 | 295 | -28.0 | -0.095 |

## Table 140.

### Thermoelectric Voltage Data for Hafnium Dioxide

| Mean Temperature °F | Specimen ΔT °F | Resultant Voltage Output Millivolts | Voltage Output Per Degree Temperature Differential Mv/°F |
|---|---|---|---|
| 1745 | 30 | -28.0 | -0.933 |
| 1750 | 20 | -28.0 | -1.400 |
| 1775 | 40 | -28.5 | -0.713 |
| 2125 | 10 | -260.0 | -26.000 |
| 2135 | 10 | -245.0 | -24.500 |
| 2553 | 35 | -42.0 | -1.200 |
| 2653 | 35 | -32.0 | -0.971 |
| 2968 | 65 | -220.0 | -3.385 |
| 2980 | 60 | -225.0 | -3.750 |
| 3395 | 70 | -32.0 | -0.457 |
| 3415 | 90 | -24.0 | -0.267 |
| 3410 | 80 | -19.5 | -0.244 |
| 3725 | 100 | 8.0 | 0.080 |
| 3728 | 95 | 8.5 | 0.090 |
| 4040 | 120 | 10.0 | 0.083 |
| 4075 | 90 | 9.5 | 0.106 |
| 4100 | 100 | 9.0 | 0.090 |
| 4320 | 100 | -2.0 | -0.020 |
| 4320 | 100 | -2.0 | -0.020 |

## Table 141.

### Thermoelectric Voltage Data for Magnesium Oxide

| Mean Temperature °F | Specimen ΔT °F | Resultant Voltage Output Millivolts | Voltage Output Per Degree Temperature Differential Mv/°F |
|---|---|---|---|
| 1810 | 100 | -0.60 | -0.006 |
| 1815 | 100 | -0.55 | -0.006 |
| 1983 | 65 | -60.00 | -0.923 |
| 2060 | 60 | -60.00 | -1.000 |
| 2370 | 40 | -95.00 | -2.375 |
| 3383 | 35 | -90.00 | -2.571 |
| 2565 | 110 | -35.00 | -0.318 |
| 2595 | 110 | -40.00 | -0.364 |
| 2818 | 165 | -45.00 | -0.273 |
| 2830 | 170 | -45.00 | -0.265 |
| 3190 | 180 | -40.00 | -0.222 |
| 3265 | 170 | -40.00 | -0.235 |
| 3465 | 330 | -70.00 | -0.212 |
| 3470 | 320 | -70.00 | -0.219 |
| 3785 | 350 | 0.00 | 0.000 |
| 3835 | 330 | 5.00 | 0.015 |

## Table 142.

### Thermoelectric Voltage Data for Thorium Dioxide

| Mean Temperature °F | Specimen ΔT °F | Resultant Voltage Output Millivolts | Voltage Output Per Degree Temperature Differential Mv/°F |
|---|---|---|---|
| 1873 | 125 | 185.0 | 1.480 |
| 1930 | 140 | 240.0 | 1.714 |
| 1990 | 150 | 205.0 | 1.367 |
| 2318 | 115 | 105.0 | 0.913 |
| 2365 | 170 | 95.0 | 0.559 |
| 2375 | 210 | 90.0 | 0.429 |
| 2500 | 200 | 100.0 | 0.500 |
| 2468 | 195 | 100.0 | 0.512 |
| 2558 | 235 | 80.0 | 0.340 |
| 2810 | 280 | 40.0 | 0.143 |
| 2788 | 285 | 40.0 | 0.140 |
| 2760 | 340 | 55.0 | 0.162 |
| 2965 | 410 | 80.0 | 0.195 |
| 2900 | 340 | 60.0 | 0.176 |
| 2930 | 360 | 45.0 | 0.125 |

## Table 143.

### Thermoelectric Voltage Data for Zirconium Dioxide

| Mean Temperature °F | Specimen ΔT °F | Resultant Voltage Output Millivolts | Voltage Output Per Degree Temperature Differential Mv/°F |
|---|---|---|---|
| 1843 | 175 | -320.0 | -1.829 |
| 1960 | 160 | -365.0 | -2.281 |
| 2083 | 155 | -400.0 | -2.581 |
| 2733 | 115 | 13.5 | 0.117 |
| 2748 | 145 | 14.0 | 0.097 |
| 2758 | 155 | 16.0 | 0.103 |
| 2958 | 185 | 32.5 | 0.176 |
| 2973 | 185 | 34.5 | 0.187 |
| 2990 | 220 | 36.0 | 0.164 |
| 3238 | 275 | 48.0 | 0.175 |
| 3263 | 225 | 50.0 | 0.222 |
| 3265 | 260 | 50.0 | 0.192 |
| 3283 | 265 | 51.0 | 0.193 |
| 3580 | 340 | 64.5 | 0.190 |
| 3580 | 320 | 64.0 | 0.200 |
| 3575 | 350 | 64.0 | 0.183 |
| 3713 | 375 | 60.0 | 0.160 |
| 3730 | 340 | 57.5 | 0.169 |
| 4060 | 300 | 43.0 | 0.143 |
| 4068 | 315 | 39.5 | 0.125 |
| 4060 | 300 | 38.5 | 0.128 |
| 4155 | 230 | 35.5 | 0.154 |
| 4215 | 310 | 19.5 | 0.063 |
| 4220 | 400 | 16.5 | 0.041 |

## Table 144.

### Thermoelectric Voltage Data for Columbium + 0.5% Zirconium

| Mean Temperature °F | Specimen ΔT °F | Resultant Voltage Output Millivolts | Voltage Output Per Degree Temperature Differential Mv/°F |
|---|---|---|---|
| 1632 | 67 | -3.80 | -0.057 |
| 1706 | 78 | -3.75 | -0.048 |
| 1740 | 81 | -3.75 | -0.046 |
| 2065 | 110 | -3.40 | -0.031 |
| 2080 | 120 | -3.40 | -0.028 |
| 2115 | 120 | -3.30 | -0.028 |
| 2343 | 125 | -3.15 | -0.025 |
| 2400 | 140 | -3.20 | -0.023 |
| 2400 | 140 | -3.25 | -0.023 |
| 2655 | 150 | -3.05 | -0.020 |
| 2680 | 170 | -3.05 | -0.018 |
| 2708 | 175 | -3.00 | -0.017 |
| 2923 | 175 | -2.00 | -0.011 |
| 2923 | 175 | -2.00 | -0.011 |
| 3198 | 235 | -1.40 | -0.006 |
| 3203 | 225 | -1.40 | -0.006 |
| 3213 | 205 | -1.40 | -0.007 |

## Table 145.

Thermoelectric Voltage Data for
Molybdenum + 0.5% Titanium

| Mean Temperature °F | Specimen ΔT °F | Resultant Voltage Output Millivolts | Voltage Output Per Degree Temperature Differential Mv/°F |
|---|---|---|---|
| 1880 | 70 | -3.85 | -0.055 |
| 1920 | 70 | -3.85 | -0.055 |
| 1928 | 65 | -3.95 | -0.061 |
| 1923 | 85 | -4.00 | -0.047 |
| 2203 | 95 | -4.00 | -0.042 |
| 2205 | 100 | -3.80 | -0.038 |
| 2210 | 90 | -3.80 | -0.042 |
| 2513 | 125 | -3.60 | -0.029 |
| 2530 | 120 | -3.60 | -0.030 |
| 2740 | 130 | -3.20 | -0.025 |
| 2755 | 130 | -3.20 | -0.025 |
| 2858 | 145 | -3.00 | -0.021 |
| 2875 | 150 | -2.95 | -0.020 |
| 2865 | 150 | -3.00 | -0.020 |
| 1708 | 45 | -3.40 | -0.076 |
| 1703 | 55 | -3.60 | -0.066 |

## Table 146.

### Thermoelectric Voltage Data for Platinum + 12. 2% Rhodium

| Mean Temperature °F | Specimen ΔT °F | Resultant Voltage Output Millivolts | Voltage Output Per Degree Temperature Differential Mv/°F |
|---|---|---|---|
| 1562 | 165 | 0. 40 | 0. 002 |
| 1575 | 160 | 0. 65 | 0. 004 |
| 1745 | 210 | 0. 95 | 0. 005 |
| 1780 | 260 | 0. 95 | 0. 004 |
| 1882 | 245 | 1. 25 | 0. 005 |
| 1880 | 240 | 1. 20 | 0. 005 |
| 1985 | 250 | 1. 80 | 0. 007 |
| 1992 | 245 | 1. 75 | 0. 007 |
| 2080 | 300 | 2. 00 | 0. 007 |
| 2102 | 295 | 2. 10 | 0. 007 |
| 2230 | 320 | 2. 60 | 0. 008 |
| 2257 | 305 | 2. 60 | 0. 009 |
| 2282 | 335 | 2. 60 | 0. 008 |
| 2292 | 355 | 2. 70 | 0. 008 |

## Table 147.

### Thermoelectric Voltage Data for Tungsten (Carborundum)

| Mean Temperature °F | Specimen ΔT °F | Resultant Voltage Output Millivolts | Voltage Output Per Degree Temperature Differential Mv/°F |
|---|---|---|---|
| | First Run, Specimen 1 | | |
| 1885 | 230 | -4.20 | -0.018 |
| 1873 | 225 | -4.20 | -0.019 |
| 2098 | 315 | -5.00 | -0.016 |
| 2100 | 300 | -5.00 | -0.017 |
| 2428 | 205 | -5.80 | -0.028 |
| 2455 | 210 | -5.80 | -0.028 |
| 2715 | 230 | -6.25 | -0.027 |
| 2735 | 230 | -6.25 | -0.027 |
| 2970 | 260 | -6.40 | -0.025 |
| 2990 | 260 | -6.40 | -0.025 |
| 3330 | 260 | -5.60 | -0.022 |
| 3325 | 250 | -5.60 | -0.022 |
| 3605 | 270 | -4.30 | -0.016 |
| 3595 | 270 | -4.25 | -0.016 |
| 3880 | 280 | -2.80 | -0.010 |
| 3873 | 265 | -2.90 | -0.011 |
| 4055 | 210 | -1.75 | -0.006 |
| 4055 | 190 | -1.65 | -0.009 |
| 4325 | 270 | -0.60 | -0.002 |
| 4355 | 330 | -0.55 | -0.002 |
| | Second Run, Specimen 1 | | |
| 1840 | 40 | -4.00 | -0.010 |
| 3405 | 130 | -3.55 | -0.027 |

## Table 148.

### Thermoelectric Voltage Data for Tungsten (General Electric)

| Mean Temperature °F | Specimen ΔT °F | Resultant Voltage Output Millivolts | Voltage Output Per Degree Temperature Differential Mv/°F |
|---|---|---|---|
| | First Run, Specimen 1 | | |
| 1750 | 40 | 1.20 | 0.030 |
| 1762 | 35 | 1.20 | 0.034 |
| 2297 | 45 | 0.95 | 0.021 |
| 2355 | 50 | 0.90 | 0.018 |
| 2455 | 50 | 0.95 | 0.019 |
| 2975 | 50 | 0.80 | 0.016 |
| 2990 | 40 | 0.70 | 0.018 |
| 3075 | 50 | 0.85 | 0.017 |
| 3445 | 50 | 0.40 | 0.008 |
| 3465 | 30 | 0.20 | 0.007 |
| 3490 | 60 | 0.60 | 0.010 |
| 3885 | 50 | -0.20 | -0.004 |
| 3830 | 20 | -0.10 | -0.005 |
| 3918 | 55 | -0.05 | -0.001 |
| 3925 | 10 | -0.05 | -0.005 |
| | Second Run, Specimen 1 | | |
| 1818 | 45 | 2.60 | 0.058 |
| 1853 | 55 | 2.40 | 0.044 |

## Table 149.

Thermoelectric Voltage Data for
ATJ Graphite

| Mean Temperature °F | Specimen ΔT °F | Resultant Voltage Output Millivolts | Voltage Output Per Degree Temperature Differential Mv/°F |
|---|---|---|---|
| 1645 | 90 | 0.15 | 0.002 |
| 1653 | 85 | 0.15 | 0.002 |
| 1833 | 55 | 0.30 | 0.005 |
| 1835 | 50 | 0.20 | 0.004 |
| 1843 | 55 | 0.20 | 0.004 |
| 1983 | 85 | 0.30 | 0.004 |
| 1985 | 60 | 0.15 | 0.003 |
| 2260 | 80 | 0.20 | 0.003 |
| 2260 | 80 | 0.20 | 0.003 |
| 2355 | 110 | 0.15 | 0.001 |
| 2360 | 110 | 0.20 | 0.002 |
| 2745 | 190 | 0.20 | 0.001 |
| 2740 | 180 | 0.20 | 0.001 |
| 2730 | 220 | 0.20 | 0.001 |
| 2835 | 110 | 0.30 | 0.003 |
| 2925 | 150 | 0.35 | 0.002 |
| 2890 | 160 | 0.30 | 0.002 |
| 3130 | 200 | 0.20 | 0.001 |
| 3130 | 210 | 0.25 | 0.001 |
| 3340 | 240 | 0.20 | 0.001 |
| 3345 | 250 | 0.25 | 0.001 |
| 3625 | 250 | 0.30 | 0.001 |
| 3613 | 225 | 0.25 | 0.001 |
| 3828 | 185 | 0.50 | 0.003 |
| 3790 | 220 | 0.45 | 0.002 |
| 3810 | 260 | 0.45 | 0.002 |
| 4010 | 260 | 0.45 | 0.002 |

Table 149 (Continued).

Thermoelectric Voltage Data for
ATJ Graphite

| Mean Temperature °F | Specimen ΔT °F | Resultant Voltage Output Millivolts | Voltage Output Per Degree Temperature Differential Mv/°F |
|---|---|---|---|
| 4000 | 240 | 0.40 | 0.002 |
| 4195 | 260 | 0.40 | 0.002 |
| 4185 | 250 | 0.50 | 0.002 |
| 4355 | 290 | 0.70 | 0.002 |
| 4310 | 220 | 0.60 | 0.003 |
| 4555 | 190 | 0.60 | 0.003 |
| 4570 | 340 | 0.60 | 0.002 |

Aeronautical Systems Division, Dir/
Materials and Processes, Physics Lab,
Wright-Patterson AFB, Ohio
Rpt Nr ASD-TDR-62-765. THE THERMAL PROPERTIES OF TWENTY-SIX SOLID MATERIALS TO 5000°F OR THEIR DESTRUCTION TEMPERATURES. Final Report, Aug 62, 420 pp incl illus. and tables.

Unclassified Report

The thermal expansion, heat capacity, thermal conductivity, total normal emittance, electric resistivity, and thermoelectric

( over )

1. Refractory materials
2. Thermophysical properties

I. AFSC Project 7381, Task 738103
II. Contract AF 33(616)-7319
III. Southern Research Institute, Birmingham, Alabama
IV. C. D. Pears et al
V. Aval fr OTS
VI. In ASTIA Collection

---

voltage were investigated for 26 refractory materials, including the borides, carbides, nitrides, oxides, ATJ graphite, tungsten, and alloys of molybdenum and columbium. The temperature range was from 500°F to 5000°F. In addition to these thermophysical properties, the density, chemical analysis before and after temperature exposure, and microscopic pictures before and after temperature exposure, are included to define the materials and assist in the analysis of the data.